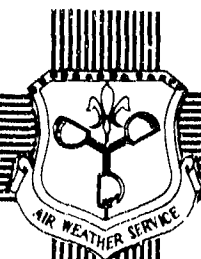


DTIC
AD-A240 437



USAFETAC/TN--91/005

movers 2



SWANEA

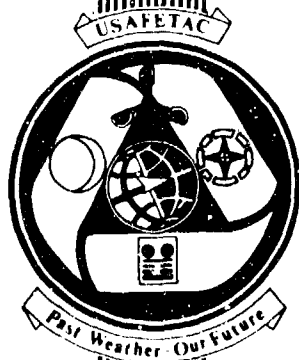
(SOUTHWEST ASIA-NORTHEAST AFRICA)

A CLIMATOLOGICAL STUDY

VOLUME IV--THE MEDITERRANEAN COAST
AND NORTHEAST AFRICA

by

1st Lt Michael J. Vojtesak
Capt Kathleen M. Traxler
Michael T. Gilford
Capt Kevin P. Martin
SSgt Gordon Hepburn



JULY 1991

APPROVED FOR PUBLIC RELEASE;
DISTRIBUTION IS UNLIMITED

91-10643



USAF
ENVIRONMENTAL TECHNICAL
APPLICATIONS CENTER

Scott Air Force Base, Illinois, 62225-5438

91 9 13 021

REVIEW AND APPROVAL STATEMENT

USAFETAC/TN-91/005, *SWANEA (Southwest Asia--Northeast Africa)--A Climatological Study, Volume IV--The Mediterranean Coast and Northeast Africa*, July 1991, has been reviewed and is approved for public release. There is no objection to unlimited distribution of this document to the public at large, or by the Defense Technical Information Center (DTIC) to the National Technical Information Service (NTIS).

FOR THE COMMANDER



WALTER S. BURGMANN

Scientific and Technical Information

Program Manager

10 July 1991

REPORT DOCUMENTATION PAGE

2. Report Date: July 1991
3. Report Type: Technical Note
4. Title and Subtitle: SWANEA (Southwest Asia--Northeast Africa)--A Climatological Study, Volume IV--The Mediterranean Coast and Northeast Africa
6. Authors: 1st Lt Michael J. Vojtesak, Capt Kathleen M. Traxler, Mr Michael T. Gilford, Capt Kevin P. Martin, SSgt Gordon K. Hepburn
7. Performing Organization Name and Address: USAF Environmental Technical Applications Center (USAFETAC/ECR), Scott AFB, IL 62225-5438.
8. Performing Organization Report Number: USAFETAC/TN--91/005
12. Distribution/Availability Statement: Approved for public release; distribution is unlimited.
13. Abstract: The fourth in a four-volume series, this volume is a climatological study of the Mediterranean Coast and Northeast Africa, an area that includes the coastlines of western and southern Turkey through Libya, plus the countries of Egypt, Libya, Chad, and Sudan. After describing the general geography of these areas, it discusses the major meteorological features of the entire study region. Each major subregion (based on "climatic commonality") is then broken into its own geography and general weather sections. Finally, the four so-called "seasons" in each of these subregions are discussed in detail.
14. Subject Terms: CLIMATOLOGY, METEOROLOGY, WEATHER, GEOGRAPHY, AFRICA, MEDITERRANEAN, Turkey, Egypt, Libya, Chad, Sudan
15. Number of Pages: 236
17. Security Classification of Report: Unclassified
18. Security Classification of this Page: Unclassified
19. Security Classification of Abstract: Unclassified
20. Limitation of Abstract: UL

Accession For	
DTIC GRA&I	<input checked="" type="checkbox"/>
DTIC TAB	<input type="checkbox"/>
Unannounced	<input type="checkbox"/>
Justification	
By	
Distribution/	
Availability Codes	
Dist	Avail and/or Special
A-1	

Standard Form 298



PREFACE

This study was prepared by the United States Air Force Environmental Technical Applications Center, Readiness Support Section (USAFETAC/ECR), in response to a support assistance request (SAR) from the 5th Weather Wing, Langley AFB, VA, under the provisions of Air Weather Service Regulation 105-18. It documents work done under USAFETAC project 807-11, and is the fourth in a four-volume series that discusses the climatology of the area known as "SWANEA" (Southwest Asia-Northeast Africa). Like its predecessors, this work is complemented by two other SWANEA studies. One describes transmittance climatology in the 3-5 and 8-12 micron bands; the other, refractive climatology. Publication of these complementary studies parallels or follows the parent work.

The project would not have been possible without the dedicated support of the many people and agencies we have listed below in the sincere hope we've not omitted anyone.

First, our deepest gratitude and appreciation to Mr Walter S. Burgmann, Mr Wayne E. McCullom, Mr William Reller, Mrs Kay Marshall, and Mrs Susan Keller of the Air Weather Service Technical Library.

To Mr Henry ("Mac") Fountain, Mr Vann Gibbs, Mr Dudley ("Lee") Foster, and other members of Operating Location A (OL-A), USAF Environmental Technical Applications Center, Asheville, NC, for providing data, data summaries, and technical support.

Thanks to Maj William F. Sjoberg, Mr Kenneth R. Walters Sr, and Capt Don D. Carter of USAFETAC's Readiness Support Section (ECR) for their hard work, assistance, and encouragement.

Thanks to Mr Robert Fett of the U.S. Naval Environmental Prediction Research Facility and Lt Cmdr Rutsh (Naval Liaison to Air Force Global Weather Central--AFGWC) for their assistance in providing supplemental data for this project.

Thanks to Mr Maurice Crew of the United Kingdom Meteorological Office for providing copies of studies unavailable elsewhere.

Thanks to Lt Col Frank Globokar, Lt Col John Erickson, Maj Daniel Ridge, Maj Roger Edson, and Capt Patrick Condray, for their cooperation in establishing and providing "peer review" of draft manuscripts.

Thanks to SSgt Thomas E. Dunker of USAFETAC's Operational Applications Section (ECO) for providing the wind roses used in this document.

Finally, all the authors owe sincere gratitude to the Technical Publications Editing Section of the AWS Technical Library (USAFETAC/LDE)-- Mr George M. Horn and Sgt Corinne M. Kawa. Without their patience and cooperation, this project could not have been completed.

CONTENTS

Chapter 1	INTRODUCTION	Page
	Area of Interest	1-1
	Geography	1-3
	Study Content	1-4
	Climatological Regimes	1-5
	Conventions	1-5
	Data Sources	1-5
	Related References	1-5
Chapter 2	MAJOR METEOROLOGICAL FEATURES OF THE MEDITERRANEAN COAST AND NORTHEAST AFRICA	
	Semipermanent Climatic Controls	2-1
	Synoptic Disturbances	2-27
	Mesoscale and Local Effects	2-43
	Regional Winds	2-57
Chapter 3	THE TURKISH COAST	
	Situation and Relief	3-2
	Winter	3-6
	Spring	3-14
	Summer	3-19
	Fall	3-24
Chapter 4	THE EASTERN MEDITERRANEAN COAST	
	Situation and Relief	4-2
	Winter	4-6
	Spring	4-15
	Summer	4-22
	Fall	4-27
Chapter 5	THE NORTH AFRICAN COAST	
	Situation and Relief	5-2
	Winter	5-7
	Spring	5-13
	Summer	5-18
	Fall	5-23
Chapter 6	THE EASTERN SAHARA	
	Situation and Relief	6-2
	Winter	6-7
	Spring	6-14
	Summer	6-20
	Fall	6-26
Chapter 7	SOUTHERN CHAD/SUDAN	
	Situation and Relief	7-2
	Dry Season	7-4
	Dry to Wet Transition	7-11
	Wet Season	7-16
	Wet to Dry Transition	7-21
	BIBLIOGRAPHY	BIB-1

FIGURES

Figure 1-1.	The Southwest Asia-Northeast Africa (SWANEA) Region.....	1-1
Figure 1-2.	The Mediterranean Coast and Northeast Africa Subregions	1-2
Figure 1-3.	Topography of the Mediterranean Coast and Northeast Africa.....	1-3
Figure 2-1a.	Mean January Sea Surface Temperatures (F).....	2-2
Figure 2-1b.	Mean April Sea Surface Temperatures (F).....	2-2
Figure 2-1c.	Mean July Sea Surface Temperatures (F).....	2-3
Figure 2-1d.	Mean October Sea Surface Temperatures (F).....	2-3
Figure 2-2a.	Mean January Position of the Azores High, Icelandic Low, Asiatic High, and Saharan High.	2-5
Figure 2-2b.	Mean April Position of the Azores High, Icelandic Low, Asiatic High, and Saharan High.	2-5
Figure 2-2c.	Mean July Position of the Azores High and Icelandic Low.	2-6
Figure 2-2d.	Mean October Position of the Azores High, Icelandic Low, and Asiatic High.....	2-6
Figure 2-3.	General Tracks For Cold Asiatic Air Into the Central and Eastern Mediterranean.....	2-7
Figure 2-4a.	Mean January Position of the Sudanese Low.....	2-8
Figure 2-4b.	Mean April Position of the Sudanese Low.....	2-8
Figure 2-4c.	Mean July Positions of the Saharan Low, Anatolian Plateau Thermal Trough, and Sudanese Trough.....	2-9
Figure 2-4d.	Mean October Position of the Sudanese Low.....	2-9
Figure 2-5.	Mean July Position of the Saudi Arabian Heat Low.	2-10
Figure 2-6.	Region Affected by the Monsoon Climate.	2-11
Figure 2-7a.	Mean March-July Monsoon Trough Positions, Chad and Sudan.....	2-12
Figure 2-7b.	Mean August-November Monsoon Trough Positions, Chad and Sudan.....	2-12
Figure 2-8a.	Summer Monsoon Trough Meteorological Pattern.	2-13
Figure 2-8b.	Satellite View of Northeast Africa Showing a Tropical Disturbance in the Monsoon Trough (Fett, 1983).	2-14
Figure 2-9.	Vertical Cross Section of the "African Interior" Monsoon Trough and the Intertropical Discontinuity (ITD) (from Omotosho, 1984).	2-15
Figure 2-10a.	Mean January Upper-Air Flow Patterns, 850 mb.	2-16
Figure 2-10b.	Mean January Upper-Air Flow Patterns, 700 mb.	2-16
Figure 2-10c.	Mean January Upper-Air Flow Patterns, 500 mb.	2-17
Figure 2-10d.	Mean January Upper-Air Flow Patterns, 300 mb.	2-17
Figure 2-10e.	Mean January Upper-Air Flow Patterns, 200 mb.	2-18
Figure 2-11a.	Mean April Upper-Air Flow Patterns, 850 mb.	2-18
Figure 2-11b.	Mean April Upper-Air Flow Patterns, 700 mb.	2-19
Figure 2-11c.	Mean April Upper-Air Flow Patterns, 500 mb.	2-19
Figure 2-11d.	Mean April Upper-Air Flow Patterns, 300 mb.	2-20
Figure 2-11e.	Mean April Upper-Air Flow Patterns, 200 mb.	2-20
Figure 2-12a.	Mean July Upper-Air Flow Patterns, 850 mb.	2-21
Figure 2-12b.	Mean July Upper-Air Flow Patterns, 700 mb.	2-21
Figure 2-12c.	Mean July Upper-Air Flow Patterns, 500 mb.	2-22
Figure 2-12d.	Mean July Upper-Air Flow Patterns, 300 mb.	2-22
Figure 2-12e.	Mean July Upper-Air Flow Patterns, 200 mb.	2-23
Figure 2-13a.	Mean October Upper-Air Flow Patterns, 850 mb.	2-23
Figure 2-13b.	Mean October Upper-Air Flow Patterns, 700 mb.	2-24
Figure 2-13c.	Mean October Upper-Air Flow Patterns, 500 mb.	2-24
Figure 2-13d.	Mean October Upper-Air Flow Patterns, 300 mb.	2-25
Figure 2-13e.	Mean October Upper-Air Flow Patterns, 200 mb.	2-25
Figure 2-14.	Mean January and July Positions of the Subtropical Ridge.	2-26
Figure 2-15.	Mean January and July Positions of the Polar Jet (PJ) and Subtropical Jet (STJ).....	2-27
Figure 2-16a.	Typical Jet Positions During Formation of Genoa Low.	2-28
Figure 2-16b.	Typical Jet Positions During Formation of Atlas Low.	2-28
Figure 2-16c.	Typical Jet Positions During Formation of Cyprus Low.....	2-29

Figure 2-17.	Mean July 200-mb Zonal Flow Showing the Tropical Easterly Jet (TEJ).	2-29
Figure 2-18.	Meridional Cross Section of Zonal Winds Near 10° E for July.	2-30
Figure 2-19.	Cross Sectional View Showing the MTEJ at 13° N in August (from Burpee, 1972).	2-30
Figure 2-20.	Mediterranean Cyclogenesis Regions.....	2-31
Figure 2-21a.	Synoptic Surface Chart (7 April 1954, 0000Z), Atlas Low.....	2-32
Figure 2-21b.	500-mb Flow (7 April, 1954, 0300Z), Atlas Low.	2-33
Figure 2-21c.	Synoptic Surface Chart (8 April 1954, 0000Z), Atlas Low.....	2-33
Figure 2-21d.	500-mb Flow (8 April, 1954, 0300Z), Atlas Low.	2-34
Figure 2-21e.	Synoptic Surface Chart (9 April 1954, 0000Z), Atlas Low.....	2-34
Figure 2-22.	Surface Circulation Causes Development of the Cyprus Low.	2-35
Figure 2-23a.	Synoptic Surface Chart (16 November 1953, 0000Z), Cyprus Low.	2-36
Figure 2-23b.	Synoptic Surface Chart (17 November 1953, 0000Z), Cyprus Low.	2-36
Figure 2-23c.	Synoptic Surface Chart (18 November 1953, 0000Z), Cyprus Low.	2-37
Figure 2-23d.	500-mb Flow (18 November 1953, 0300Z), Cyprus Low.....	2-37
Figure 2-24a.	500-mb Contour Chart Over a Cyprus Low With No Severe Thunderstorms or Heavy Precipitation.....	2-38
Figure 2-24b.	Surface Chart Depicting Cyprus Low Position Beneath a Weak Mid-Level Trough With No Severe Thunderstorms or Heavy Precipitation.	2-38
Figure 2-24c.	500-mb Contour Chart Over an Intense Cyprus Low With Severe Thunderstorms and Heavy Precipitation.....	2-39
Figure 2-24d.	Surface Chart Depicting Cyprus Low Position Beneath a Strong Mid-Level Trough With Severe Thunderstorms and Heavy Precipitation.....	2-39
Figure 2-25a.	Primary (solid arrow) and Secondary (dashed arrow) Mid-Latitude Storm Tracks, November. ...	2-40
Figure 2-25b.	Primary (solid arrow) and Secondary (dashed arrow) Mid-Latitude Storm Tracks, December, January, and February.	2-40
Figure 2-25c.	Primary (solid arrow) and Secondary (dashed arrow) Mid-Latitude Storm Tracks, March and April.....	2-40
Figure 2-26.	Basic Cloud and Wind Pattern with a Tropical Wave (from Leroux, 1983).	2-41
Figure 2-27.	Formation of an African Squall Line (vertical cross-section) (from Hayward, 1987).	2-42
Figure 2-28.	The "Common" Daytime Sea Breeze (A) and Nighttime Land Breeze (B).	2-43
Figure 2-29a.	Gradient Flow With Offshore Wind Component Slopes Gently Over Dense, Cooler Marine Boundary Layer.	2-43
Figure 2-29b.	Increased Compacting Tightens Pressure Gradient Along Land-Sea Interface.....	2-43
Figure 2-29c.	Maximum Compacting of the Marine Boundary Layer.	2-43
Figure 2-29d.	Frontal Sea Breeze Accelerates Towards Shore.	2-44
Figure 2-29e.	Sea Breeze "Front" Reaches the Coast.	2-44
Figure 2-29f.	Land/Sea Breeze Mechanism in Full Swing.....	2-44
Figure 2-30a.	Mean Monthly Relative Humidities for Izmir, Turkey.....	2-44
Figure 2-30b.	Mean Monthly Relative Humidities for Beirut, Lebanon.....	2-45
Figure 2-30c.	Mean Monthly Relative Humidities for Bet Dagan, Israel.	2-45
Figure 2-30d.	Mean Monthly Relative Humidities for Matruh, Egypt.	2-45
Figure 2-30e.	Mean Monthly Relative Humidities for Benghazi, Libya.	2-46
Figure 2-31a.	Typical Daytime Mountain/Valley Circulation (from Flohn, 1969).	2-47
Figure 2-31b.	Typical Nighttime Mountain/Valley Circulation (from Flohn, 1969).	2-47
Figure 2-32a.	Typical Mountain/Valley Wind Circulation Life Cycle: SUNRISE	2-48
Figure 2-32b.	MORNING.	2-48
Figure 2-32c.	MIDDAY.....	2-48
Figure 2-32d.	LATE AFTERNOON.....	2-48
Figure 2-32e.	SUNSET.....	2-48
Figure 2-32f.	EVENING.....	2-48
Figure 2-32g.	MIDNIGHT.....	2-49
Figure 2-32h.	PRE-DAWN.....	2-49
Figure 2-33.	Fully Developed Lee Wave System (from Wallace and Hobbs, 1977).	2-49

Figure 2-34.	Three-Dimensional View of Longitudinal Vortices in the Boundary Layer (from Hanna, 1969).....	2-51
Figure 2-35.	Cross-Sectional View of Dune and Cloud Formation Mechanism (from Hanna, 1969).....	2-51
Figure 2-36.	WBGT Heat Stress Index Activity Guidelines.....	2-52
Figure 2-37a.	Average Maximum WBGT--January.....	2-53
Figure 2-37b.	Average Maximum WBGT--April.....	2-54
Figure 2-37c.	Average Maximum WBGT--July.....	2-55
Figure 2-37d.	Average Maximum WBGT--October.....	2-56
Figure 2-38.	Typical Low-Pressure System Track Creating Khamsin Conditions.....	2-57
Figure 2-39.	Khamsin-Type Conditions Associated With a Rare Eastward-Moving Atlas Low.....	2-58
Figure 2-40.	Active Storm Track For Sharav Winds.....	2-59
Figure 2-41.	Deep Trough Producing Sirocco Winds.....	2-60
Figure 2-42.	Regional Harmattan.....	2-61
Figure 2-43a.	METEOSAT Imagery of Harmattan-Produced Duststorm Over Chad and Sudan (6 March 1991, 1030Z).....	2-62
Figure 2-43b.	Surface Data: Harmattan-Produced Duststorm Over Northeast Africa (6 March 1991, 1200Z).....	2-63
Figure 2-44.	Source Region For "Habob" Development (from Hammer, 1970).....	2-64
Figure 3-1a.	The Turkish Coast.....	3-2
Figure 3-1b.	Climatological Summaries for Selected Stations on the Turkish Coast.....	3-3
Figure 3-2.	Topographical Features of the Turkish Coast.....	3-4
Figure 3-3.	Mean Winter Frequencies of Ceilings Below 3,000 Feet (915 meters), Turkish Coast.....	3-5
Figure 3-4.	Mean Winter Frequencies of Visibilities Below 3 Miles, Turkish Coast.....	3-6
Figure 3-5.	January Surface Wind Roses, Turkish Coast.....	3-7
Figure 3-6a.	Mean Annual Upper-Air Wind Directions, Isparta, Turkey.....	3-8
Figure 3-6b.	Mean Annual Upper-Air Wind Directions, Izmir, Turkey.....	3-8
Figure 3-7.	Mean Winter Monthly Precipitation, Turkish Coast.....	3-9
Figure 3-8a.	A Favored Track for Heavy Precipitation along the Western Turkish Coast.....	3-10
Figure 3-8b.	A Favored Track for Heavy Precipitation along the Southern Turkish Coast.....	3-10
Figure 3-9.	Mean Winter Thunderstorm Days, Turkish Coast.....	3-11
Figure 3-10.	Mean Winter Daily Maximum/Minimum Temperatures (F), Turkish Coast.....	3-12
Figure 3-11.	Mean Spring Frequencies of Ceilings Below 3,000 Feet (915 meters), Turkish Coast.....	3-13
Figure 3-12.	Mean Spring Frequencies of Visibilities Below 3 Miles, Turkish Coast.....	3-14
Figure 3-13.	April Surface Wind Roses, Turkish Coast.....	3-15
Figure 3-14.	Mean Spring Monthly Precipitation, Turkish Coast.....	3-16
Figure 3-15.	Mean Spring Thunderstorm Days, Turkish Coast.....	3-17
Figure 3-16.	Mean Spring Daily Maximum/Minimum Temperatures (F), Turkish Coast.....	3-18
Figure 3-17.	Mean Summer Frequencies of Ceilings Below 3,000 Feet (915 meters), Turkish Coast.....	3-19
Figure 3-18.	Mean Summer Frequencies of Visibilities Below 3 Miles, Turkish Coast.....	3-20
Figure 3-19.	July Surface Wind Roses, Turkish Coast.....	3-21
Figure 3-20.	Mean Summer Monthly Precipitation, Turkish Coast.....	3-22
Figure 3-21.	Mean Summer Thunderstorm Days, Turkish Coast.....	3-23
Figure 3-22.	Mean Summer Daily Maximum/Minimum Temperatures (F), Turkish Coast.....	3-24
Figure 3-23.	Mean Fall Frequencies of Ceilings Below 3,000 Feet (915 meters), Turkish Coast.....	3-25
Figure 3-24.	Mean Fall Frequencies of Visibilities Below 3 Miles, Turkish Coast.....	3-26
Figure 3-25.	October Surface Wind Roses, Turkish Coast.....	3-27
Figure 3-26.	Mean Fall Precipitation, Turkish Coast.....	3-28
Figure 3-27.	Mean Fall Thunderstorm Days, Turkish Coast.....	3-29
Figure 3-28.	Mean Fall Daily Maximum/Minimum Temperatures (F), Turkish Coast.....	3-30
Figure 4-1a.	The Eastern Mediterranean Coast.....	4-2
Figure 4-1b.	Climatological Summaries for Selected Stations on the Eastern Mediterranean Coast.....	4-3
Figure 4-1c.	More Climatological Summaries for Selected Stations on the Eastern Mediterranean Coast.....	4-4
Figure 4-2.	Mean Winter Frequencies of Ceilings Below 3,000 Feet (915 meters), Eastern Mediterranean Coast.....	4-7
Figure 4-3.	Mean Winter Frequencies of Visibilities Below 3 Miles, Eastern Mediterranean Coast.....	4-8

Figure 4-4.	January Surface Wind Roses, Eastern Mediterranean Coast.....	4-9
Figure 4-5a.	Upper-level Annual Mean Wind Direction, Beirut, Lebanon.....	4-10
Figure 4-5b.	Upper-level Annual Mean Wind Direction, Bet Dagan, Israel.....	4-10
Figure 4-6.	Mean Winter Monthly Precipitation, Eastern Mediterranean Coast.....	4-11
Figure 4-7.	Mean Winter Thunderstorm Days, Eastern Mediterranean Coast.....	4-12
Figure 4-8.	An Example of 500-mb Flow Causing Widespread Snow in the Eastern Mediterranean.....	4-13
Figure 4-9.	Mean Winter Daily Maximum/Minimum Temperatures (F), Eastern Mediterranean Coast.....	4-14
Figure 4-10.	Mean Spring Frequencies of Ceilings Below 3,000 Feet (915 meters), Eastern Mediterranean Coast.....	4-16
Figure 4-11.	Mean Spring Frequencies of Visibilities Below 3 Miles, Eastern Mediterranean Coast.....	4-17
Figure 4-12.	April Surface Wind Roses, Eastern Mediterranean Coast.....	4-18
Figure 4-13.	Mean Spring Monthly Precipitation, Eastern Mediterranean Coast.....	4-19
Figure 4-14.	Mean Spring Thunderstorm Days, Eastern Mediterranean Coast.....	4-20
Figure 4-15.	Mean Spring Daily Maximum/Minimum Temperatures (F), Eastern Mediterranean Coast.....	4-21
Figure 4-16.	Mean Summer Frequencies of Ceilings Below 3,000 Feet (915 meters), Eastern Mediterranean Coast.....	4-23
Figure 4-17.	Mean Summer Frequencies of Visibilities Below 3 Miles, Eastern Mediterranean Coast.....	4-24
Figure 4-18.	July Surface Wind Roses, Eastern Mediterranean Coast.....	4-25
Figure 4-19.	Mean Summer Daily Maximum/Minimum Temperatures (F), Eastern Mediterranean Coast.....	4-26
Figure 4-20.	Mean Fall Frequencies of Ceilings Below 3,000 Feet (915 meters), Eastern Mediterranean Coast.....	4-28
Figure 4-21.	Mean Fall Frequencies of Visibilities Below 3 Miles, Eastern Mediterranean Coast.....	4-29
Figure 4-22.	October Surface Wind Roses, Eastern Mediterranean Coast.....	4-30
Figure 4-23.	Mean Fall Monthly Precipitation, Eastern Mediterranean Coast.....	4-31
Figure 4-24.	Mean Fall Thunderstorm Days, Eastern Mediterranean Coast.....	4-32
Figure 4-25.	Mean Fall Daily Maximum/Minimum Temperatures (F), Eastern Mediterranean Coast.....	4-33
Figure 5-1a.	The North African Coast.....	5-2
Figure 5-1b.	Climatological Summaries for Selected Stations on the North African Coast.....	5-2
Figure 5-1c.	More Climatological Summaries for Selected Stations on the North African Coast.....	5-3
Figure 5-1d.	Still More Climatological Summaries for Selected Stations on the North African Coast.....	5-4
Figure 5-2.	The Nile Delta, Showing Primary Rivers, Lakes, and Cities.....	5-5
Figure 5-3.	Mean Winter Frequencies of Ceilings Below 3,000 Feet (915 meters), North African Coast.....	5-7
Figure 5-4.	Mean Winter Frequencies of Visibilities Below 3 Miles, North African Coast.....	5-8
Figure 5-5.	January Surface Wind Roses, North African Coast.....	5-9
Figure 5-6a.	Upper-level Annual Mean Wind Direction, Tripoli, Libya.....	5-9
Figure 5-6b.	Upper-level Annual Mean Wind Direction, Benghazi, Libya.....	5-10
Figure 5-7.	Mean Winter Monthly Precipitation, North African Coast.....	5-10
Figure 5-8.	Typical Northeast Track of the Genoa Low.....	5-11
Figure 5-9.	Mean Winter Thunderstorm Days, North African Coast.....	5-11
Figure 5-10.	Mean Winter Daily Maximum/Minimum Temperatures (F), North African Coast.....	5-12
Figure 5-11.	Mean Spring Frequencies of Ceilings Below 3,000 Feet (915 meters), North African Coast.....	5-13
Figure 5-12.	Mean Spring Frequencies of Visibilities Below 3 Miles, North African Coast.....	5-14
Figure 5-13.	April Surface Wind Roses, North African Coast.....	5-15
Figure 5-14.	Mean Spring Monthly Precipitation, North African Coast.....	5-16
Figure 5-15.	Mean Spring Daily Maximum/Minimum Temperatures (F), North African Coast.....	5-17
Figure 5-16.	Mean Summer Frequencies of Ceilings Below 3,000 Feet (915 meters), North African Coast.....	5-18
Figure 5-17a.	Summer Source Regions for Cumulus Development in the Akhdar Mountains.....	5-19
Figure 5-17b.	Summer Source Region for Sea-Breeze Cumulus Development in the Nafusah Mountains.....	5-19
Figure 5-18.	Mean Summer Frequencies of Visibilities Below 3 Miles, North African Coast.....	5-20
Figure 5-19.	July Surface Wind Roses, North African Coast.....	5-21
Figure 5-20.	Summer Short Waves Affecting the Eastern Mediterranean.....	5-21
Figure 5-21.	Mean Summer Daily Maximum/Minimum Temperatures (F), North African Coast.....	5-22
Figure 5-22.	Mean Summer Frequencies of Ceilings Below 3,000 Feet (915 meters), North African Coast.....	5-23
Figure 5-23.	Mean Fall Frequencies of Visibilities Below 3 Miles, North African Coast.....	5-24

Figure 5-24.	October Surface Wind Roses, North African Coast.....	5-24
Figure 5-25.	Mean Fall Monthly Precipitation, North African Coast.....	5-25
Figure 5-26.	Mean Fall Thunderstorm Days, North African Coast.....	5-25
Figure 5-27.	Mean Fall Daily Maximum/Minimum Temperatures (F), North African Coast.....	5-26
Figure 6-1a.	The Eastern Sahara.....	6-2
Figure 6-1b.	Climatological Summaries for Selected Stations in the Eastern Sahara.....	6-3
Figure 6-1c.	More Climatological Summaries for Selected Stations in the Eastern Sahara.....	6-4
Figure 6-2.	Mean Winter Cloudiness (Isopleths) and Frequencies of Ceilings Below 3,000 Feet (915 meters), Eastern Sahara.....	6-7
Figure 6-3.	Mean Winter Frequencies of Visibilities Below 3 Miles, Eastern Sahara.....	6-8
Figure 6-4.	January Surface Wind Roses, Eastern Sahara.....	6-9
Figure 6-5a.	Mean Annual Wind Direction for Dongola, Sudan.....	6-10
Figure 6-5b.	Mean Annual Wind Direction for Kufra, Libya.....	6-10
Figure 6-5c.	Mean Annual Wind Direction for Sabha, Libya.....	6-11
Figure 6-6.	Mean Winter Monthly/Maximum 24-hour Precipitation, Eastern Sahara.....	6-12
Figure 6-7.	Mean Winter Daily Maximum/Minimum Temperatures (F), Eastern Sahara.....	6-13
Figure 6-8.	Mean Spring Cloudiness (Isopleths) and Frequencies of Ceilings Below 3,000 Feet (915 meters), Eastern Sahara.....	6-14
Figure 6-9.	Mean Spring Frequencies of Visibilities Below 3 Miles, Eastern Sahara.....	6-16
Figure 6-10.	April Surface Wind Roses, Eastern Sahara.....	6-17
Figure 6-11.	Mean Winter Monthly/Maximum 24-hour Precipitation, Eastern Sahara.....	6-18
Figure 6-12.	Mean Spring Daily Maximum/Minimum Temperatures (F), Eastern Sahara.....	6-19
Figure 6-13.	Mean Spring Cloudiness (Isopleths) and Frequencies of Ceilings Below 3,000 Feet (915 meters), Eastern Sahara.....	6-20
Figure 6-14.	Mean Summer Frequencies of Visibilities Below 3 Miles, Eastern Sahara.....	6-21
Figure 6-15.	July Surface Wind Roses, Eastern Sahara.....	6-22
Figure 6-16.	Mean Summer Monthly/Maximum 24-hour Precipitation, Eastern Sahara.....	6-23
Figure 6-17a.	Gradient-Level Flow, Widespread Summer Rain and Thunderstorms.....	6-24
Figure 6-17b.	700-mb Flow, Widespread Summer Rain and Thunderstorms.....	6-24
Figure 6-18.	Summer Mean Daily Maximum/Minimum Temperatures (F), Eastern Sahara.....	6-25
Figure 6-19.	Mean Fall Cloudiness (Isopleths) and Frequencies of Ceilings Below 3,000 Feet (915 meters), Eastern Sahara.....	6-26
Figure 6-20.	Mean Fall Frequencies of Visibilities Below 3 Miles, Eastern Sahara.....	6-27
Figure 6-21.	October Surface Wind Roses, Eastern Sahara.....	6-28
Figure 6-22.	Mean Fall Monthly/Maximum 24-hour Precipitation, Eastern Sahara.....	6-29
Figure 6-23.	Mean Fall Daily Maximum/Minimum Temperatures (F), Eastern Sahara.....	6-30
Figure 7-1a.	Southern Chad and Sudan.....	7-2
Figure 7-1b.	Climatological Summaries For two Stations, Southern Chad and Sudan.....	7-4
Figure 7-2.	Mean Dry Season Cloudiness (Isopleths) and Frequencies of Ceilings Below 3,000 Feet (915 meters), Southern Chad and Sudan.....	7-5
Figure 7-3.	Mean Dry Season Frequencies of Visibilities Below 3 Miles, Southern Chad and Sudan.....	7-6
Figure 7-4.	Mean Dry Season Surface Wind Roses, Southern Chad and Sudan.....	7-7
Figure 7-5a.	Upper-level Annual Mean Wind Direction, Khartoum, Chad.....	7-7
Figure 7-5b.	Upper-level Annual Mean Wind Direction, N'Djamena, Chad.....	7-8
Figure 7-5c.	Upper-level Annual Mean Wind Direction, Sarh, Chad.....	7-8
Figure 7-6.	Mean Annual 30,000-foot (9 km) Wind Direction, Southern Chad and Sudan.....	7-9
Figure 7-7.	Mean Dry Season Monthly/Maximum 24-hour Precipitation, Southern Chad and Sudan.....	7-10
Figure 7-8.	Mean Dry Season Thunderstorm Days, Southern Chad and Sudan.....	7-10
Figure 7-9.	Mean Dry Season Daily Maximum/Minimum Temperatures (F), Southern Chad and Sudan.....	7-11
Figure 7-10.	Mean Dry-to-Wet Transition Cloudiness (Isopleths) and Frequencies of Ceilings Below 3,000 Feet (915 meters), Southern Chad and Sudan.....	7-12
Figure 7-11.	Mean Dry-to-Wet Transition Frequencies of Visibilities Below 3 Miles, Southern Chad and Sudan.....	7-13
Figure 7-12.	Mean Dry-to-Wet Transition Surface Wind Roses, Southern Chad and Sudan.....	7-14

Figure 7-13.	Mean Dry-to-Wet Transition Monthly/Maximum 24-hour Precipitation, Southern Chad and Sudan.	7-15
Figure 7-14.	Mean Dry-to-Wet Transition Thunderstorm Days, Southern Chad and Sudan.	7-16
Figure 7-15.	Mean Dry-to-Wet Transition Daily Maximum/Minimum Temperatures (F), Southern Chad and Sudan.	7-16
Figure 7-16.	Mean Wet Season Cloudiness (Isopleths) and Frequencies of Ceilings Below 3,000 Feet (915 meters), Southern Chad and Sudan.	7-17
Figure 7-17.	Mean Wet Season Frequencies of Visibilities Below 3 Miles, Southern Chad and Sudan.	7-18
Figure 7-18.	July Surface Wind Roses, Southern Chad and Sudan.	7-19
Figure 7-19.	Mean Wet Season Monthly/Maximum 24-hour Precipitation, Southern Chad and Sudan.	7-20
Figure 7-20.	Mean Wet-Season Thunderstorm Days, Southern Chad and Sudan.	7-20
Figure 7-21.	Mean Wet-Season Daily Maximum/Minimum Temperatures (F), Southern Chad and Sudan.	7-21
Figure 7-22.	Mean Wet-to-Dry Transition Cloudiness (Isolines) and Frequencies of Ceilings Below 3,000 Feet (915 meters), Southern Chad and Sudan.	7-22
Figure 7-23.	Mean Wet-to-Dry Transition Frequencies of Visibilities Below 3 Miles, Southern Chad and Sudan.	7-22
Figure 7-24.	October Surface Wind Roses, Southern Chad and Sudan.	7-24
Figure 7-25.	Mean Wet-to-Dry Transition Monthly/Maximum 24-hour Precipitation, Southern Chad and Sudan.	7-24
Figure 7-26.	Mean Wet-to-Dry Transition Thunderstorm Days, Southern Chad and Sudan.	7-25
Figure 7-27.	Mean Wet-to-Dry Transition Daily Maximum/Minimum Temperatures (F), Southern Chad and Sudan.	7-25

Chapter 1

INTRODUCTION

AREA OF INTEREST. This study--the fourth of four volumes that cover the entire "SWANEA" (Southwest Asia-Northeast Africa) region shown in Figure 1-1--describes the geography, climatology and meteorology of the Mediterranean Coast and Northeast Africa. The Mediterranean Coast comprises the coastal regions of Turkey, Syria, Jordan, Israel, Lebanon, and

northern Africa. The Northeast Africa portion comprises Libya, Egypt, Chad, Sudan, and a small section of Ethiopia. The study region has been further divided into five zones of "climatic commonality" (the Turkish Coast, the Eastern Mediterranean Coast, the North African Coast, the Eastern Sahara, and Southern Chad/Sudan), as shown in Figure 1-2, next page.

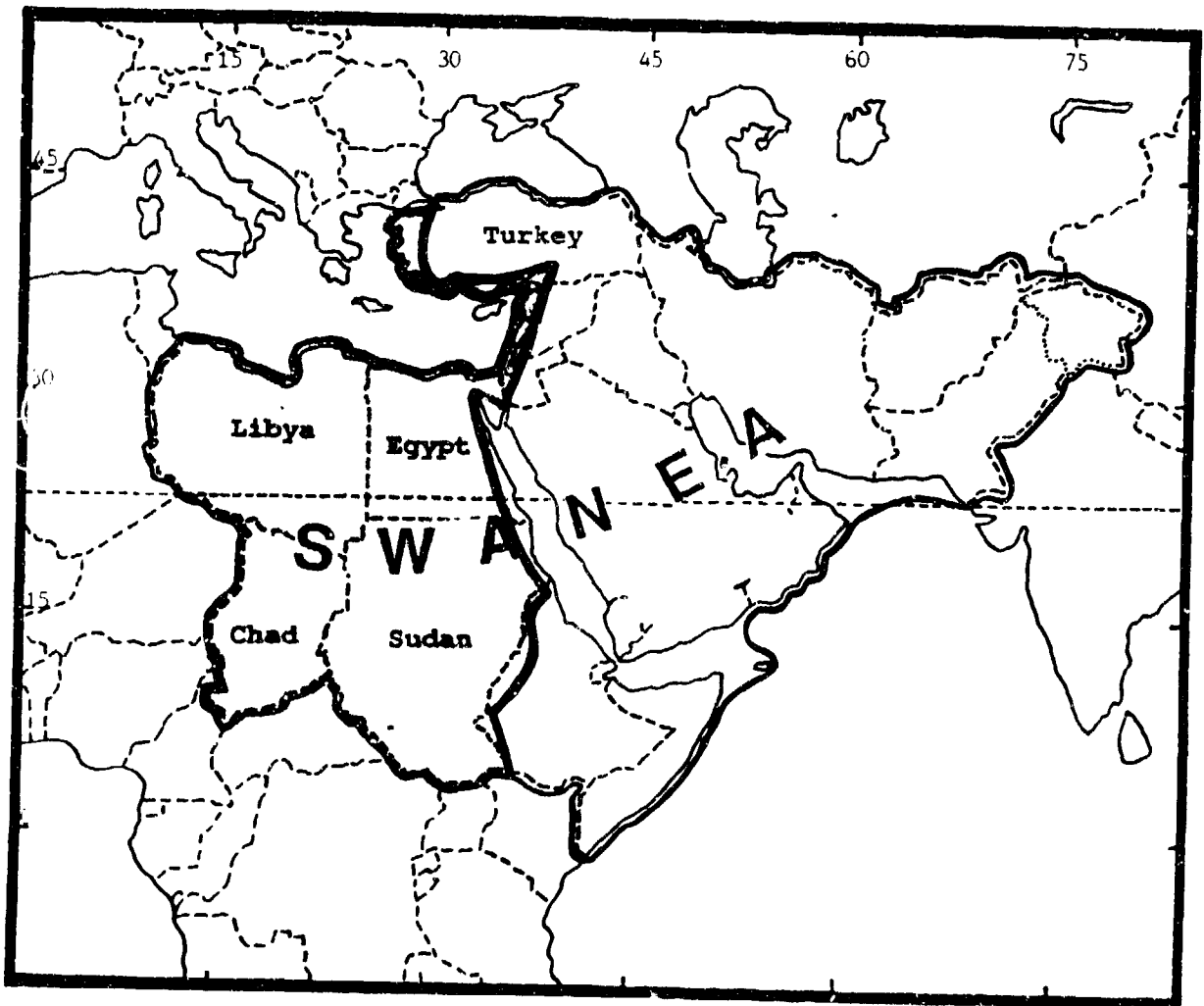


Figure 1-1. The Southwest Asia-Northeast Africa (SWANEA) Region. The shaded areas mark the Northeast Africa/Mediterranean Coast study region.

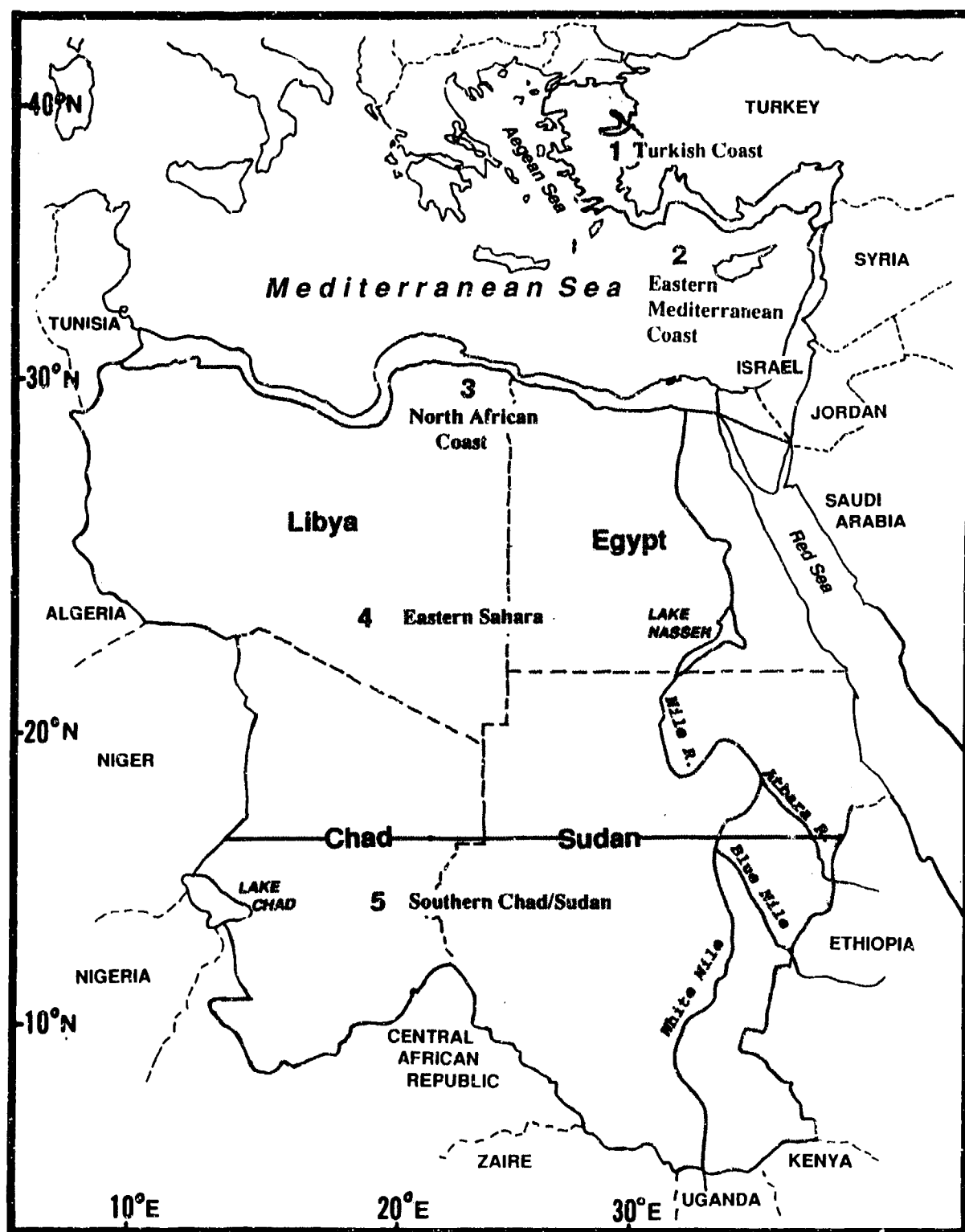


Figure 1-2. The Mediterranean Coast and Northeast Africa. The study area is shown subdivided into its five "zones of climatic commonality": (1) The Turkish Coast, (2) the Eastern Mediterranean Coast, (3) The North African Coast, (4) The Eastern Sahara, and (5) Southern Chad/Sudan.

GEOGRAPHY. The Mediterranean Coast comprises all of Israel and Lebanon, and part of Jordan; it includes the coasts of northern Africa and the coastal areas (averaging about 20 NM wide) that run from the Tunisia-Libya border to northwestern Turkey near 40° N, 29° E. Also included are inland portions of western Turkey below

3,280 feet (1,000 meters) between 37° and 41° N where strong marine characteristics are present; average width of this section is 150 NM. Northeast Africa, a mostly barren and arid region, includes Libya, Egypt, Chad, and Sudan. Figure 1-3 shows the topography and main geographical features of the entire study area.



Figure 1-3. Topography of the Mediterranean Coast and Northeast Africa.

Moisture availability is the most important climatic element in this region. The extreme aridity in most places (notably the Sahara, Negev, Sinai, and Libyan Deserts) contrasts with the Turkish coast, where lakes, ponds, and permanent rivers abound.

The Egyptian Nile Delta and the Jordan Rift Valley in Israel and Jordan are unique features. The Nile Delta is a vast alluvial flood plain (11,310 sq NM) with extensive irrigation canals. The Jordan Rift Valley forms the northern end of the Great Rift System of Africa. The Jordan River cuts a valley 5-12 NM wide and slopes southward to the Dead Sea, which is 1,292 feet (396 meters) below mean sea level.

Several mountain ranges parallel the Mediterranean Sea; their windward slopes are the wettest places in the region. The Taurus Mountains (with peaks over 13,000 feet/3,963 meters) back the Turkish coastline. The Lebanon Ranges (with elevations up to 10,000 feet/3,050 meters) MSL extend along the eastern Mediterranean coast; the Akhdar and Nafusah Mountains in Libya lie along the southern Mediterranean coast.

The Sahara is Northeast Africa's most prominent geographical feature, comprising 70% of its land surface (about 4.7 million sq NM). Only 20% of the Sahara, however, is true sand desert; the rest is rocky stubble eroded by persistent winds and infrequent rainfall. The Sahara includes elevated plains between 600 and 1,200 feet (183-366 meters) MSL, lowlands (with oases), and depressions, the largest of which is the Qattara Depression in northwestern Egypt; it covers about 7,200 square NM and is 436 feet (133 meters) below sea level. "Inselbergs" are isolated, steep-sided hills and rocky outcrops that rise above the desert floor at scattered locations throughout the Sahara. The highest of these reaches 6,345 feet (1,934 meters) MSL, but many are less than 100 feet (33 meters) high.

Several prominent mountain ranges in Chad and Sudan (the Tibesti in northern Chad and the Marrah in southwestern Sudan) rise above 10,000 feet (3,050 meters) MSL.

STUDY CONTENT. Chapter 2 provides a detailed discussion of the major climatic controls that affect the Mediterranean Coast and Northeast Africa. These controls range from the macroscale ("semipermanent climatic controls"), through the synoptic ("synoptic disturbances"), to the mesoscale. The individual

treatments of each climatic subregion in subsequent chapters do not include repeated descriptions of these phenomena, but provide specifics unique to the individual subregion by focusing on mean distributions and local anomalies of sky cover, visibility, winds, precipitation, and temperature. Meteorologists using this study should read and consider the general discussion in Chapter 2 before trying to understand or apply the individual climatic zone discussions in Chapters 3-7. This is particularly important because the study was designed first as a master reference to the entire region, and second as a modular reference to its subregions. Chapters 3-7 discuss "situation and relief" and "general weather" for each of the five subregions, by season.

The Turkish Coast (Chapter 3) includes those portions of western and southern Turkey where elevations reach the top of the marine boundary layer (3,280 feet/1,000 meters MSL). The Mediterranean and Aegean Seas provide moisture for frontal systems moving through this subregion. The storm track shifts north in the summer, allowing the sea breeze to dominate.

The Eastern Mediterranean Coast (Chapter 4) extends from Syria south to the Suez Canal. This subregion's precipitation maximum is in winter due to cyclonic activity that develops in the Mediterranean Sea. The sea breeze is a factor, particularly in summer, but subsidence aloft usually caps cloud development and minimizes precipitation.

The North African Coast (Chapter 5) extends from the Suez Canal to the Libya-Tunisia border. Most precipitation occurs in winter because of cyclonic activity. The sea breeze can advect some moisture inland, but the limited rainfall is not enough to change this subregion's desert environment.

The Eastern Sahara (Chapter 6) includes most of Libya and Egypt, as well as those portions of Chad and Sudan north of 16° N. The climate is dry year-round. Cyclonic activity usually only results in a wind shift, some cloudiness, and duststorms. The Mediterranean Sea is the only moisture source. The Nile River is in the eastern portion of the subregion.

Southern Chad/Sudan (Chapter 7) includes those portions of Chad and Sudan that lie south of 16° N. This is the only subregion that has "wet" and "dry" seasons. The summer wet season is produced by the Monsoon Trough.

CLIMATOLOGICAL REGIMES. The Mediterranean Coast sees mainly mid-latitude weather with migratory high pressure cells, cyclonic activity, and polar air surges. Land/sea breezes are an important factor close to shorelines. The traditional four seasons (winter, spring, summer, fall) are found here.

Northeast Africa is dominated by large deserts. The Eastern Sahara subregion is in the subtropics; climate is primarily affected by Mediterranean weather, including migratory high pressure cells, cyclonic activity, and polar air surges. There is seldom enough moisture, however, to produce precipitation.

South of 16° N, Northeast Africa is dominated by seasonal wind reversals that produce wet and dry seasons.

The climate between 11° and 16° N is that of a semidesert steppe; the weather is more tropical than Mediterranean. Because of this, phenomena such as the Monsoon Trough and squall lines will be stressed.

CONVENTIONS. The spellings of cities and geographical features are those used by the United States Defense Mapping And Aerospace Center (DMAAC), but expect wide variations in the English spelling of many place names in North Africa. Distances are in nautical miles (NM), except for visibilities which are given in statute miles. Ceilings and cloud bases are in feet/meters above ground level (AGL)*, but cloud tops are above mean sea level (MSL). Elevations are in feet with a meter or kilometer (km) equivalent immediately following. Temperatures are in Fahrenheit (F) with a Celsius (C) conversion following. Wind speeds are in knots (kt). Precipitation amounts are in inches with a millimeter (mm) conversion following. Most synoptic chart times are given in Greenwich Mean Time (GMT or Z). When synoptic charts are not provided, only local standard time (LST) is used.

***NOTE:** The AGL cloud bases given in this study are generalized over large areas. Readers must consider terrain in applying these generalized values. For example, the AGL cloud bases of the Marrah Mountains are generally representative of valley reporting stations, but not of locations in surrounding mountains, where ceilings and cloud bases would be lower, and where, in fact, many locations would be obscured.

DATA SOURCES. Most of the information used in preparing this study came from two sources, both within the United States Air Force Environmental Technical Applications Center (USAFETAC). Studies, books, atlases, and so on were supplied, with rare exceptions, by the Air Weather Service Technical Library, or AWSTL, which is the only dedicated atmospheric sciences library in the Department of Defense and the largest such library in the United States. Climatological data came direct from the Air Weather Service Climatic Database or through Operating Location A, USAFETAC--the branch of USAFETAC responsible for maintaining and managing this database.

RELATED REFERENCES. This study, while more than ordinarily comprehensive, is certainly not the only source of meteorological and climatological information for the military meteorologist concerned with the Mediterranean Coast and Northeast Africa. USAFETAC's Readiness Support Section (ECR) occasionally prepares special narrative climatologies for smaller areas or points within this region; contact ECR directly for information on such studies. Station Climatic Summaries for Africa and Asia provide summarized observational data for many stations in the study region. Staff weather officers and forecasters are urged to contact the Air Weather Service Technical Library for as much data on the region as is currently available.

Chapter 2

MAJOR METEOROLOGICAL FEATURES OF THE MEDITERRANEAN COAST AND NORTHEAST AFRICA

The "major meteorological features" of the Mediterranean Coast and Northeast Africa are listed below as they appear and are described in this chapter. These features affect the weather and climate of the region during part or all of the year. The same features may be discussed in more detail in subsequent chapters as they relate to individual subregions of the study area.

	Page
Semipermanent Climatic Controls	2-2
Sea Surface Temperatures	2-2
The Azores High	2-4
The Icelandic Low	2-4
The Asiatic High	2-4
The Saharan High	2-4
The Anatolian Plateau High	2-7
Thermal Lows	2-7
The Sudanese Heat Low	2-7
The Anatolian Plateau Thermal Trough	2-7
The Saharan Heat Low	2-8
The Saudi Arabian Heat Low	2-10
The Monsoon Climate	2-11
The Monsoon Trough	2-12
Mean Mid- and Upper-Level Flow	2-15
The Subtropical Ridge	2-26
Synoptic Disturbances	2-27
Jet Streams	2-27
The Polar and Subtropical Jets (PJ and STJ)	2-27
Tropical Easterly Jet (TEJ)	2-29
Mid-Tropospheric Easterly Jet (MTEJ)	2-30
Mid-Latitude Cyclogenesis	2-31
The Genoa Low	2-31
The Atlas Low	2-32
The Cyprus Low	2-35
Storm Tracks	2-40
African Waves	2-41
Tropical Squall Lines	2-41
Mesoscale and Local Effects	2-43
Land/Sea Breeze	2-43
Marine Inversions	2-44
Mountain/Valley Winds	2-47
Mountain Waves	2-49
Duststorms	2-50
Sand Streets	2-51
Wet-Bulb Globe Temperature Index (WBGT)	2-52
Regional Winds	2-57
Khamsin	2-57
Sharav	2-59
Sirocco	2-60
Harmattan	2-61
Haboob	2-64
Etesian	2-65

SEMI-PERMANENT CLIMATIC CONTROLS

SEA SURFACE TEMPERATURES (SSTs). The Mediterranean and Aegean Seas strongly influence the climate of the coastal subregions by modifying temperatures in the marine boundary layer. The southern

and eastern portions of the Mediterranean Sea are warmest, while the Aegean Sea is always coolest. Figures 2-1a-d give seasonal SSTs for these water bodies.

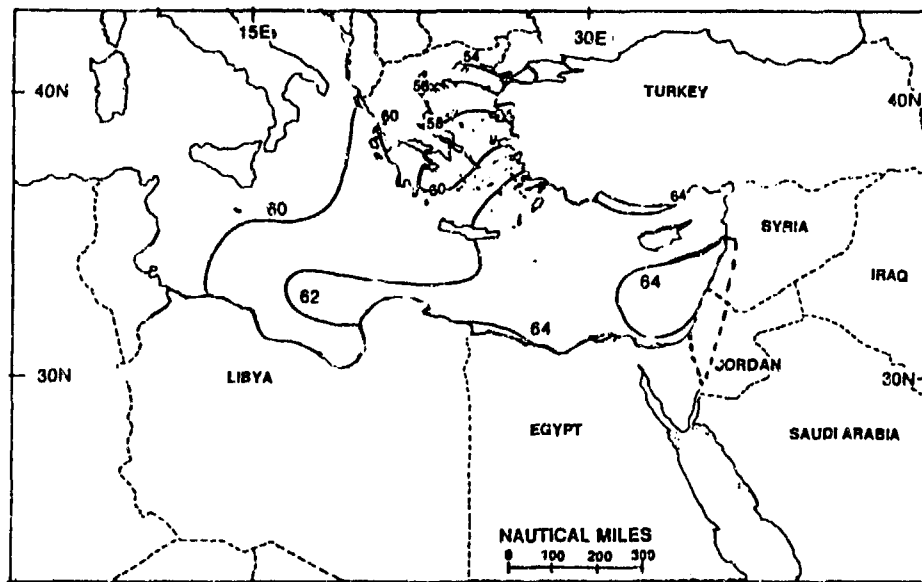


Figure 2-1a. Mean January Sea Surface Temperatures (F). January SSTs have a large temperature gradient, particularly across the Aegean Sea. The cooler waters are the result of cold continental air masses moving over them, as well as subsurface mixing in the Mediterranean Sea. Water temperatures are 8-15° F (5-9° C) higher along the sheltered southern Turkish coast. Mediterranean Sea SSTs are higher in the east; cold European polar air and subsurface mixing have more of an effect on western areas.

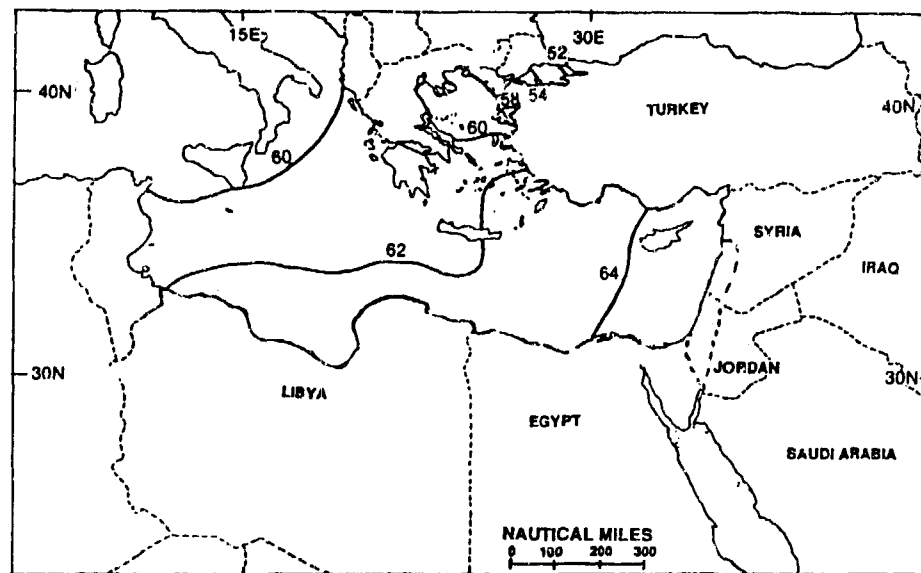


Figure 2-1b. Mean April Sea Surface Temperatures (F). General warming in spring produces a slight increase in April SSTs. Warmer water surfaces moderate polar air masses crossing the region.

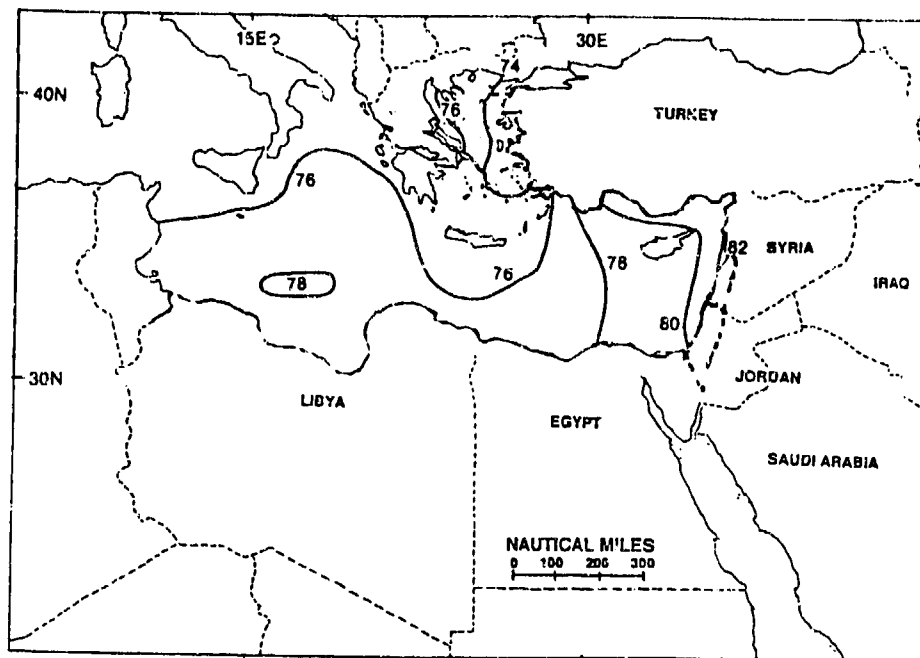


Figure 2-1c. Mean July Sea Surface Temperatures (F). By July, water temperatures peak throughout the basin. The warmest water is along the eastern Mediterranean coast and Gulf of Sidra.

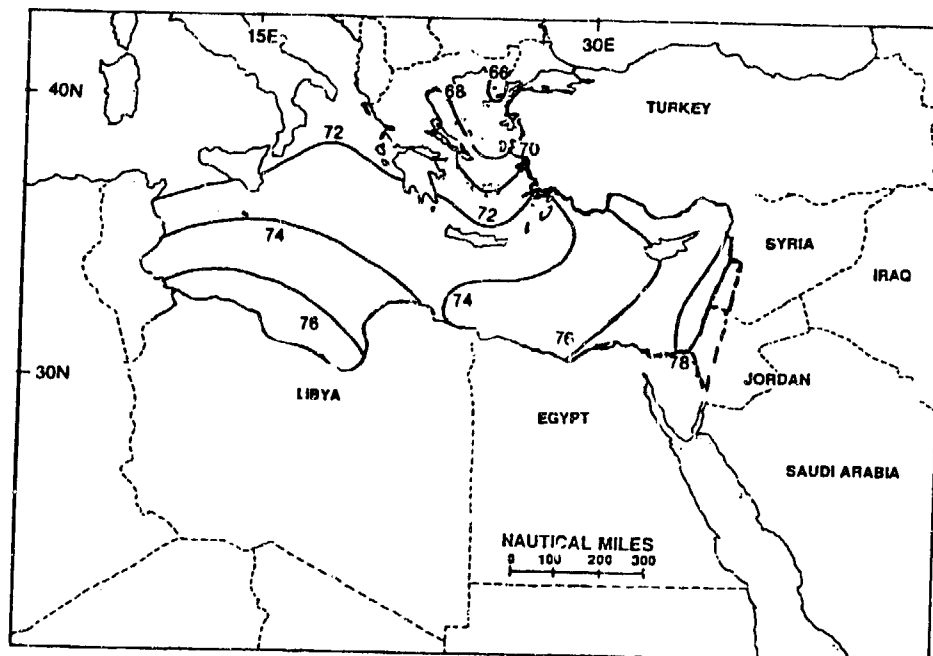


Figure 2-1d. Mean October Sea Surface Temperatures (F). Fall SSTs remain high in the Mediterranean, but the Aegian Sea cools faster.

THE AZORES HIGH helps regulate cyclonic activity into the Mediterranean Sea basin and is an important part of the subtropical circulation pattern. This semi-permanent high-pressure cell's mean position varies from 29° N, 29° W in January to 37° N, 37° W in July. Mean sea-level pressure varies from 1021 mb in January to 1025 mb in July. The strength and position of the high can channel mid-latitude systems into the area or form a "blocking" pattern of strong ridging in the eastern Atlantic Ocean. Mean positions of the Azores High are shown in Figures 2-2a-d.

THE ICELANDIC LOW is a dominant surface feature in the North Atlantic throughout the year. It represents the mean position of numerous migratory lows in the vicinity of Iceland. The area is a good cyclogenesis region due to the relatively warm North Atlantic waters and the cold air from Greenland. Lows typically move west to east and can become very intense. The pressure gradient between the Icelandic Low and the Azores High produces a broad field of westerlies over the Northeast Atlantic, directing a constant stream of storms into western Europe. Most of these lows track northeast into the Norwegian Sea and occlude; however, secondary lows frequently form on the trailing cold front and move along a southeastern track from the British Isles to the Mediterranean Sea.

THE ASIATIC HIGH is a strong but very shallow semipermanent high pressure system that dominates much of the Asian continent from late September to late April. It is produced primarily by radiational cooling. Migratory Arctic air masses moving southward to central Asia temporarily reinforce and intensify this high. Centered over western Mongolia, its mean central pressure is strongest in January (see Figure 2-2a) and February. Vertical extent rarely exceeds 850 mb. The Asiatic High may exceed 1,050 mb for 1-3 day periods; highest recorded pressure is 1,083 mb.

The Asiatic High also plays a part in determining the tracks of surface lows. Strong high pressure extending into eastern Europe usually forces Mediterranean lows eastward or southeastward into the Middle East. When the Asiatic High is weak and restricted to central Asia, these lows track in the direction of upper-level flow. The Asiatic High provides a source of low-level cold air into the Adriatic, Aegean, and eastern Mediterranean Seas. Cold air enters these waters through mountain passes along the Yugoslavian coast and across the Sea of Marmara into the Aegean Sea, where it enhances cyclogenesis--see Figure 2-3.

THE SAHARAN HIGH is the only mean, large-scale, high pressure feature in the eastern Sahara during late fall, winter, and early spring. It develops in October or November and dissipates by May, but ridging from the Azores High extends into northeast Africa year-round (see Figures 2-2a-d). This high is part of the subtropical belt of high pressure and is of dynamic origin. Strong radiative cooling enhances its surface strength. Its day-to-day position and strength vary as deep polar troughs enter northern Africa, particularly between January and early April. The Saharan High generally moves eastward ahead of the disturbance or disappears entirely off the synoptic chart. It usually reforms at the surface within 12-24 hours after a frontal passage. Saharan High outflow is dry and cool, averaging 3-5 knots during fair weather periods.

Figures 2-2a and 2-2b show January and April locations and mean sea-level pressures of the Saharan High. The two features often produce an extensive high-pressure ridge over northern Libya and west-central Egypt. The Saharan High's mean April position shifts slightly eastward to 22° E due to increased daytime heating and the increase in cyclonic activity over the Atlas Mountains.

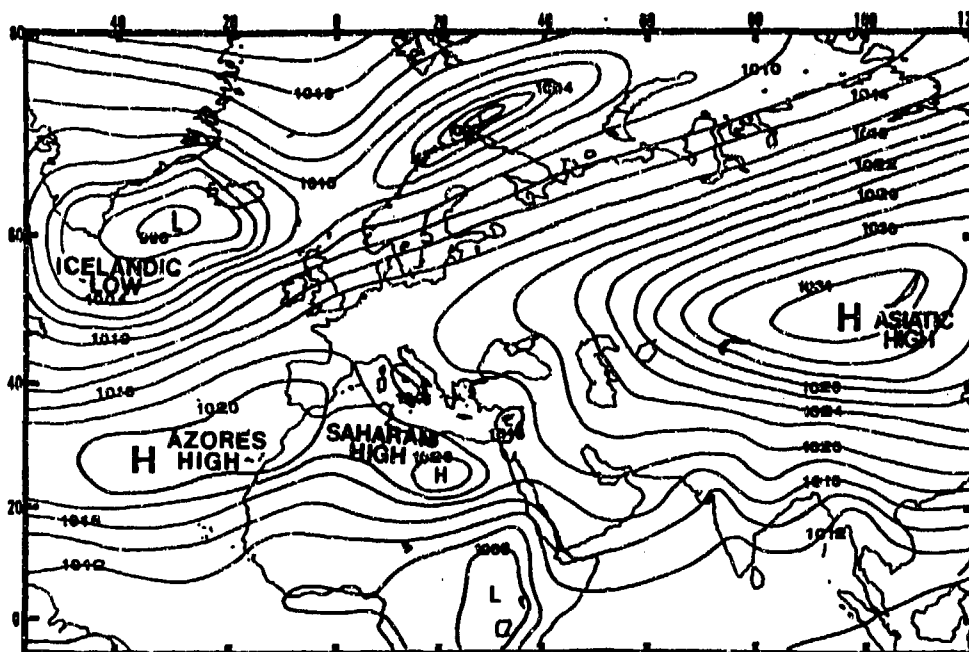


Figure 2-2a. Mean January Position of the Azores High, Icelandic Low, Asiatic High, and Saharan High. From December to February, the Azores High extends eastward over the western Sahara, reinforcing mean westerly surface flow into the region. Occasionally, a strengthening Azores High ridges northward over the coastal waters of western Europe for 5 to 10 days. This allows the Polar Jet to slide southward along the north and east side of the Azores High into the north central Sahara, producing cold weather outbreaks in the Mediterranean region. The Icelandic Low is usually below 1,000 mb in winter.

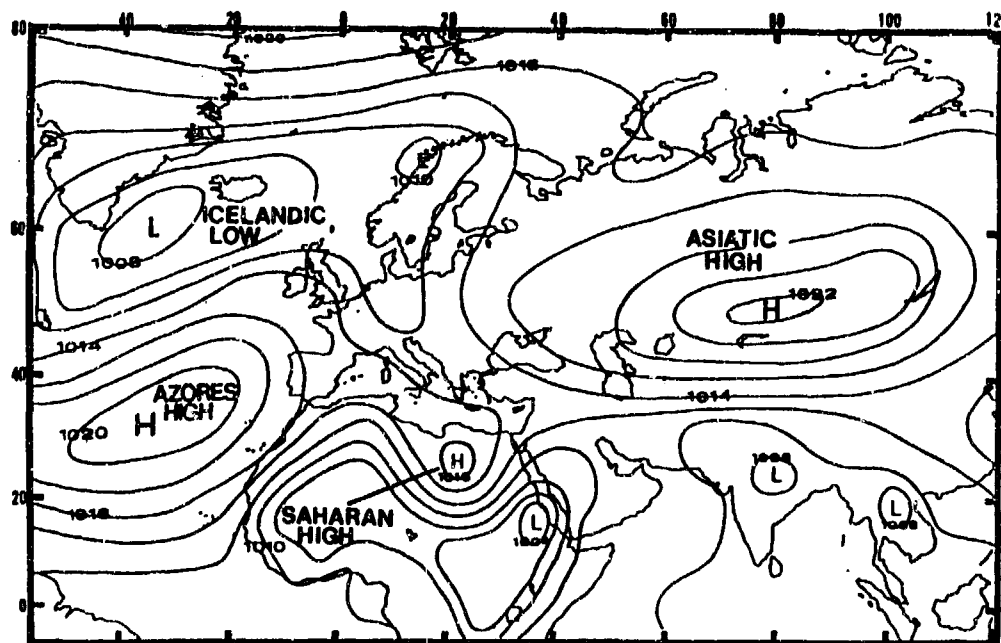


Figure 2-2b. Mean April Position of the Azores High, Icelandic Low, Asiatic High, and Saharan High. From March to May, the Azores High moves slowly WNW to near 30° N, 32° W. Its westerly spring migration away from the African continent weakens the mean high-pressure ridge over North Africa. Cyclonic activity (and its main storm track--see Storm Tracks) dips southward over the western Mediterranean Sea. Intense duststorms are common as strong winds sweep across the dry Sahara (see Khamsin). In March and April, the Asian landmass warms quickly, weakening support for the Asiatic High; mean pressure decreases to 1022 mb and shifts westward.

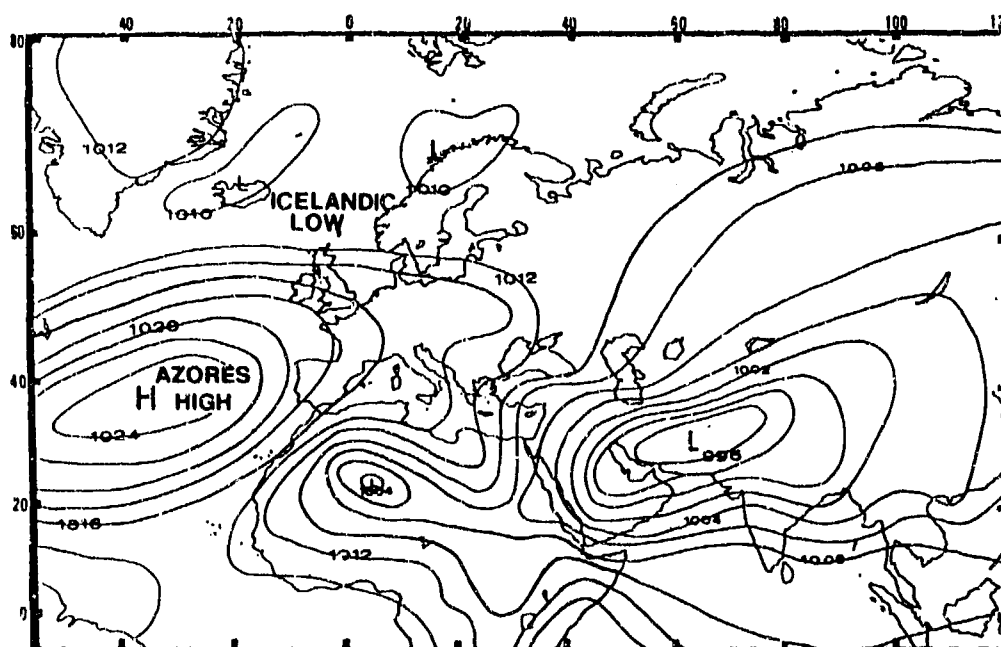


Figure 2-2c. Mean July Position of the Azores High and Icelandic Low. From June to September, the Azores High strengthens to a mean of 1025 mb and reaches its northernmost position near 37° N, 37° W. The High effectively blocks cyclonic activity into the Mediterranean Sea basin by producing a strong ridge over western Europe. Cyclonic activity can penetrate southward only when the ridge is weak and low pressure off Iceland is strong. The Icelandic Low is much less prominent in summer, with central pressures averaging near 1010 mb.

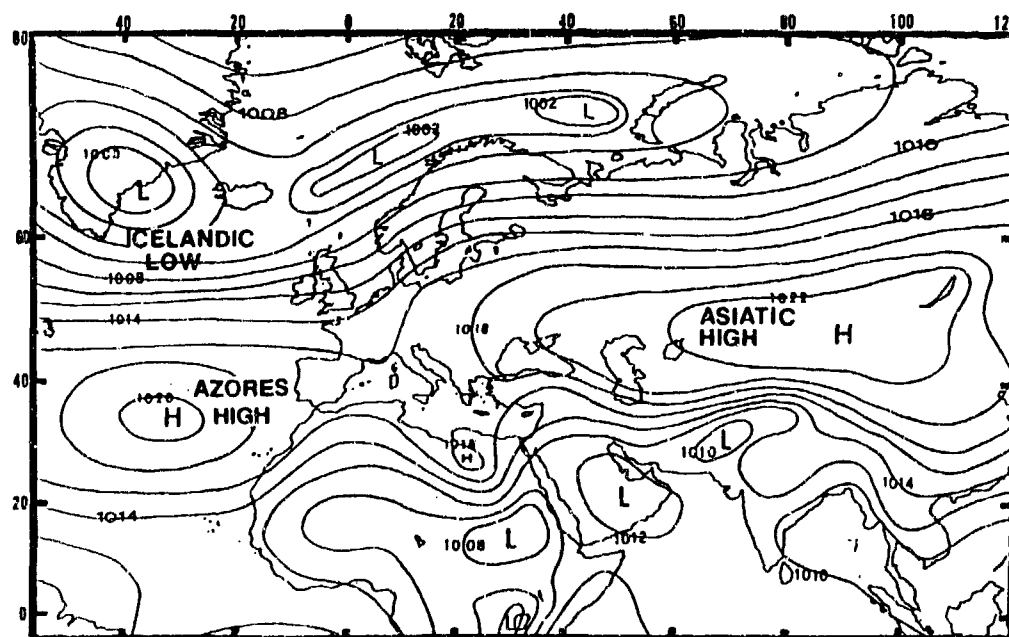


Figure 2-2d. Mean October Position of the Azores High, Icelandic Low, and Asiatic High. In October, the Azores High moves ESE to a mean position of 35° N, 30° W. Note that the Azores High ridge axis has retreated from the western European coast.

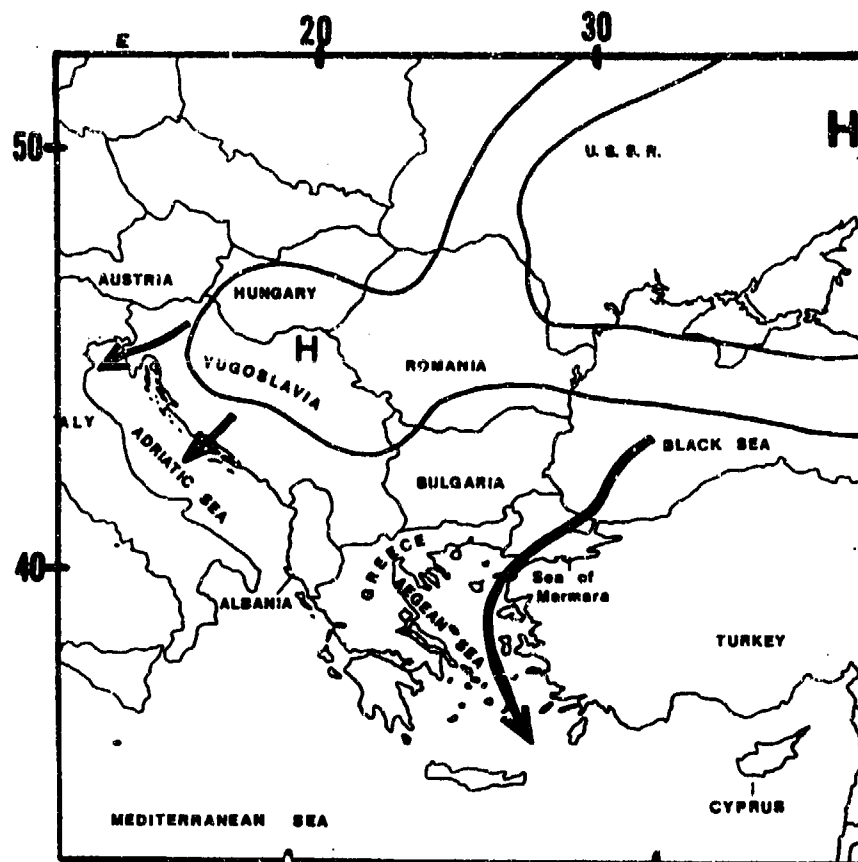


Figure 2-3. General Tracks For Cold Asiatic Air Into the Central and Eastern Mediterranean.

THE ANATOLIAN PLATEAU HIGH forms in central Turkey during the winter due to radiative cooling. It is connected to the east with similar highs over the Iranian highlands. With calm conditions, the short-lived high pressure cell often forms southeast of Ankara. Turkey's mountainous terrain creates a natural barrier to eastward-moving systems, and the high pressure reinforces this barrier. Strong winter and early spring cyclones can break down the ridge and move directly across Turkey. This high is not persistent enough to show on mean pressure charts.

THERMAL LOWS. Four well-defined thermal lows or troughs affect this region directly or indirectly during different parts of the year; they are the Sudanese Low, the Anatolian Plateau Thermal Trough, the Saharan Heat Low, and the Saudi Arabian Heat Low.

The Sudanese Heat Low is present during most of the year--see Figures 2-4a-d. It is responsible for southerly

winds that advect moist, warm air ahead of eastward-moving Atlas and Cyprus Lows. The Red Sea is the source of this moisture, which can result in thunderstorm activity over the northeastern Sahara.

The Anatolian Plateau Thermal Trough is a daytime surface feature produced by strong surface heating over the Anatolian Plateau of Turkey from May to September--see Figure 2-4c. The trough, sometimes becoming a weak low, may appear to be part of the large-scale low pressure trough over Africa, the Middle East, and South Asia; it is, however, a local phenomenon. This is particularly evident in the fall when cool air penetrates into the region and destroys the trough, while the large-scale low pressure trough remains intact over southwest Asia. This thermal trough is responsible for creating the Etesians (which see), a local northerly wind circulation through the Aegean Sea. Flow along the trough's northwestern quadrant reinforces these winds.

The Saharan Heat Low develops over the Sahara Desert near 25° N, 3° E in late March or early April and lasts until mid-October. It is sustained by intense solar radiation through the summer and can extend up to 750 mb. This low anchors the western end of the large-scale low pressure trough extending from Pakistan westward to the Sahara. In March and April, it is the origin for hot, dust-laden air masses that affect the eastern Sahara and

Mediterranean coast. It also assists in Atlas Low development. In northwestern Libya, west of 22° E, dry low-level winds blow from 45 to 170 degrees and average 8 to 15 knots. This persistent circulation introduces large amounts of dust into the atmosphere. By July, the semipermanent Saharan Low has a mean surface pressure of 1004 mb--see Figure 2-4c.

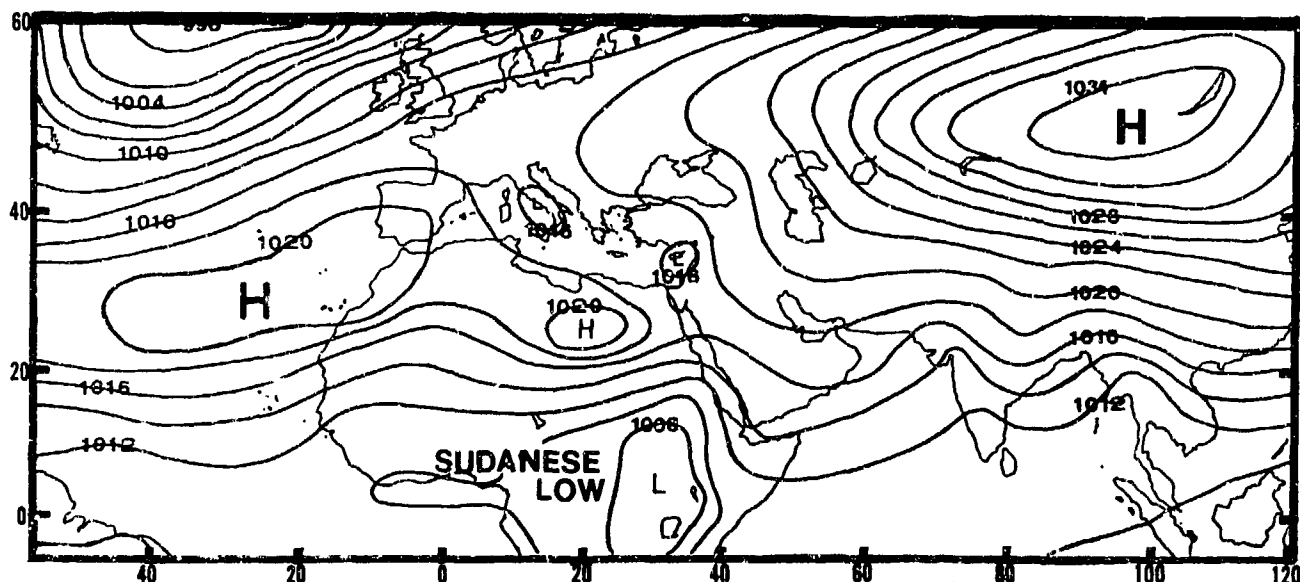


Figure 2-4a. Mean January Position of the Sudanese Low. Between December and March, the Sudanese Low lies over the elevated plateaus of southwestern Ethiopia and southeastern Sudan at 7° N, 32° E.

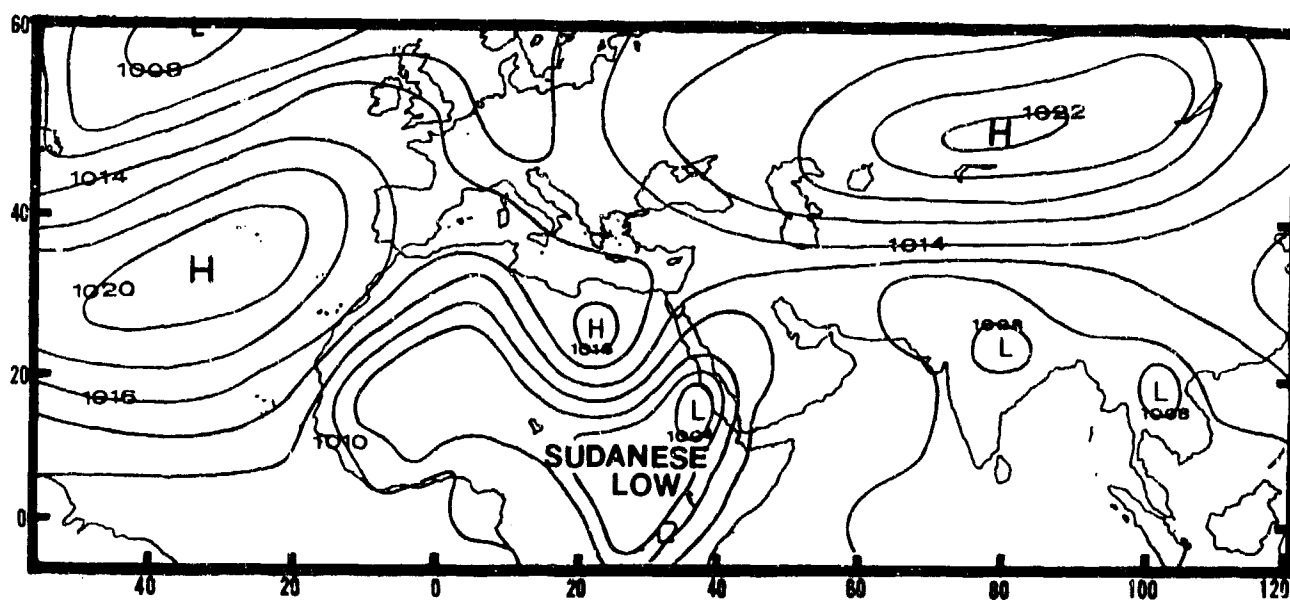


Figure 2-4b. Mean April Position of the Sudanese Low. In April and May, the Sudanese Low migrates northward to 15-20° N.

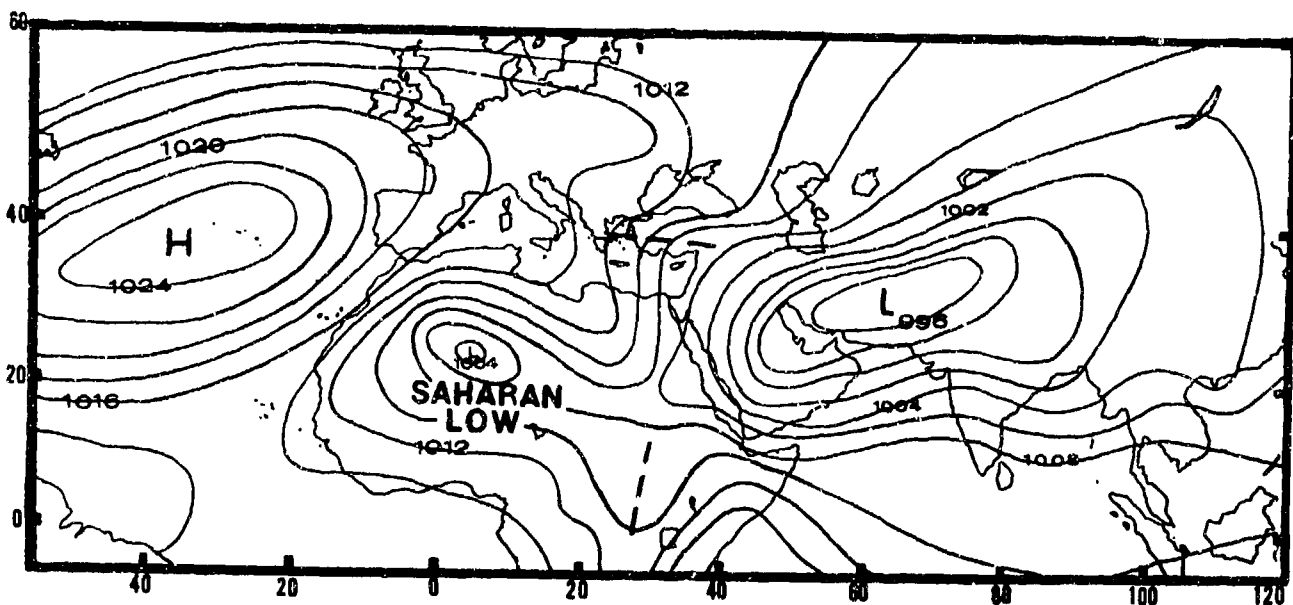


Figure 2-4c. Mean July Positions of the Saharan Low, Anatolian Plateau Thermal Trough, and Sudanese Trough. Between June and September, the Sudanese Low becomes part of the large-scale thermal trough extending from the western Sahara to northwest India, as shown.

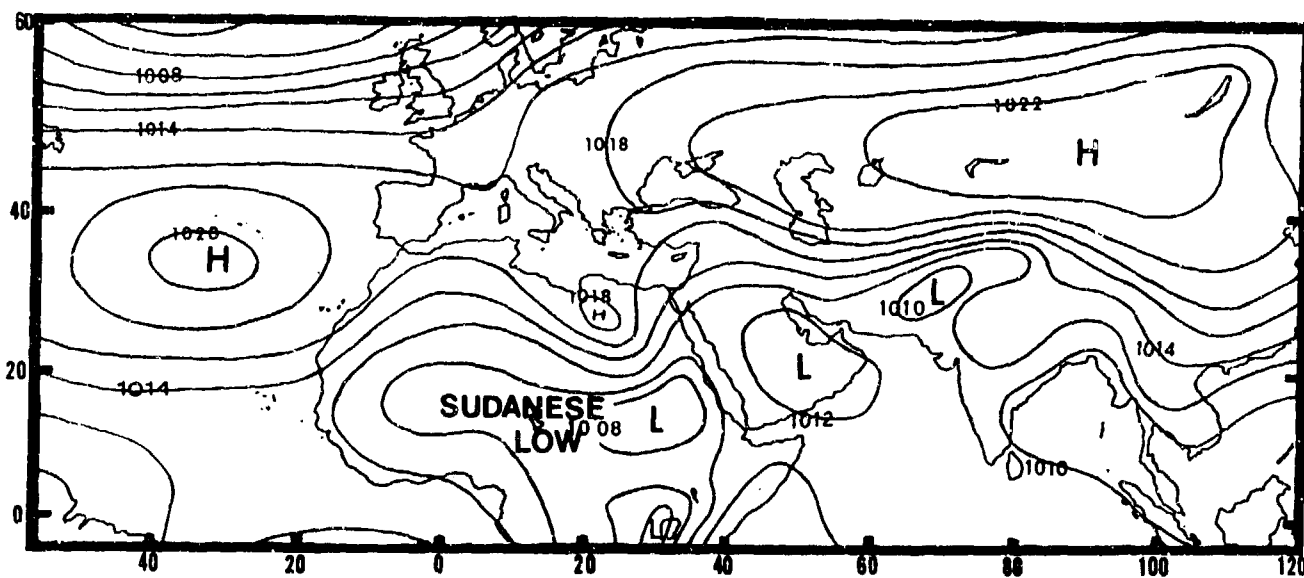


Figure 2-4d. Mean October Position of the Sudanese Low. In fall, the Sudanese Low reappears as the closed circulation shown here.

The Saudi Arabian Heat Low is present from April to late October. It can extend to 650 mb. Its summer position and strength is regulated by intense surface heating over the Rub al Khali Desert. Its mean position (20° N, 48° E) varies little. The low weakens at night, producing descending air and dry northeasterlies in the

Red Sea and eastern Egypt/Sudan; speeds are 5 to 15 knots. Since it does not appear on mean pressure charts for July, the gradient-level streamline flow over the eastern Sahara and Middle East Peninsula is shown in Figure 2-5.

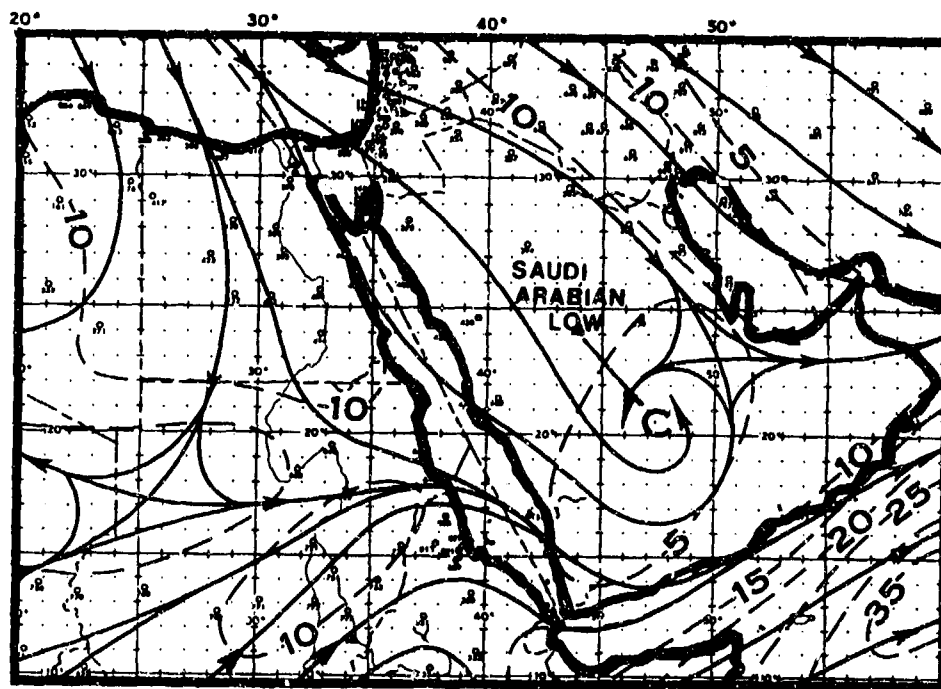


Figure 2-5. Mean July Position of the Saudi Arabian Heat Low. Streamlines (solid lines) show direction of flow. Isotachs (dashed lines) are in knots.

THE MONSOON CLIMATE. The term "monsoon" is generally applied to areas where there is a seasonal reversal of the prevailing surface winds. The generally accepted definition of a "monsoon" climate incorporates the following criteria (after Ramage, 1971):

- Prevailing seasonal wind directions between summer and winter must change by at least 120 degrees;

- Both summer and winter mean wind speeds must equal or exceed 10 knots (5 meters/sec);

- Wind directions and speeds must exhibit high degrees of steadiness; and

- No more than one cyclone/anticyclone couplet occurs during January or July in any 2-year period within any 5 degree grid square.

Figure 2-6 shows the northern limit of the monsoon climate (shaded area) lying across Northeast Africa as defined by Ramage.

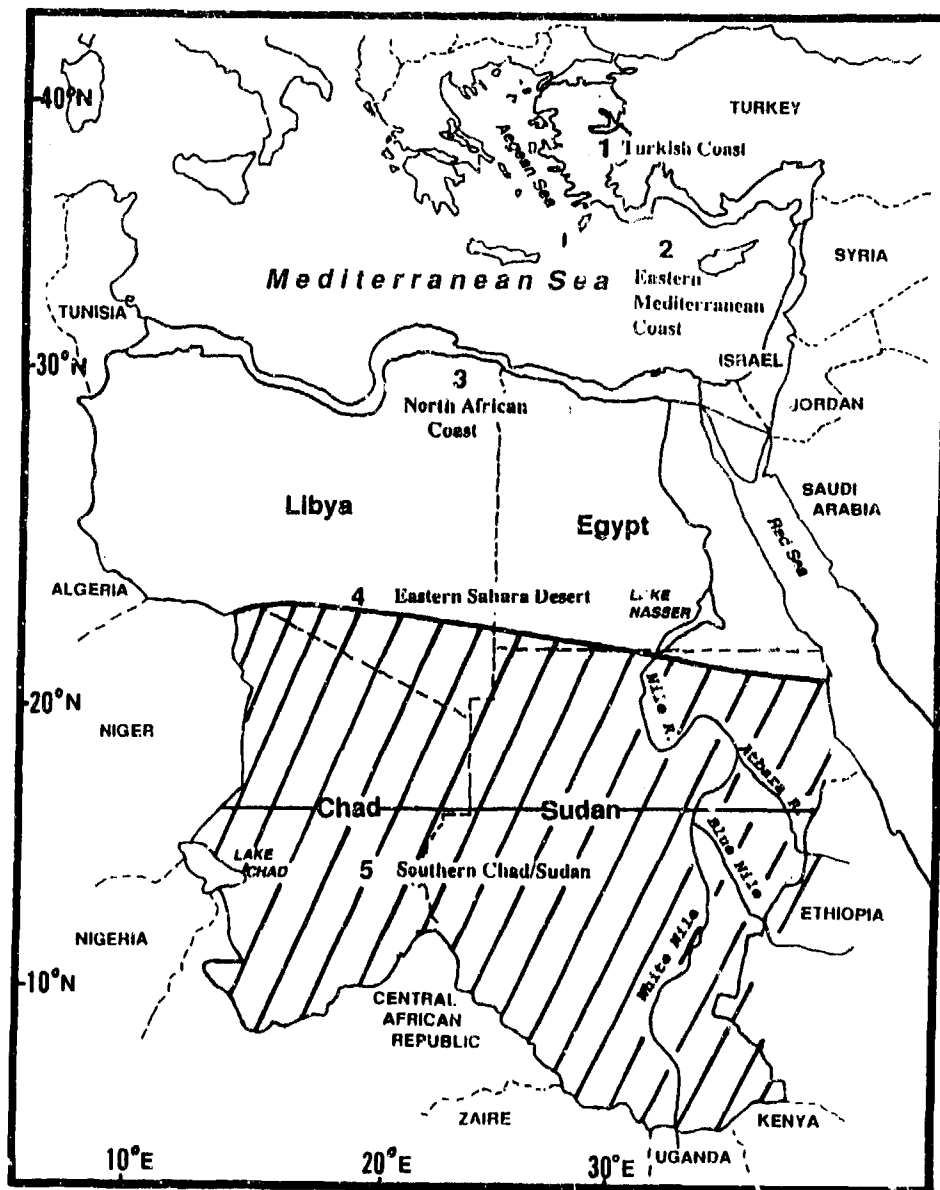


Figure 2-6. Region Affected by the Monsoon Climate. The hatched area shows the northern extent of the "monsoon climate" according to Ramage.

THE MONSOON TROUGH forms from the convergence of Azores and South Atlantic High outflow. Oriented WSW to ENE across equatorial Africa, it separates the dry subtropical Saharan air from the moist equatorial Atlantic air. A series of lows develop along the trough axis where the northerly winds meet the

southwesterlies. The Monsoon Trough's northward movement from March to July is more gradual than the southward movement from August to November. The trough is farthest north in July and August. Figure 2-7a shows its positions as it moves into Chad and Sudan; Figure 2-7b shows its positions as it moves out.

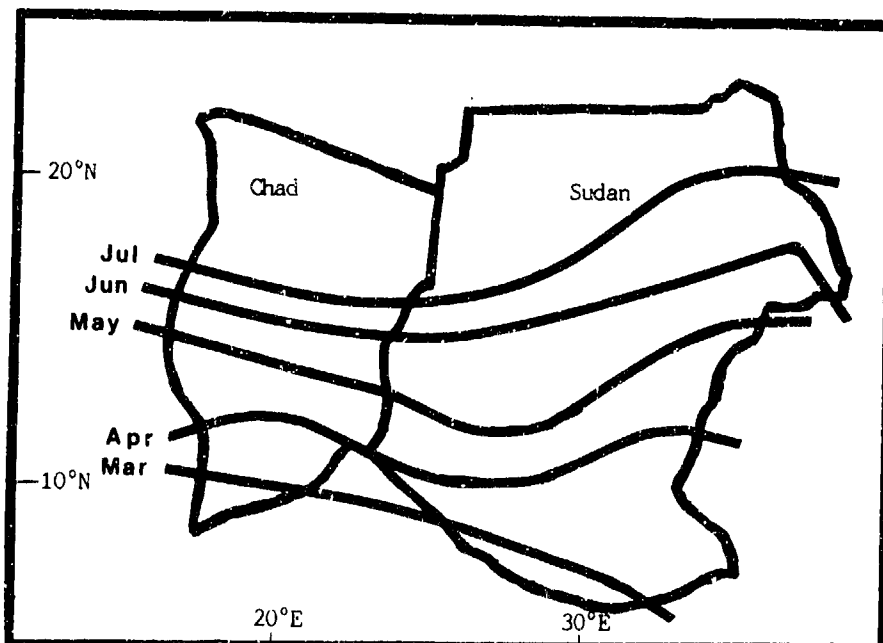


Figure 2-7a. Mean March-July Monsoon Trough Positions, Chad and Sudan.

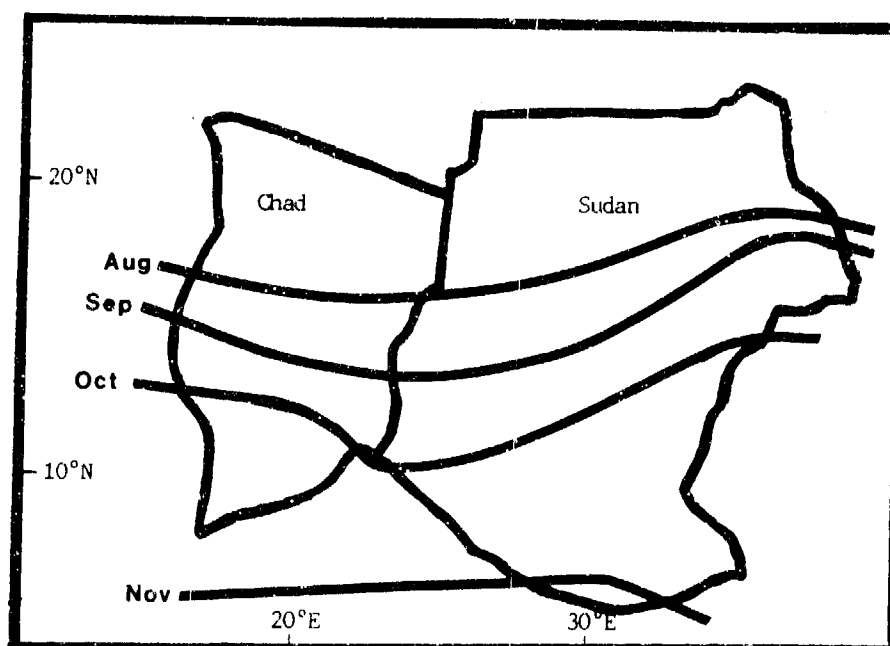


Figure 2-7b. Mean August-November Monsoon Trough Positions, Chad and Sudan.

From March to May, surface Monsoon Trough movements are characterized by brief 1-3 day northward surges when deep Atlas Lows (which see) temporarily replace or weaken the Azores/Saharan High pressure ridge over the Sahara. The Monsoon Trough moves northward 20-50 NM in response to the lower pressure and is driven southward again when high pressure builds behind the front. These highs are still strong in March, but they are much weaker and less frequent in April and May, allowing the surface Monsoon Trough to gradually move northward in the spring. Between December and July, the South Atlantic High also strengthens and moves from 32° S to 26°S, driving the trough northward. As the Monsoon Trough approaches and moves north of a

station, the mean surface winds back through the north and west.

During the summer, ridging from the Azores and Saharan Highs is replaced by the Saharan Heat Low. Cyclonic activity and transitory highs shift northward. The average position of the surface Monsoon Trough remains fairly constant during the summer. Figure 2-8a shows the general summer meteorological pattern with the broad Monsoon Trough, actually a wide belt of thermal lows stretching across the African continent and dominated by the hot, dry, Saharan air mass. Figure 2-8b is a satellite view of an active Monsoon Trough in June with a tropical disturbance over southwest Sudan.

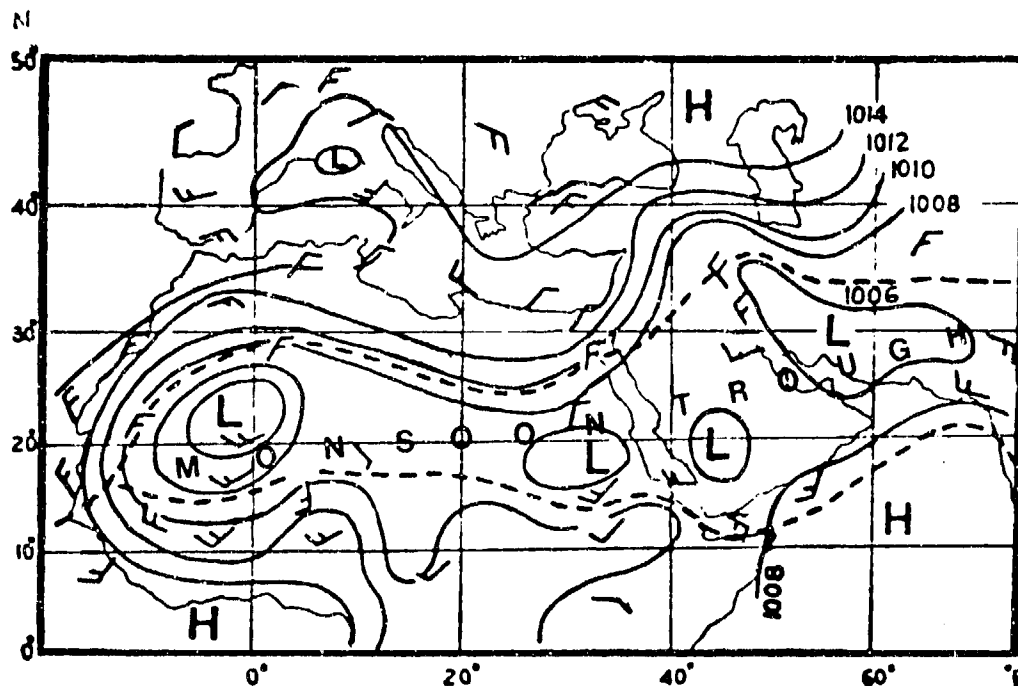


Figure 2-8a. Summer Monsoon Trough Meteorological Pattern.



JE-11a. METEOSAT. Enlarged View. Infrared Picture. 1155 GMT 13 June 1979.

Figure 2-8b. Satellite View of Northeast Africa Showing a Tropical Disturbance in the Monsoon Trough (Fett, 1983). The low is identified as a tropical disturbance over southwest Sudan. The suspended dust of a Haboob (which see) is evident north of Khartoum. Thunderstorms were reported south of Khartoum, and suspended dust and duststorms were reported north and west of the city.

The boundary separating the Saharan air mass from the cooler, moister equatorial air to the south is often referred to by African meteorologists as the "Intertropical Discontinuity," or ITD. Other meteorologists may use other terms for the ITD, which is shown as the hatched line in Figure 2.9. The ITD slopes southward and extends upward to 700-600 mb. It is a baroclinic zone, with stable Saharan air over moist, conditionally unstable equatorial air. The ITD's mean summer position is 15°

N at 850 mb and 5° N at 700 mb. It is marked by wind shifts and humidity contrasts. On the north of the ITD, winds are generally northerly or easterly at low- and mid-levels, while winds to the south are southwesterly or westerly. The two contrasting air masses also produce the thermally driven Mid-Tropospheric Easterly Jet (which see) that produces localized areas of divergence, enhancing cloud cover and rainfall.

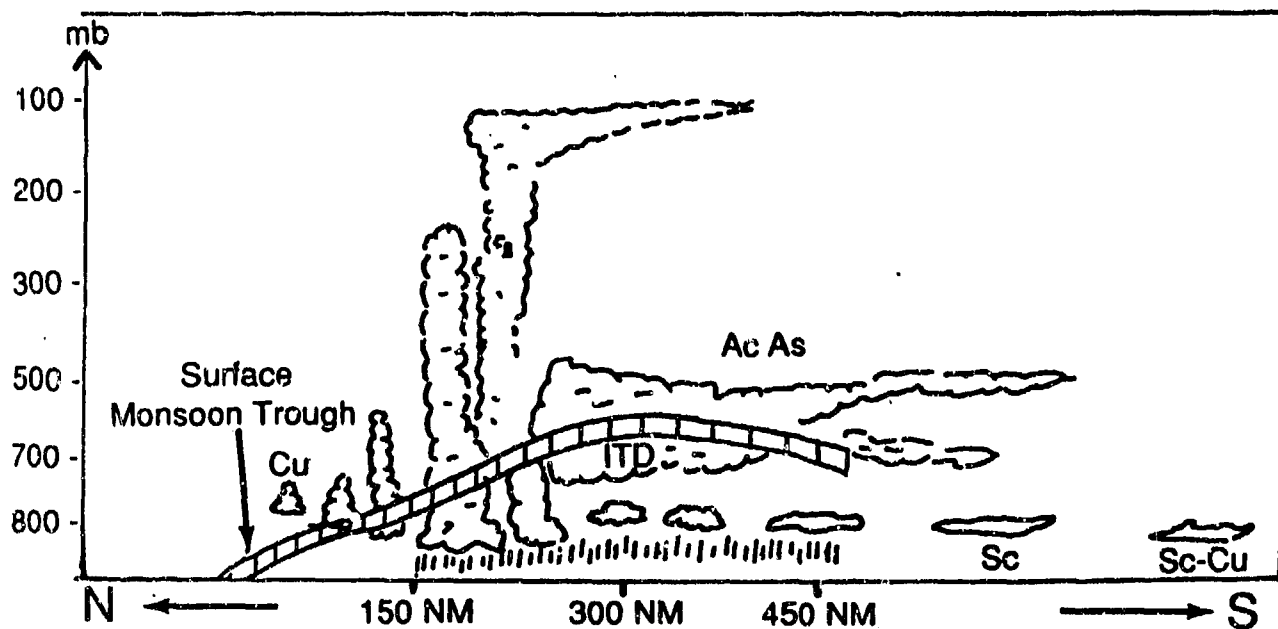


Figure 2-9. Vertical Cross Section of the "African Interior" Monsoon Trough and the Intertropical Discontinuity (ITD) (from Omotosho, 1984). Note that precipitation associated with the Monsoon Trough and the ITD occurs well south of the Monsoon Trough's surface position.

MEAN MID AND UPPER-LEVEL FLOW. Figures 2-10 through 2-13 show January, April, July, and October streamline flow at 850, 700, 500, 300, and 200 millibars over the entire SWANEA study area.

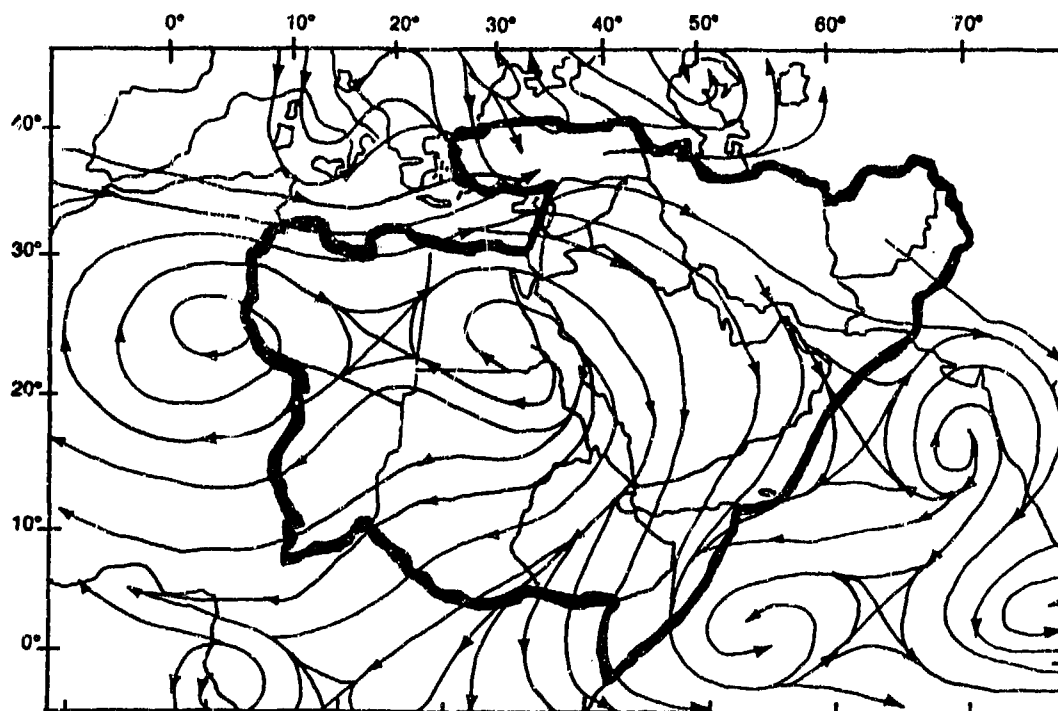


Figure 2-10a. Mean January Upper-Air Flow Patterns, 850 mb.

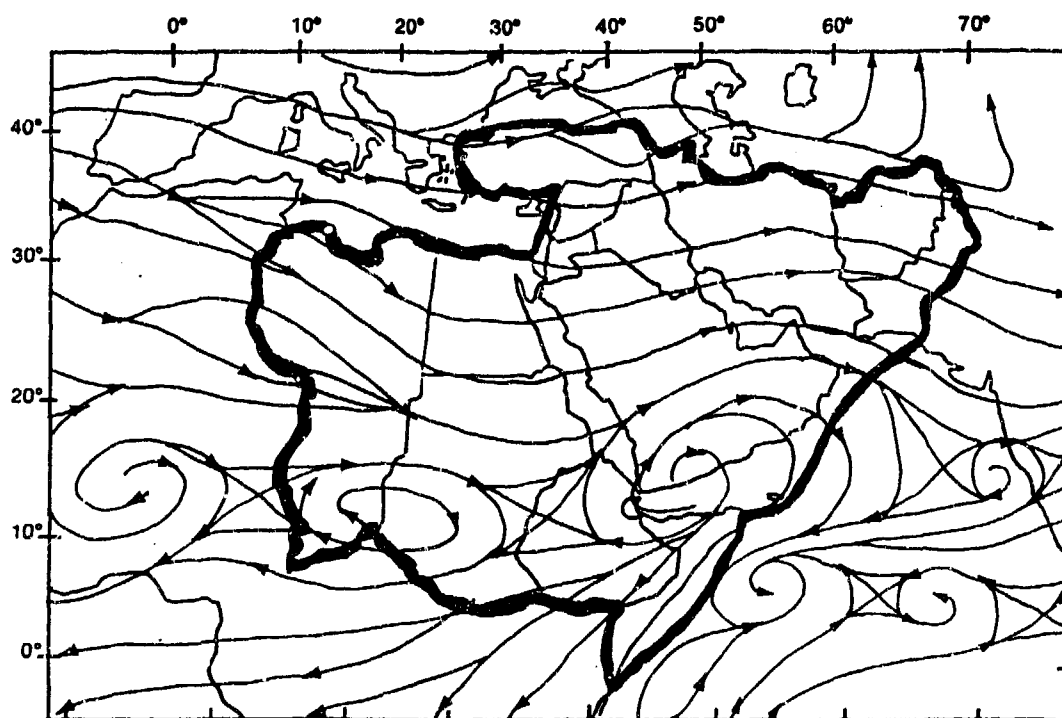


Figure 2-10b. Mean January Upper-Air Flow Patterns, 700 mb.

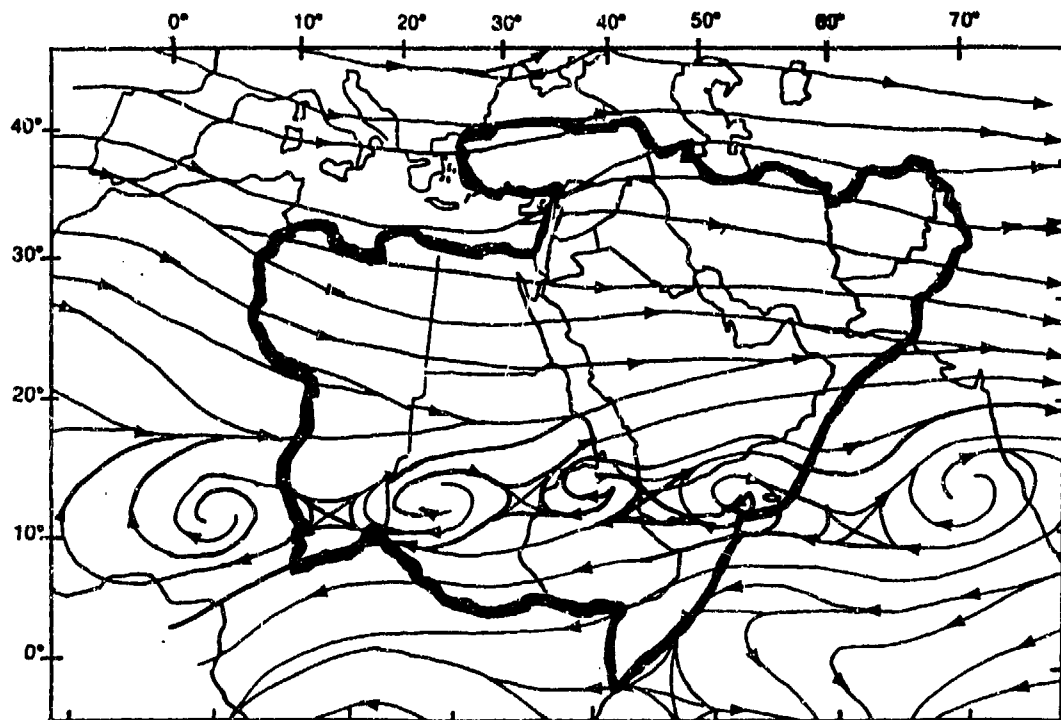


Figure 2-10c. Mean January Upper-Air Flow Patterns, 500 mb.

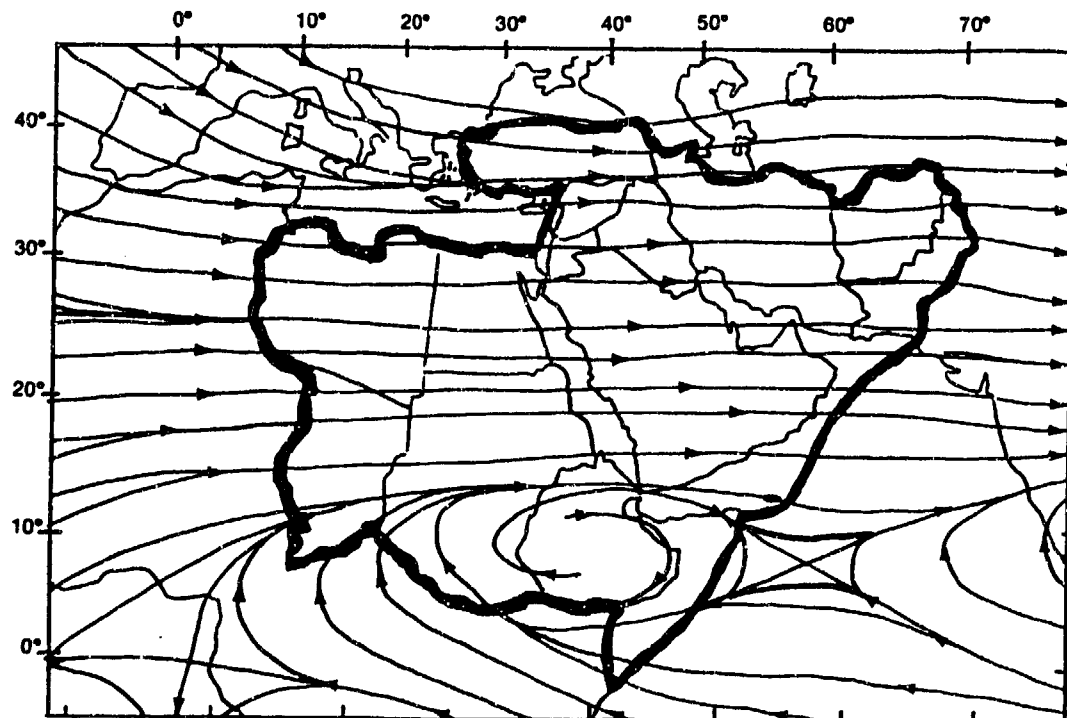


Figure 2-10d. Mean January Upper-Air Flow Patterns, 300 mb.

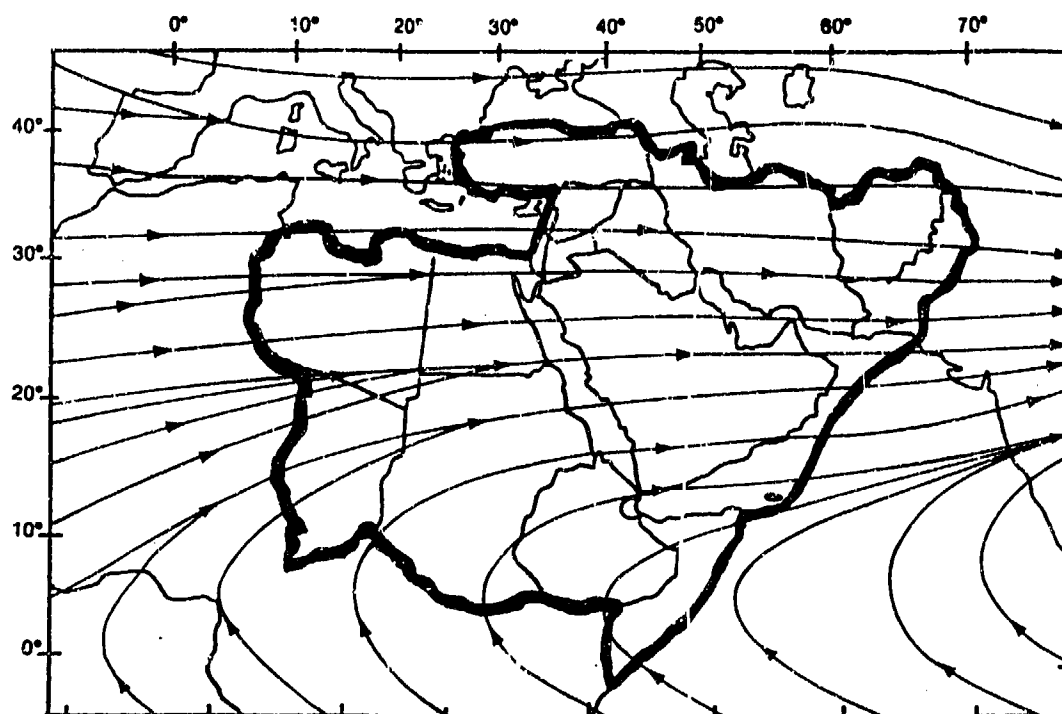


Figure 2-10e. Mean January Upper-Air Flow Patterns, 200 mb.

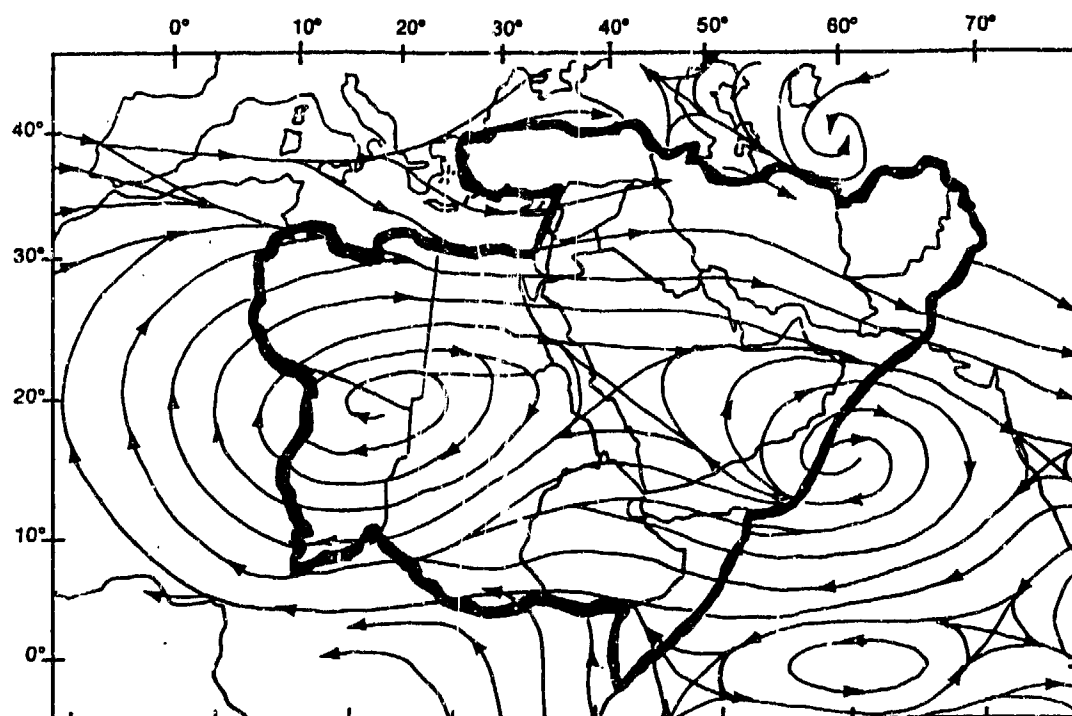


Figure 2-11a. Mean April Upper-Air Flow Patterns, 850 mb.

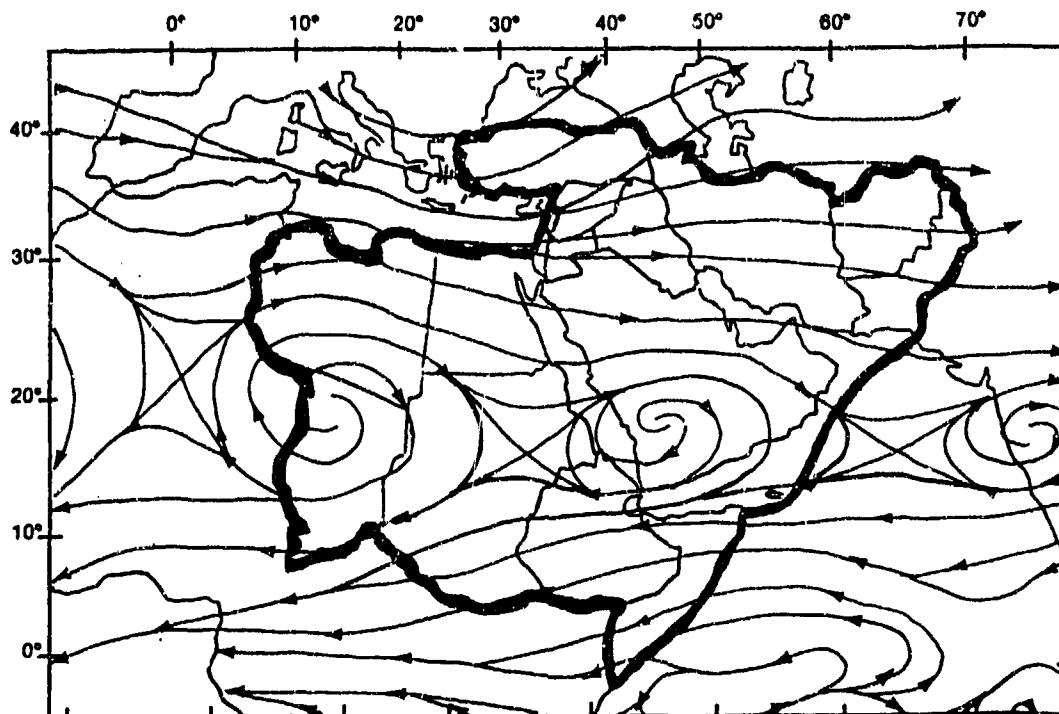


Figure 2-11b. Mean April Upper-Air Flow Patterns, 700 mb.

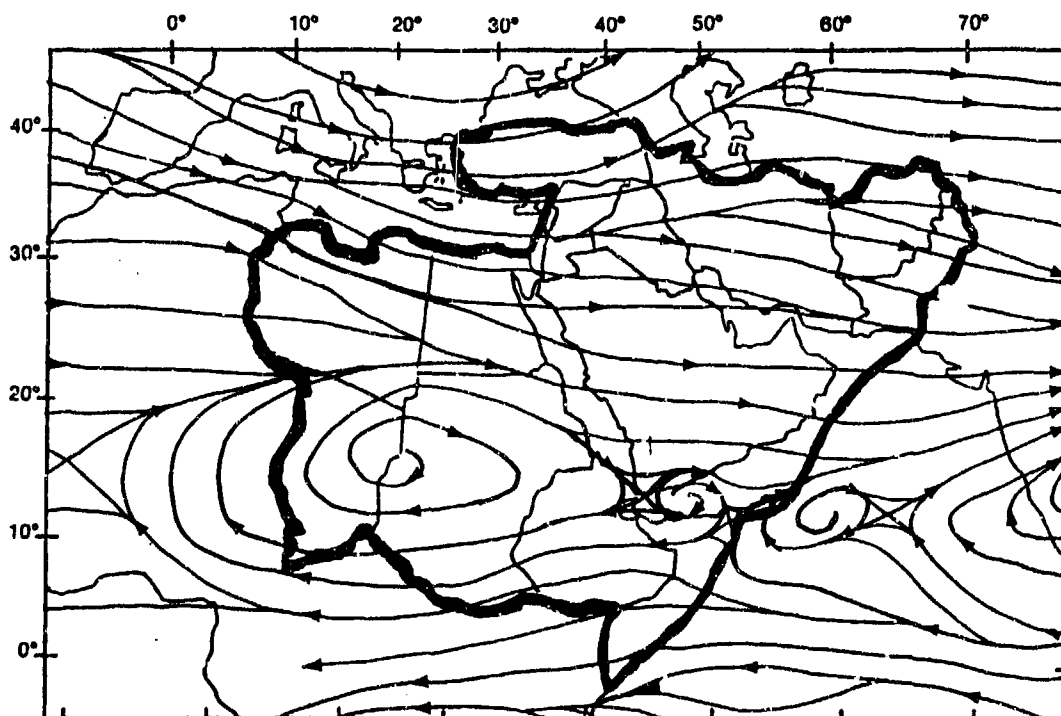


Figure 2-11c. Mean April Upper-Air Flow Patterns, 500 mb.

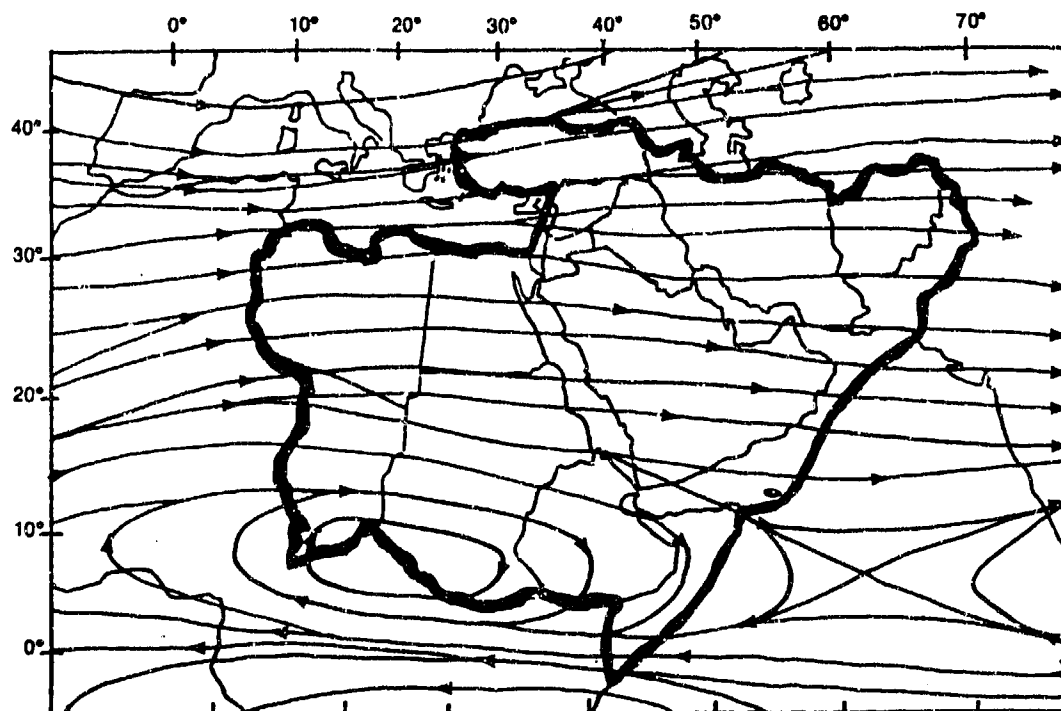


Figure 2-11d. Mean April Upper-Air Flow Patterns, 300 mb.

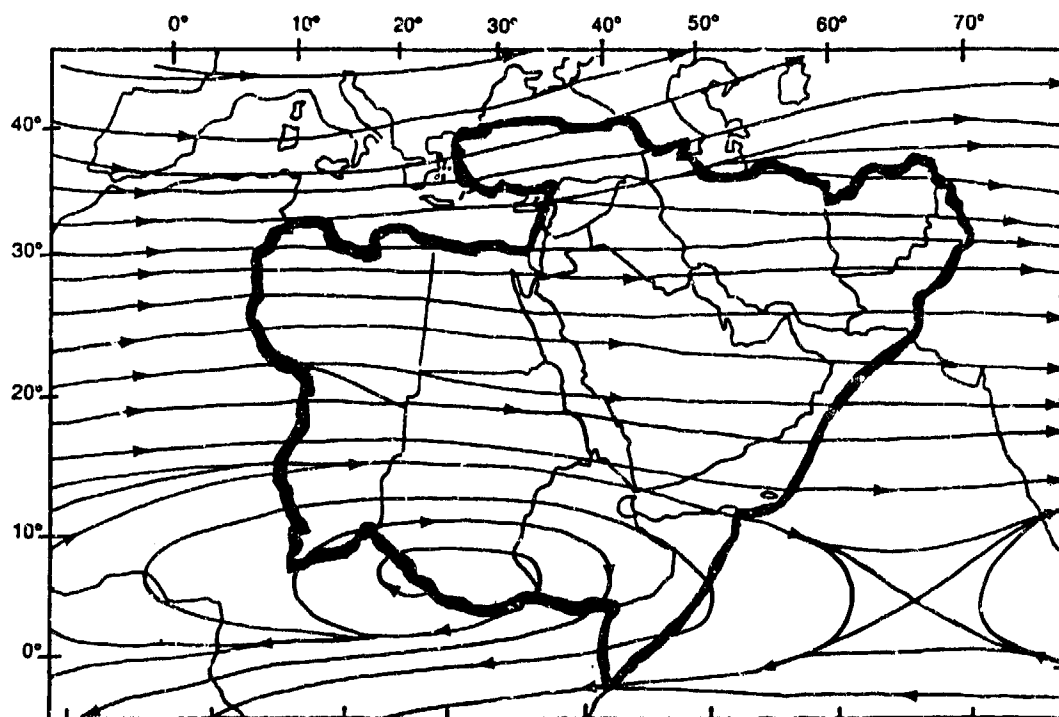


Figure 2-11e. Mean April Upper-Air Flow Patterns, 200 mb.

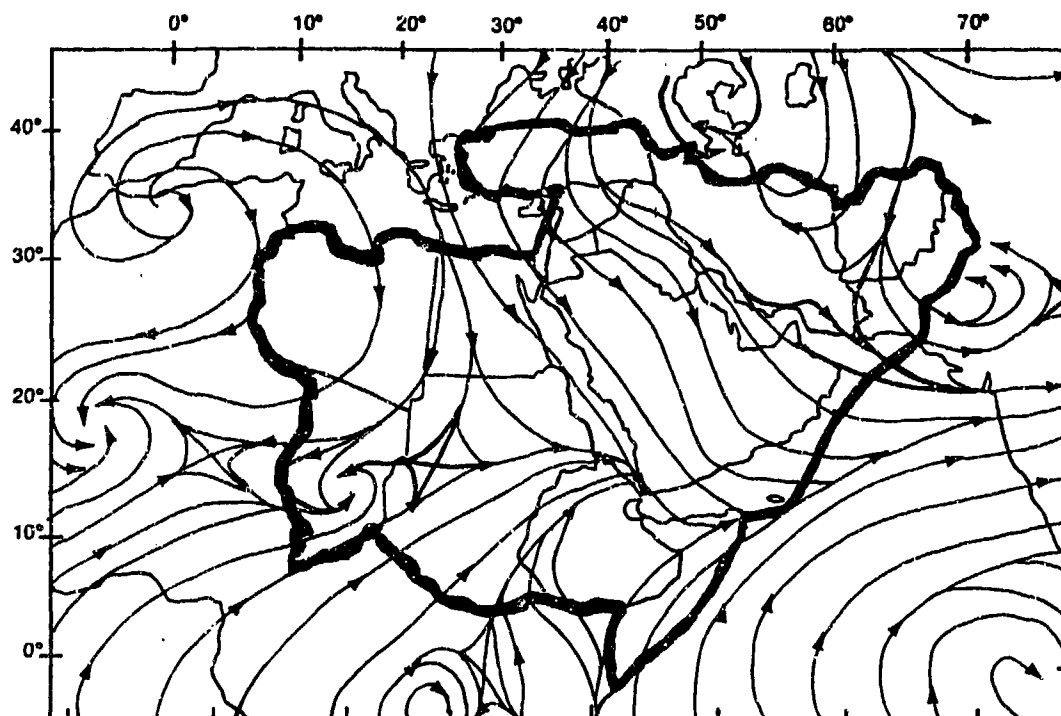


Figure 2-12a. Mean July Upper-Air Flow Patterns, 850 mb.

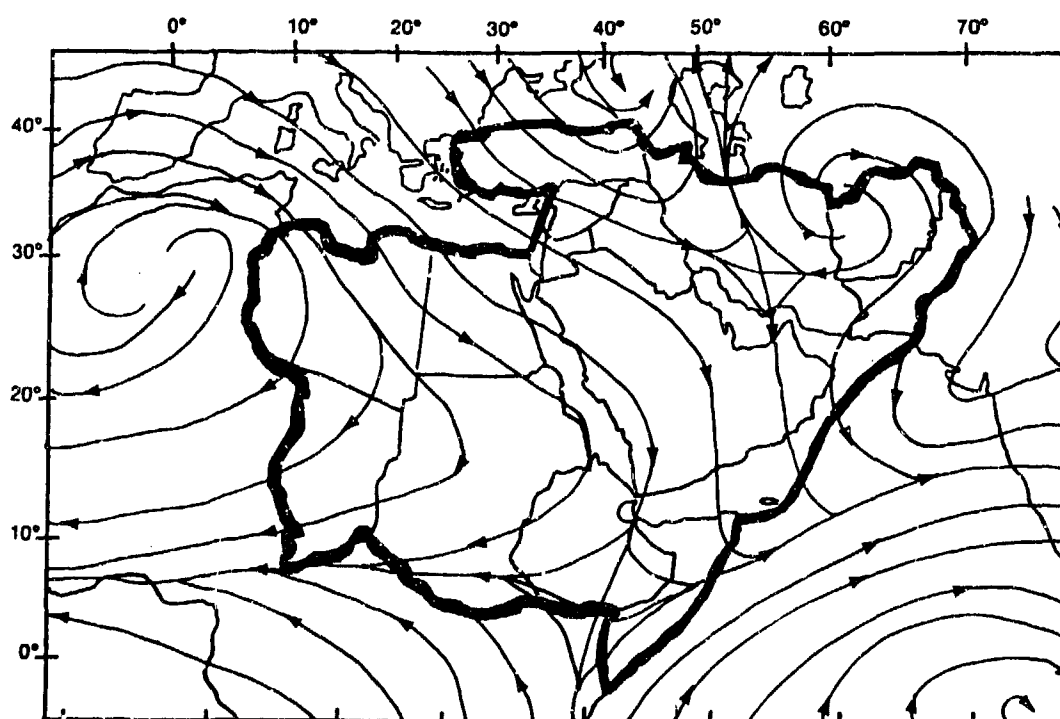


Figure 2-12b. Mean July Upper-Air Flow Patterns, 700 mb.

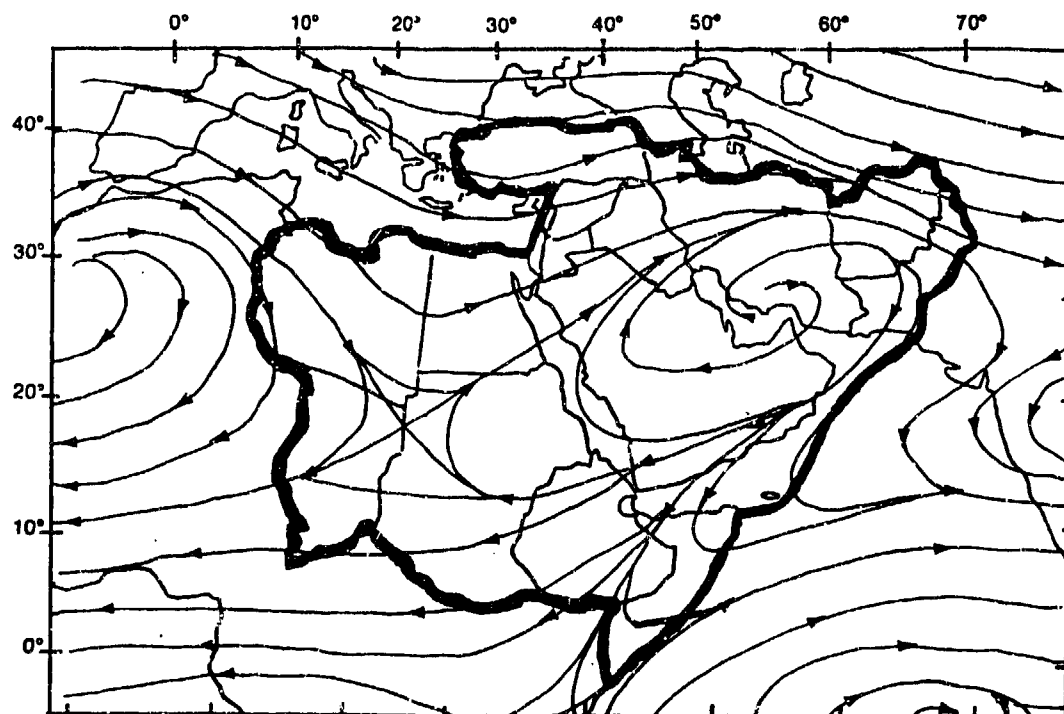


Figure 2-12c. Mean July Upper-Air Flow Patterns, 500 mb.

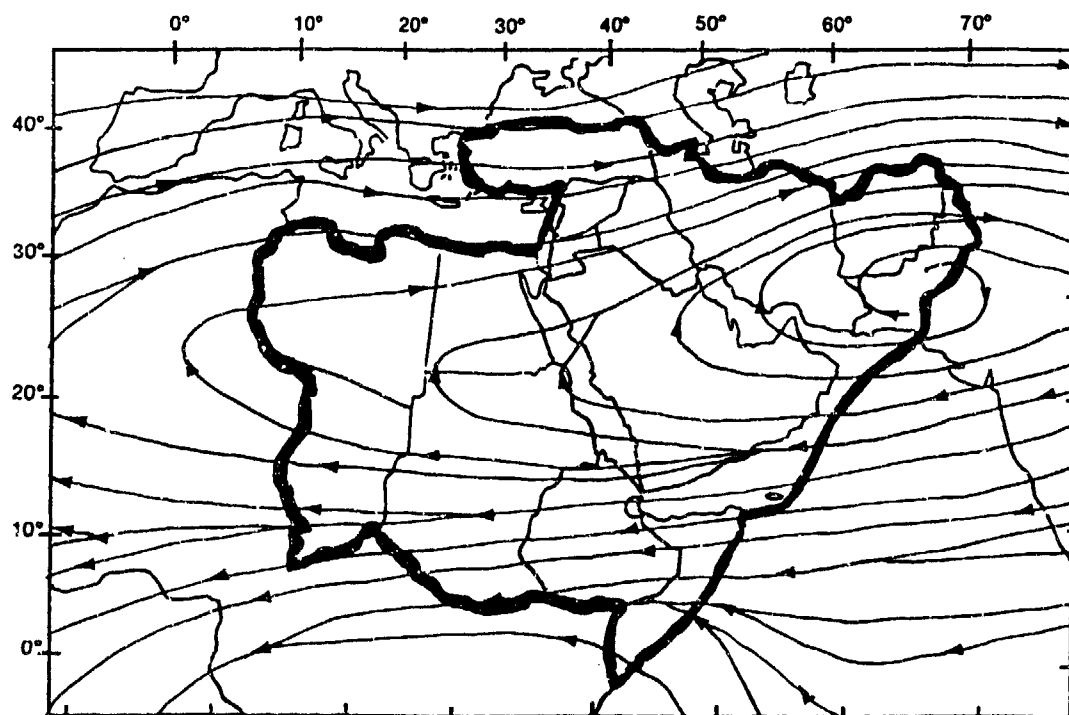


Figure 2-12d. Mean July Upper-Air Flow Patterns, 300 mb.

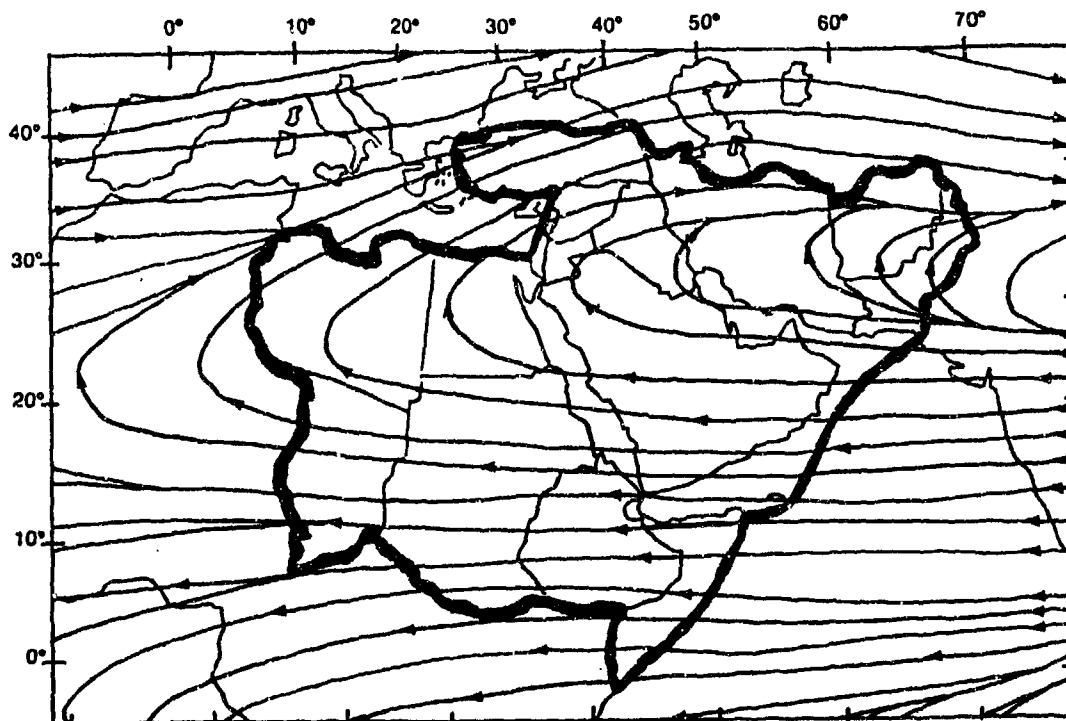


Figure 2-12e. Mean July Upper-Air Flow Patterns, 200 mb.

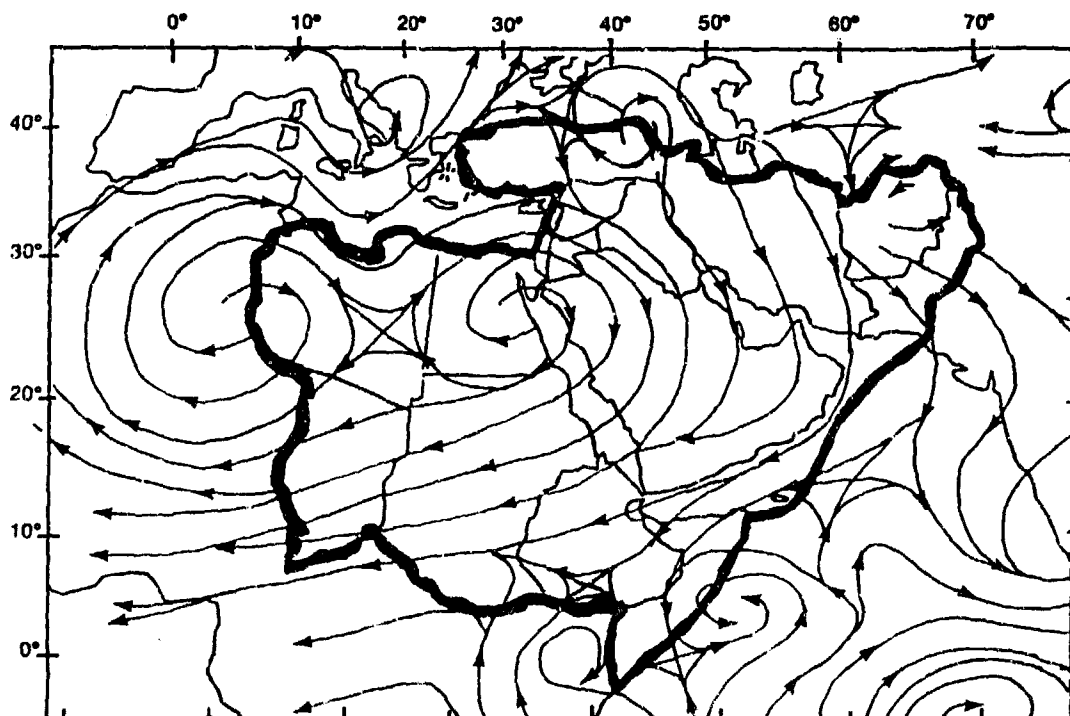


Figure 2-13a. Mean October Upper-Air Flow Patterns, 850 mb.

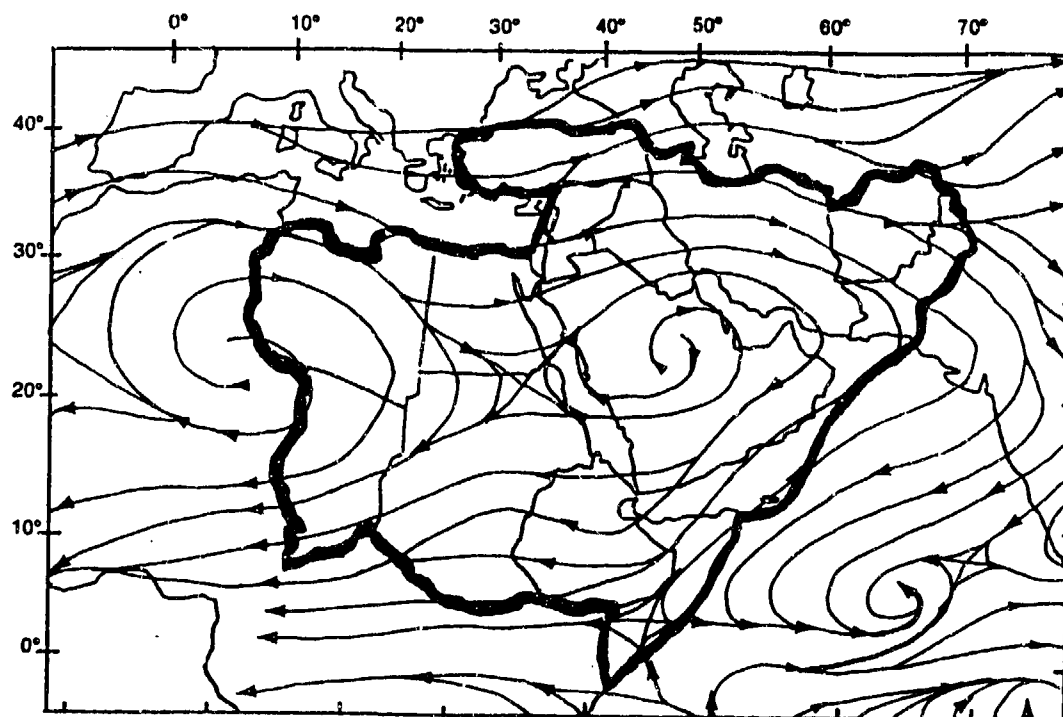


Figure 2-13b. Mean October Upper-Air Flow Patterns, 700 mb.

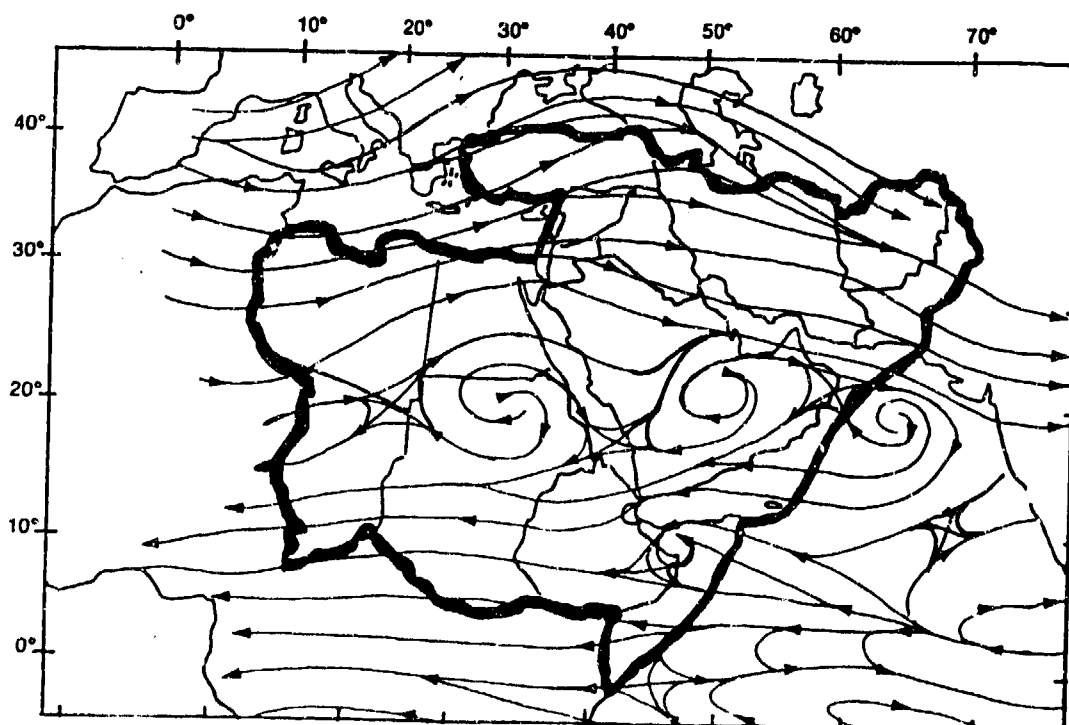


Figure 2-13c. Mean October Upper-Air Flow Patterns, 500 mb.

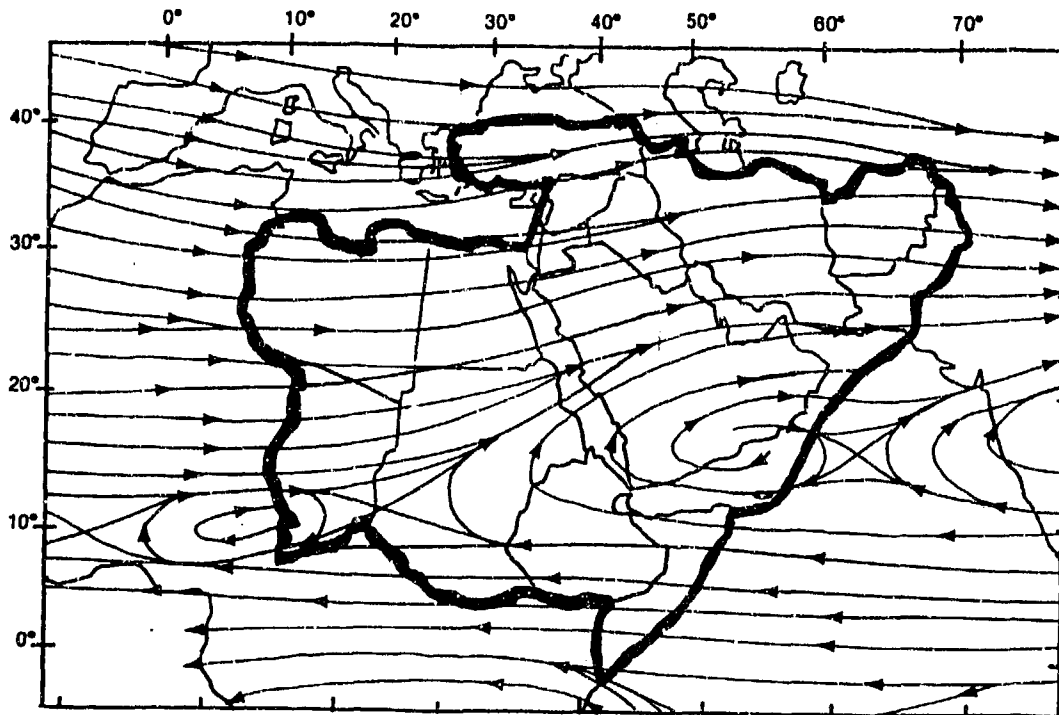


Figure 2-13d. Mean October Upper-Air Flow Patterns, 300 mb.

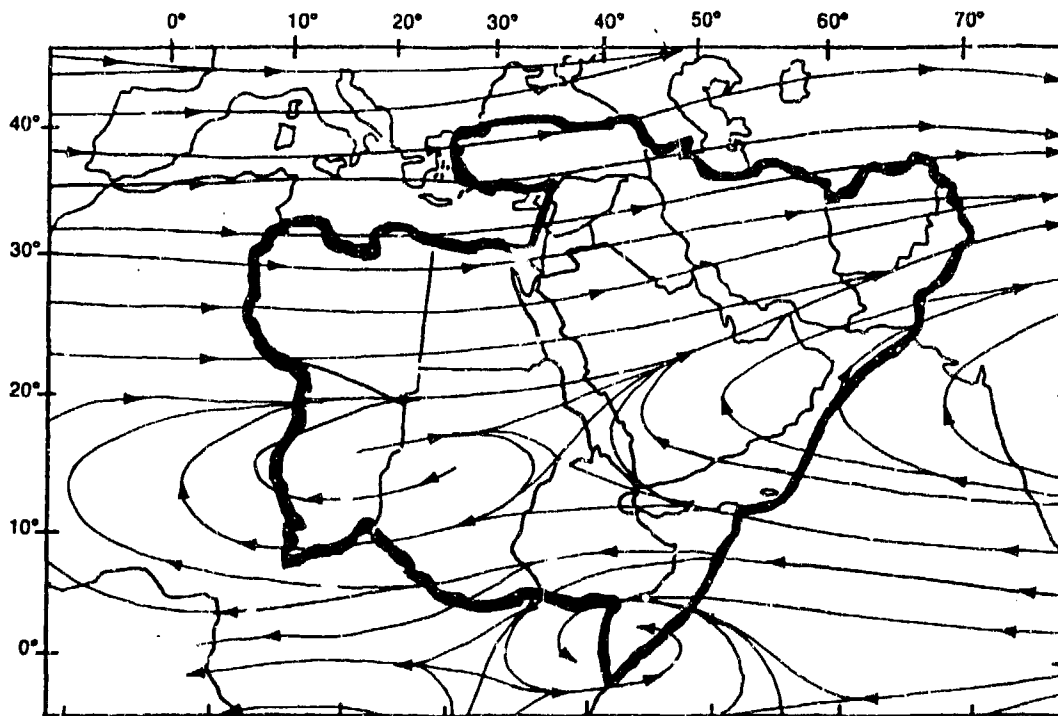


Figure 2-13e. Mean October Upper-Air Flow Patterns, 200 mb.

THE SUBTROPICAL RIDGE. This upper-level feature, represented graphically by the 200-mb ridge axis line, marks the division between upper-level westerly and easterly flow. As shown in Figure 2-14, the Subtropical Ridge oscillates from 6° N in January to $24-27^{\circ}$ N in July. This oscillation provides the region

with alternating periods of westerly and easterly upper-level flow. Upper-level westerly flow occurs throughout the year north of 30° N. In October, southerly or easterly flow only occurs south of 20° N. April and October positions can be inferred from Figures 2-11e and 2-13e.

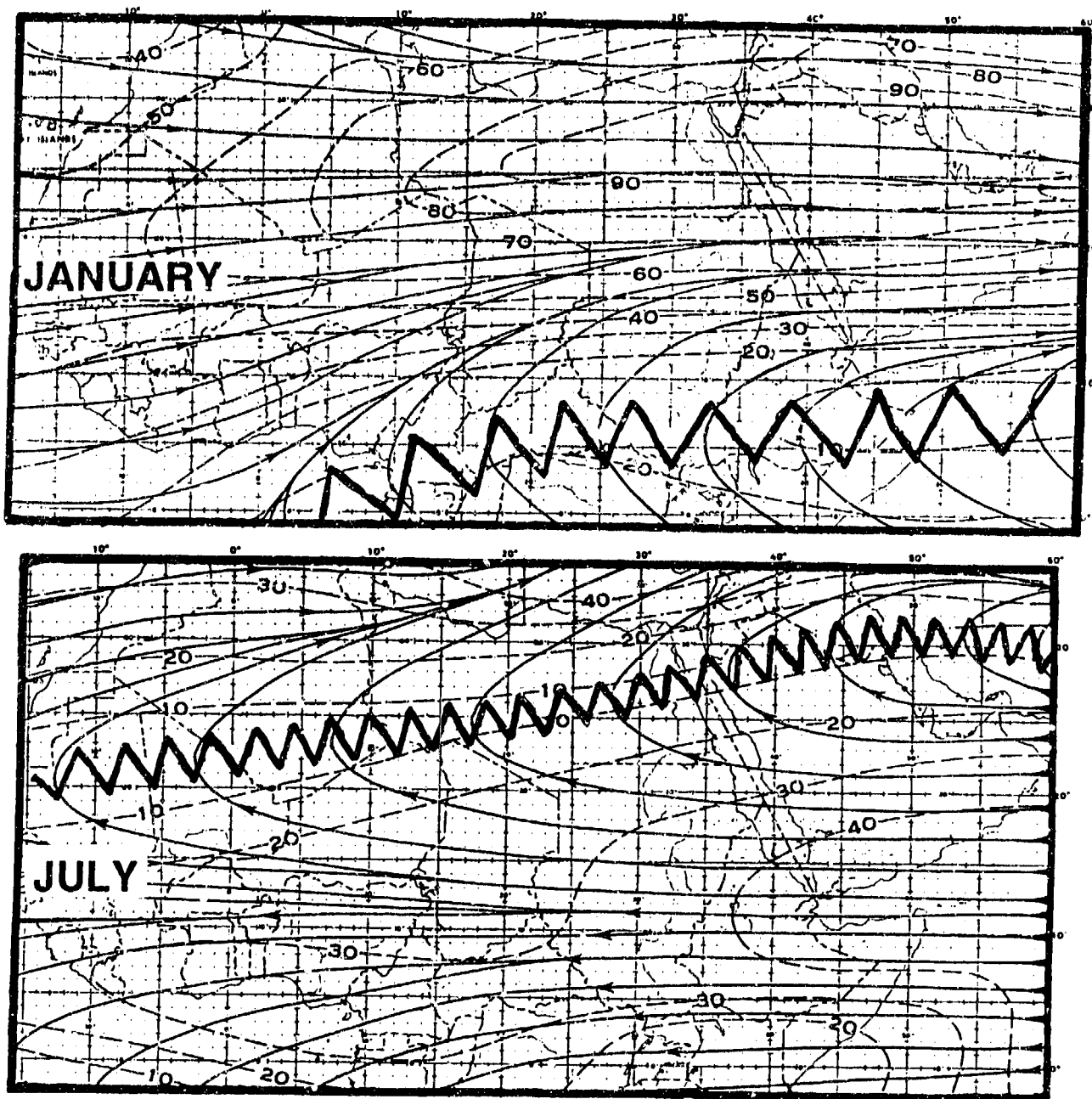


Figure 2-14. Mean January and July Positions of the Subtropical Ridge. The jagged line denotes the mean ridge axis position. Dashed lines are isotachs (kt).

SYNOPTIC DISTURBANCES

JET STREAMS. Four different jet streams affect this region: the Polar Jet (PJ), the Subtropical Jet (STJ), the Tropical Easterly Jet (TEJ), and the Mid-Tropospheric Easterly Jet (MTEJ).

The Polar and Subtropical Jets (PJ and STJ) are important to the formation and movement of weather

systems throughout the Mediterranean Basin. The PJ's position and movements control cold air advection and mid-level direction for developing Mediterranean cyclones; the STJ provides steering, shear, and outflow in the upper layers. These jets affect all of the study area except sub-Saharan Chad and Sudan. Figure 2-15 shows the mean jet positions in January and July.

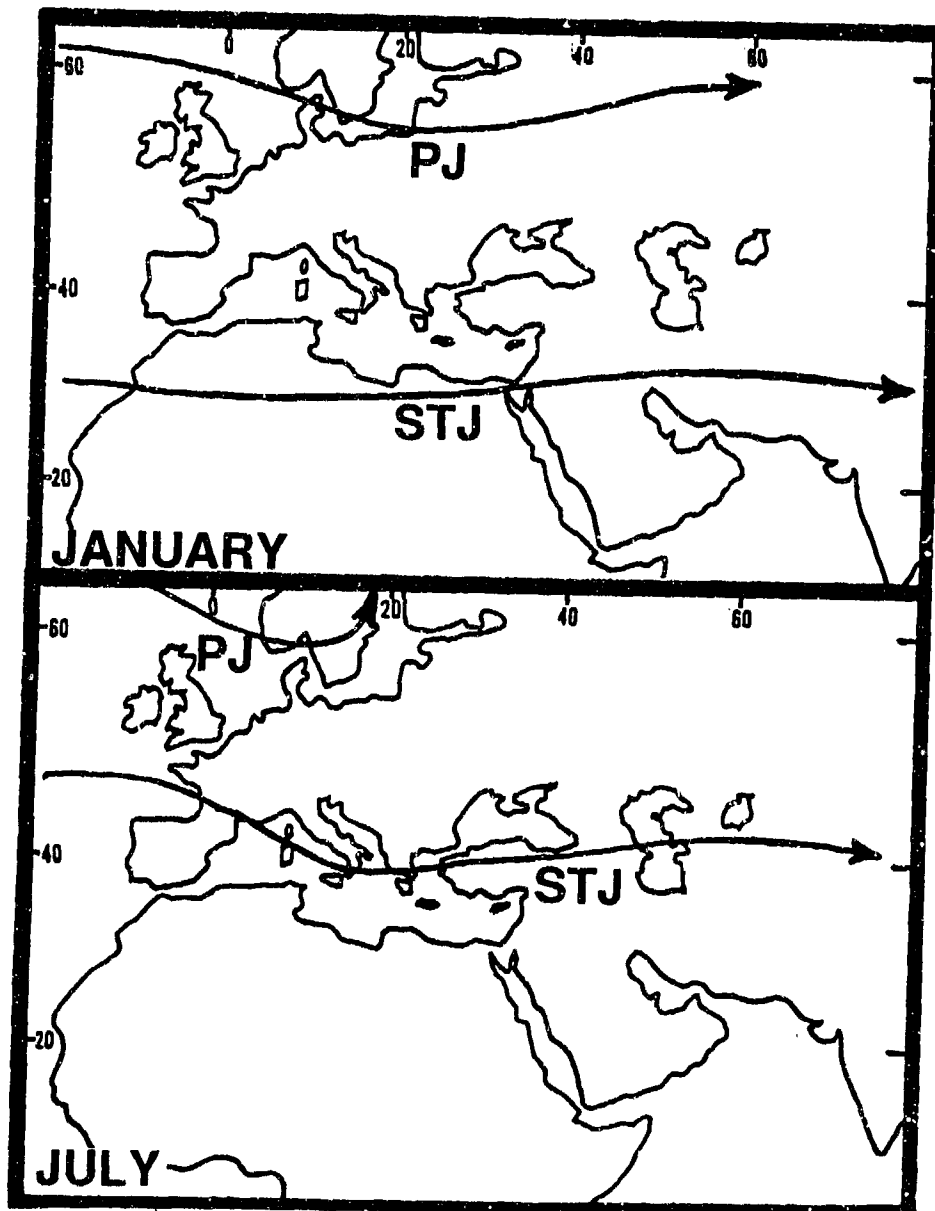


Figure 2-15. Mean January and July Positions of the Polar Jet (PJ) and Subtropical Jet (STJ).

Mean PJ positions vary from north to south over Europe from 55° to 65° N. Maximum wind speeds from December to March vary from 60 to 160 knots. The PJ is usually found near 30,000 feet (9,146 meters) MSL. Southward deviations (to $30\text{--}45^{\circ}$ N) are most frequent between December and March, but the PJ enters the eastern Sahara on rare occasions in April, May, or June. The April-June PJ is found between 30,000 and 34,000 feet (9,146-10,365 meters) MSL; maximum wind speeds are between 60 and 140 knots.

Although the STJ shows less variability in its daily position, seasonal variability is greater than that of the PJ. Mean STJ positions over the subtropics range from 25° to 45° N. Maximum wind speeds between December and April are between 80 and 180 knots at a mean height of 39,000 feet (12,195 meters) MSL. Speeds between May and November are between 30 and 60 knots at 39,000-43,000 feet (12,195-13,110 meters) MSL. The STJ is weakest in July and August, seldom extending south of 35° N.

Initially, surface low-pressure cells develop when a strong PJ digs south of 30° N and forms a deep upper-level trough. Northerly flow often develops on the east side of a blocking high-pressure ridge over the eastern Atlantic. The PJ and upper-level trough may intensify surface lows over the Mediterranean Sea and in the lee of the Atlas Mountains of northwestern Africa. Northerly flow ensures that the trough and the surface cyclone move eastward into the eastern Mediterranean.

The preferred area of low-pressure center intensification is often under the southeast quadrant of the upper-level trough. The low often deepens in the area between the two jets. Jet stream interaction most frequently occurs with Atlas Lows between 25° and 30° N--nearest the mean position of the STJ. Figures 2-16a-c illustrate generalized PJ/STJ interaction and low-pressure intensification area for Genoa, Atlas, and Cyprus Lows, respectively.

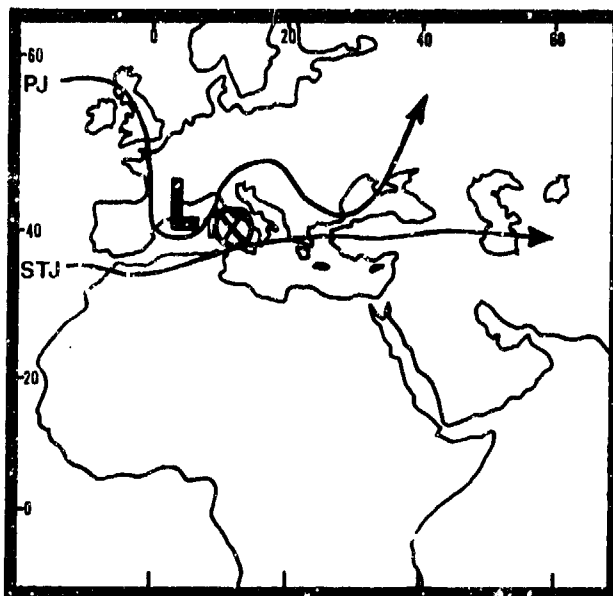


Figure 2-16a. Typical Jet Positions During Formation of Genoa Low. The surface low formation/intensification area is denoted by the circled X.

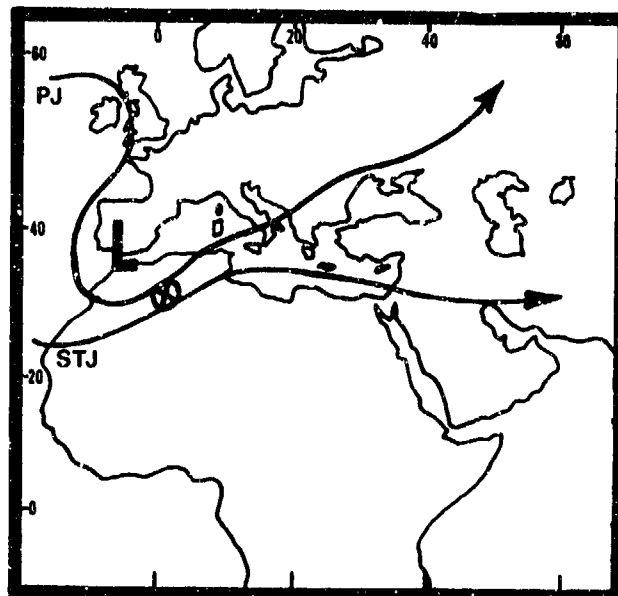


Figure 2-16b. Typical Jet Positions During Formation of Atlas Low. The surface low formation/intensification area is denoted by the circled X.

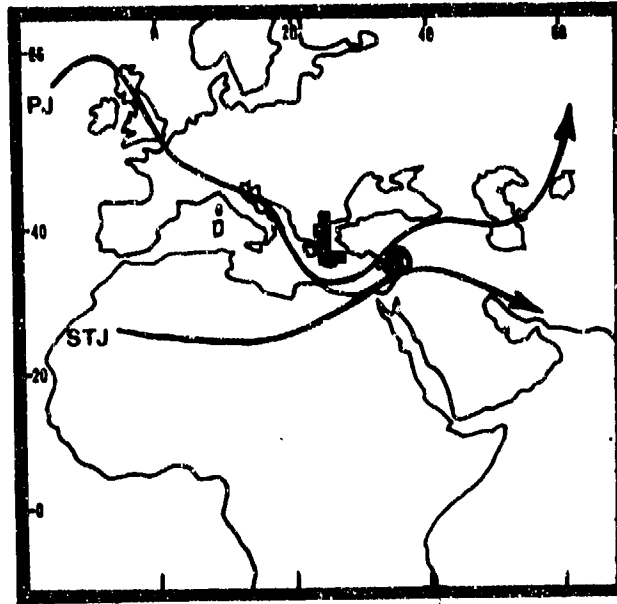


Figure 2-16c. Typical Jet Positions During Formation of Cyprus Low.
The surface low formation/intensification area is denoted by the circled X.

Tropical Easterly Jet (TEJ). This summer feature in the upper-level easterlies develops as outflow from the southern edges of the Tibetan 200-mb circulation. The TEJ provides an outflow mechanism for Monsoon Trough convection, thus sustaining convection in sub-Saharan Chad and Sudan. Changes in the TEJ may cause surges in Monsoon Trough convection. Its mean

position lies at about 10° N, but it oscillates between $7^{\circ}30'$ and 18° N (see Figure 2-17). Highest wind speeds (90 knots) are found between 100 and 200 mb. The TEJ normally lies about $4-5^{\circ}$ south of the surface Monsoon Trough over the African continent west of the Ethiopian Highlands.

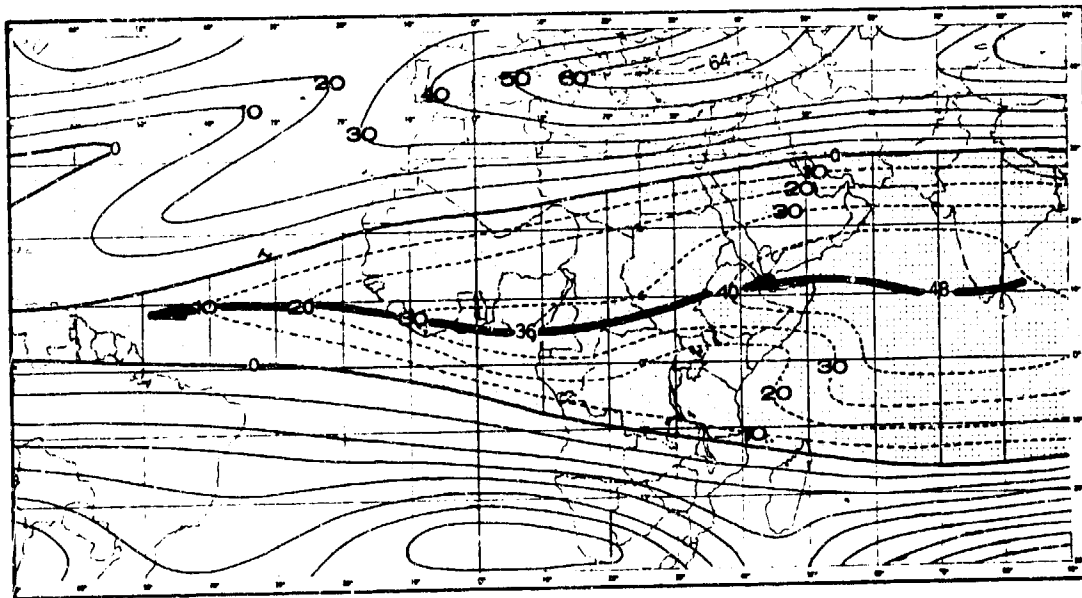


Figure 2-17. Mean July 200-mb Zonal Flow Showing the Tropical Easterly Jet (TEJ). The dark arrow is the TEJ. The stippled area represents easterly flow. Dashed lines are isotachs in knots. Solid lines are westerly flow isotachs.

Mid-Tropospheric Easterly Jet (MTEJ). This mid-level jet occurs over subtropical Africa between May and October. The MTEJ develops from the thermal contrast along the ITD as hot, dry Saharan air lies over

the cooler, moister equatorial air. The gradient is strongest during the summer when surface temperatures reach their maximum over the Sahara, but change little over equatorial regions.

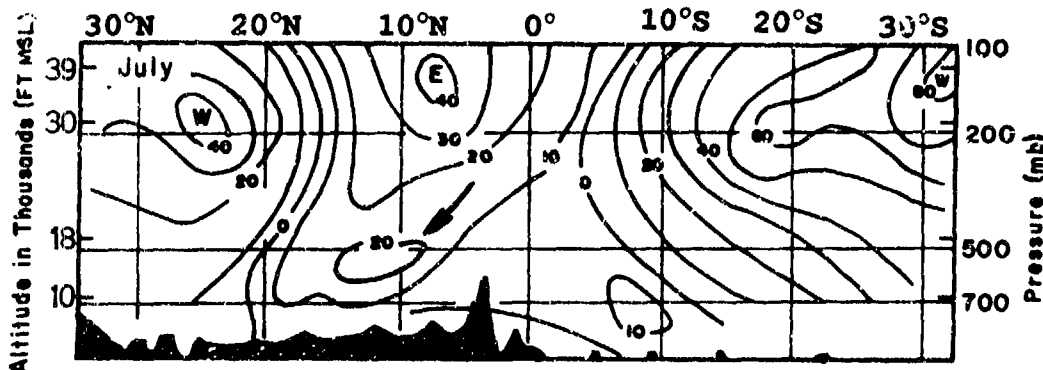


Figure 2-18. Meridional Cross Section of Zonal Winds Near 10° E for July. Solid lines are isotachs in knots. The arrow points out the location of the MTEJ.

The MTEJ develops along the Ethiopian Highland foothills (the southeasternmost penetration of Saharan air) and extends westward to the Atlantic Ocean. Mean jet core winds average 25 knots; maximum speeds can reach 50 knots. Figure 2-19 shows an MTEJ latitudinal

cross section at 13° N in August. The dotted line shows the jet axis. The MTEJ steers African Waves (which see) westward between Khartoum and N'Djamena from June through September.

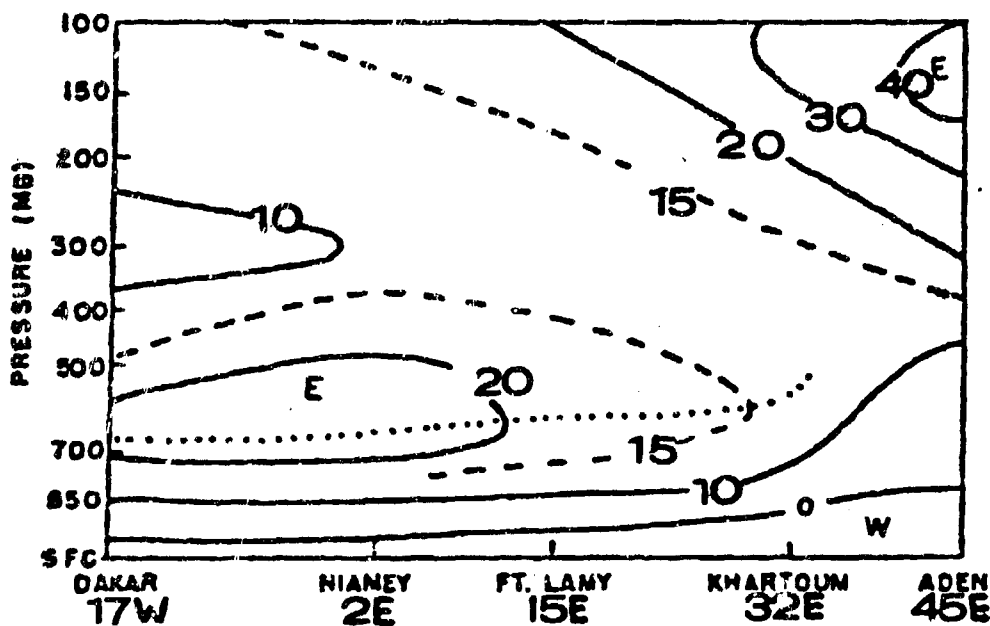


Figure 2-19. Cross Sectional View Showing the MTEJ at 13° N in August (from Burpee, 1972). Solid lines are isotachs in knots. The dotted line shows the jet axis. The easterly wind maximum correlates well with the mean height of the Intertropical Discontinuity (ITD) at 13° N during August.

MID-LATITUDE CYCLOGENESIS. Areas of cyclogenesis for Genoa Lows, Atlas Lows, and Cyprus Lows are shown in Figure 2-20. These systems affect the eastern Mediterranean Coast and northeast Africa most

frequently between November and March. Deep Cyprus Lows produce thunderstorms in the northern Nile River Valley of Egypt. One winter thunderstorm in this area brings 70 to 90% of the entire seasonal rainfall total.

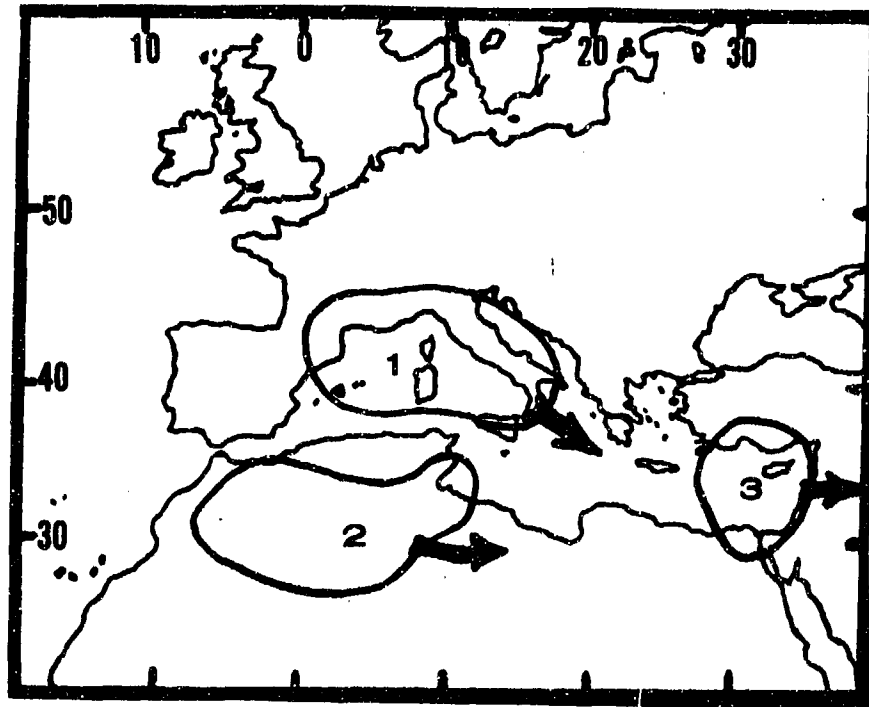


Figure 2-20. Mediterranean Cyclogenesis Regions. The three primary areas of cyclogenesis are shown for (1) Genoa Lows, (2) Atlas Lows, and (3) Cyprus Lows. Arrows indicate general direction of movement.

Synoptic considerations dictate specific areas for cyclone formation and movement. Surface pressure patterns, shortwave troughs, vorticity advection, and jet-stream positions determine cyclone strength. The entire Mediterranean coast is affected by these systems. Surface cold fronts extend southward into northern Libya and Egypt and provide most significant weather in these areas. Only abnormally deep surface troughs can bring even weak temperature changes and wind shifts south to 18° N. Cold fronts moving south of this area weaken into a shear line.

The Genoa Low forms primarily from December to March in the Gulf of Genoa (the northern part of the Ligurian Sea); it accounts for 69% of Mediterranean basin cyclones. Airflow over the Swiss Alps produces lee-side troughing off the coast of Italy; transient disturbances intensify in this trough. These storms

normally intensify over a 12-48 hour period before moving off into the north-central Mediterranean.

There are three common patterns for Genoa Low development. One is the movement of a surface cold front into the Gulf of Genoa from the west in advance of an upper-level trough, which produces southwesterly flow aloft in the warm sector. Unstable cold air advected by strong northerly surface winds through the Rhone Gap in southern France produce cyclonic turning at the lower levels. The warm Mediterranean Sea supplies moisture to the developing low, which moves southeastward into the Mediterranean, then turns eastward toward Turkey. The primary track is ESE into Cyprus, with a secondary track ENE into the Black Sea. The cold front will normally extend 200 NM inland into northern Africa, but the southern end is weak.

A second common synoptic pattern for Genoa Low development is the establishment of a blocking 500-mb ridge over the eastern Atlantic along the European coast that brings north to northwesterly mid-level flow into the Mediterranean basin. Icelandic Lows passing to the north extend cold fronts southeastward over Spain and France. The blocking long-wave ridge steers shortwaves into the Gulf of Genoa. Cold air aloft, warm water at the surface, and lee-side troughing combine to intensify the shortwaves. The low normally tracks southeastward over the central Mediterranean Sea. These migratory lows may bring short periods of light showers, drizzle, or virga to areas east of 15° E and north of 23° N.

A third synoptic situation for Genoa Low formation occurs when cyclonic shear over the Strait of Gibraltar produces an upper-level cutoff low in the western Mediterranean. About 10% of these vortices reach the Gulf of Genoa and intensify into a Genoa Low. These troughs bring mid- and upper-level clouds, but no precipitation in northeastern Africa south as far as 25° N.

The Atlas Low. From March to April and from October to early December, transitory lows form in the north-central interior of Algeria southeast of the Atlas Mountains near 30° N, 2° E. An Atlas Low generally forms when a mid- or upper-level trough, oriented NE-SW over Spain, is positioned over a weak surface low or slow-moving cold front.

In March and April, the mean Azores High moves northwestward, shifting the mean mid-level flow pattern from zonal to more meridional. This can cause a southward movement of disturbances along the Polar Jet, which often digs along the backside of the 500-mb trough, producing lifting along the Atlas Mountains. Mid-level cold air and moisture cross the Atlas range as a cold-core cut-off low or shortwave. These storms seldom develop or penetrate very far into the eastern Sahara without strong northerly flow and mid-level cold air support. The Subtropical Jet provides strong outflow and divergence aloft; mean wind speed is 80 knots over western Africa in the spring.

The lows normally move northeast over the south-central Mediterranean along the polar-subtropical jet axes. They produce strong south or southwesterly winds within the cyclone's warm sector (see Sirocco and Khamsin regional winds). When a sustained northerly flow pattern persists for more than 3 days, the Polar Jet and the mean Atlas Low storm track shift southward with the lows moving east across the northern Sahara; polar air surges south of 30° N. Southerly winds are greater than 25 knots, producing Khamsin winds over central portions of the eastern Sahara. Strong surface high pressure (see Harmattan) normally moves in behind the system. Figures 2-21a through e depict a 3-day sequence during which Atlas Low cyclogenesis and movement is east-southeastward over the northern Sahara.

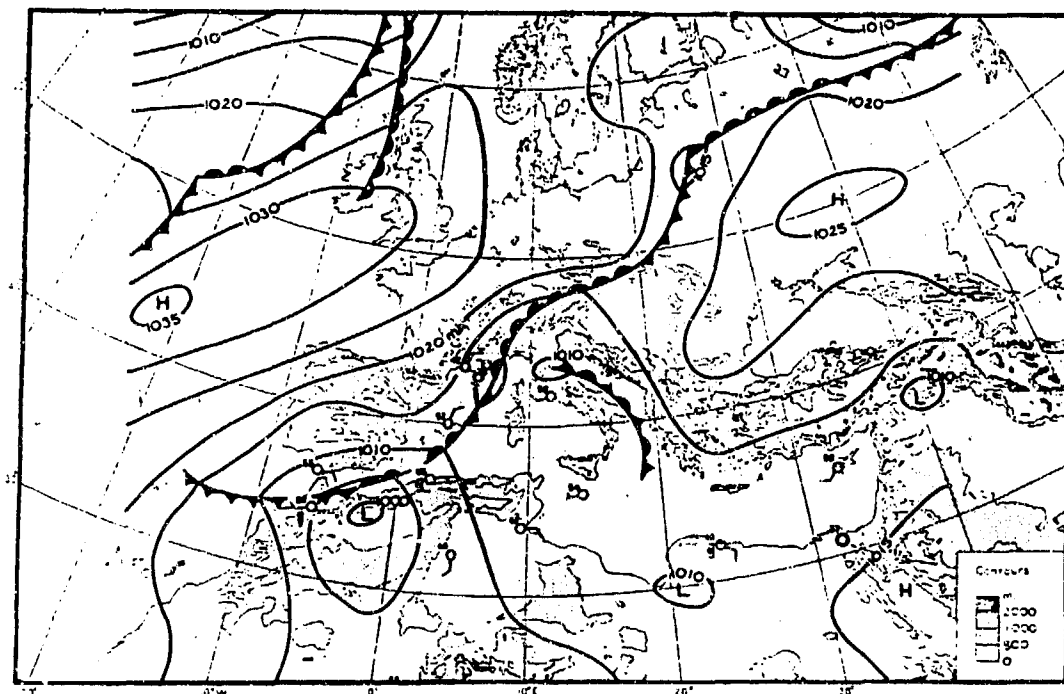
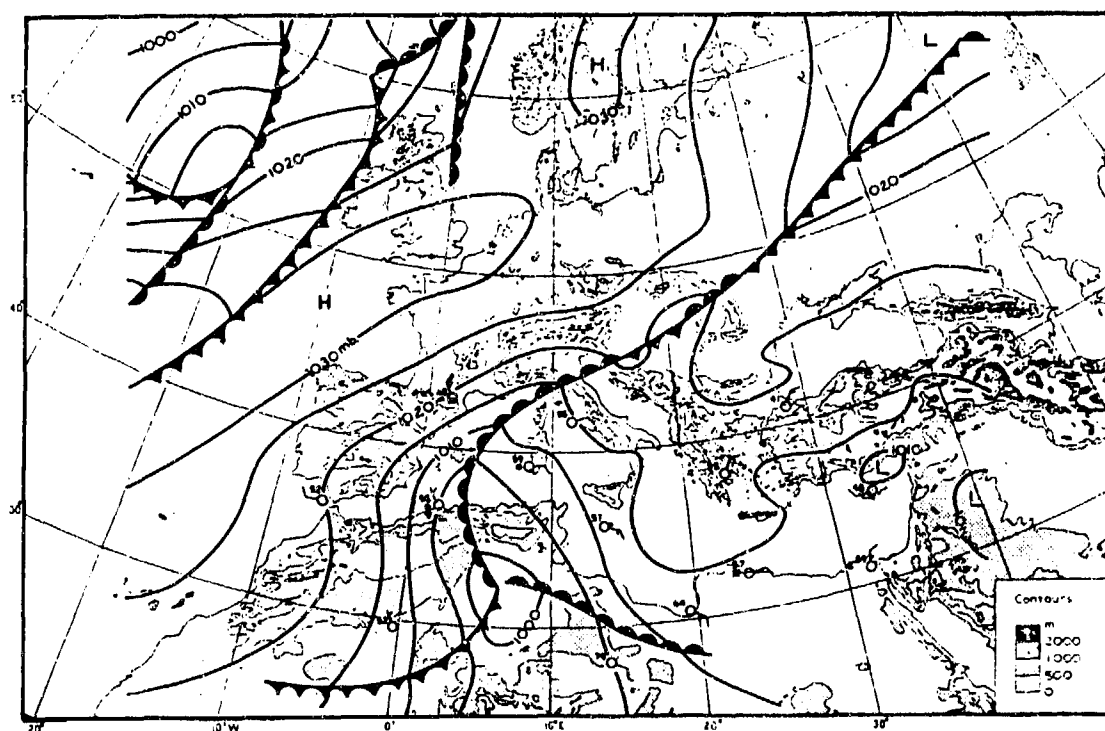
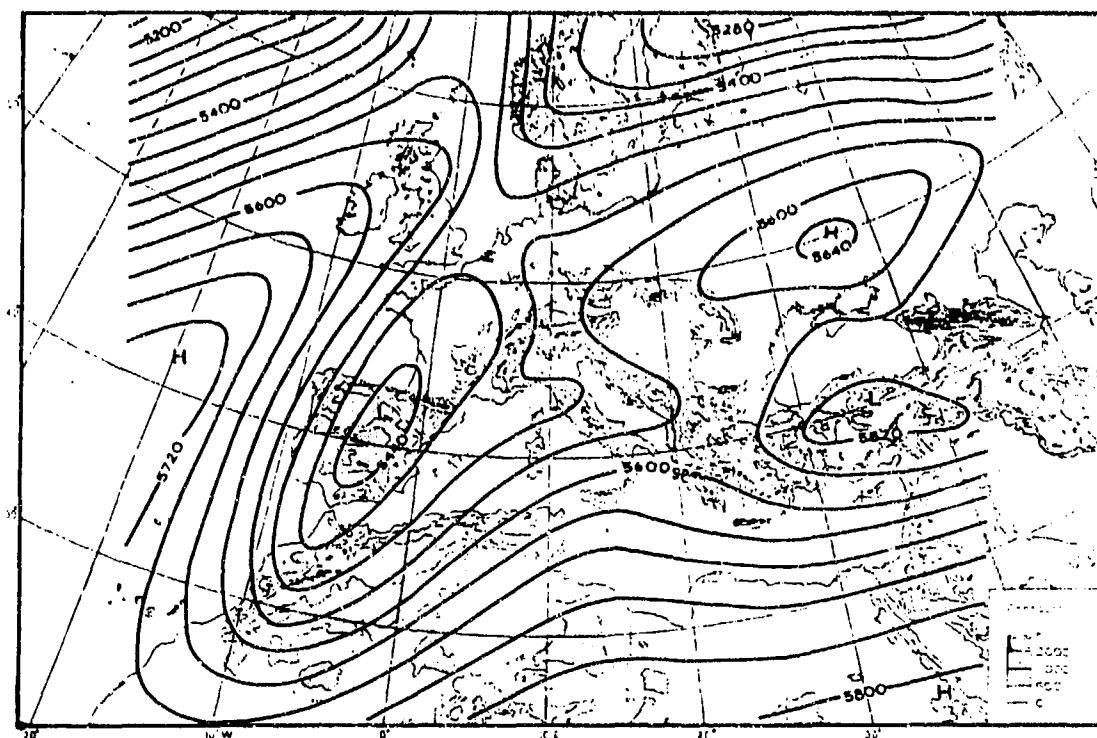


Figure 2-21a. Synoptic Surface Chart (7 April 1954, 0000Z), Atlas Low. Pressures in millibars.



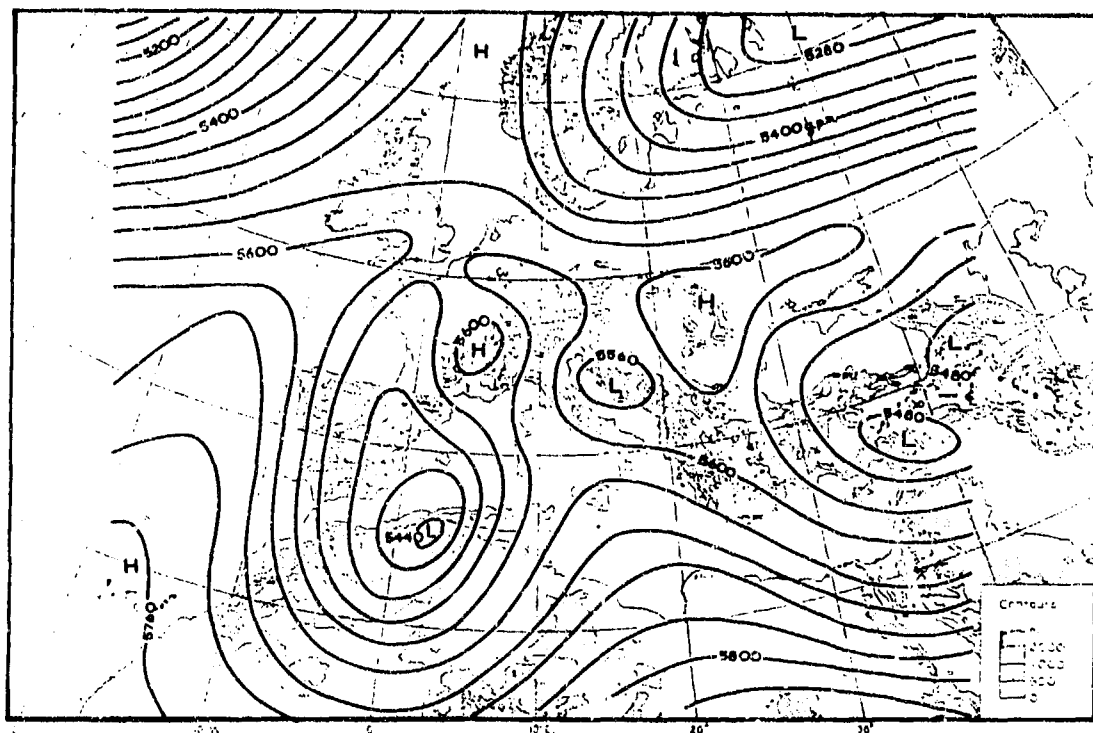


Figure 2-21d. 500-mb Flow (8 April, 1954, 0300Z), Atlas Low. Contours are heights in geopotential meters (gpm). The 500-mb trough is moving southeastward from central Spain into northern Algeria, forming a cut-off low at 35° N, 3° E.

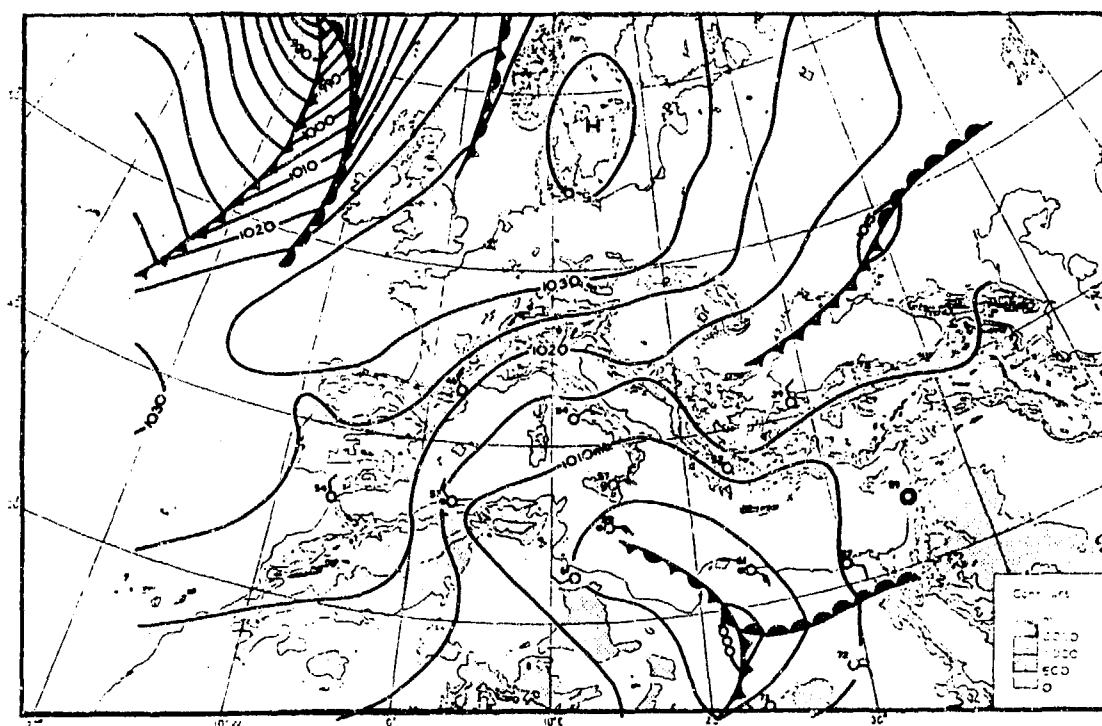


Figure 2-21e. Synoptic Surface Chart (9 April 1954, 0000Z), Atlas Low. Pressures in millibars. The Atlas Low is positioned along the Libya-Egypt border.

The Cyprus Low. This migratory low can create heavy thunderstorm activity between November and March. Two factors contribute to Cyprus Low cyclogenesis: low-level inflow of northwesterlies from the Aegean Sea over warm eastern Mediterranean waters (see Figure

2-22) and instability aloft caused by cold slow-moving migratory (mid- and upper-level) polar troughs. One or two Cyprus Lows produce extensive thunderstorm outbreaks every winter.

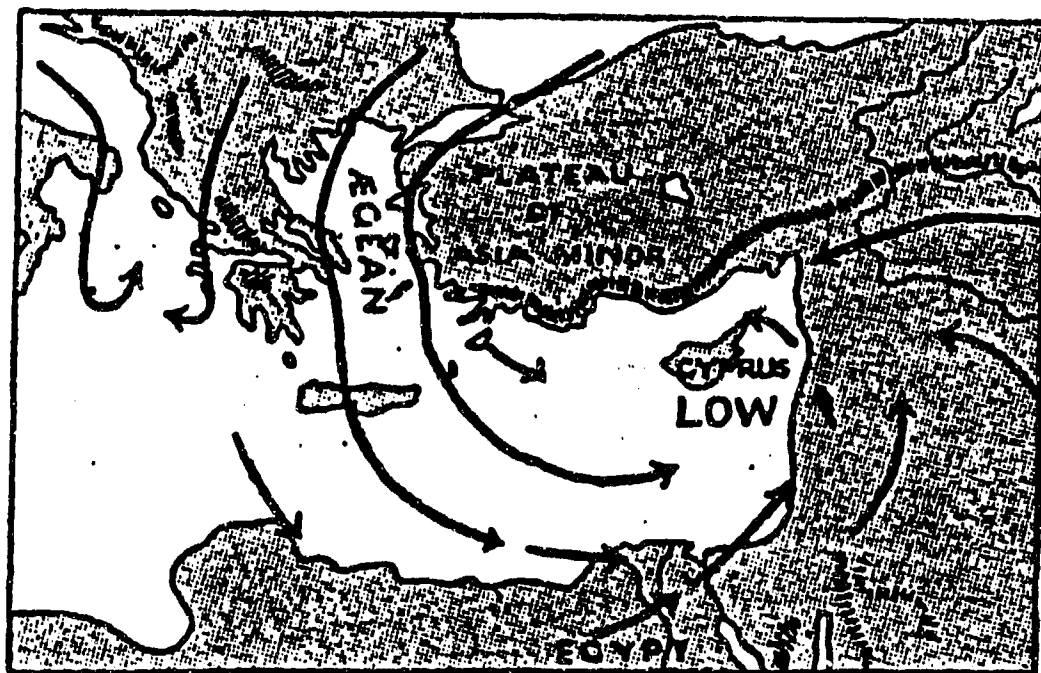


Figure 2-22. Surface Circulation Causes Development of the Cyprus Low.

The Cyprus Low develops over a warm water surface. As a result, less instability is needed to sustain lower surface pressures. Favorable mid- and upper-level flow (westerlies) occur frequently throughout the December-March period, whereas the Atlas Low cyclogenesis area requires a sustained northerly flow pattern, common only during transition seasons.

Figures 2-23a-d illustrate a mid-November sequence for Cyprus Low formation. Figures 2-23a-c are surface charts showing the 16-18 November 1953 development of the low, and 2-23d is the 18 November 500-mb chart.

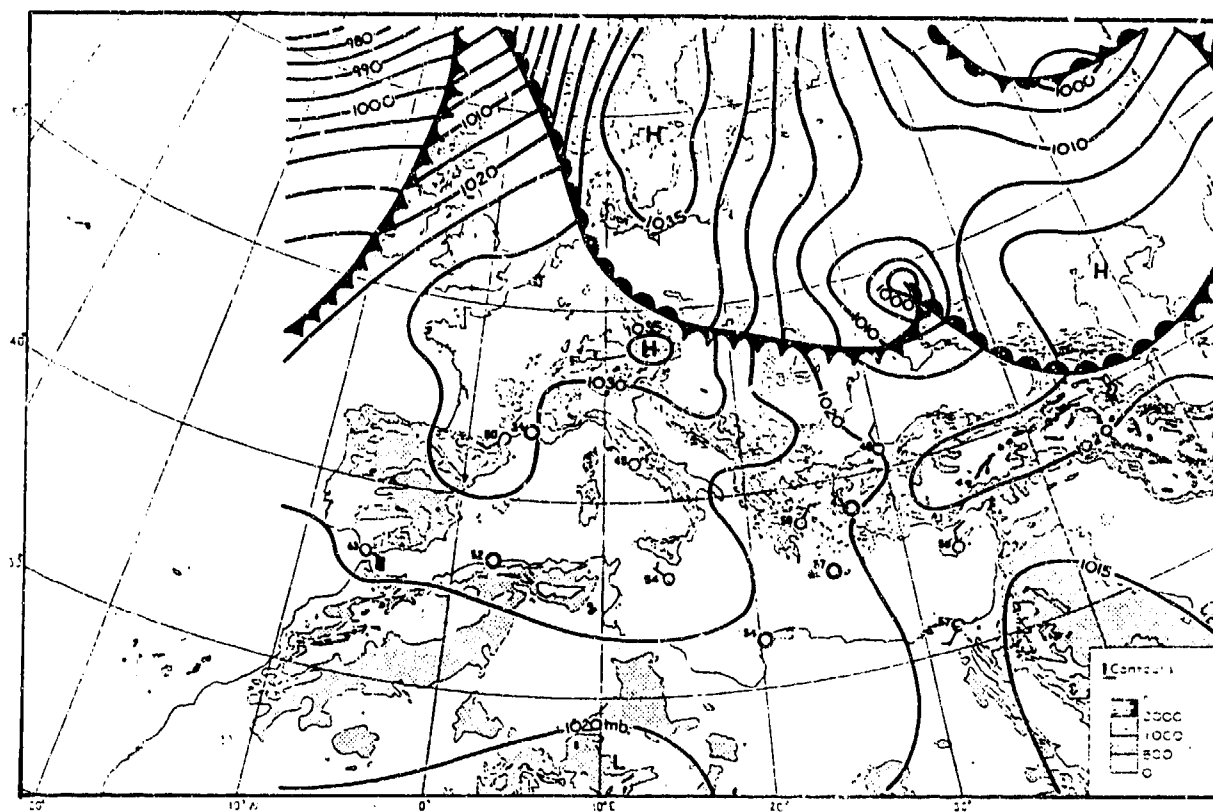


Figure 2-23a. Synoptic Surface Chart (16 November 1953, 0000Z), Cyprus Low. Pressures in millibars.

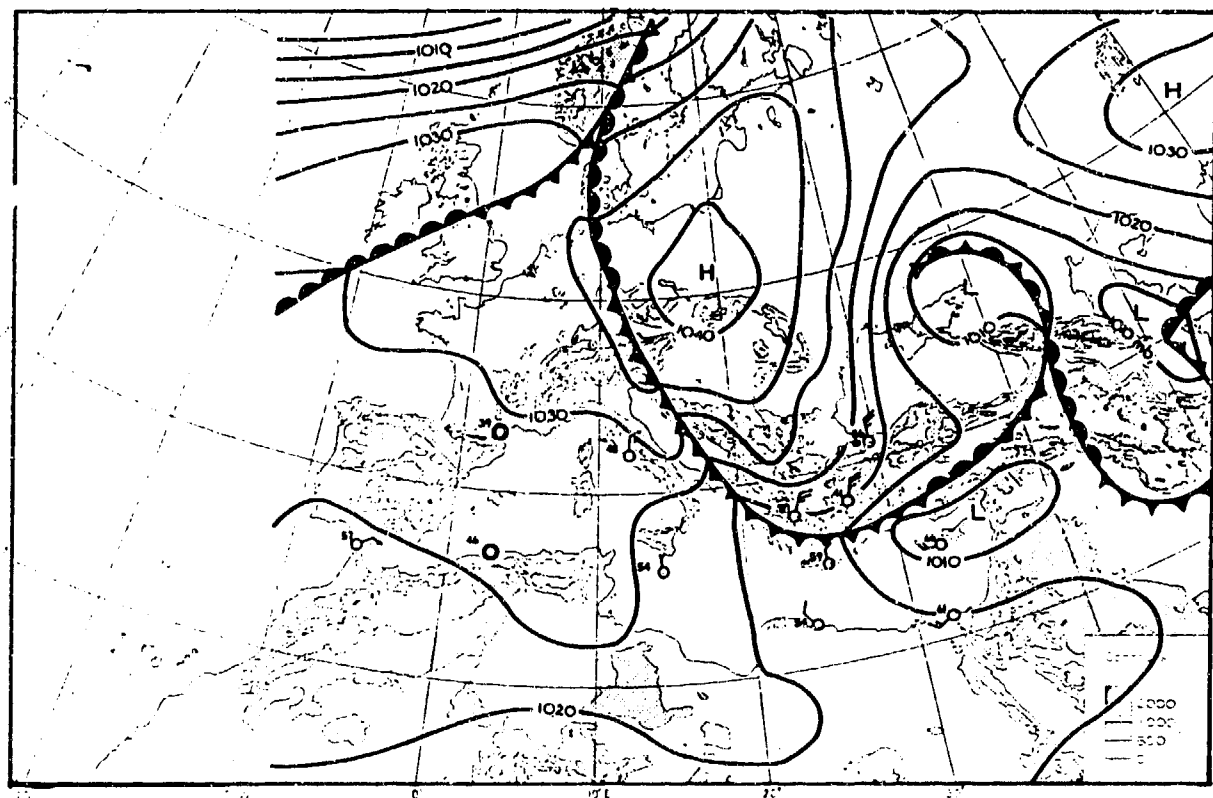


Figure 2-23b. Synoptic Surface Chart (17 November 1953, 0000Z), Cyprus Low. Pressures in millibars.

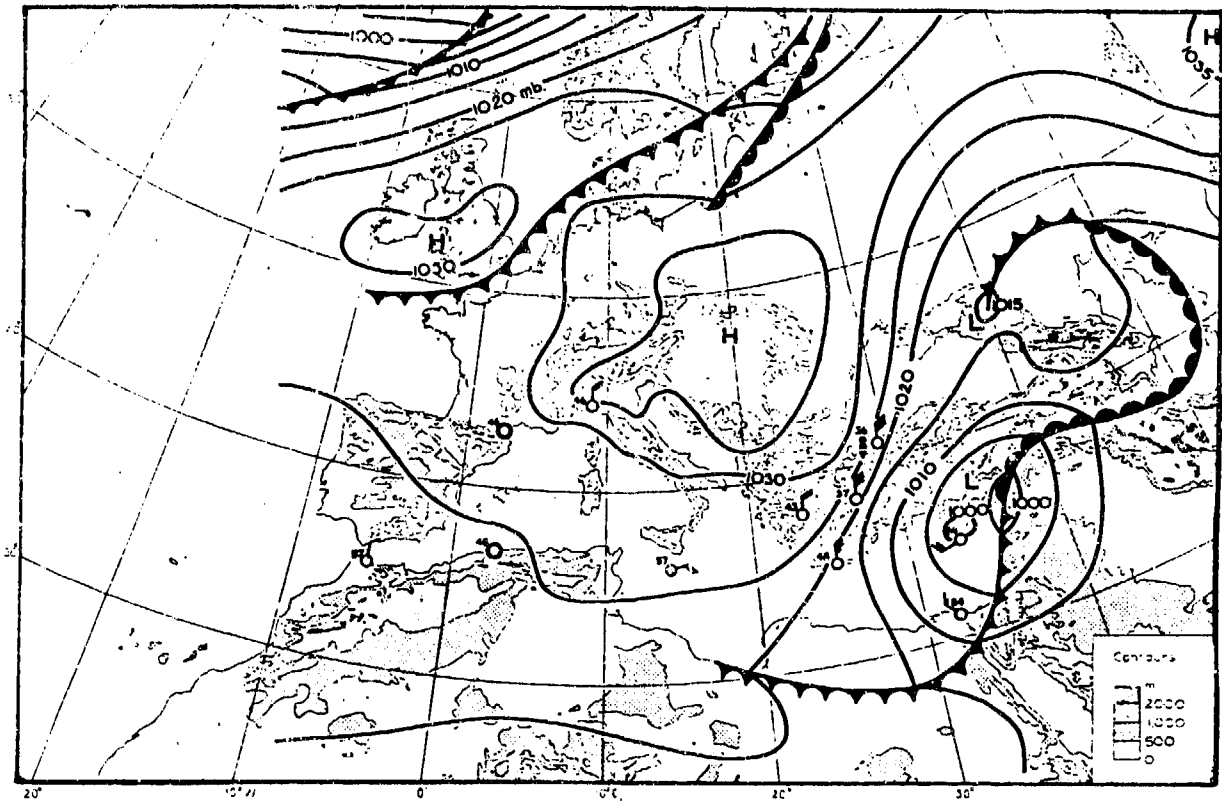


Figure 2-23c. Synoptic Surface Chart (18 November 1953, 0000Z), Cyprus Low. Pressures in millibars.

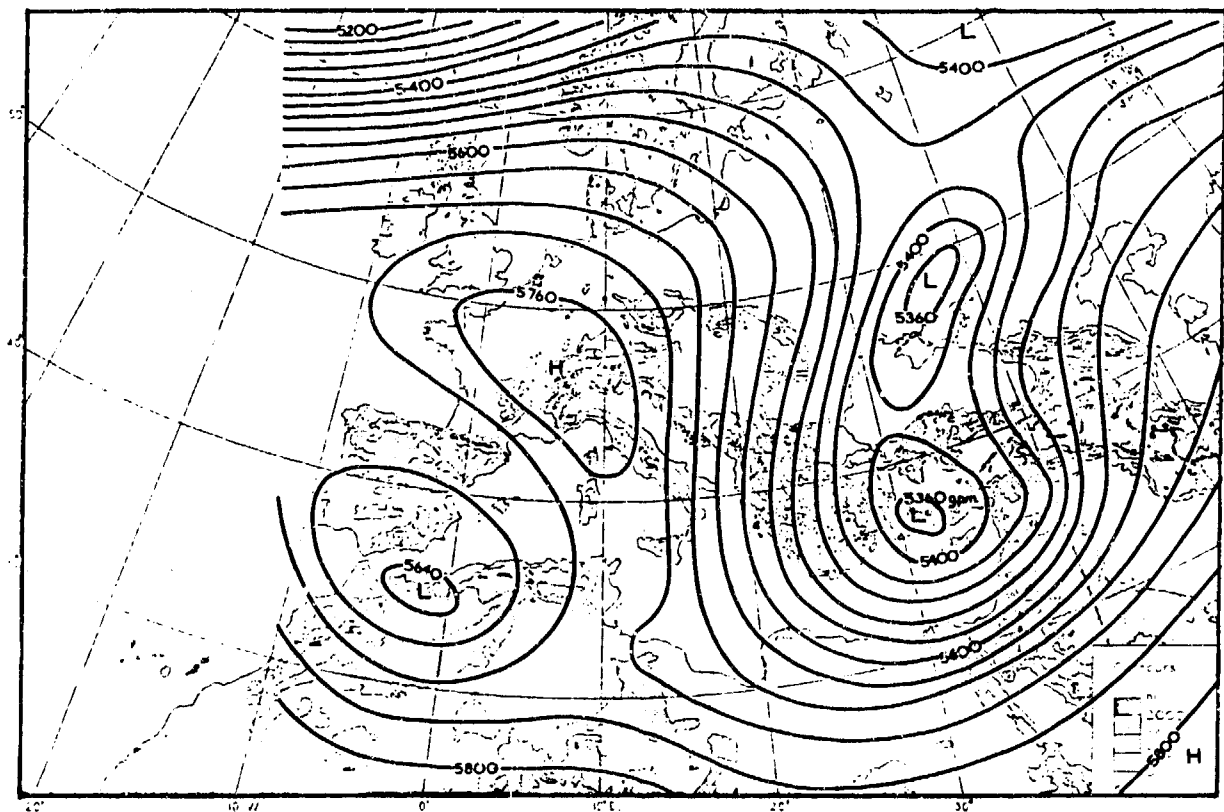


Figure 2-23d. 500-mb Flow (18 November 1953, 0300Z), Cyprus Low. Contours are in geopotential meters (gpm).

A thunderstorm outbreak with significant rainfall requires cold air between 700 and 500 mb, usually 15 to 18° F (8-10° C) colder than the environment. Occasionally, very cold polar troughs penetrate the eastern Mediterranean Sea with moist low-level support. Warm Saharan surface air advected ahead of the cold front creates favorable conditions for Cyprus Low development and severe thunderstorm activity. Significant positive vorticity advection is required to

trigger the development, otherwise only light, short-lived showers occur.

For the rare heavy rainfall or snowfall to occur, strong mid- and upper-level troughs must accompany the surface low. Figures 2-24a through d show two different Cyprus Lows in the eastern Mediterranean Sea; the rare heavy rainfall event is only produced by the synoptic patterns in Figures 2-24c and d.

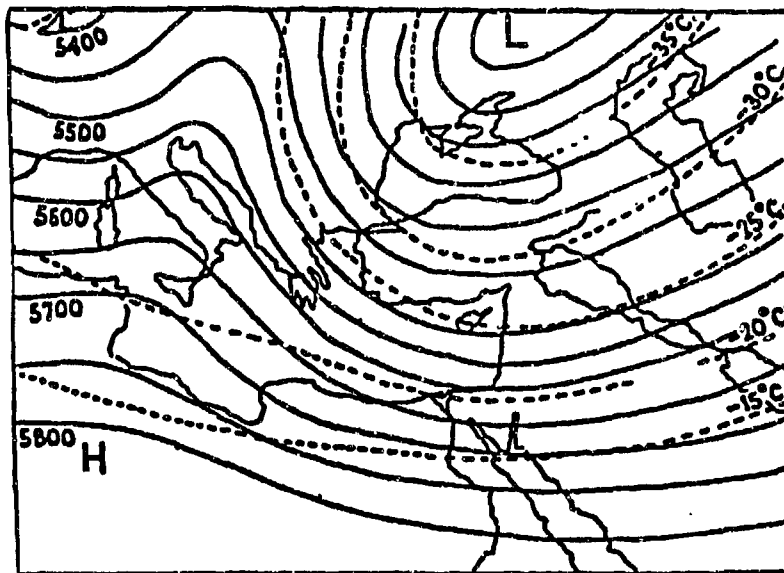


Figure 2-24a. 500-mb Contour Chart Over a Cyprus Low With No Severe Thunderstorms or Heavy Precipitation. Dashed lines are isotherms (C) at 5-degree intervals; solid lines are geopotential height (gpm) at 50-meter intervals.

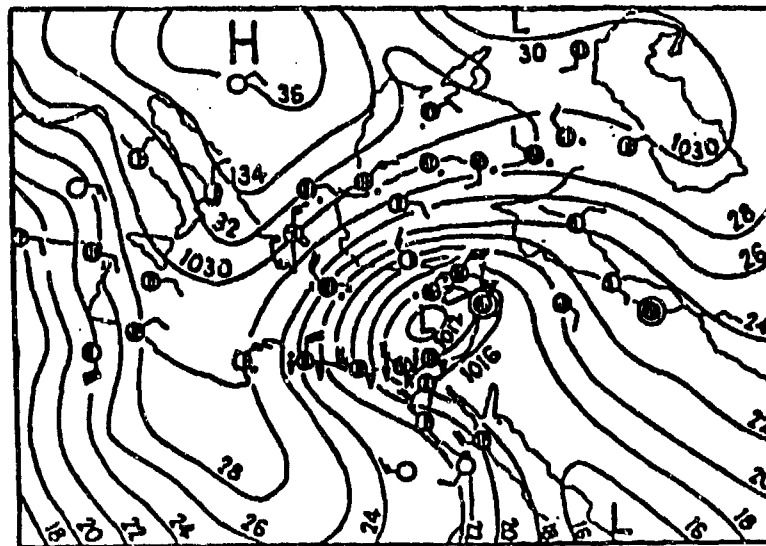


Figure 2-24b. Surface Chart Depicting Cyprus Low Position Beneath a Weak Mid-Level Trough With No Severe Thunderstorms or Heavy Precipitation. Solid lines are surface pressure isobars at 2-mb intervals. Arrow shows system movement.

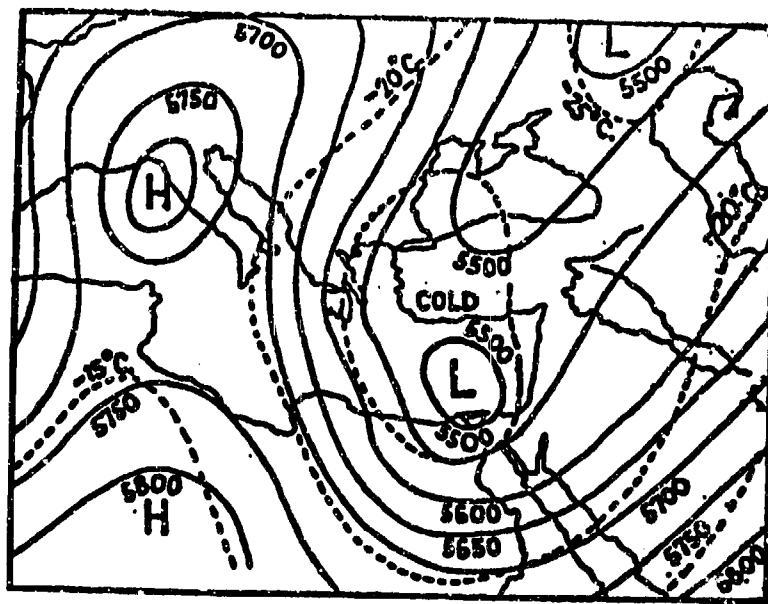


Figure 2-24c. 500-mb Contour Chart Over an Intense Cyprus Low With Severe Thunderstorms and Heavy Precipitation. Dashed lines are isotherms (C) at 5-degree intervals; solid lines are geopotential height (gpm) at 50-meter intervals.

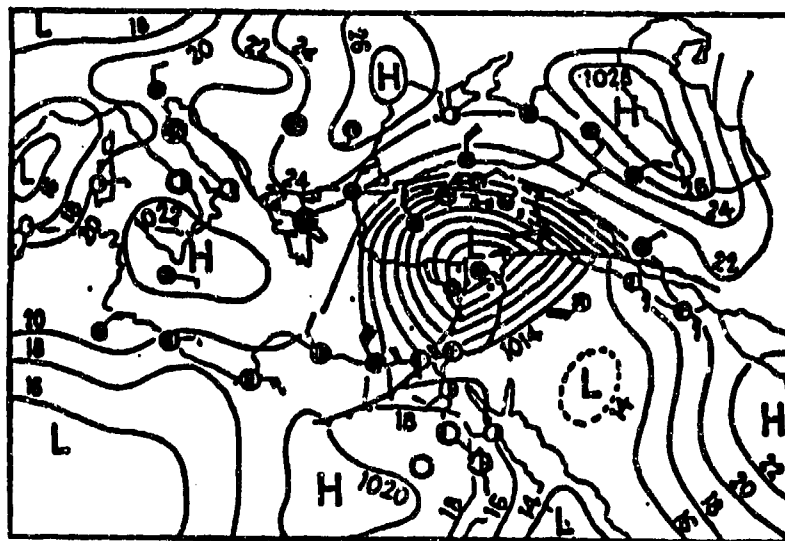


Figure 2-24d. Surface Chart Depicting Cyprus Low Position Beneath a Strong Mid-Level Trough With Severe Thunderstorms and Heavy Precipitation. Solid lines are surface pressure isobars at 2-mb intervals. Arrow shows system movement. Snow occurs when this synoptic pattern is supplemented by extremely cold low- and mid-level Asiatic air advection into the back of the primary low (see Figure 2-3). Although such events are rare (the average is one every 5 years), they can occur in any given winter when synoptic conditions are favorable. The snow in these events falls over the eastern Mediterranean coastal plain and in the hills and mountains behind the primary cold front. Amounts at elevations above 500 feet (150 meters) MSL can be significant; Jerusalem got nearly 10 inches during a March 1960 storm.

STORM TRACKS. From May to October, mid-latitude storms are very rare in the Mediterranean Sea. The mean November storm tracks shown in Figure 2-25a reflect the southward movement of the Polar Jet. Figure 2-25b shows the December-February storm tracks as they affect the eastern Mediterranean Sea. Figure 2-25c shows the storm tracks that affect the region in March and April. Leaside troughing along the Atlas Mountains initiates Atlas Low cyclogenesis inland over northwest Africa.



Figure 2-25a. Primary (solid arrow) and Secondary (dashed arrow) Mid-Latitude Storm Tracks, November. Most November cyclones affecting the region are Genoa Lows that move ENE across southern Europe. Most November cyclonic activity in the eastern Mediterranean Sea involves secondary cyclogenesis along active Genoa Low cold fronts.



Figure 2-25b. Primary (solid arrow) and Secondary (dashed arrow) Mid-Latitude Storm Tracks, December, January, and February. Genoa and Cyprus Lows are the main sources of cyclonic activity. Primary tracks (solid arrows) pass through the Gulf of Genoa and eastern Mediterranean basin. The secondary track (dashed line) is for Atlas Lows.

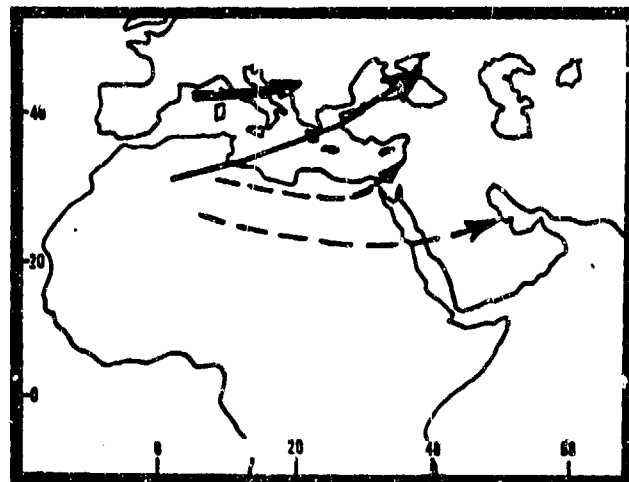


Figure 2-25c. Primary (solid arrow) and Secondary (dashed arrow) Mid-Latitude Storm Tracks, March and April. Atlas Lows produce the majority of significant spring weather. Genoa Lows can also develop in the Bay of Biscay along northern Spain and western France, but these move ENE across southern Europe.

AFRICAN WAVES originate over southern Chad/Sudan at the 700-mb level between 10° and 15° N from May to October. The trough is usually tilted slightly--see Figure 2-26. These waves move from east to west at 10-15 knots. Successive waves can develop every 2 to 5 days, from 1,200 to 2,200 NM apart. Much controversy still surrounds wave genesis over Southern Chad/Sudan, but apparently the MTEJ creates a shearing environment, assisted by positive vorticity and latent heat release.

Very little weather is associated with these disturbances before late June. Since moisture is limited, weak troughs seldom produce more than an increase in mid-level cloud cover. In the weaker troughs, mid-level winds are lighter than surface winds; convergence, cloud cover, and precipitation are on the east side of the trough.

By late July, the surface Monsoon Trough moves to near 20° N, bringing more moisture into southern Chad/Sudan. The MTEJ is also well-established, increasing the likelihood for increased cloud development and rainfall on the west, rather than on the east, side of the trough. Slight increases in surface wind speeds significantly increase convective development. Wind speeds of 40 knots have been observed.

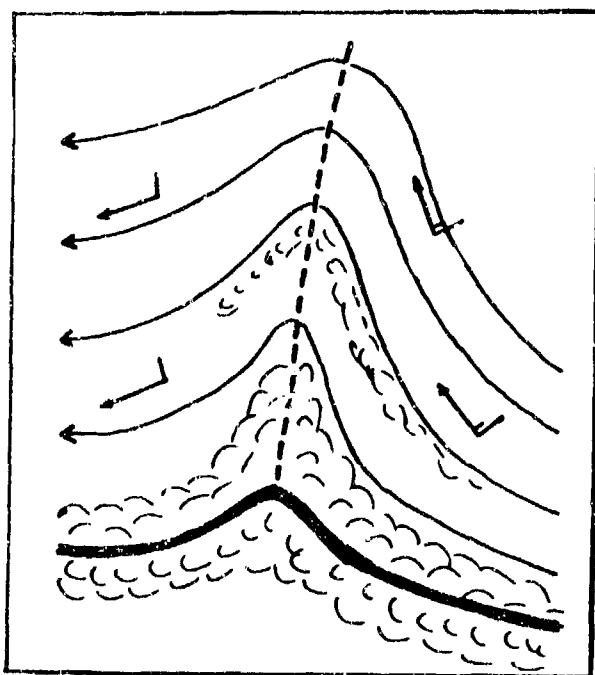


Figure 2-26. Basic Cloud and Wind Pattern with a Tropical Wave (from Leroux, 1983). The trough axis is shown by a dashed line. The solid line represents the 700-mb position of the ITD. Wind speeds are in knots.

TROPICAL SQUALL LINES develop in southern Chad/Sudan during the summer and move westward at 20-30 knots. The leading edge is often a sharply defined, north-south arc that contains convective cells in various stages of growth; there are multiple outflow boundaries. The cirrus outflow merges into a solid shield. Three synoptic conditions are necessary for tropical squall line development. They are (from Fortune, 1980):

- Shear and instability along the Intertropical Discontinuity (ITD)
- The Monsoon Trough, which supplies large amounts of moisture, is located between 15° and 20° N
- Convergence is occurring through a deep layer of the mid-troposphere.

The tropical squall line is strictly a summertime phenomenon south of 16° N. There are two main differences between tropical squall lines and those of the mid-latitude type: (1) the anvil cloud extends behind (east) of the squall lines--not in front, and (2) new convective squall lines develop to the *west* of the outflow boundary.

Intense downdrafts and outflow boundaries can occur beneath individual convective cells. Cold downdrafts cause rapid temperature decreases and can raise large amounts of dust and sand into the air; visibilities can be reduced to less than 1/2 mile. Brief and intense rainfall is common, but coverage is extremely variable. Downdraft speeds average 20 to 30 knots over flat terrain, increasing to 40 knots in the Marrah Mountains of west-central Sudan.

In northeastern Chad, experienced American meteorologists have observed squall line gusts in excess of 50 knots with near-zero visibilities caused by dust and sand. Strong north-south outflow boundaries vary from 5 to 150 NM in length.

Figure 2-27 shows a possible formation sequence of an African squall line. A common source is near Lake Chad, where additional moisture is available and where easterly flow is channeled between the Tibesti and Marrah Mountains.

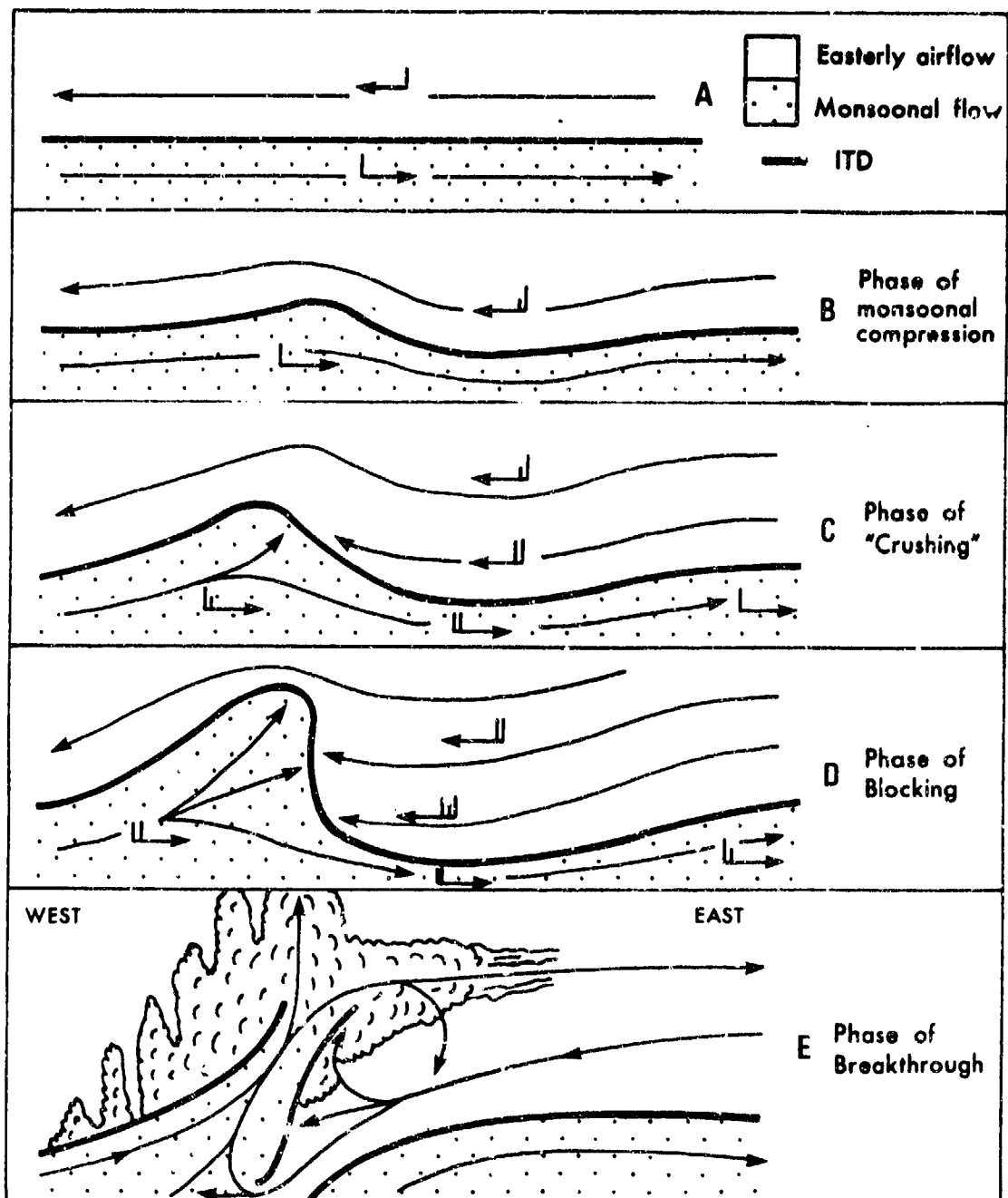


Figure 2-27. Formation of an African Squall Line (vertical cross-section) (from Hayward, 1987). The sequence of diagrams from A to E depict the development of an African squall line south of the surface Monsoon Trough. Shearing along the ITD creates waves along the boundary. The blocking phase can be reached in the presence of an active MTEJ. The easterly flow is forced to spread to the north and south, leading to the actual thunderstorm line--a north-south arc--when the mid-level flow breaks through the ITD and reaches the surface. Westerly flow is forced aloft, producing heavy rain and thunderstorms. Easterly flow drives the storms west.

MESOSCALE AND LOCAL EFFECTS

LAND/SEA BREEZE. Differential surface heating along coasts generates this diurnal phenomenon. The marine boundary layer rarely extends above 3,000 feet (915 meters) AGL or beyond 15 NM inland unless augmented by synoptic flow; then it may reach 5,000 feet (1,525 meters) and extend up to 80 NM inland. In general, sea breeze penetration reaches a maximum by mid-afternoon. Nighttime land-sea temperature differences are normally smaller; wind speeds are lower and maximum offshore penetration is limited to 5 NM. Sea breezes average 8-14 knots; land breezes average 4-8 knots. Two types of land/sea breezes are found along the Mediterranean Coast: "common" and "frontal".

"Common" land/sea breezes affect all coastal areas of the Mediterranean and Aegean Seas. Figure 2-28 illustrates the "common" land/sea breeze circulation under calm conditions with no topographic influences and a uniform coastline. Onshore (A) and offshore (B) flow intensifies in proportion to daily heat exchanges between land and water. Common land/sea breezes normally reverse at dawn and dusk.

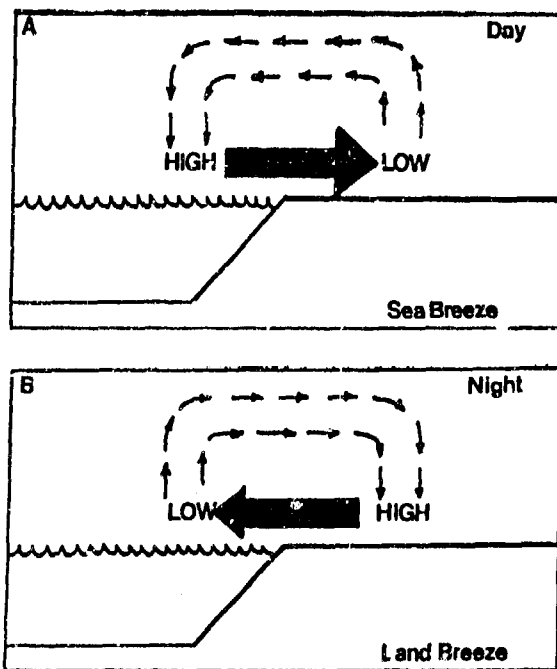


Figure 2-28. The "Common" Daytime Sea Breeze (A) and Nighttime Land Breeze (B). Thick arrows represent pressure gradient and direction of flow.

"Frontal" land/sea breezes are the product of the "front" between land and sea air masses. The transition for wind reversal is delayed by 1 to 4 hours as gradient flow prevents the sea breeze boundary layer or "front" from moving ashore. Figure 2-29a-f shows a typical "frontal" land/sea breeze sequence. Solid blocks denote the land surface, while dashed lines represent water. Vertical lines show the sea breeze boundary layer and arrows represent wind circulation.



Figure 2-29a. Gradient Flow With Offshore Wind Component Slopes Gently Over Dense, Cooler Marine Boundary Layer. Shearing action along the "front", or land-sea air mass interface, compacts the layer. Gradient flow strength determines the magnitude of compacting.

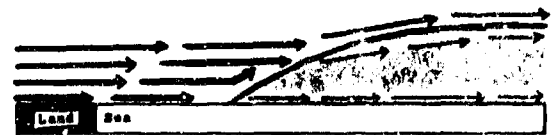


Figure 2-29b. Increased Compacting Tightens Pressure Gradient Along Land-Sea Interface. If the gradient is weak, land surfaces heat rapidly. As a result, the surface pressure gradient and winds resemble those in Figure 2-29a.



Figure 2-29c. Maximum Compacting of the Marine Boundary Layer. At this instant, the surface winds inside the marine boundary layer show onshore direction. The marine layer surface flow may take several hours to reach the coast. Momentum accelerates wind speed with time.

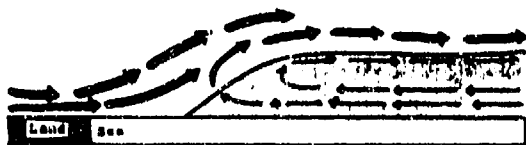


Figure 2-29d. Frontal Sea Breeze Accelerates Towards Shore. Initial "frontal" sea breezes may sustain 20-knot winds for 15-45 minutes.

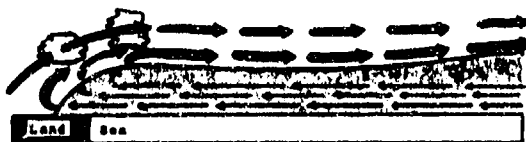


Figure 2-29e. Sea Breeze "Front" Reaches the Coast. Note the increased depth of onshore flow in the marine boundary layer. Compare with Figure 2-29c.

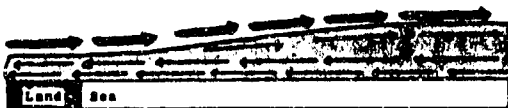


Figure 2-29f. Land/Sea Breeze Mechanism in Full Swing. Offshore flow aloft, onshore flow at surface.

The synoptic flow causes directional variations of 10-45 degrees and can increase or decrease wind speeds. With weak synoptic flow, the sea breeze triggers shallow cumulus along the coast by late afternoon. Shoreline configuration and topography can trigger orographic lifting, cloudiness, and precipitation under otherwise

stable conditions. The Nafusah and Akhdar Mountains of Libya are prime locations for sea-breeze cumulus development regardless of the strength of synoptic flow.

Early morning stratus and stratocumulus often develop along the Libyan and Egyptian coastlines during the land-sea breeze transition between 0700 and 0900 LST. Cool air is produced through radiative cooling over land. After midnight, the land breeze pushes the cooler air over the warmer water, and stratus forms by condensation. Stratus and stratocumulus seldom form above 5,000 feet (1,525 meters) or below 2,000 feet (610 meters). When the sea breeze develops at roughly 0800 LST, weak onshore flow moves the stratus and stratocumulus over the coast. The stratus averages 500 feet (150 meters) thick and quickly burns off over land by 1000 LST.

MARINE INVERSIONS separate the marine boundary layer from the warmer, drier air aloft over the Mediterranean coast. The marine layer normally extends 5 to 20 NM inland, but it can reach to 80 NM inland if supported by the synoptic flow. The marine boundary layer varies considerably in depth throughout the year. This is particularly evident in the relative humidities provided in Figures 2-30a-e for Mediterranean coastal stations. The marine air layer is cooler, moister, and stabler than the interior air masses, particularly along the desert coasts. The inversion is less pronounced during summer at Izmir, Turkey, where there is enough moisture to produce clouds, usually stratocumulus, but dry air aloft prevents any significant vertical development. In winter, the marine boundary layer is uniform throughout the region, extending above 5,000 feet (1,525 meters). The layer is very shallow during the summer with subsidence aloft.

FEET	JAN	FEB	MAR	APR	MAY	JUN	JUL	AUG	SEP	OCT	NOV	DEC
5,000	70	66	62	60	55	51	48	48	51	56	61	67
4,000	71	68	64	60	55	50	48	49	52	58	62	68
3,000	72	68	64	59	55	50	48	49	52	59	64	68
2,000	70	67	65	59	56	50	48	50	53	60	65	68
1,000	69	66	65	59	57	51	49	51	54	61	66	67

Figure 2-30a. Mean Monthly Relative Humidities for Izmir, Turkey.

FEET	JAN	FEB	MAR	APR	MAY	JUN	JUL	AUG	SEP	OCT	NOV	DEC
5,000	63	61	54	44	42	37	34	38	42	42	57	64
4,000	63	61	55	46	45	41	39	46	49	46	58	65
3,000	62	60	56	49	50	48	47	57	57	52	58	64
2,000	62	60	57	54	57	57	57	67	64	59	58	62
1,000	61	59	60	58	63	66	65	70	65	63	57	60

Figure 2-30b. Mean Monthly Relative Humidities for Beirut, Lebanon.

FEET	JAN	FEB	MAR	APR	MAY	JUN	JUL	AUG	SEP	OCT	NOV	DEC
5,000	62	58	52	40	34	32	30	32	36	47	56	62
4,000	64	59	55	44	37	36	35	39	45	52	57	63
3,000	64	60	58	48	43	43	46	52	58	57	58	64
2,000	62	60	60	53	52	55	60	66	68	62	58	63
1,000	61	61	61	58	61	65	69	72	71	66	59	63

Figure 2-30c. Mean Monthly Relative Humidities for Bet Dagan, Israel.

FEET	JAN	FEB	MAR	APR	MAY	JUN	JUL	AUG	SEP	OCT	NOV	DEC
5,000	59	52	49	41	36	36	36	38	42	49	56	60
4,000	60	54	51	43	39	38	39	41	46	53	58	62
3,000	60	56	53	47	42	42	44	47	52	58	59	63
2,000	60	58	56	52	48	43	52	55	58	61	61	62
1,000	59	60	60	58	58	58	64	65	64	63	61	61

Figure 2-30d. Mean Monthly Relative Humidities for Matruh, Egypt.

FEET	JAN	FEB	MAR	APR	MAY	JUN	JUL	AUG	SEP	OCT	NOV	DEC
5,000	63	56	48	38	32	32	35	38	44	51	57	62
4,000	66	58	51	41	34	35	40	42	47	53	60	63
3,000	68	61	54	45	38	40	46	48	52	55	60	64
2,000	67	62	57	51	44	47	52	56	58	57	61	64
1,000	67	63	59	54	50	55	60	62	60	59	61	65

Figure 2-30e. Mean Monthly Relative Humidities for Banghazi, Libya. The reporting station is 25 NM inland.

MOUNTAIN/VALLEY WINDS develop with fair skies and light and variable synoptic flow. They are common in the Turkish Taurus Mountains, the Jordan Rift Valley, the Nafusah and Akhdar Mountains in northern Libya, the Tibesti Mountains in northern Chad, and the Marrah Mountains and Ethiopian Highland foothills of Sudan. There are two types of terrain-induced winds: the mesoscale mountain/valley wind, and the localized, microscale "slope" (upslope/downslope) wind. The key differences lie in the temporal and spatial scales.

Mesoscale Mountain/Valley Winds average 6-12 knots. Daytime valley winds (Figure 2-31a) are strongest (10-15 knots) between 650 and 1,300 feet (200-400 meters) AGL. Nighttime mountain winds (Figure 2-31b) average only 3-7 knots at the same level. Deep valleys develop more nocturnal cloud cover than shallow valleys because nocturnal airflow convergence is stronger. The mesoscale-valley circulation has a maximum vertical extent of 6,560 feet (2,000 meters) AGL, depending on valley depth and width, the strength of prevailing winds in the mid-troposphere, and the breadth of microscale slope winds.

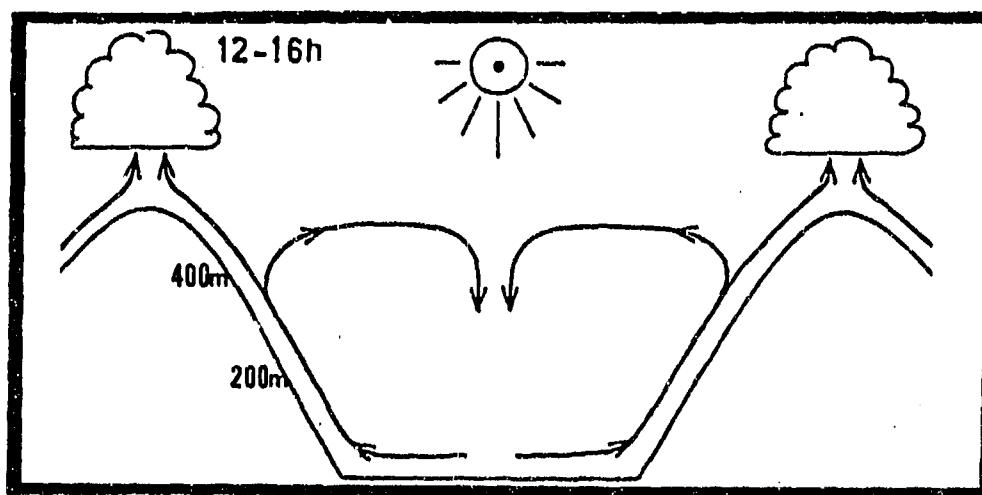


Figure 2-31a. Typical Daytime Mountain/Valley Circulation (from Flohn, 1969).

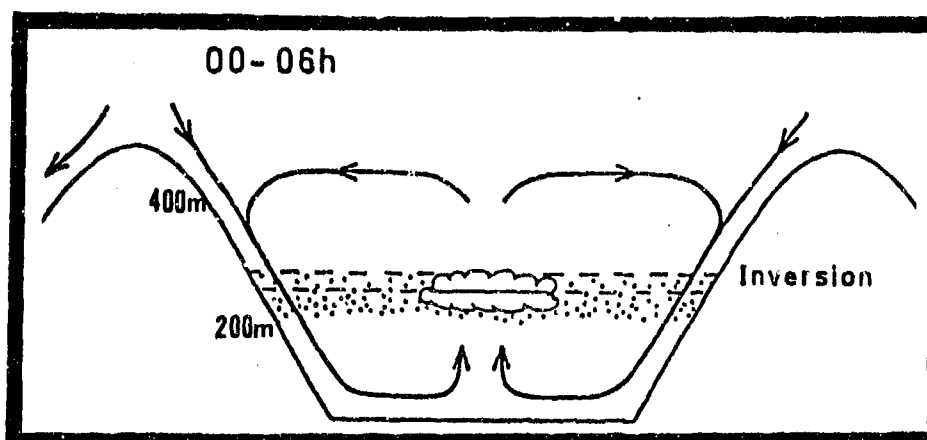


Figure 2-31b. Typical Nighttime Mountain/Valley Circulation (from Flohn, 1969).

Microscale Slope Winds develop along the surface boundary layer (0-500 feet/ 0-150 meters AGL) of mountains and large hills. Mean daytime upslope wind speeds are 6-8 knots; mean nighttime downslope speeds are 4-6 knots. These speeds are found at elevations no higher than 130 feet (40 meters) AGL. Downslope mountain winds are strongest between November and March, while upslope valley winds are strongest between April and October. Upslope winds are strongest on slopes with southerly exposures. Figures 2-32a-h (from Geiger, 1961) show the life cycle of a typical mountain/valley wind circulation. The light arrows represent microscale circulation; the dark arrows, mesoscale circulation.

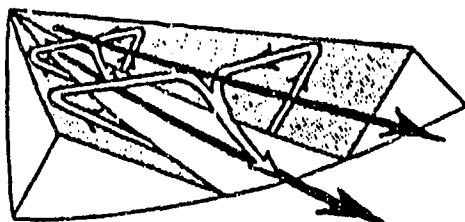


Figure 2-32a. SUNRISE. Sunshine almost immediately generates upslope wind development, but the downslope mountain wind persists as mesoscale flow overrides microscale flow. Generally the transition between Figures 2-32a and b occurs between 0700 and 1000 LST, but local terrain determines how soon sunlight can start the microscale upslope wind, which is not fully developed until the entire valley surface is heated enough to stop the mesoscale downslope mountain wind.

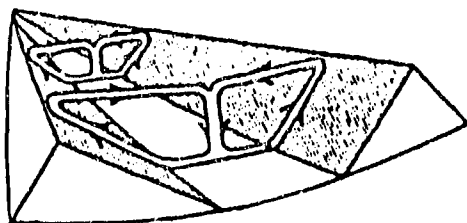


Figure 2-32b. MORNING. Widespread surface heating continues to generate microscale upslope flow, cutting off any downslope mountain circulation.

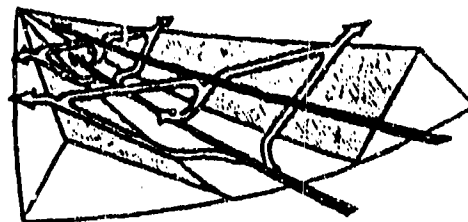


Figure 2-32c. MIDDAY. Sunshine covers the entire valley floor, and upslope flow feeds the valley circulation.

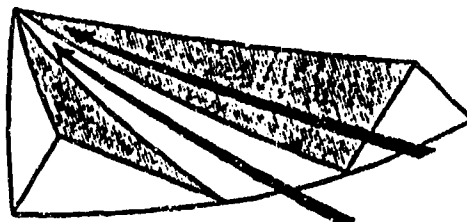


Figure 2-32d. LATE AFTERNOON. East-facing slopes begin to cool; upslope flow weakens.

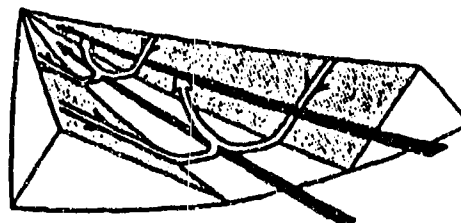


Figure 2-32e. SUNSET. Although microscale downslope wind components dominate the surface boundary layer, mesoscale upslope valley flow retains weak momentum.

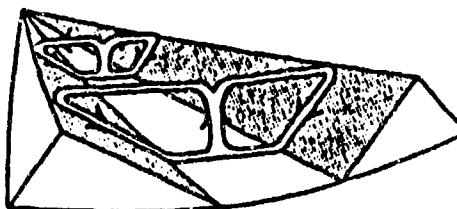


Figure 2-32f. EVENING. Downslope winds dominate.

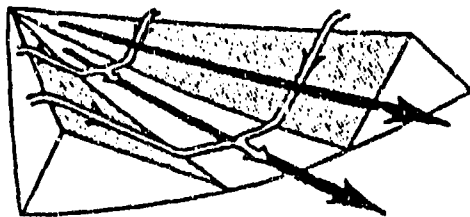


Figure 2-32g. **MIDNIGHT.** Downslope winds feed the mountain circulation.

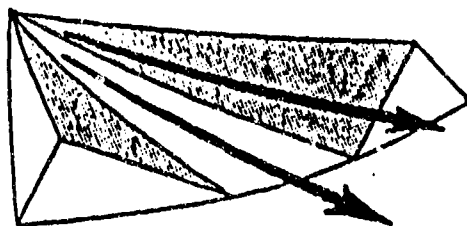


Figure 2-32h. **PRE-DAWN.** Winds are calm just before surface heating begins at the microscale; the mesoscale downslope mountain circulation retains its momentum. Microscale downslope winds end just before sunrise; upslope winds begin again at first light.

Orographic uplift may accentuate mesoscale mountain-valley convergence above 6,000-7,000 feet (1,830-2,135 meters), producing short-lived convective cells. Mountain winds and land breezes flow in the same direction and work together where ranges such as the Akhdar Mountains parallel the coast. Valley winds and sea breezes can also combine to create higher wind

speeds than if only one wind system were present.

Mountain inversions develop when cold air builds up along wide valley floors where nighttime downslope wind convergence is weak. The cold air descends from the slopes, undercutting warmer air in the valley and forming an inversion. Moisture in the inversion layer often traps smoke, or produces fog and thin stratus.

MOUNTAIN WAVES develop when air at lower levels is forced up and over the windward sides of ridges; turbulence is usually moderate to severe. Mid- and upper-level troughs in the westerlies may produce mountain waves in the ranges rimming the Mediterranean Sea, as well as in the Tibesti Mountains in northern Chad. The Ethiopian Highland's western foothills and the Marrah Mountains may produce mountain wave turbulence during the summer with an MTEJ present. Criteria for mountain wave formation include sustained winds of 15-25 knots and flow within 30 degrees of perpendicular to the ridge.

Wavelength amplitude depends on wind speed and lapse rate above the ridge. Light winds follow the contour of the ridge with little displacement above and rapid damping beyond. Stronger winds displace air above the stable inversion layer; upward displacement of air can reach the tropopause. Downstream, the wave propagates an average distance of 50 times the ridge height. Lenticular clouds form in the lee waves. Rotor clouds form when there is a core of strong wind moving over the ridge, but only when the core does not exceed 1.5 times the ridge height. Turbulence in rotor clouds is strongest due to the sudden directional shear. Figure 2-33 shows a fully developed lee wave system.

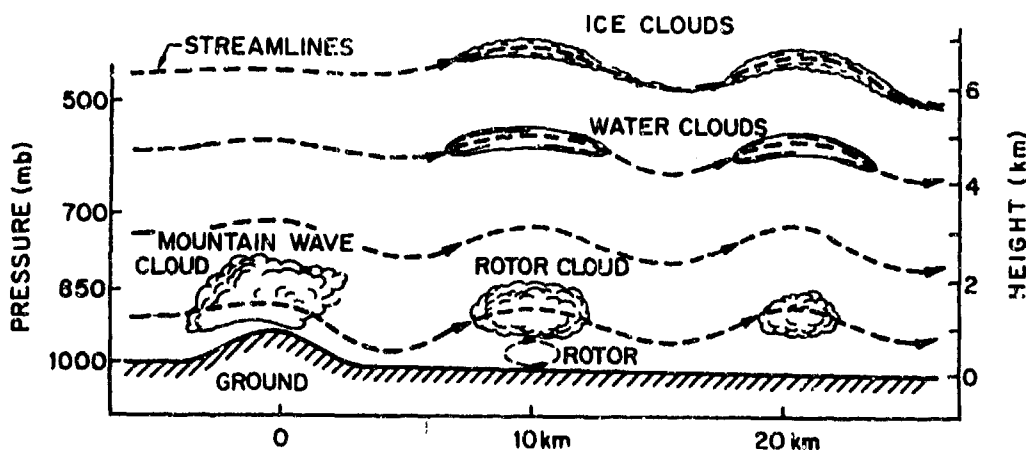


Figure 2-33. Fully Developed Lee Wave System (from Wallace and Hobbs, 1977).

DUSTSTORMS. Given the right conditions, duststorms are dominant features in and near the deserts of the region. Duststorms carry suspended particles over long distances, often reducing visibility to less than 30 feet (10 meters). Season of occurrence, wind direction, amount of particulate matter, and duration vary by locality. Large-scale duststorms often persist for 1 or 2 days before a frontal passage (such as with an Atlas or Cyprus Low), or with a synoptic-scale squall line. Mesoscale squall lines may reduce visibility to less than 1/2 mile for several minutes to an hour. Vehicles crossing the sand break through the crust easily; even light winds can raise dust. Sandstorms differ from duststorms only in the size of the suspended particles. Sand is seldom raised to more than 3-6 feet (1-2 meters) above the ground; particles settle quickly.

Dust devils are miniature tornados, but their wind speeds are not as high. They are set off by intense summer heating. Diameters range from 10 to 300 feet (3-91 meters). Dust devils move at about 10 knots and may last for 1 to 5 minutes. Visibilities are near zero in the vortex.

The origin and nature of duststorms depend upon general synoptic conditions, local surface conditions, and diurnal/seasonal considerations, as shown below.

Synoptic Conditions--

Active cold fronts. From November to April, duststorms may develop with frontal passages. Gusts of 15 to 20 knots are sufficient to lift dust and sand, but a pressure gradient of 6 to 8 mb/100 NM produces widespread duststorms. Strong fronts can increase the size of the area affected considerably, extending southward to include Chad and Sudan.

Convective activity. Convection produces local downdrafts that commonly reach 30 knots, while squall lines organize over a larger area to produce cloud bands up to 100 NM long and from 10 to 20 NM wide. Visibilities can be greatly reduced within minutes. Convection associated with the Monsoon Trough in southern Chad and Sudan frequently produces Haboobs (which see).

Stagnant Transitory High Surface Pressure. The Saharan and Saudi Arabian Highs normally strengthen over the subtropics during extended fair weather periods

between November and March. Only a 4- to 6-mb/100 NM surface pressure gradient is necessary to generate dust-laden surface winds. These highs can produce severe and widespread duststorm activity and are the most difficult to forecast. Although such situations are easy to recognize, precise locations (timing/areal extent) and severity are difficult to infer with so little data available. Stagnant air aloft provides little ventilation to remove the dust.

Local Surface Conditions--

Soil type and condition control the amount of particulate matter that can be raised into the atmosphere. Dry sand or silt, for example, is easily lifted by 10-15 knot winds. Haze is a persistent feature of the sandy deserts. The fine dust, sand, salt, or silt can be suspended for weeks and travel hundreds, even thousands, of miles from the source. Harmattan winds (which see) blow dust from the Sahara into southern Chad. On rare occasion, the particles can precipitate back to the surface as "mud rain." Strong frontal passages can reduce visibilities to near zero.

Seasonal Considerations--

October to March. Large areas of dust haze develop when there is subsidence aloft and a lack of turbulent mixing. Most duststorms develop along frontal boundaries. Synoptic scale winds of only 10-15 knots can lower visibility below 3 miles over 1,000 sq NM for up to 12 hours.

April to September. Convection produces most duststorms, but late-spring frontal systems, particularly Atlas Lows, can also produce them. Local visibilities below 3 miles occur in areas where the soil is dry.

Diurnal Considerations--

Daytime. The lowest visibilities occur around 0900 LST, shortly after the inversion breaks and turbulent surface mixing raises the dust. Distant tree tops can be visible at this time, but their bases are obscured by the dust haze. Daytime heating produces turbulent mixing in the lowest layers. Hot, dry winds transport dust aloft to the base of the large-scale subsidence inversion over the Sahara. Persistent dryness allows dust to reach 10,000 feet (3,050 meters) MSL, where it can remain suspended for days or weeks.

Nighttime. Cooler surface temperatures create stable conditions in the surface layer. Turbulent mixing is minimized; visibilities improve during the night and are best between 2000 and 0600 LST as the temperature inversion produces light surface winds. The dust settles beneath the inversion layer throughout the night; visibilities improve to 4-7 miles.

SAND STREETS. Vast longitudinal dune formations, about 1-1/4 NM apart, create localized wind circulations in western Libya, Egypt, and northern Chad. They parallel the mean wind direction. These dunes average 60 to 160 feet (20-50 meters) high and 330 feet (100 meters) wide. They vary from 1,000 feet (305 meters) to 100 NM long. Sand streets develop along the dune crest. The three-dimensional circulation pattern is shown in Figure 2-34.

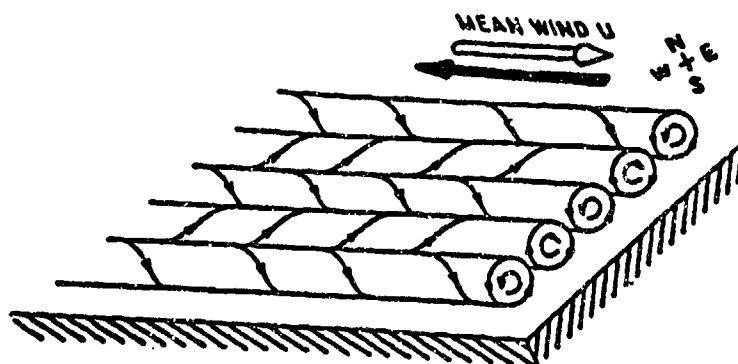


Figure 2-34. Three-Dimensional View of Longitudinal Vortices in the Boundary Layer (from Hanna, 1969). Southeast winds (dark arrow) may also develop roll vortices, but northwest flow (light arrow) is more common. The roll vortex diameter approximates the thickness of the boundary layer.

Figure 2-35 shows a cross-section of airflow over successive dunes. For sand streets to form, there should be little variation of wind direction with height, above average wind speeds, unstable lapse rates near the surface, and an inversion above the convective layer. Roll vortices, which parallel prevailing airflow, converge

over dune crests, producing clouds whenever enough moisture is present. Synoptic-scale streeting, however, requires large amounts of moisture to produce low-level clouds and is therefore rare. Only spring or fall frontal activity with rare surges of moist air ahead of the cold front produces low-level cloud streets.

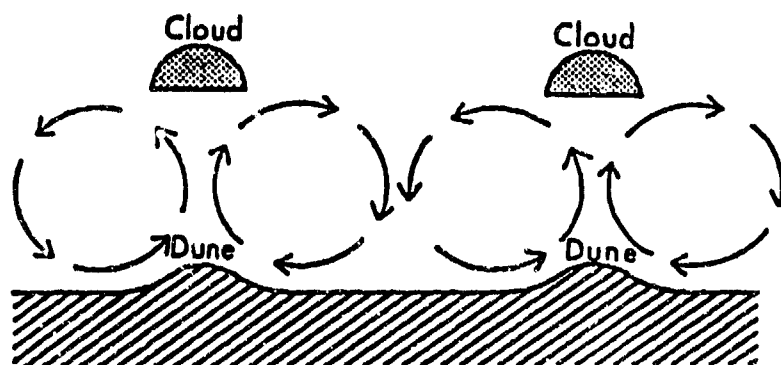


Figure 2-35. Cross-Sectional View of Dune and Cloud Formation Mechanism (from Hanna, 1969). Cloud formation is unlikely when boundary layer air is extremely dry.

WET-BULB GLOBE TEMPERATURE (WBGT) HEAT STRESS INDEX. The WBGT heat stress index provides values that can be used to calculate the effects of heat stress on individuals. WBGT is computed by using the formula:

$$\text{WBGT} = 0.7\text{WB} + 0.2\text{BG} + 0.1\text{DB}$$

where: WB = wet-bulb temperature
BG = Vernon black-globe temperature
DB = dry-bulb temperature

A complete description of the WBGT heat stress index and the apparatus used to derive it is given in Appendix A of TE MED 507, *Prevention, Treatment and Control of Heat Injury*, July 1980, published by the Army, Navy, and Air Force. The physical activity guidelines shown in Figure 2-36 are based on those used by the three services. Note that the wear of body armor or NBC gear adds 10° F to the WBGT, and activity should be adjusted accordingly.

Figures 2-37a-d give average maximum WBGTs for January, April, July, and October. For more information, see USAFETAC/TN-90/005, *Wet-Bulb Globe Temperature, A Global Climatology*.

WBGT (°F)	WATER REQUIREMENT	WORK/REST INTERVAL	ACTIVITY RESTRICTIONS
90-up	2 quarts/hour	20/40	Suspend all strenuous exercise.
88-90	1.5-2 quarts/hour	30/30	No heavy exercise for troops with less than 12 weeks hot weather training.
85-88	1-1.5 quarts/hour	45/15	No heavy exercise for unacclimated troops, no classes in sun, continue moderate training 3rd week.
82-85	.5-1 quart/hour	50/10	Use discretion in planning heavy exercise for unacclimated personnel.
75-82	.5 quart/hour	50/10	Caution: Extremely intense exertion may cause heat injury.

Figure 2-36. WBGT Heat Stress Index Activity Guidelines.

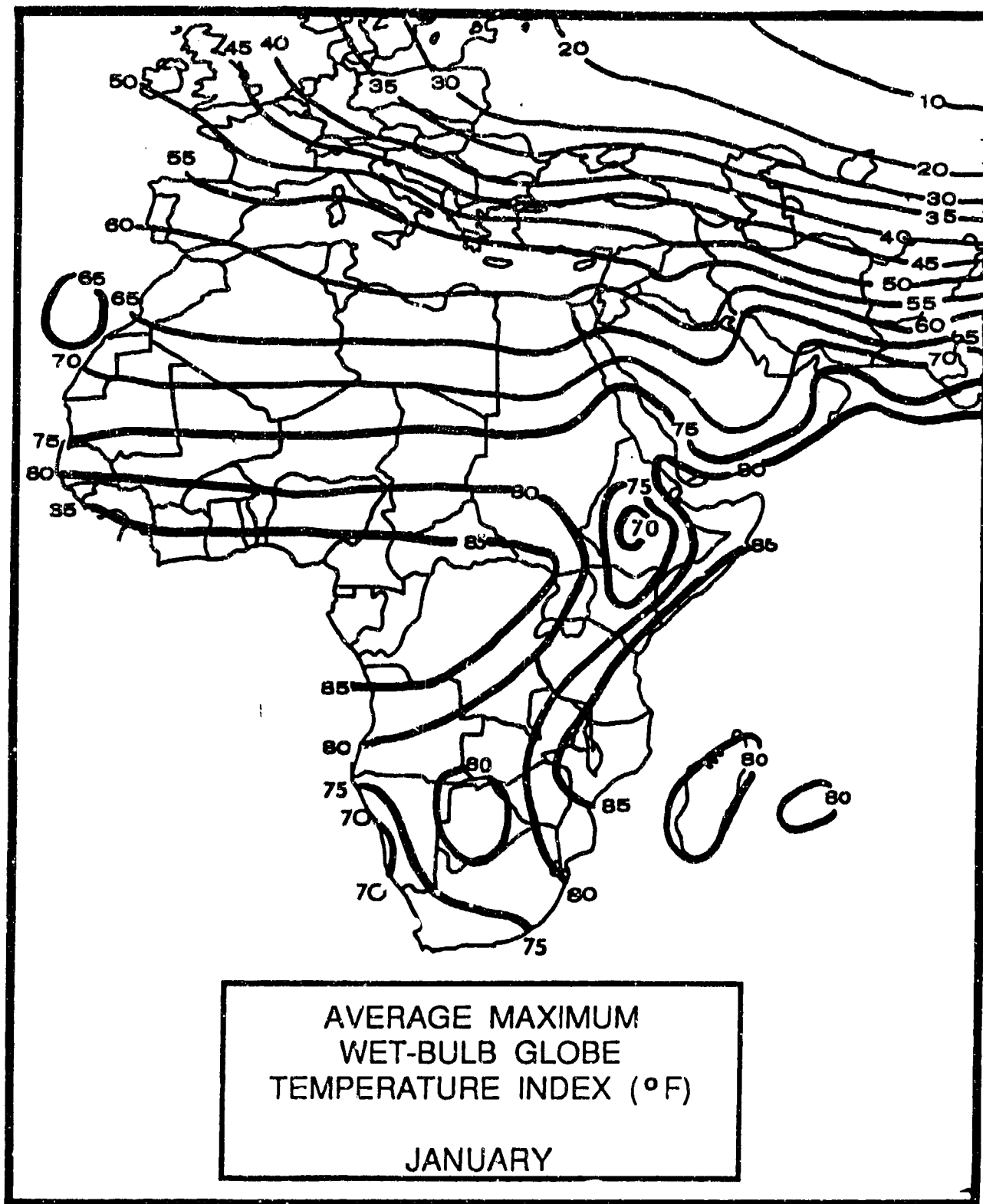


Figure 2-37a. Average Maximum WBGT--January.

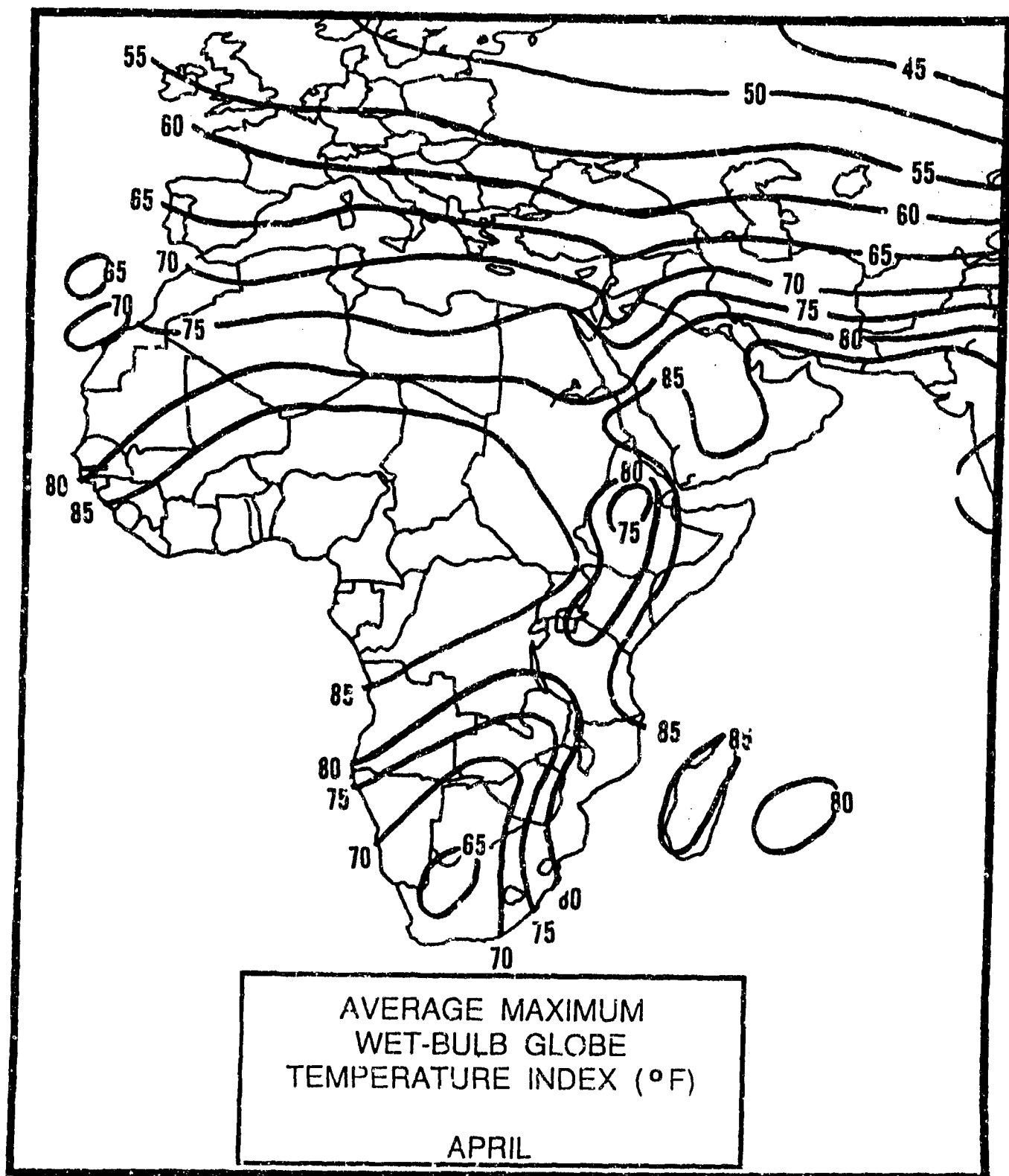


Figure 2-37b. Average Maximum WBGT--April.

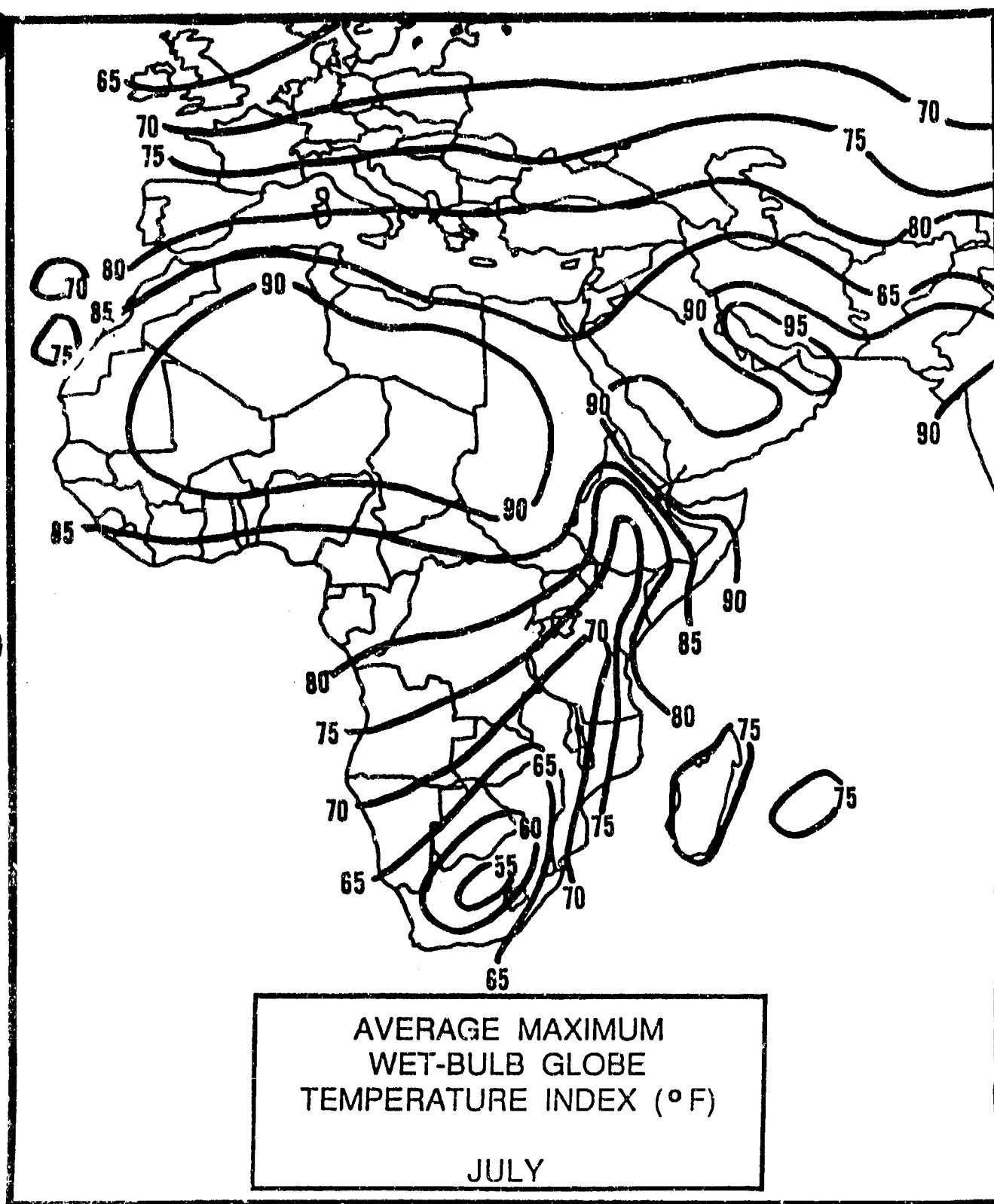


Figure 2-37c. Average Maximum WBGT--July.

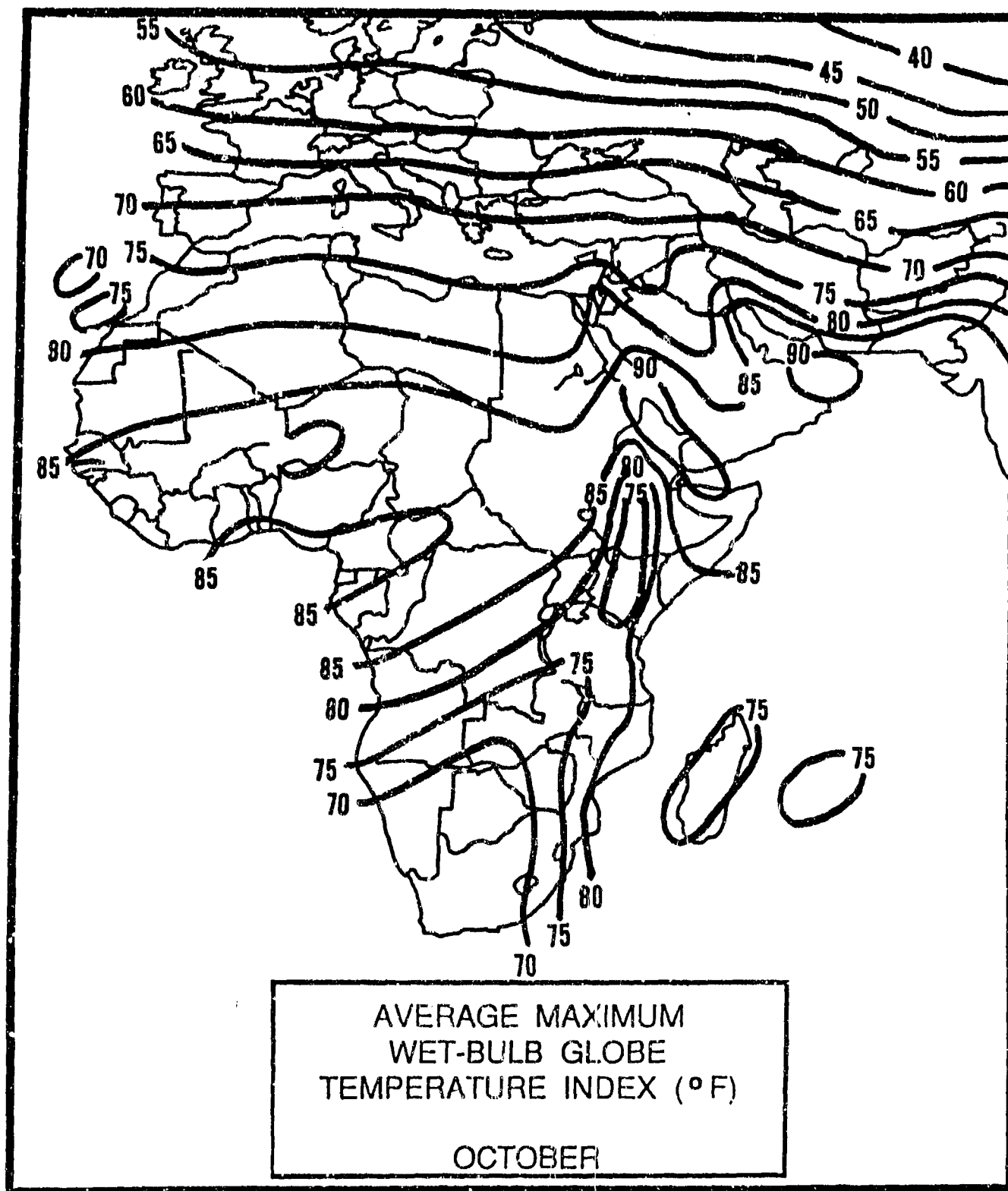


Figure 2-37d. Average Maximum WBGT--October.

REGIONAL WINDS

Local meteorologists and laymen commonly refer to certain surface winds by their local names rather than by the synoptic conditions causing them. These winds produce moderate to severe duststorms, low visibilities, and strong gusts over portions of the Mediterranean coast and Northeast Africa. They affect areas ranging in size from 500 to 100,000 sq NM. The following sections describe the most common local winds and their causes.

KHAMSIN. The Arabic word means "fifty," referring to the 50 days after Coptic Easter when this hot and dry southerly wind occurs. In Libya, the Khamsin is called the "Ghibli." The Sharav and Sirocco are similar meteorologically and are discussed later. Although they can occur anytime between February and June, Khamsins are most frequent during March and April. Khamsin conditions (hot, extremely dry southerly surface winds, low visibility, and thick dust) develop when Atlas Lows move eastward over the dry Sahara.

During intense Khamsin conditions, winds average 20-30 knots ahead of the front and 15-30 knots behind. Temperatures are normally 20° F (11° C) lower behind the front, and relative humidities rise from 10-15% to 25-30%. Khamsins last for 1 to 3 days, but slow-moving Atlas Lows may produce widespread dust conditions that persist up to 10 days.

Khamsin visibilities are 1/4 to 3 miles; they vary both diurnally and seasonally. Turbulent mixing keeps visibilities low in the daytime. Duststorms restrict visibilities for 5-8 hours, usually until several hours after sunset, when rapid cooling at the surface forms a radiation inversion that caps airborne dust. Visibilities improve to 3-6 miles. Wind speeds of more than 30 knots prevent formation of the inversion. Winter Khamsin duststorms are less severe than in the spring or early summer.

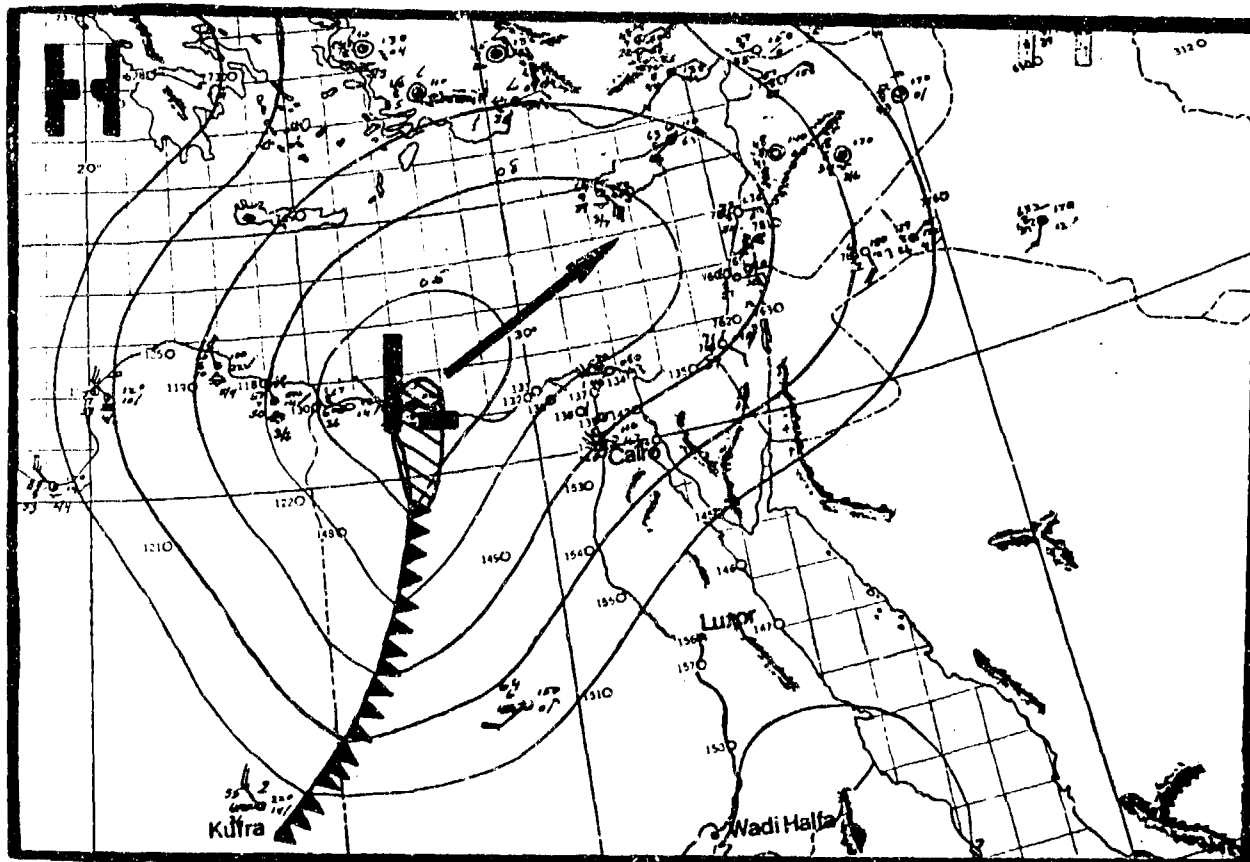


Figure 2-38. Typical Low-Pressure System Track Creating Khamsin Conditions. "True" Khamsin conditions are shown as hatched oval-shaped area.

"True" Khamsin conditions occur within an elongated oval area located parallel to the cold front (the hatched area under the low in Figure 2-38). Egyptian meteorologists define a "true" Khamsin as "any low-pressure system that approaches Cairo, Egypt, from the west or southwest producing 15 to 25 knot southeasterly surface winds." These winds are always hot and extremely dry. The northwesterly flow behind the front also produces widespread duststorm activity; this is not a "true" Khamsin, but locals will probably use the term to describe it anyway.

Deep, slow-moving Atlas Lows moving eastward over the central Sahara (Figure 2-39) produce "embedded" Khamsin conditions. In the hatched areas, there is widespread dust and 3- to 6-mile visibilities, but soil conditions determine the actual size of the affected area. Dust is normally less severe to the north of the low-pressure system. If the Atlas Low turns northeastward at 30° E, southeasterlies intensify Khamsin conditions along the Nile River Valley between Luxor and Wadi Halfa.

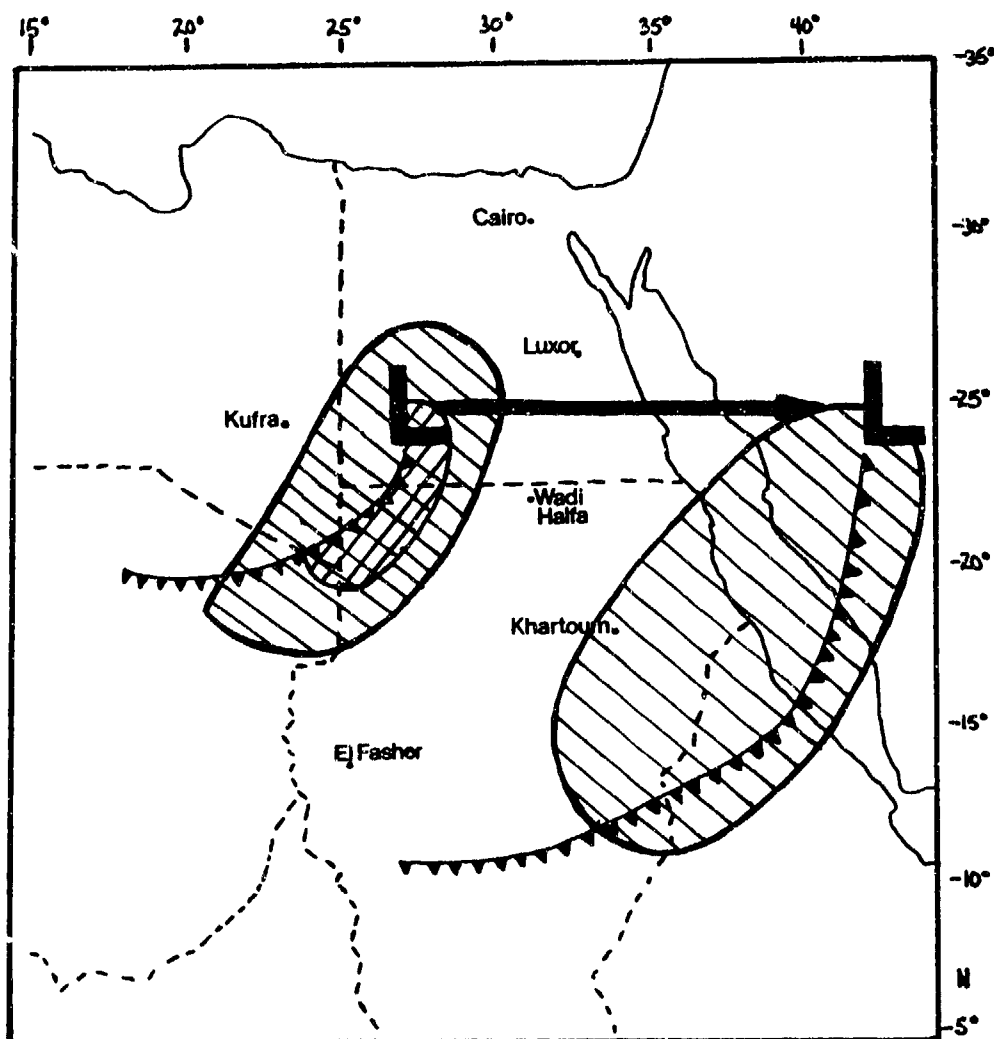


Figure 2-39. Khamsin-Type Conditions Associated With a Rare Eastward-Moving Atlas Low. Cross-hatched zone represents "true" Khamsin conditions; hatched areas denote widespread duststorm activity.

SHARAV. This is a hot, dry, and dusty wind that occurs with lows over the eastern Mediterranean Sea. Transition periods, primarily May and October, have the highest occurrence of Sharavs, which seldom occur from June to September.

Sharavs are not identified by direction--even though they're usually associated with east to southwest winds--but by relative humidity and temperature change. Specifically, the Sharav is defined by a temperature increase of at least 9° F (5° C) and a relative humidity decrease of at least 25% from the mean of the previous 5 days. Sharav air temperatures often reach 104° F (40° C) and sometimes exceed 120° F (49° C). In the Hills of Judea, strong Sharavs can drop relative humidity to below 10%.

Strong Sharav conditions occur most commonly with desert air moving northward in the warm air sector of Atlas Lows or stalled Cyprus Lows. Figure 2-40 shows the normal desert low path that produces Sharav conditions. The most severe Sharavs occur when the surface low moves due east over the Sinai Peninsula, then turns northeast. If the upper-level trough slows down and deepens, the low may turn northeast early enough to cross the eastern Mediterranean Sea and prevent strong Sharav conditions along the eastern coast.

Other synoptic conditions can produce Sharav winds. For example, a trough over the Red Sea or persistent high-pressure east of Israel can advect hot, dry desert air in from the Arabian Desert. Stagnant high pressure is the most favorable condition for persistent Sharav conditions, which can last for 2-4 days.

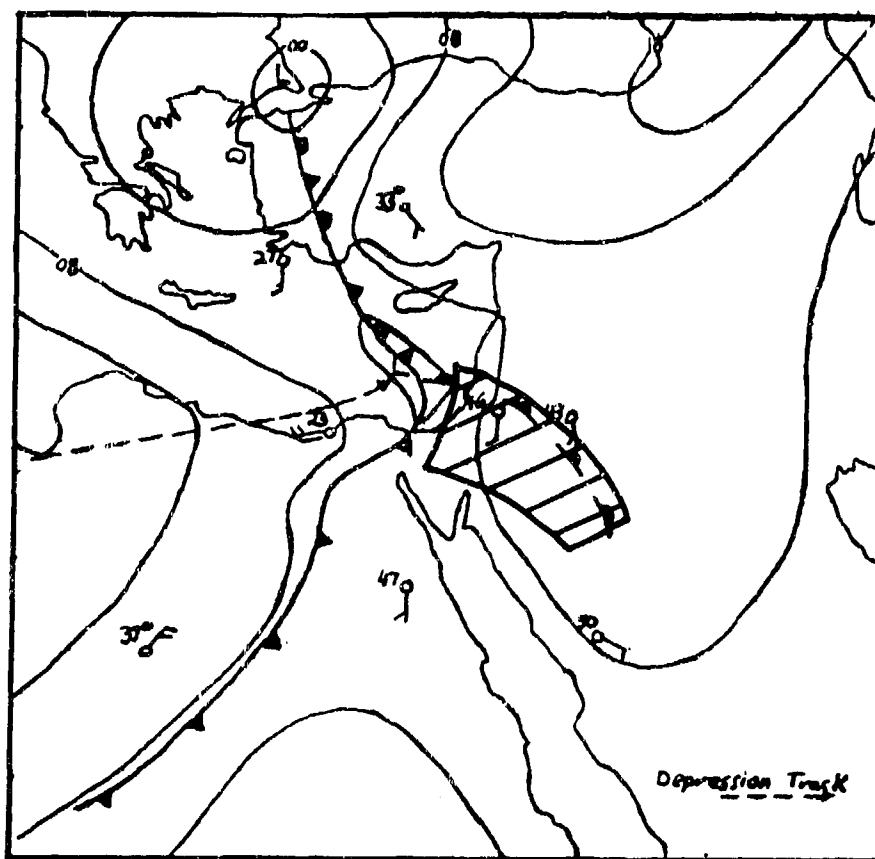


Figure 2-40. Active Storm Track For Sharav Winds. The hatched area represents strong southerly flow where the most severe Sharav conditions occur. The dashed arrow depicts typical storm track movement. Temperatures are °C.

SIROCCO winds are similar to Khamsin and Sharav winds in that they, too, are hot and dry southerly or southeasterly winds in the warm sectors of advancing lows. Air from the deserts of northern Africa, Israel, or Syria is advected into southern Turkey. Temperatures are over 100° F (38° C) and relative humidities drop below 30%. The strong southerly winds normally transport Saharan dust to 6,000-7,000 feet (1,830-2,130 meters).

Siroccos, most common in the spring, can develop with Atlas, Genoa, or Cyprus Lows. The storm track determines severity and location. With a deep upper-level trough, the low moves northeast over the eastern Mediterranean Sea, as shown in Figure 2-41. Southerly winds average 15-25 knots and persist for 1 to 6 hours. Peak gusts are 30 to 45 knots. After the low passes, cold northerly flow drops temperatures as much as 30° F (17° C); relative humidities can increase to 80% within 2-3 hours.

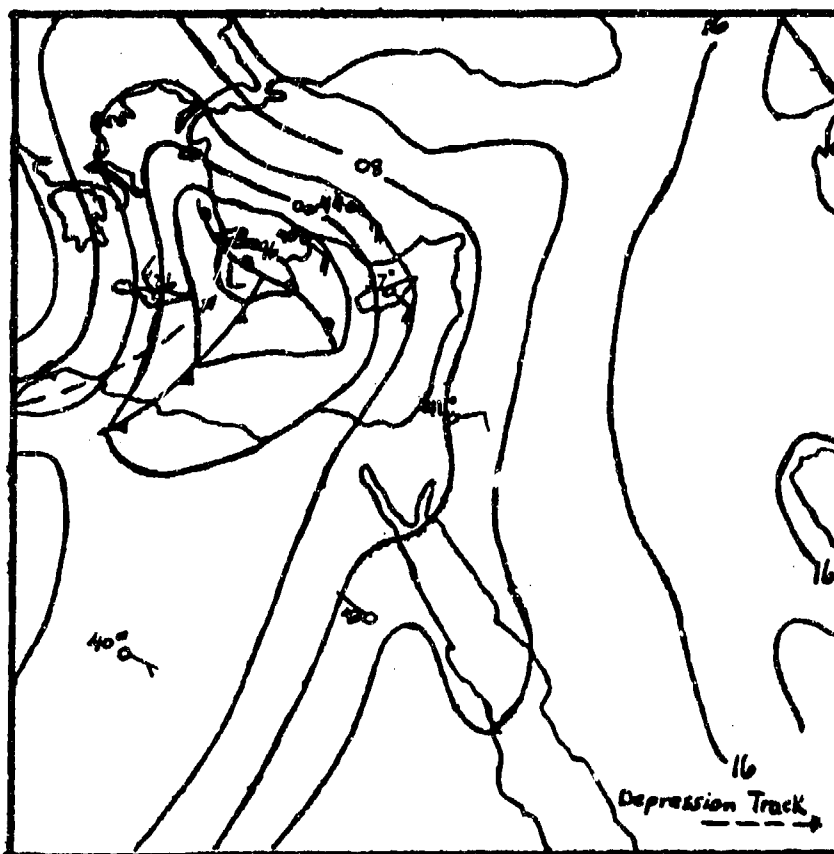


Figure 2-41. Deep Trough Producing Sirocco Winds. Dashed arrow depicts typical storm track movement. Temperatures are °C.

HARMATTAN winds are dry, dust-bearing winter northeasterlies. They originate in the Sahara as outflow from the Saharan and Azores Highs and average 8-12 knots over Africa during the winter. In combination with the dry, dust-laden air, they produce "Harmattan Haze." Severe Harmattan episodes occur behind strong cold fronts with winds reaching 30-45 knots. Turbulent surface mixing produces a thick dust haze that normally reaches 1,000 feet (305 meters) AGL, but that can reach 10,000-12,000 feet (3,050-3,660 meters) MSL and extend southward to 5° N.

Harmattan Haze can persist for extended periods. Dust that reaches the surface Monsoon Trough is lifted over it along the ITD because the dry, dust-laden air is warmer and less dense. Horizontal visibilities actually increase south of the Monsoon Trough as the dust layer

is forced aloft, but slant-range visibilities are lower. Horizontal visibilities average 3-6 miles; slant-range, only 1-3 miles.

Harmattan episodes occur behind intense cold fronts, mainly from Atlas Lows, when flow from the Saharan High is northeasterly at 30-45 knots. Northern Chad and western Sudan experience three to five strong Harmattan episodes from January to May. Central and eastern Sudan also see Harmattan winds, but less frequently. Severe duststorms, extremely low visibility, and high winds occur for 12 to 24 hours. Figure 2-42 shows the area affected by a strong Harmattan (hatched area) in relation to the Saharan High and the remnant of the cold front (a shear line). Figures 2-43a and b show a Harmattan episode over Northeast Africa.

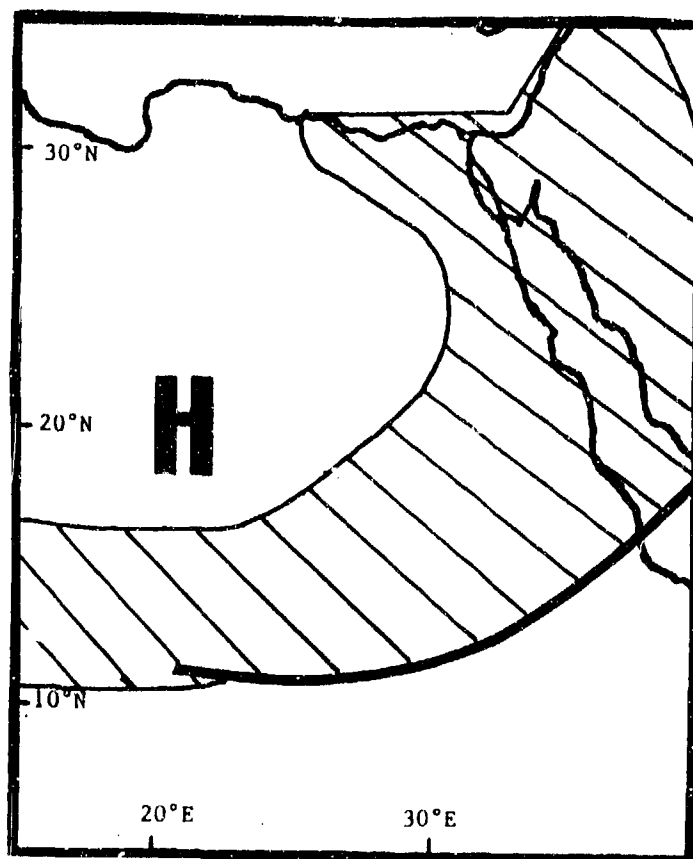


Figure 2-42. Regional Harmattan. The hatched area shows the location of the widespread dust in relation to the Saharan High. The solid line is the shear line extending from the active frontal system.

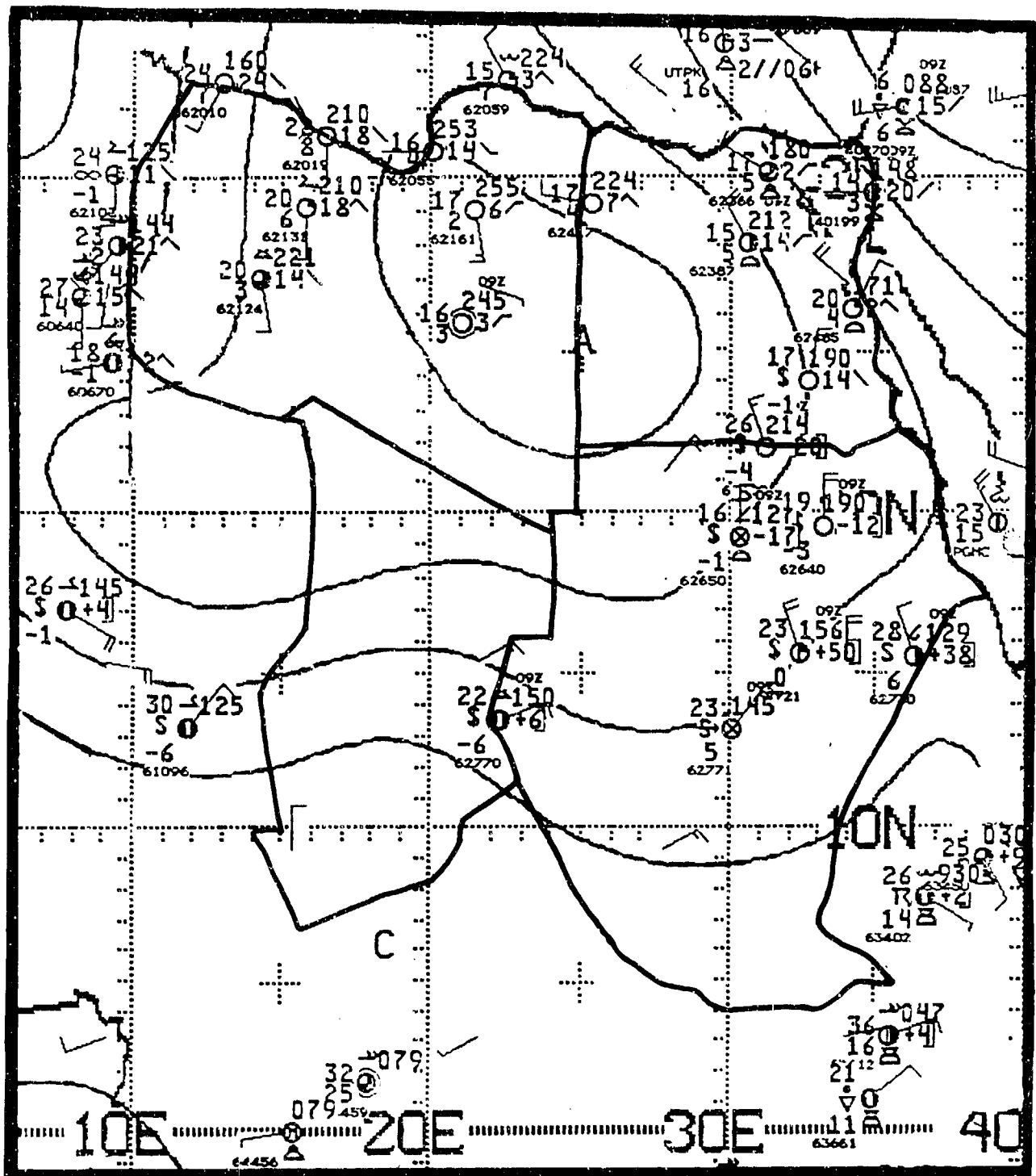


Figure 2-43b. Surface Data: Harmattan-Produced Duststorm Over Northeast Africa (6 March 1991, 1200Z). Wind barbs without station data are satellite-derived. Duststorms/sandstorms and suspended dust are evident in observations throughout the area.

The **HABOOB** of northern and central Sudan is a strong wind with sandstorms or duststorms produced by individual thunderstorms or squall lines. The name is from the Arabic *habb* meaning "wind." Convective downbursts, microbursts, and outflow boundaries

produce "walls of dust" and debris in advance of the storm cell and precipitation. These "walls" may be several hundred feet high and 1-2 NM across. Figure 2-44 shows the area in which Haboobs frequently develop.

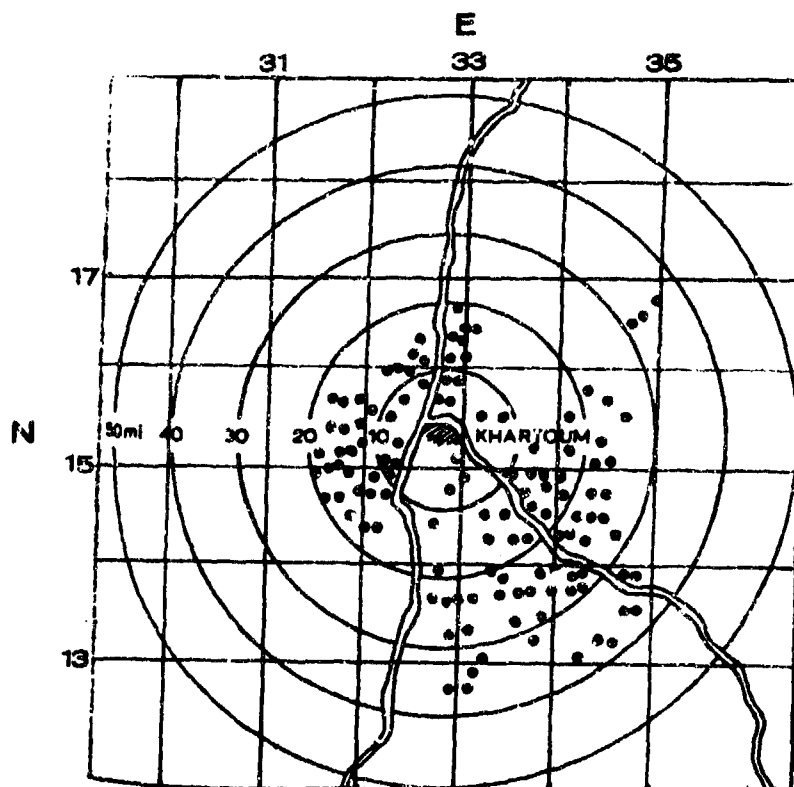


Figure 2-44. Source Region For "Haboob" Development (from Hammer, 1970). Each dot represents the initial development of cumulus clouds from July to September of 1964 and 1965. Development usually begins between 1000 and 1300L. Convection develops to the southeast and west of Khartoum primarily due to available moisture. The water system feeding into the Nile River flows through Khartoum from the southeast. Over 80% of all Haboobs at Khartoum approach the Nile River Valley from the southeast quadrant.

Haboobs occur mainly during the summer with the presence of the Monsoon Trough. Peak frequency is in June, normally in the afternoon. These "walls of dust" move rapidly ahead of the storm cell. Figure 2-8b is a satellite view of a Haboob moving northeast from Monsoon Trough convection. Spring and early summer Haboob conditions last 1/2 to 2 hours; those generated after mid-June seldom persist for more than 15 minutes because the soil is more moist.

Weather in a Haboob is severe. Visibilities are usually less than 1/8 NM within the "wall of dust." Winds average 25 to 50 knots; a peak gust of 105 knots

was recorded at Khartoum, Sudan. Wind direction is typically south to southeast because Haboobs are more likely to occur in the dry dust of the Sahara on the north side of the Monsoon Trough. Suspended dust from these events have been observed at over 15,000 feet (4,570 meters). Normal thunderstorm hazards are present. Rainfall actually improves visibility as heavy rain removes the dust.

Low-level moisture is available south of the Monsoon Trough; however, a northward surge in the surface Monsoon Trough is needed to increase the 700 mb moisture, generally to 40% or greater to sustain

convective activity and generate a Haboob. These northward surges are more likely to occur in the early part of the wet season as the Monsoon Trough moves into the area. Low-level moisture availability, orographic lifting along the Ethiopian Highlands, and the MTEJ all contribute to Haboob development.

ETESIAN winds are northerlies that occur from May through October and affect the coastlines of western and southern Turkey, Syria, and Israel. The Anatolian Plateau Thermal Trough and high pressure over the Balkans combine to produce these steady northerly winds that can persist for 5 days. Etesian wind strength

and frequency peak in July and August when speeds occasionally reach 30 knots. Speeds are normally persistent at 10-15 knots, but higher speeds result from channeling through the islands near the Turkish coast. The northerly Etesians normally extend up to 6,500 feet (1,980 meters) MSL, with peak winds around 3,300 feet (1,000 meters) MSL. Rare northeasterly winds over Libya suggest that Etesian winds may occasionally penetrate that far. An Etesian regime is established after a cold front moves through to the southeast. Although Etesian winds normally produce good weather, they occasionally bring in clouds or produce duststorms where they cross a dry desert.

Chapter 3

THE TURKISH COAST

The Turkish Coast region comprises the western and southern Turkish coasts below the 3,280-foot (1,000 meter) contour. The Mediterranean and Aegean Seas form its southern and western boundaries. After discussing the area's situation and relief, this chapter discusses "general weather conditions" by season.

	Page
Situation and Relief	3-2
Winter--December-February	3-6
General Weather	3-6
Sky Cover.....	3-6
Visibility	3-7
Winds.....	3-8
Precipitation	3-10
Temperature	3-13
Spring--March-May	3-14
General Weather	3-14
Sky Cover.....	3-14
Visibility	3-15
Winds.....	3-15
Precipitation	3-16
Temperature	3-18
Summer--June-August	3-19
General Weather	3-19
Sky Cover.....	3-19
Visibility	3-20
Winds.....	3-20
Precipitation	3-21
Temperature	3-23
Fall--September-November	3-24
General Weather	3-24
Sky Cover.....	3-24
Visibility	3-25
Winds.....	3-25
Precipitation	3-26
Temperature	3-28

THE TURKISH COAST

SITUATION AND RELIEF

GEOGRAPHY. As shown in Figure 3-1a, the Turkish Coast region extends from the southern coast of the Sea of Marmara south, then east to the Turkey/Syria border. It includes the coasts of the Sea of Marmara, the Aegean Sea, and the Mediterranean Sea to the 3,280-foot (1,000-meter) contour. Its northern boundary runs from the Dardanelles along the Sea of Marmara's southern coast to the town of Mudanya. A straight line joins the

boundary to the 3,280-foot (1,000-meter) contour at Bursa. The boundary follows this contour south, then east to the Turkey/Syria border, and thence along the border to the Mediterranean coast. Climatological data summaries for selected stations are provided by Figure 3-1b; information for other stations is available in USAFETAC/DS-89/035, *Station Climatic Summaries, Asia*.



Figure 3-1a. The Turkish Coast. The Turkish Coast (in dark shading) extends from the northwestern coast of Turkey to the Turkey/Syria border.

STATION: ANTALYA TURKEY													
LAT/LON: 38 53 N 30 42 E ELEV: 138 FT													
ELEMENTS	JAN	FEB	MAR	APR	MAY	JUN	JUL	AUG	SEP	OCT	NOV	DEC	ANN
XTRM MAX	75	79	82	91	102	107	110	112	109	102	91	74	112
AVG MAX	59	60	64	70	77	86	93	93	87	80	71	62	76
AVG MIN	43	44	47	52	59	67	73	73	67	60	52	46	56
XTRM MIN	18	24	30	38	43	53	59	57	51	44	32	28	18
AVG PRCP	9.7	6.3	3.5	1.1	1.3	0.4	0.1	0.1	0.5	2.0	4.1	10.9	40.6
MAX MON	24.1	19.4	11.3	7.2	7.6	3.1	1.3	2.0	3.9	14.0	16.1	26.0	64.8
TS DAYS	4	3	2	2	4	3	1	1	2	3	3	4	32

* = LESS THAN 0.05 INCHES OR LESS THAN 0.5 DAYS

STATION: CANAKKALE TURKEY													
LAT/LON: 40 08 N 28 24 E ELEV: 10 FT													
ELEMENTS	JAN	FEB	MAR	APR	MAY	JUN	JUL	AUG	SEP	OCT	NOV	DEC	ANN
XTRM MAX	68	70	81	87	93	98	99	102	94	88	82	72	102
AVG MAX	49	50	54	63	72	81	87	87	79	70	61	53	67
AVG MIN	37	37	39	45	53	60	65	65	60	53	48	41	50
XTRM MIN	12	11	17	29	38	44	50	49	43	34	19	13	11
AVG PRCP	3.9	2.9	2.7	1.5	1.1	1.0	0.4	0.4	0.9	1.9	3.3	3.9	24.0
MAX MON	8.0	6.2	6.4	2.9	2.8	4.4	1.6	2.8	5.8	6.8	8.2	7.2	33.1
SMO DAYS	1	2	1									1	5
MAX DEP	6.0	8.4	8.4	1.6							0.4	8.0	9.4
YS DAYS	1	2	1	1	2	2	1	1	1	2	2	2	18
FOG DAYS	1	1	1	*	*	0	0	*	0	*	1	1	5
HZ/SMK	2	2	5	3	2	*	2	2	2	3	3	2	28

* = LESS THAN 0.05 INCHES OR LESS THAN 0.5 DAYS

STATION: INCIRLIK AB, TURKEY													
LAT/LON: 37 00 N 35 28 E ELEV: 239 FT													
ELEMENTS	JAN	FEB	MAR	APR	MAY	JUN	JUL	AUG	SEP	OCT	NOV	DEC	ANN
XTRM MAX	72	79	87	98	106	109	108	114	108	106	93	80	114
AVG MAX	58	60	66	74	81	89	93	96	91	83	72	62	77
AVG MIN	41	42	46	52	58	65	71	71	66	59	51	45	56
XTRM MIN	17	20	23	32	41	48	52	58	48	38	24	24	17
AVG PRCP	4.5	3.4	3.1	2.4	2.4	0.9	0.2	0.1	0.5	1.2	1.7	5.3	25.6
MAX MON	9.9	10.5	5.1	6.3	7.9	4.5	1.3	1.8	2.7	3.4	6.6	13.4	35.1
MAX DLY	2.1	1.2	1.8	3.5	4.5	2.0	1.3	1.8	2.6	2.2	3.4	3.6	4.5
TS DAYS	2	2	3	3	5	3	1	1	2	3	2	2	28
FOG DAYS	2	3	3	4	4	6	8	7	4	2	1	2	48
APP TEMP	58	60	66	75	82	92	100	102	99	93	72	62	

* = LESS THAN 0.05 INCHES OR LESS THAN 0.5 DAYS
NOTE: ALPHEGE JUST BLOWING SAND DUNE OCCUR

STATION: IZMIR TURKEY													
LAT/LON: 38 24 N 27 04 E ELEV: 82 FT													
ELEMENTS	JAN	FEB	MAR	APR	MAY	JUN	JUL	AUG	SEP	OCT	NOV	DEC	ANN
XTRM MAX	70	75	86	91	103	105	108	109	102	100	90	80	109
AVG MAX	54	56	61	69	78	87	92	92	84	76	66	58	73
AVG MIN	40	42	44	50	58	65	70	70	63	57	51	45	55
XTRM MIN	15	17	25	32	40	49	52	53	42	38	27	21	15
AVG PRCP	5.3	4.2	2.8	1.8	1.5	0.3	0.1	0.1	0.6	1.9	3.4	5.6	27.7
MAX MON	15.6	11.7	12.0	7.2	4.6	1.9	2.4	0.8	4.1	15.6	10.3	14.1	44.0
FOG DAYS	*	*	- OCCURS -										*
TS DAYS	3	3	2	2	3	1	*	*	1	2	3	3	23

* = LESS THAN 0.05 INCHES OR LESS THAN 0.5 DAYS

Figure 3-1b. Climatological Summaries for Selected Stations on the Turkish Coast. These summaries are based on several references covering different periods of record from 10 to 50 years.

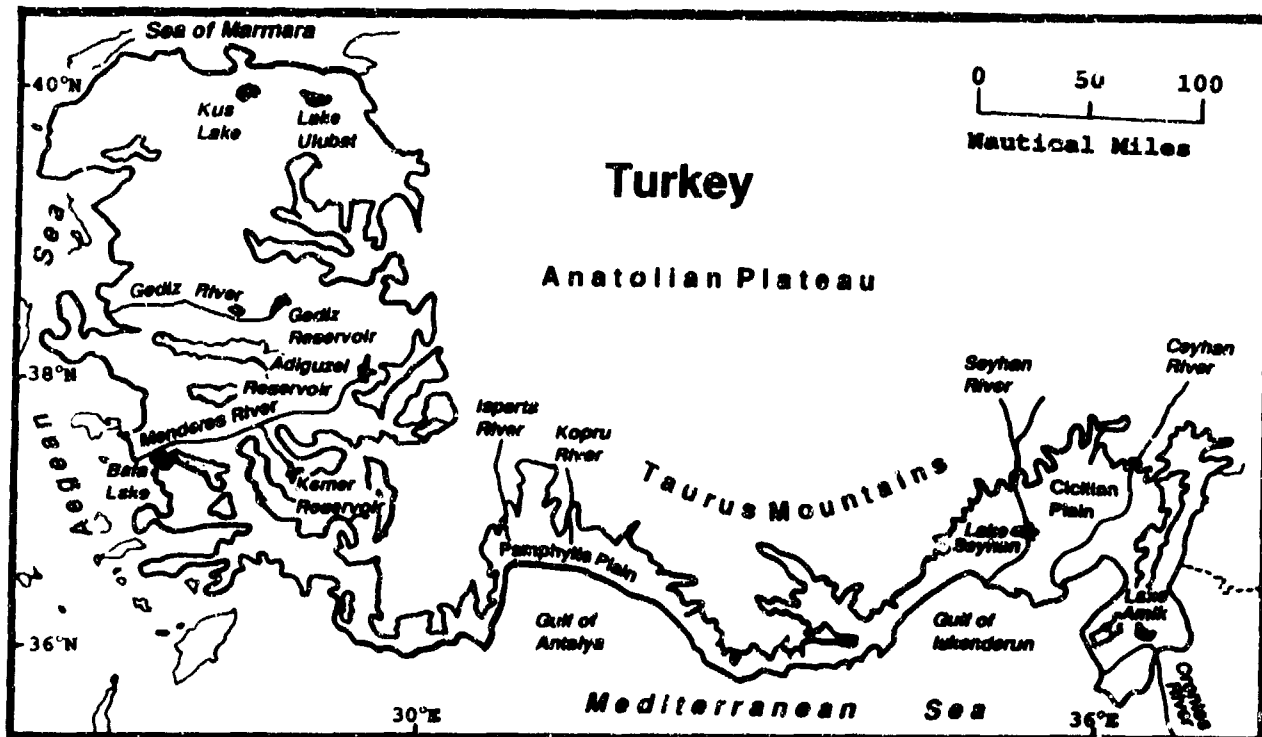


Figure 3-2. Topographical Features of the Turkish Coast. The shaded areas denote areas above 3,280 feet (1,000 meters).

TOPOGRAPHY. As shown in Figure 3-2, the Aegean Sea and the Sea of Marmara coastal plains, which vary from 50 to 175 NM wide, comprise 80% of the area. Steep, elongated ridges extend from the Anatolian Plateau westward to within 50 NM of the coast. Ridges average 3,300 feet (1,005 meters), but reach to 8,000 feet (2,440 meters). Large river valleys that separate the parallel ridges average 7 NM in width and extend 130 NM east from the Aegean Sea. The Menderes and Gediz Valleys are the largest.

Turkey's Mediterranean coastal plains are extremely narrow, averaging less than 4 NM in width. They parallel the Taurus Mountains, which rise to 7,000 feet (2,135 meters) within 17 NM of the coast. The highest peaks reach 13,000 feet (3,960 meters) near Adana. Several large coastal valleys run inland from the coast. The Pamphylia Plain, about 80 NM long and 100 NM wide, surrounds the Gulf of Antalya. The Cilician Plain extends 130 NM around the Gulf of Iskenderun's coast and 140 NM inland. The Orontes River Valley, near the Syrian border, extends 43 NM inland and stretches 13 to 17 NM along the coast.

RIVERS AND DRAINAGE SYSTEMS. Numerous permanent rivers and streams flow from the Anatolian Plateau's lakes, springs, and ponds, as well as from the

snow-capped Taurus Mountains. The major rivers are over 175 NM long. They cut narrow valleys that dissect the mountainous interior. Many smaller streams descend from the mountains and form tributaries within the major systems. The Gediz and Menderes Rivers, flowing westward into the Aegean Sea, are the most extensive systems. The Isparta and Koprü Rivers run through the Pamphylia Plain. The Seyhan and Ceyhan Rivers flow through the Cilician Plain. They all drain into the Mediterranean from the highest peaks in the Taurus Ranges. The Orontes (or Asi) River is the only river of significance in the extreme southeast.

LAKES AND RESERVOIRS. Most lakes and reservoirs are in Turkey's western sections. The largest, Kus Lake and Lake Ulubat, have a combined surface area of over 85 square miles and are within 13 NM of the Sea of Marmara. Lake Seyhan and Lake Annik are the only major fresh water lakes along the southeastern coasts. The Gediz, Adiguzel, and Kemer Reservoirs are man-made flood control waterways within the Gediz and Menderes river systems.

VEGETATION. Mediterranean scrub and grasses abound. Citrus and cotton are the chief cash crops. Evergreens, spruce, and mountain shrubs dominate on the moist, cool valley slopes.

THE TURKISH COAST WINTER

December-February

GENERAL WEATHER. Genoa and Cyprus Lows affect the Turkish Coast region every 3 to 7 days, causing heavy rainfall, thunderstorms, and/or snow. The Asiatic High causes northeasterly flow into the Sea of Marmara. Severely cold air masses move south from the Asiatic High once or twice a winter.

SKY COVER. Nocturnal stratus forms during fair weather off the Aegean and Mediterranean coasts. Bases are 3,000 to 5,000 feet (915 to 1,525 meters) tops extend to 7,000 feet (2,135 meters) MSL. These clouds blow

inland with the sea breeze and form stratocumulus along seaward-facing slopes. Heating and orographic uplift further enhance cumulus development over ridges until cloud tops reach 13,000 feet (3,960 meters) MSL. The stratus along the Sea of Marmara coast is lower due to the persistent cold onshore flow; bases are 200 to 1,000 feet (60 to 305 meters), and tops are 4,000 feet (1,220 meters) MSL. As shown in Figure 3-3, ceilings below 3,000 feet (915 meters) occur most frequently near the Sea of Marmara, and inland of the Aegean coast.

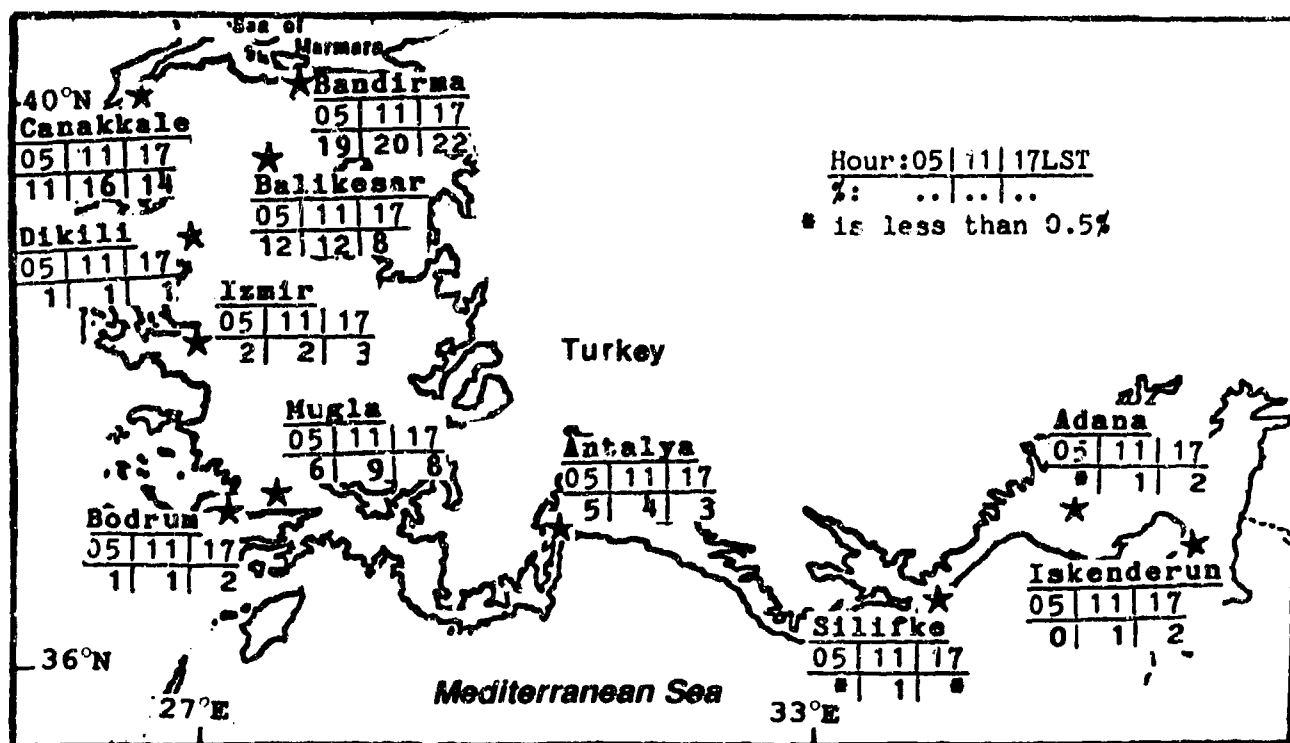


Figure 3-3. Mean Winter Frequencies of Ceilings Below 3,000 Feet (915 meters), Turkish Coast.

THE TURKISH COAST

WINTER

December-February

Mean cloudiness reaches its peak during winter, mostly due to transitory lows. Cloudiness inland of the Aegean coast and near the Sea of Marmara averages 65-75%, while the Mediterranean coast averages 50-60%. Lows moving along the southern Turkish coast produce dense cloud cover about 14 times each winter. Orographically lifted stratus or stratocumulus hide thick layers of mid- and upper-level cloud cover from a ground-based observer. Bases are normally between 2,500 and 4,000 feet (760 and 1,220 meters), but may be as low as 1,500 feet (455 meters). Tops of layered clouds extend to 20,000 feet (6 km) MSL.

Lows moving into the Black Sea spread fewer clouds over the region than the lows that move along the southern Turkish coast. Warm sector stratocumulus and cold front cumulus are the main low-level cloud types. Bases are between 3,000 and 4,000 feet (915 and 1,220 meters). Considerable mid- and high-level clouds may also be present with tops to 18,000 feet (5,485 meters) MSL. With either type of low, ceilings can go below 500 feet (150 meters) with heavy precipitation. Thin

cirrus occurs near jet streams and from thunderstorm blow-off. Bases are above 18,000 feet (5,485 meters) and tops are as high as 40,000 feet (12 km).

VISIBILITY. Fog is common throughout the region in winter, especially along the Aegean Sea and Sea of Marmara coasts where visibilities below 3 miles are most common. Radiation fog forms in fair weather with light winds between 0600 and 0800 LST, but normally dissipates by 1300 LST. Sea fogs move inland with the sea breeze or strong synoptic flow, occasionally lasting for days and extending well inland through the mountain valleys. Stratus obscures the higher ridges.

Low visibilities along the Mediterranean Coast are produced by precipitation. Steady rain, drizzle, or even snow reduces visibility to below 7 miles; with fog, to below 3 miles. Snow can reduce visibility to below a mile. Heavy rain showers and thunderstorms (in the warm sector or with cold fronts) can lower visibilities to between 2 and 6 miles for brief periods.

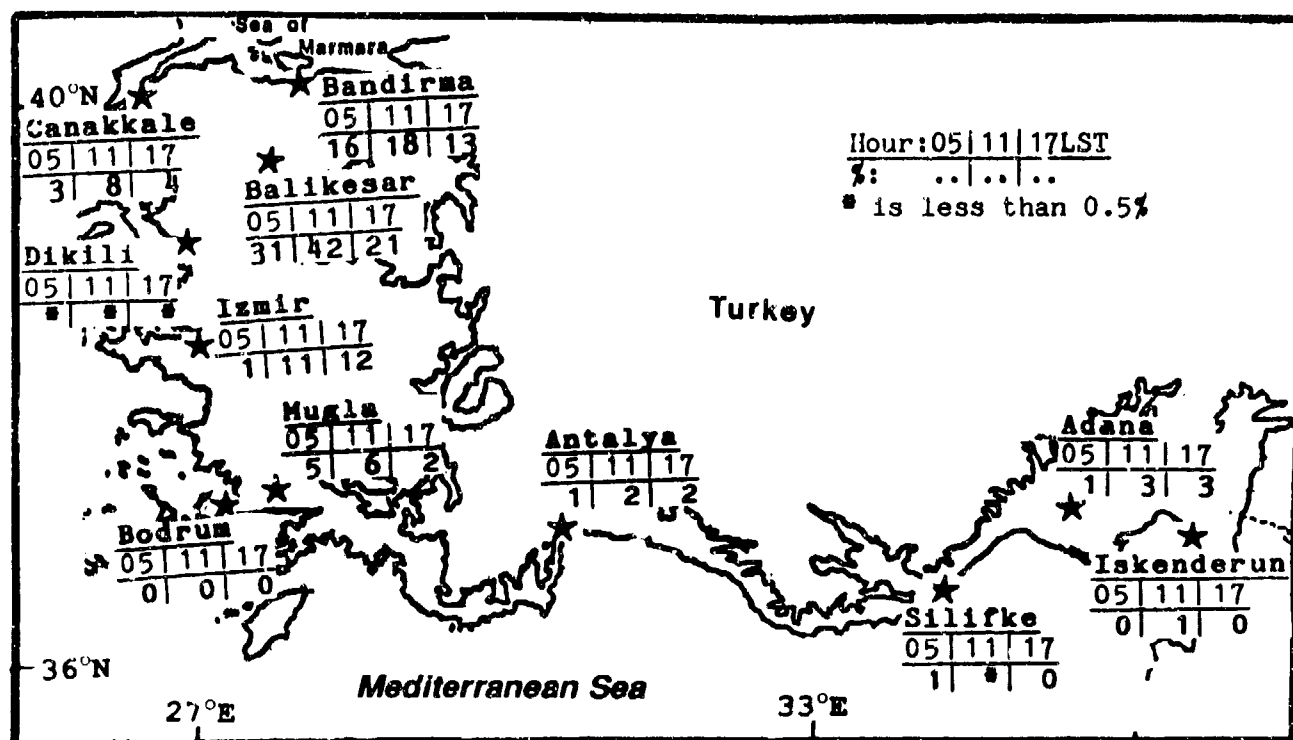


Figure 3-4. Mean Winter Frequencies of Visibilities Below 3 Miles, Turkish Coast.

THE TURKISH COAST WINTER

December-February

Strong southerly winds or siroccos ahead of very deep lows suspend large amounts of dust from the Sahara. This dust lowers visibilities to less than a mile about once a winter. It is common to observe a reddish haze aloft at 20,000-foot (6-km) MSL. Surface haze rarely reduces visibility to below 3 miles, but it is often reported at Izmir in the 3-6 mile range. Haze and fog are common there because its fjord-like inlet traps pollution and marine moisture under a low-level inversion with high-pressure stagnation. Smoke is a rare source of obscuration, but it is observed most frequently along the Sea of Marmara coast to an area south of Balıkesir; visibility rarely drops to less than 3 miles.

WINDS. The extensive river valleys and mountain ranges along the Anatolian Plateau generate strong mountain/valley circulations. These mountains, combined with a very irregular coastline, cause the high

variabilities in speed and direction shown in Figure 3-5. The plateaus are large-scale sources of cold air; they provide valleys with cold air drainage throughout the day. This is most striking at Silifke, where an extensive valley system extending to the northwest dominates winds.

The land/sea breeze circulation affects most of the coast. Large-scale outflow from the Asiatic High generates persistent northeasterly surface flow along the Sea of Marmara's southeastern coasts. Northeasterly flow converges with westerlies near 40° N, while the northeasterlies curl southward around the plateau and into the northern Aegean Sea. Mean speeds are 5 to 10 knots; the northeasterlies are stronger at 7 to 13 knots. The highest recorded wind speed (56 knots from the NNW at Antalya) was due to an exceptionally strong low.



Figure 3-5. January Surface Wind Roses, Turkish Coast.

THE TURKISH COAST

WINTER

December-February

Above 850 mb, the prevailing synoptic flow is westerly at 20 knots. Figures 3-6a-b give upper-air wind directions at three levels. Isparta is in the Atlas Mountains just north of the region at an elevation of 3,270 feet (997 meters). An 8,000-foot (2,440-meter)

ridge separates it from the coast and affects its 5,000-foot winds. Winds above this level are probably representative of the Mediterranean coast's predominantly westerly flow. Maximum speeds of 60 knots are found around 35,000 feet (10.5 km).

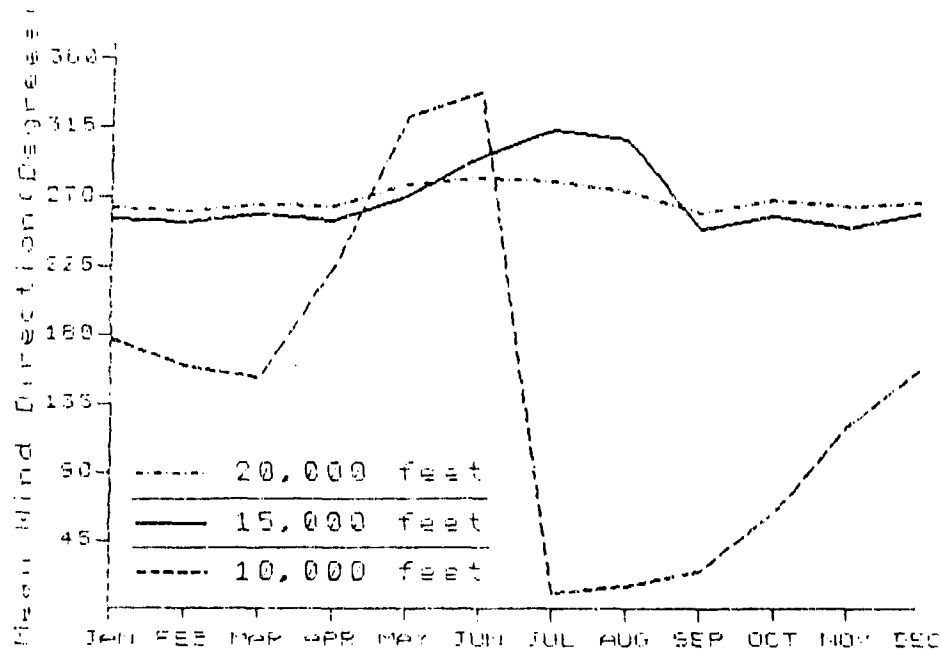


Figure 3-6a. Mean Annual Upper-Air Wind Directions, Isparta, Turkey.

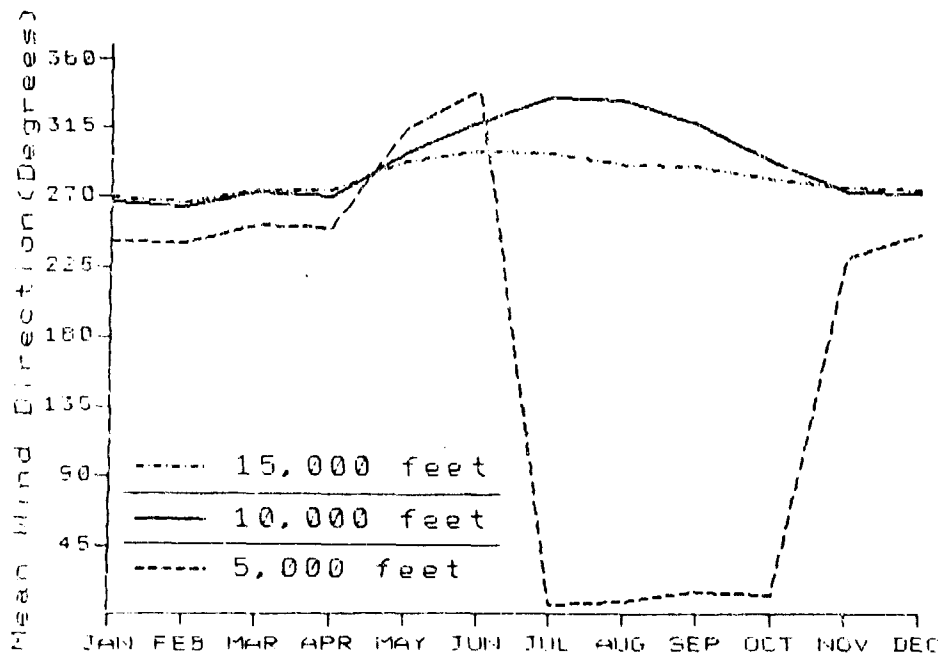


Figure 3-6b. Mean Annual Upper-Air Wind Directions, Izmir, Turkey.

THE TURKISH COAST

WINTER

December-February

PRECIPITATION. As shown in Figure 3-7, precipitation is greatest in early winter; in December, 11 inches (280 mm) of rain falls along the southwest Turkish coast, which is affected by both Genoa and Cyprus Lows. Precipitation amounts decrease from west to east along the southern Turkish coast as fewer Cyprus lows penetrate eastward into the Gulf of Iskenderun. Mean precipitation also decreases south to north along

the western Turkish Coast. Cyprus Lows do not affect this area, and 80% of lows which do affect it move quickly into the Black Sea, where they bring rain for 2 days or less. Figures 3-8a-b illustrate those situations that cause the heaviest precipitation. Lighter precipitation occurs with lows tracking along the North African Coast.

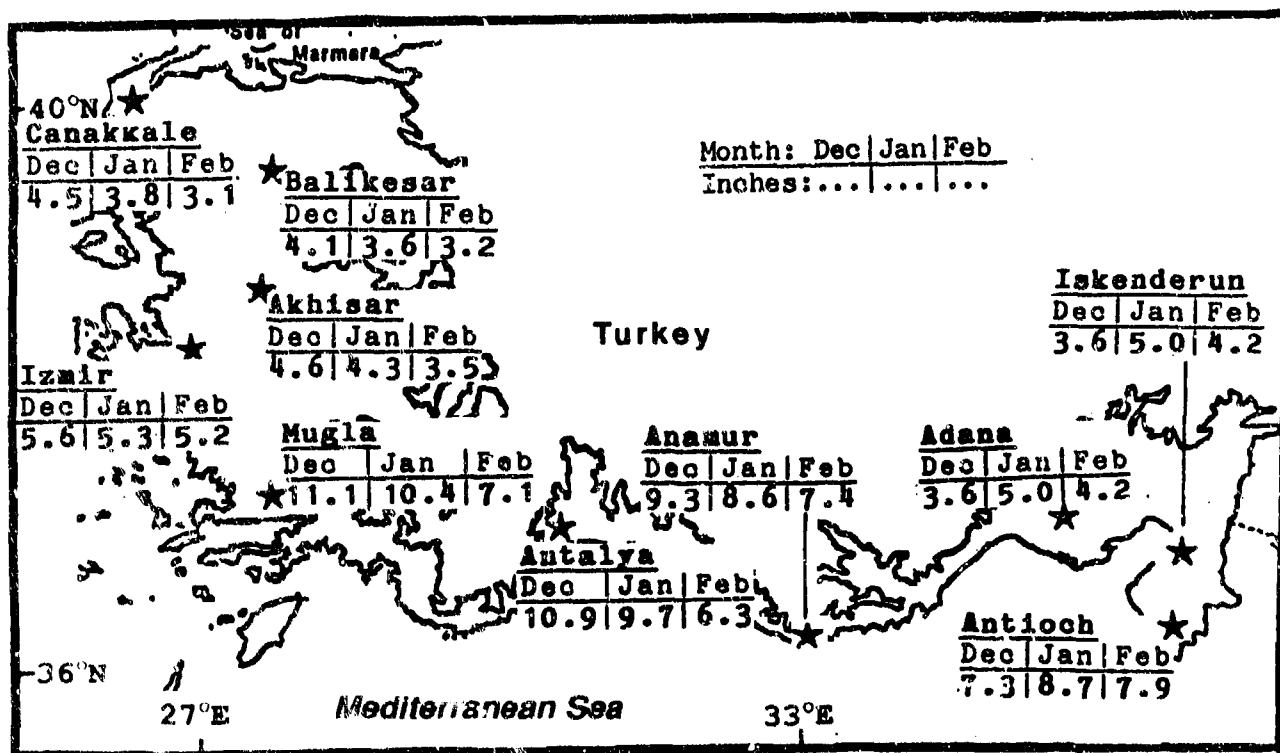


Figure 3-7. Mean Winter Monthly Precipitation, Turkish Coast.

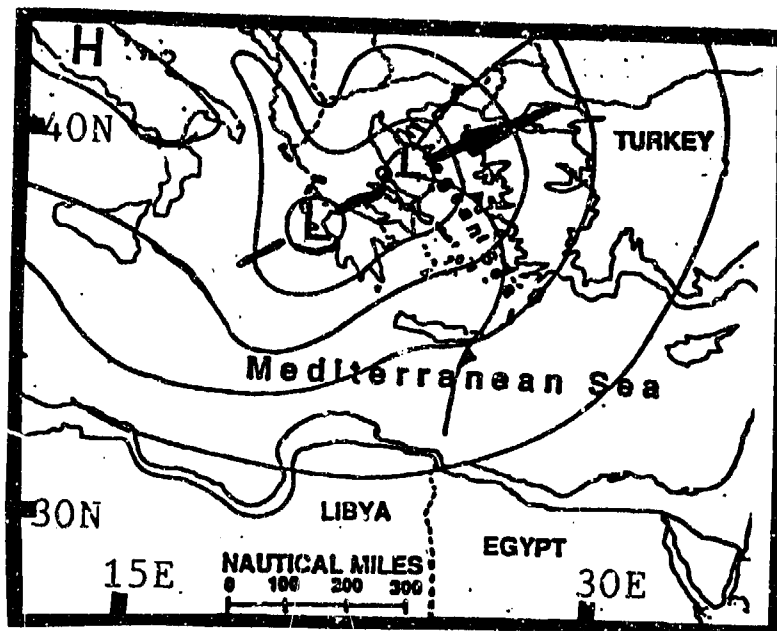


Figure 3-8a. A Favored Track for Heavy Precipitation along the Western Turkish Coast.

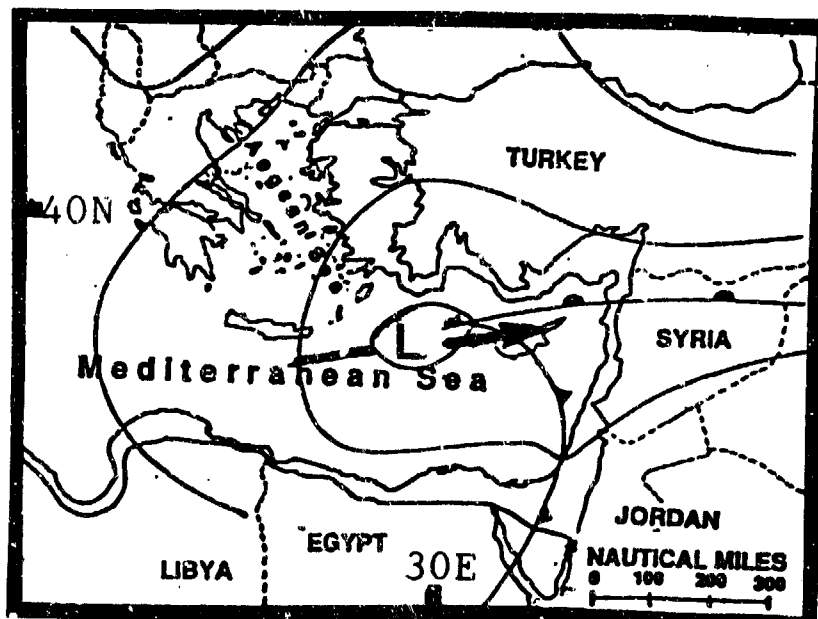


Figure 3-8b. A Favored Track for Heavy Precipitation along the Southern Turkish Coast.

THE TURKISH COAST

WINTER

December-February

Snow falls on less than 1 day a year along the Mediterranean coast. It is more common along the Aegean coast, where it falls on 5-10 days a winter, normally above the 3,000-foot (915-meter) level. Snow falls about 13 days a winter in the plains and hills just south of the Sea of Marmara.

Winter thunderstorms are associated with cold fronts, most frequently along the southwest Turkish coast, which sees 15 to 20 thunderstorm days. The average drops away from this area, with 9 thunderstorm days in the east and 3 to 6 days in the north. Tops do not normally exceed 40,000 feet (12 km) MSL.

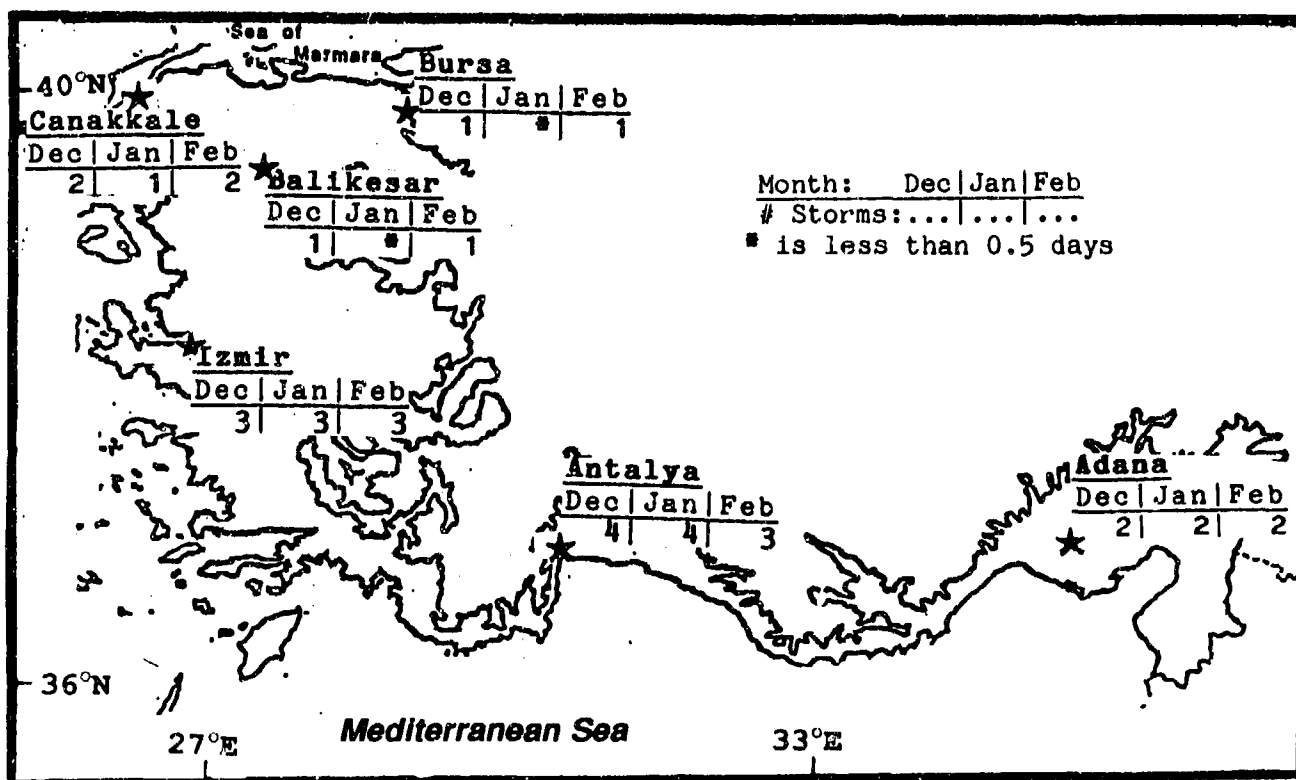


Figure 3-9. Mean Winter Thunderstorm Days, Turkish Coast.

THE TURKISH COAST WINTER

December-February

TEMPERATURE. Winters are mild. Mean daily highs, as shown in Figure 3-10, are between 47 and 64° F (8 and 18° C). Temperatures are lower near the Sea of Marmara. Record highs range from 69° F (21° C) at Mugla to 81° F (27° C) at Silifke, along the Mediterranean coast. Daily lows range from 33 to 50° F (1 to 10° C). When the Asiatic High is strong, bitterly

cold air affects the region. Temperatures are well below freezing even after air warms adiabatically as it descends the Anatolian Plateau and mixes with warmer maritime air from the coast. Examples are the record lows of -8° F (-22° C) at Balikesar, 6° F (-14° C) at Antioch and 26° F (-3° C) at Iskenderun.

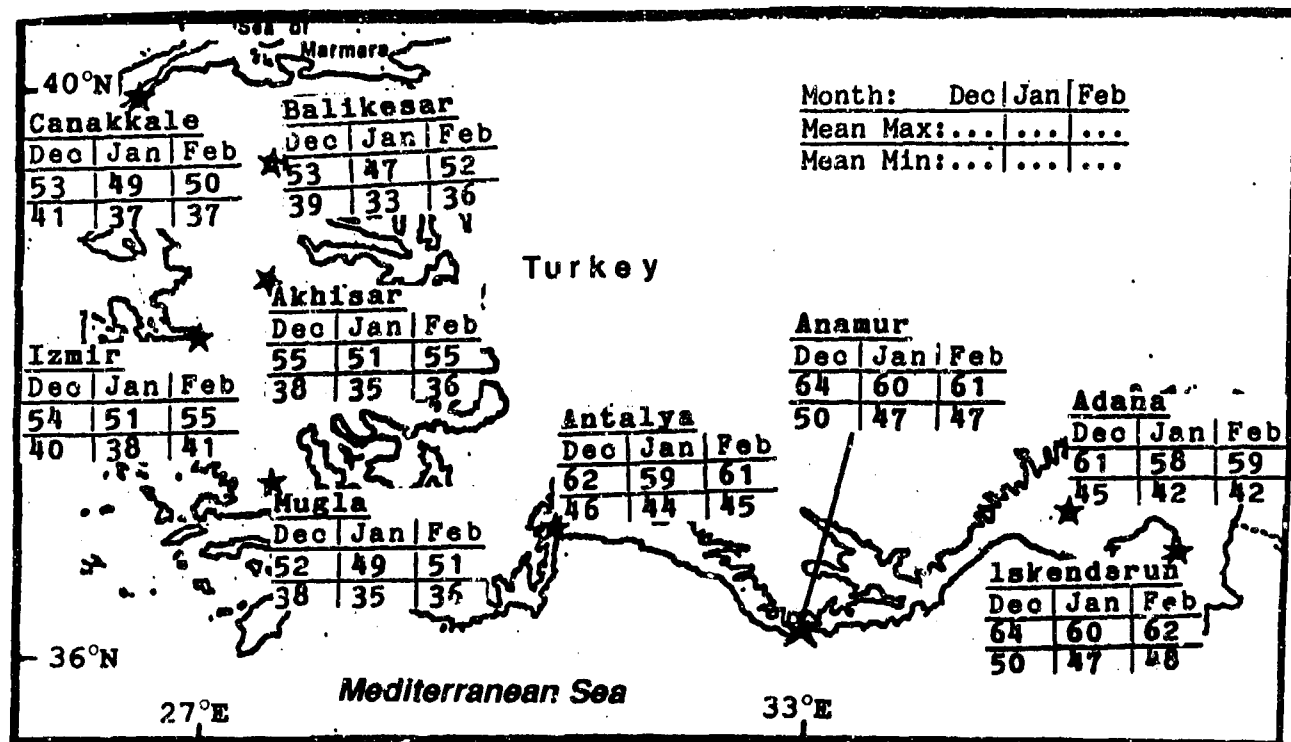


Figure 3-10. Mean Winter Daily Maximum/Minimum Temperatures (F), Turkish Coast.

THE TURKISH COAST SPRING

March-May

GENERAL WEATHER. As the Azores High strengthens and moves north, favored areas for cyclogenesis shift from the Mediterranean to the Atlas Mountains in North Africa. Atlas Lows, which typically move over the eastern Mediterranean and into the Sea of Marmara, bring drier air to the Turkish Coast; wind speeds are 10 to 15 knots stronger.

SKY COVER. There is a gradual decrease in cloud cover during the spring. March cloud cover patterns are similar to winter's, but by mid-May, mean cloudiness decreases by almost 25%. As shown in Figure 3-11, northwestern locations have higher frequencies of ceilings below 3,000 feet (915 meters) because they are exposed to moist northeasterly flow that produces stratus. Diurnal stratocumulus and cumulus are common during fair weather periods, when bases are between 2,500 and 4,000 feet (760 and 1,220 meters) and less than 2,000 feet (610 meters) thick. Stratocumulus forms when cold air drainage from the Anatolian Plateau moves over warmer coastal waters. After sunrise, the sea breeze reverses the flow; the stratocumulus moves inland and develops into fair-weather cumulus. Orographic uplift produces cumulus along the windward ridges of coastal

ranges. Fair-weather morning stratus forms along the northern coast; bases are between 400 and 1,000 feet (120 and 305 meters) and tops are below 1,500 feet (450 meters) MSL.

The cloudiest days on the Mediterranean coast occur when a March Genoa Low or an April-May Atlas Low moves through the eastern Mediterranean basin. Multilayered clouds form, with bases as low as 1,000 feet (305 meters) and tops to 45,000 feet (13.5 km) MSL. Atlas Lows that travel northeastward into the Black Sea and the Soviet Union are relatively cloud-free. Cumulus and cumulonimbus, with 2,500- to 4,000-foot (760- to 1,220-meter) bases and 25,000-foot (7.5-km) MSL tops, form ahead of and along the cold front. Stratocumulus forms in the warm sector as North African air moves over the Mediterranean Sea and thickens due to orographic uplift along the western Taurus Mountains. Bases range from 2,500 to 4,000 feet (760 to 1,220 meters); tops are less than 6,000 feet (1,830 meters) MSL. Mid- and upper-level clouds occur when an upper-level trough imposes itself on the Atlas Low. Extremely low ceilings (500 feet/150 meters) occur during heavy showers and thunderstorms.

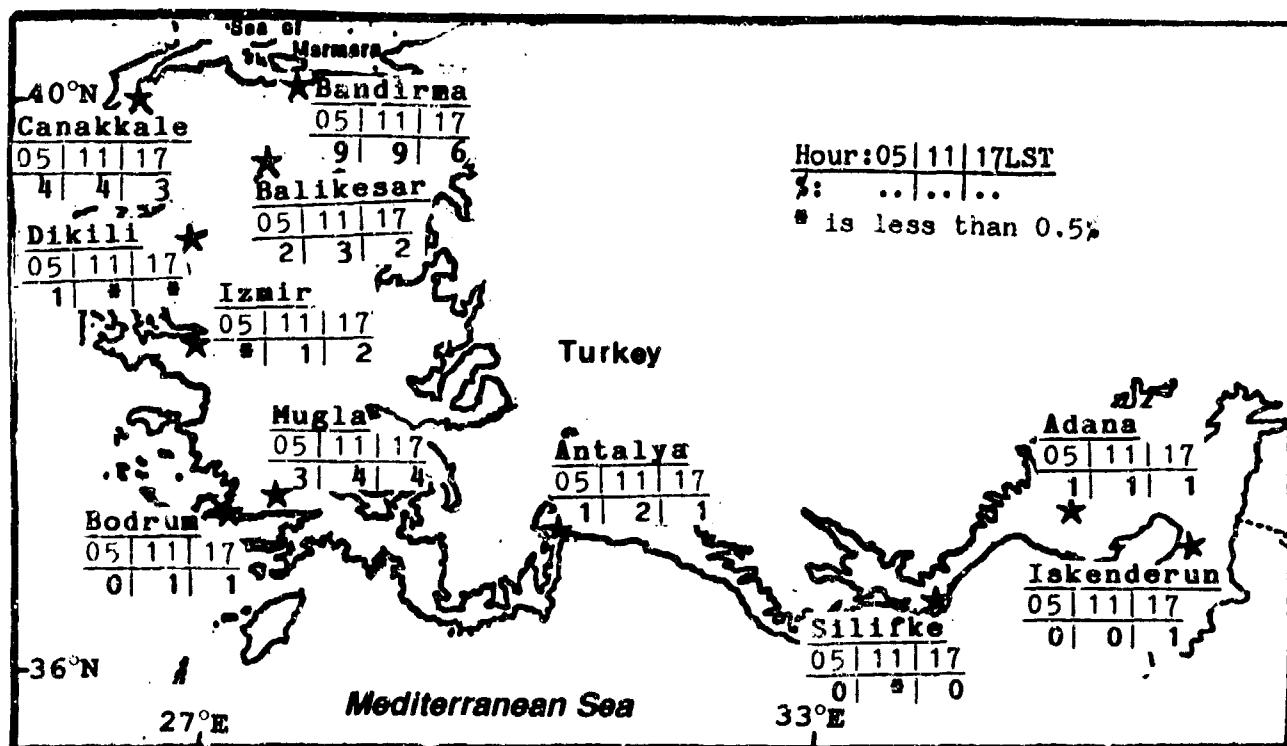


Figure 3-11. Mean Spring Frequencies of Ceilings Below 3,000 Feet (915 meters), Turkish Coast.

THE TURKISH COAST SPRING

March-May

VISIBILITY. The effects of migratory lows on fog and precipitation intensity weaken steadily. Frequencies of visibilities below 7 miles decrease; fog is the primary visibility restriction. Radiation fog forms between 0500 and 1200 LST with light winds and stagnant high pressure; visibility is below 3 miles if enough moisture is present. Sea fog is possible in early spring, but is less frequent when sea surface temperatures rise by late May. Sea fogs develop near the Marmara and northern Aegean Sea coasts and can persist until the prevailing synoptic flow clears out the stagnant air mass. Thick fog may form ahead of warm fronts or behind cold fronts when temperature changes are abrupt and the air masses are moist, but visibilities rarely drop below 3 miles. Thin stratus obscures higher ridges.

Precipitation restricts visibility in spring, but less frequently by May. Genoa or Atlas Lows that track through the eastern Mediterranean basin usually produce 3- to 7-mile visibilities in steady rain or drizzle. Visibilities can go below 3 miles if precipitation combines with fog. Rare spring snow squalls can reduce visibility to less than a mile. Heavy rain showers and thunderstorms along cold fronts or in the sea breeze convergence can lower visibilities to 3 miles for brief periods. Most visibilities below 3 miles occur along the Sea of Marmara coast and inland from the Aegean coast, as shown in Figure 3-12. Southern Turkey rarely sees visibilities below 3 miles.

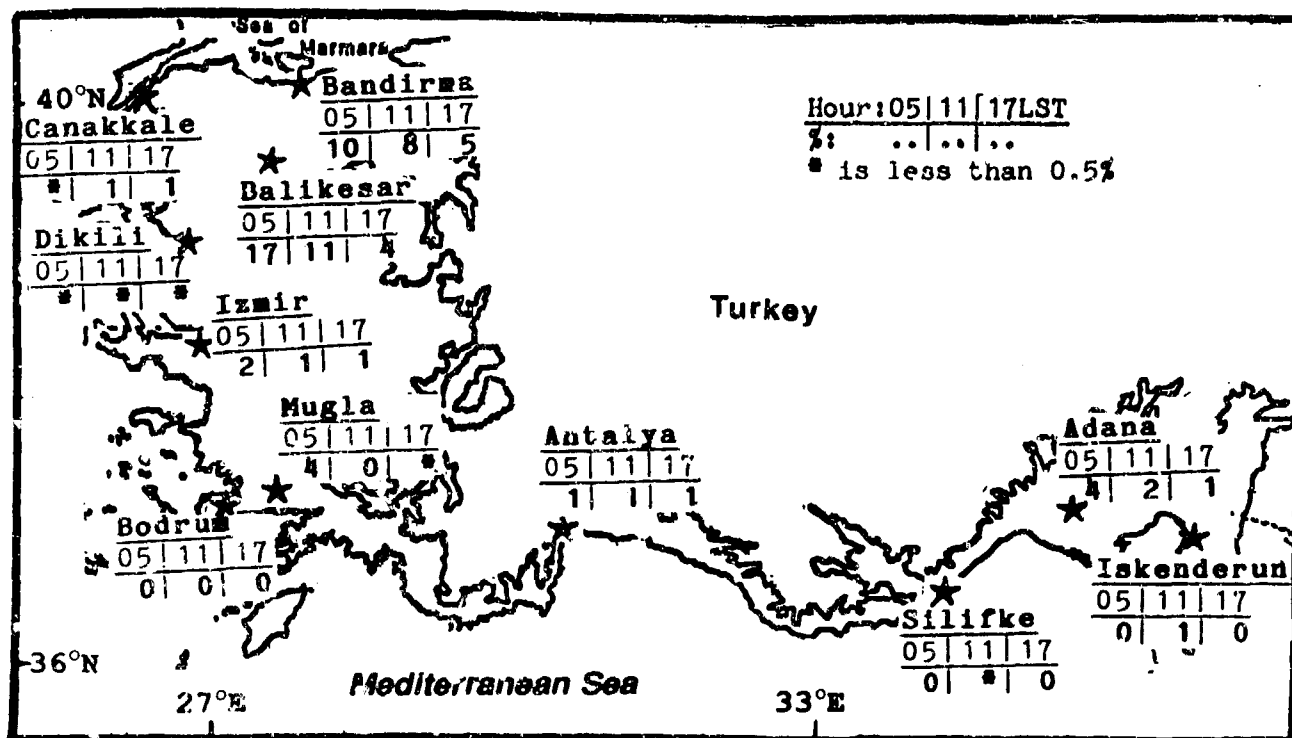


Figure 3-12. Mean Spring Frequencies of Visibilities Below 3 Miles, Turkish Coast.

Dust, haze, and smoke are rare, but southerly flow from Atlas Lows brings in dust from North Africa on 1 or 2 days each spring. Blowing dust from intense Atlas Lows may lower visibilities to less than a mile. Dust aloft can remain suspended for several hours up to 20,000 feet (6 km) MSL, producing a reddish haze. Rainfall mixing with this haze causes "red rains." Haze

and smoke reduces visibility to 3 to 6 miles only when enhanced by local topography and urbanization. Haze is common at Izmir, on a fjord-like inlet. Smoke, which accumulates under inversions in stagnant air masses, is common in the industrial and agricultural areas between the Sea of Marmara and Balikesar.

THE TURKISH COAST SPRING

March-May

WINDS. Flow is consistently southwesterly at 5 to 10 knots except on the immediate Sea of Marmara coast, where winds are northeasterly at 8 to 13 knots. Winds are strongest in March Siroccos, when speeds up to 55 knots are possible. Large-scale warming on the Anatolian Plateau lessens cold air drainage and mountain wind strength. Land/sea and mountain/valley breezes are well-defined during spring except along the Sea of

Marmara, where Asiatic High outflow still dominates. Figure 3-13 provides April surface wind roses.

The springtime winds aloft shown in Figure 3-6 shift to summer's northwesterly flow by May between 5,000 and 20,000 feet (1,525 and 6,100 meters) MSL. Peak speeds (40 to 50 knots) are near 35,000 feet (10.5 km) MSL.

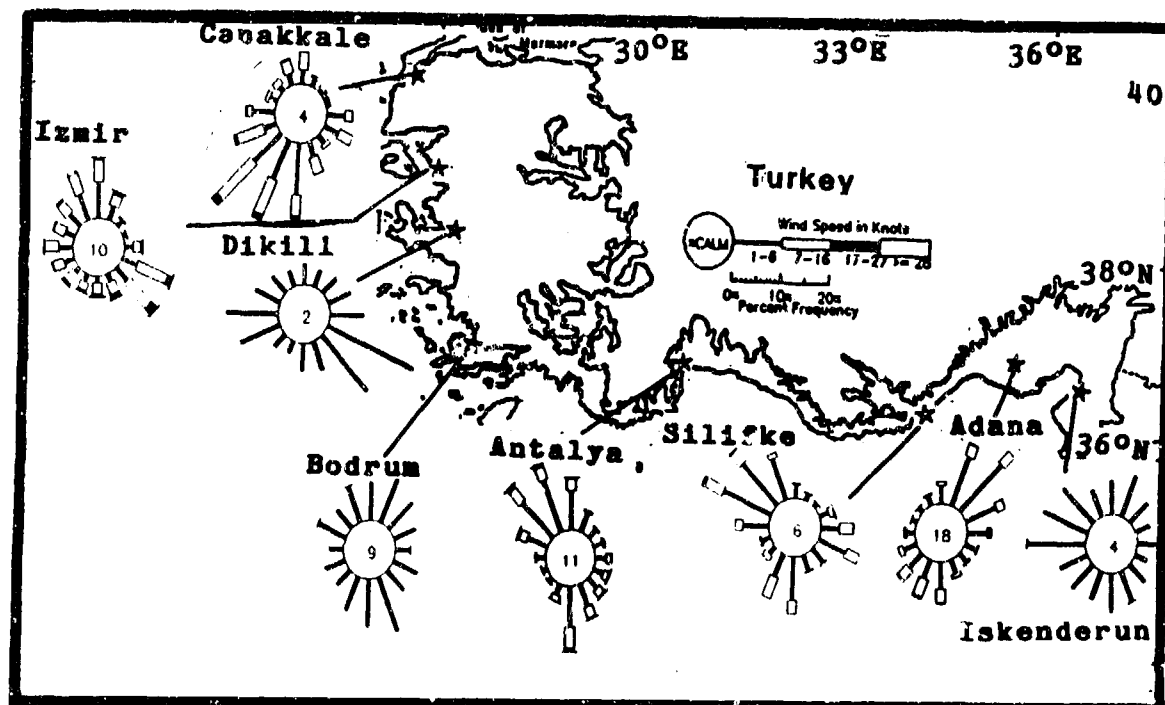


Figure 3-13. April Surface Wind Roses, Turkish Coast.

THE TURKISH COAST
SPRING

March-May

PRECIPITATION. As the Genoa Low storm track gradually migrates northward, mean precipitation decreases across the area, as shown in Figure 3-14.

Genoa or Atlas Lows tracking along the Mediterranean coast produce heavy rain, drizzle, or even snow.

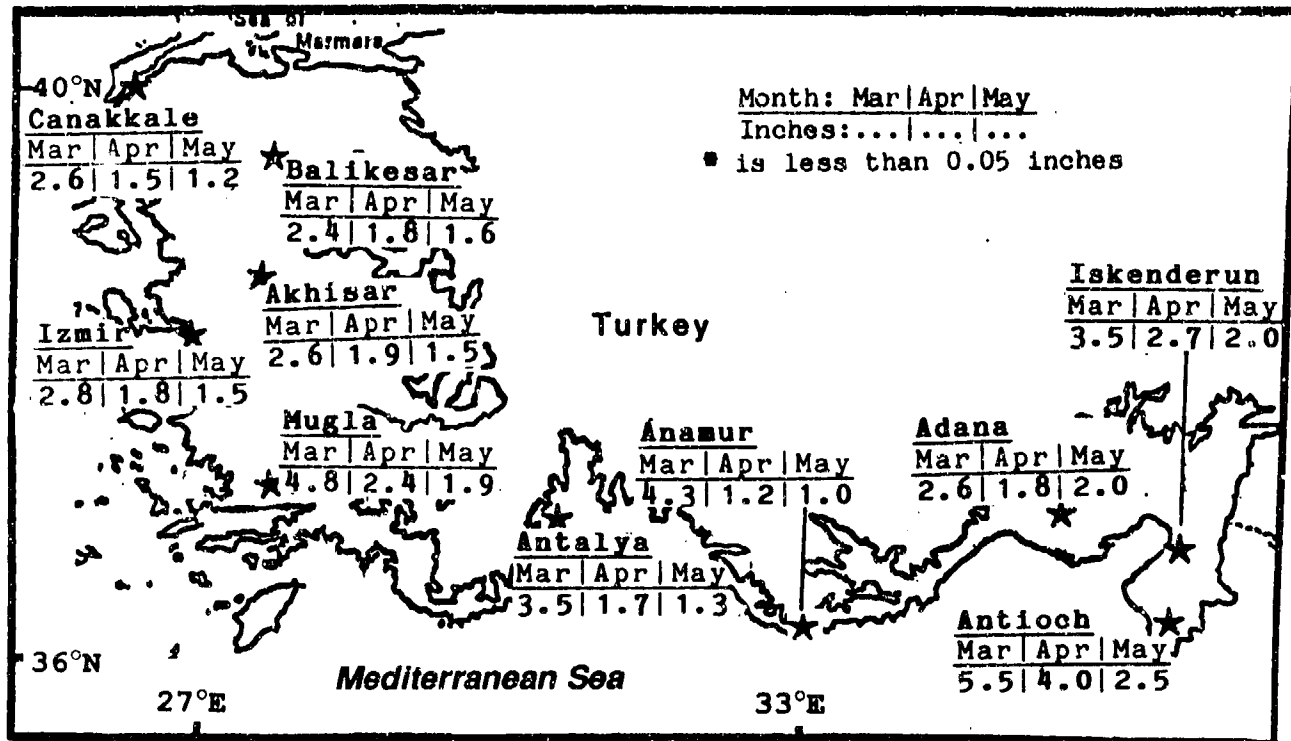


Figure 3-14. Mean Spring Monthly Precipitation, Turkish Coast.

THE TURKISH COAST SPRING

March-May

The entire region averages between 3 and 11 spring thunderstorm days, as shown in Figure 3-15. Thunderstorm frequency increases to a yearly maximum in May or early June as intense surface heating enhances frontally produced thunderstorms. Many stations record

half or more of their spring thunderstorm days in May. The strong winds from Atlas Lows induce orographic showers and thunderstorms near the Taurus Mountains. Rain showers and thunderstorms may form along the sea-breeze front.

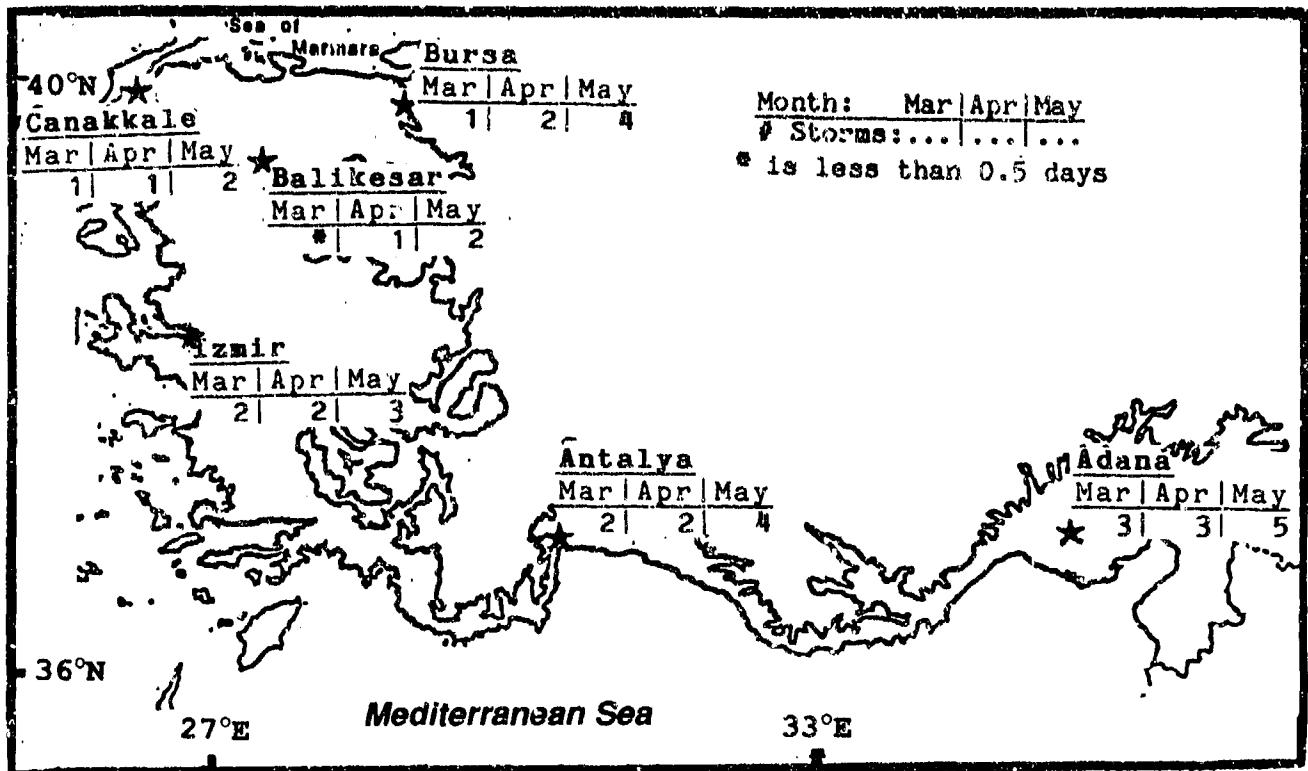


Figure 3-15. Mean Spring Thunderstorm Days, Turkish Coast.

THE TURKISH COAST SPRING

March-May

TEMPERATURE. Mean daily highs, given in Figure 3-16, range from 54 to 81° F (12 to 27° C). Highest temperatures (93° F/34° C at Canakkale and 109° F/43° C at Antioch) occur in May. Temperatures can rise suddenly into the 90's° F (32 to 34° C) in late March when an Atlas Low brings extremely hot and dry Saharan air (Sirocco) into the region; extremely high

temperatures may persist for 1 to 3 days. Mean daily lows range from the high 30's° F (3° C) to the low 60's° F (16° C). Temperatures are seldom below freezing after mid-April. Record lows include 17° F (-8° C) at Canakkale, 34° F (1° C) at Anamur, and 23° F (-5° C) at Adana.

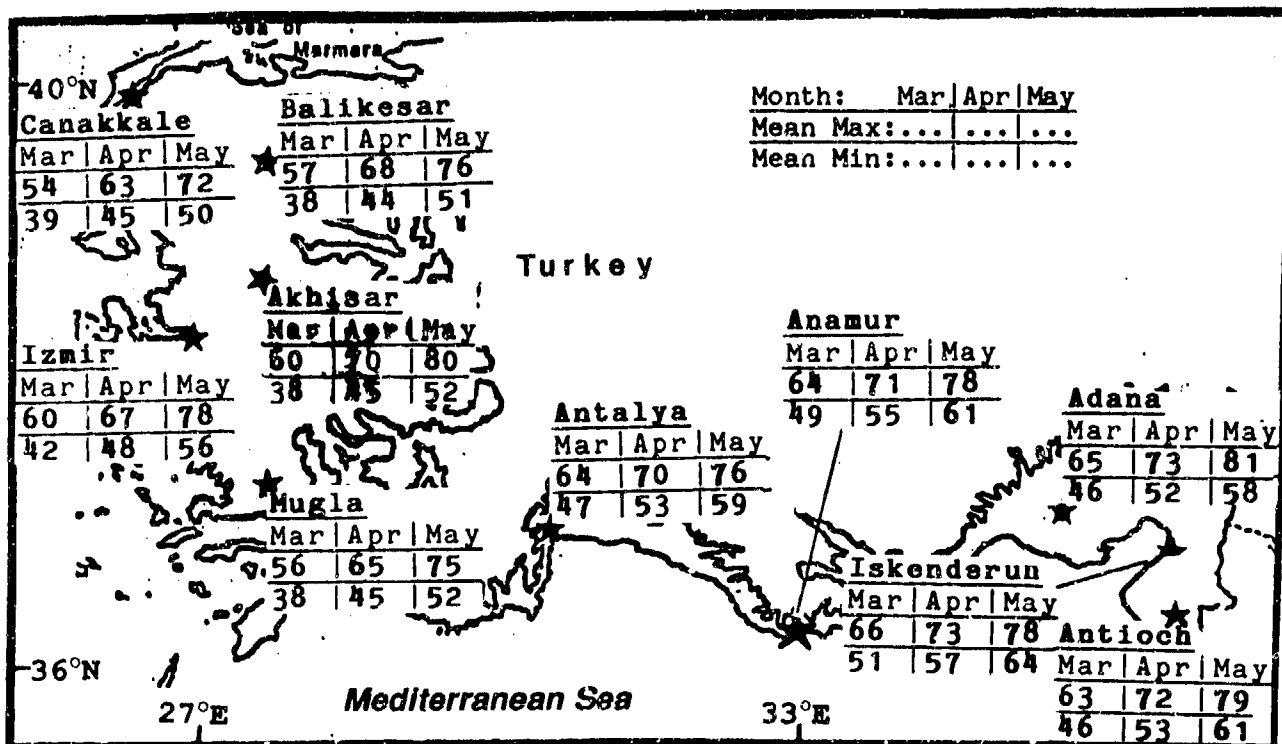


Figure 3-16. Mean Spring Daily Maximum/Minimum Temperatures (F), Turkish Coast.

GENERAL WEATHER. Weak cyclonic activity, diurnal convection, and the Etesian winds are now in control. Although the summer storm track is displaced over northern Europe, upper-air disturbances reach the Turkish Coast on 1 to 2 days a month and touch off isolated showers and thunderstorms. Thunderstorm activity is enhanced by strong daytime surface heating and a well-defined sea-breeze circulation. The sea breeze supplies the moisture for orographic showers along the Taurus Mountains. The Anatolian Plateau Thermal Trough produces a persistent northerly gradient flow (the Etesian, which see) in July and August.

SKY COVER. Only one weak low a month crosses the region. Diurnal cumulus provides most summertime cloud cover. Mean summer cloud cover averages about 30% along the Marmara coast and in the southeast, but less than 10% in the southwest. Ceilings below 3,000 feet (915 meters) are rare during summer; as shown in Figure 3-17, they are reported less than 6% of the time, normally near sunrise. Etesian winds enhance the stratocumulus and fair-weather cumulus that develops along the Sea of Marmara coast. Stratocumulus develops

from morning stratus with bases at 200 to 1,000 feet (60 to 305 meters), and is seldom more than 300 feet (90 meters) thick. The sea breeze along the southern coast enhances the fair-weather cumulus associated with orographic uplift. Stratocumulus and fair-weather cumulus bases are between 3,000 and 4,000 feet (915 and 1,220 meters), but stratocumulus bases may form at 1,500 feet (455 meters) along the southern slopes of the Taurus Mountains; tops go to 12,000 feet (3,655 meters) MSL.

Middle and high clouds form with weak summer disturbances and jet streams that produce thin cirrus with 20,000-foot (6-km) MSL bases. Rare cold fronts and upper-level disturbances may produce frontal cumulus, towering cumulus and cumulonimbus. Typically, cloud bases are in the 3,000- to 6,000-foot (915- to 1,830-meter) range. Cumulus tops reach 15,000 feet (4,570 meters) MSL, but towering cumulus and cumulonimbus may reach 50,000 feet (15 km) MSL. Cloud bases are near 500 feet (150 meters) in heavy downpours.

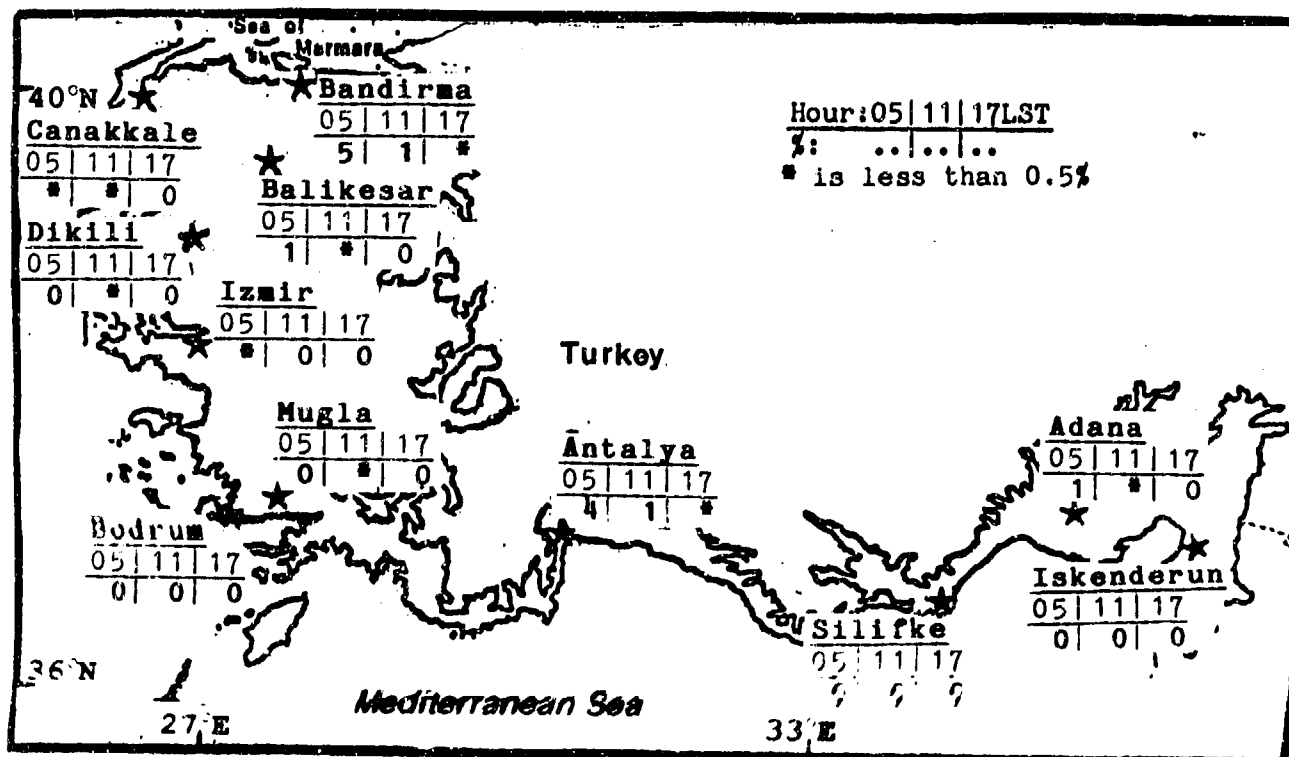


Figure 3-17. Mean Summer Frequencies of Ceilings Below 3,000 Feet (915 meters), Turkish Coast.

THE TURKISH COAST SUMMER

June-August

VISIBILITY. Visibilities after June are generally good. Figure 3-18 shows that summer visibilities below 3 miles are rare. Greatest low-visibility frequencies occur along the Sea of Marmara coast south to Balıkesar and around Adana. Morning radiation fog causes most poor

visibilities, but with June cyclonic activity, heavy precipitation can reduce visibilities to between 3 and 7 miles. Rain showers and thunderstorms along sea-breeze fronts also lower visibilities. June migratory lows cause most visibility reductions in precipitation.

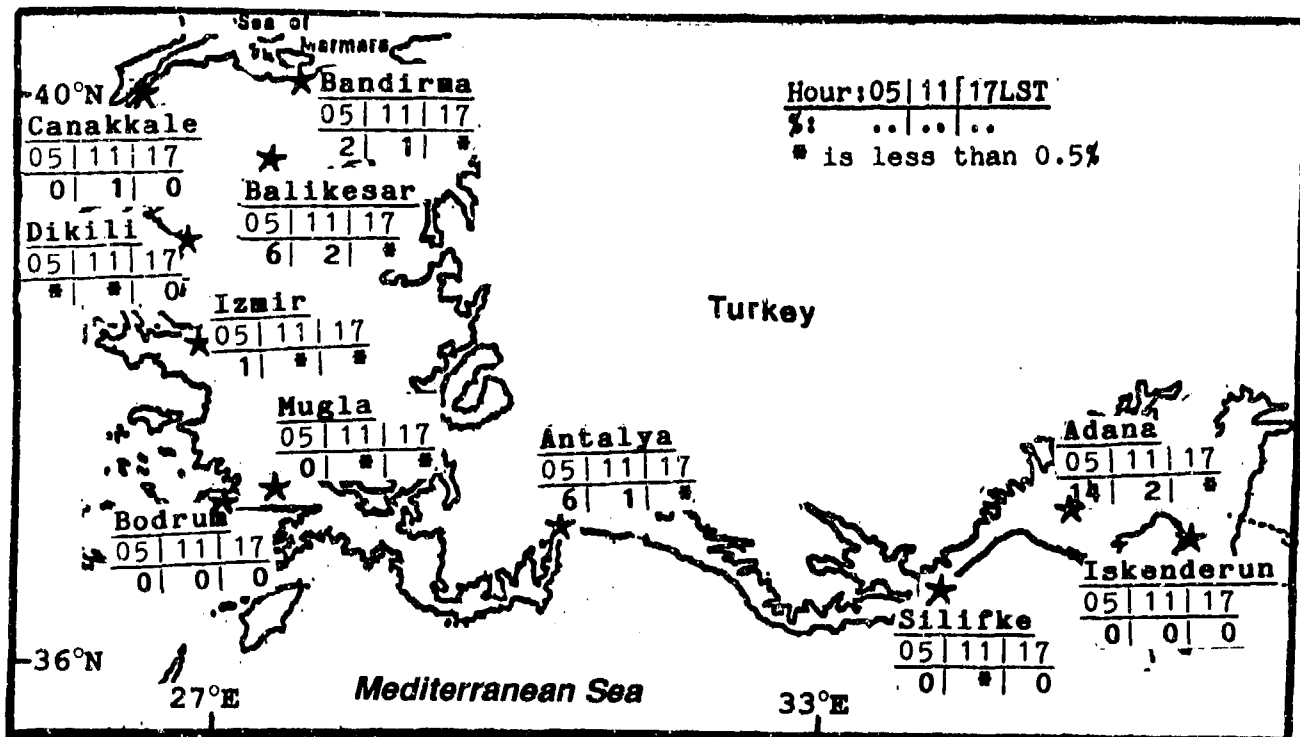


Figure 3-18. Mean Summer Frequencies of Visibilities Below 3 Miles, Turkish Coast.

Dust, haze, and smoke are rare. Local microbursts from thunderstorms or sea-breeze gusts in open beach areas may transport dust or sand, but visibilities rarely go below 6 miles. Rare June Atlas Lows can bring in North African dust. Haze and smoke rarely reduce visibilities to less than 3 miles. Izmir is most likely to report haze with 3- to 6-mile visibilities because of its topography, urbanization, and large-scale stagnant air problems. Smoke is confined to the industrial and agricultural areas between Canakkale and Golcuk, and south to Balıkesar.

WINDS. Etesian northerly surface flow at 10 to 15 knots dominates the western and southwestern Turkish Coast between mid-July and mid-August. These winds

penetrate southward to the western Mediterranean Sea coast, but the Taurus Mountains block direct northerly flow east of Antalya. Tight surface pressure gradients between the Anatolian Plateau Thermal Trough and the Balkan High produced the highest recorded summer wind gusts (31 knots from the NE at Canakkale and 42 knots from the NNE at Izmir). The prevailing northerlies almost completely overpower the land/sea breeze west and north of Antalya, except at Dikili. At stations east of Antalya, pronounced land/sea and mountain/valley circulations overcome the prevailing north-northwesterly flow. Summer winds at Izmir and Antalya, because of the rugged terrain, are almost the same as in winter, but speeds are less. See Figure 3-19.

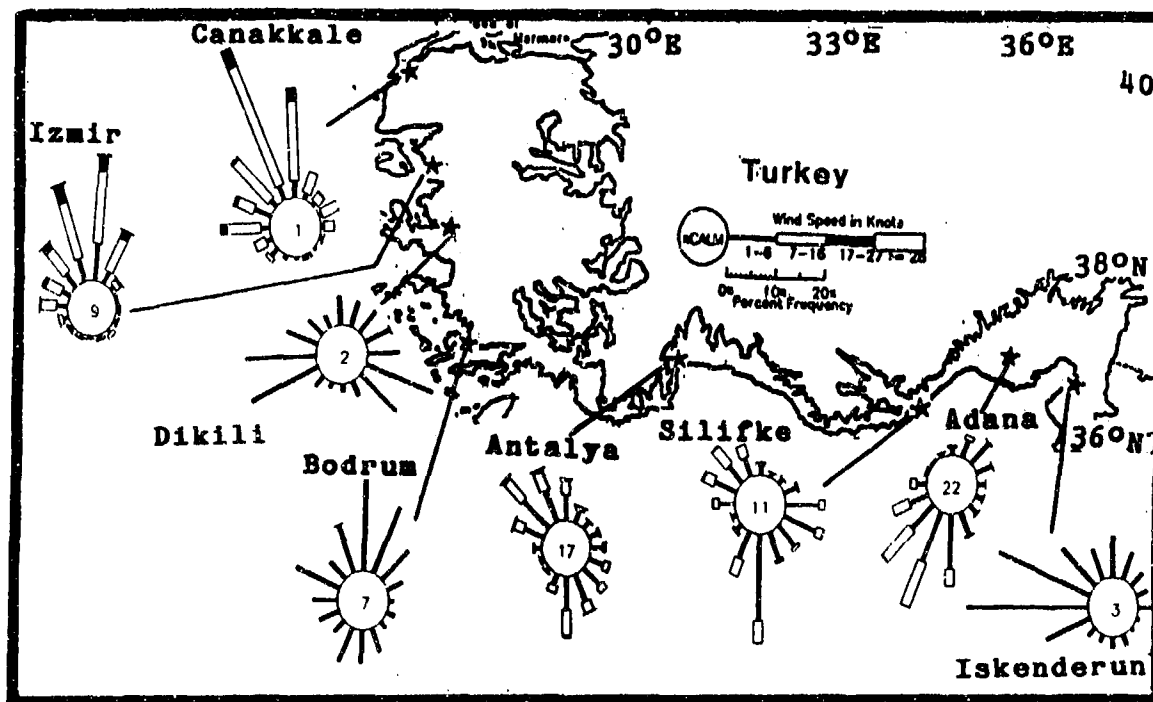


Figure 3-19. July Surface Wind Roses, Turkish Coast.

As shown in Figure 3-6, summer winds aloft are northwesterly below 20,000 feet (6 km) MSL, backing to westerly at higher levels. Peak speeds, about 60 knots at 40,000 feet (12 km) MSL, are highest in the summer.

THE TURKISH COAST SUMMER

June-August

PRECIPITATION. Summer is the driest season. As shown in Figure 3-20, precipitation averages less than 1.3 inches (32 mm) a month, and many locations get less

than 0.3 inches (8 mm) a month. In July and August, rainshowers are isolated. The most rain falls south of the Taurus Mountains above 1,600 feet (485 meters).

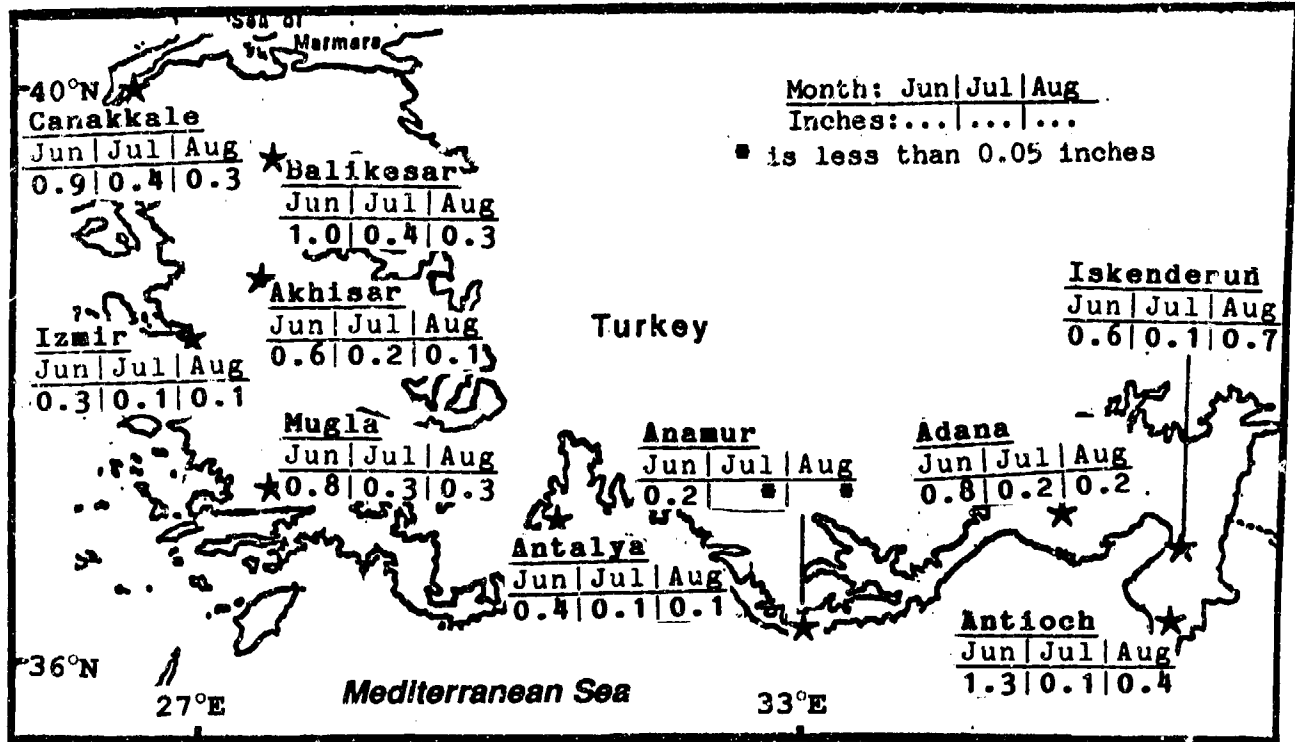


Figure 3-20. Mean Summer Monthly Precipitation, Turkish Coast.

THE TURKISH COAST SUMMER

June-August

Figure 3-21 suggests that, except in protected areas such as Izmir, there are between 4 and 7 thunderstorm days a summer. Thunderstorm activity is concentrated along the Taurus Mountains and western Anatolian

Plateau due to the orographic uplift of moist sea breezes. Also, Etesian winds cause a thunderstorm increase along the Sea of Marmara coast. Occasionally, a weak upper-level disturbance triggers squall lines.

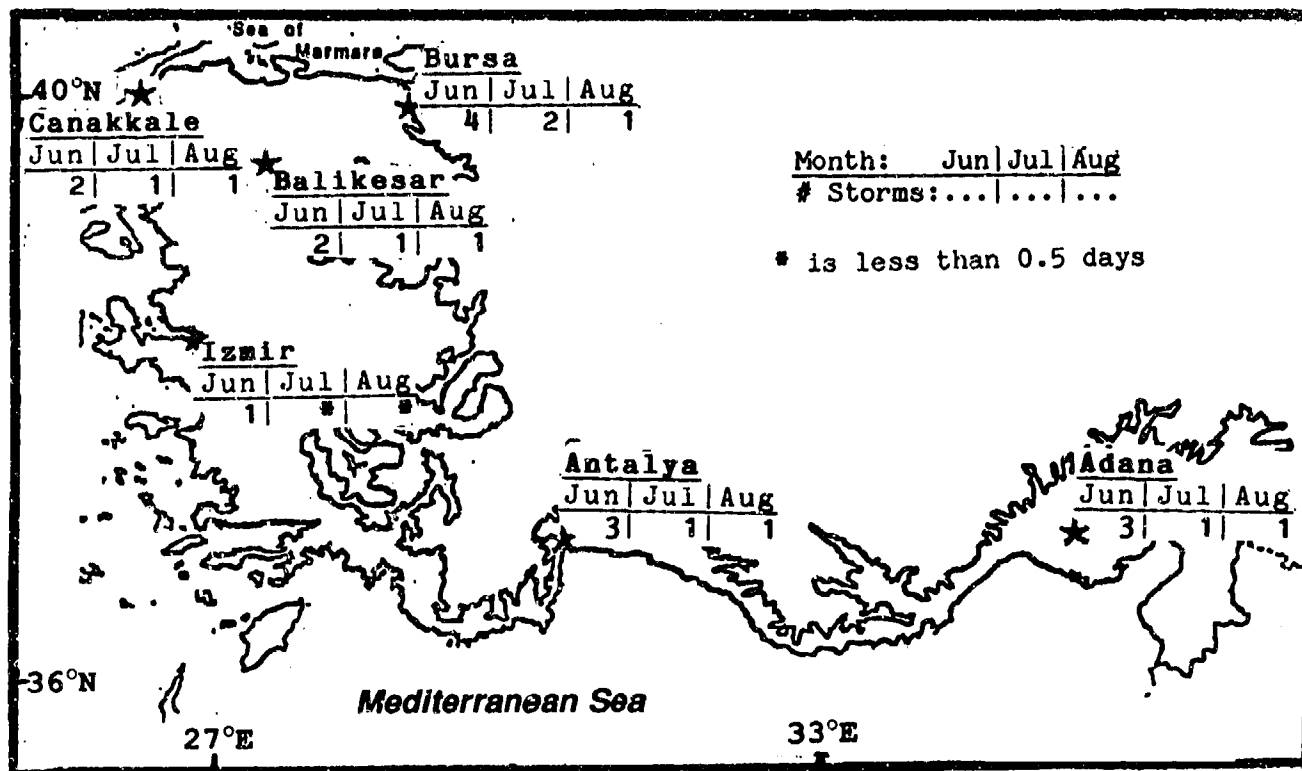


Figure 3-21. Mean Summer Thunderstorm Days, Turkish Coast.

THE TURKISH COAST SUMMER

June-August

TEMPERATURE. As shown by Figure 3-22, southwest Turkey is the warmest part of the region during the summer. Mean daily highs range from 81° F (24° C) to 94° F (34° C). Record highs exceed 100° F (38° C) everywhere, and Adana's 114° F (46° C) is the region's highest temperature. Mean daily lows range

from 53° F (12° C) to 77° F (25° C). The lower range of these temperatures is confined to the Sea of Marmara coast where Etesian winds moderate coastal temperatures. Record lows are 39° F (4° C) at Balıkesir, 49° F (9° C) at Adana, and 59° F (14° C) at Iskenderun.

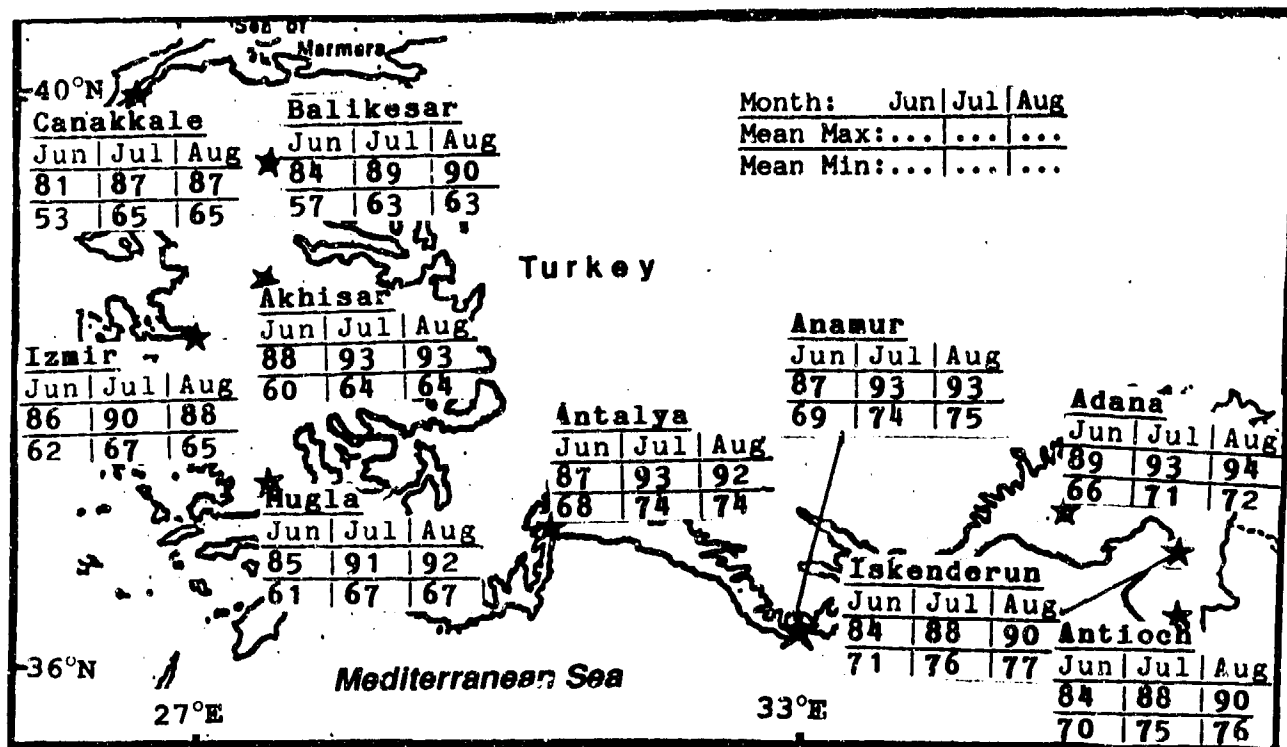


Figure 3-22. Mean Summer Daily Maximum/Minimum Temperatures (F), Turkish Coast.

GENERAL WEATHER. A large-scale trough centered over the Mediterranean Sea forms between the Azores and Asiatic Highs, and directs late-fall cyclonic storms through the Mediterranean basin. Polar air surges, heavy rains, and snow reach the Turkish Coast by late October.

SKY COVER. Mean cloud cover increases by about 30% during the fall as more lows (either Atlas or Genoa), migrate through the region. Cyclonic activity produces multilayered clouds. Lows moving northeastward through the Sea of Marmara usually form thicker cumulus, towering cumulus, and cumulonimbus within 50 to 100 NM of the low-pressure center. Cloud bases are 3,000 to 6,000 feet (915 to 1,830 meters), with towering cumulus and cumulonimbus tops reaching 45,000 feet (13.5 km) MSL. Bases may lower to 500 feet (150 meters) in heavy showers. Cirrus and altocumulus provide upper cloud cover. Cirrus is thin, forming above 18,000 feet (5,485 meters) MSL; altocumulus forms between 8,000 and 16,000 feet (2,440 and 4,875 meters) MSL. If the low moves over the

eastern Mediterranean Sea, these clouds form up to 200 miles from the low's center. Bases are usually lower, between 1,000 and 3,000 feet (305 and 915 meters). Thicker clouds become more common by November with Atlas Lows. In November, cool Aegean and Mediterranean Seas and warm North African air advection enhance these lows' warm-front stratocumulus.

Stratocumulus is common on Turkey's southern coast. Cold air drainage from the Anatolian Plateau or coastal Taurus Mountains flows offshore over the warmer water between 0400 and 0700 LST and forms stratocumulus that moves onshore with the sea breeze. The stratocumulus, with bases between 400 and 1,000 feet (120 and 305 meters), is lifted orographically to 1100 LST until its tops reach 3,000 to 4,000 feet (915 to 1,220 meters) MSL. Ceilings below 3,000 feet (915 meters) increase in late fall in the northwestern corner of the region as lower stratocumulus is advected onshore. See Figure 3-23.

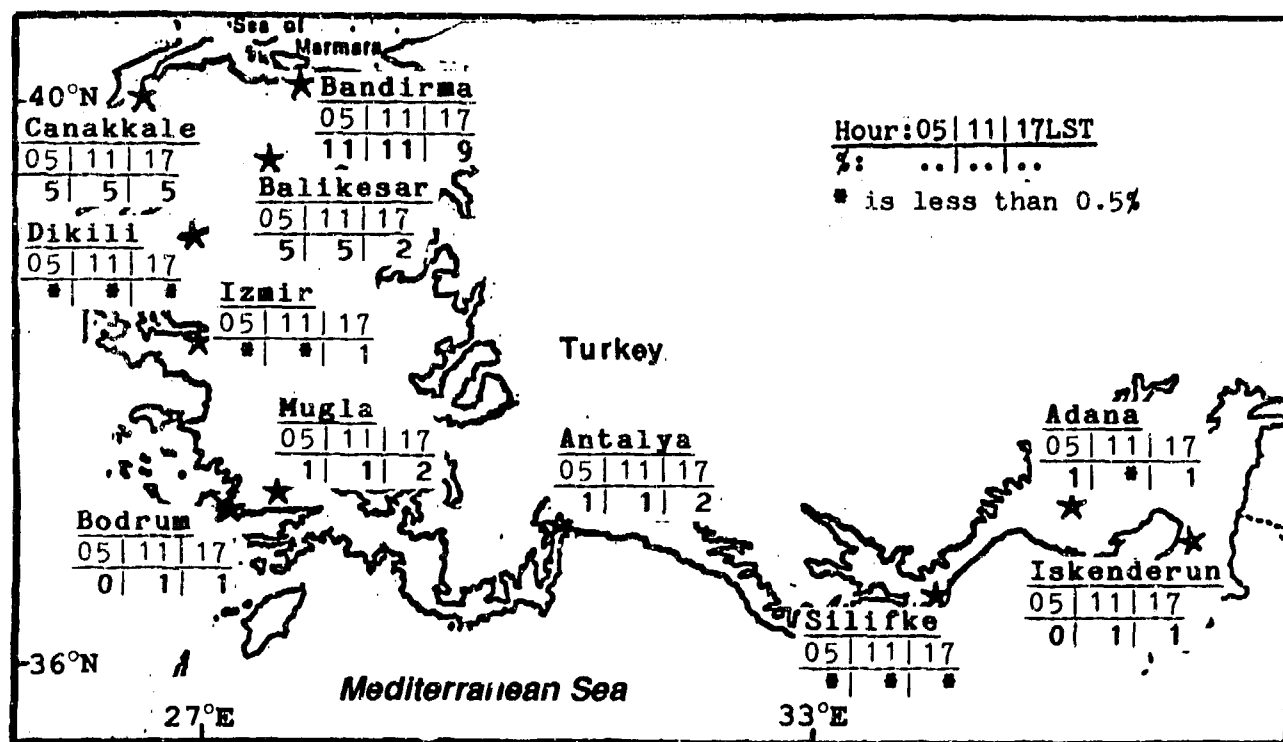


Figure 3-23. Mean Fall Frequencies of Ceilings Below 3,000 Feet (915 meters), Turkish Coast.

VISIBILITY. Fall visibilities are generally good, but they go below 7 miles slightly more frequently between the end of summer and October. The frequency of visibilities below 3 miles increases another 10-20% north of Mugla in November. Morning radiation fog, the primary fall visibility restriction, often drops visibilities to less than 3 miles. By late October, increasingly intense frontal and migratory low precipitation also reduces visibilities below 3 miles. Local topography that enhances synoptically-caused restrictions is another cause of visibilities below 3 miles.

Warm fronts cause advection fog in November when the land surface is cold, especially on the western Turkish Coast if the warm sector airmass is moist and slow-moving. Sea fogs form along the Sea of Marmara during weak synoptic flow. Rain showers and thunderstorms occurring with cyclonic activity may lower visibility to less than a mile for periods of less than an hour. Visibility in steady rain, drizzle, and snow squalls is usually 5 to 7 miles, but 3 miles when combined with fog. Rare November snow squalls can reduce visibility to less than a mile.

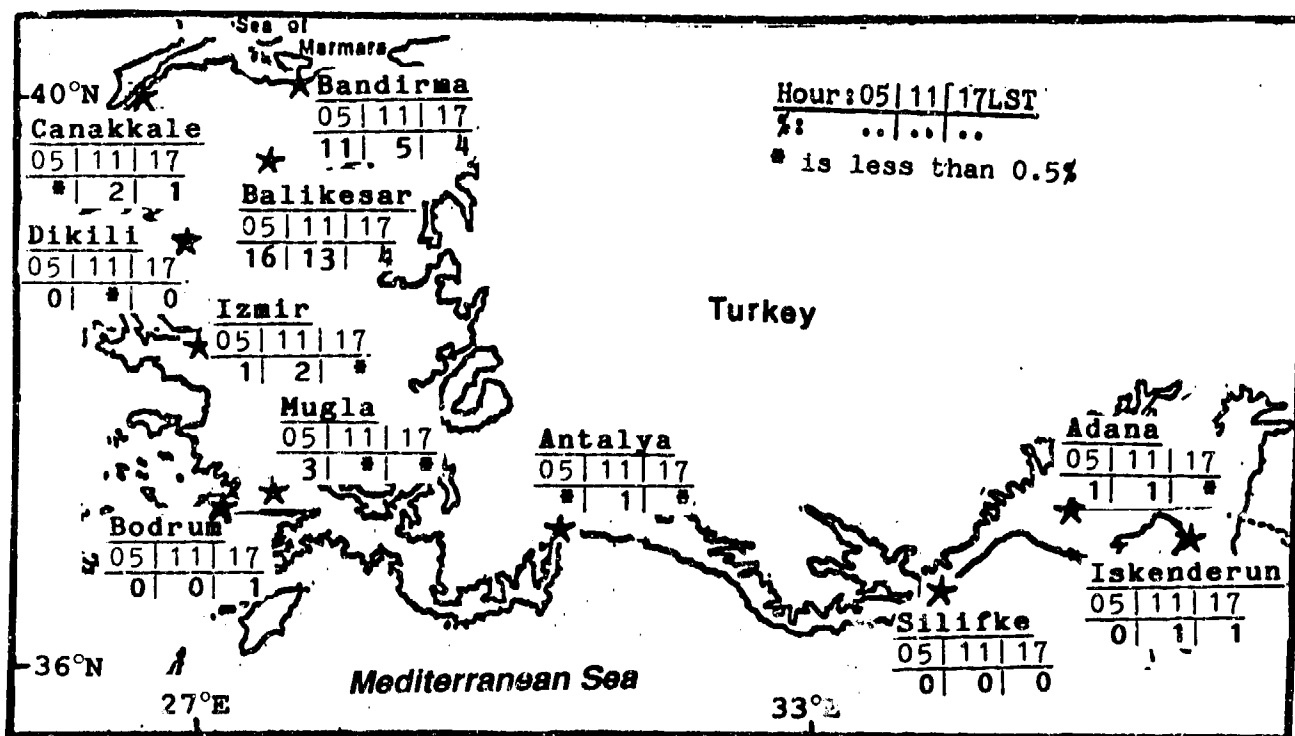


Figure 3-24. Mean Fall Frequencies of Visibilities Below 3 Miles, Turkish Coast.

Dust, haze, and smoke are rare. Atlas Lows and thunderstorm gust fronts produce blowing dust and sand if the winds are very strong (greater than 25 knots); visibility can drop to less than a mile. Haze forms with lighter winds. Dust persists at 20,000 feet (6,100 meter) MSL after a strong Atlas Low, producing a reddish haze.

Haze and smoke rarely reduce visibilities to below 3 miles. Izmir consistently reports haze between 3 and 6 NM because local terrain traps industrial smoke and marine moisture between elevated ridges. The industry and agriculture between Canakkale and Golcuk and then south to Balikesar produces a rare report of smoke.

THE TURKISH COAST FALL

September-November

WINDS. The flow along the western coast of Turkey transitions from the summer Etesians in mid-September to north-northwesterly flow from the strengthening Asiatic High, channeled by terrain into the Aegean Sea. This north-northwesterly flow seldom penetrates south of 38° N in the fall. The Taurus Mountains shelter the southern Turkish Coast from this flow; synoptic flow (originating from the Azores High) is southwesterly in this area. The two distinct flow patterns meet between Bodrum and Silifke. Wind speeds over the entire area

are about 5 to 10 knots. Land/sea breezes are less pronounced in the fall, especially in the northwest. Drainage winds from the Anatolian Plateau and Atlas Mountains increase and channel down the valleys, as shown by the wind roses in Figure 3-25.

During the fall, winds aloft shift back to westerly above 5,000 feet (1,525 meters) MSL as the storm track moves south (see Figure 3-6).

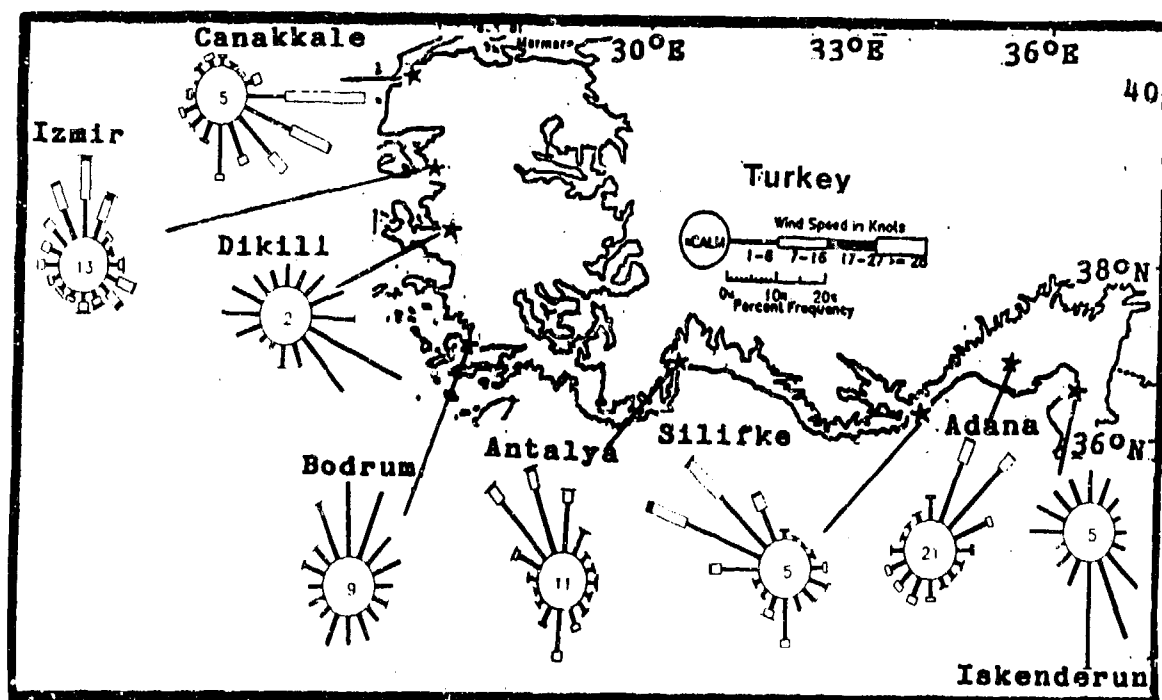


Figure 3-25. October Surface Wind Roses, Turkish Coast.

THE TURKISH COAST FALL

September-November

PRECIPITATION. The mean fall precipitation amounts shown in Figure 3-26 reflect increasing November cyclonic storm frequencies. Lows tracking across the eastern Mediterranean cause extensive areas of rain and drizzle. Rain showers and thunderstorms occur

near cold fronts traveling northeastward. These fronts become more frequent as fall progresses. Snow showers are possible late in the season, and contribute to Iskenderun's and Antioch's high precipitation amounts.

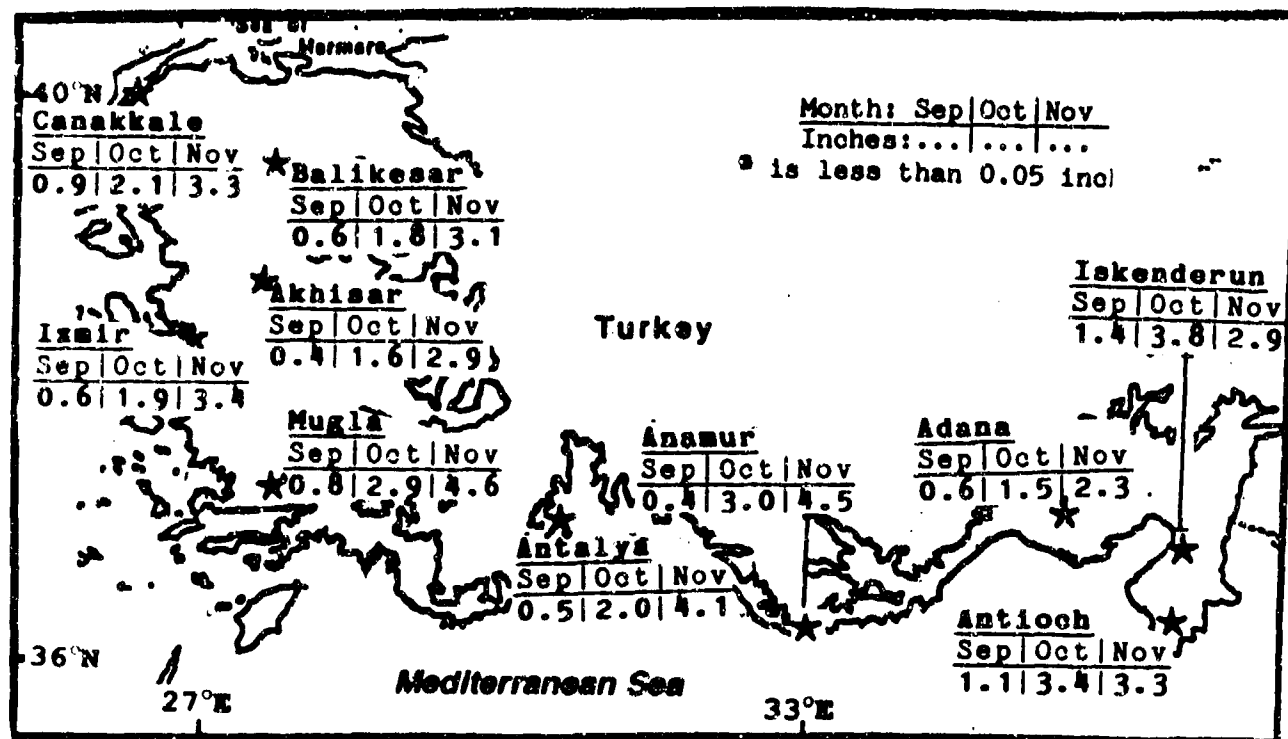


Figure 3-26. Mean Fall Monthly Precipitation, Turkish Coast.

THE TURKISH COAST FALL

September-November

As shown in Figure 3-27, thunderstorm days increase because of increasing frontal activity. Thunderstorm

frequency diminishes along the immediate Sea of Marmara coast due to the cessation of the Etesian winds.

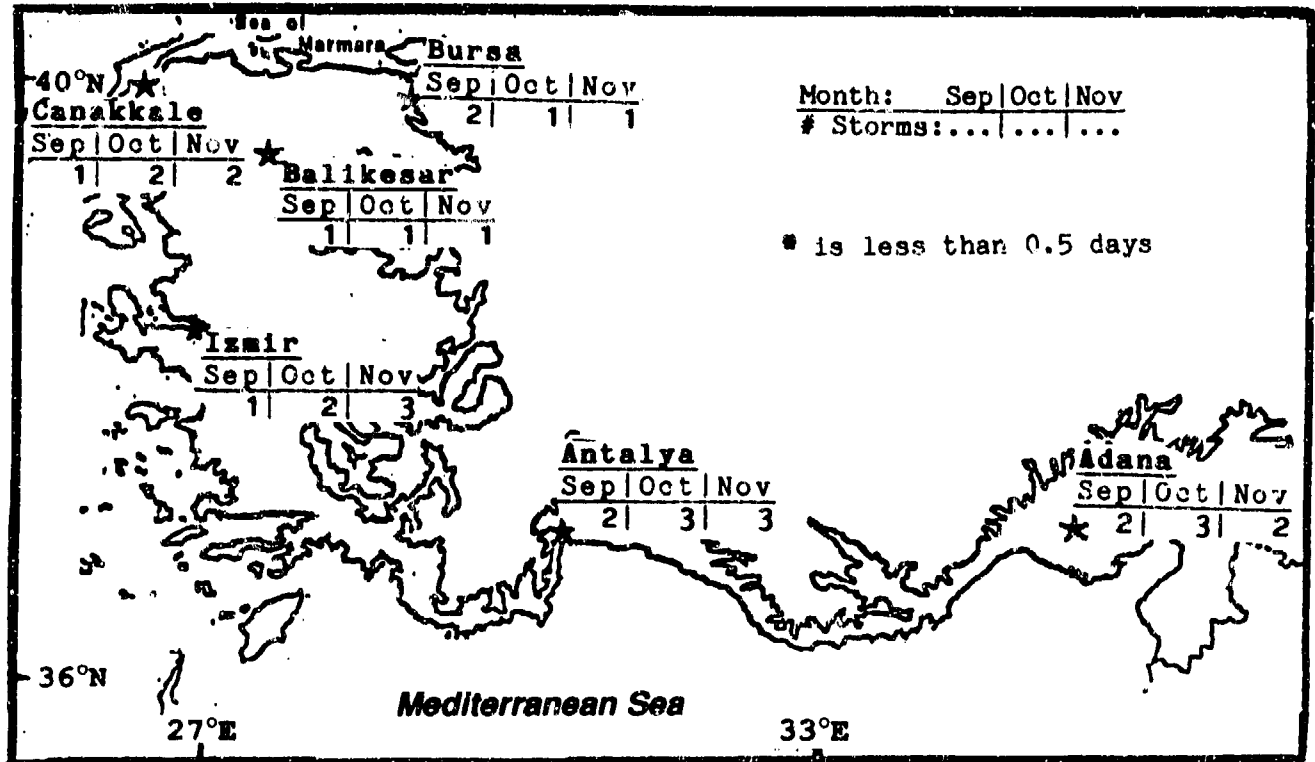


Figure 3-27. Mean Fall Thunderstorm Days, Turkish Coast.

THE TURKISH COAST FALL

September-November

TEMPERATURE. Mean daily highs range from 61° F (16° C) to 94° F (34° C), as shown in Figure 3-28. The lowest temperatures are found along the Sea of Marmara coast. Record highs are 94° F (34° C) at Canakkale and 109° F (43° C) along the Mediterranean coast. An Atlas

Low's hot, dry winds can push afternoon temperatures into the 100-105° F (38-39° C) range. Mean daily lows range from the mid 40's° F (6-8° C) to the low 70's° F (21-23° C). Record lows are 13° F (-11° C) at Akhisar, 24° F (-4° C) at Adana, and 39° F (4° C) at Anamur.

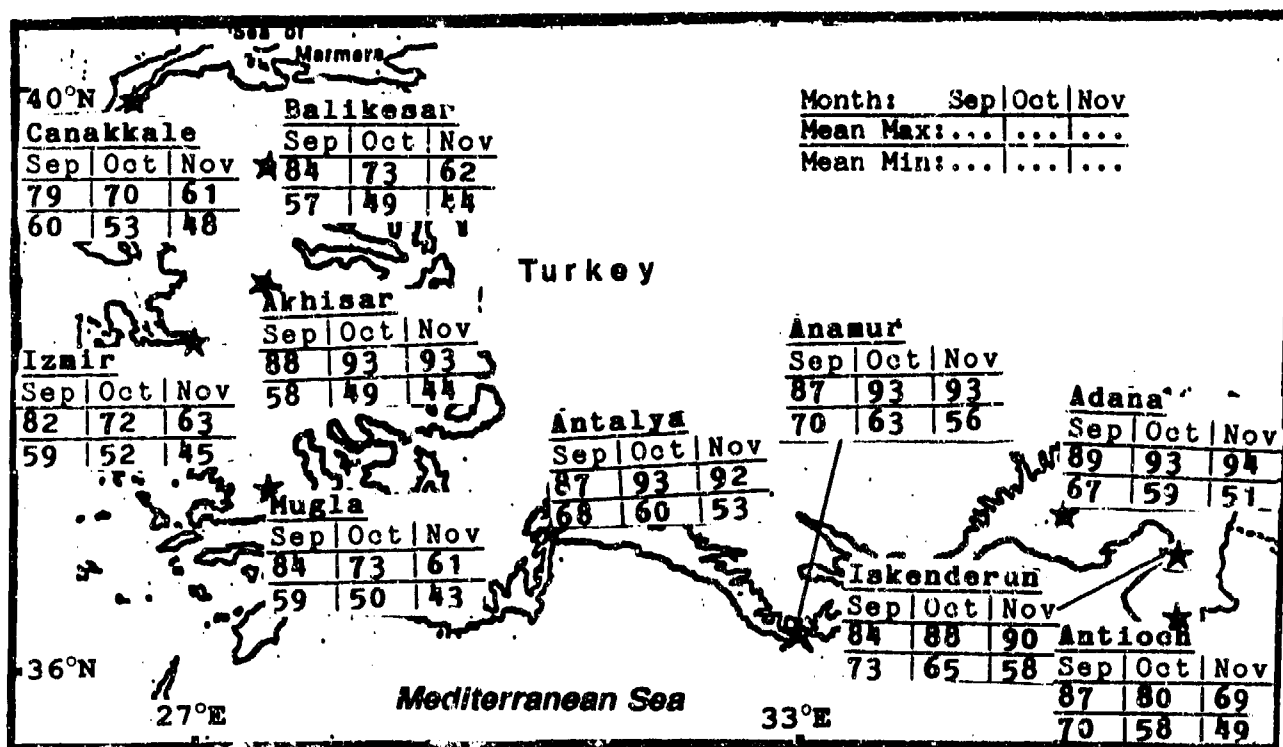


Figure 3-28. Mean Fall Daily Maximum/Minimum Temperatures (F), Turkish Coast.

Chapter 4

THE EASTERN MEDITERRANEAN COAST

The Eastern Mediterranean Coast region extends from the Syria/Turkey border southward and westward to the Suez Canal. It includes all of Israel and Lebanon, western Jordan, small portions of Syria, and Egypt's northern Sinai Desert. After describing the area's situation and relief, this chapter discusses "general weather conditions" by season.

	Page
Situation and Relief	4-2
Winter--December-February	4-6
General Weather ..	4-6
Sky Cover.....	4-6
Visibility	4-8
Winds	4-9
Precipitation	4-11
Temperature	4-14
Spring--March-May	4-15
General Weather	4-15
Sky Cover.....	4-15
Visibility	4-17
Winds	4-18
Precipitation	4-19
Temperature	4-20
Summer--June-August	4-22
General Weather	4-22
Sky Cover.....	4-22
Visibility	4-24
Winds	4-25
Precipitation	4-26
Temperature	4-26
Fall--September-November	4-27
General Weather	4-27
Sky Cover.....	4-27
Visibility	4-29
Winds	4-30
Precipitation	4-31
Temperature	4-33

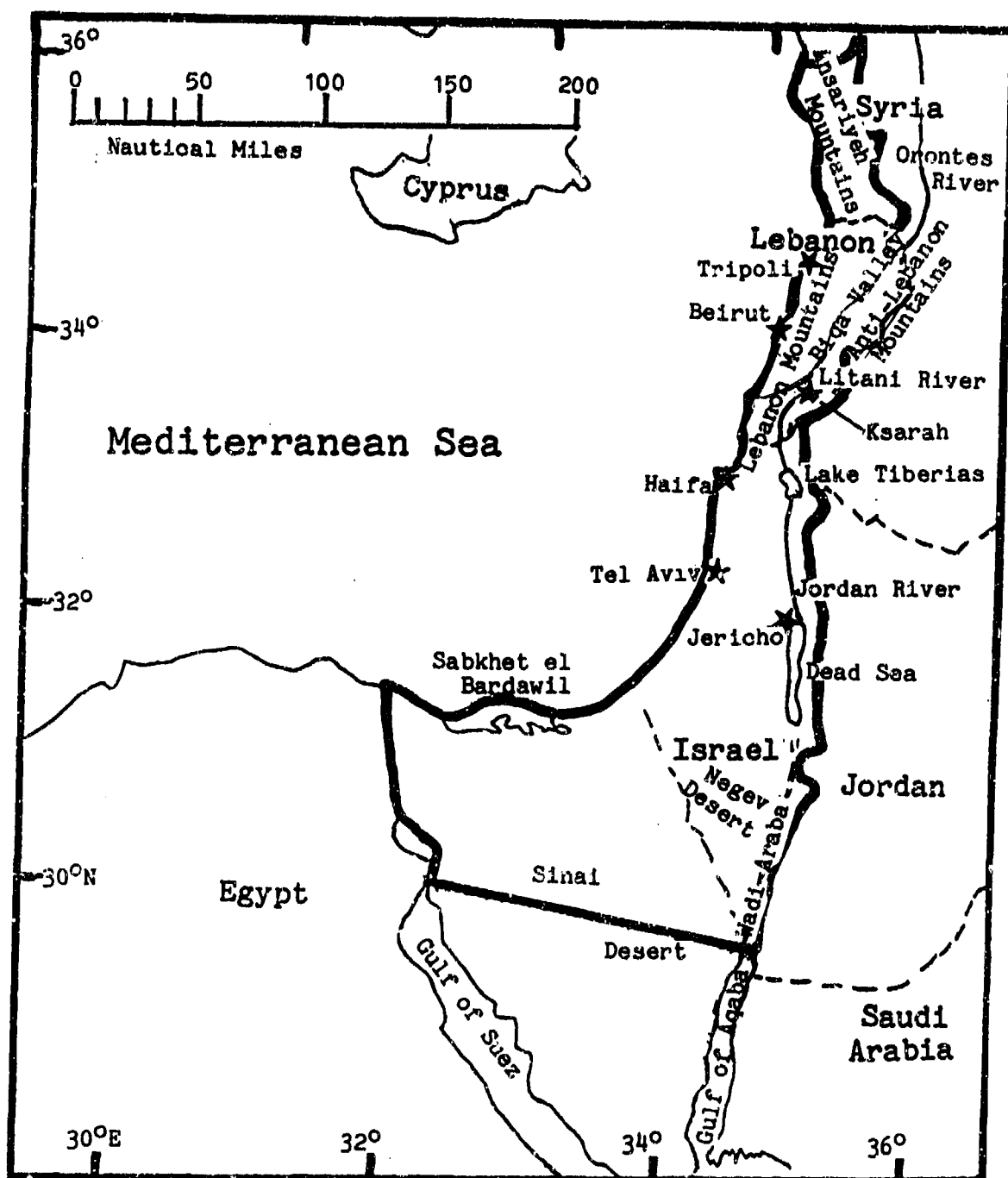


Figure 4-1a. The Eastern Mediterranean Coast. The Eastern Mediterranean Coast (enclosed by the bold lines) extends from the Syria/Turkey border southward, then westward to the Suez Canal. Many political borders are in dispute; some have been omitted for clarity.

STATION: TRIPOLI LEBANON													
LAT/LON: 34 27 N 35 48 E						ELEV: 33 FT							
ELEMENTS	JAN	FEB	MAR	APR	MAY	JUN	JUL	AUG	SEP	OCT	NOV	DEC	ANN
XTRM MAX	74	75	85	92	103	96	93	95	101	99	90	77	103
AVG MAX	62	62	67	72	78	82	86	88	87	83	74	66	76
AVG MIN	48	49	52	55	62	68	71	72	70	64	58	49	59
XTRM MIN	31	32	37	41	51	58	61	65	55	52	45	38	31
AVG PRCP	7.6	8.0	3.6	1.7	0.8	*			0.6	1.9	5.0	6.4	35.6
MAX MON													
TS DAYS	4	3	4	1	2	*			1	4	2	5	27

* = LESS THAN 0.05 INCHES OR LESS THAN 0.5 DAYS

STATION: BEIRUT LEBANON													
LAT/LON: 33 49 N 35 29 E						ELEV: 53 FT							
ELEMENTS	JAN	FEB	MAR	APR	MAY	JUN	JUL	AUG	SEP	OCT	NOV	DEC	ANN
XTRM MAX	77	87	97	99	107	104	98	99	99	101	91	84	107
AVG MAX	62	63	66	72	78	83	87	89	86	81	73	65	75
AVG MIN	51	51	54	58	64	69	73	74	73	69	61	55	63
XTRM MIN	31	30	36	43	46	56	64	62	60	52	41	30	30
AVG PRCP	7.5	8.2	3.7	2.2	0.7	0.1	*	*	0.2	2.0	5.2	7.3	35.1
MAX DLY	4.0	3.5	3.6	3.7	1.6	2.4	0.4	0.3	2.1	5.5	4.7	3.9	5.5
FOG DAYS													
TS DAYS	3	3	2	1	1	*	*	0	1	2	4	3	21
DUST DAYS	1	*	1	*	*	*	0	0	*	0	*	*	3
APP TEMP	62	63	66	73	80	89	94	99	93	85	75	65	

* = LESS THAN 0.05 INCHES OR LESS THAN 0.5 DAYS

STATION: KSARAH OBSERVATORY LEBANON													
LAT/LON: 33 50 N 35 53 E						ELEV: 3012 FT							
ELEMENTS	JAN	FEB	MAR	APR	MAY	JUN	JUL	AUG	SEP	OCT	NOV	DEC	ANN
XTRM MAX	68	71	82	91	97	97	101	104	103	93	86	70	104
AVG MAX	51	53	61	69	78	84	87	90	86	79	66	55	72
AVG MIN	34	37	40	46	52	57	61	61	57	52	45	38	48
XTRM MIN	17	19	26	31	38	45	50	50	44	39	30	20	17
AVG PRCP	5.6	6.0	2.0	2.0	0.4	0.1	0.0	*	*	0.7	2.7	4.9	24.6
MAX MON													
MAX DLY	3.1	2.8	1.5	2.9	1.6	0.2	*	*	0.2	1.1	3.0	3.2	
TS DAYS	2	3	2	2	2	1	0	*	1	3	4	3	23
SNOW DAYS	3	3	*	*								1	7

* = LESS THAN 0.05 INCHES OR LESS THAN 0.5 DAYS

Figure 4-1b. Climatological Summaries for Selected Stations on the Eastern Mediterranean Coast.

STATION: HAIFA ISRAEL													
LAT/LON: 32 49 N 35 00 E ELEV: 26 FT													
ELEMENTS	JAN	FEB	MAR	APR	MAY	JUN	JUL	AUG	SEP	OCT	NOV	DEC	ANN
XTRM MAX	79	87	104	109	112	109	99	99	107	108	97	90	112
AVG MAX	65	66	72	76	83	86	88	90	88	85	79	68	79
AVG MIN	49	50	52	58	65	70	76	76	74	68	60	52	62
XTRM MIN	29	27	33	40	50	56	63	61	61	47	43	33	28
AVG PRCP	7.1	5.7	0.8	0.7	0.1	0.0	0.0	0.0	0.0	0.5	2.7	8.7	24.4
MAX MON	12.1	10.5	6.0	4.2	2.1	0.6	*	*	0.8	6.2	13.6	16.7	44.6
MAX DLY	3.6	5.1	2.7	1.6	1.5	0.3	*	*	0.8	2.2	5.4	10.7	
TS DAYS	2	1	0	2	0	0	0	0	0	1	0	0	6
FOG DAYS	2	2	3	2	*	2	*	1	1	3	5	1	21
HAZE DAYS	9	10	14	15	19	20	23	21	16	18	14	12	190
DUST DAYS	*	0	1	*	*	*	*	*	0	0	*	*	2
APP TEMP	65	66	73	77	87	93	99	104	98	92	81	68	

* = LESS THAN 0.05 INCHES OR LESS THAN 0.5 DAYS

STATION: TEL AVIV, ISRAEL													
LAT/LON: 32 06 N 34 47 E ELEV: 4 FT													
ELEMENTS	JAN	FEB	MAR	APR	MAY	JUN	JUL	AUG	SEP	OCT	NOV	DEC	ANN
XTRM MAX	79	91	95	106	109	109	100	99	108	107	95	88	109
AVG MAX	62	65	69	76	81	85	87	87	85	82	74	65	77
AVG MIN	46	47	49	54	58	64	69	70	67	62	54	48	57
XTRM MIN	32	32	32	38	46	52	50	63	56	48	41	32	32
AVG PRCP	5.0	3.3	1.5	0.5	0.1	*	*	*	*	0.7	3.3	5.9	20.3
MAX MON	11.4	8.0	6.3	1.5	0.6	*	*	*	0.6	5.7	16.3	16.5	33.0
MAX DAY													
TS DAYS	3	3	3	1	0	0	0	0	*	1	4	4	18
DUST DAYS													
APP TEMP													

* = LESS THAN 0.05 INCHES OR LESS THAN 0.5 DAYS

STATION: JERICHO JORDAN													
LAT/LON: 31 52 N 35 29 E ELEV: -902 FT													
ELEMENTS	JAN	FEB	MAR	APR	MAY	JUN	JUL	AUG	SEP	OCT	NOV	DEC	ANN
XTRM MAX	84	89	100	117	120	118	114	117	117	107	99	85	120
AVG MAX	68	71	78	87	97	101	103	103	100	94	84	72	88
AVG MIN	50	51	55	60	67	73	75	76	74	69	61	53	64
XTRM MIN	37	37	35	47	50	59	59	64	63	57	46	36	36
AVG PRCP	1.4	1.2	0.7	0.3	0.1	0.0	0.0	0.0	0.0	0.1	0.7	1.1	5.6
MAX MON	2.6	2.3	0.9	1.0	1.0	0.2	0.1	0.0	0.0	0.7	2.0	3.6	7.3
HAZE DAYS	2	1	3	3	5	6	12	9	3	2	2	4	53
TS DAYS	1	1	1	1	1	0	0	0	0	1	2	1	9
DUST DAYS	1	3	2	3	3	4	2	1	2	*	1	4	26
APP TEMP	68	70	78	87	97	103	107	109	106	102	87	72	

* = LESS THAN 0.05 INCHES OR LESS THAN 0.5 DAYS

Figure 4-1c. More Climatological Summaries for Selected Stations on the Eastern Mediterranean Coast.

GEOGRAPHY. The northern boundary of the Eastern Mediterranean Coast runs from the Mediterranean Sea along the Turkey/Syria border to the 3,280-foot (1,000-meter) contour. The eastern boundary follows this contour through Syria to the Syria/Lebanon border. The Syrian border with Lebanon and Israel serves as the boundary southwards to the 1,640-foot (500-meter) contour. The boundary then follows this contour southward to Aqaba in southern Jordan. The southern boundary is a straight line from Aqaba to the southern end of the Suez Canal, near Suez, Egypt. The western boundary is the Suez Canal and the Mediterranean shore north to the Turkish border. A number of political boundaries in this region remain in dispute and are not shown in Figure 4-1a.

The region's Syrian and Lebanese coasts are 5 to 30 NM wide, with extensive coastal mountain ranges separating the harsh desert environment to the east from the maritime climate to the west. The Ansariyeh Mountains of Syria average 3,500 feet (1,065 meters) but some peaks reach 5,000 feet (1,525 meters). The Lebanon and Anti-Lebanon Ranges of Lebanon and western Syria average 5,000 feet (1,525 meters) with many peaks rising above 9,000 feet (2,745 meters). The Biqa Valley separating these two ranges is between 3 and 9 NM wide and about 100 NM long. The mountain ranges and the Biqa Valley comprise over 70% of the land surface in the Syrian/Lebanese part of the area.

In the less mountainous southern portion, the Judean Hills extend along the Israeli coast into Jordan. They are highest in the south, reaching about 3,500 feet (1,065 meters) high. The long, narrow Jordan Rift Valley lies east of these hills and forms the eastern border. It is part of a gigantic rift system running from southern Turkey through the Red Sea to East Africa. Average elevation along its 175-NM length is 300 feet (90 meters); however, it drops to 1,292 feet (393 meters) below sea level at the Dead Sea. It lies much lower than the surrounding landscape; the valley walls are steep, bare, and broken only by gorges formed by wadis or seasonal water courses. A wide coastal plain extends southeastward in the area's Egyptian and southern Israeli portions; it slopes gently to 1,640 feet (500 meters). The Negev and Sinai Deserts are extremely rugged plateaus. Rocky stubble, shallow canyons and dunes dominate the landscape. Elevations average 1,640 feet (500 meters) MSL.

RIVERS AND DRAINAGE SYSTEMS. The Jordan and Litani Rivers form the most extensive drainage

basins in the area. The Jordan River flows along the 10 to 30 NM wide Jordan Rift Valley floor. Its 5- to 12-NM wide flood plain is the lowest on Earth, reaching almost 1,300 feet (395 meters) below sea level. The Jordan River flows southward 100 NM from the southern Anti-Lebanon ranges to the Dead Sea. The Litani River runs southward along the Biqa Valley's length before turning westward to the Mediterranean Sea. Its average elevation is 3,000 feet (915 meters) MSL and it's 78 NM long.

An abundance of wadis, mostly dry water courses, line the Jordan Rift Valley south of the Dead Sea. Largest of these is the Wadi Araba, extending southeastward from within 20 NM of the Dead Sea to the Gulf of Aqaba.

The other two significant drainage systems are the Orontes River and the Kinneret-Negev Conduit. The latter is a man-made irrigation system extending southwestward from Lake Tiberias to the Gaza Strip and is used for irrigating the coastal plains. The Orontes River flows northeastward from the area's northeastern corner. Most of its 450-NM course is outside the region in Syria and Turkey.

LAKES AND RESERVOIRS. The Jordan River connects Lake Tiberias, also known as Lake Kinneret or the Sea of Galilee, with the Dead Sea. Lake Tiberias (6 by 13 NM) is 675 feet (205 meters) below sea level. The Dead Sea (the area's largest waterbody at 3-9 NM wide by 42 NM long) is 1,292 feet (393 meters) below sea level. Numerous small freshwater lakes dot the Lebanon and Anti-Lebanon Mountains. Lake Litani, the major water body along the Litani River, is 6 NM long and 2 NM wide. It lies at 3,300 feet (1,005 meters) in the Biqa Valley. Egypt's shallow Sabkhet el Bardawil is separated from the Mediterranean Sea by a narrow spit with two narrow connecting channels. It extends 40 NM along the Sinai Desert's coast, reaching 12 NM inland at its widest. It is surrounded by extensive salt flats and salt lakes.

VEGETATION. Where it exists, most vegetation is scrub and clumps of short grasses. Most cash crops (citrus) and grasses lie along the fertile coastal strips of Syria, Lebanon, and northern Israel. Isolated evergreens are found above 5,000 feet (1,525 meters) in the Lebanese mountain ranges. The northern river valleys support extensive agriculture, as well as thickets of reeds, shrubs, and small trees. The only plants around the Dead Sea are small, salt-tolerant reeds.

GENERAL WEATHER. Genoa and Cyprus Lows produce rainfall, severe thunderstorms with hail, and even significant snowfall at elevations above 5,000 feet (1,525 meters). The rare Cyprus Low with significant cold air advection can lower the snow line to 500 feet (150 meters) MSL. Warm Mediterranean waters, which average 63° F (17° C), provide enough moisture for heavy precipitation. Winter flow is moist; it develops an extensive marine boundary layer that averages 5,000 feet (1,525 meters) in thickness.

SKY COVER. Fair-weather stratus or stratocumulus forms over warm coastal waters at night because of the land breeze between 0400 and 0700 LST. The sea breeze that starts between 0700 and 0900 LST shifts the developing clouds onshore. The resulting stratus, with 200- to 1,000-foot (60- to 305-meter) bases, and stratocumulus, with 1,400- to 3,500-foot (425-1,065-meter) bases, normally dissipate by 1200 LST.

Occasionally, fair weather cumulus forms within the moist sea breeze. The moisture and land surface heating under clear winter skies allow the cumulus to build past 1600 LST, with bases between 2,500 and 4,000 feet (760 and 1,220 meters). Tops reach 13,000 feet (3,960 meters) MSL.

On the windward sides of coastal mountains, there is increased low-level cloud cover near places like Beirut. Cloud bases at mountain locations are lower than on coastlines and in the Negev Desert.

Genoa and Cyprus Lows may both track directly over the region. Multilayered low- and mid-level cloud cover dominates the area near a transitory low. A cold front's cumuliform clouds have bases between 2,500 and 6,000 feet (760 and 1,830 meters); tops may reach 40,000 feet (12 km) MSL. Ceilings below 500 feet (150 meters) occur with heavy showers or in mountains. Mid-level clouds form with bases between 8,000 and 15,000 feet (2,440 and 4,570 meters). Altocumulus tops are below 18,000 feet (5,480 meters) but altostratus tops may go to 30,000 feet (9.2 km) MSL. Thin cirrus with bases at or above 18,000 feet (5,480 meters) develops near jet streams, within migratory lows, and with thunderstorms. Thicker cirrus develops with lows and thunderstorms. Thunderstorm "blow-off" reaches 40,000 feet (12 km) MSL.

Depending on elevation, ceilings in the northern section are below 3,000 feet (915 meters) 11 to 30% of the time. Low ceilings in the Sinai and Negev deserts are rare. Most afternoon low ceilings are caused by cumulus that develops along seaward-facing slopes. Morning low stratus or fog concentrated along the coast causes most low ceilings, but a transitory low is another major cause. Latakia reports fewer low ceilings than other northern coastal stations; most cloud cover here results in ceilings between 3,000 and 4,000 feet (915 and 1,220 meters). Ceilings in this range occur 30-40% of the time at Latakia because the marine inversion layer is deeper here than at stations farther south.

THE EASTERN MEDITERRANEAN COAST
WINTER

December-February

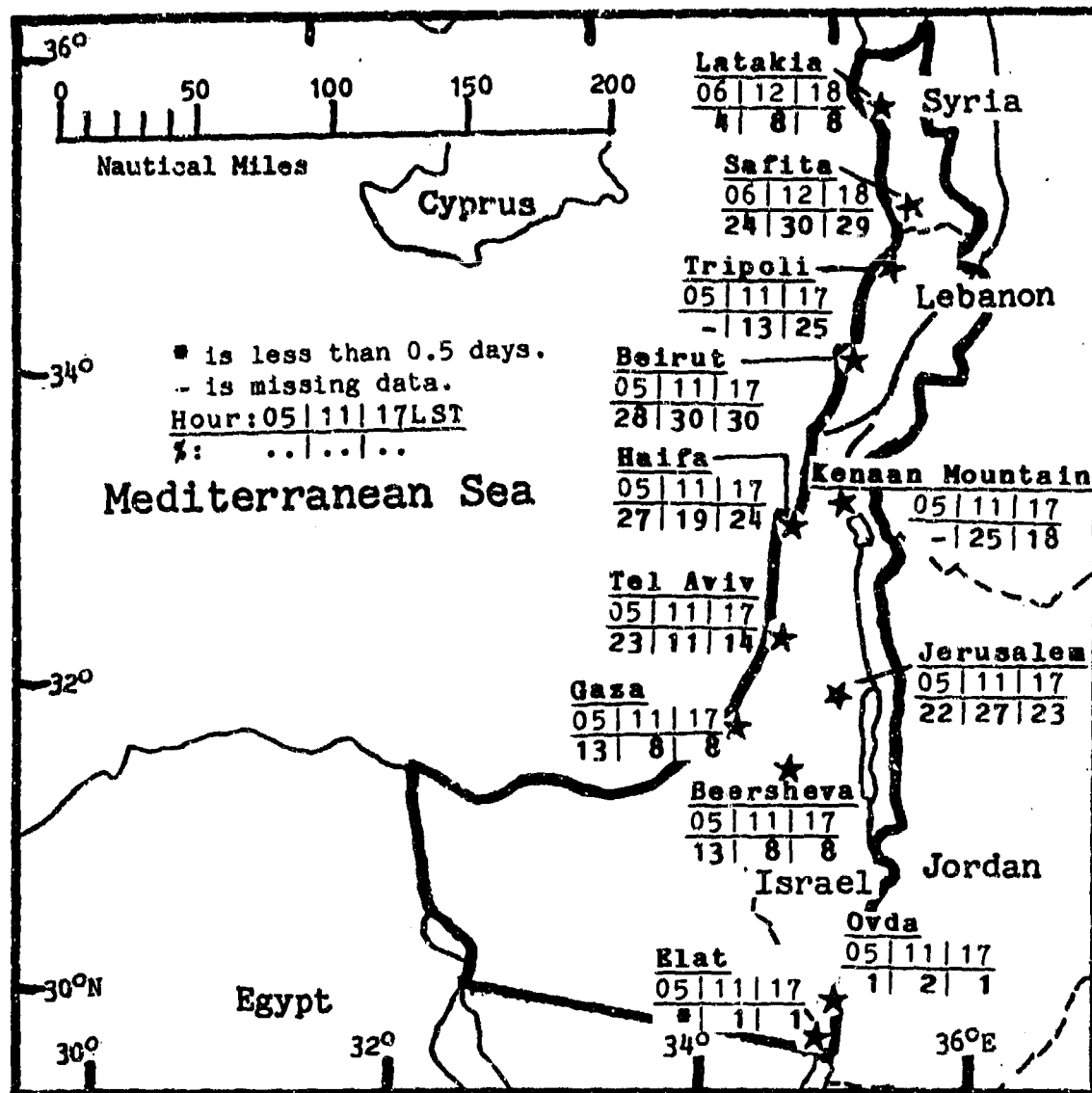


Figure 4-2. Mean Winter Frequencies of Ceilings Below 3,000 Feet (915 meters), Eastern Mediterranean Coast.

THE EASTERN MEDITERRANEAN COAST WINTER

December-February

VISIBILITY. Morning radiation fog forms during fair weather or after significant rainfall, particularly in the Lebanon Mountains and the Biqa Valley. Raised dust and marine moisture from the Gulf of Aqaba and the Red Sea cause dust haze in the Negev and Sinai Deserts, usually only reducing visibilities to about 5 miles. Winter visibilities are below 3 miles less than 7% of the time except in the Lebanon and Anti-Lebanon Mountains where frequencies are around 30%. See Figure 4-3.

Rain and drizzle often reduce visibility to below 7 miles during low passages. Fog north of a warm front, combined with steady rain or drizzle, can reduce visibility to 3 miles. Elevations above 2,000 feet (610

meters) get low ceilings and 1- to 4-mile visibilities in stratus and fog under these conditions. Rainshowers and thunderstorms along a cold front may lower visibility to 3 miles with heavy downbursts along the coastline. Fast-moving fronts limit low visibilities to less than an hour. Visibilities in snow can drop to near zero, especially in the higher mountains.

Intense low-pressure systems may cause Sirroccos that transport dust and sand from the Sinai Desert. Lowest visibility is in the Negev and Sinai Deserts. Severe thunderstorms and hail are common with these lows.

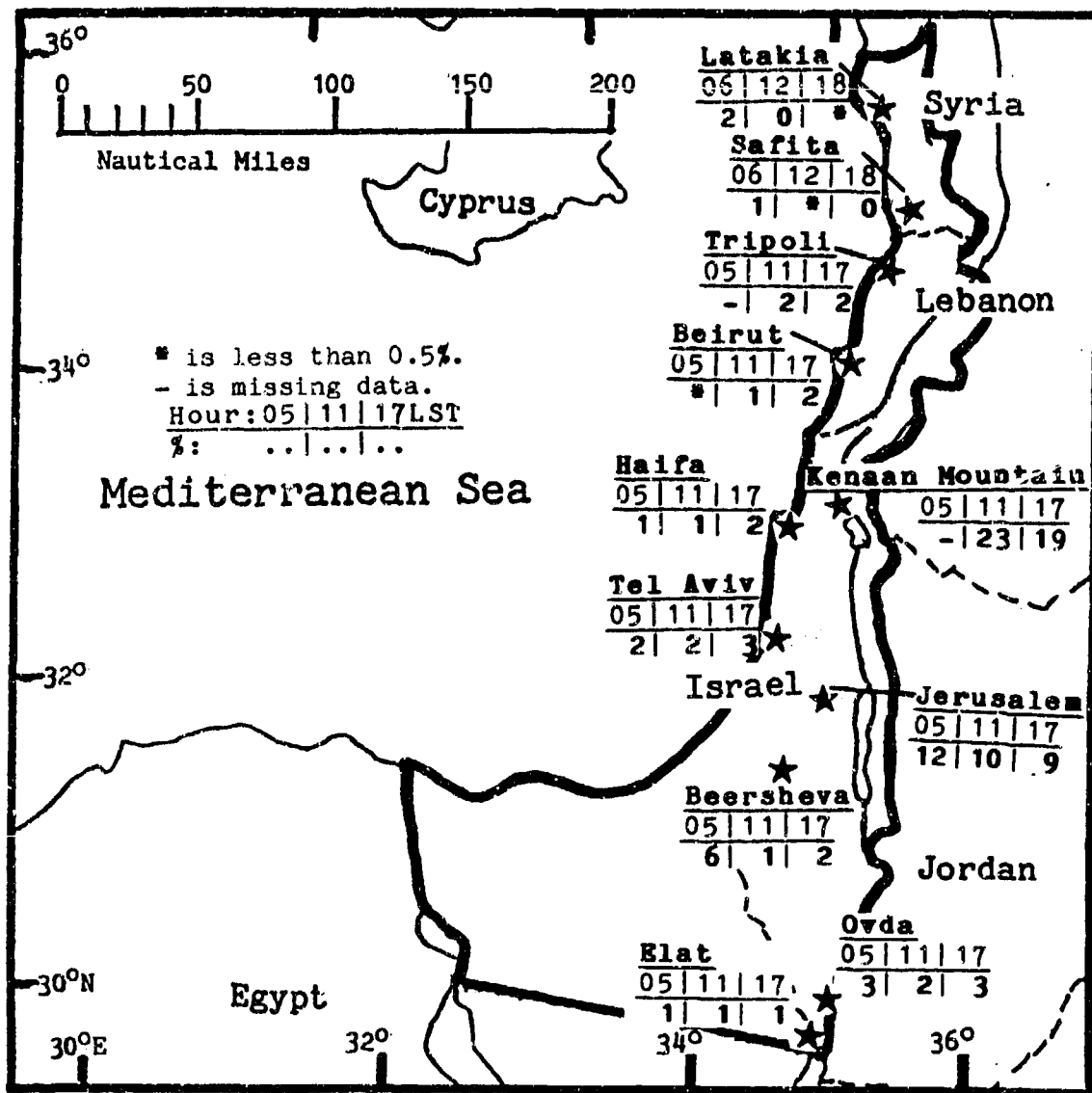


Figure 4-3. Mean Winter Frequencies of Visibilities Below 3 Miles, Eastern Mediterranean Coast.

THE EASTERN MEDITERRANEAN COAST WINTER

December-February

WINDS. Prevailing winter flow is westerly to west-southwesterly. Peak gusts, associated with Genoa and Cyprus Lows, are near 50 knots and usually westerly. Daytime sea breezes average 7 knots at Beirut and 9 knots at Tel Aviv. The winter sea breeze is active between 1200 and 1700 LST. Stronger ones may push inland to the Dead Sea by 1400 LST.

The Lebanon and Ansariyeh Mountains form the sea breeze's eastern edge in Lebanon and Syria, but it channels inland along the Litani River and into the Bika Valley. Persistent, 7-knot, northeasterly winds drain from the Jordan Rift Valley, affecting the northern Gulf of Aqaba and Elat. Figure 4-4 gives wind roses for the area.

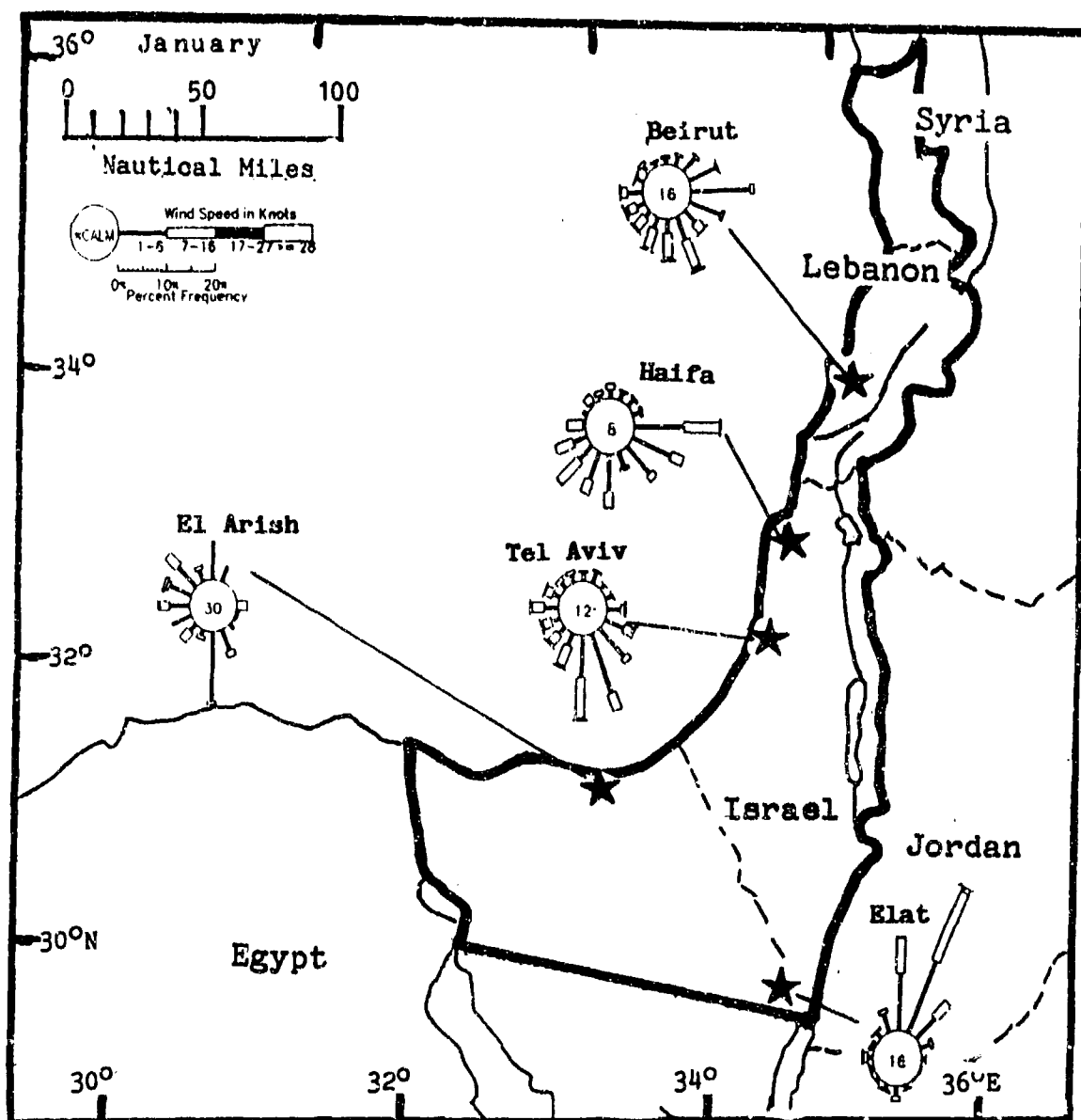


Figure 4-4. January Surface Wind Roses, Eastern Mediterranean Coast.

Winds aloft are normally westerly, as shown in Figures 4-5a and b. Bet Dagan's high mean speed (94

knots at 42,000 feet/13 km), indicates that this station is close to the Subtropical Jet's mean position in February.

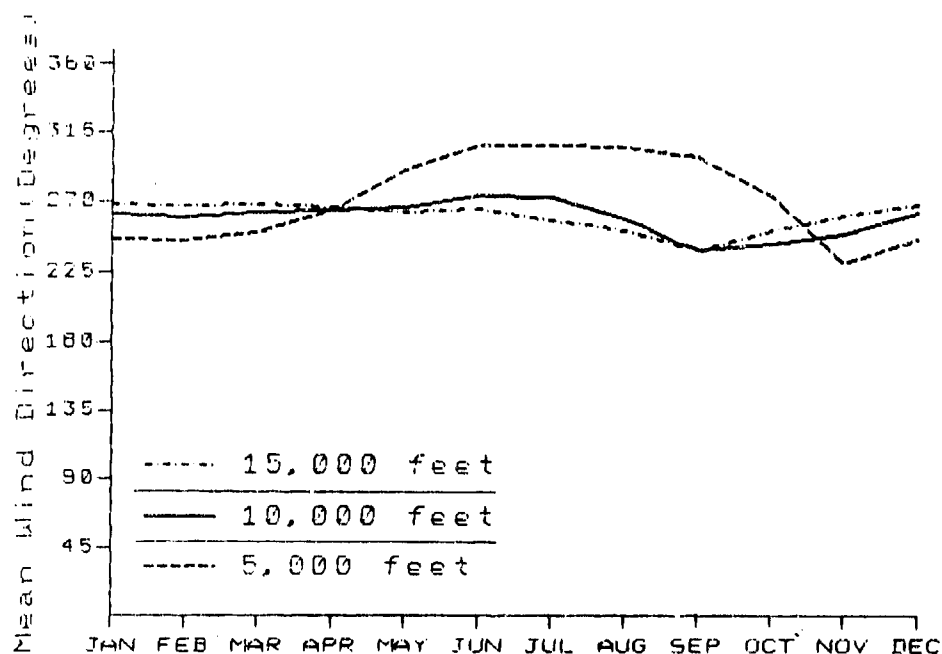


Figure 4-5a. Upper-level Annual Mean Wind Direction, Beirut, Lebanon.

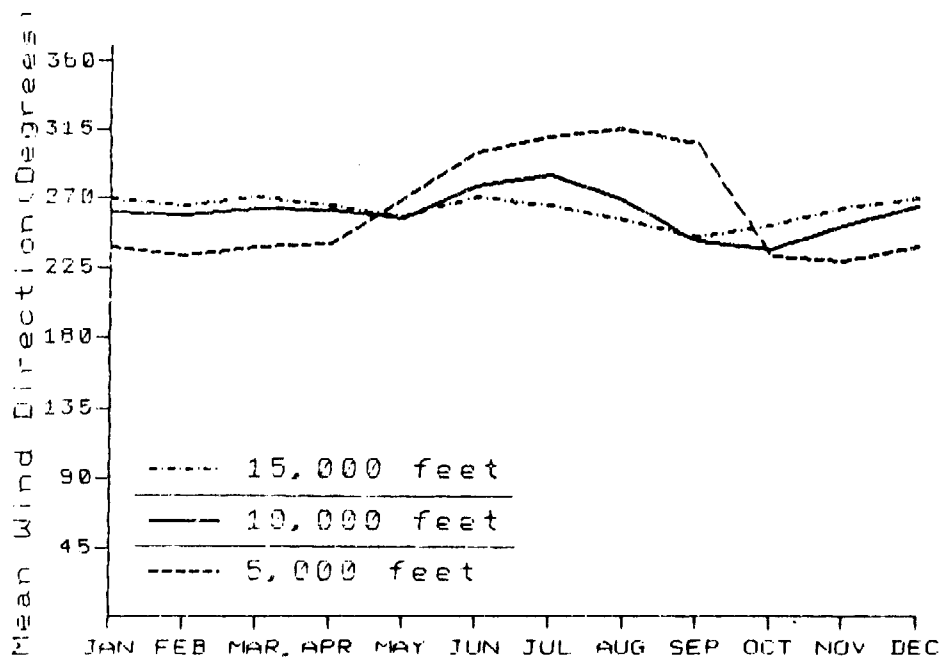


Figure 4-5b. Upper-level Annual Mean Wind Direction, Bet Dagan, Israel.

THE EASTERN MEDITERRANEAN COAST WINTER

December-February

PRECIPITATION. The Eastern Mediterranean Coast gets 50-70% of its mean annual precipitation from December to February. The coasts and the Lebanon Mountains' windward slopes receive 11 to 37 inches (280 to 920 mm) per winter month. Precipitation decreases eastward, as shown in Figure 4-6. The Jordan Rift Valley receives from 1 to 16 inches (25 to 400 mm), decreasing from north to south. Most falls in showers,

but rain and drizzle are common north of warm fronts. The Lebanon Mountains and the Judcan Hills produce a rain shadow in the Biqa Valley and the Jordan Rift Valley. An average of 14 low-pressure systems penetrate the region each winter. A rare stationary frontal boundary occasionally produces heavy rain that can persist for 5-10 days, most often in February.

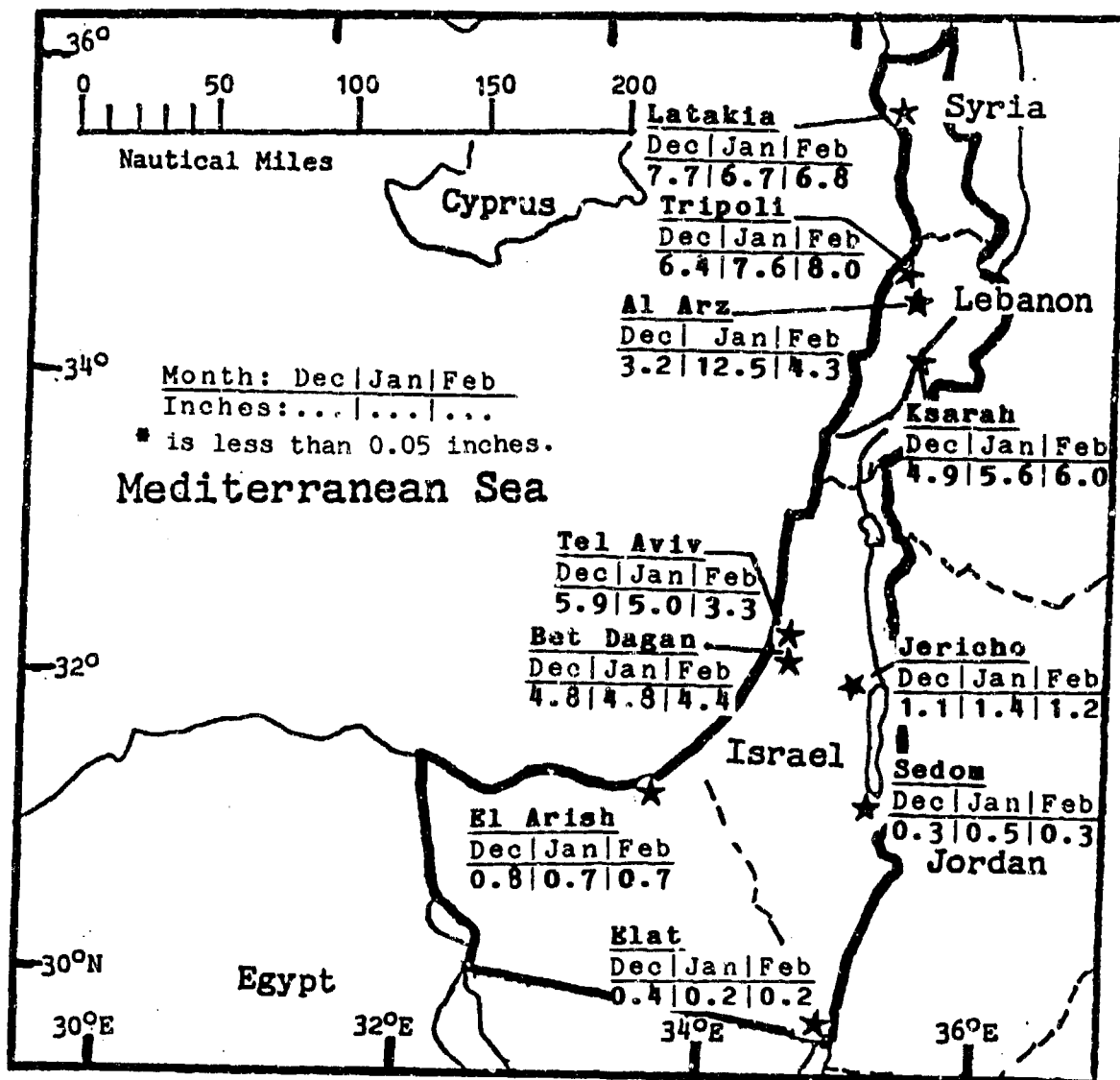


Figure 4-6. Mean Winter Monthly Precipitation, Eastern Mediterranean Coast.

THE EASTERN MEDITERRANEAN COAST WINTER

December-February

Strong Genoa or Cyprus Lows cause most of the winter thunderstorms shown in Figure 4-7. They occur on 1-21 days a season. Latakia, Syria, averages 7 thunderstorms a winter month, but Jericho (in the Jordan

Rift Valley) averages only 1. Hail is common in winter thunderstorms; it occurs with about 25% of them. Hail larger than 3/4 inch (17 mm), however, is extremely rare.

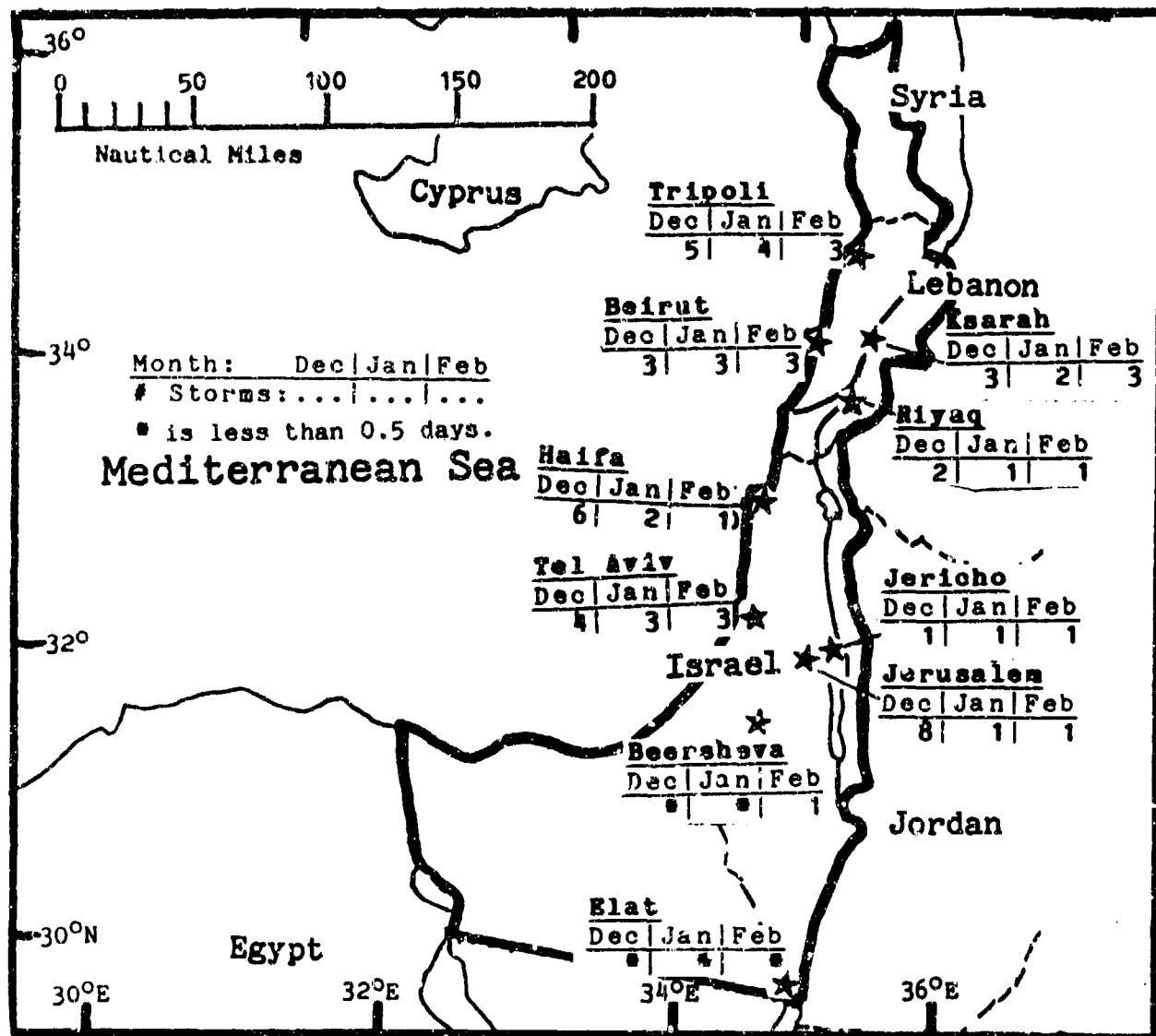


Figure 4-7. Mean Winter Thunderstorm Days, Eastern Mediterranean Coast.

Significant winter snowfall is normally confined to the Lebanon Mountains' higher elevations (above 5,000 feet/1,525 meters) MSL. Depth rarely exceeds 12 inches (306 mm). Snowfall in the Lebanon Mountains averages 2 to 30 days a season depending on elevation and latitude. Snow is rare at sea level, occurring about once

every 3 to 5 years; it melts within 3 hours and depths are normally less than 2 inches (50 mm). However, 10 to 12 inches of snow have fallen above 1,000-foot (305-meter) elevations with deep, closed lows. Figure 4-8 illustrates a common 500-mb pattern for significant snowfall.

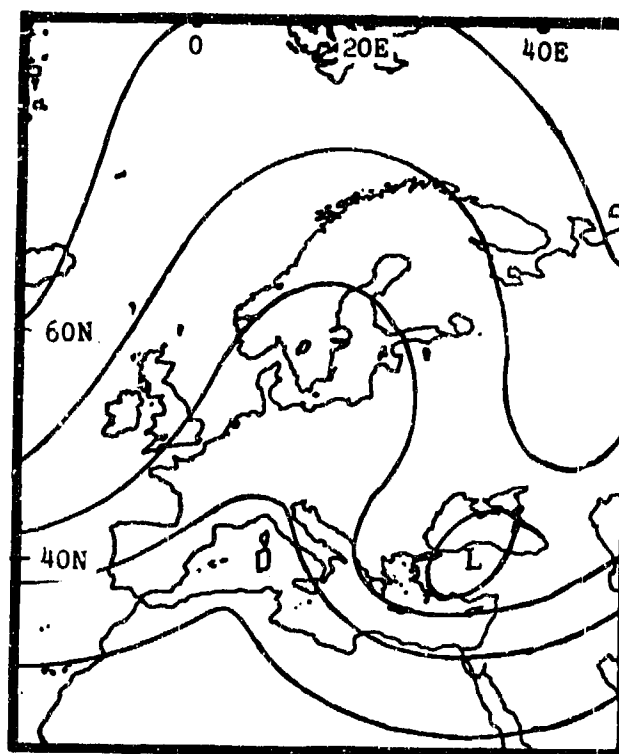


Figure 4-8. An Example of 500-mb Flow Causing Widespread Snow in the Eastern Mediterranean. This example shows a deep trough over Eastern Europe and a strong ridge over Western Europe. Cold short waves drop into the eastern Mediterranean and reform in the Cyprus area. Severe winter thunderstorms may develop with small hail if warm, moist air is present.

THE EASTERN MEDITERRANEAN COAST

WINTER

December-February

TEMPERATURE. Winter highs average 54° F (12° C) in the mountains and 73° F (23° C) in the Jordan Rift Valley--see Figure 4-9. The Lebanon Mountains' highest elevations experience the lowest temperatures; the mean high at Al Arz (elevation 6,283 feet/1,916 meters) is 35° F (2° C). Extreme highs normally occur

with southeasterly winds; they decrease with elevation from 93 to 71° F (35 to 21° C). Elat and Bet Dagan reach 93° F (35° C). Mean lows range from 33° F (2° C) to 56° F (12° C). Extreme lows result from polar surges out of Eastern Europe and range from 7° F (-14° C) at Riyaq to 36° F (2° C) at Sedom.

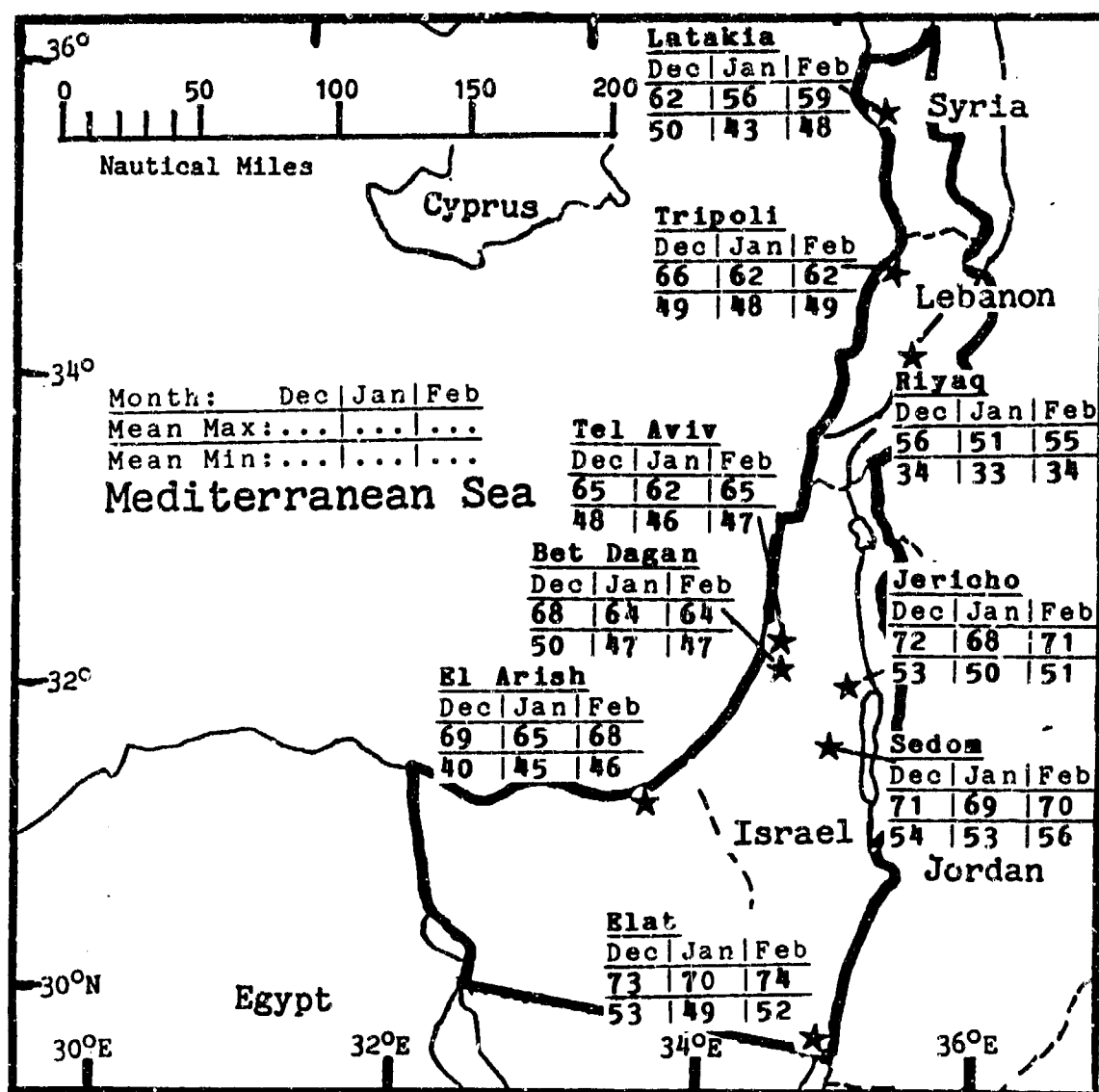


Figure 4-9. Mean Winter Daily Maximum/Minimum Temperatures (F), Eastern Mediterranean Coast.

THE EASTERN MEDITERRANEAN COAST

SPRING

March-May

GENERAL WEATHER. The primary cyclogenesis region shifts southward to the Atlas Mountains in the western Sahara. Stronger winds, warmer temperatures, and less rainfall accompany an Atlas Low. The Sirocco is common between late March and early May. Atlas Low activity peaks in April. Polar air may still penetrate the eastern Mediterranean in March.

SKY COVER. Mean spring cloud cover is similar to winter's, although it increases in the coastal deserts because intense surface heating develops a stronger sea breeze in May. Stratocumulus (reported as stratus at higher elevations) moves onshore with the sea breeze but dissipates before noon with the increasing onshore flow and the hot, dry land. Bases range from 1,400 to 3,200 feet (425 to 975 meters); tops seldom exceed 4,000 feet (1,220 meters) MSL. Higher elevations report ceilings as low as 400 feet (120 meters). Orographic uplift sustains cumulus along the Lebanon Mountains. Frequently, walls of fair-weather cumulus are observed east of Beirut and Haifa, causing the low-ceiling frequencies seen in Figure 4-10. Bases are usually 2,500 to 4,000 feet (760 to 1,220 meters). Cloud tops quickly dissipate above 6,000 feet (1,830 meters) MSL in drier air above the marine boundary layer before reaching the interior. The

Anti-Lebanon Mountains and the lee side Lebanon Mountains experience morning low cloud or fog, but little fair-weather cumulus. Inland stations on the plateaus, such as Beersheva, rarely observe extensive late afternoon cumulus because the sea-breeze moisture and land surface air mix thoroughly. The spring sea breeze off the Gulf of Aqaba causes low ceilings in the southern Negev. Latakia seldom reports ceilings below 3,000 feet (915 meters) because its marine inversion layer is higher than at other stations.

Lows entering the area north of Latakia produce a few clouds (mainly cumulus and altocumulus) along the cold front. Bases range from 2,500 to 6,000 feet (760 to 1,830 meters); tops reach 14,000 feet (4,265 meters) MSL. Accompanying towering cumulus and cumulonimbus have similar bases, but tops reach 20,000 to 45,000 feet (6 to 13.5 km) MSL. Lows passing south of Latakia produce multilayered cloud decks as more warm moisture is advected along the warm front and the Subtropical Jet is present. These clouds extend from 2,500 feet (760 meters) to 45,000 feet (13.5 km) MSL. Ceilings in heavy showers can go much lower (near 500 feet/150 meters), but nimbostratus is rare.

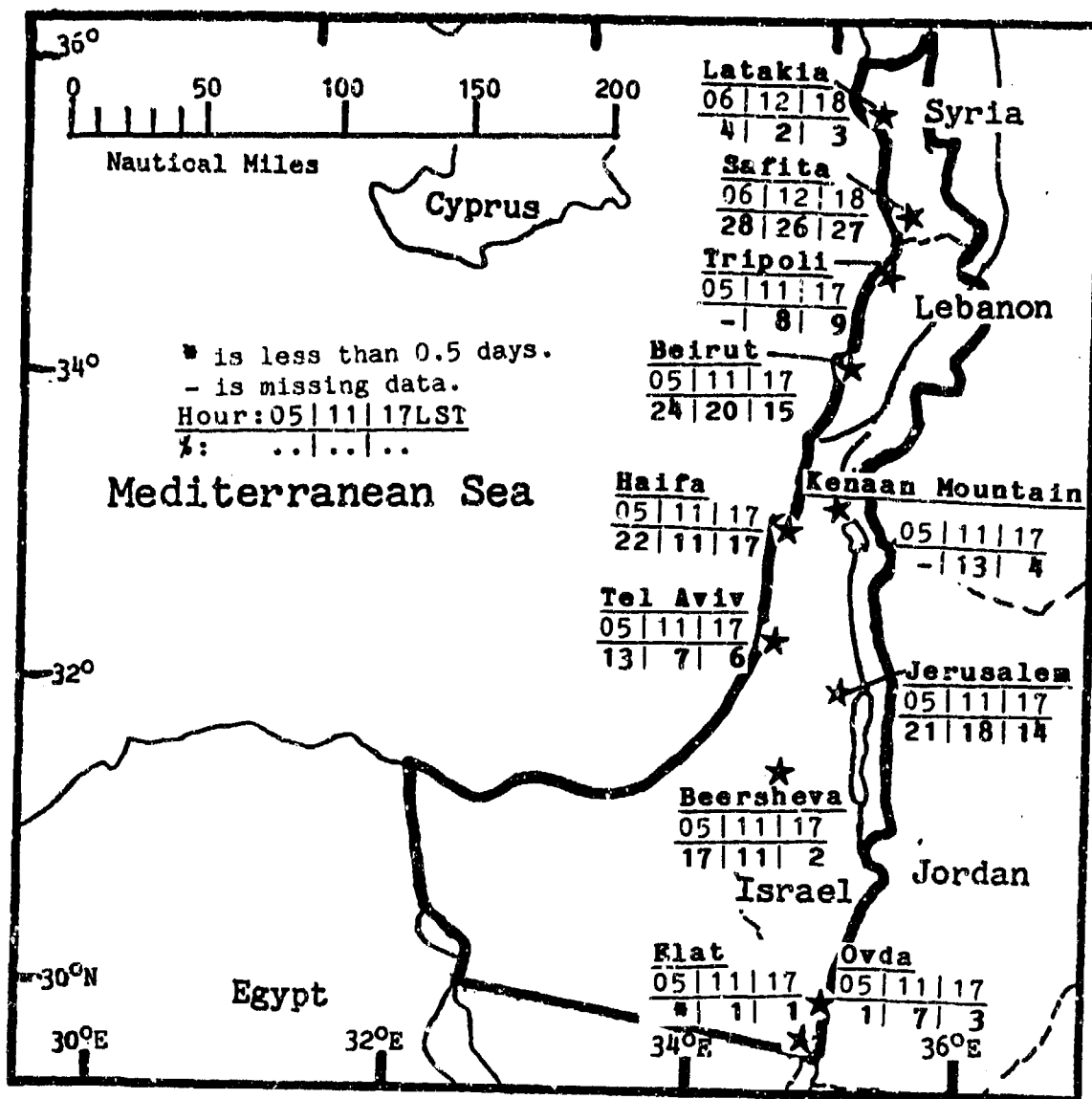


Figure 4-10. Mean Spring Frequencies of Ceilings Below 3,000 Feet (915 meters), Eastern Mediterranean Coast.

THE EASTERN MEDITERRANEAN COAST SPRING

March-May

VISIBILITY. Visibilities are below 3 miles less than 11% of the time throughout the region, as shown in Figure 4-11. Low visibilities are most common in the morning between 0600 and 0900 LST. They vary from 2% during the morning on the coast to 23% in mountains and valleys. Large-scale precipitation is responsible for most 5- to 6-mile visibilities in early spring, but fog becomes the primary factor in late spring. Radiation fog forms from 0700 to 0900 LST in stable atmospheric conditions in residual moisture left by rainfall or during the land/sea breeze transition. In May, radiation fog is common in interior mountain and valley locations and on

the coast. Dust haze is common in the Negev and Sinai deserts, but it seldom reduces visibility to below 5 miles.

Atlas Lows become less frequent during late spring. Low visibility with rain, drizzle, and fog occurs more often at northern stations because the lows cross the central and northern coast. Southern stations get sea fog and stratus in the accompanying warm air advection ahead of the low. Strong Siroccos (which see) bring North African dust and sand into the region. Visibilities are less than 3 miles with active frontal thunderstorms, heavy rain showers, and blowing dust.

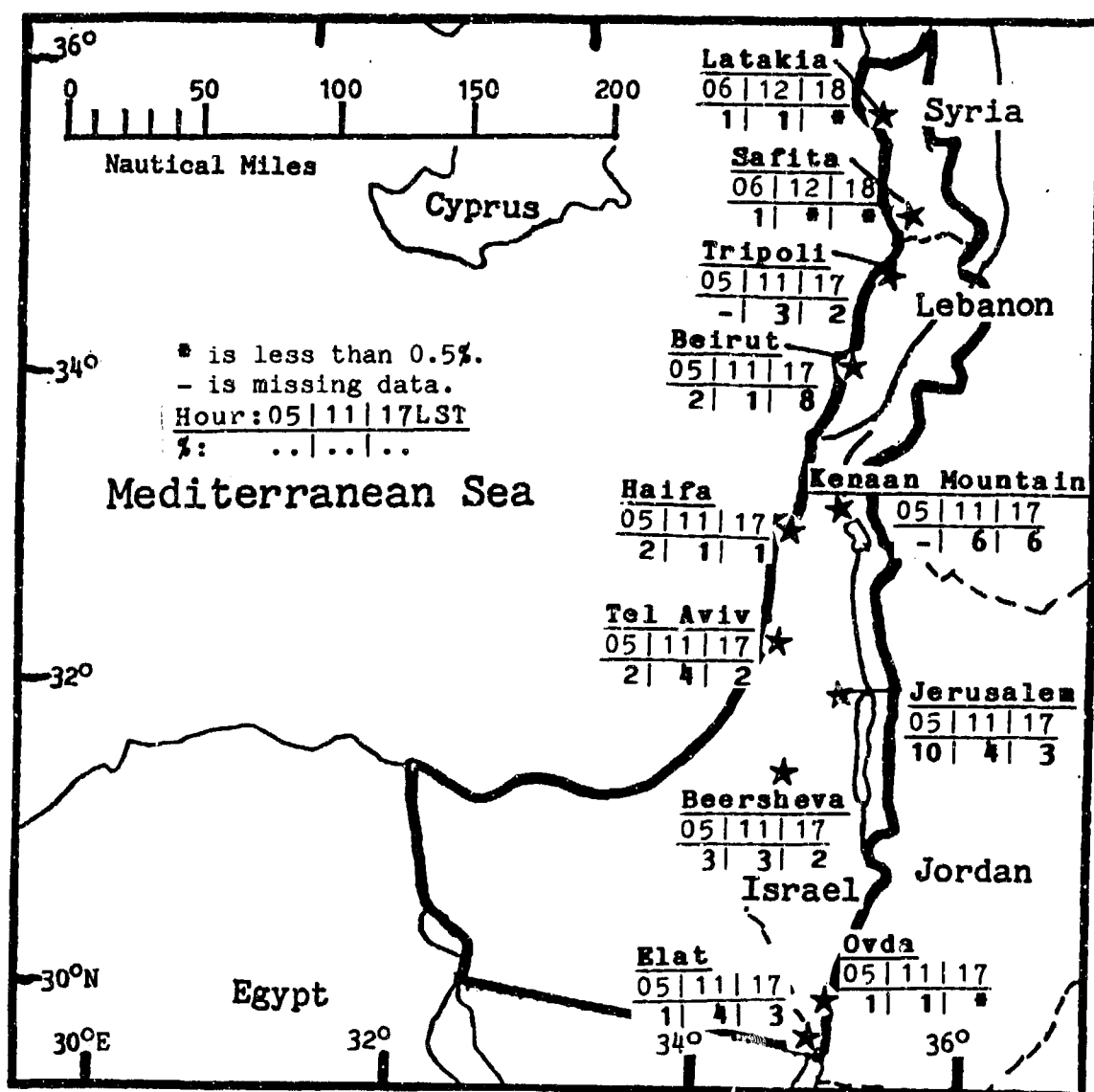


Figure 4-11. Mean Spring Frequencies of Visibilities Below 3 Miles, Eastern Mediterranean Coast.

WINDS. Prevailing flow is southwesterly to west-southwesterly; it reinforces the sea breeze. Synoptic-scale wind gusts, commonly caused by Atlas or Cyprus Lows, reach 50 knots. Winds are strongest along the coast but weaken substantially to between 15 and 25 knots inland. Surface wind roses are shown in Figure 4-12.

Surface winds display well-defined land/sea and mountain/valley breezes. Coastal sea breezes average 7 knots south of and 9 knots north of Beirut. Normally, the easterly land breeze is 3 knots slower than the westerly sea breeze. Mountain/valley winds are southwesterly or northeasterly in the Biqa Valley. The Jordan Rift Valley has a unique mountain/valley circulation that develops in

late April. Northerly nocturnal drainage winds average 11 knots, penetrating southward along the Jordan Valley to Elat where they diminish to 5 knots. The Dead Sea generates an easterly 5-knot lake breeze along its western edge by day; however, a strong sea breeze surges into the region from the west, usually after 1400 LST. The wind reversal is abrupt; westerlies may reach 20 knots and persist until 1700 LST.

Mid-level winds shift to the northwest as the Azores High and the desert heat lows strengthen--refer to Figure 4-5. The shift is damped at higher levels. Mean wind speeds diminish as the Subtropical Jet moves north. By May, highest speeds are 60 knots at 40,000 feet (12 km) MSL.

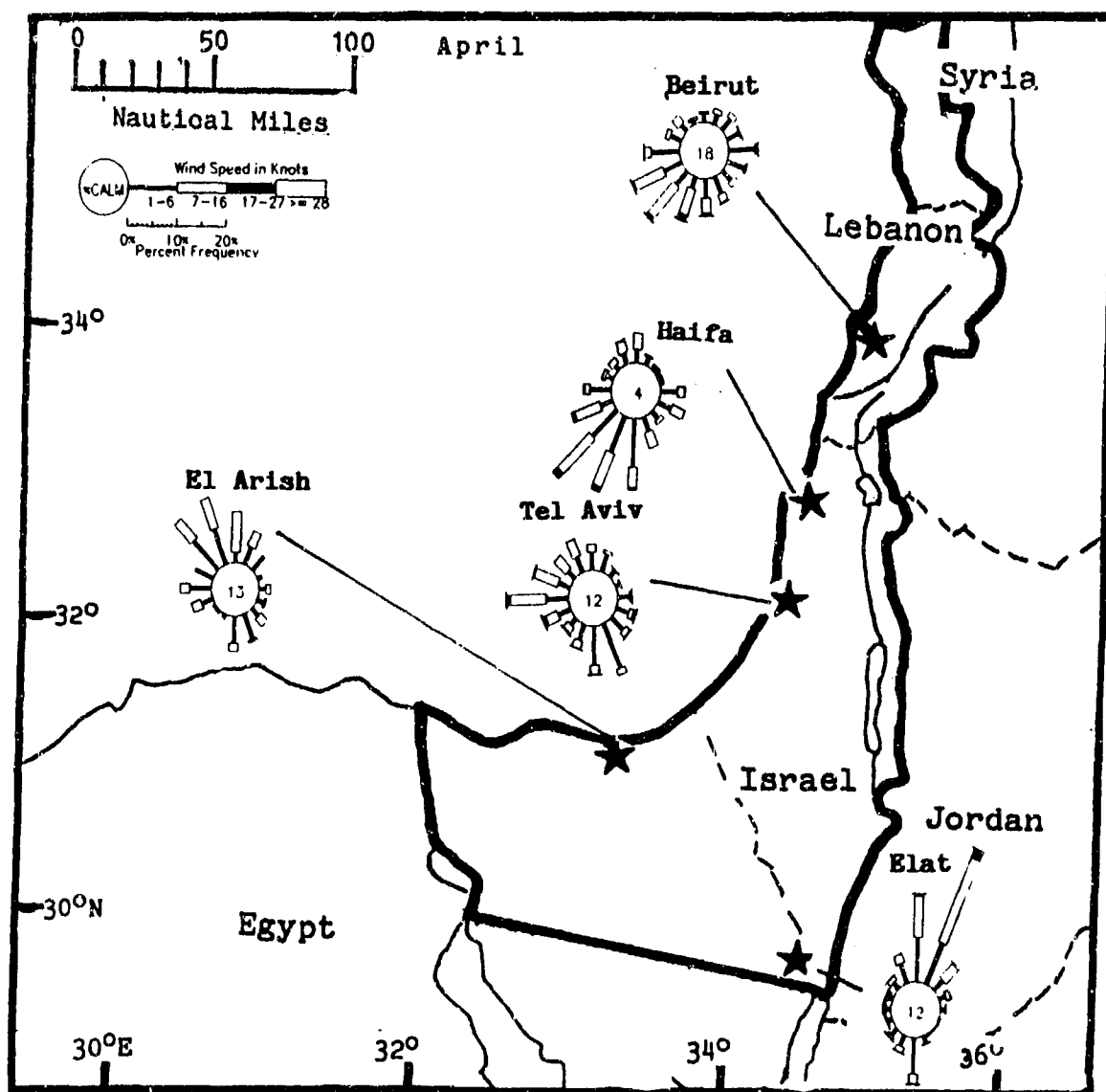


Figure 4-12. April Surface Wind Roses, Eastern Mediterranean Coast.

THE EASTERN MEDITERRANEAN COAST SPRING

March-May

PRECIPITATION. As the storm track moves north of the area, rainfall decreases--see Figure 4-13. Most precipitation falls in showers and thundershowers. Thunderstorm frequency decreases only slightly through the spring as Atlas Low activity peaks in April--see

Figure 4-14. Extensive thunderstorms form along the southern Lebanon and Anti-Lebanon Mountains. Heavy morning dew adds 1-2 inches (25-50 mm) to mean spring precipitation totals.

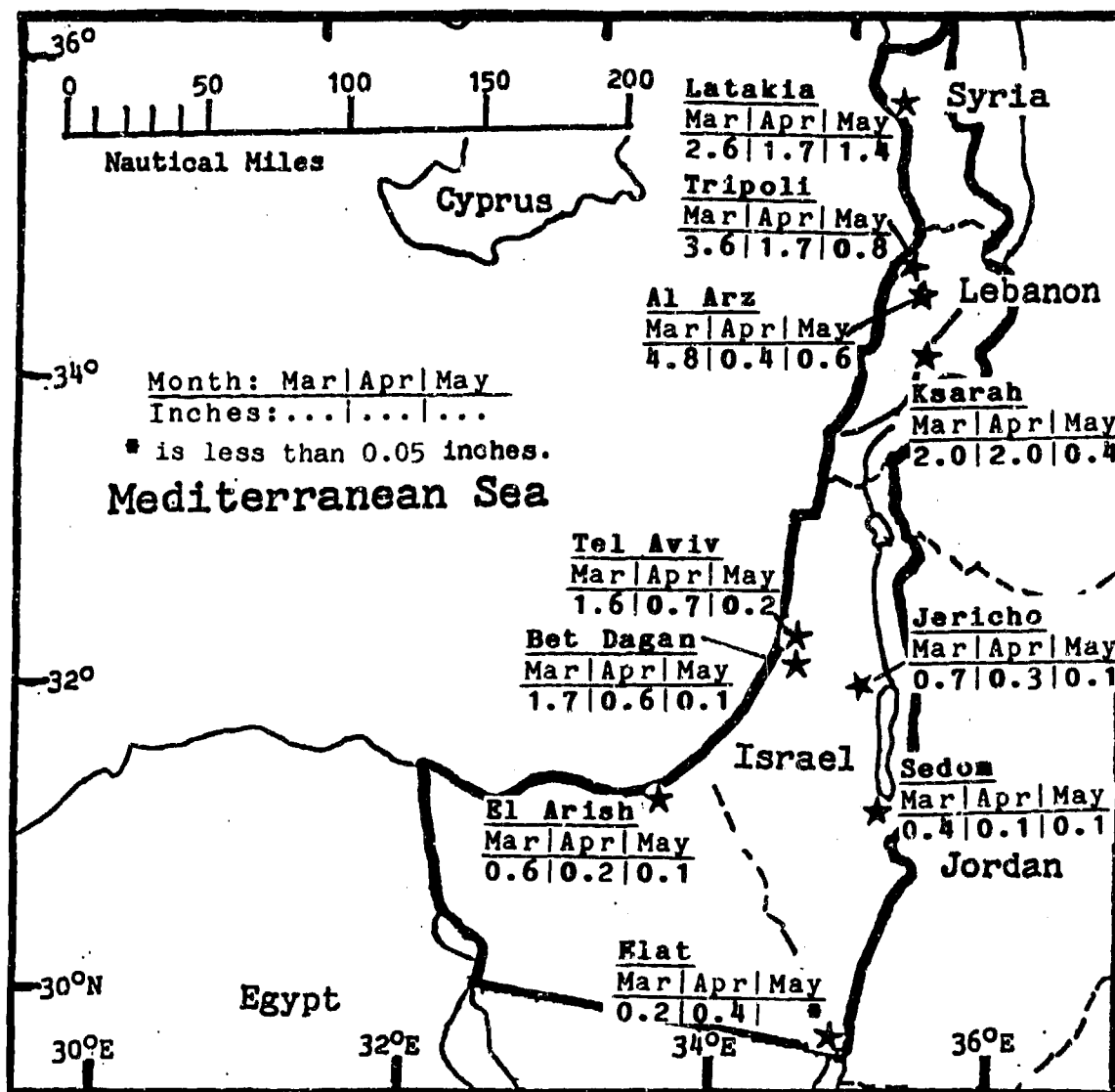


Figure 4-13. Mean Spring Monthly Precipitation, Eastern Mediterranean Coast.

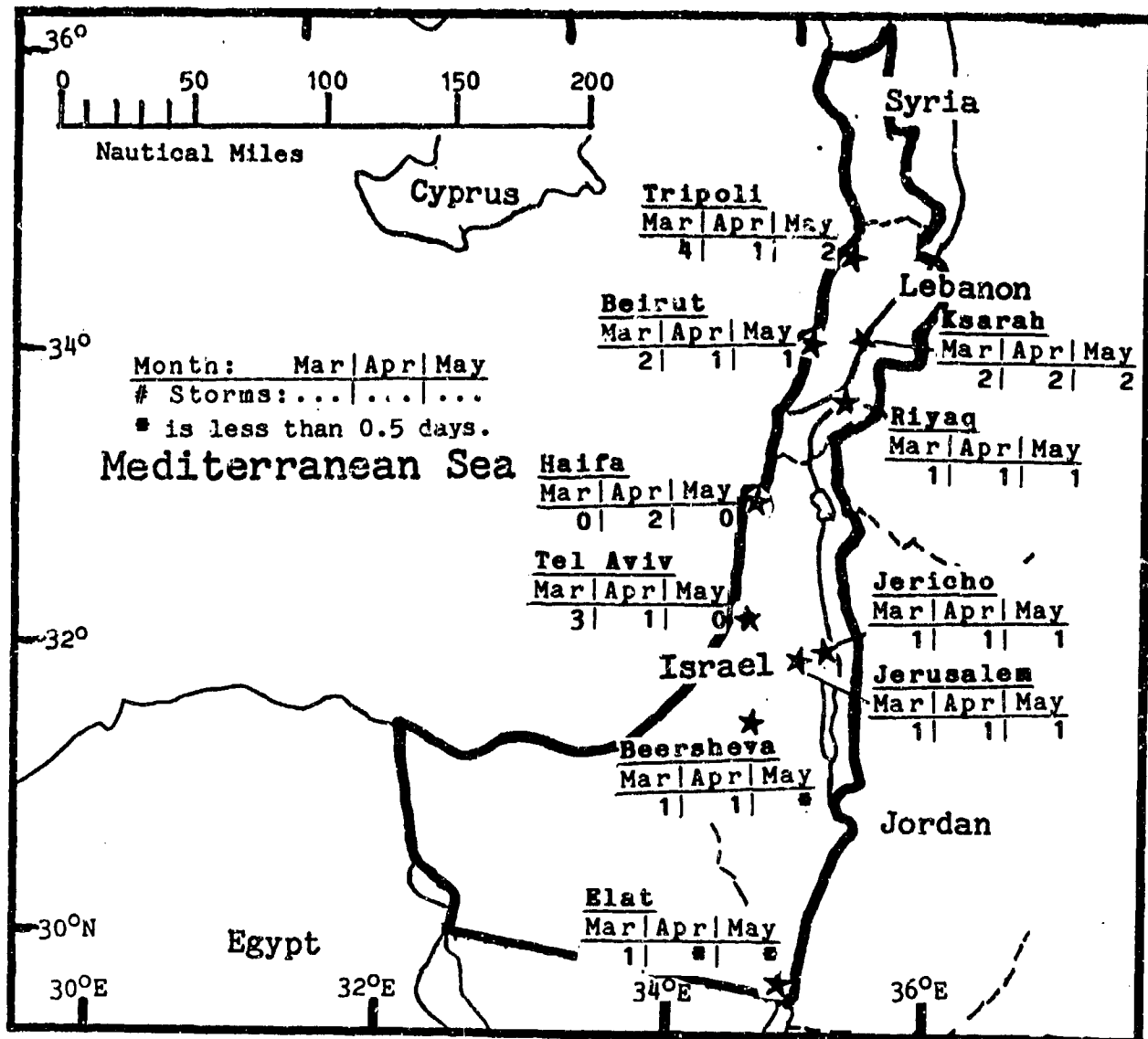


Figure 4-14. Mean Spring Thunderstorm Days, Eastern Mediterranean Coast.

THE EASTERN MEDITERRANEAN COAST SPRING

March-May

TEMPERATURE. Mean daily highs, shown in Figure 4-15, vary from 61° F (16° C) to 79° F (26° C) in March. Higher elevations are colder; Al Arz (elevation 6,283 feet/1,916 meters) has a mean March high of 39° F (4° C). By May, highs range from 70° F (21° C) along the coast to 97° F (36° C) in the southern Jordan Rift Valley. Sharav winds (which see) produce drastic temperature increases. The highest springtime

temperatures range from 90° F (32° C) in the Lebanon Mountains to 120° F (48° C) at Jericho. Mean daily lows vary from 44 to 64° F (7 to 18° C) along the coasts, but they are more variable inland, ranging from 36° F (2° C) at Al Arz to 75° F (24° C) at Sedom. Extreme lows range from 19° F (-7° C) at Riyaq to 43° F (6° C) at Sedom.

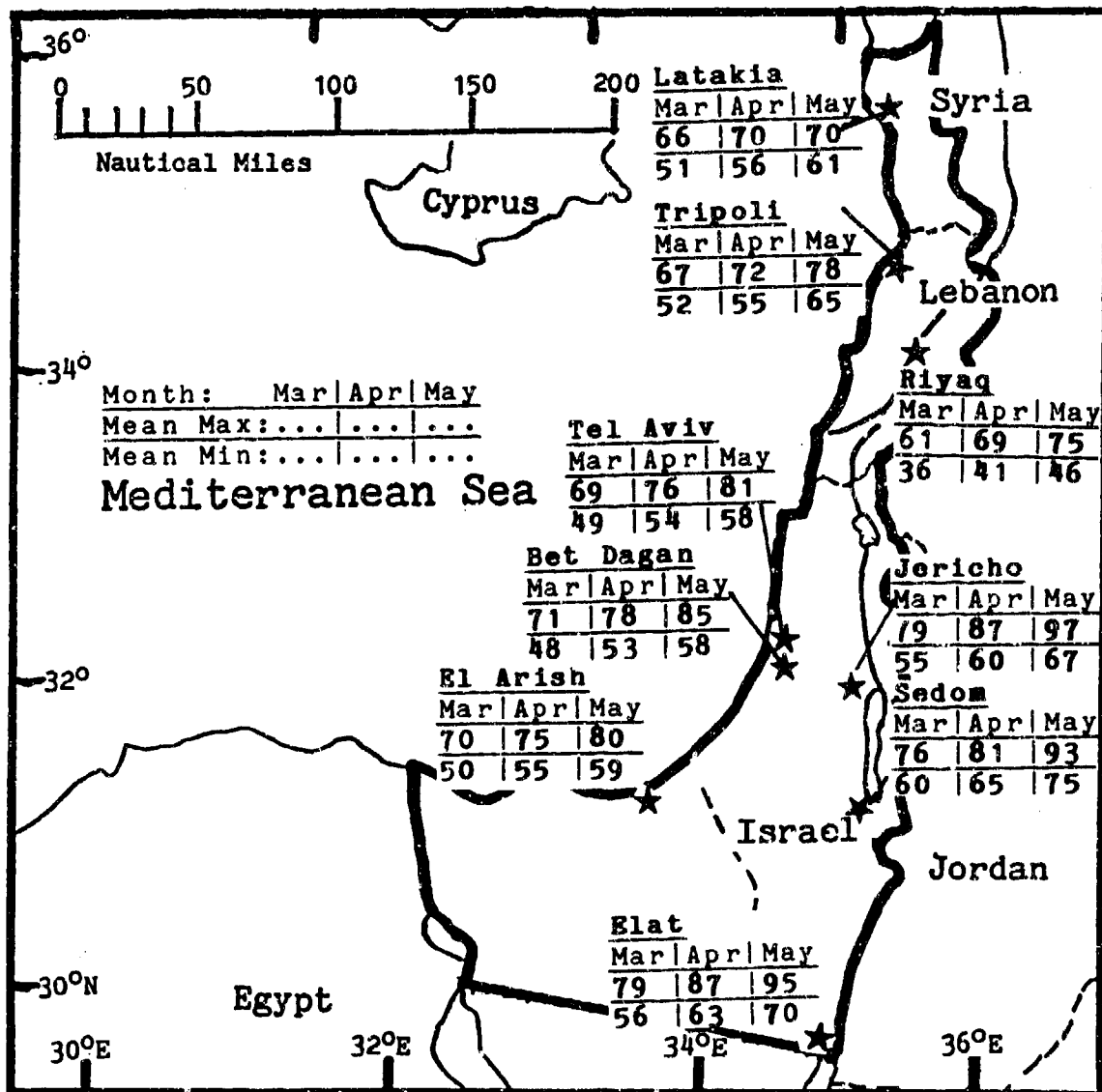


Figure 4-15. Mean Spring Daily Maximum/Minimum Temperatures (F), Eastern Mediterranean Coast.

THE EASTERN MEDITERRANEAN COAST

SUMMER

June-August

GENERAL WEATHER. The Azores High is strongest in the summer; heat lows dominate the area. The region is dry all summer as subsidence caps the marine boundary layer at 2,000 feet (610 meters). Orographic uplift of sea-breeze moisture produces isolated convection, but cumulus is short-lived in the dry air aloft. Cyclonic activity and upper-air disturbances are extremely rare and weak, but they may generate frontal showers and isolated thunderstorms.

SKY COVER. Cloud cover is limited to morning stratus/stratocumulus, afternoon cumulus, and cirrus; summer transitory low activity is rare. Summer stratus or stratocumulus develops when air cooled by radiation flows offshore at night and forms a thin cloud cover over the warm coastal waters. The sea breeze moves these clouds over land, causing the morning low-ceiling frequencies shown in Figure 4-16. Stratus bases are from 500 to 1,000 feet (150 to 305 meters) AGL and stratocumulus bases are mostly between 1,400 and 4,000 feet (425 and 1,220 meters). These clouds may be as low

as 100 feet (30 meters) on windward mountain slopes. Tops range from 1,000 to 6,000 feet (305 to 1,830 meters). Fair-weather cumulus, with bases averaging 3,000 feet (915 meters), forms when the sea breeze moisture is lifted against the coastal ranges to produce cloud lines that can be 10 to 50 NM long. The drier air above the marine inversion dissipates this cumulus by 1500 LST. Midday low ceilings are associated with these clouds. Fair-weather cumulus rarely reaches 8,000 feet (2,400 meters) MSL unless upper-level disturbances enhance them, in which case towering cumulus and cumulonimbus reach 25,000 to 50,000 feet (7.5-15 km) MSL over the Lebanon Mountains. Clear summer skies prevail over the Negev and Sinai Deserts.

The rare upper-level disturbance causes multilayered altocumulus and cirrus, with bases near 12,000 feet (3,660 meters) and tops to 40,000 feet (12 km) MSL. Cirrus near jet streams is less than 400 feet (120 meters) thick with bases near 20,000 feet (6,100 meters) MSL; thunderstorm cirrus can reach 50,000 feet (15 km) MSL.

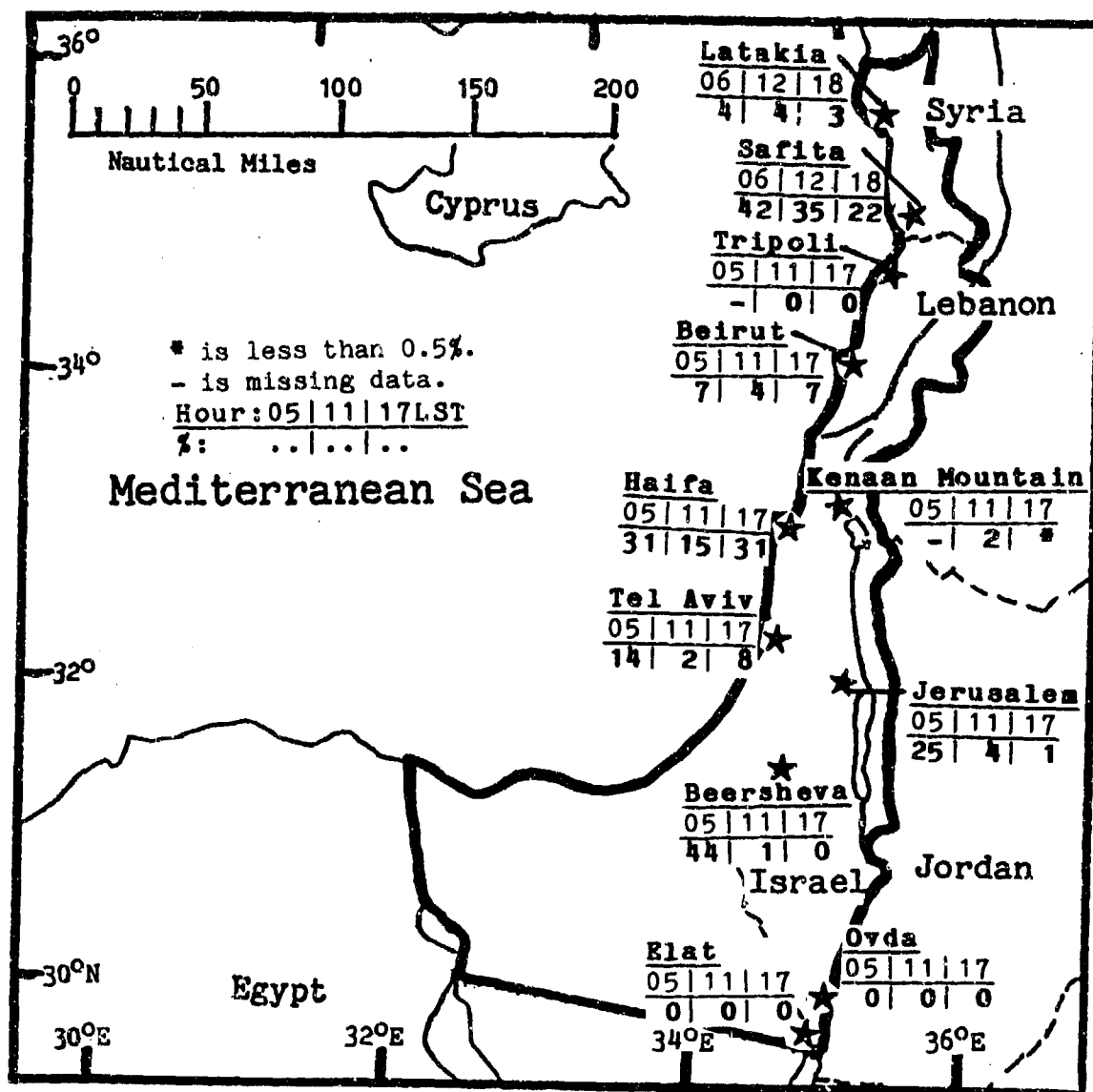


Figure 4-16. Mean Summer Frequencies of Ceilings Below 3,000 Feet (915 meters), Eastern Mediterranean Coast.

VISIBILITY. Fog and haze are the main causes of reduced summer visibilities. Fair weather dominates as the strong sea breeze penetrates deep into the interior. The land breeze is weak; radiation fog forms with light or calm winds. Thin, patchy ground fog lowers the visibility to between 3 and 6 miles about 1 day in 5 inland between Tripoli and Beersheva. Occasionally, this produces the below 3-mile visibilities shown in Figure 4-17. Dust devils raise dust in the Negev and

Sinai Deserts, producing about 6-mile visibilities. Dust haze at Ovda and Elat reduces visibility to 3-6 miles. Industrial smoke can lower visibility to about 3 miles with extended periods of stagnant weather conditions (stationary high pressure). Most industrial activity is located near Tel Aviv and Haifa. Smoke and haze are often observed between 0800 and 1100 LST, but they are usually dispersed by the sea breeze.

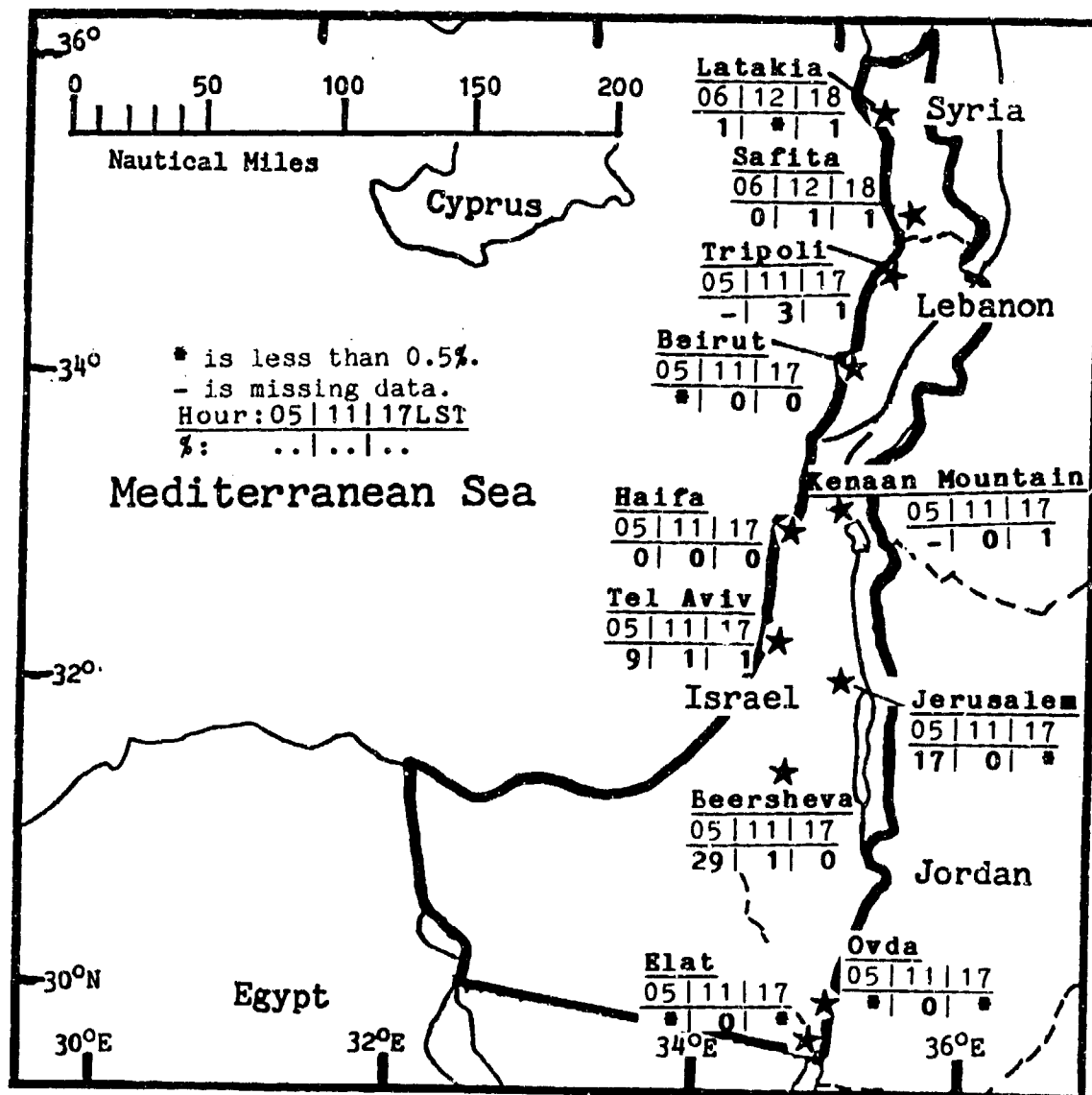


Figure 4-17. Mean Summer Frequencies of Visibilities Below 3 Miles, Eastern Mediterranean Coast.

WINDS. Prevailing flow aloft is northwesterly; surface wind speeds decrease from 23 knots in June to 14 knots in August. The large decrease is caused by weak cyclonic activity and a stronger Azores High. Peak wind gusts are less than 25 knots, usually associated with rare cyclonic activity. Gusts are more likely to affect the extreme north; both Latakia, Syria, and Tripoli, Lebanon, have reported gusts above 30 knots. Figure 4-18 gives surface wind roses.

The sea breeze is well-defined but limited from the surface to 2,000 feet (610 meters) by the subsidence inversion. Sea breezes often penetrate to Lake Tiberias and the Dead Sea. They average 10 knots at Tripoli. A delayed sea-breeze front reaches the Dead Sea around 1400 LST, averaging 8 knots. Winds are northerly at 8

knots along the Jordan Rift Valley from the Dead Sea to Elat. The Gulf of Aqaba's sea breeze overrides this flow between 1200 and 1700 LST on its northern shore. The Lebanon Mountains stop the marine boundary near the northern coast, but onshore flow channels 60 miles into the Lebanese interior along the Litani River Valley. Stations backed by mountains, such as Beirut and Haifa, have a local nocturnal drainage flow that accelerates offshore flow.

Winds veer to westerly at the 10,000-foot (3,000-meter) level in the summer, as was shown in Figure 4-5. The Subtropical Jet is well north of the area; mean speeds are at a yearly low in August, with a 30-knot maximum.

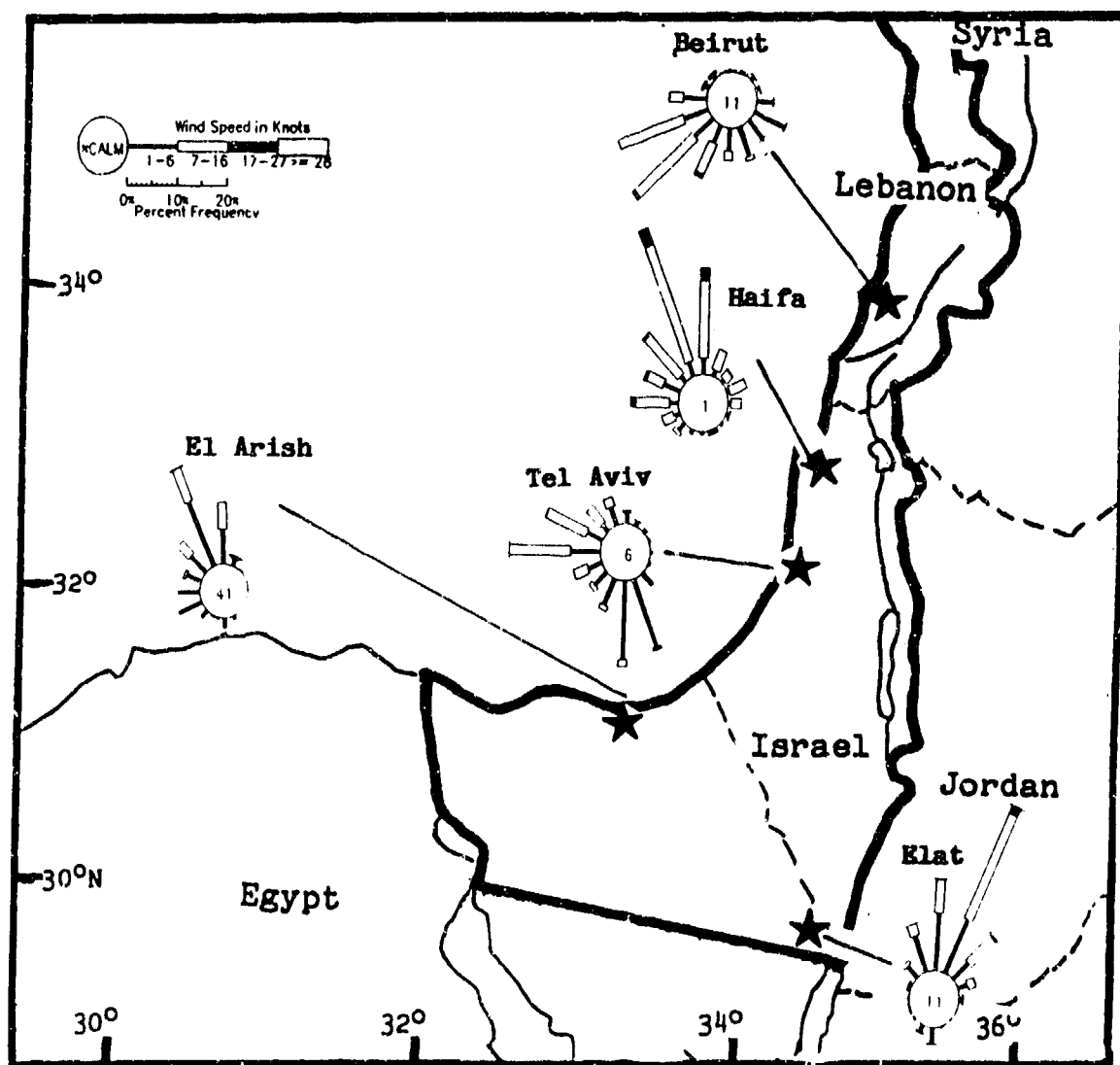


Figure 4-18. July Surface Wind Roses, Eastern Mediterranean Coast.

THE EASTERN MEDITERRANEAN COAST SUMMER

June-August

PRECIPITATION. Summers are extremely dry except for the rare upper level disturbance or cyclonic storm that brings scattered rainshowers and isolated thunderstorms to the highest elevations. Summer rainfall is less than 0.1 inches (3 mm) a month; for that reason, the usual precipitation figure has been omitted. Thunderstorms occur on less than 1 day a summer throughout the region.

TEMPERATURE. Mean daily highs range from 82° F (27° C) to 104° F (41° C), as shown in Figure 4-19. The Jordan Rift Valley has the highest mean daily highs, at 86-104° F (30-41° C). Extreme highs are 95° F (35° C) at Tripoli and 123° F (51° C) at Sedom. Mean daily lows range from 51° F (10° C) to 74° F (23° C) except in the Jordan Rift Valley, where temperatures do not normally go below 80° F (26° C). Lowest summer temperatures are in June, when they range from 37° F (3° C) at Riyaq to 73° F (23° C) at Sedom.

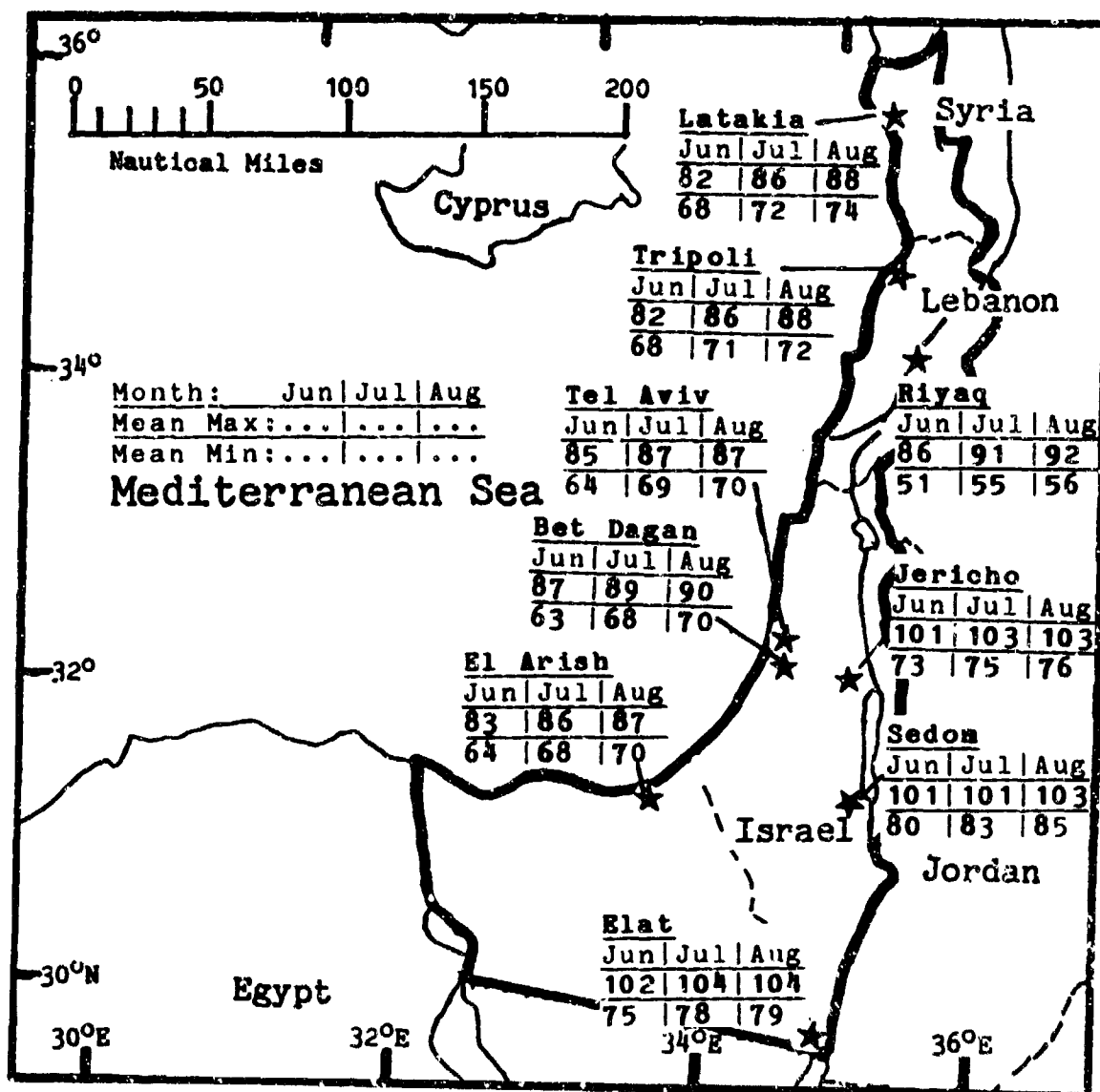


Figure 4-19. Mean Summer Daily Maximum/Minimum Temperatures (F), Eastern Mediterranean Coast.

GENERAL WEATHER. The region retains its characteristic dry summer weather until mid-October. The Azores High shifts southward by November. Genoa Low movement is normally northeastward over northern Turkey and southern Europe, but a secondary storm track crosses the area by late fall. Genoa Lows produce rain showers and thunderstorms. Snow is possible above 5,000-foot (1,525-meter) elevations. Weak flow concentrates sea breeze moisture in the marine boundary layer to below 1,500 feet (455 meters) MSL.

SKY COVER. Mean cloud cover increases with the return of cyclonic activity. Cloud cover with early fall low pressure systems is confined to cold fronts and to cumulus along the mountains. The cumulus has 2,500-6,000 foot (760-1,830 meter) bases and is 8,000 feet (2,440 meters) thick. Stratus and stratocumulus frequently develop in November behind intense lows. Bases are between 1,400 and 3,200 feet (425 and 975 meters) and tops reach 5,000 feet (1,525 meters) MSL. Embedded cumulonimbus, towering cumulus, and thick cirrus reaches 50,000 feet (15 km). Altocumulus and

altostratus form with bases between 8,000 and 15,000 feet (2,440 and 4,570 meters) and tops to 30,000 feet (9,145 meters) MSL. Nimbostratus forms when the low moves directly over the region; bases are as low as 1,000 feet (305 meters); tops reach 20,000 feet (6,100 meters) MSL.

Early morning stratus/stratocumulus continues to be brought in by the sea breeze until late October, but a decrease in cloudiness from summer is reflected in the low incidence of early morning ceilings below 3,000 feet (915 meters) shown in Figure 4-20. Only Beirut's low-ceiling frequency increases in the fall; morning stratus persists there, enhanced by convergence with increasing drainage winds off the Lebanon Mountains. Morning stratus bases are usually between 200 and 1,000 feet (60 and 305 meters); stratocumulus bases develop between 1,400 and 3,200 feet (425 and 975 meters). Tops range from 2,000 to 5,200 feet (610 and 1,585 meters) MSL. These clouds may form 100-foot (30-meter) ceilings along coastal hillsides.

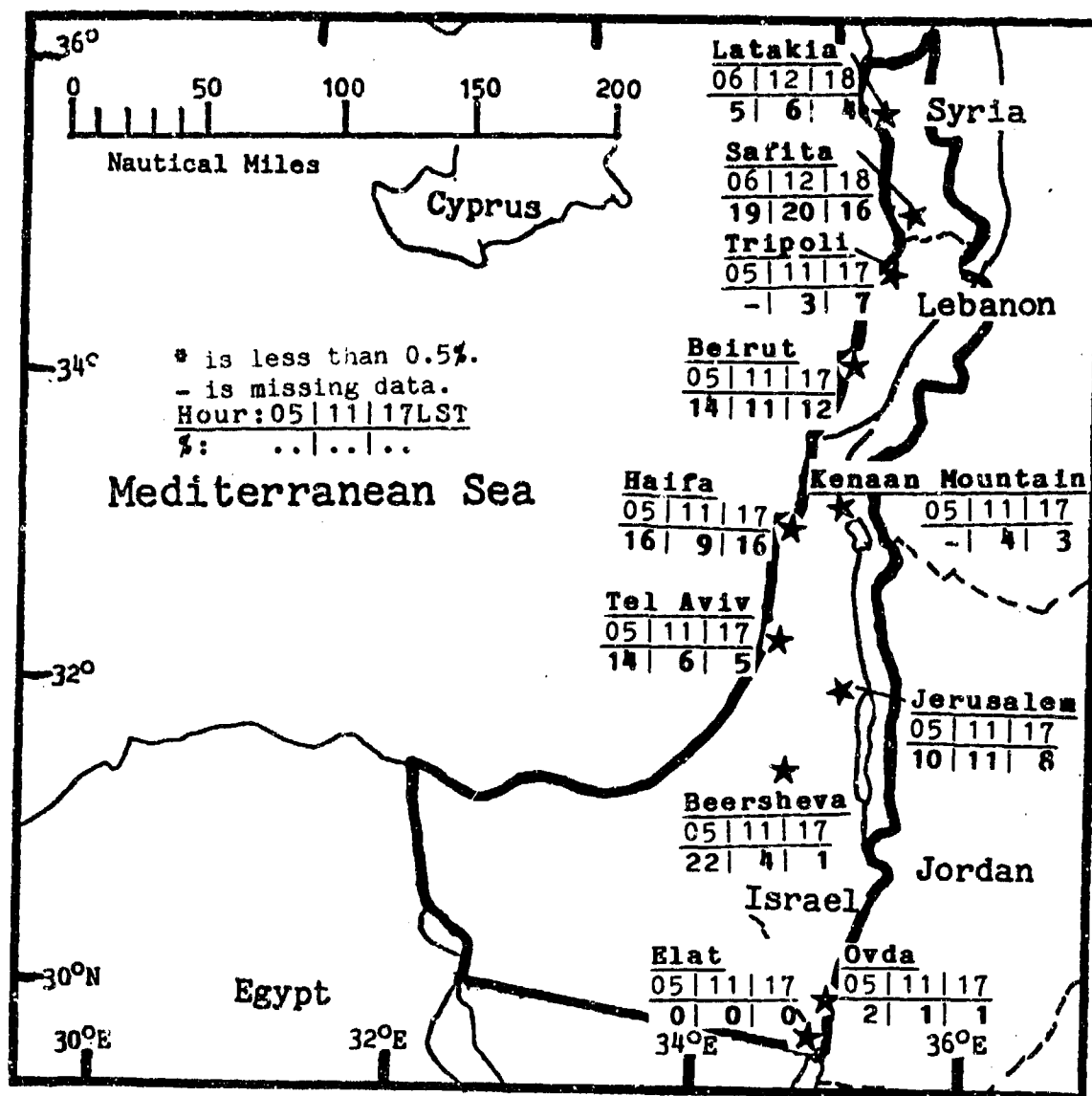


Figure 4-20. Mean Fall Frequencies of Ceilings Below 3,000 Feet (915 meters), Eastern Mediterranean Coast.

VISIBILITY. Radiation fog develops in moist air advected into the region by the sea breeze; the result is 3- to 6-mile visibilities along the coast and in the mountain valleys between Tripoli and Beersheva. Advection fogs occur along the coast, but not in the valleys. These fog types combine to produce 3-mile visibilities on 30-60% of fall mornings. Both burn off rapidly in late-morning heating. Haifa reports 60% fog frequencies at 0800 LST in the 3- to 6-mile range. Only Beersheva reports visibilities below 3 miles in this fog with any frequency (13%). Radiation fog produced by Gulf of Aqaba moisture occasionally causes the low morning visibilities at Ovda indicated by Figure 4-21.

Fall frequencies of visibility below 3 miles are identical to summer's until November, when fog also forms in moisture left by heavy rain showers and thunderstorms. Frontal rain showers and thunderstorms may reduce visibility to less than 3 miles for brief periods.

Coastal stations such as Tel Aviv and Haifa have the most industrial smoke and haze, which lower visibilities to between 2 and 4 miles in September and October under stagnant conditions. This is most frequent in the early morning before the sea breeze sets in. Smoke is a more recent phenomenon at Beirut due to the city's civil war; it lowers visibility to about 5 miles.

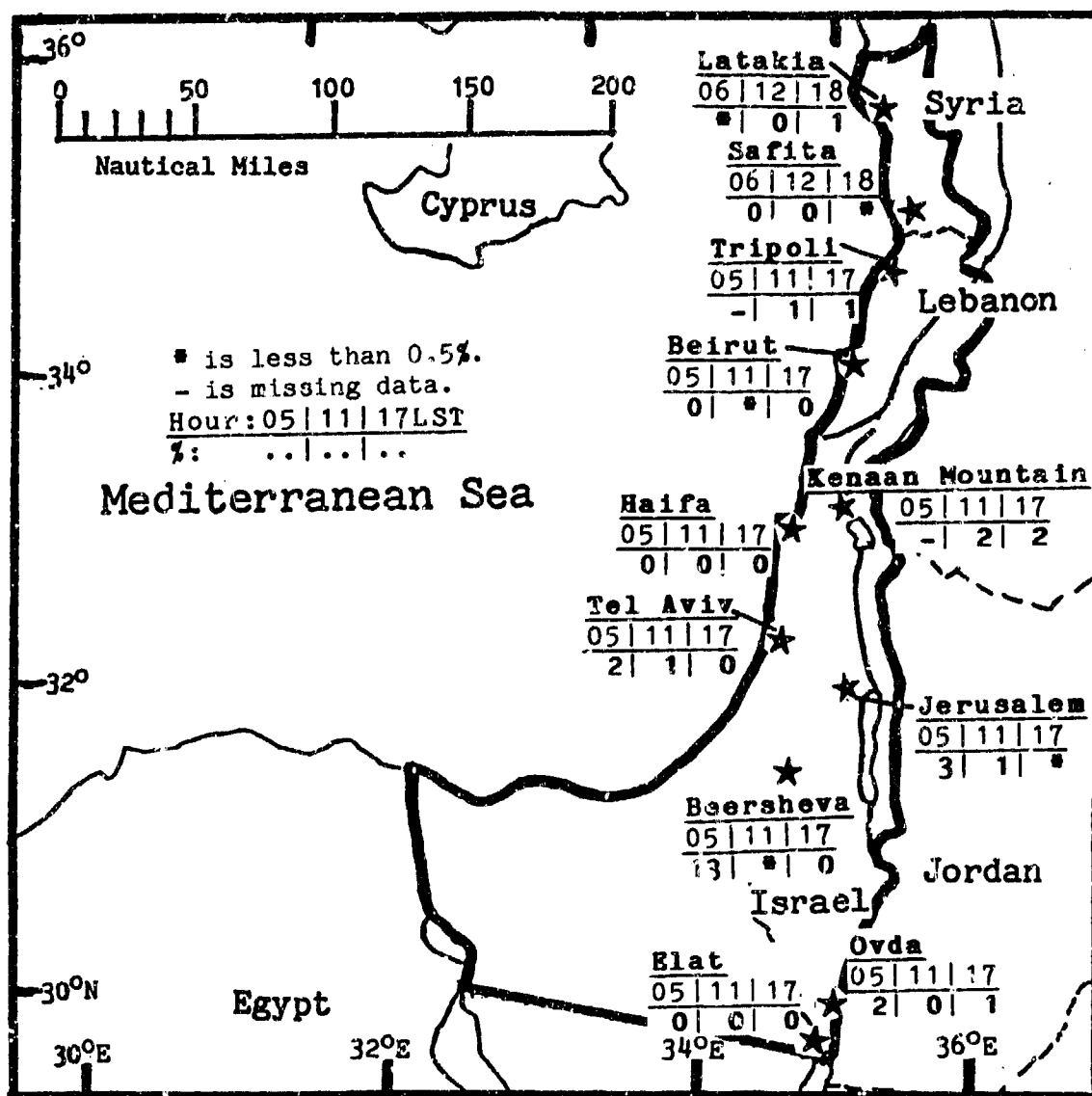


Figure 4-21. Mean Fall Frequencies of Visibilities Below 3 Miles, Eastern Mediterranean Coast.

THE EASTERN MEDITERRANEAN COAST FALL

September-November

WINDS. Fall prevailing winds are southwesterly at 9 to 18 knots. The sea breeze is well-defined near shore, but it can move inland beyond 25 NM over flat terrain. Mountains higher than 2,000 feet (610 meters) block it entirely from the northern interior. The sea breeze is between 5 and 9 knots at all coastal sites and between 3 and 6 knots at interior locations. Land breezes, normally less than 5 knots, are enhanced at coastal stations backed by mountains. Cooler air in the coastal mountains

increases northern stations' nocturnal drainage flow. Cyclonic activity produces the highest wind speeds. All gusts above 30 knots occur in November, with Tripoli (WSW at 54 knots) and Beirut (S at 41 knots) recording the highest wind speeds in the region. Figure 4-22 gives surface wind roses for selected stations. Winds aloft back to westerly, as was shown in Figure 4-5. Speeds increase to 70 knots at 42,000 feet (13 km) by November.

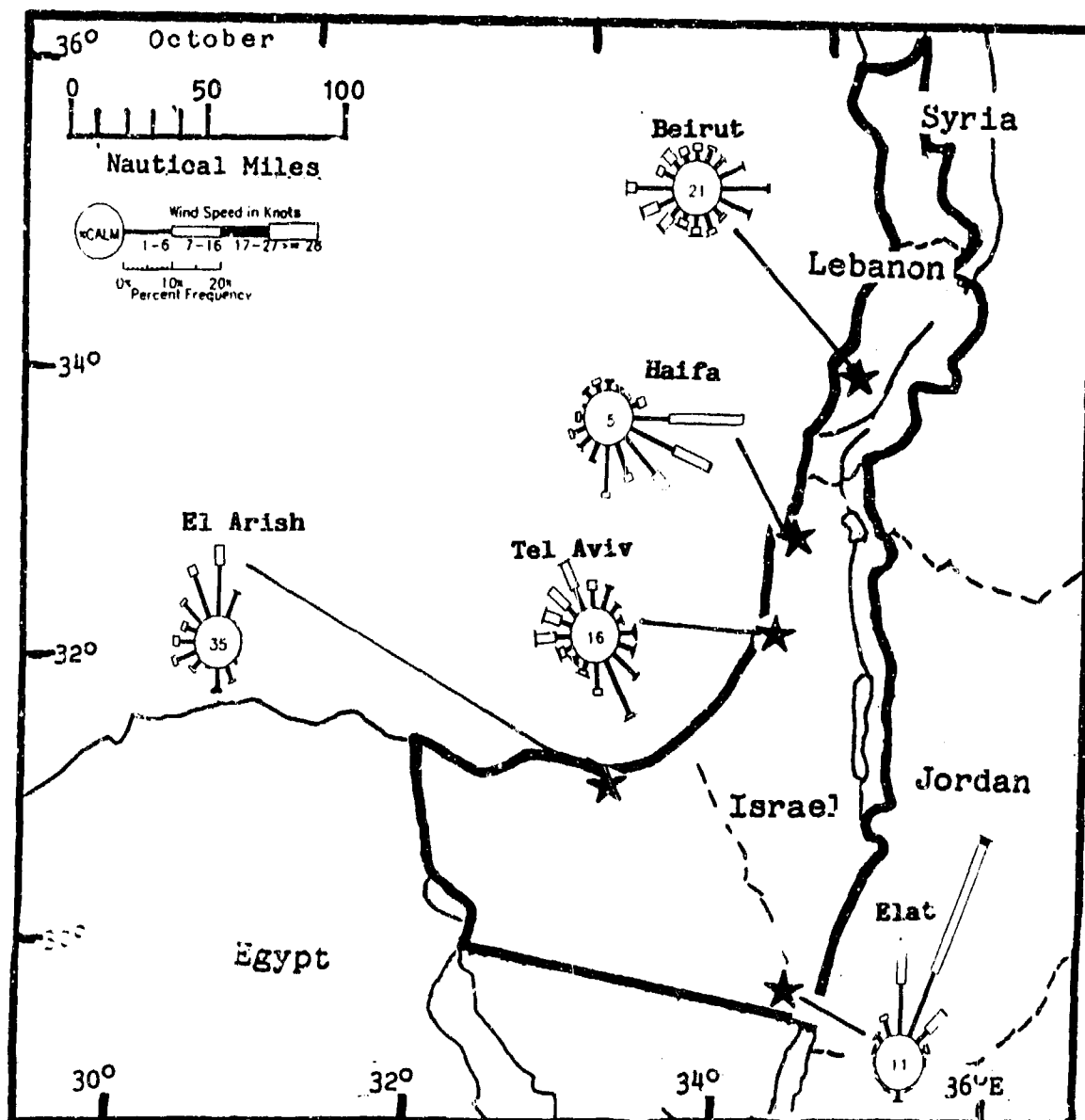


Figure 4-22. October Surface Wind Roses, Eastern Mediterranean Coast.

THE EASTERN MEDITERRANEAN COAST FALL

September-November

PRECIPITATION. September rainfall is scarce, as shown in Figure 4-23. The prevailing southwesterly flow is very dry, and the storm track is north of the region. Rainfall increases in late October along the northern coast as Genoa Lows begin to affect the region. The Lebanon Mountains produce a rain shadow effect to their northeast. Rainfall amounts increase through the

fall from less than 0.6 inch (15 mm) in September to 2-5 inches (50-125 mm) in November along the coast.

Fall thunderstorm frequencies increase in the north. Windward mountain slopes get more than six thunderstorms a season.

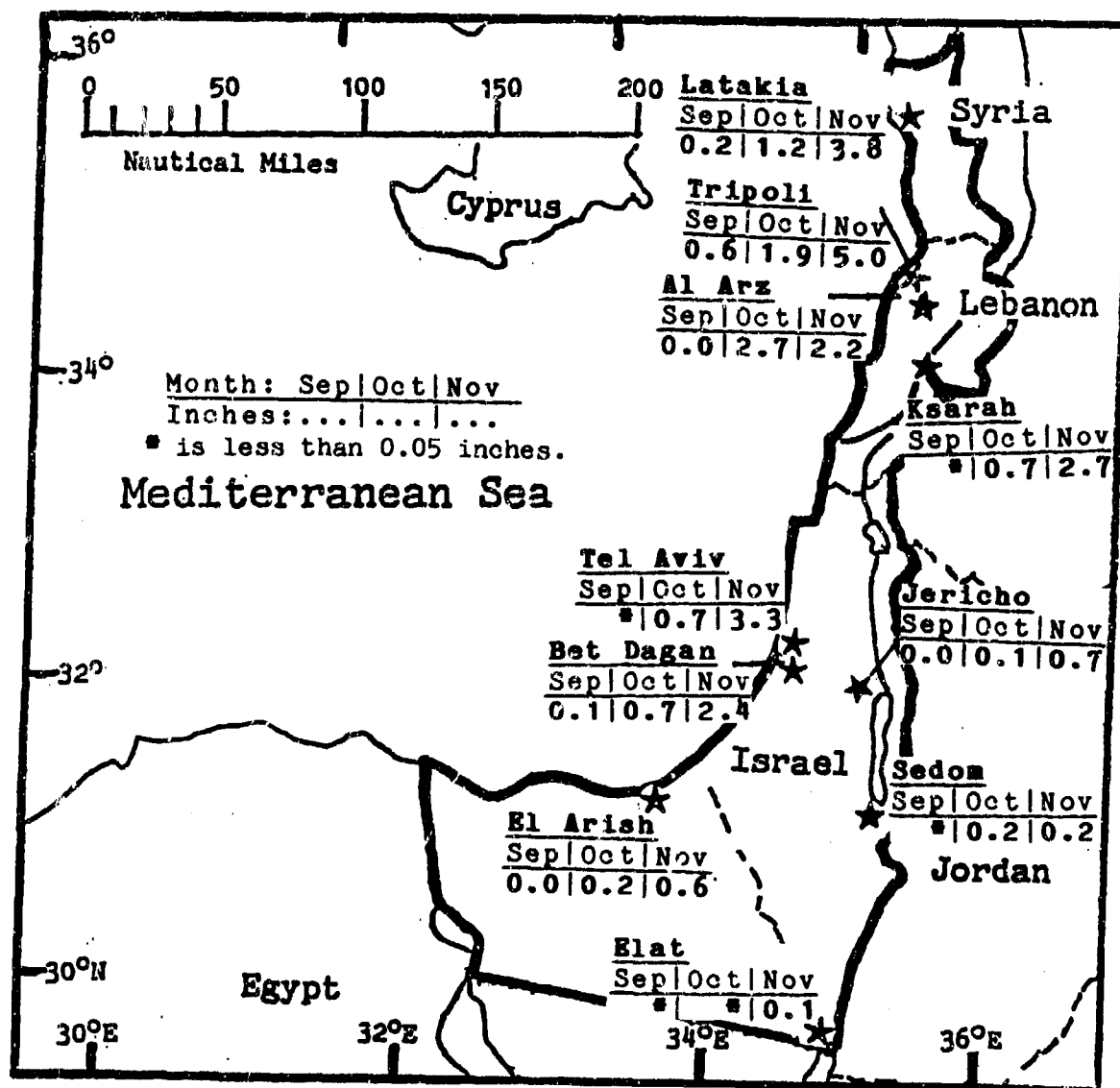


Figure 4-23. Mean Fall Monthly Precipitation, Eastern Mediterranean Coast.

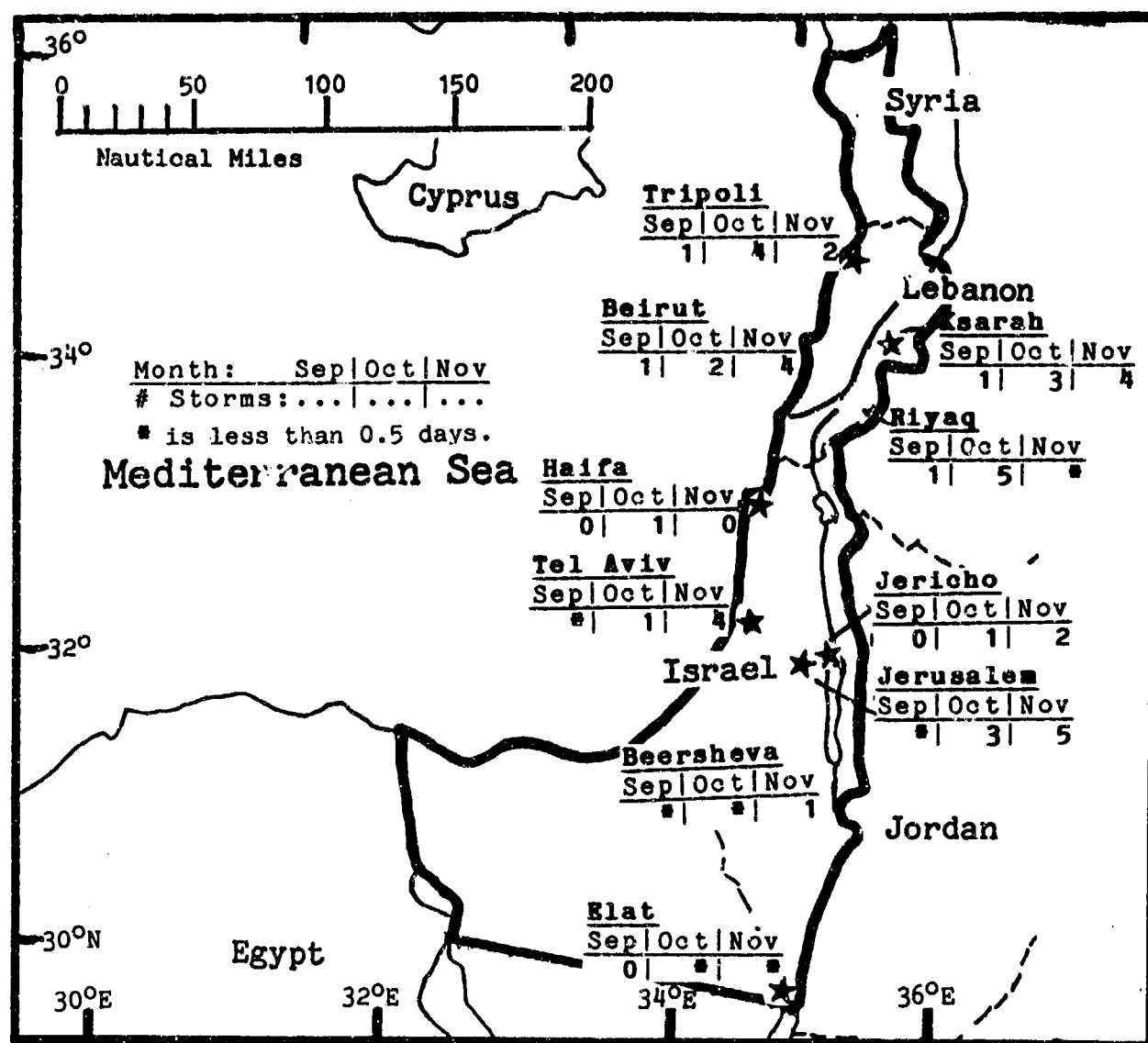


Figure 4-24. Mean Fall Thunderstorm Days, Eastern Mediterranean Coast.

TEMPERATURE. Mean daily highs range from 74° F to 88° F (23° C to 31° C) along the coast. They are about 15° F (8° C) lower in the mountains above 2,000 feet (1,500 meters) and reach 51° F (10° C) at Al Arz (6,283 feet/1,916 meters in elevation).

Temperatures are highest in the Jordan Rift Valley. The record high temperature at Marj Uyan (at 2,516 feet/767 meters) is 93° F (34° C) and 117° F (47° C) at

Jericho. Mean daily lows range from 41° F (4° C) to 81° F (27° C). Lows on the immediate coastline are between 50 and 70° F (10 and 21° C).

Sub-freezing temperatures only occur above 5,000 feet (1,525 meters). The area's record low temperatures include 25° F (-4° C) at Riyaq and 52° F (11° C) at Sedom. Figure 4-25 gives mean temperature data for the area.

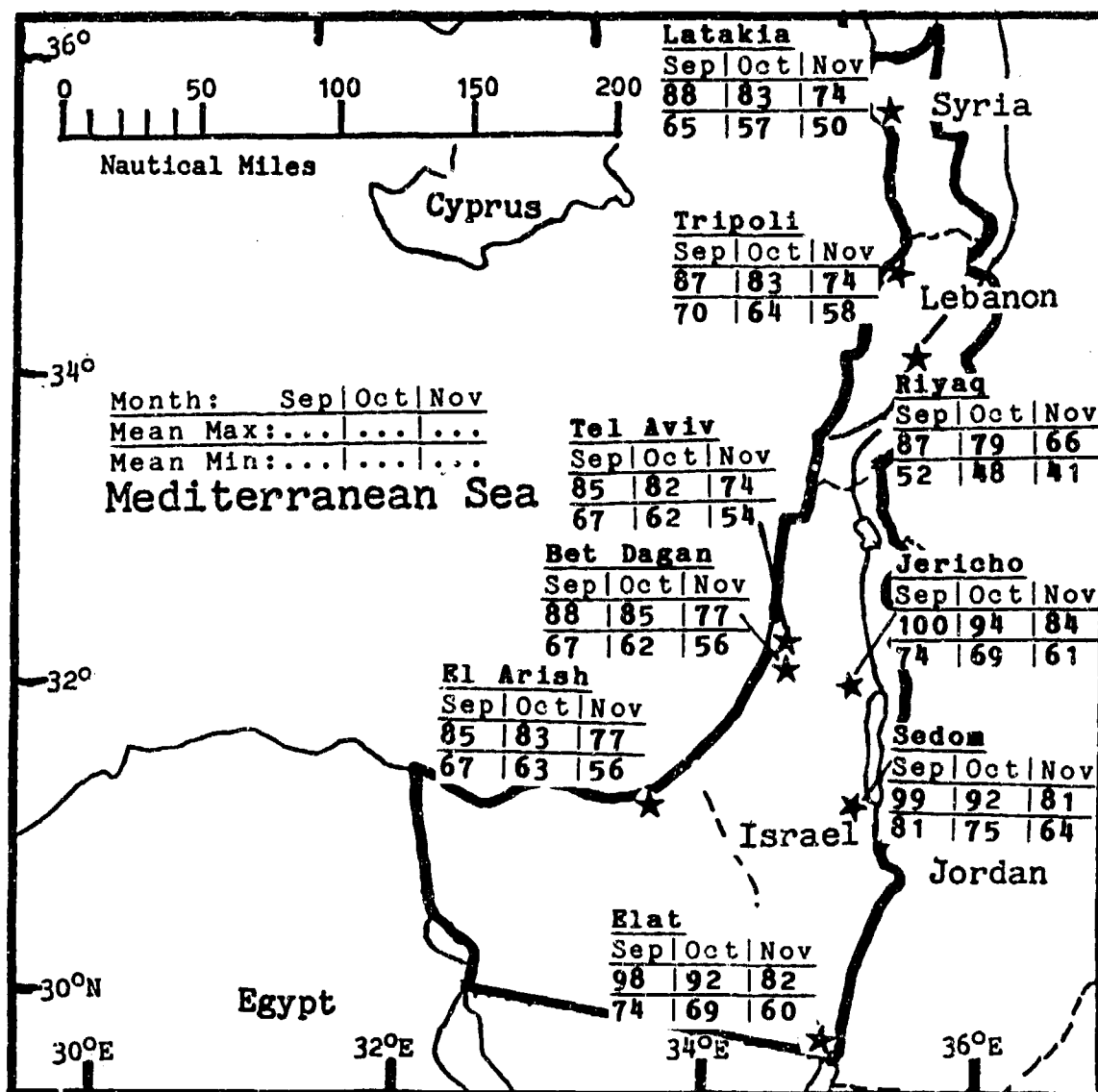


Figure 4-25. Mean Fall Daily Maximum/Minimum Temperatures (F), Eastern Mediterranean Coast.

Chapter 5

NORTH AFRICAN COAST

The North African Coast comprises the coastal fringes of Egypt and Libya west of the Suez Canal. It includes most of the Akhdar Mountains and the northern slopes of the Nafusah Mountains. After describing the area's situation and relief, this chapter discusses "general weather conditions" by season.

	Page
Situation and Relief	5-2
Winter--December-February	5-7
General Weather	5-7
Sky Cover.....	5-7
Visibility	5-8
Winds	5-9
Precipitation	5-10
Temperature	5-12
Spring--March-May	5-13
General Weather	5-13
Sky Cover.....	5-13
Visibility	5-14
Winds	5-15
Precipitation	5-16
Temperature	5-17
Summer--June-August	5-18
General Weather	5-18
Sky Cover.....	5-18
Visibility	5-20
Winds	5-21
Precipitation	5-21
Temperature	5-22
Fall--September-November	5-23
General Weather	5-23
Sky Cover.....	5-23
Visibility	5-24
Winds	5-24
Precipitation	5-25
Temperature	5-26

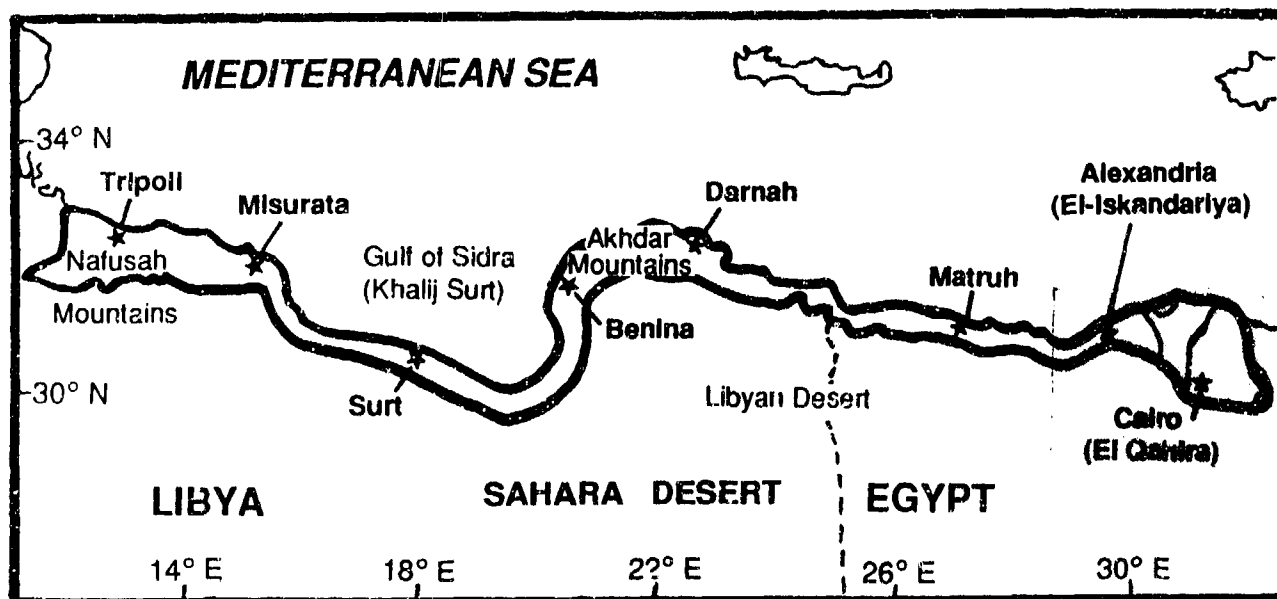


Figure 5-1a. The North African Coast. This region includes the flat, sandy plain that stretches for 1,100 NM along the southern Mediterranean Sea coast from the Libyan-Tunisian border eastward to the northern Sinai Peninsula and the Suez Canal. The spelling of place-names here varies widely. DMAAC spelling, transliterated from the Arabic, is used except for well-known places like Cairo and the Gulf of Sidra; in such cases, both spellings are given. The shaded rectangle defines the area described by Figure 5-2.

STATION: <u>Darnah, LY</u>													
LAT/LON: <u>32 47 N</u>		<u>22 38 E</u>						ELEV: <u>7M</u>					
ELEMENTS	JAN	FEB	MAR	APR	MAY	JUN	JUL	AUG	SEP	OCT	NOV	DEC	ANN
XTRM MAX	88	91	108	104	111	114	112	110	108	103	100	91	114
AVG MAX	85	85	87	73	77	82	84	85	83	80	74	87	78
AVG MIN	60	49	62	68	60	68	72	73	89	84	59	51	69
XTRM MIN	34	31	35	36	44	50	53	57	54	45	38	34	31
AVG PRCP	2.3	1.8	1.1	0.4	0.4	*	*	*	0.2	0.6	2.0	2.4	11.0
MAX MON	8.7	5.8	5.4	2.2	1.7	0.1	*	0.4	2.4	7.4	8.8	6.4	21.9
MAX DAY	1.9	1.7	0.9	1.1	1.0	*	*	0.4	2.0	5.9	2.4	2.0	
TS DAYS	1	1	1	1	1	*	0	*	1	1	1	1	9
DUST DAYS	*	0	0	*	0	0	0	0	0	0	0	0	1
APP TEMP	73	75	88	115	120	130+	110	100	115	110	93	75	

STATION: <u>Misurata, LY</u>													
LAT/LON: <u>32 25 N</u>		<u>15 08 E</u>						ELEV: <u>5M</u>					
ELEMENTS	JAN	FEB	MAR	APR	MAY	JUN	JUL	AUG	SEP	OCT	NOV	DEC	ANN
XTRM MAX	91	97	102	113	113	124	118	123	118	115	98	90	124
AVG MAX	84	85	70	75	80	87	90	92	89	84	75	68	79
AVG MIN	46	47	51	58	62	67	72	72	71	65	57	50	60
XTRM MIN	32	32	34	34	43	50	59	57	50	48	41	36	32
AVG PRCP	2.0	1.3	0.8	0.3	0.3	*	*	*	0.4	1.0	1.9	2.2	10.2
MAX MON	7.1	5.8	4.2	2.2	1.8	0.1	*	0.4	2.4	8.7	8.8	6.2	18.3
MAX DAY	1.8	1.3	0.9	0.7	1.0	0.1	*	0.4	2.0	3.1	2.4	2.4	
TS DAYS	1	1	*	1	1	1	*	*	1	2	*	1	9
DUST DAYS	2	3	4	4	4	2	1	*	2	2	2	2	28
APP TEMP	64	64	70	75	83	95	100	103	98	89	75	68	

* = LESS THAN 0.05 INCHES OR LESS THAN 0.5 DAYS

Figure 5-1b. Climatological Summaries for Selected Stations on the North African Coast.

STATION: <u>Benina, LY</u>													
LAT/LON: <u>32 08 N</u> <u>20 04 E</u> ELEV: <u>28M</u>													
ELEMENTS	JAN	FEB	MAR	APR	MAY	JUN	JUL	AUG	SEP	OCT	NOV	DEC	ANN
XTRM MAX	84	90	101	108	113	113	108	111	108	100	88	88	113
AVG MAX	83	84	70	75	82	84	84	88	83	80	75	83	78
AVG MIN	48	50	53	58	62	67	72	72	68	64	58	52	60
XTRM MIN	32	32	34	39	43	50	50	57	50	51	43	32	32
AVG PRCP	2.7	1.8	0.8	0.2	0.1	*	*	*	0.1	0.7	1.8	2.8	10.5
MAX MON	10.2	5.8	3.5	2.8	2.1	1.2	0.2	0.2	9.5	3.8	7.9	9.3	24.3
MAX DAY	3.3	1.4	1.5	2.8	2.1	0.8	0.2	0.2	1.4	2.5	1.7	2.2	3.3
TS DAYS	1	1	1	*	*	*	*	*	*	1	*	*	5
DUST DAYS	1	1	1	1	1	1	1	*	1	3	2	1	14
APP TEMP	63	64	69	81	83	87	89	93	87	84	77	68	

STATION: <u>Surt, LY</u>													
LAT/LON: <u>31 12 N</u> <u>18 35 E</u> ELEV: <u>22M</u>													
ELEMENTS	JAN	FEB	MAR	APR	MAY	JUN	JUL	AUG	SEP	OCT	NOV	DEC	ANN
XTRM MAX	84	99	101	113	114	124	118	118	111	108	100	88	124
AVG MAX	84	88	72	75	79	84	88	88	87	82	78	67	77
AVG MIN	48	48	52	57	62	68	71	73	70	64	57	50	59
XTRM MIN	35	33	35	40	43	49	50	63	59	52	43	36	33
AVG PRCP	1.8	1.0	0.8	0.1	0.1	*	0	0	0.5	0.8	1.2	1.8	7.8
MAX MON	5.2	4.1	3.1	1.0	0.8	0.4	0	0	1.8	2.5	4.8	4.0	13.7
MAX DAY	1.7	2.2	0.9	0.4	0.6	0.4	0	*	1.8	2.6	2.1	1.8	
TS DAYS	*	*	*	*	*	*	0	0	1	1	*	1	3
DUST DAYS	3	3	2	2	2	1	0	*	1	1	2	2	19
APP TEMP	72	81	90	118	130+	130+	130+	130+	130	115	97	78	

STATION: <u>Tridoli, LY</u>													
LAT/LON: <u>32 54 N</u> <u>13 11 E</u> ELEV: <u>20M</u>													
ELEMENTS	JAN	FEB	MAR	APR	MAY	JUN	JUL	AUG	SEP	OCT	NOV	DEC	ANN
XTRM MAX	83	98	104	111	115	117	118	118	117	108	99	88	118
AVG MAX	82	88	69	78	84	92	99	95	89	81	71	64	79
AVG MIN	45	47	50	57	66	72	73	74	70	63	54	48	60
XTRM MIN	30	30	34	37	41	48	55	57	54	45	37	32	30
AVG PRCP	2.7	1.5	0.8	0.3	0.2	0.1	*	*	0.4	1.4	2.1	3.1	12.8
MAX MON	5.1	6.4	3.9	3.2	1.3	0.7	0.4	1.1	4.3	7.7	11.5	14.9	29.8
MAX DAY	2.1	4.9	2.0	2.0	0.8	0.4	0.4	1.1	3.1	3.2	5.1	2.8	
TS DAYS	1	1	*	*	*	*	*	*	1	2	2	1	9
DUST DAYS	4	4	4	4	3	3	1	1	3	3	2	2	34
APP TEMP	70	75	88	108	115	130+	130+	125	115	110	90	75	

* = LESS THAN 0.05 INCHES OR LESS THAN 0.5 DAYS

Figure 5-1c. More Climatological Summaries for Selected Stations on the North African Coast.

THE NORTH AFRICAN COAST

SITUATION AND RELIEF

STATION: <u>Alexandria, UB</u>													
LAT/LON: <u>31 12 N</u> <u>29 53 E</u> ELEV: <u>23 FT</u>													
ELEMENTS	JAN	FEB	MAR	APR	MAY	JUN	JUL	AUG	SEP	OCT	NOV	DEC	ANN
XTRM MAX	82	91	106	108	113	115	111	108	108	104	97	90	115
AVG MAX	68	67	70	76	79	85	87	86	85	82	77	68	77
AVG MIN	49	51	53	57	63	68	71	73	70	66	60	53	62
XTRM MIN	37	37	39	43	48	57	61	61	57	54	45	37	37
AVG PRCP	1.4	0.8	0.4	0.2	0.1	*	*	*	0.2	0.2	1.2	1.7	6.2
MAX MON	5.0	3.6	2.3	2.0	0.9	0.1	*	*	0.9	2.9	8.9	15.3	15.3
MAX DAY	1.9	1.3	1.2	1.2	0.7	0.1	*	*	0.9	2.3	4.6	2.2	4.6
TS DAYS	2	2	1	*	1	*	0	0	*	2	1	2	11
DUST DAYS	2	1	3	2	1	1	0	*	*	*	*	2	12
APP TEMP	68	67	70	76	82	93	97	93	90	85	77	68	

STATION: <u>Matruh, UB</u>													
LAT/LON: <u>30 22 N</u> <u>27 14 E</u> ELEV: <u>98 FT</u>													
ELEMENTS	JAN	FEB	MAR	APR	MAY	JUN	JUL	AUG	SEP	OCT	NOV	DEC	ANN
XTRM MAX	79	86	104	105	111	113	98	103	104	102	93	85	113
AVG MAX	64	65	68	72	75	80	82	83	83	80	75	68	75
AVG MIN	47	48	51	56	61	67	71	72	70	65	58	51	60
XTRM MIN	34	36	36	43	46	55	61	61	57	52	45	38	34
AVG PRCP	1.6	1.0	0.5	0.1	0.1	0.0	0.0	*	*	0.5	1.0	1.3	6.1
MAX MON	8.3	2.4	2.0	1.8	0.7	2.3	0.0	0.4	0.5	4.0	3.7	5.2	15.2
MAX DAY	2.1	1.7	1.5	1.0	0.6	1.9	0.0	0.4	0.5	3.0	1.7	3.9	3.9
TS DAYS	1	1	*	1	0	0	0	0	*	1	1	1	6
DUST DAYS	3	3	4	4	3	2	1	1	1	2	1	5	30
APP TEMP	64	65	68	72	77	86	89	91	90	85	77	68	

STATION: <u>Port Said, UB</u>													
LAT/LON: <u>31 18 N</u> <u>32 19 E</u> ELEV: <u>20 FT</u>													
ELEMENTS	JAN	FEB	MAR	APR	MAY	JUN	JUL	AUG	SEP	OCT	NOV	DEC	ANN
XTRM MAX	84	92	100	105	113	111	107	99	104	100	98	88	113
AVG MAX	68	68	70	74	80	85	88	89	87	84	77	69	78
AVG MIN	51	52	56	60	65	71	74	75	73	70	64	55	64
XTRM MIN	37	36	37	49	50	58	66	68	64	55	48	32	32
AVG PRCP	0.7	0.5	0.4	0.2	0.2	*	0.0	0.0	*	0.1	0.4	0.6	3.0
MAX MON	2.8	2.3	1.7	1.7	1.3	1.3	*	*	0.3	3.4	2.7	3.5	7.3
MAX DAY	1.5	2.3	0.6	1.4	1.1	1.3	*	*	0.3	1.6	1.9	2.1	2.3
TS DAYS	*	*	*	1	*	*	0	0	0	1	*	1	4
DUST DAYS	2	2	3	2	1	1	*	*	*	*	1	2	14
APP TEMP	68	68	70	74	83	91	96	96	94	89	77	69	

* * * LESS THAN 0.05 INCHES OR LESS THAN 0.5 DAYS

Figure 5-1d. Still More Climatological Summaries for Selected Stations on the North African Coast.

GEOGRAPHY. The eastern border of the North African Coast runs from Port Said south along the Suez Canal to the northern tip of the Gulf of Suez, then west to the Nile River south of Cairo. It then follows the Nile flood plain north to a point just south of Alexandria. Continuing west, the rest of the region is made up of the narrow coastal plain from Alexandria along the Akhdar Mountains' southern slopes, along the Gulf of Sidra, and along the Nafusah Mountains' northern slopes to the Tunisia border.

This region's width varies from 5 to 130 NM. It is widest on both ends and narrowest between the Gulf of Sidra and the Akhdar Mountains. Except in the Akhdar and Nafusah Mountains, elevations are below 660 feet (200 meters) MSL.

Flat coastal plains with sandy or rocky soils make up 85% of this region. Although much of the Sahara is rocky, there are extensive sand dunes in the Libyan and Sinai Deserts. There are also isolated salt marshes and tidal lagoons. The Nile Delta is arid even though the Nile and its many branches flow through it.

The Nafusah and Akhdar Mountains interrupt the gently sloping coastal plains. They average 2,000 feet (610 meters) MSL, with several peaks above 3,000 feet (915 meters) MSL. The Nafusah Mountains parallel the coast about 70 to 90 NM inland. The Akhdar Mountains hug the coastline along the northeastern Gulf of Sidra coast.

DRAINAGE AND RIVER SYSTEMS. The River Nile, the region's only permanent drainage basin, is one of the world's largest. Figure 5-2 is an expanded view of the Nile Delta, which extends 85 NM inland and 130 NM along the coast. It contains hundreds of meandering streams and canals. The Nile splits into two branches--the Damietta on the east and the Rosetta on the west--17 NM north of Cairo. These rivers are lined with salt marshes and small lakes formed during seasonal flooding.

Many semipermanent streams (wadis) dissect the Nafusah and Akhdar Mountains. These wide but shallow stream beds reach the Mediterranean Sea only during the winter. The Suez Canal is a man-made waterway linking the Red and Mediterranean Seas.

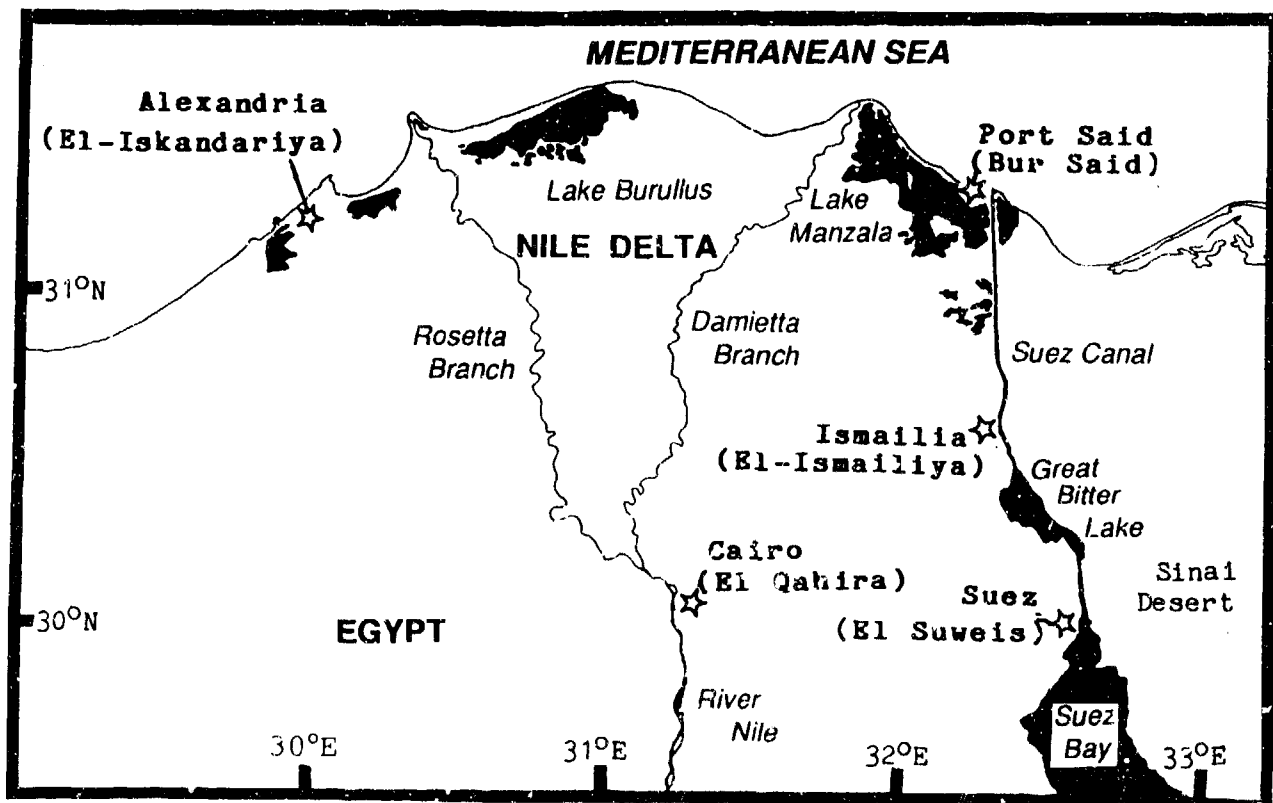


Figure 5-2. The Nile Delta, Showing Primary Rivers, Lakes, and Cities.

LAKES AND RESERVOIRS. The only lakes and reservoirs in the region are in the Nile Delta or along the Suez Canal. Many are seasonally flooded. The Great Bitter Lake was created during construction of the canal.

VEGETATION. The deserts are mostly barren, but short scrub grows in protected areas where water is available. Irrigation in the Nile Delta allows cultivation of palms and citrus. Isolated open woodland, evergreen, and scrub vegetation are found in the Nafusah and Akhdar Mountains.

GENERAL WEATHER. Although moderate frontal showers and thunderstorms occur with stronger cold fronts, many only produce drizzle and light rain. Moist northwesterly flow from the Azores High, assisted by upper-level jets, steer low-pressure troughs through the region regularly.

SKY COVER. The combination of morning stratus or stratocumulus and the effects of transitory low-pressure systems make winter the cloudiest season. Morning stratus/stratocumulus forms over the water during fair weather when the nocturnal land breeze pushes air cooled by radiation over warmer coastal waters. The sea breeze sets up at sunrise and pushes the clouds onshore. The amount of stratus/stratocumulus at a given location is a function of its proximity to the coast and mountainous terrain. Morning stratus/stratocumulus bases are about 2,500 feet (760 meters), but below 500 feet (150 meters) in the mountains. These clouds cause some of the low morning ceilings shown in Figure 5-3. Tops are normally below 6,000 feet (1,830 meters) MSL. Clouds burn off within 2 hours after sunrise in the warmer air. Morning stratus (bases at 700-1,100 feet/215-335 meters) forms in the Nile Delta from the moisture trapped under a nocturnal radiation inversion.

Cumulus forms at midday; bases are normally 4,000 feet (1,225 meters) but can be as low as 2,500 feet (760 meters). Tops are normally below 7,000 feet (2,135 meters) MSL. Most non-frontal afternoon ceilings below 3,000 feet (915 meters) are caused by this cumulus.

The effects of transitory lows depend on the system's origin. Mediterranean systems (such as Genoa Lows) are cloudier than North African systems (such as Atlas Lows) because of their overwater trajectories. Genoa Lows tracking along this coast cause the most extensive cloud cover, with multilayered decks from 4,000 feet (1,220 meters) and tops to 20,000 feet (6 km) MSL. Embedded cumuliform clouds can extend to 40,000 feet (12 km) MSL. Cloud bases may lower to 500 feet (150 meters) during heavy showers.

South-to-southwest winds ahead of an Atlas Low passing through the Gulf of Sidra force moisture over the Akhdar Mountains and increase cloudiness on the western slopes. On rare occasions, Atlas lows travel eastward south of the region. Skies are almost cloudless with these lows except on the Akhdar Mountains' eastern slopes, where enough moisture from the sea is present for cumulus to form.

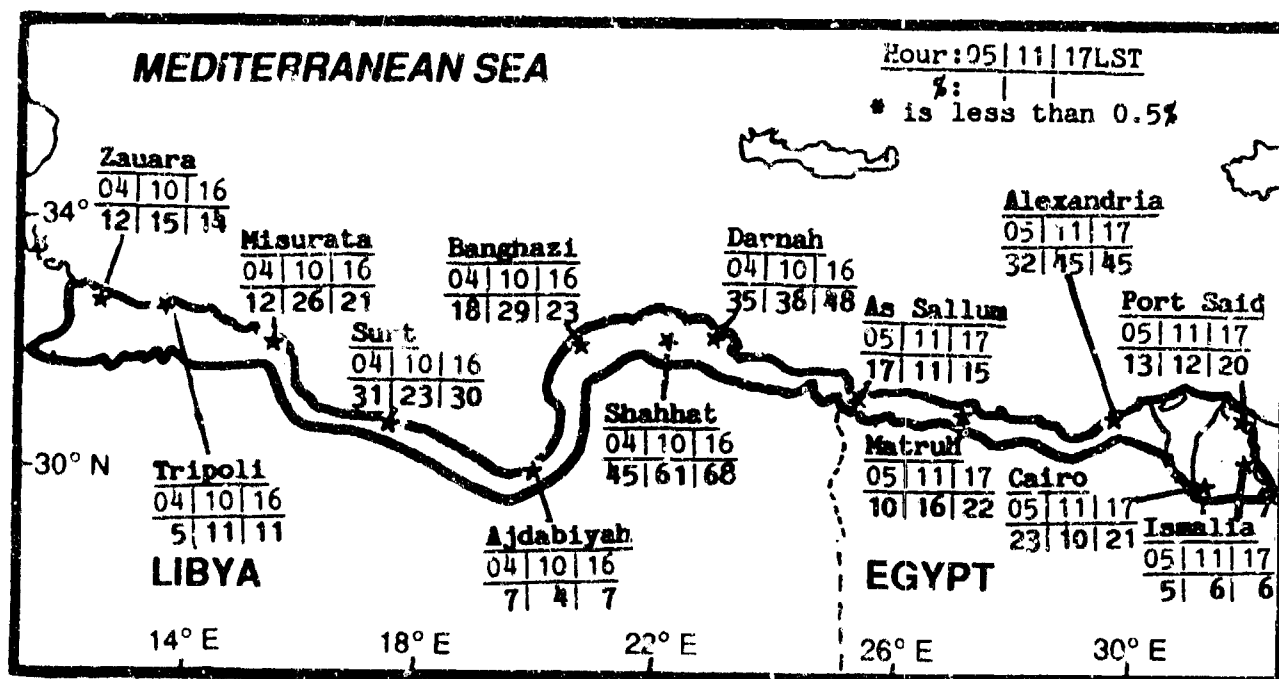


Figure 5-3. Mean Winter Frequencies of Ceilings Below 3,000 Feet (915 meters), North African Coast.

THE NORTH AFRICAN COAST WINTER

December-February

VISIBILITY. Winter visibilities are usually above 3 miles throughout the region, but they are below 3 miles 1-7% of the time along the coast (in the marine boundary layer) and 6-13% of the time inland. Figure 5-4 shows that low visibilities are more common in the east and in the mountains. Dust is often raised with 10-15 knot winds; the amount raised and particle sizes vary with wind speed, atmospheric stability, and local ground type and moisture content. Dust and haze combine at some inland locations such as Cairo and Adjabiya. Although dust haze normally only lowers visibilities to 5-6 miles, they can go below 3 miles. Low visibility is less of a problem west and north of the Akhdar Mountains where winds are more westerly than southwesterly and carry less dust.

Morning fog forms along the Nile Delta's rivers and canals, along the coast, and near lagoons. Heavy frontal rain showers and thunderstorms restrict visibilities to 1-3 miles. Morning stratus often obscures higher seaward-facing slopes in the Akhdar and Nafusah Mountains, causing 1-3 mile visibilities. Daytime heating lifts these fogs into thin stratocumulus or cumulus decks by late morning.

Sand and dust carried by winds over 25 knots near transitory lows and around their trailing cold fronts can drop visibilities below 1 mile for 1-6 hours. These duststorms often lift dust to 20,000 feet (6 km) MSL. The Akhdar Mountains shelter areas to the north from southerly, dust-laden winds. Transitory lows also cause heavy rain showers and thunderstorms that may reduce visibilities below 3 miles for short periods.

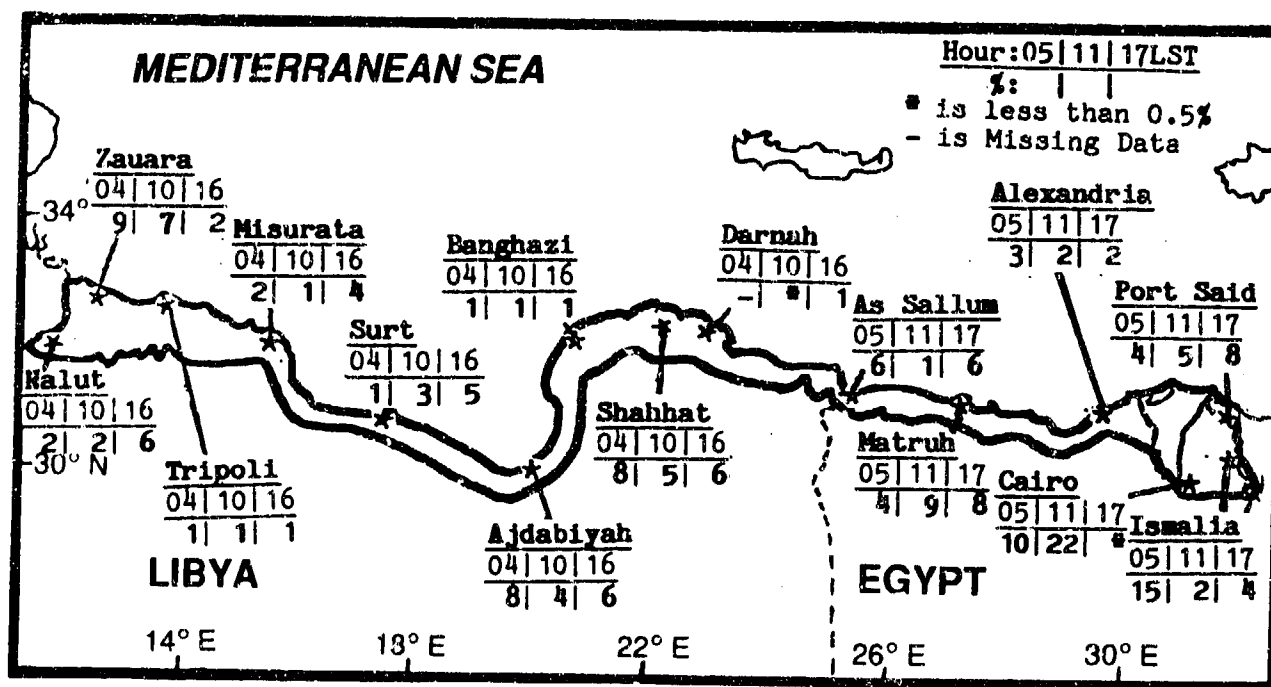


Figure 5-4. Mean Winter Frequencies of Visibilities Below 3 Miles, North African Coast.

WINDS. Mean wind speeds generally decrease from west to east as the Azores High's influence declines with distance away from its mean winter position. Highest observed wind speeds are always associated with cyclonic activity, usually Genoa Lows. Strong and gusty west to northwest winds accompany intense cold fronts. Peak gusts average 30 knots, but 45- to 55-knot gusts have been reported at Tripoli and Darnah, both exposed coastal locations. Stations farther from the coast have

lower mean wind speeds, as shown in Figure 5-5. The land or sea breeze augments prevailing westerlies along coasts that are perpendicular to the flow. Westerlies dominate areas where coastlines are parallel to the flow. Nocturnal drainage winds dominate around the Akhdar and Nafusah Mountains.

Upper-level winds, shown in Figures 5-6a and 5-6b, are westerly under the Azores High's influence.

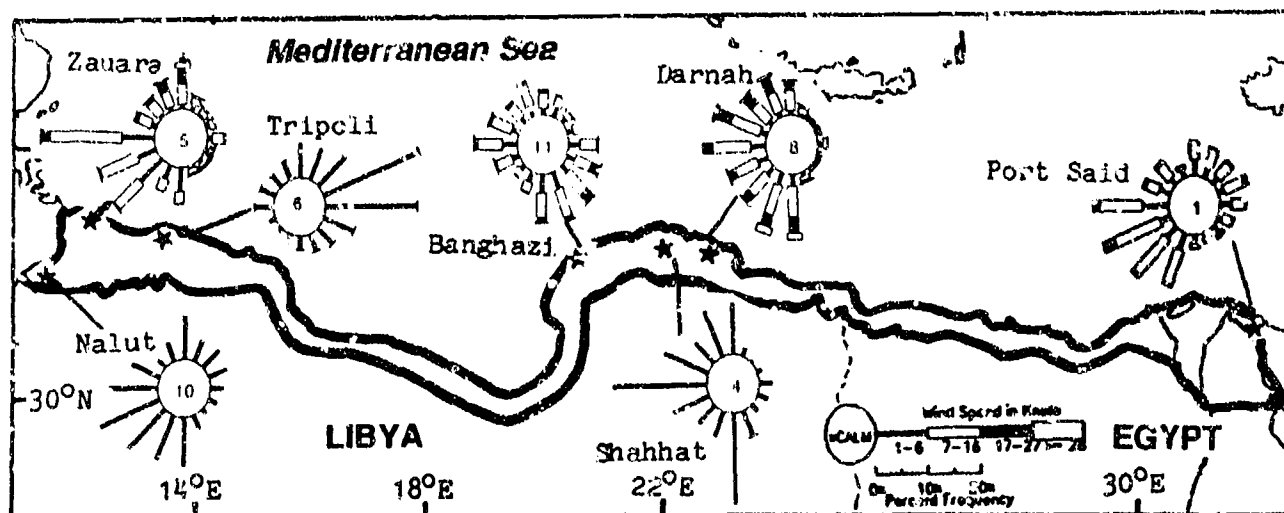


Figure 5-5. January Surface Wind Roses, North African Coast.

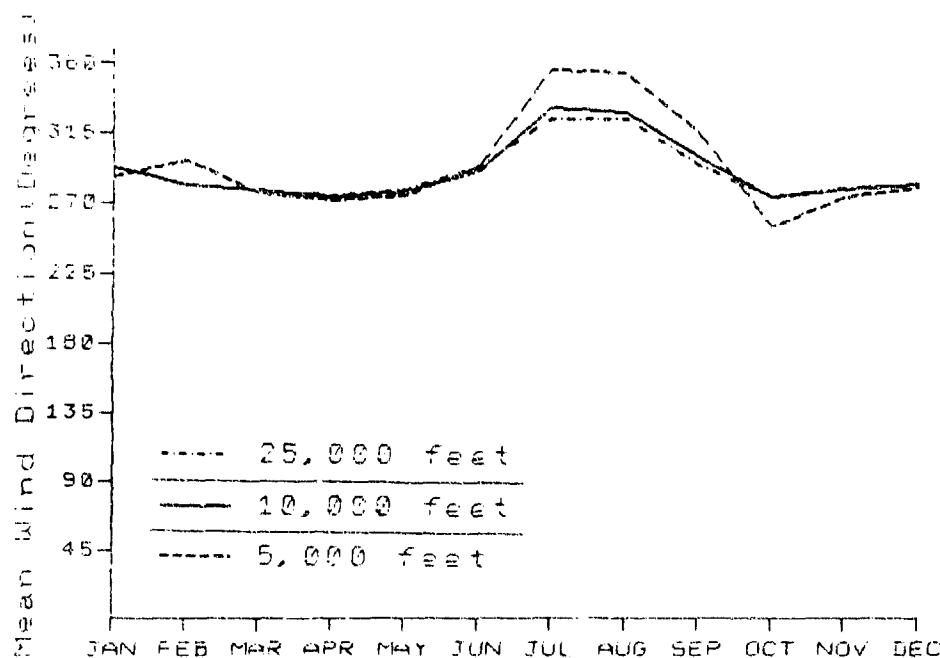


Figure 5-6a. Upper-level Annual Mean Wind Direction, Tripoli, Libya.

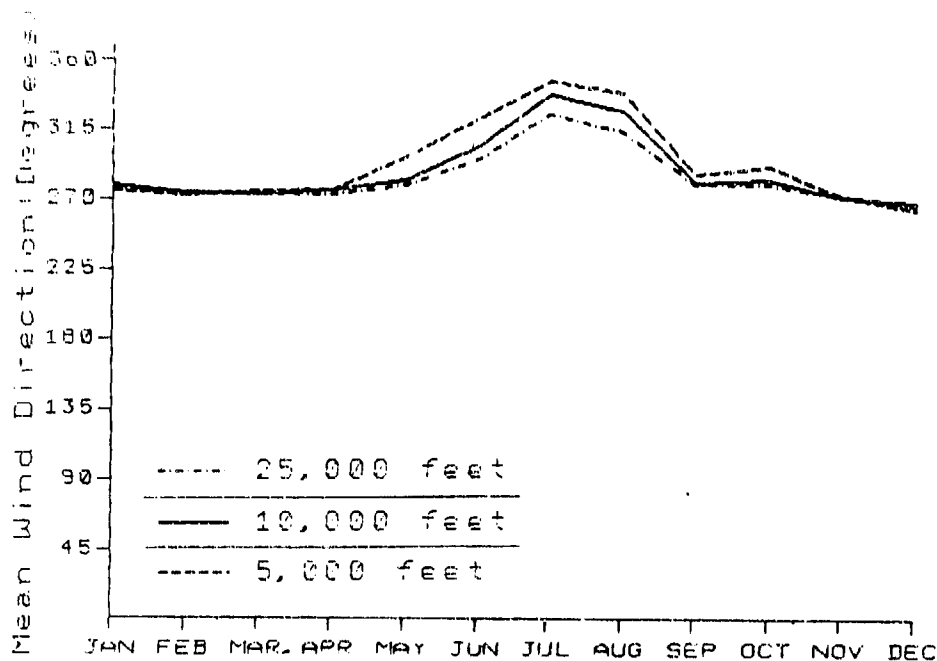


Figure 5-6b. Upper-level Annual Mean Wind Direction, Benghazi, Libya.

PRECIPITATION. Most rainfall is convective. As shown in Figure 5-7, the region gets 1 to 16 inches of rain in the winter, depending on proximity to the mean storm track, proximity to the mountains, and coastal orientation. Northwestern mountains slopes get the most. Light rain or drizzle falls above 2,000-foot (610-meter) elevations with transitory lows. As illustrated by the Genoa Low track in Figure 5-8, less

rain falls along flat desert coasts oriented west-to-east and parallel to advancing cold fronts. Southeastern slopes and east-facing coasts get even less. Port Said, on the region's extreme eastern edge where fronts seldom penetrate, gets the least rainfall. Snow falls on less than 1 day a winter. It seldom lasts more than 2 hours, but can persist for up to 6 hours above 1,500 feet (455 meters) after a frontal passage.

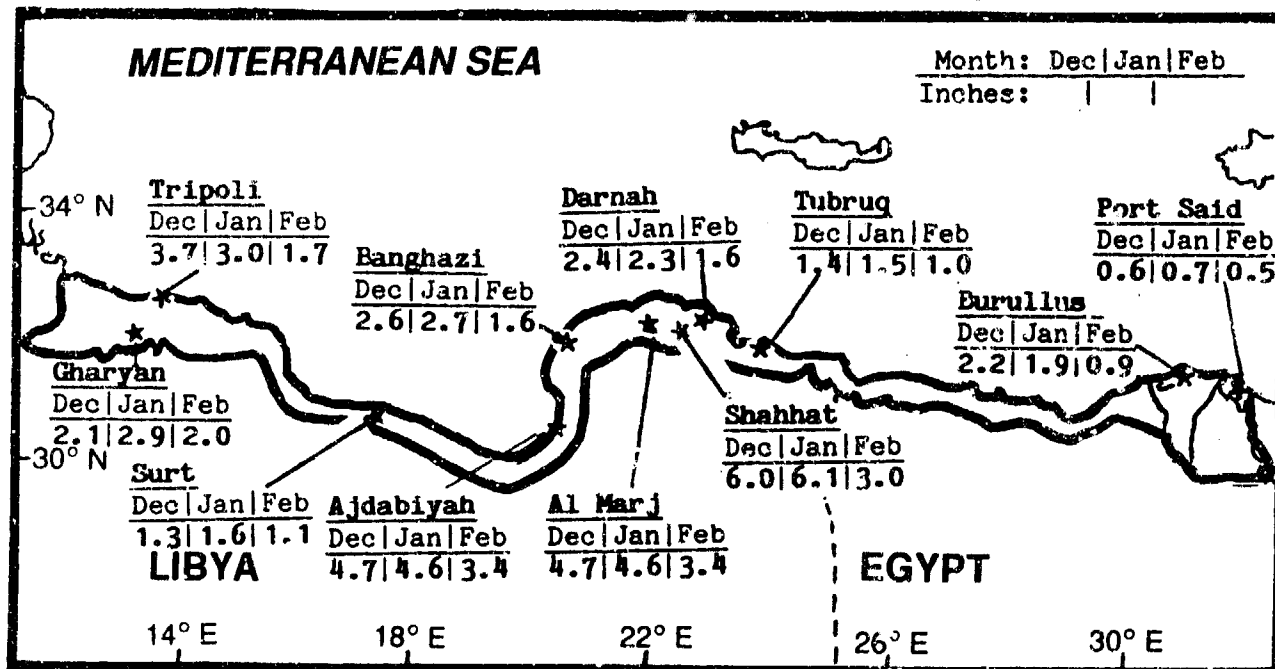


Figure 5-7. Mean Winter Monthly Precipitation, North African Coast.

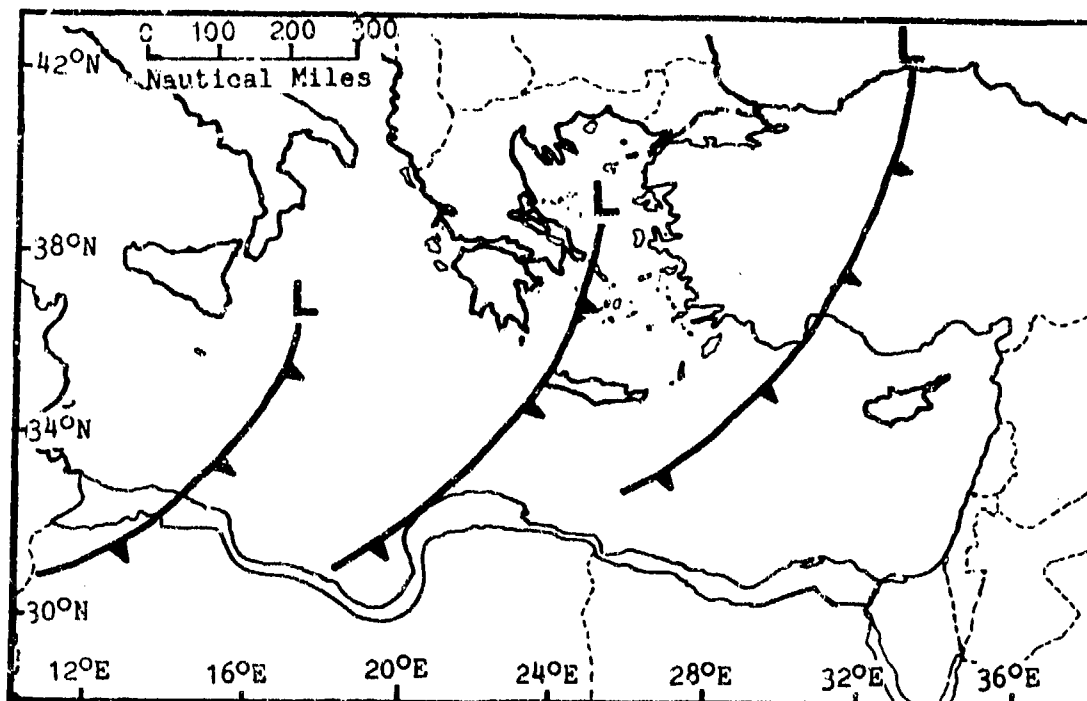


Figure 5-8. Typical Northeast Track of the Genoa Low.

Most stations report one or two thunderstorms a month in winter, as shown in Figure 5-9. Areas on windward slopes get the most. Tops are about 35,000 feet (10.5 km) MSL.

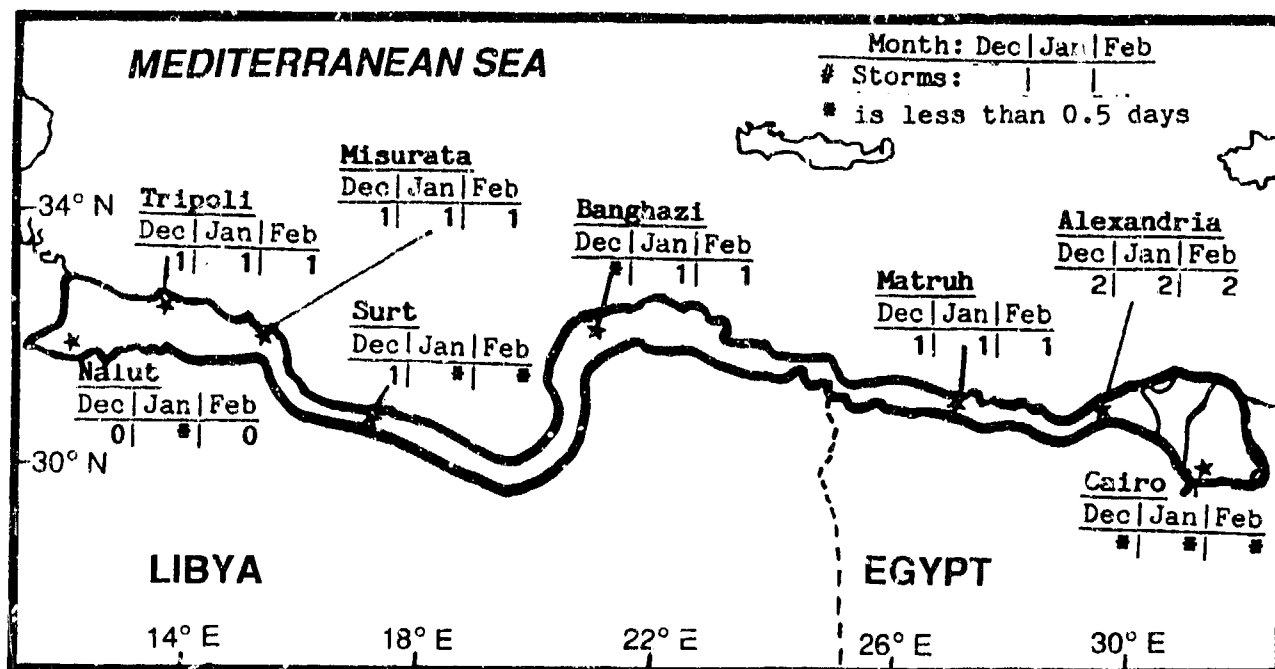


Figure 5-9. Mean Winter Thunderstorm Days, North African Coast.

THE NORTH AFRICAN COAST WINTER

December-February

TEMPERATURE. Mean daily highs in winter range from 54° F (12° C) at Shahhat to 71° F (22° C) inland over the Nile Delta. Lows range from 39° F (4° C) at Nalut to 57° F (14° C) at the Rosetta Lighthouse on the Nile Delta coast. Southerly winds bring extreme highs of 80-99° F. Continental polar surges from Europe bring

sub-freezing temperatures to the western two-thirds of the region. Extreme lows along coastal plains vary from 25° F (-4° C) at Tripoli to 32° F (0° C) at Benghazi. In the Nile Delta, extreme lows range from 28° F (-2° C) at Gharyan to 37° F (3° C) at Alexandria. Nalut's extreme low is 19° F (-7° C) in January.

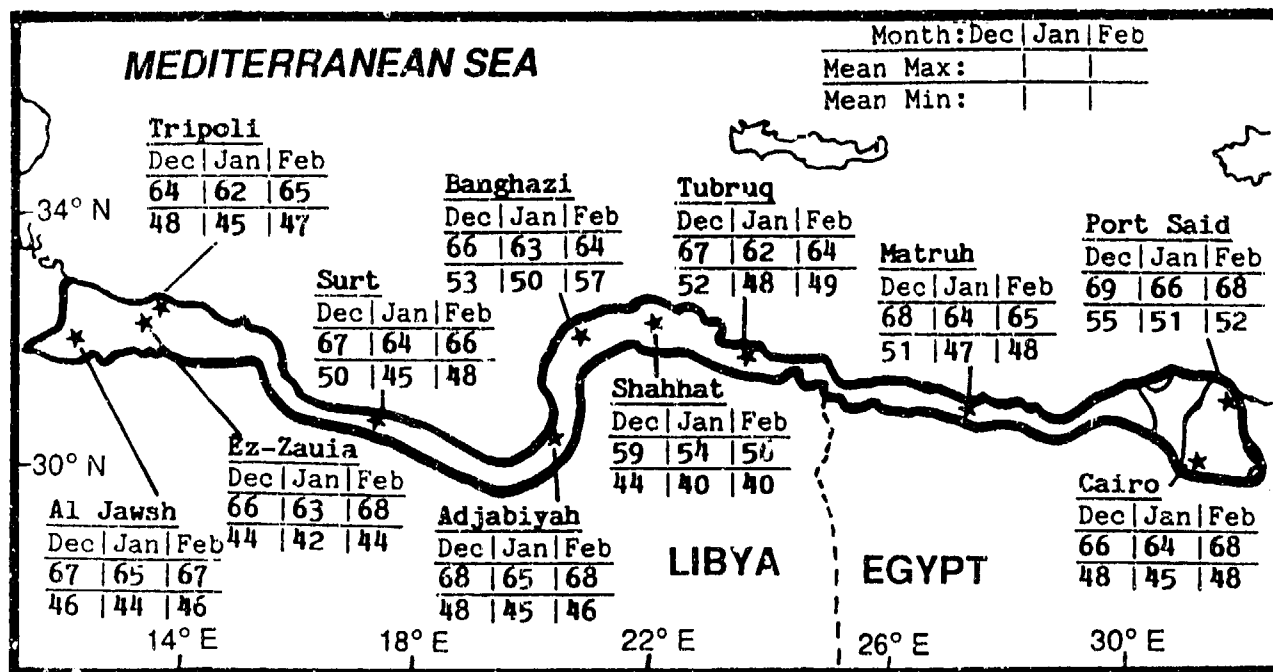


Figure 5-10. Mean Winter Daily Maximum/Minimum Temperatures (F), North African Coast.

GENERAL WEATHER. Movement of the Azores High shifts the mean Polar Jet into the western Mediterranean Basin while the Subtropical Jet intensifies over west-central Africa. The Saharan Heat Low builds during the spring, creating weak southeasterly flow in the region's western portion. A prominent area of cyclogenesis develops along the Atlas Mountains, spawning lows that often track northeastward through the Gulf of Sidra. After March (but most frequently in later April), hot and dry southerly winds from the Sahara (the Khamsin or Ghibli) bring dust, sand, high winds and high temperatures to the region, but little rainfall. The Polar and Subtropical Jets may interact with surface low pressure to produce strong, well-developed cells. There are about eight low passages during a typical spring.

SKY COVER. Although cloudiness diminishes in the spring, Atlas Lows and moist air keep cloud cover relatively high. At sunrise, the sea breeze pushes extensive stratus and stratocumulus decks onshore. Localized amounts of stratus/stratocumulus are functions of land/sea breeze strength and terrain. Bases are generally 2,000-3,000 feet (610-915 meters), but mountain stations may report similar clouds with 500-foot (150-meter) bases. Tops are 3,000 to 6,000 feet (915 to 1,830 meters) MSL on windward slopes. Over

the Nile Delta, stratus with bases of 800-1,200 feet (245-365 meters) forms from moisture trapped under the nocturnal inversion layer. These decks dissipate between 0900 and 1100 LST in the warmer, drier air. Fair-weather cumulus forms in the afternoon along the coast with bases at 4,000-5,000 feet (1,220-1,520 meters) and tops to 7,500 feet (2,285 meters); they usually dissipate by late afternoon. Ceilings below 3,000 feet (915 meters) are common in these fair-weather clouds; Figure 5-11 shows relative frequencies.

Clouds associated with transitory lows diminish after mid-April. Nimbostratus is very rare, but scattered cumulonimbus or towering cumulus can occur along cold fronts; bases are 4,000-5,000 feet (1,220-1,525 meters), tops from 25,000 to 50,000 feet (7.5-15 km) MSL. Bases may lower to 500 feet (150 meters) in heavy showers. Although altocumulus and altostratus occur with Atlas Lows and upper-level disturbances, they are not extensive because Atlas Lows are normally dry. Bases are between 8,000 and 15,000 feet (2,440 and 4,570 meters) and tops in multilayered clouds reach to 21,000 feet (6,400 meters). Thin cirrus develops at 18,000 feet (5,485 meters) near Subtropical Jets, Atlas Lows, weak upper-level disturbances, and thunderstorms. Thunderstorm blow-off may reach 50,000 feet (15 km) MSL.

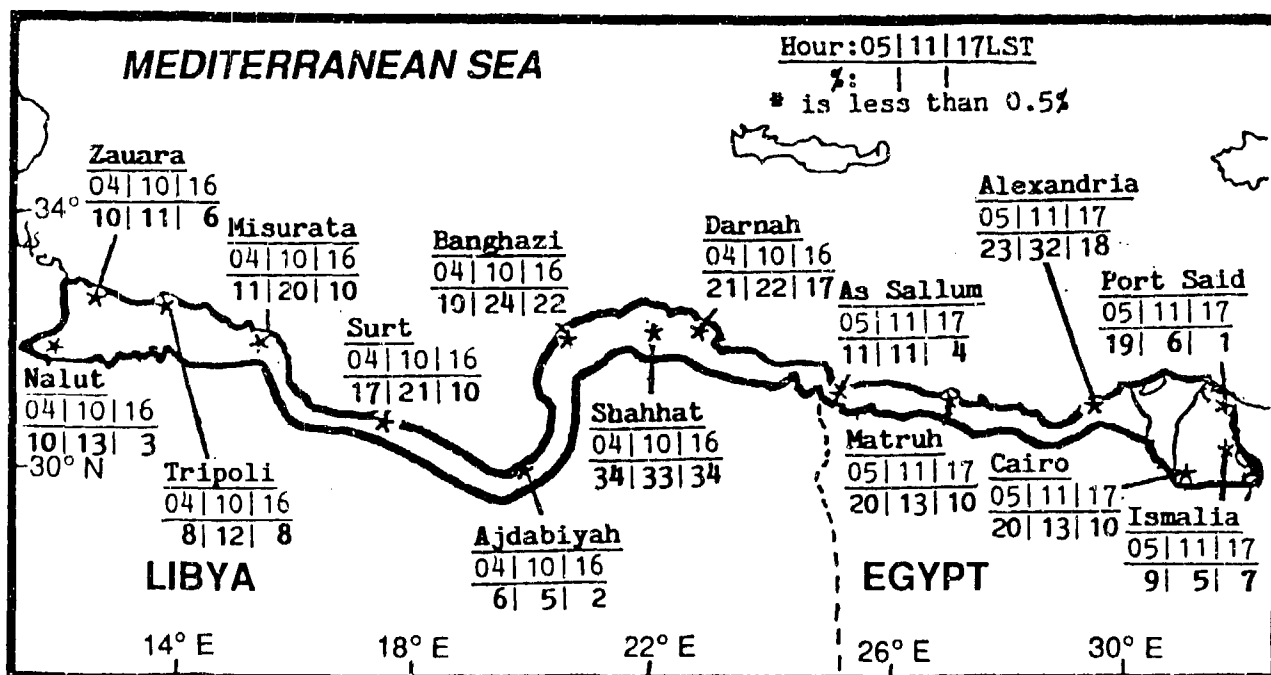


Figure 5-11. Mean Spring Frequencies of Ceilings Below 3,000 Feet (915 meters), North African Coast.

THE NORTH AFRICAN COAST SPRING

March-May

VISIBILITY. Spring visibilities are generally poor as frequent Atlas Lows raise dust and sand. As shown in Figure 5-12, visibilities are below 3 miles 1-14% of the time along immediate coasts, 6-25% inland.

Winds above 25 knots near Atlas Lows and their trailing cold fronts can reduce visibilities to 1 mile. Hot, extremely dry winds gusting to 30 knots create massive dust storms. Walls of dust several hundred feet high and a mile or two long are common. Dust can extend up to 20,000 feet (6 km) MSL.

Early morning fog causes most low visibilities in the Akhdar Mountains and the Nile Delta. Low clouds become fog on higher slopes.

Flow from the Saharan Heat Low transports dust into the area above the marine boundary layer, where it settles and combines with haze. Haze alone rarely lowers visibilities to less than a mile; they normally remain above 6 miles. Visibility may drop below a mile in dust haze, which is particularly dense around Adjabiya, but 5 or 6 miles is more common. Heavy showers and thunderstorms can also lower visibility below a mile briefly.

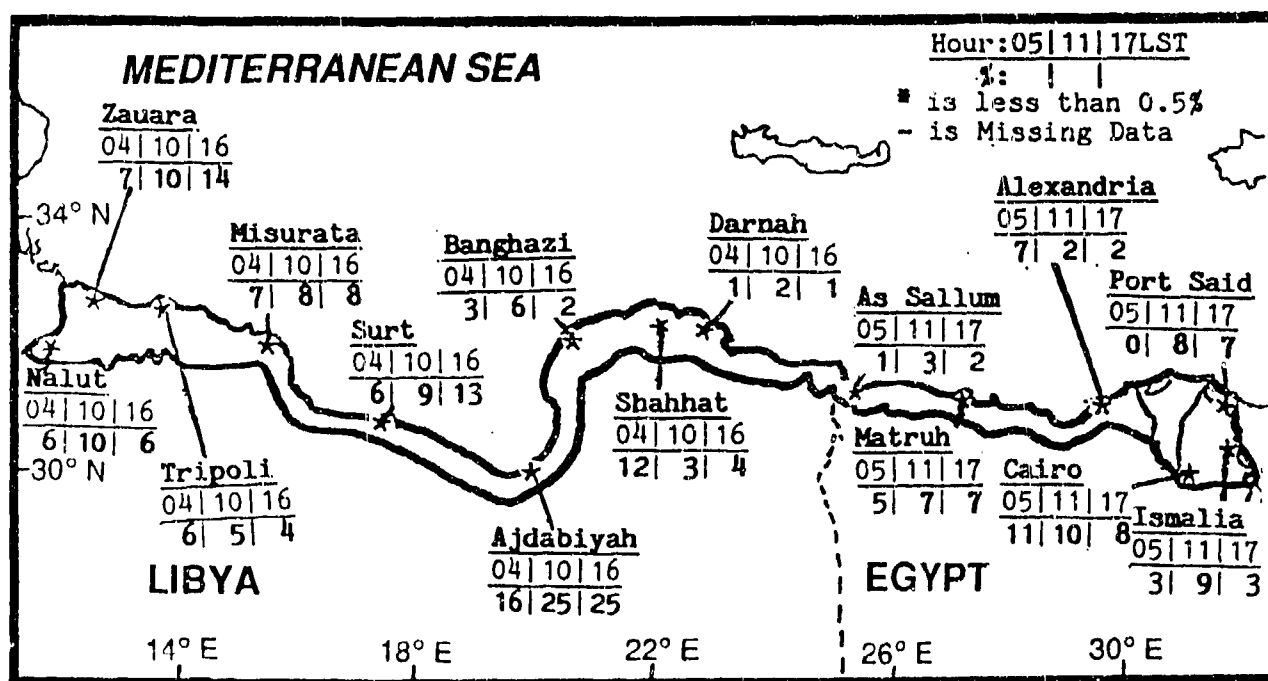


Figure 5-12. Mean Spring Frequencies of Visibilities Below 3 Miles, North African Coast.

WINDS. Although the prevailing synoptic flow is due westerly, intense spring surface heating enhances the land/sea breeze circulation and makes it dominant, as shown in Figure 5-13. Coastal stations have the strongest winds, primarily in directions perpendicular to the coastline. Nalut and Shahhat--both inland stations--have the lightest winds. Tripoli is a coastal station, but relatively light winds are reported at the airport, which is about 15 miles inland.

The Saharan Heat Low induces weak southeasterly flow in the region's western portion. This flow penetrates to the coast, usually above the marine boundary layer. The southeasterlies begin in April and persist through the summer. The frequency of

northwesterlies diminishes in the spring at most stations, indicating that Genoa Lows (the primary synoptic cause) become less frequent.

Atlas Lows generate the region's strongest spring winds, primarily from the south or southeast. These are locally known as the "Khamsin" or "Ghibli". Gusts to 31 knots have been reported at Surt, 43 knots at Benina, and 45 knots at Darnah.

Upper-level winds begin to shift toward the northwest by May, as was shown in Figures 5-6a & b. This change, brought about by a combination of the strengthening Azores High and the weak high above the Saharan Heat Low, affects western sections first.

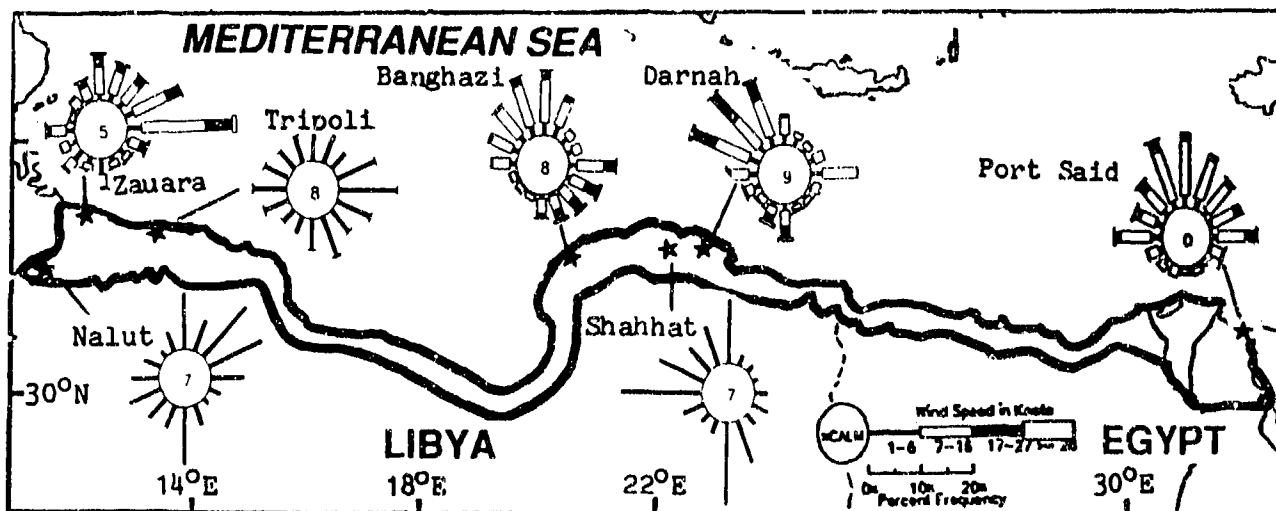


Figure 5-13. April Surface Wind Roses, North African Coast.

THE NORTH AFRICAN COAST SPRING

March-May

PRECIPITATION. Most April-May rainfall is from orographic rainshowers in the mountains (see Figure 5-14). Atlas Lows are mostly responsible, but actual amounts depend on the path of the individual low. The northeast track extends from northwestern Libya across the Gulf of Sidra and into the eastern Mediterranean. The secondary eastward track is along or south of the Egyptian coast. Lows traveling along the southern route

trigger thunderstorms northwest of the low. These become severe as they approach the Nile. They occasionally cause flooding when a low interacts with an inverted Sudanese Low pressure trough (see the Sudanese Low discussion in Chapter 2). Isolated thunderstorms are most common in April, especially in Egypt where lows draw on Red Sea moisture; frequencies are at or below 1 a month.

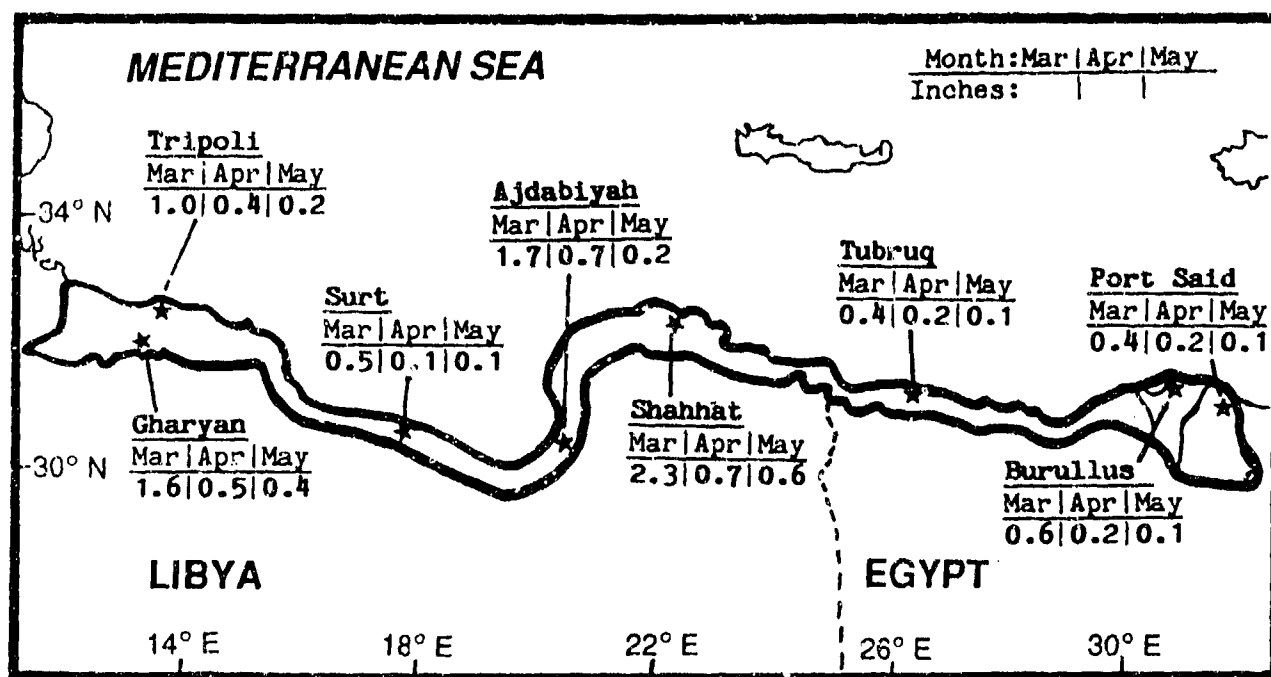


Figure 5-14. Mean Spring Monthly Precipitation, North African Coast.

THE NORTH AFRICAN COAST SPRING

March-May

TEMPERATURE. Spring mean daily highs vary from 61° F (17° C) at Shahhat in March to 92° F (33° C) at Al Jawsh in May. Mean daily lows range from 43 to 67° F (6 to 18° C). Khamsin or Ghibli winds from Atlas Lows pass over the southern Nafusah and Akhdar Mountains; they warm the air adiabatically while descending the

northern slopes and result in the region's highest temperatures, including 102° F (39° C) at Alexandria and 121° F (49° C) at Ez-Zauia. Temperatures are lowest in March when rare Polar Jet surges reach the area. Extreme lows range from 22° F (-5° C) at Shahhat to 44° F (7° C) at Alexandria.

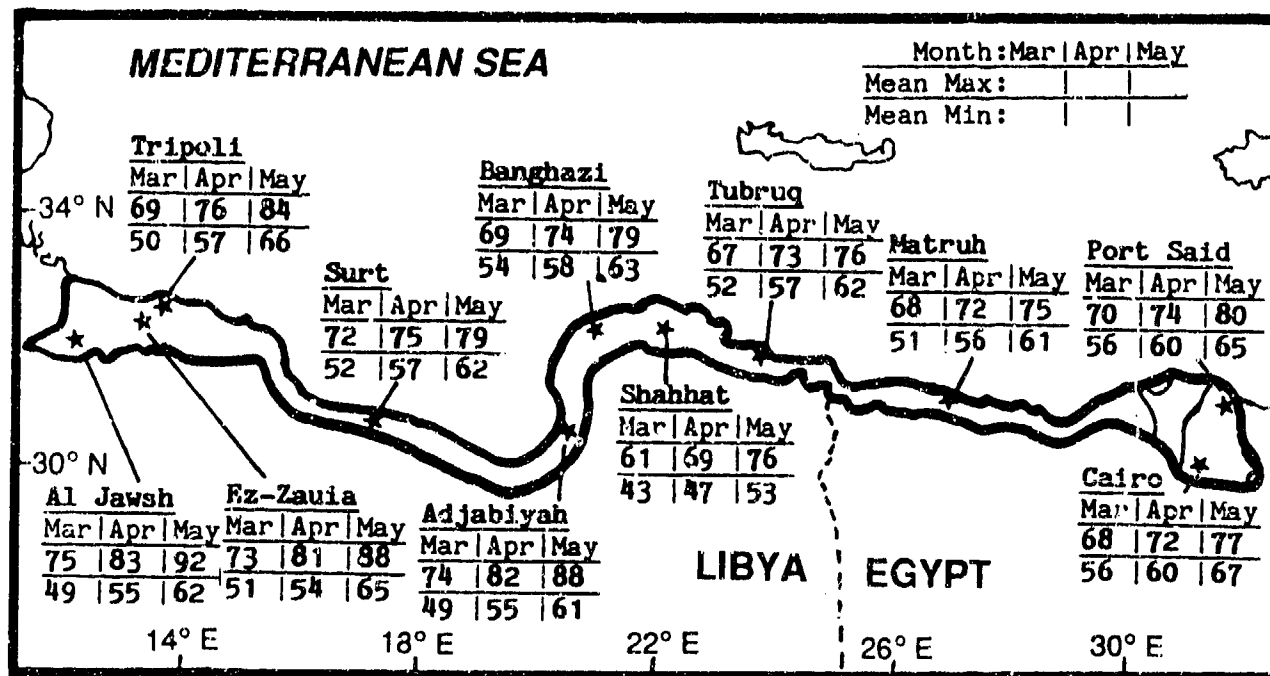


Figure 5-15. Mean Spring Daily Maximum/Minimum Temperatures (F), North African Coast.

THE NORTH AFRICAN COAST SUMMER

June-August

GENERAL WEATHER. Summers are extremely dry as the Azores High's strong subsidence results in clear skies over most of the region. The Saharan Heat Low is strongest in summer. Transitory systems are rare. The only significant cloud cover and rainfall occur along the mountains' northern slopes from orographic lift.

SKY COVER. Where the land/sea breeze is well-developed, stratus and stratocumulus form over the sea at night and move over the coast with the sea breeze. These clouds only move inland for about 10-20 NM, however, because of the extreme aridity. Nile Delta moisture also produces high amounts of low morning stratus, as shown in Figure 5-16. Ceilings are 2,000-3,000 feet (610-915 meters) on the coast, but less than 500 feet (150 meters) in the mountains. Tops are

below 5,000 feet (1,525 meters) MSL. Stratus normally dissipates over the warm land between 0900-1100 LST.

Rare upper-level troughs or early June Atlas Lows produce the only mid- or upper-level clouds. Altocumulus bases are 10,000-18,000 feet (3,050-5,485 meters); tops are 20,000 feet (6 km) MSL. Cirrus develops above 20,000 feet (6 km) MSL. These rare disturbances also produce cumulus with bases at 4,000-8,000 feet (1,220-2,440 meters) and tops to 10,000 feet (3,050 meters). Cumulus from Atlas Lows have bases at or below 1,000 feet (305 meters) in the mountains and 2,500 feet (760 meters) on the coast. Tops of the rare thunderstorm may exceed 50,000 feet (15 km) MSL. During heavy showers, ceilings can lower to 500 feet (150 meters).

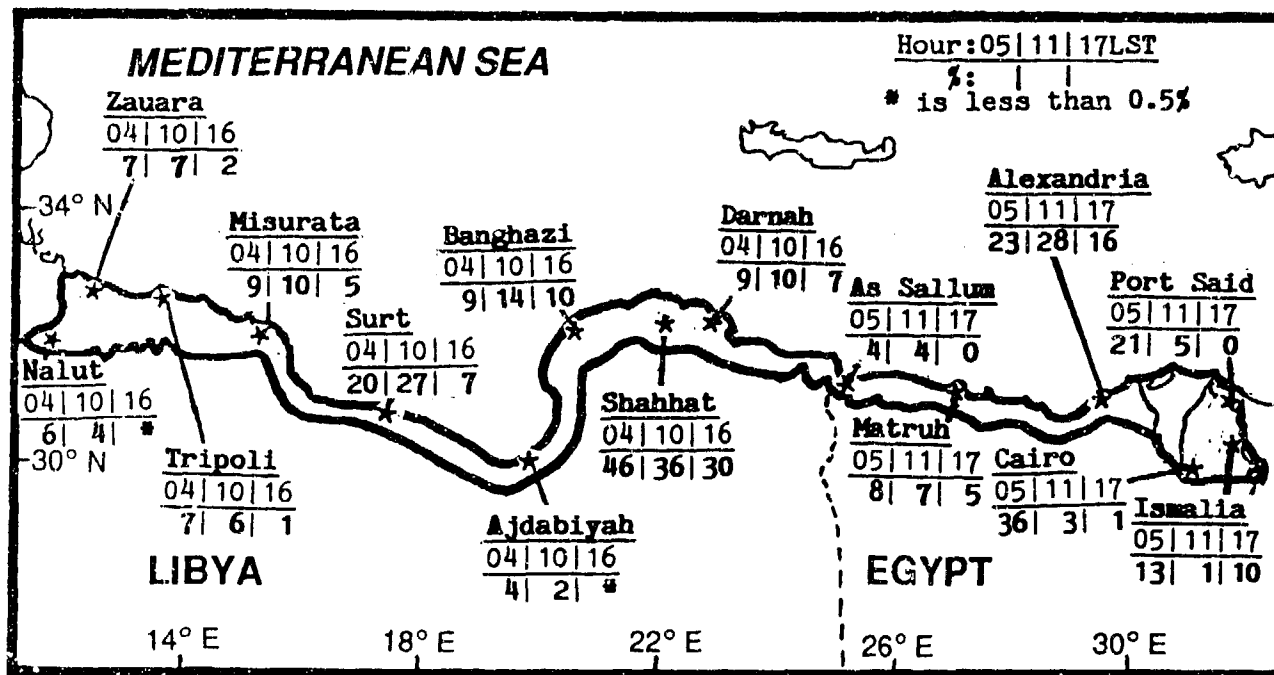


Figure 5-16. Mean Summer Frequencies of Ceilings Below 3,000 Feet (915 meters), North African Coast.

The mid-morning stratocumulus that causes the low ceilings near Surt may develop into coastal fair-weather cumulus that rarely reaches above 5,000 feet (1,525 meters) MSL or beyond 20 NM from shore; it generally dissipates in the afternoon. More extensive areas of

cumulus (shown in Figure 5-17a) develop in the Akhdar Mountains where terrain slopes sharply upward from the coast. Cumulus development along the Nafusah Mountains, 40-60 NM from the sea, is less extensive--see Figure 5-17b.

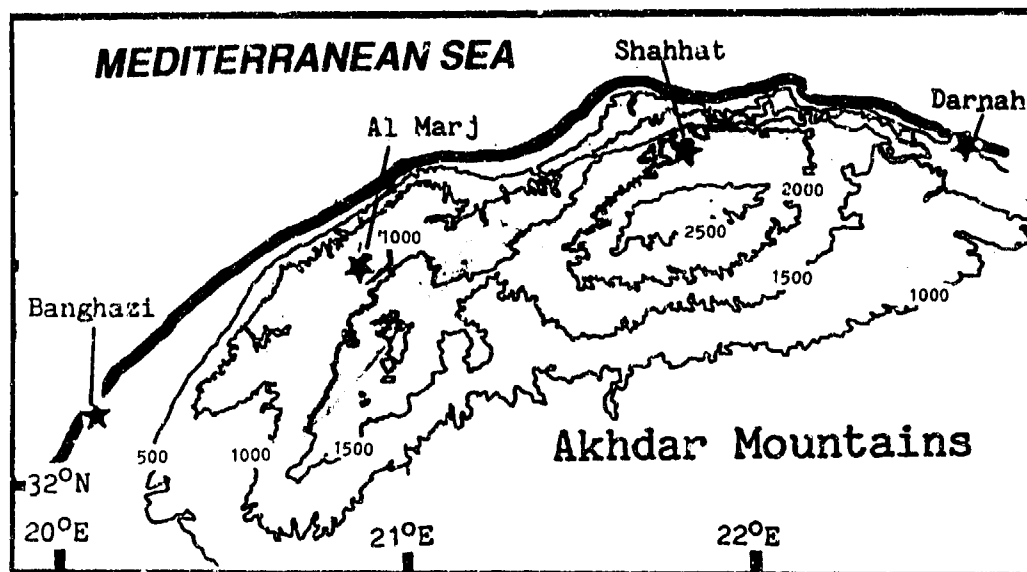


Figure 5-17a. Summer Source Regions for Cumulus Development in the Akhdar Mountains. The two primary source regions (shaded) are separated by a natural break between two extensive ridges. Except for the rare frontal passage, this area gets the only summer rainfall in the region. Contours are at 500-foot (150-meter) intervals.

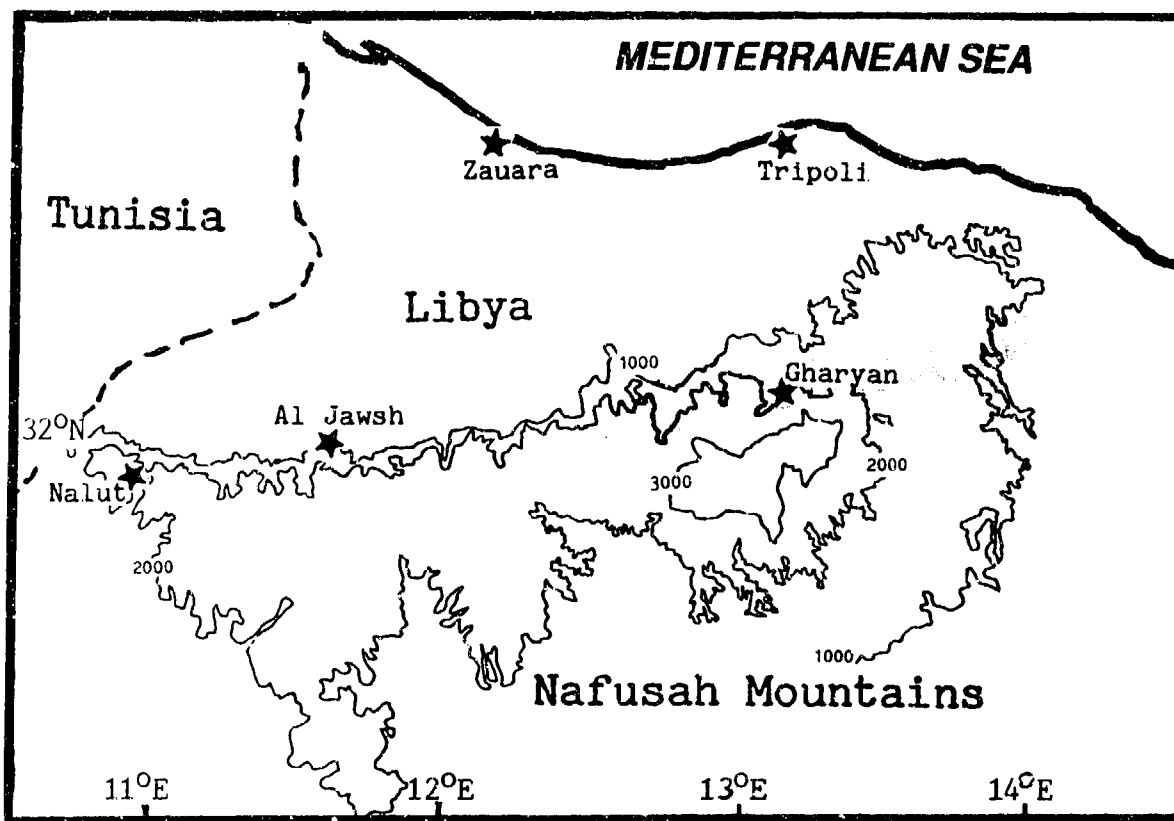


Figure 5-17b. Summer Source Region for Sea-Breeze Cumulus Development in the Nafusah Mountains. Sea-breeze moisture rarely penetrates west of the source area (shaded). Downwind development only occasionally reaches Misurata and the Gulf of Sidra. Contours are at 1,000-foot (305-meter) intervals.

VISIBILITY. Morning fog is the major visibility restriction throughout the region. Figure 5-18 shows that morning visibilities are below 3 miles 0-14% of the time along the coast, 4-36% in the mountains. Radiational cooling or morning low clouds in the high mountains cause most fog, which normally burns off by 1100 LST.

Afternoon visibilities are generally good. The sea breeze at Misurata is strong enough to carry dust and sand from the shoreline over the airfield, causing lowered visibilities in the afternoon. Winds above 25 knots with June Atlas Lows result in poor visibilities with blowing dust and sand. Local thermal turbulence and rare

thunderstorm downbursts can produce short (1- to 30-minute) duststorms that significantly lower visibility near large sand dunes, such as at Misurata, Adjabiya, or Port Said.

Afternoon haze that forms within the marine boundary layer or in the residual moisture of dissipated radiation fogs lowers visibility to 4-6 miles at some locations. Thick dust haze forms near Adjabiya in the afternoon as sea breeze moisture combines with dust--not only local dust, but suspended Saharan dust that settles into the marine boundary layer. Rain restricts visibility only during a brief and rare thunderstorm.

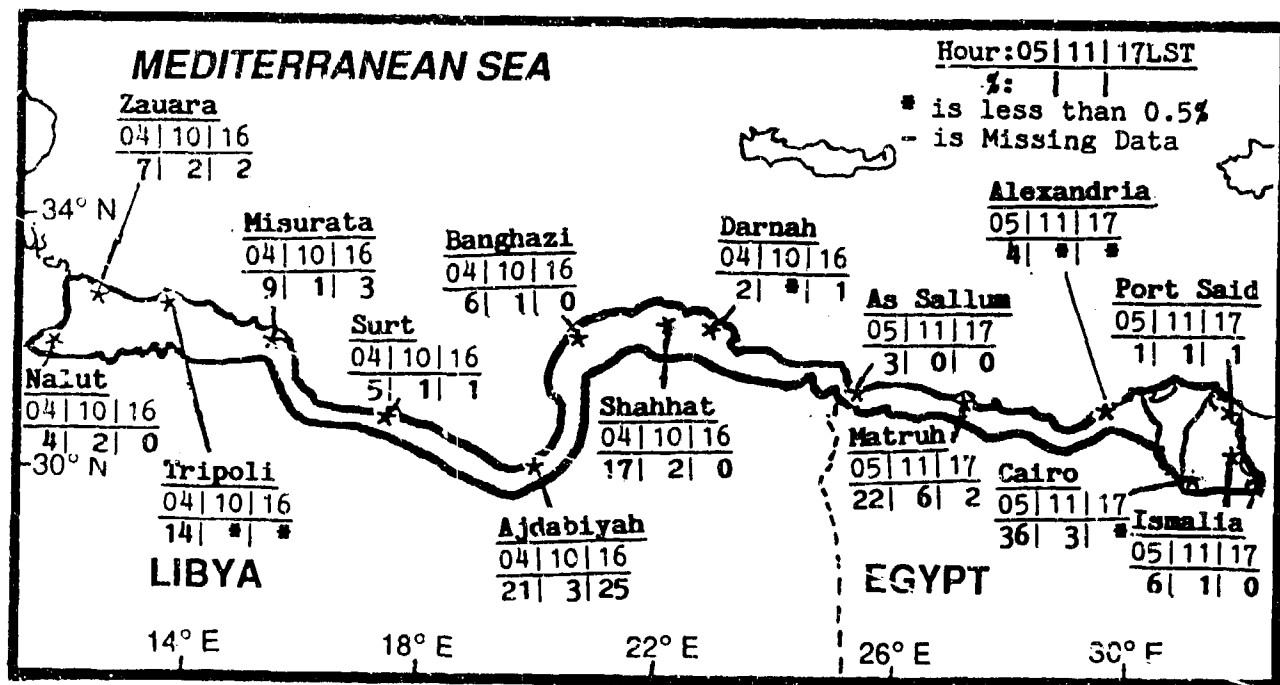


Figure 5-18. Mean Summer Frequencies of Visibilities Below 3 Miles, North African Coast.

WINDS. Flow is north-northwesterly with little variation; at most locations it reinforces the sea breeze and suppresses the land breeze. As shown in Figure 5-19, wind directions are mostly perpendicular to the coastline and least variable in the summer. The sea breeze is strongest in the summer, often penetrating 40 NM inland. Speeds are highest, 7-16 knots, at the coast.

The mountains shelter southern locations from the sea breeze; synoptic flow combines with mountain/valley breezes to provide speeds below 7 knots.

Upper-level winds, under the influence of the Azores High, are northwesterly, as shown in Figures 5-6a & b.

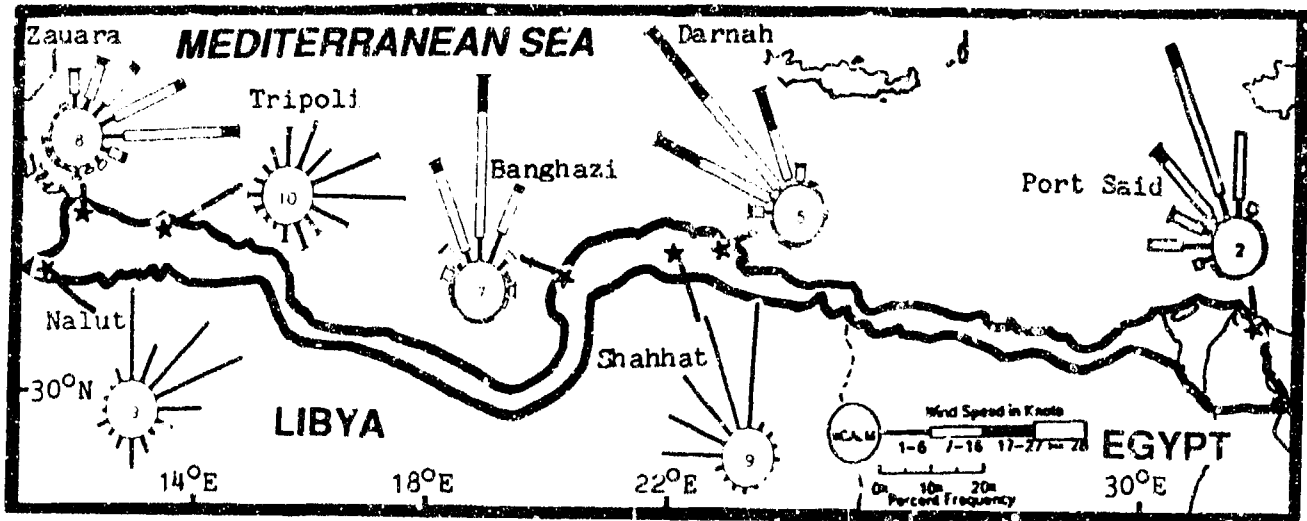


Figure 5-19. July Surface Wind Roses, North African Coast.

PRECIPITATION. Rainfall is so scarce in summer (mean rainfall accumulation 0.1 inch/3 mm or less) that the customary figure showing its extent has not been provided. Instead, refer to the shaded areas in Figures 5-17a and b, which show where the only regular summer rainfall occurs. Light mist, drizzle, and brief showers fall in the mountains above 1,500 feet (455 meters) MSL.

Rare summer showers are caused by upper-level disturbances generated by cold upper-level troughs or short waves; Figure 5-20 gives an example. Some locations in the Nafusah Mountains average one thunderstorm a summer, usually in June. East of Benghazi, thunderstorms may not occur at all for several summers in succession.

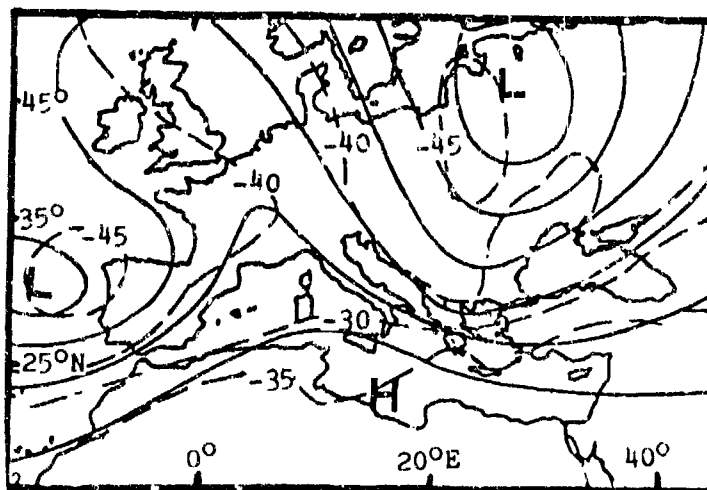


Figure 5-20. Summer Short Waves Affecting the Eastern Mediterranean. The solid lines are 300 mb contours; the dashed lines are 300-mb temperatures (°C).

THE NORTH AFRICAN COAST SUMMER

June-August

TEMPERATURE. Mean daily highs range from 80 to 104° F (27 to 40° C). The record high is 133° F (56° C) at Ez-Zauia. The marine boundary layer moderates temperatures on the coast. The daily high is usually reached before 1200 LST from late June through August. A well-developed sea breeze may lower temperatures by

15° F (9° C) in an hour, but when the land breeze returns (1900-2100 LST), the temperature rises again by as much as 15° F (9° C). Although not shown in Figure 5-21, summer mean daily lows can range from 57 to 77° F (14 to 20° C). Record lows include 40° F (5° C) at Shahhat and 62° F (17° C) at Alexandria.

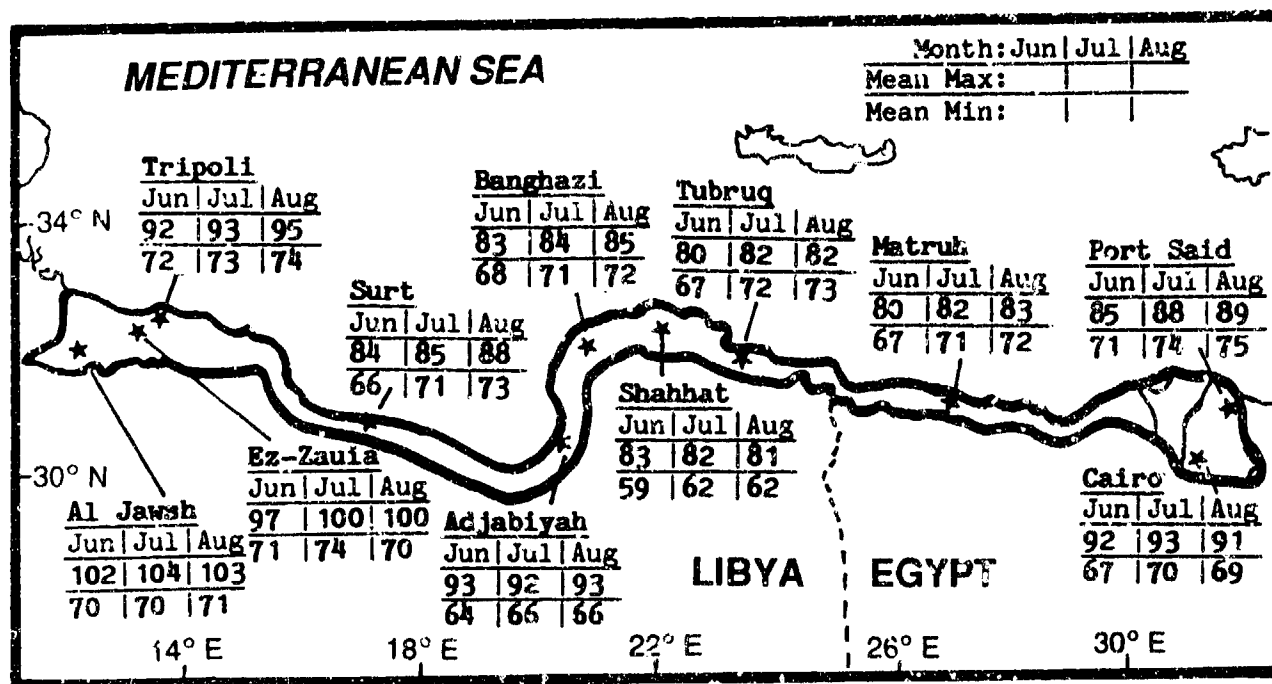


Figure 5-21. Mean Summer Daily Maximum/Minimum Temperatures (F), North African Coast.

GENERAL WEATHER. The Azores High dominates. Northwesterly flow strengthens and gradually introduces moisture to the area, beginning in the west. Cyclonic activity increases. Although an average of six low-pressure systems travel through the central Mediterranean Basin during the fall, only three pass over the North African Coast region.

SKY COVER. Morning stratus and afternoon cumulus become more pronounced in fall. Stratus and stratocumulus form over coastal waters during the night

and move onshore with the sea breeze. Bases may be as low as 500 feet (150 meters) in the mountains. Radiation fog becoming stratus causes low morning ceilings throughout the Nile Delta; this stratus, which usually dissipates within 2 hours as the land surface heats, is responsible for the high frequency of low ceilings shown in Figure 5-22. Cumulus forms in the warm, moist fall air as the sea breeze is sustained into the afternoon. Cumulus bases are 4,000-8,000 feet (1,220-2,440 meters), and tops range from 6,000 to 10,000 feet (1,830 to 3,050 meters) MSL.

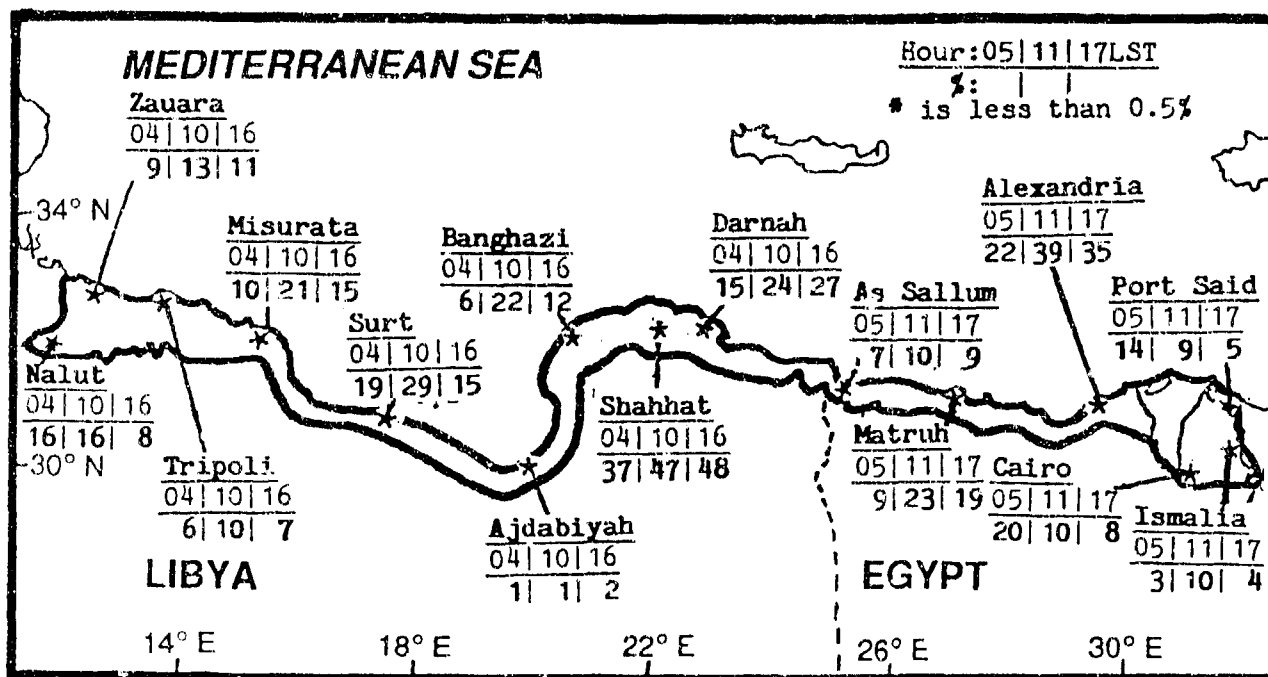


Figure 5-22. Mean Summer Frequencies of Ceilings Below 3,000 Feet (915 meters), North African Coast.

Transitory systems, such as Genoa Lows, become more common. Thin cirrus forms near the Subtropical and Polar Jets; bases are above 18,000 feet (5,485 meters). Mid- and upper-level clouds become more common. Deep Mediterranean lows follow their southern tracks in late fall and spread extensive cloud cover over the region. Cirrus, with bases near 18,000 feet (5,485 meters), reaches 50,000 feet (15 km) MSL.

near thunderstorms. Multilayered altocumulus and altostratus form with bases between 8,000 and 15,000 feet (2,440 and 4,570 meters) and tops to 20,000 feet (6 km) MSL. Mediterranean lows also generate cumulus with 2,500-foot (760-meter) bases and tops from 25,000 to 50,000 feet (7.5 to 15 km). In heavy showers, bases may lower to 500 feet (150 meters) AGL. Nimbostratus, however, is very rare.

VISIBILITY. The incidence of fog and low visibility decreases in fall, but they are still common in the morning west of the Gulf of Sidra, in the mountains, and within the Nile Delta (see Figure 5-23). Dust haze is common between 1200 and 1600 LST; visibilities are

normally 4-6 miles, but are below 3 miles near Adjabiyah. Dust and sand carried by winds over 25 knots reduce visibilities to a mile or less and can lift dust to 20,000 feet (6 km) MSL.

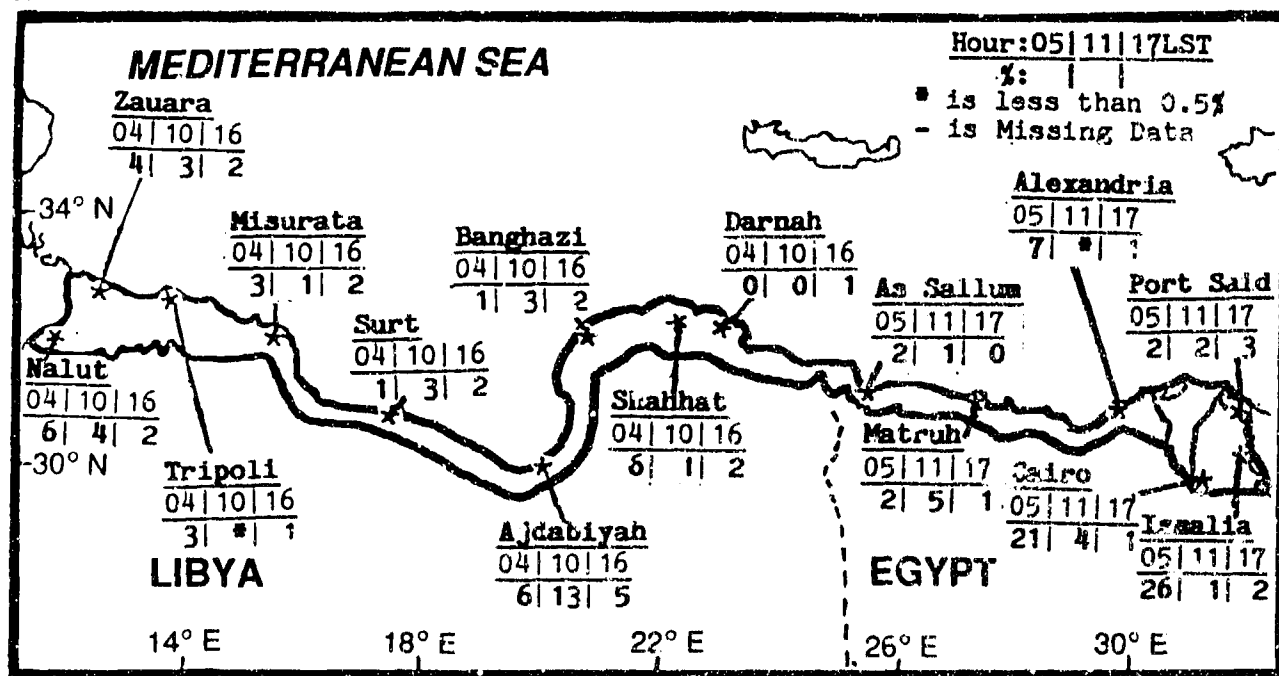


Figure 5-23. Mean Fall Frequencies of Visibilities Below 3 Miles, North African Coast.

WINDS. Surface flow is westerly to west-northwesterly at 8-15 knots. The strongest winds rarely exceed 40 knots and usually occur with frontal passages. Figure 5-24 shows that land/sea breezes are pronounced along most of the coast. The prevailing flow overshadows the weak (3-5 knot) land breeze along the Nile Delta's coast and maintains a strong marine inversion over the land on

most nights. Elsewhere, land breezes average 5 knots; sea breezes vary from 8 knots at Tripoli to 12 knots at Misurata. Speeds are highest along immediate coasts. Drainage winds from the Akhdar Mountains intensify the nocturnal circulation; Benina has 10-17 knot winds at night and 6-10 knot winds during the day.

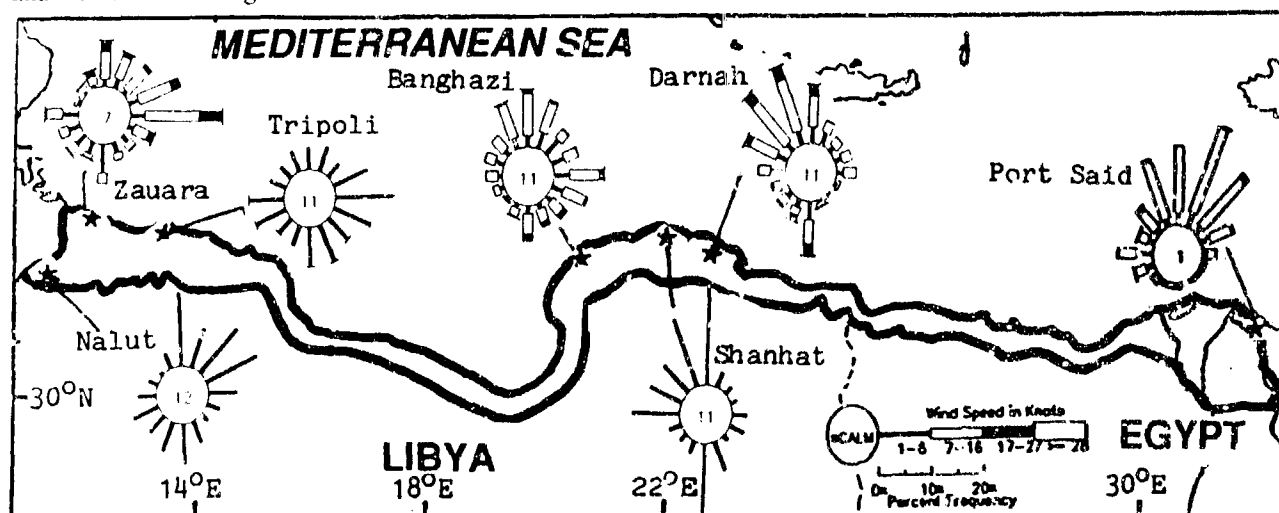


Figure 5-24. October Surface Wind Roses, North African Coast.

THE NORTH AFRICAN COAST FALL

September-November

PRECIPITATION. Frontal activity increases dramatically in November; at most stations, rainfall is more than doubled from September to November. Most rain falls in the mountains; the least, in the east and

along southward-indented coasts. Figure 5-25 gives mean monthly precipitation totals. There is also an increase in thunderstorm frequency, as shown in Figure 5-26.

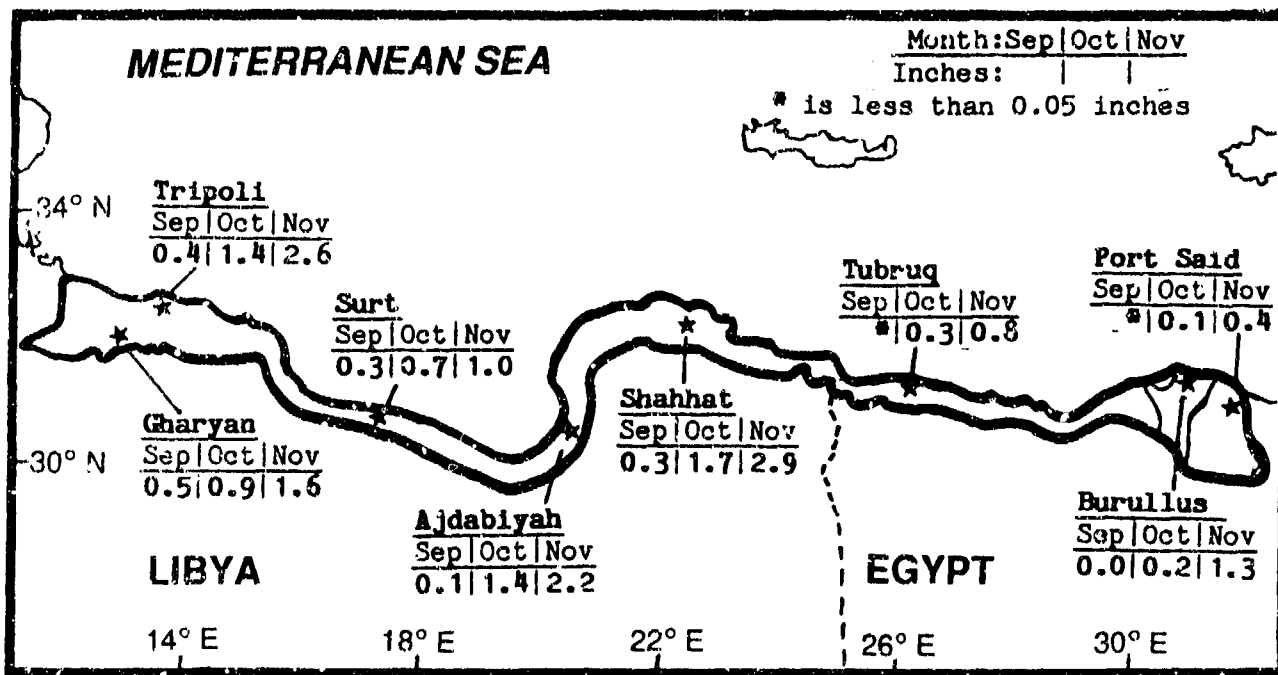


Figure 5-25. Mean Fall Monthly Precipitation, North African Coast.

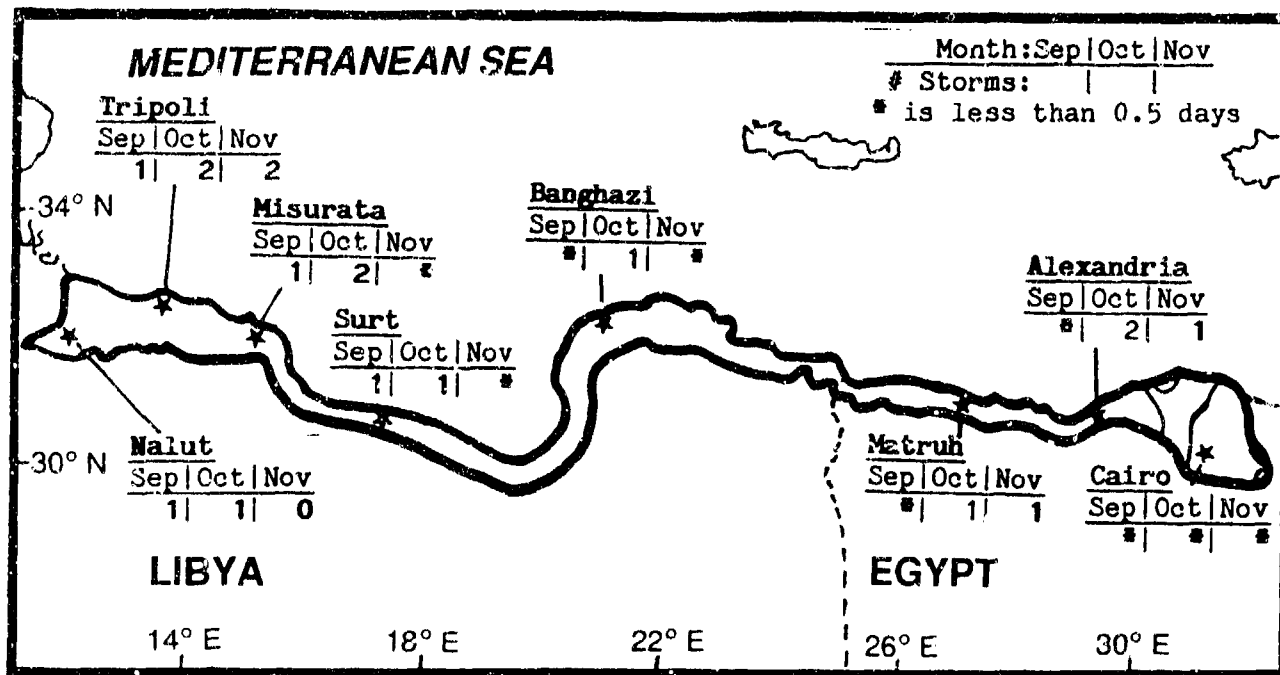


Figure 5-26. Mean Fall Thunderstorm Days, North African Coast.

THE NORTH AFRICAN COAST

FALL

September-November

TEMPERATURE. Mean daily highs range from 67 to 98° F (19 to 37° C). The record high is 136° F (58° C), at Ez-Zauia. This is also the world's official record high temperature. It occurred when an Atlas Low brought strong southerly winds to the area. Mean daily lows

range from 50 to 76° F (9 to 24° C). Extreme lows range from 24° F (-4° C) at Shāhhat to 48° F (9° C) at Port Said. Al Marj and Damah have both recorded 33° F (1° C). Shāhhat is the only location that records sub-freezing temperatures during the fall.

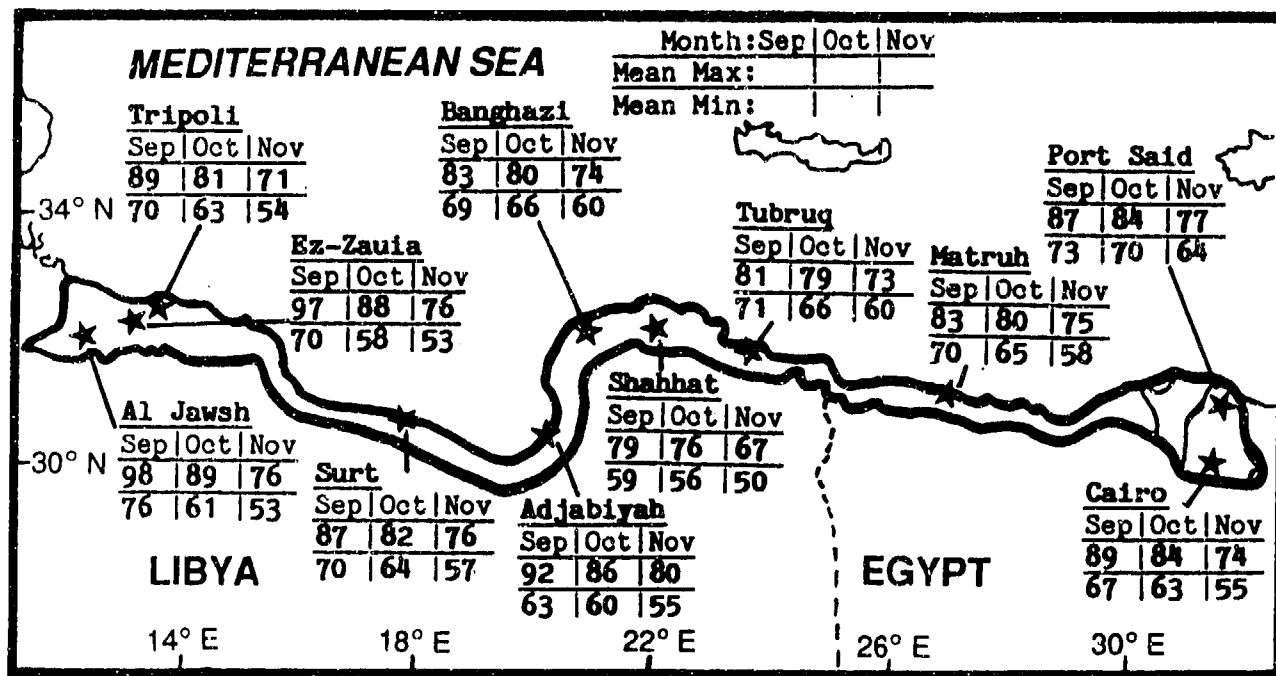


Figure 5-27. Mean Fall Daily Maximum/Minimum Temperatures (F), North African Coast.

Chapter 6

THE EASTERN SAHARA

The Eastern Sahara region comprises most of Libya and Egypt, the northern portions of Chad and Sudan, and a small part of Ethiopia. The region includes the Libyan Desert, the Nubian Desert, and the Nile Delta. After describing the area's situation and relief, this chapter discusses "general weather conditions" by season.

	Page
Situation and Relief	6-2
Winter--December-February.....	6-7
General Weather	6-7
Sky Cover	6-7
Visibility	6-8
Winds	6-9
Precipitation	6-12
Temperature	6-13
Spring--March-May	6-14
General Weather	6-14
Sky Cover	6-14
Visibility	6-15
Winds	6-17
Precipitation	6-18
Temperature	6-19
Summer--June-August	6-20
General Weather	6-20
Sky Cover	6-20
Visibility	6-21
Winds	6-22
Precipitation	6-23
Temperature	6-25
Fall--September-November.....	6-26
General Weather	6-26
Sky Cover	6-26
Visibility	6-27
Winds	6-28
Precipitation	6-29
Temperature	6-30

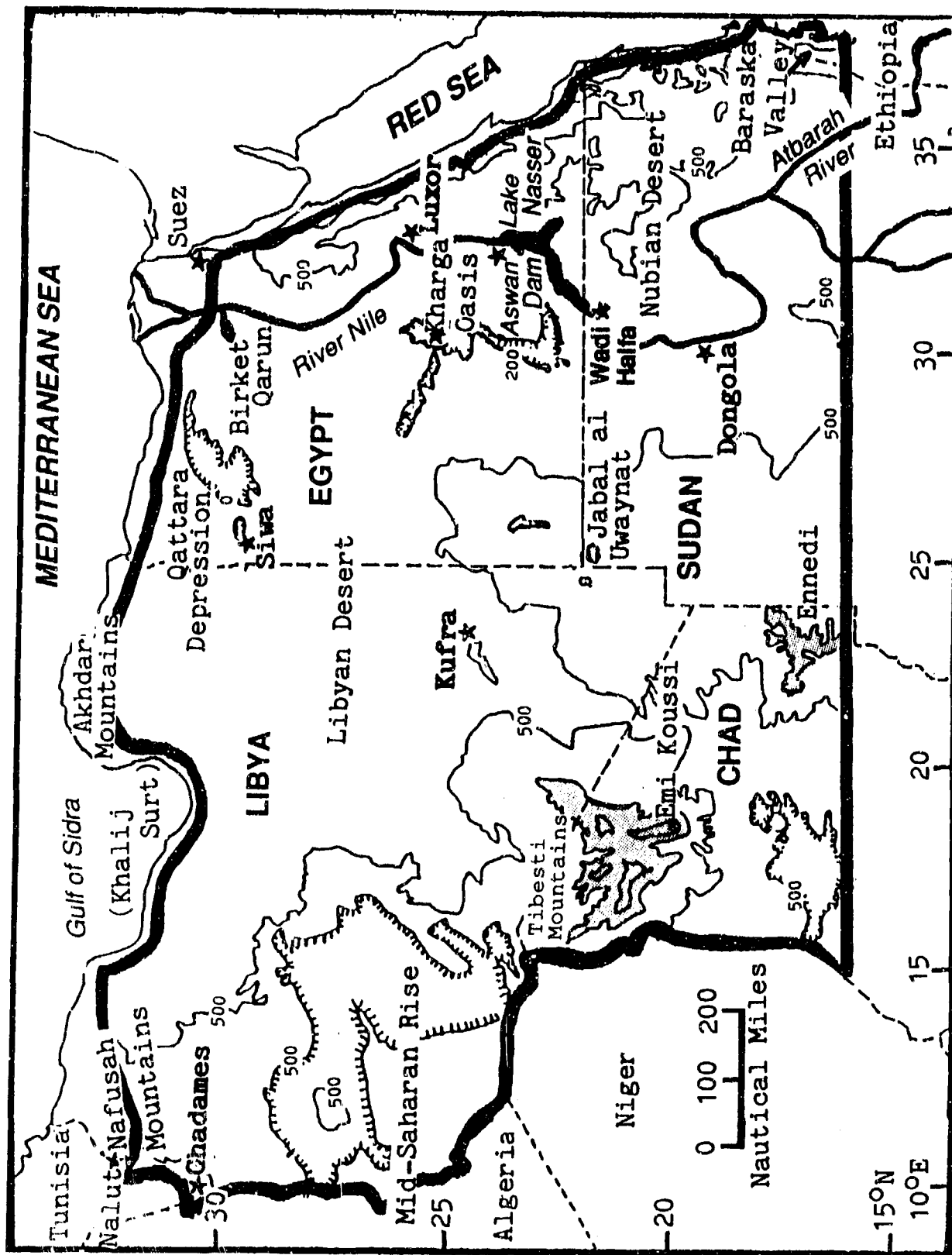


Figure 6-1a. The Eastern Sahara. As shown, the Eastern Sahara region extends south from the northeastern coasts of Libya and Egypt into central Chad and Sudan. It includes a small portion of Ethiopia. The shaded areas are above 3,280 feet (1,000 meters). Climatic summaries for selected stations are provided in Figures 6-1b and c.

STATION: GHADAMES (GHUDAMIS) LIBYA													
LAT/LON: 30 08 N 8 40 E ELEV: 380M													
ELEMENTS	JAN	FEB	MAR	APR	MAY	JUN	JUL	AUG	SEP	OCT	NOV	DEC	ANN
EXT MAX	80	83	100	113	120	131	128	120	122	110	102	87	131
AVG MAX	84	70	79	90	99	107	109	107	101	90	78	68	88
AVG MIN	37	40	47	55	85	72	72	72	67	59	49	40	56
EXT MIN	20	26	30	39	44	57	59	55	50	38	35	26	20
AVG PRCP	0.2	0.1	0.2	0.1	*	*	*	*	*	0.2	0.2	0.1	1.1
MAX MON	1.6	1.4	0.8	0.8	0.4	0.3	*	0.1	0.8	0.9	1.4	1.0	3.1
MAX DAY	0.3	0.2	0.7	0.4	0.4	0.3	*	0.1	0.2	0.7	0.2	1.0	
TS DAYS	*	0	0	*	*	0	0	*	0	*	0	0	1
DUST DAYS	5	7	10	12	3	5	2	1	4	3	5	2	58
APP TEMP	79	84	100	108	120	125	125	120	115	110	92	76	

STATION: SIRTE (SURT) LIBYA													
LAT/LON: 31 12 N 16 35 E ELEV: 22M													
ELEMENTS	JAN	FEB	MAR	APR	MAY	JUN	JUL	AUG	SEP	OCT	NOV	DEC	ANN
EXT MAX	84	89	101	113	114	124	118	118	111	106	100	88	124
AVG MAX	84	88	72	75	78	84	85	88	87	82	76	67	77
AVG MIN	45	48	52	57	82	88	71	73	70	64	57	50	59
EXT MIN	35	33	35	40	43	49	50	63	59	52	43	36	33
AVG PRCP	1.6	1.0	0.8	0.1	0.1	*	0	0	0.5	0.8	1.2	1.6	7.5
MAX MON	5.2	4.1	3.1	1.0	0.8	0.4	0	0	1.8	2.8	4.8	4.0	13.7
MAX DAY	1.7	2.2	0.9	0.4	0.5	0.4	0	*	1.8	2.8	2.1	1.5	
TS DAYS	*	*	*	*	*	*	0	0	1	1	*	1	3
DUST DAYS	3	3	2	2	2	1	0	*	1	1	2	2	19
APP TEMP	72	81	90	118	130	130	130	130	130	115	97	76	

STATION: KUFRA (AL KUFRAH) LIBYA													
LAT/LON: 24 13 N 23 20 E ELEV: 381M													
ELEMENTS	JAN	FEB	MAR	APR	MAY	JUN	JUL	AUG	SEP	OCT	NOV	DEC	ANN
EXT MAX	90	99	104	111	118	122	111	115	108	108	101	91	122
AVG MAX	70	73	81	91	99	102	100	100	97	90	81	72	88
AVG MIN	41	45	50	59	88	72	73	73	70	61	52	43	59
EXT MIN	26	28	33	45	48	60	62	63	58	39	37	30	26
AVG PRCP	0	*	0	0	*	0	0	*	*	*	0	*	0.1
MAX MON	*	0.3	*	*	0.1	0	0	0.4	0.2	*	*	0.1	0.5
MAX DAY	*	0.2	*	*	0.1	0	0	0.4	0.2	*	*	0.1	
TS DAYS	0	0	*	0	*	0	0	0	*	0	0	0	1
DUST DAYS	*	*	1	1	1	*	0	0	0	*	*	*	3
APP TEMP	68	76	79	91	100	105	102	102	97	90	79	70	

STATION: DONGOLA SUDAN													
LAT/LON: 19 10 N 30 29 E ELEV: 774 FT													
ELEMENTS	JAN	FEB	MAR	APR	MAY	JUN	JUL	AUG	SEP	OCT	NOV	DEC	ANN
XTRN MAX	104	108	113	117	120	121	121	119	117	116	108	103	121
AVG MAX	83	85	93	102	107	110	108	109	107	102	93	85	99
AVG MIN	49	52	58	65	71	78	76	78	76	69	60	51	65
XTRN MIN	37	37	40	50	54	62	63	66	59	49	43	40	37
AVG PRCP	0.0	*	0.0	0.0	0.1	*	0.3	0.5	*	*	0.0	0.0	0.9
MAX MON	0.2	*	*	*	0.8	*	1.9	2.2	0.1	0.1	*	*	2.4
MAX DAY	0.2	*	*	*	0.6	*	1.3	1.4	0.1	0.1	*	*	1.4
TS DAYS	0	0	*	0	1	0	2	3	1	1	0	0	8
DUST DAYS	2	5	8	8	6	9	3	5	3	3	1	1	50
APP TEMP	83	81	89	97	102	107	110	117	105	100	92	83	

* = LESS THAN 0.06 INCHES OR LESS THAN 0.5 DAYS

Figure 6-1b. Climatological Summaries for Selected Stations in the Eastern Sahara.

STATION: WADI HALFA SUDAN													
LAT/LON: 21 58 N 31 20 E ELEV: 413 FT													
ELEMENTS	JAN	FEB	MAR	APR	MAY	JUN	JUL	AUG	SEP	OCT	NOV	DEC	ANN
XTRN MAX	100	108	118	127	120	120	119	118	118	117	115	102	127
AVG MAX	78	80	88	98	105	107	108	108	101	98	87	78	94
AVG MIN	48	48	54	62	71	74	74	78	73	67	58	49	62
XTRN MIN	32	34	38	45	52	58	63	57	58	42	38	28	28
AVG PRCP	*	*	*	*	0.1	0.0	*	*	*	*	*	*	0.1
MAX MON	0.2	0.3	0.3	*	0.4	0.0	1.2	*	*	0.7	0.3	0.2	1.2
MAX DAY	0.2	0.3	0.3	*	0.4	0.0	0.8	*	*	0.8	0.3	0.2	0.8
TS DAYS	*	0	*	*	1	0	*	*	0	0	*	0	2
DUST DAYS	3	5	6	7	9	9	3	4	2	1	1	2	52
APP TEMP	72	77	85	93	100	100	100	104	98	98	83	78	

STATION: SIWA EGYPT													
LAT/LON: 28 12 N 25 29 E ELEV: -46 FT													
ELEMENTS	JAN	FEB	MAR	APR	MAY	JUN	JUL	AUG	SEP	OCT	NOV	DEC	ANN
XTRN MAX	88	98	108	113	118	120	118	117	111	108	108	93	120
AVG MAX	87	71	77	88	94	100	101	100	95	90	80	70	88
AVG MIN	38	41	48	53	61	68	69	68	64	58	50	41	55
XTRN MIN	24	27	32	39	47	53	53	60	52	43	38	27	24
AVG PRCP	*	*	*	*	0.1	*	0.0	0.0	0.0	*	*	0.1	0.4
MAX MON	0.3	0.8	0.4	0.3	0.8	*	*	0.0	*	0.4	0.2	1.1	1.1
MAX DAY	0.5	0.4	0.4	0.3	0.8	*	*	0.0	*	0.3	0.2	1.1	1.1
TS DAYS	*	0	*	*	*	0	0	0	*	*	*	*	1
DUST DAYS	2	3	4	5	3	1	1	*	*	*	1	2	22
APP TEMP	67	69	77	87	98	107	110	110	100	95	81	70	

STATION: LUXOR EGYPT													
LAT/LON: 25 40 N 32 42 E ELEV: 290 FT													
ELEMENTS	JAN	FEB	MAR	APR	MAY	JUN	JUL	AUG	SEP	OCT	NOV	DEC	ANN
XTRN MAX	90	101	108	116	119	119	118	119	118	113	108	91	119
AVG MAX	74	79	88	95	104	108	107	108	103	98	87	78	94
AVG MIN	42	44	50	59	69	70	73	73	71	65	54	45	60
XTRN MIN	32	28	38	43	54	59	64	66	62	50	39	34	28
AVG PRCP	0.0	0.0	0.0	*	0.0	0.0	0.0	0.0	0.0	*	0.0	0.0	*
MAX MON	0.1	0.1	*	*	0.2	0.0	0.0	0.0	*	*	*	*	0.24
MAX DAY	0.1	0.1	*	*	0.2	0.0	0.0	0.0	*	*	*	*	0.24
TS DAYS	0	0	0	0	*	0	0	0	0	*	0	0	*
DUST DAYS	1	2	4	5	3	*	*	1	*	*	1	1	18
APP TEMP	74	78	82	92	100	102	103	103	103	99	87	77	

STATION: ASWAN DAM EGYPT													
LAT/LON: 23 57 N 32 45 E ELEV: 200 FT													
ELEMENTS	JAN	FEB	MAR	APR	MAY	JUN	JUL	AUG	SEP	OCT	NOV	DEC	ANN
XTRN MAX	100	102	111	118	118	124	124	120	118	115	108	99	124
AVG MAX	74	78	87	98	103	107	108	108	103	98	87	78	94
AVG MIN	50	52	58	66	74	78	80	80	75	71	62	53	67
XTRN MIN	38	35	41	48	52	68	88	67	61	54	37	37	35
AVG PRCP	0.0	0.0	*	*	0.07	0.0	0.0	0.0	0.0	*	*	0.0	0.1
MAX MON	*	*	*	0.1	0.2	*	0.0	0.0	*	0.2	*	*	0.2
MAX DAY	*	*	*	0.1	0.2	*	0.0	0.0	*	0.2	*	*	0.2
TS DAYS	0	0	0	0	0	0	0	0	*	*	*	0	*
DUST DAYS	1	3	5	6	4	3	2	2	1	1	1	2	30
APP TEMP	72	74	84	92	100	106	104	104	103	98	85	78	

* = LESS THAN 0.05 INCHES OR LESS THAN 0.5 DAYS

Figure 6-1c. More Climatological Summaries for Selected Stations in the Eastern Sahara.

GEOGRAPHY. The northern border of the Eastern Sahara begins in the west near Nalut, Libya, and runs east across the Nafusah Mountains' southern slopes to within approximately 20 miles of the Mediterranean coastline along the Gulf of Sidra. The coastal strip widens along the Akhdar Mountains' southern slopes east and south of Banghazi, Libya, and joins the eastern border along the Red Sea Hill's western slopes southwest of Suez, Egypt.

The eastern boundary follows the 610-foot (185-meter) contour along the eastern Red Sea Hills southward to Tokar, Sudan. It then jumps to the 1,620-foot (495-meter) contour, which it follows southward along Ethiopia's Baraska Valley to 16° N. The southern boundary continues along 16° to the Chad/Niger border. The western boundary follows the western borders of Chad and Libya north to the Nafusah Mountains.

Two mountain ranges help divide the coast from the Sahara. The Nafusah Mountains, in the extreme northwest, extend 185 miles along the Mediterranean coast and average about 3,000 feet (915 meters) in height. The Akhdar Mountains are further east; they extend 145 miles along the Gulf of Sidra's east coast. Average height is 2,500 feet (760 meters).

The Eastern Sahara is a vast plateau covered with sand and rock. Elevations range from 600 to 1,200 feet (180 to 365 meters). Isolated lowlands contain the only ground water and vegetation.

The Nile Valley, a broad, silt-filled feature from 1 to 13 miles wide, covers the entire eastern portion of the region. It spans 1,200 miles from south to north. Steep cliffs that reach 1,640 feet (500 meters) MSL cut through the sandstone plateau. The Nile Valley divides the Sahara into two deserts: the Libyan Desert in the west and the Nubian Desert in the east.

The Libyan Desert includes the Mid-Saharan Rise, a large plateau extending eastward from Algeria to 20° E. This desolate feature is covered by gravel and sand. It slopes downward to the east, averaging 1,640 feet (500 meters) in the west and 660 feet (200 meters) in the east. Ancient lava flows offer slight variation to the monotonous terrain; the highest of these reach 4,000 feet (1,220 meters), but generally average 2,100 feet (640 meters). Hundreds of isolated and weathered rock outcroppings protrude above the Libyan Desert floor;

the highest of these is Sudan's Jabal al-Uwaynat, at 6,343 feet (1,934 meters).

The Nubian Desert is a large sandstone plateau averaging 1,640 feet (500 meters) in elevation. It is cut by numerous wadis (semipermanent stream beds) sloping westward out of the Red Sea Hills and creating shallow, silt-filled valleys. The Nubian Desert gradually slopes up eastward from the Nile Valley to the base of the Red Sea Hills, a mountainous rift zone on the Red Sea from the Gulf of Suez to the Ethiopian border. The eastern slopes of this narrow mountain range are steep, characterized by parallel ridges with rugged, isolated peaks that reach 7,412 feet (2,259 meters).

The Tibesti Mountains lie southeast of the Mid-Saharan Rise and cover 38,600 square miles in northwestern Chad and southern Libya. Extremely rugged rock formations shaped by intense wind erosion rise abruptly from the desert floor. The highest point in the region (Emi Koussi, at 11,204 feet/3,415 meters) is in the Tibesti Massif. Emi Koussi is the largest of five volcanic peaks over 10,000 feet (3,050 meters). The Ennedi Plateau in northeastern Chad contains sandstone peaks at more than 4,700 feet (1,430 meters) MSL.

DRAINAGE AND RIVER SYSTEMS. The Eastern Sahara's only permanent river is the Nile, which flows northward 1,200 NM through Sudan and Egypt to the Mediterranean. Seasonal flooding produces a fertile, 10 to 13 mile-wide, silt-filled floodplain that contrasts with the barren desert. The Atbarah River, which rises in the Ethiopian Highlands and joins the Nile in the region's southeast corner, is its only permanent tributary. Navigable in the flood season between June and August, it dries to a series of pools after August. The Nubian Desert contains many wadis that fill with surface runoff after an infrequent rainfall; none normally join the Nile.

LAKES AND RESERVOIRS. The Eastern Sahara is dotted by numerous fertile oases and barren depressions with salt marshes and salt pans--thin, sun-baked surfaces with spongy muck beneath the crust. Elevations are mostly below 330 feet (100 meters), and several depressions and oases are below sea level. The largest oasis is the Kharga in south-central Egypt. Its basin is 200 miles long and 30 miles wide. The Siwa Oasis, in northwest Egypt, is 100 feet (30 meters) below sea level. The Siwa basin is 50 miles long and 10 miles wide. It contains several small salt lakes.

The Birket Karun, a freshwater lake 2.5 miles long and 4 miles wide in northeastern Egypt, is separated from the Nile by a narrow strip of desert. It is 150 feet (45 meters) below sea level. Also known as the Al Fayyum Depression, this lake was once connected to the Nile by an ancient Egyptian canal system.

The Qattara Depression covers 7,200 square miles in northwestern Egypt at 436 feet (133 meters) below sea level. Its surface is salt marsh and desert salt pan.

The Aswan Dam forms Lake Nasser, the region's largest man-made reservoir. The lake extends south 300

miles from the dam to the Egypt/Sudan border. Width varies from 6 to 36 NM.

VEGETATION. The landscape is barren except for isolated clumps of grass and small shrubs along wadis. Lush grasses and palm trees grow in oases. The Nile Valley contains 98% of the region's plants. There, aquatic grasses and acacia trees grow, along with irrigated cash crops. Small shrubs are mixed with isolated grass clumps in isolated mountain ranges. The Tibesti supports some agriculture. Isolated open woodlands and savannah thrive in cooler surroundings above 5,000 feet (1,525 meters).

GENERAL WEATHER. The Azores High is at its southernmost position; westerly flow at all levels is reinforced by the Saharan High. Cyclonic activity and frontal showers characterize winter weather. A cold front moves southward over the region every 3 to 5 days. Winter low-pressure systems, such as Cyprus and Atlas Lows, move northeast or east over the Mediterranean Sea, which, along with the North Atlantic Ocean, feeds the lows with moisture. Significant cloud cover and frontal precipitation is normally limited to the immediate vicinity of low-pressure centers and cold fronts, which weaken appreciably south of 25° N as moisture dwindles.

SKY COVER. Winter is the cloudiest season over the northern two-thirds of the region, but least cloudy over the southern third. Mean cloud cover decreases from 35% in the northwest (closest to storm tracks) to 14% in the southeast. Fronts cause formation of stratocumulus, altocumulus, and cirrus in layers between 2,000 and

20,000 feet (610 and 6,100 meters). Embedded towering cumulus or cumulonimbus reaches 50,000 feet (15 km) MSL. Cloud bases can be as low as 500 feet (150 meters) in heavy showers. All clouds remain close to the frontal boundary. Altocumulus castellus can develop during disturbed weather. Rain may fall from these clouds, but it rarely reaches the ground.

Afternoon stratocumulus with 2,500-foot (760-meter) bases forms over local moisture sources, such as oases. This results in the higher frequencies of ceilings below 3,000 feet (915 meters) at Siwa shown in Figure 6-2. Stratocumulus and cumulus ceilings between 3,000 and 5,000 feet (915 and 1,525 meters) are between 5 and 10 times more frequent than those at 2,500 feet (760 meters). Stratus is very rare. Most ceilings below 3,000 feet (915 meters) south of a line from Sabhah to Asyut are the result of blowing dust; most of these ceilings are below 800 feet (245 meters).

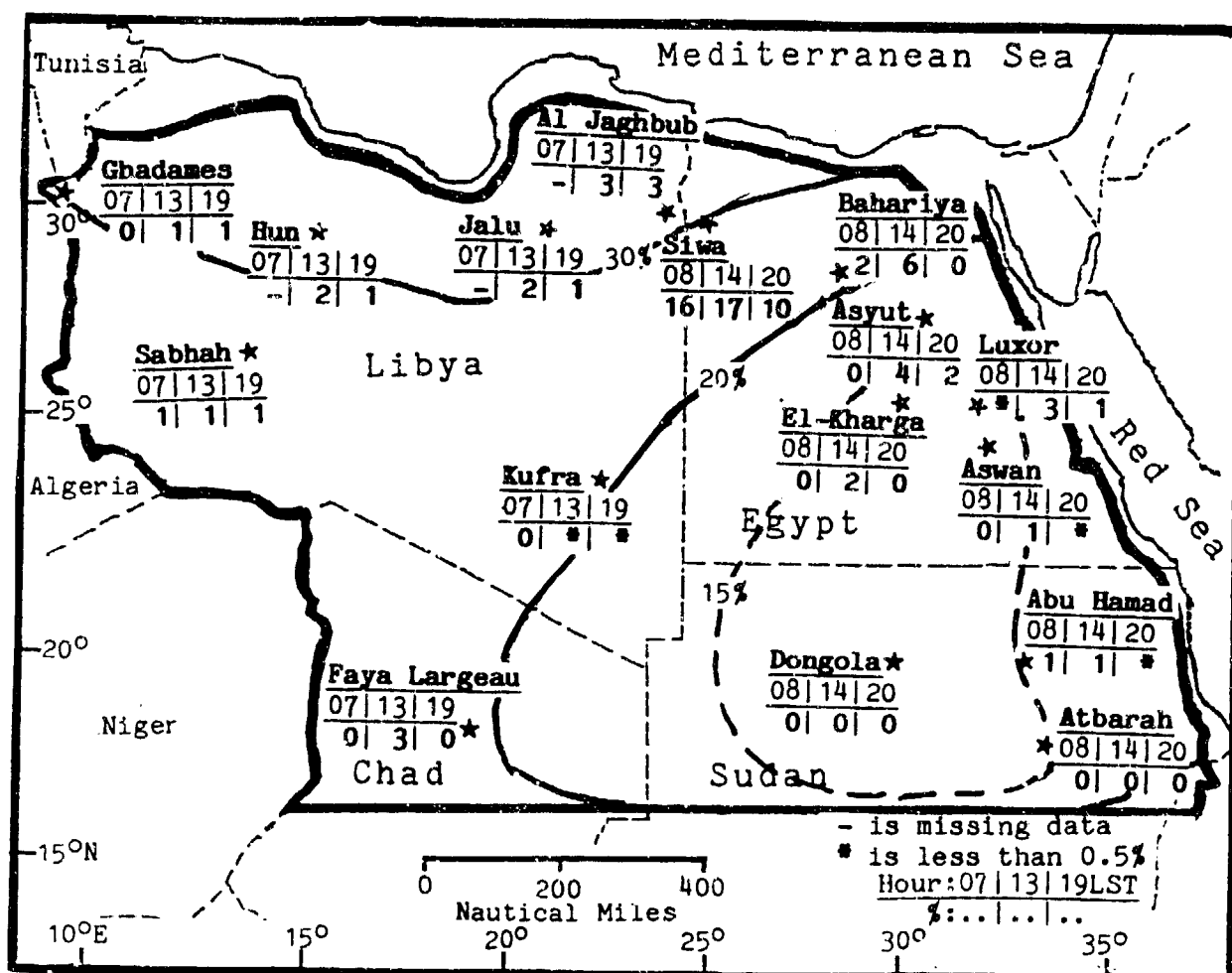


Figure 6-2. Mean Winter Cloudiness (Isopleths) and Frequencies of Ceilings Below 3,000 Feet (915 meters), Eastern Sahara.

Fronts dry as they move over the Sahara. Subsidence and surface heating reduce cloud development further, but intense Atlas Lows occasionally pull significant amounts of moisture northward from the equatorial Atlantic and temporarily suppress subsidence over the Sahara. Upward motion and moisture aloft produce extensive cloud cover and rain.

VISIBILITY. Suspended dust is the greatest cause of reduced visibilities. Dust haze restricting visibility to between 3 and 6 miles is common. Cold fronts, followed by strong, cold Saharan Highs, commonly cause most dust and sand storms. The strong highs increase pressure gradients between themselves and the Monsoon Trough,

thereby increasing the northeasterly Harmattan winds, which raise more dust and lower visibilities drastically in Harmattan Haze (which see) south of 20° N.

Fog and haze form between 2000 and 0700 LST in the extreme north behind cold fronts when there is strong northerly flow off the Mediterranean Sea. This is the reason for the 4% frequency of low visibility at Asyut shown in Figure 6-3. Morning fog and haze, with visibilities between 4 and 6 miles, develop under stable conditions near localized moisture sources such as the Nile Valley, desert depressions with salt marshes like the Qattara, and large oases. A rare heavy precipitation event can drop visibilities briefly to 3 miles or less.

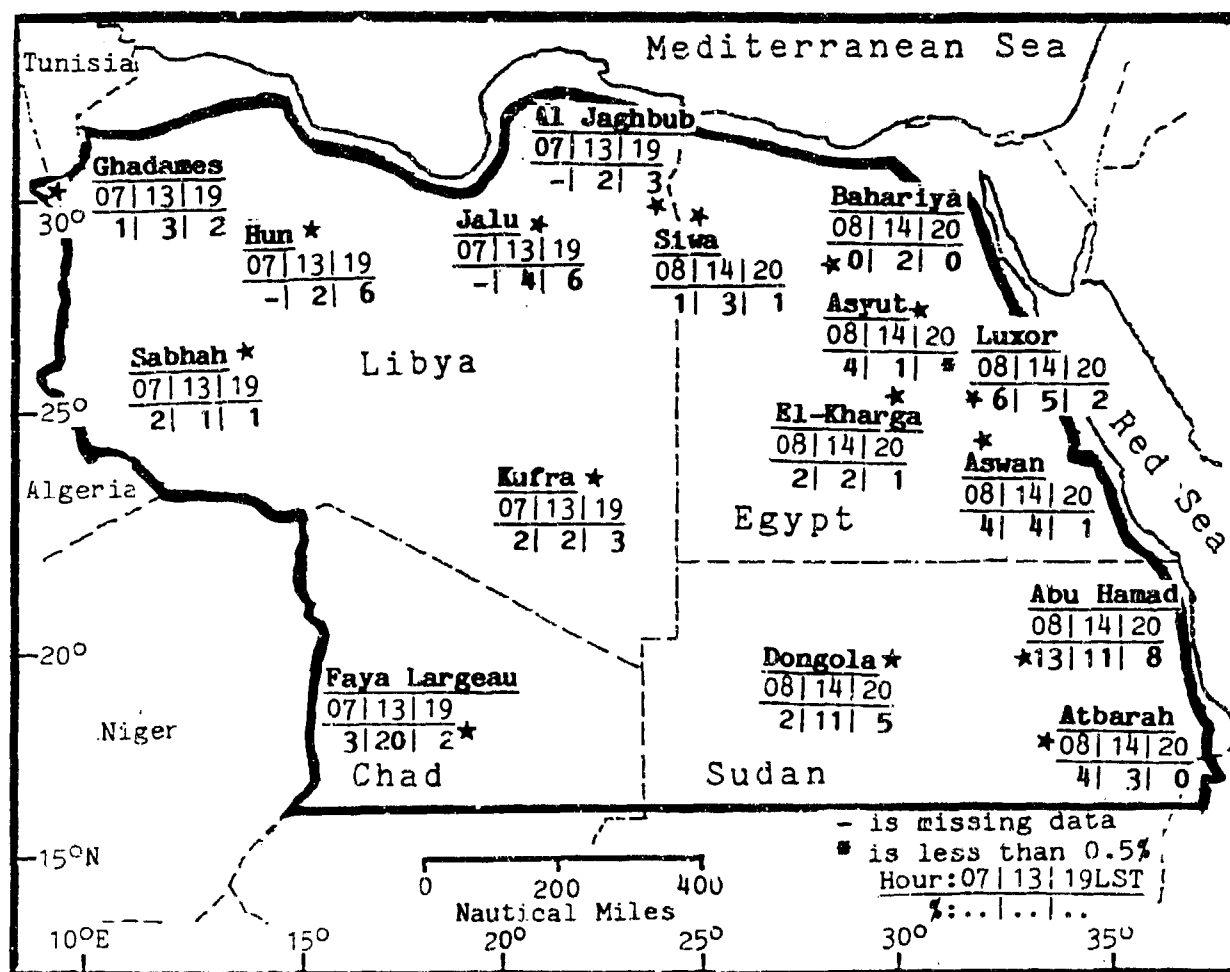


Figure 6-3. Mean Winter Frequencies of Visibilities Below 3 Miles, Eastern Sahara.

Khamsin or Ghibli winds (which see) cause duststorms that lower visibilities to near zero across Egypt and Libya. These storms last for several days. They diminish during the night and strengthen during the day along slow-moving cold fronts. The low visibility frequency shown at Faya Largeau and Dongola in Figure 6-3 shows that these storms make visibility worst during the afternoon. These two stations are affected most because they are surrounded by the easily-lifted, fine sand and dust of the Libyan Desert.

Khamsin- or Ghibli-generated duststorms may affect an area 120 miles wide ahead of the front; dust may reach 20,000 feet (6 km) and visibility can be less than 1/2 mile. Turbulent mixing and strong west to northwest

winds behind the cold front also raise dust and sand, but conditions are less severe and less persistent.

WINDS. The Azores and Saharan Highs determine low-level wind flow; a station's location relative to the average position of the Saharan High (22° N, 20° E) determines its prevailing winds. Prevailing directions in the southern and eastern parts of the region vary little because the few synoptic disturbances that reach them are weak. Faya Largeau and Aswan are in valleys that channel winds in the same direction as the synoptic flow; speeds average about 8 knots. Highest speeds are at Faya Largeau (15 knots), where winds that have swept unimpeded across the Libyan Desert are channeled.

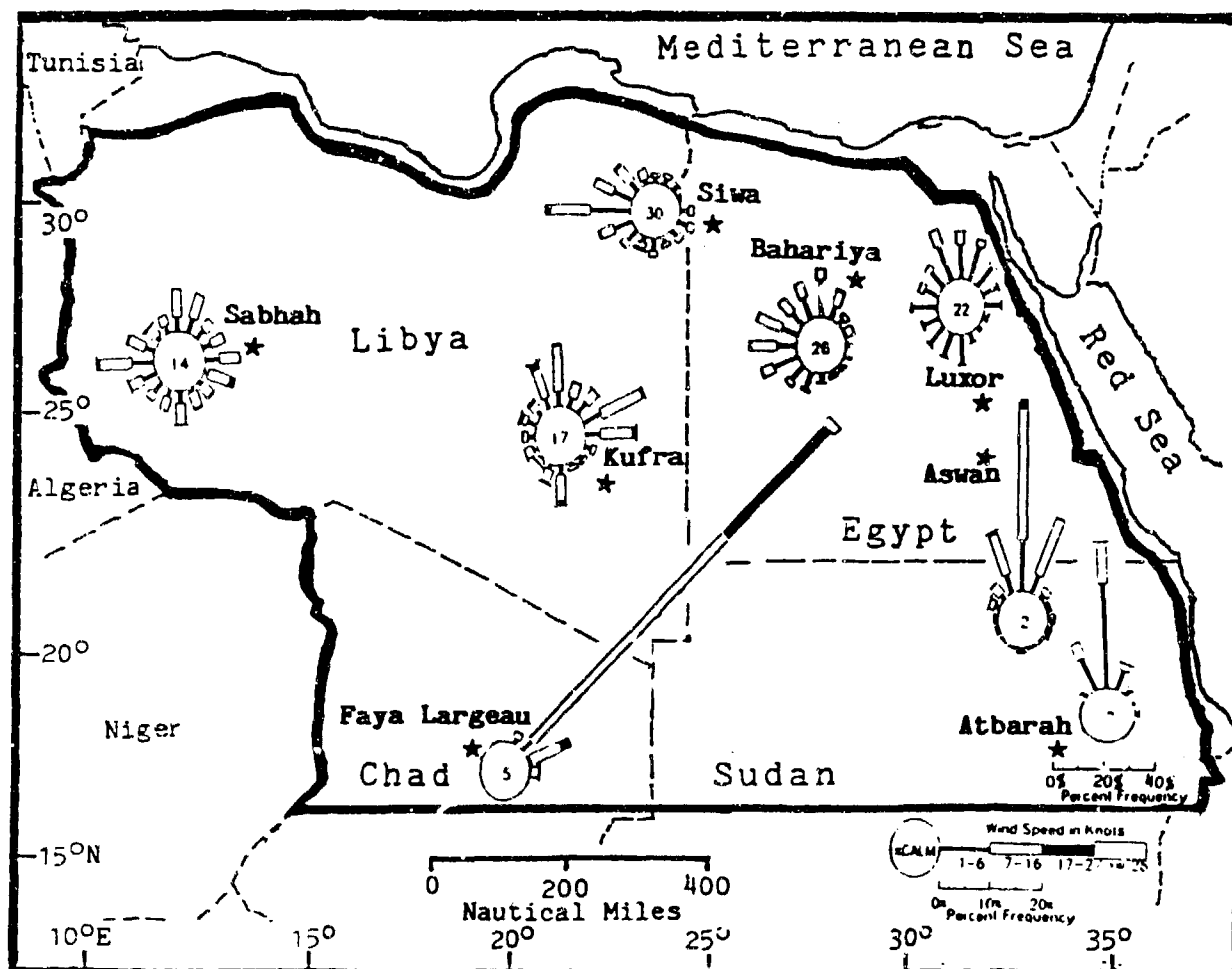


Figure 6-4. January Surface Wind Roses, Eastern Sahara. Note that the scale for the direction frequency at Atbarah is half that of the other stations.

Winds at 10,000 feet (3 km) are westerly to northwesterly. Monthly mean wind speeds at 30,000 feet (9 km) are usually between 50 and 80 knots, but they vary significantly with height because the Subtropical Jet

Stream core is centered over the region. Figures 6-5a-c show wind directions aloft at selected stations; note that the wind direction axis in these figures has been shifted 180 degrees.

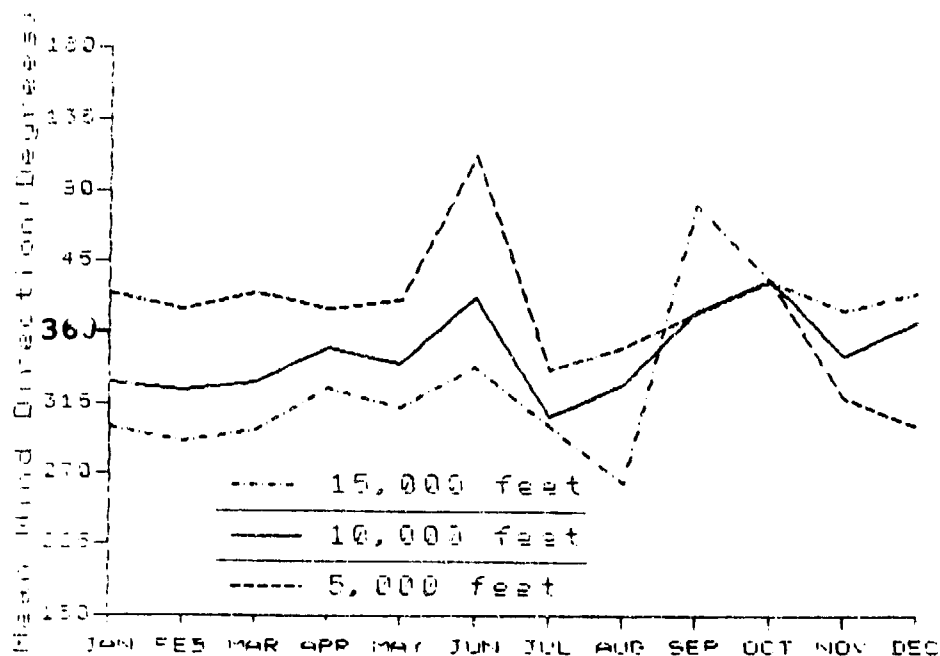


Figure 6-5a. Mean Annual Wind Direction for Dongola, Sudan.

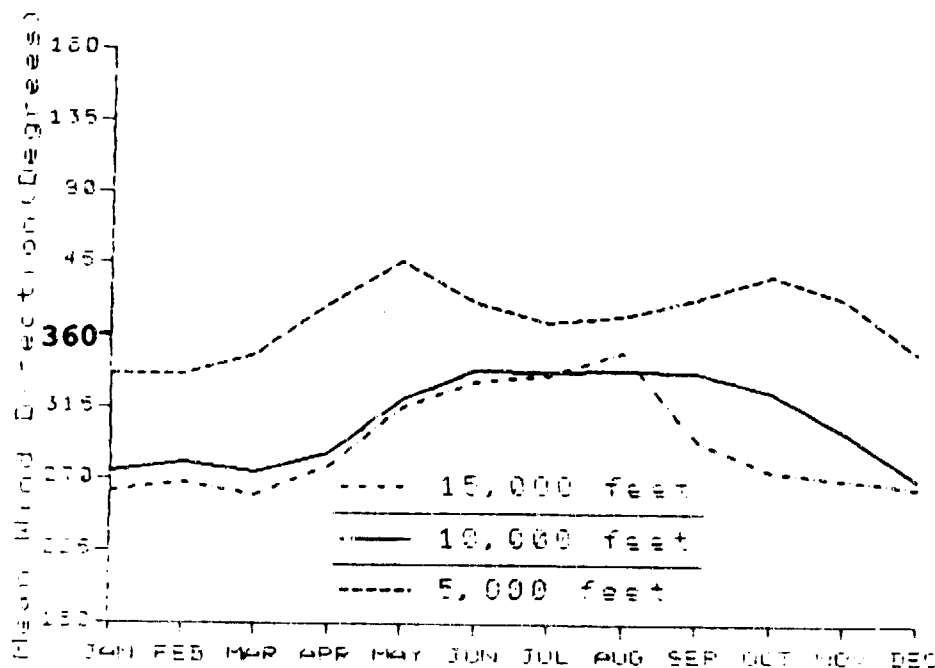


Figure 6-5b. Mean Annual Wind Direction for Kufra, Libya.

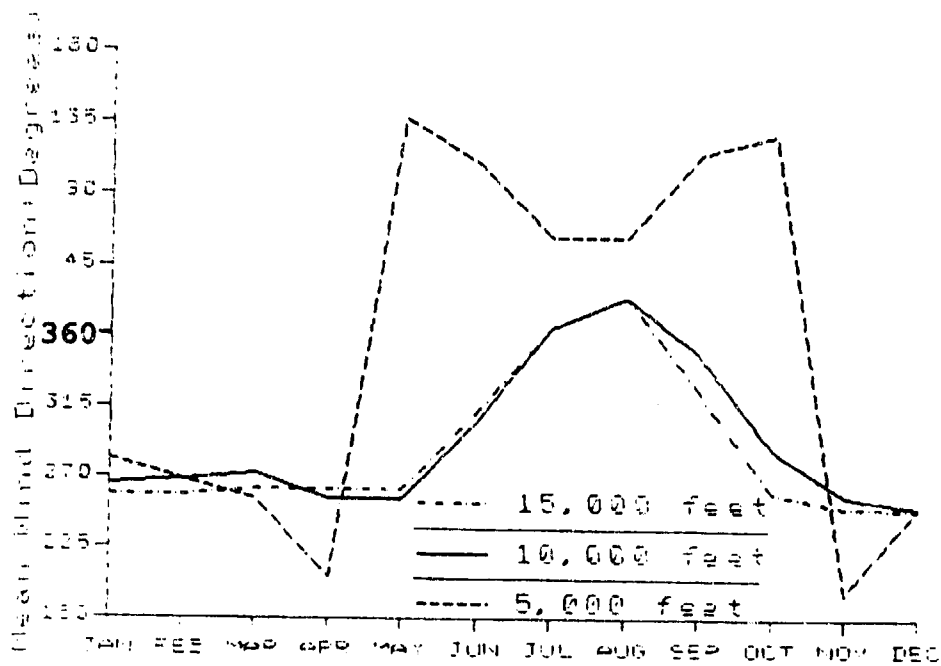


Figure 6-5c. Mean Annual Wind Direction for Subhah, Libya.

PRECIPITATION. The Libyan Desert is one of the driest areas in the world. Frontal showers and thunderstorms cause most winter precipitation; steady rain and drizzle are very rare. Snow is extremely rare except at elevations above 3,000 feet (915 meters). Significant winter rainfall episodes (above 0.1 inches--2 mm) are nonfrontal; they occur beneath a cold upper-level trough or a closed low, such as with the intense Cyprus Low shown in Chapter 2 (which see).

South of 30° N, the frequency of showers and thunderstorms varies significantly from year to year. One rainshower or thunderstorm can account for 90% of

the site's seasonal rainfall total for a 2- or 3-year period. Rainfall occurs once or twice a month north of 26° N along trailing cold fronts. The area south of 26° N averages less than one rainfall day a winter. Mean precipitation statistics are not an accurate reflection of potential rainfall accumulation or potential flood damage that might result from a single thunderstorm. Maximum 24-hour precipitation in Figure 6-6 is more representative of this hazard. Semipermanent stream beds, or wadis, fill rapidly and can carry water for significant distances. Upper-level instability, rather than migratory low central-pressure readings, determines the difference between rainfall and virga.

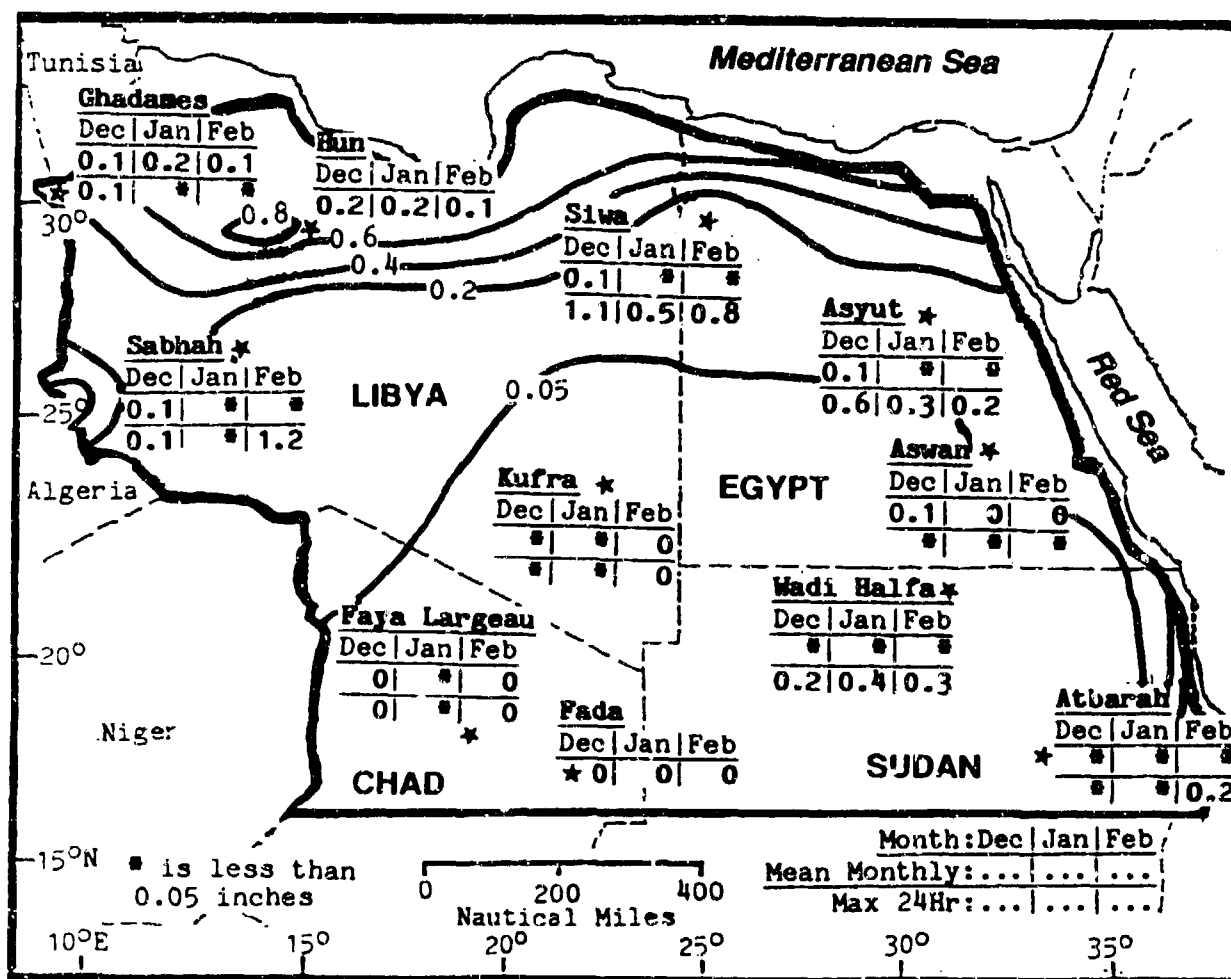


Figure 6-6. Mean Winter Monthly/Maximum 24-hour Precipitation, Eastern Sahara. Isohyets represent mean seasonal rainfall totals. Maximum 24-hour precipitation statistics for Hun and Fada are not available.

THE EASTERN SAHARA WINTER

December-February

TEMPERATURE. As shown in Figure 6-7, winter nights are cool and days are mild. Radiative processes produce large diurnal temperature ranges. The highest winter temperatures occur with subsidence aloft when transitory continental high pressure intensifies over northern Africa. Jalu has reached 89° F (32° C) under these conditions. Faya Largeau's winter extreme high is

109° F (43° C). Temperatures above 100° F (37° C) occur in every winter month throughout Chad and Sudan because fronts do not consistently penetrate south of 20° N. Extreme lows range from 16° F (-9° C) at Hun to 41° F (5° C) at Abu Hamed. It is estimated that temperatures have dropped to as low as 10° F (-12° C) over the Tibesti Mountains above 7,000-foot (2,135-meter) elevations.

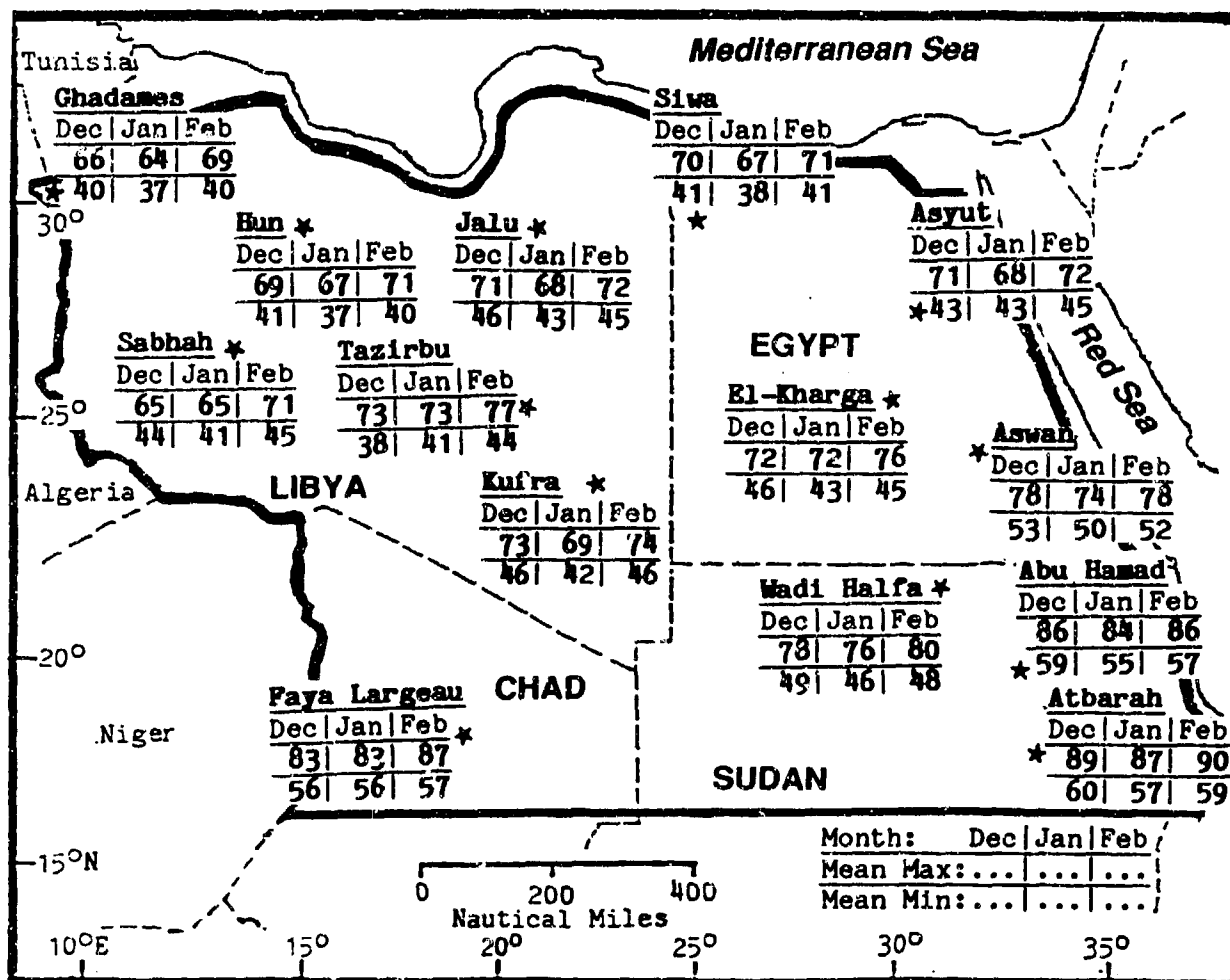


Figure 6-7. Mean Winter Daily Maximum/Minimum Temperatures (F), Eastern Sahara.

GENERAL WEATHER. The Saharan Heat Low forms in April and erodes the quasi-stationary high-pressure ridge over northern Africa. It establishes a low-level southerly or easterly flow of dry desert air over the subregion's western half.

The Azores High's northwestward shift produces a southward migration of cyclonic activity from the Mediterranean Sea to the Atlas Mountains. Hot, dry winds and frequent duststorms are common with these Atlas Lows. The Monsoon Trough surges northward for 1-3 day periods south of 18° N, but it occasionally moves northward to Dongoia and Abu Hamed. Low-level moisture and southerly flow produce isolated rainshowers by late May.

SKY COVER. Mean cloud cover increases to 18-25% in the southern third, but decreases to 20-30% in the northern two-thirds despite an increase in Atlas Low activity. Mid- and upper-level cloud cover increase slightly, but higher surface temperatures and dry Saharan air reduce cloud amounts below 8,000 feet (2,440 meters). Moist and cool Mediterranean air carried southeastward behind Atlas Low cold fronts creates stratocumulus and cumulus inland over the northern Sahara. Bases are 3,000 to 7,000 feet (915 to 2,135 meters) and tops reach 9,000 feet (2,745 meters). Embedded towering cumulus and cumulonimbus can extend to 50,000 feet (15 km). Bases can drop to 500 feet (150 meters) in heavy rainshowers.

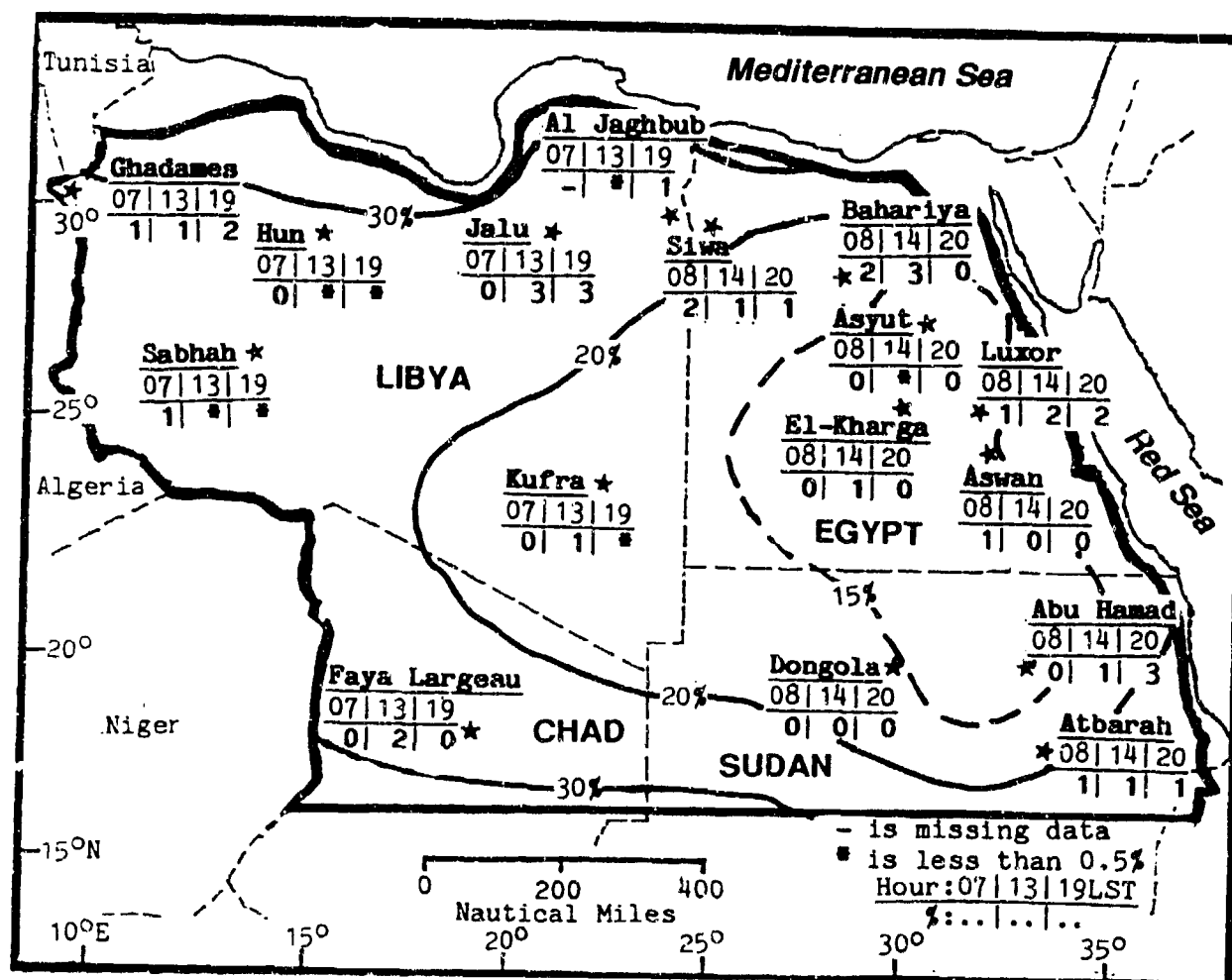


Figure 6-8. Mean Spring Cloudiness (Isopleths) and Frequencies of Ceilings Below 3,000 Feet (915 meters), Eastern Sahara.

The invading cool Mediterranean air mass warms and dries rapidly over land; cloudiness disappears 100 miles inland. Equatorial moisture occasionally moves northward within the warm sector of deep Atlas Lows. The Atlas Low center must track eastward between 27° and 30° N before broken to overcast cirrus and/or altocumulus can develop along the Tibesti Mountains. The altocumulus forms between 10,000 and 18,000 feet (3,050 and 5,485 meters); tops reach 20,000 feet (6 km) MSL. Altocumulus castellanus can develop along cold fronts, occasionally producing virga; tops can reach 40,000 feet (12 km) MSL.

Stratocumulus forms in stable morning air near large localized moisture sources. Morning cloud cover has its bases at or above 2,000 feet (610 meters) and tops below 4,000 feet (1,220 meters) MSL. Stratus is rare in the Eastern Sahara. Most low ceilings shown in Figure 6-8 and almost all ceilings below 1,000 feet (305 meters) are caused by blowing dust or sand obscurations. These ceilings are usually reported as being below 800 feet (245 meters).

The Monsoon Trough moves north in May and oscillates along the subregion's southern edge. Maritime tropical (mT) air temporarily replaces continental tropical (cT) air. The shallow mT air mass produces low and middle clouds. With northward surges of the Monsoon Trough, towering cumulus and cumulonimbus can form at Atbara and, to a lesser extent, at Faya Largeau, Dongola, and Abu Hamed. These clouds form when the Monsoon Trough is north of 20° N and mT air is 3,000-5,000 feet (915-1,525 meters) deep. Bases are between 4,000 and 8,000 feet (1,220 and 2,440 meters); tops can reach 60,000 feet (18 km) MSL. Isolated storm cells may also appear in northern Sudan. Altocumulus forms within and around dissipating towering cumulus/cumulonimbus, occurring most frequently (6-9% of the time) at night and in the early morning. Bases range from 12,000 to 20,000 feet (3,660 to 6,100 meters) with 13,000- to 22,000-foot (3,960- to 6,700-meter) MSL tops.

VISIBILITY. Low visibilities are most common in the spring when high winds from Atlas Lows combine with dry conditions to raise dust. Duststorms develop with Khamsin or Ghibli winds in the Atlas Low's warm

sector. Strong Khamsin winds may drop visibilities to near zero for 6-12 hours during the day. Although visibility improves during the night, it deteriorates again the next day. This cycle may repeat for several days in succession with slow-moving lows. Airborne dust can affect an area 120 miles wide and reach heights of 20,000 feet (6 km) MSL. Atlas Lows, accompanied by deep upper-level troughs, can produce a number of smaller surface lows that produce localized duststorms near their centers. These small lows affect the region for periods of 7-10 days. Even after the winds die down, dust in suspension blankets the area for several days.

High pressure moves into the area behind passing cold fronts, bringing strong northerly winds and more duststorms. The extent and duration of post-frontal duststorms depend upon the air mass temperature differences on either side of the front. Also, low visibility is more common at stations surrounded by silt or fine sand than at stations surrounded by rock or salt marsh. The fine sand is more common in the east and south, causing the increase in the area's low visibility frequencies shown in Figure 6-9.

Large and intense high-pressure areas may temporarily tighten pressure gradients just north of the Monsoon Trough. The tighter gradients strengthen the Harmattan winds, causing Harmattan Haze (which see) in Chad and western Sudan. Visibilities are poorest in the morning (0700 to 0900 LST), when they are between 1/2 and 1 mile.

The Monsoon Trough moves northward and oscillates over the region throughout the spring. When the Monsoon Trough is at its northernmost position, strong southerly winds produce duststorms with visibilities below a mile immediately south of the trough.

Fog and damp haze are rare, occurring only at locations with large quantities of surface water such as the Nile Valley and Qattara Depression. The salt marsh east of Al Jaghbub helps form nocturnal radiation fog or damp haze that reduces visibility at Al Jaghbub to 1 to 6-mile visibilities about 25% of the time. Heavy rainshowers along cold fronts may also reduce visibility for brief periods.

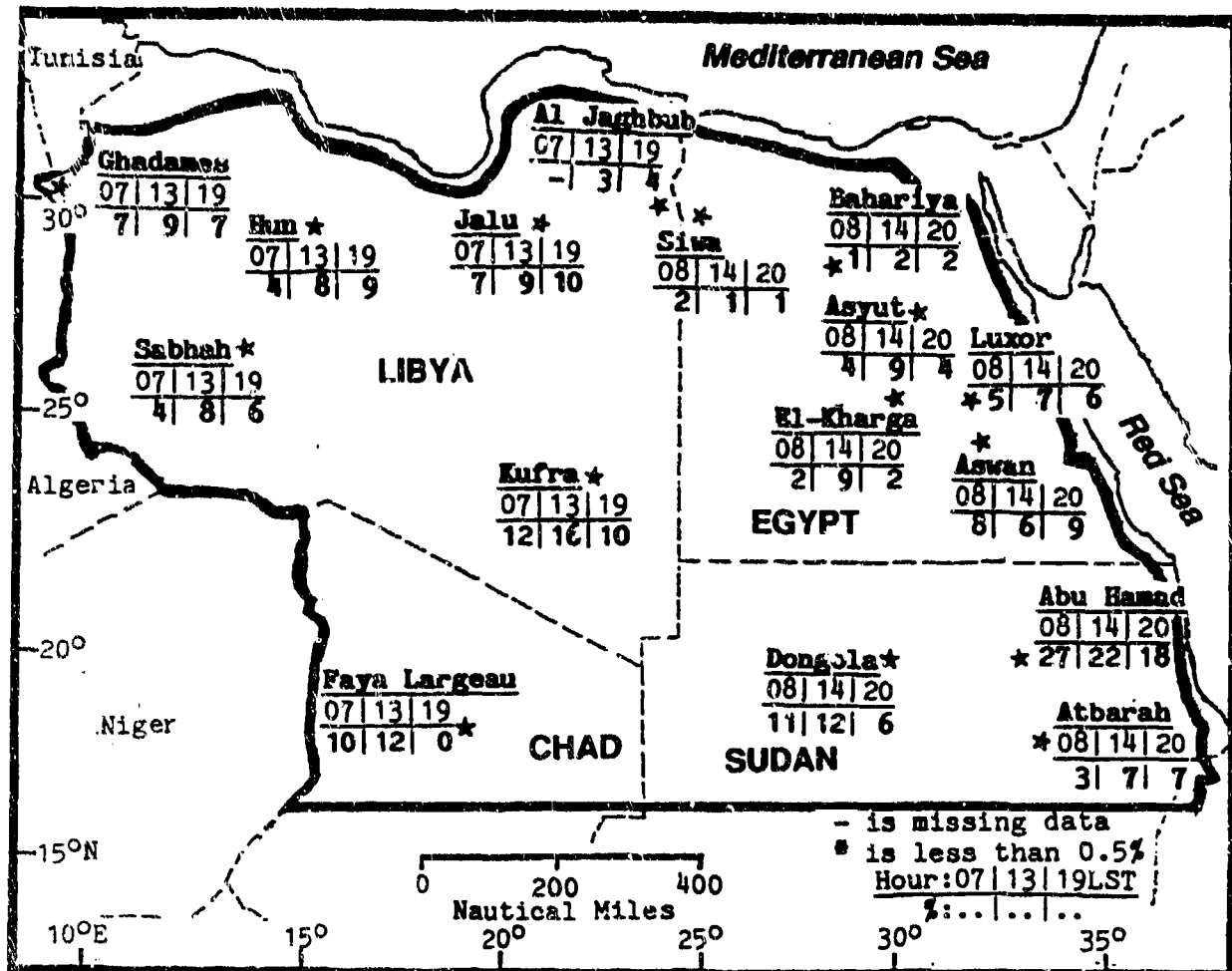


Figure 6-9. Mean Spring Frequencies of Visibilities Below 3 Miles, Eastern Sahara.

THE EASTERN SAHARA SPRING

March-May

WINDS. Surface winds change direction as the Azores High migrates northwestward. Directions are more variable than in winter because of the increased frequency of Atlas Lows, which also make winds above 17 knots more common than in winter. Western stations are more affected than those in the east. The cliffs around both Aswan and Faya Largeau cause channeling.

Mid- and upper-level winds are sustained west-southwesterly. Wind speeds are 40-90 knots above 20,000 feet (6,100 meters) in March, but they decrease significantly by May. Speeds peak at 38,000 feet (11.6 km).

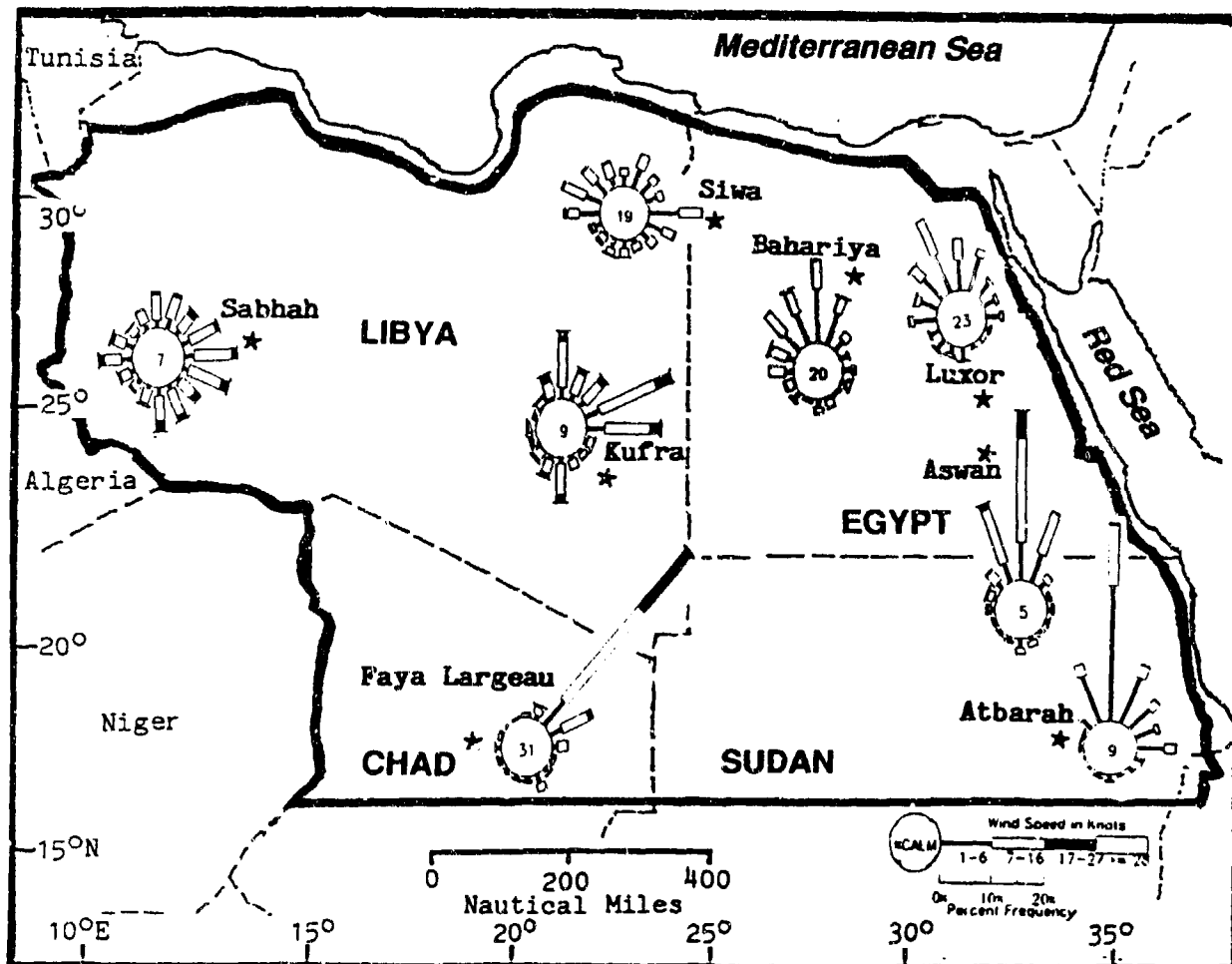


Figure 6-10. April Surface Wind Roses, Eastern Sahara.

THE EASTERN SAHARA SPRING

March-May

PRECIPITATION. Precipitation in northern Libya and Egypt decreases from its winter maximum. Stations south of 28° N receive less than a trace until May. Despite this, rainfall peaks in the spring between 24° N and 26° N. Although Atlas Lows are most common in spring, storm tracks that penetrate the interior seldom

bring heavy rainshowers. This is evident in the spring 24-hour maximum rainfall data shown in Figure 6-11. A cold and deep upper-level trough can trigger afternoon or early evening thunderstorms even in the absence of a

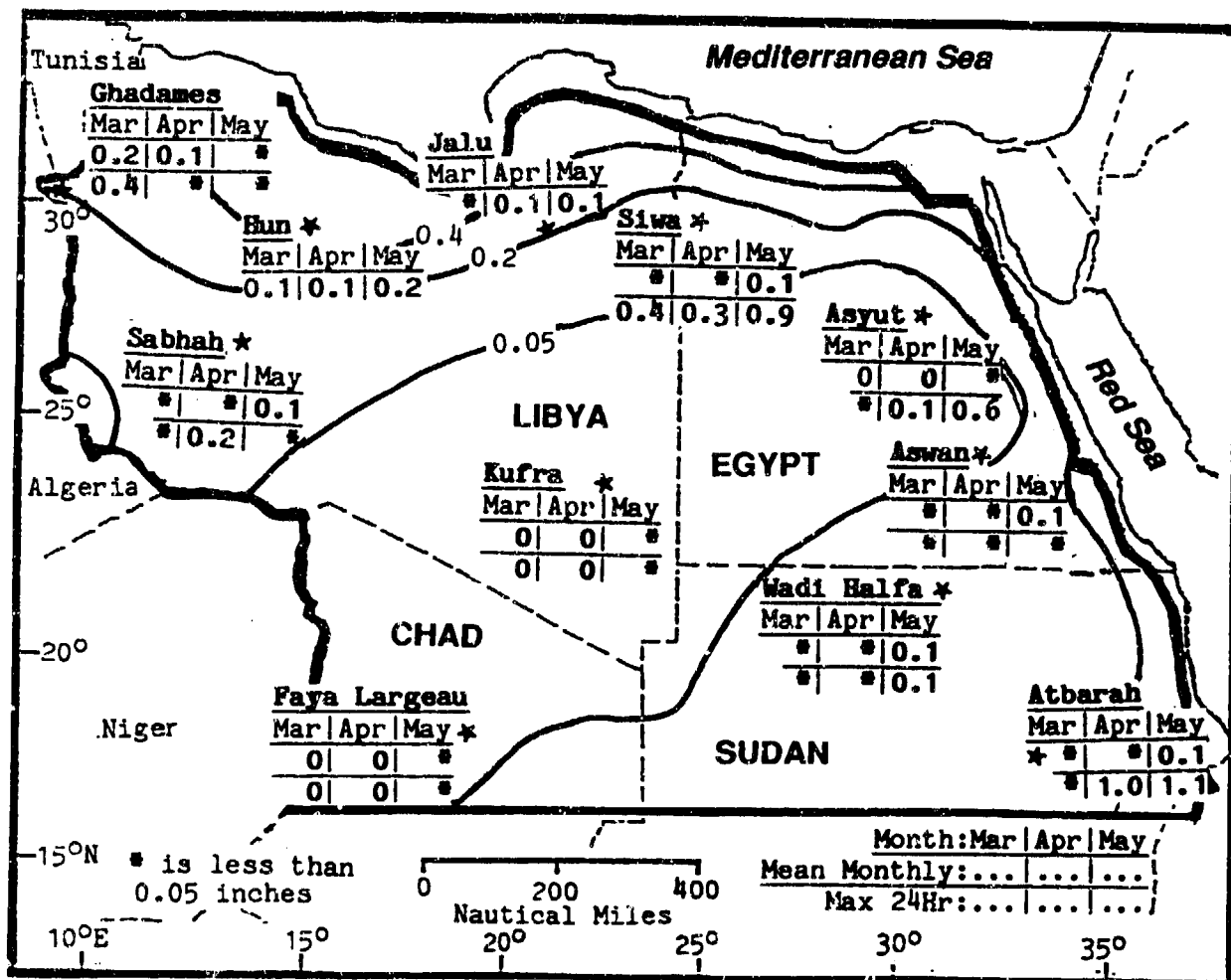


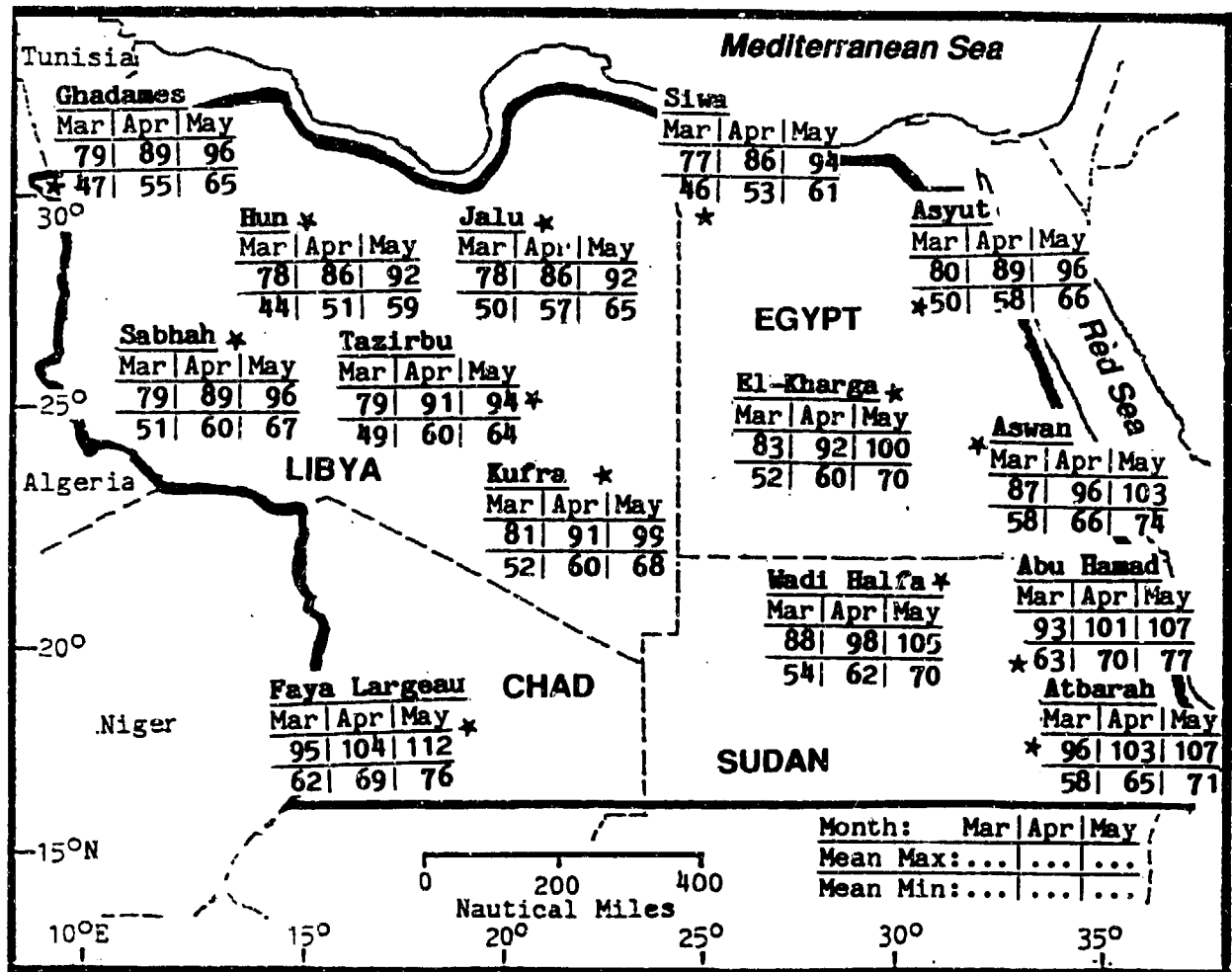
Figure 6-11. Mean Winter Monthly/Maximum 24-hour Precipitation, Eastern Sahara. Isohyets represent mean seasonal rainfall totals.

THE EASTERN SAHARA SPRING

March-May

TEMPERATURE. Mean spring temperatures are lowest in the northwest in March, but highest in the south just before the Monsoon Trough arrives. In the south, daily highs are usually above 100° F (38° C) in April and May. Atlas Lows' Khamsin or Ghibli winds often result in the highest spring temperatures. Record highs

range from 106° F (41° C) to 126° F (52° C), but air temperatures in remote areas may exceed 126° F (52° C). Ground temperatures may exceed 140° F (59° C). Diurnal variations (as much as 35° F/19° C) are most extreme in the spring. Extreme lows range from 25° F (-4° C) at Hun, to 52° F (11° C) at Faya Largeau.



GENERAL WEATHER. The Monsoon Trough, the major summer weather feature, is at about 18° N. Its high humidity and precipitation seldom extends north of 20° N for more than 3 days in a row. North of the Trough's influence, it is extremely dry.

The Subtropical Ridge (which see) is centered over the subregion during summer. It divides upper-level westerlies to the north from easterlies to the south.

SKY COVER. With few lows traveling over the Mediterranean, mean summer cloud cover over the northern two-thirds of the region drops to less than 15%. Cloud cover over the southern third, which is affected by the Monsoon Trough, increases to up to 55% and makes summer the cloudiest season. Most low ceilings shown in Figure 6-13, however, are caused by the suspended dust that occurs with thunderstorms, rainshowers, Tropical Squall Lines, and the thermal turbulence that results from intense surface heating. Duststorms commonly produce ceilings below 800 feet (245 meters).

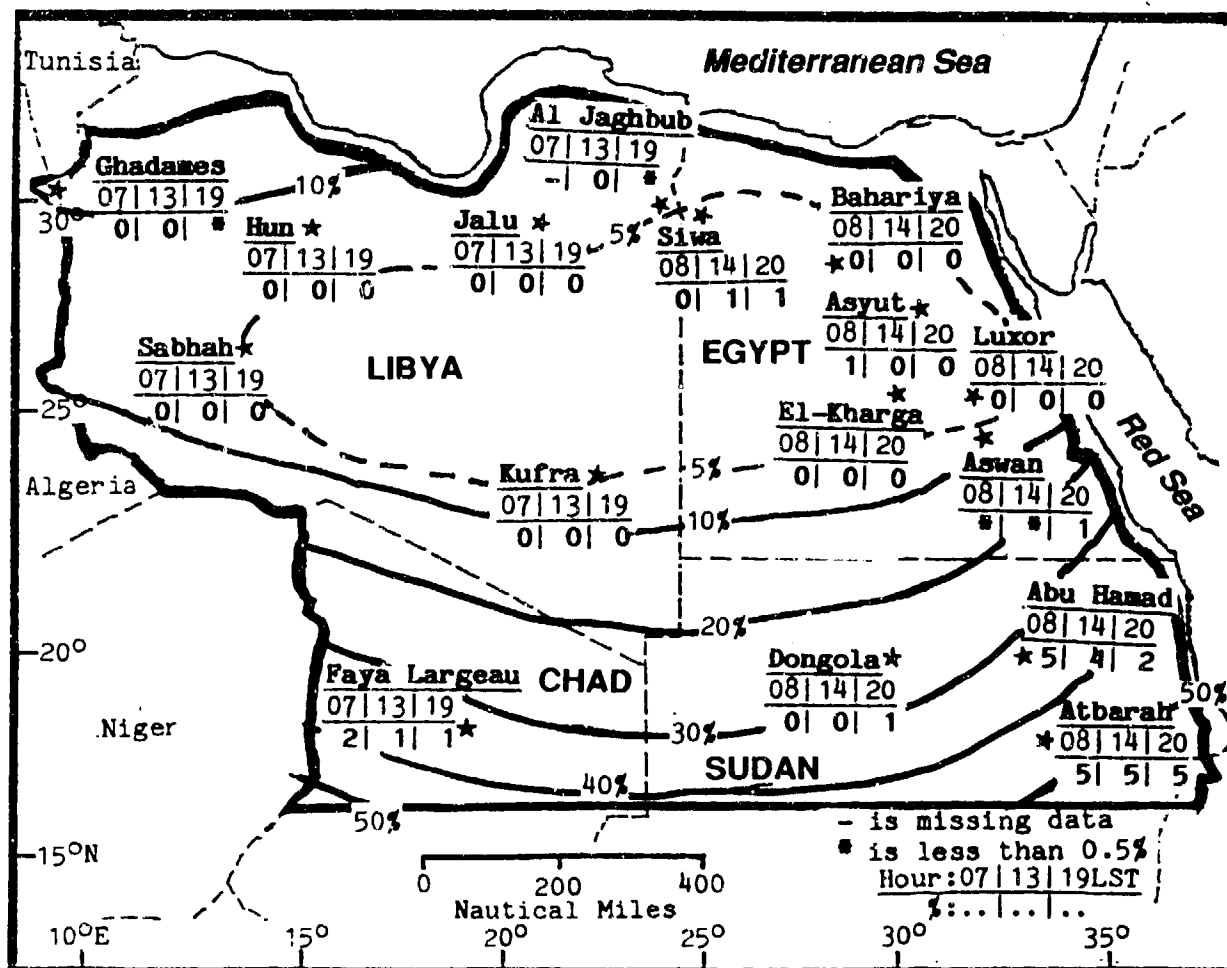


Figure 6-13. Mean Spring Cloudiness (Isopleths) and Frequencies of Ceilings Below 3,000 Feet (915 meters), Eastern Sahara.

Most cloud cover in the north is associated with the weakened Subtropical Jet (cirrus and altocumulus). Scattered to broken cumulus, along with very isolated cumulonimbus, can form along rare cold fronts crossing the region's northern fringes. This occurs only when the summer high-pressure ridge over Europe temporarily weakens and allows weak cyclonic activity to penetrate

into the southern Mediterranean. Broken morning stratocumulus is reported at Hun and Jalu about once every 5-7 years. It probably develops in the Gulf of Sidra and penetrates inland with abnormally strong northwesterly flow. Bases are 1,500-2,500 feet (455-760 meters), tops below 5,000 feet (1,525 meters) MSL.

THE EASTERN SAHARA SUMMER

June-August

Cloud amounts increase in a band between 50 and 250 miles south of the Monsoon Trough. Cumulus, towering cumulus, and cumulonimbus form within the maritime tropical (mT) airmass layer, normally when the layer is 3,000-5,000 feet (915-1,525 meters) thick. Fair-weather cumulus forms daily with about 6,000-foot (1,830 meters) bases and tops below 10,000 feet (3,050 meters) MSL. Altocumulus forms in and near the Mid-Tropospheric Easterly Jet and within the outflow boundary of expanding cumulonimbus and towering cumulus. Altocumulus can also form as the continental tropical (cT) airmass overrides an mT airmass along the Intertropical Discontinuity. Bases are 15,000 to 25,000 feet (4,570 to 7,620 meters) and tops are between 16,000 and 27,000 feet (4,875 and 8,230 meters) MSL. Cumulonimbus and towering cumulus can form an organized, westward-moving line of convection called a

"Tropical Squall Line," which see. Bases are 4,000 to 8,000 feet (1,220 to 2,440 meters); tops reach 60,000 feet (18 km). Altostratus and stratocumulus decks may form under stable conditions after a Tropical Squall Line passage and persist for 6 to 8 hours. Altostratus bases range from 8,000-12,000 feet (2,440-3,660 meters) MSL with tops to 20,000 feet (6 km) MSL. Stratus is very rare, forming in the early morning hours after heavy rains.

VISIBILITY. Summer duststorms are rare north of the surface Monsoon Trough because few synoptic disturbances affect the area. However, turbulence caused by intense surface heating raises some dust and results in the slight mid-day increase in low visibilities shown in Figure 6-14.

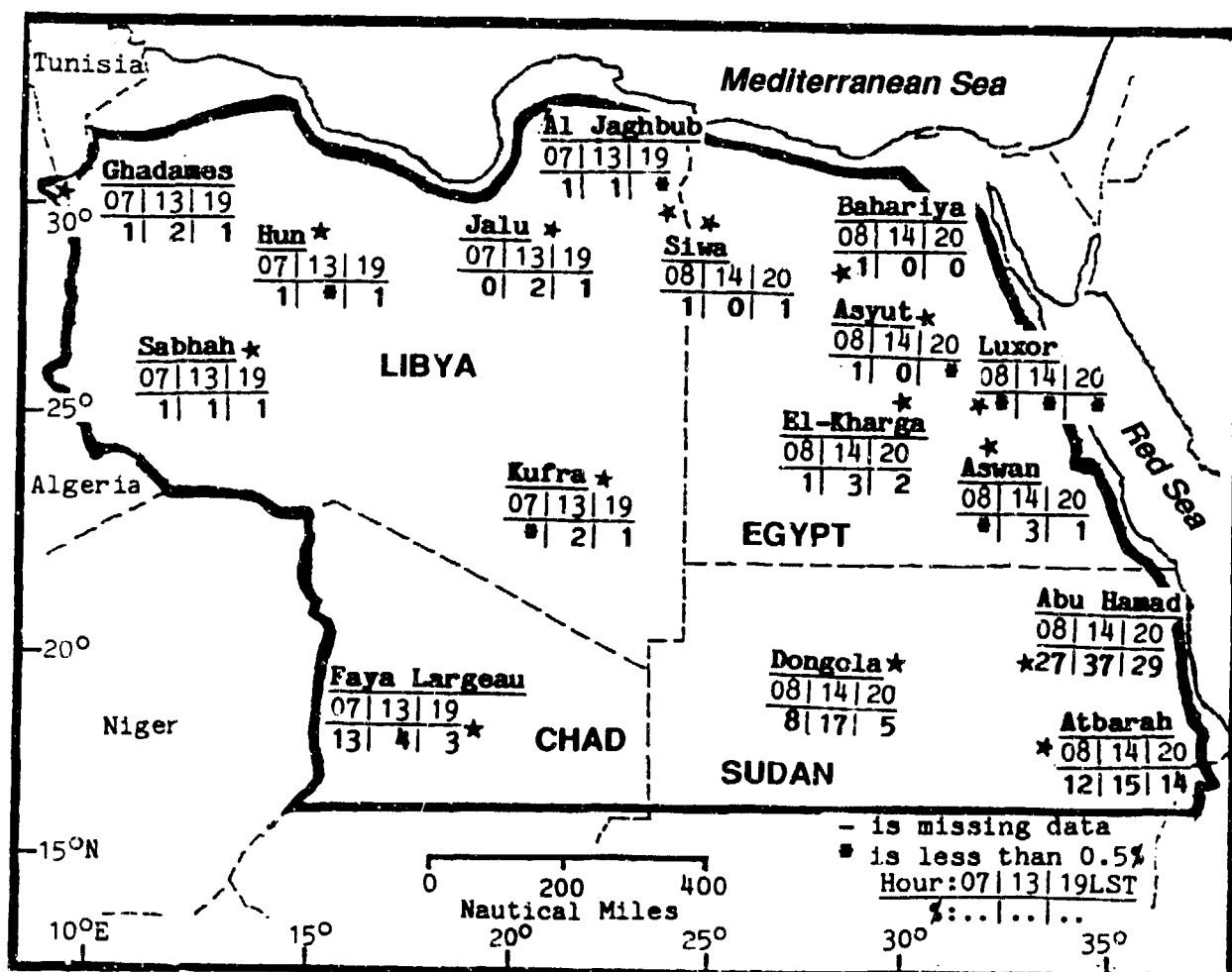


Figure 6-14. Mean Summer Frequencies of Visibilities Below 3 Miles, Eastern Sahara.

THE EASTERN SAHARA SUMMER

June-August

Visibilities below 3 miles are much more common in the region's southern third, where frequencies are more than 30%. Abu Hamed and Atbarah see more dust-related low visibilities during the summer than at any other time as the Monsoon Trough oscillates through the area every day throughout much of July and August. Large-scale movements in the Monsoon Trough cause widespread blowing dust or duststorms to its immediate south. These storms can last for several hours, raising enough sand and dust to bury roads and train tracks.

Farther south, thunderstorm and squall line downdrafts cause duststorms, usually within a 50 to 250-mile band south of the surface Monsoon Trough. These storms can reduce visibilities to 100 yards, affecting an area 150 miles in diameter and lasting for less than an hour. Tropical Squall Lines can produce "walls of dust" that are a few hundred feet high. These severe duststorms are called "Haboobs" in Sudan. They are usually most severe in early summer.

Thunderstorm precipitation, most common south of the Monsoon Trough, may briefly lower visibility to below a mile. Morning fog with 2-5 mile visibilities can form after nocturnal showers. Damp haze with 4-6 mile visibilities can form around salt marshes and in the Nile Valley. Otherwise, fog and damp haze are very rare in the Sahara.

WINDS. The Azores High keeps winds blowing steadily out of the north through most of the summer, but south of 20° N they turn to northeasterly. Southwesterly winds prevail south of the Monsoon Trough's surface position. Surface wind speeds range from 5 knots at Luxor to 15 knots at Ghadames. Winds aloft are primarily northwesterly to northeasterly, as was shown in Figure 6-5. Mean wind speeds aloft are generally below 15 knots because the axis of the Subtropical Ridge is directly over the region.

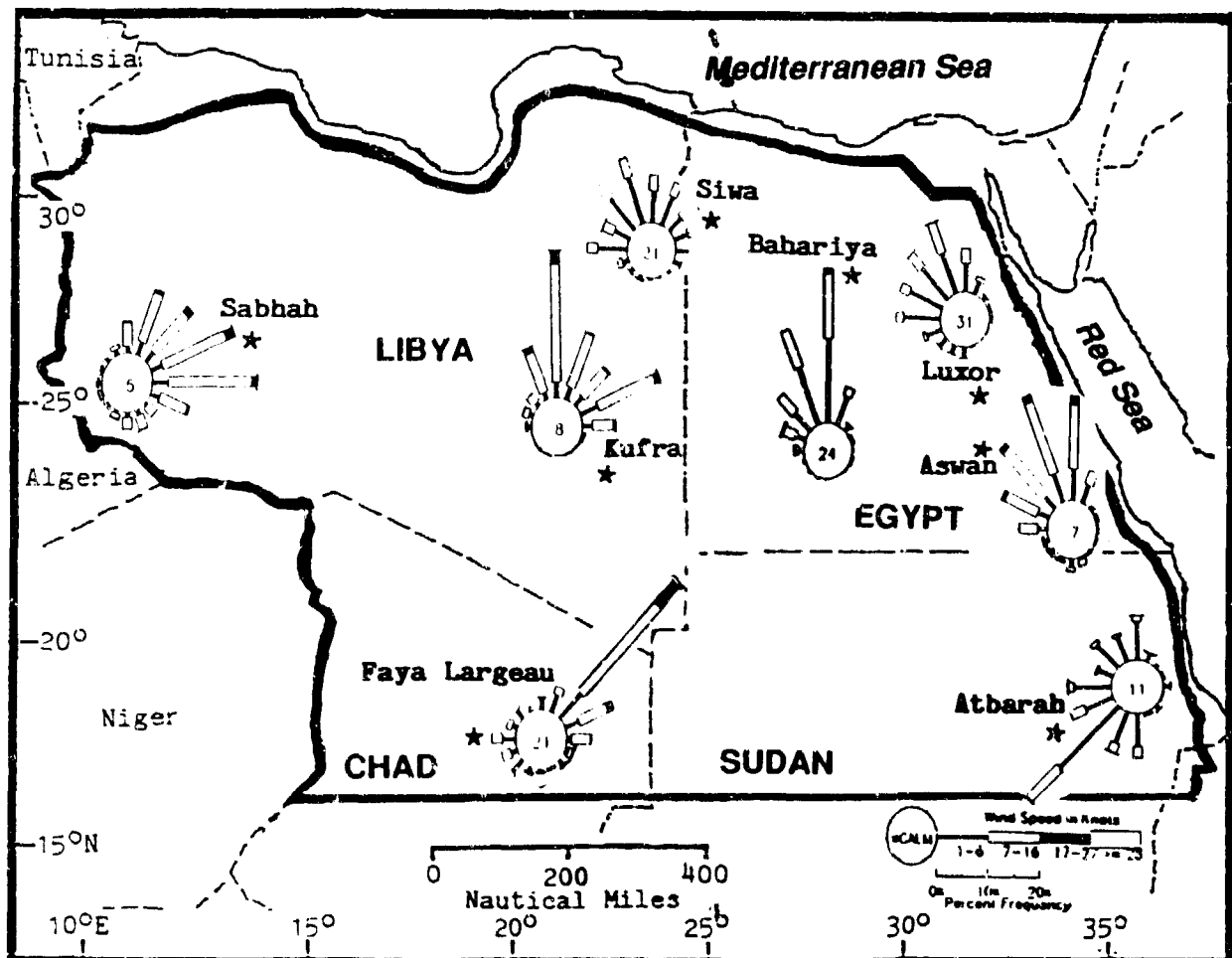


Figure 6-15. July Surface Wind Roses, Eastern Sahara.

THE EASTERN SAHARA SUMMER

June-August

PRECIPITATION. Summers are dry north of 20° N; most stations average no rain at all. Precipitation increases slightly in the northwest corner because of

orographic lift along the Nafusah Mountains' windward side, but even here average rainfall is less than 0.2 inches a month.

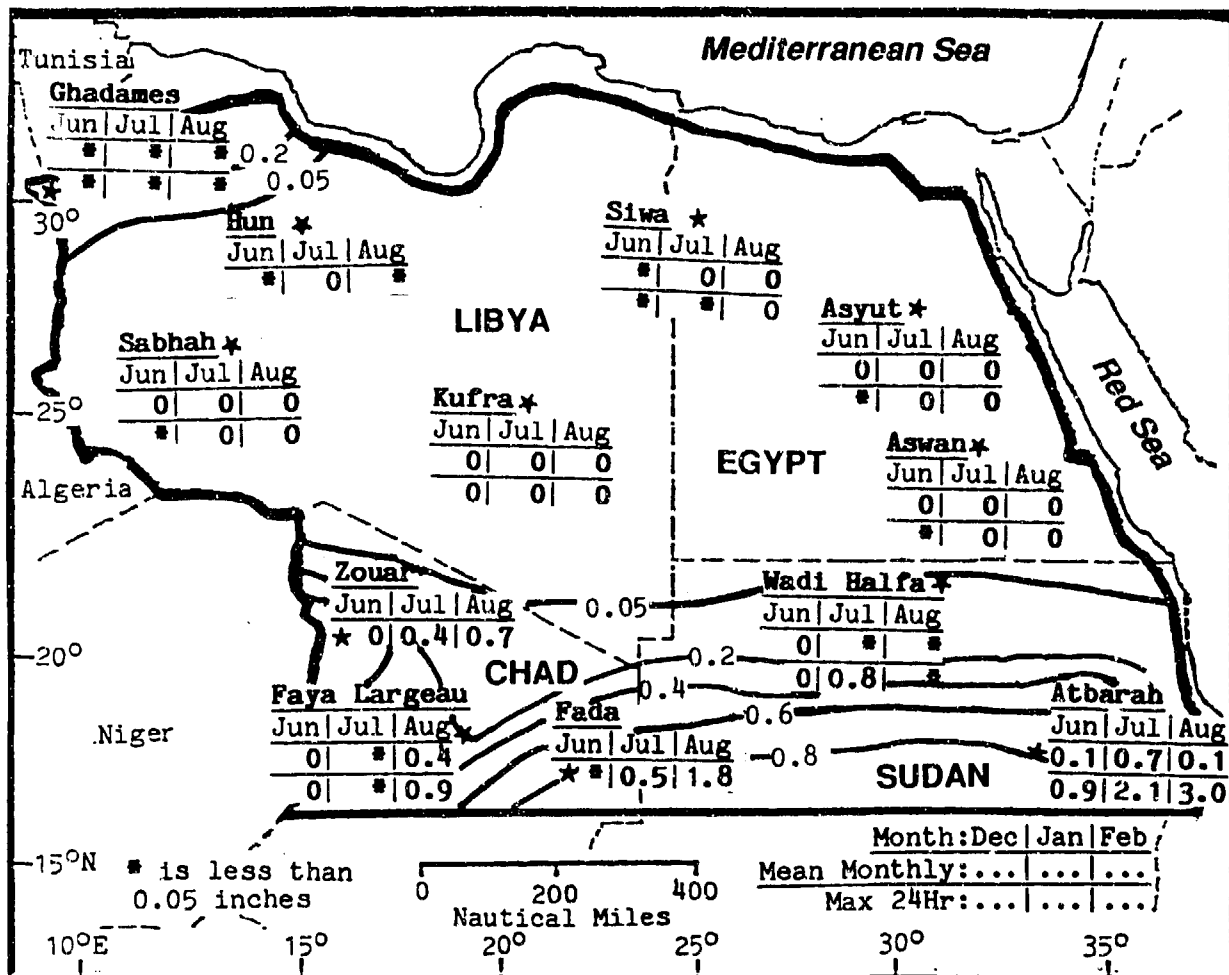


Figure 6-16. Mean Summer Monthly/Maximum 24-hour Precipitation, Eastern Sahara. Isohyets represent mean seasonal rainfall totals.

South of 20° N, the Monsoon Trough produces some rainfall in July and August when showers develop more than 150 miles south of and parallel to the surface Trough. Monsoon Trough air is 3,000 to 5,000 feet (915 to 1,525 meters) deep there--a necessary condition for strong convection. Although rainfall is reasonably predictable south of 20° N, it varies widely from year to year. Nearly 70% of summer rain falls from only two or three rainshowers or thunderstorms. Monthly rainfall

totals have reached 5 inches (125 mm) at some locations, but these amounts are extremely rare. The rare heavy rain can produce 0.1 (3 mm) to 1 inch (25 mm) in an hour and cause flash floods. Widespread showers with embedded thunderstorms can occur when flow above 750 mb is southerly or southeasterly. Figures 6-17a and 6-17b depict flow at the gradient and 700-mb levels in such a case.

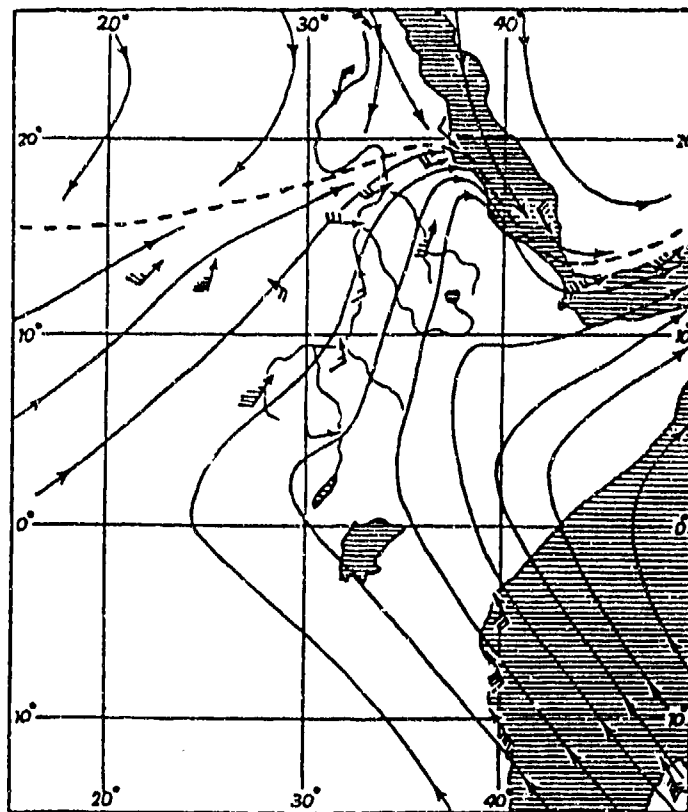


Figure 6-17a. Gradient-Level Flow, Widespread Summer Rain and Thunderstorms.

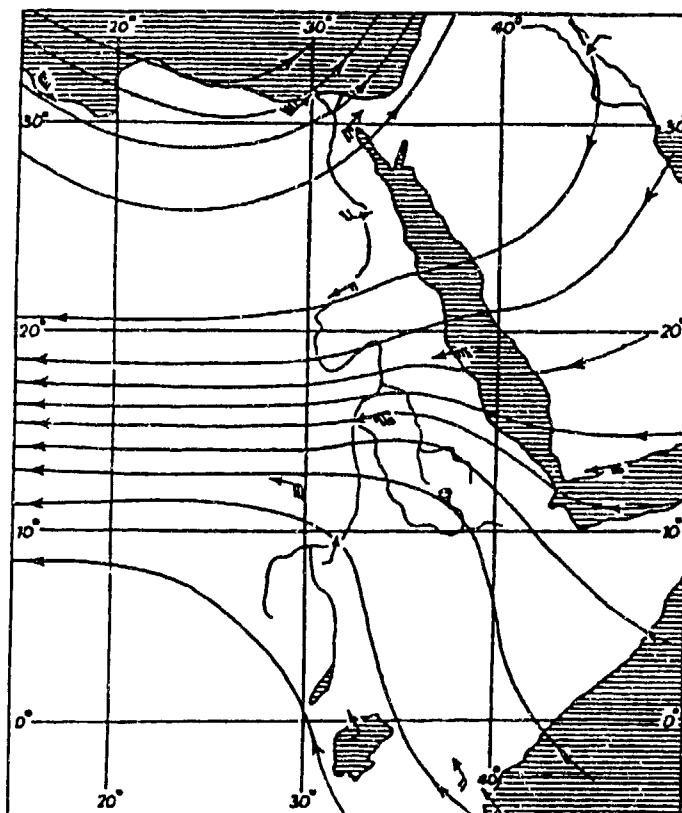


Figure 6-17b. 700-mb Flow, Widespread Summer Rain and Thunderstorms.

THE EASTERN SAHARA

SUMMER

June-August

Strong squall lines with cloud tops exceeding 55,000 feet (16.7 km) produce thunderstorms with hail and frequent lightning. A strong upper-level equatorial moisture surge usually causes the Monsoon Trough to move abnormally northward, resulting in rain where it is least expected. Although it only happens every 20-50 years, even Kufra can get a heavy downpour in August when the Monsoon Trough surges north of 25° N. Northern Chad's Tibesti Mountains provide some orographic uplift. Normally, the Monsoon Trough is not far enough north to produce more than isolated fair-weather cumulus, but Tibesti vegetation suggests that scattered but brief showers do occur. Although there are no observing stations in the mountains, at least 2 inches (50 mm) is likely above 5,000 feet (1,525 meters) during the summer.

TEMPERATURE. June and July are hottest in the south, as shown in Figure 6-18. Mean daily highs are above 100° F (38° C) throughout the region except in areas within 200 miles of the Mediterranean Sea. They are as high as 111° F (44° C) at Faya Largeau in June. The highest temperatures occur in stagnant air masses before northward surges of cooler Monsoon Trough air. Extreme highs range from 113° F (45° C) at Tazerbo to 131° F (55° C) at Ghadames. The rare observing data available indicates that temperatures reach 140° F (59° C) in the remote Sahara. Soil surfaces are even hotter. Extreme summer lows range from 49° F (9° C) at Jalu to 70° F (21° C) at Abu Hamed.

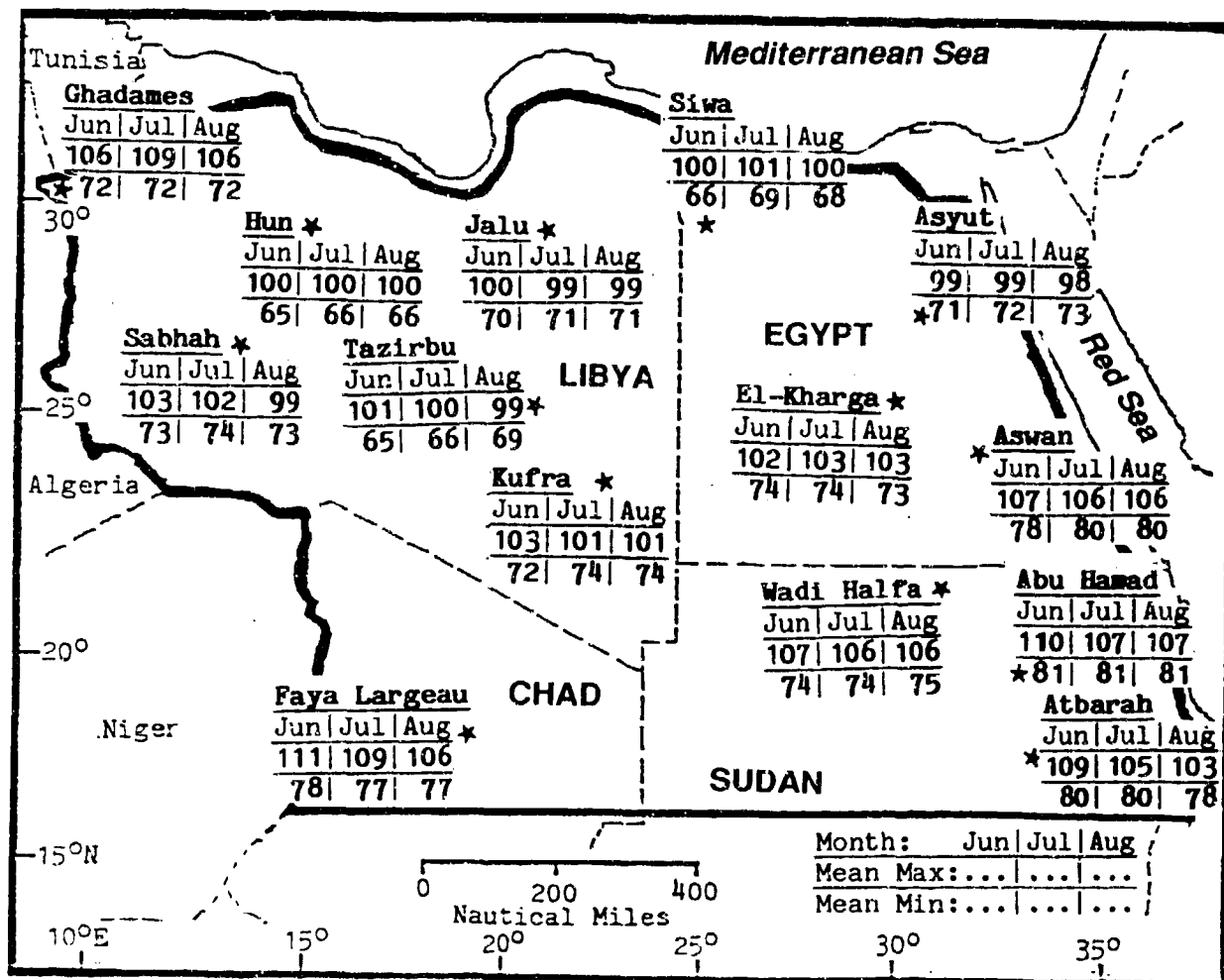


Figure 6-18. Summer Mean Daily Maximum/Minimum Temperatures (F), Eastern Sahara.

GENERAL WEATHER. During the fall the Azores High slowly migrates southward toward its winter position. Large-scale northwesterly low- and mid-level flow returns to the Eastern Sahara. The Saharan High replaces the Saharan Heat Low and reinforces northwesterly flow. Southern and western Libya are the only places where the Saharan Heat Low persists through October. Surface heating in the Saharan interior permits a shallow thermal low-pressure cell to maintain cyclonic low-level flow. Cold fronts, cloudiness, and precipitation begin to re-enter the region.

As the Monsoon Trough migrates rapidly southward, the unsettled weather (showers, thundershowers, and duststorms) also moves south. The Trough is usually south of the region after September.

SKY COVER. Increasing cyclonic activity increases mean cloudiness in the north to about 25%, mostly in the northwest. Cold fronts spread cirrus and altocumulus (mostly layered) with bases above 10,000 feet (3,050 meters). Cirrus tops are often above 40,000 feet (12 km). Altocumulus castellanus also forms along the cold front, spreading virga. Cumulus and isolated cumulonimbus also form along the cold front; bases are 3,000 to 6,000 feet (915 to 1,830 meters). Cumulonimbus tops are 60,000 feet (18 km). Bases may lower to 500 feet (150 meters) in heavy thunderstorms. Stratocumulus may form in the extreme north after frontal passage, with 2,000- to 5,000-foot (610- to 1,525-meter) bases, tops to 7,000 feet (2,135 meters). The cooler, less dry air allows stratocumulus and cumulus to form around salt marshes in the afternoon and after frontal passage; bases are 2,500 feet (760 meters). Siwa and Bahariya are affected most, as shown in Figure 6-19.

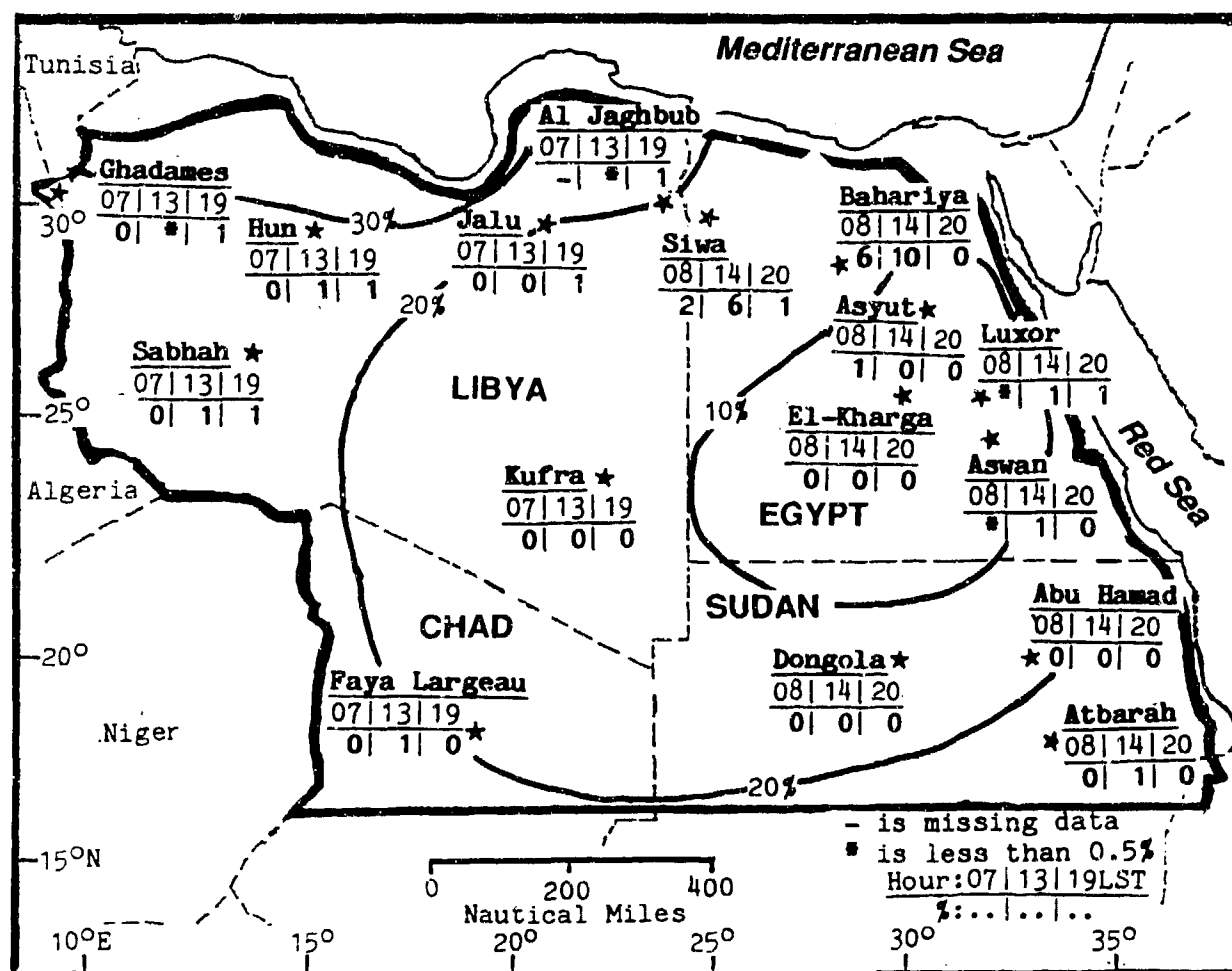


Figure 6-19. Mean Fall Cloudiness (Isopleths) and Frequencies of Ceilings Below 3,000 Feet (915 meters), Eastern Sahara.

Cloudiness decreases in the south to about 20% as the Monsoon Trough recedes. The Trough affects the southernmost locations in September, but disappears by mid-October, leaving almost cloudless skies. Cirrus may form in outflow from cumulonimbus or along the Tropical Easterly Jet. Altocumulus forms near the Mid-Tropospheric Easterly Jet and the outflow boundaries of large cumulonimbus and towering cumulus. It also forms in continental tropical (cT) airmasses that slope equatorward over maritime tropical (mT) air along the Intertropical Discontinuity. Bases average 15,000 feet (4,570 meters) and tops reach 22,000 feet (6,700 meters). Cumulus forms within the moist mT airmass with 4,000 to 8,000-foot (1,220- to 2,440-meter) bases and tops to 10,000 feet (3,050 meters).

Cumulonimbus and towering cumulus develop within a 150-250 mile band south of the surface Monsoon Trough where mT air is 3,000-5,000 feet (915-1,525 meters) deep. Tops reach 60,000 feet (18 km).

Most ceilings are above 3,000 feet (915 meters), and most low ceilings in the south are the result of dust. Fall stratus is rare, but it may form after a heavy September rainfall south of the Monsoon Trough.

VISIBILITY. Visibilities are best during the fall because the synoptic-scale disturbances that generate duststorms are absent. The Monsoon Trough leaves the subregion by October, and there is no mid-latitude cyclonic activity until November.

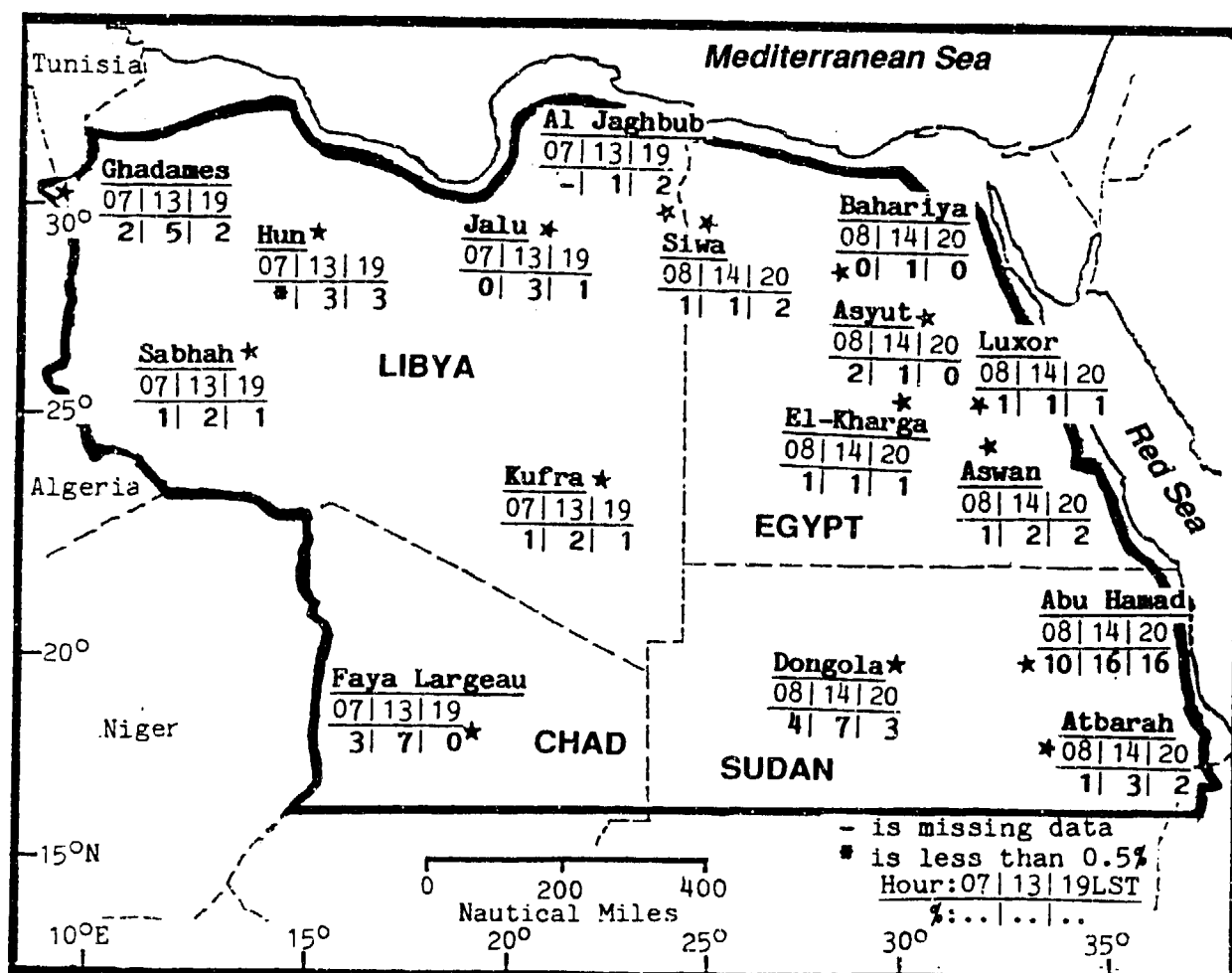


Figure 6-20. Mean Fall Frequencies of Visibilities Below 3 Miles, Eastern Sahara.

The few instances of low visibility are primarily caused by blowing dust and sand. Duststorms form with strong winds around cold fronts, most often in November. The transitory high behind the cold front intensifies the Harmattan (northeasterlies) and triggers Harmattan Haze in Chad. Visibilities can drop below 3 miles in this haze if winds are strong; they can drop below a mile for up to an hour with sustained winds of 30 knots or greater if conditions are dry.

Frontal showers occur in November at stations north of a line running from Ghadames to Bahariya. Fog and damp haze may develop during stable conditions near local water sources, including the Nile Valley and desert depressions with oases or salt marshes.

The Monsoon Trough only affects the region in September when a surge of southwesterly flow pushes the Trough northward over Abu Hamed and Atbara and triggers widespread duststorms immediately south of its surface position. This is the dominant synoptic situation that lowers visibilities below a mile in the northern Sudan.

WINDS. Surface winds assume winter's pattern as the Saharan High builds (Figure 6-21). The receding Monsoon Trough causes Atbarah's wind shift from southwesterly during the summer to northerly. The northeasterlies at Faya Largeau are enhanced by channeling through nearby canyons, which raises mean wind speeds to 15 knots in the fall. Luxor's light northwesterly winds are caused by the steep cliffs surrounding the Nile Valley. Surface winds tend to funnel along the valley floor.

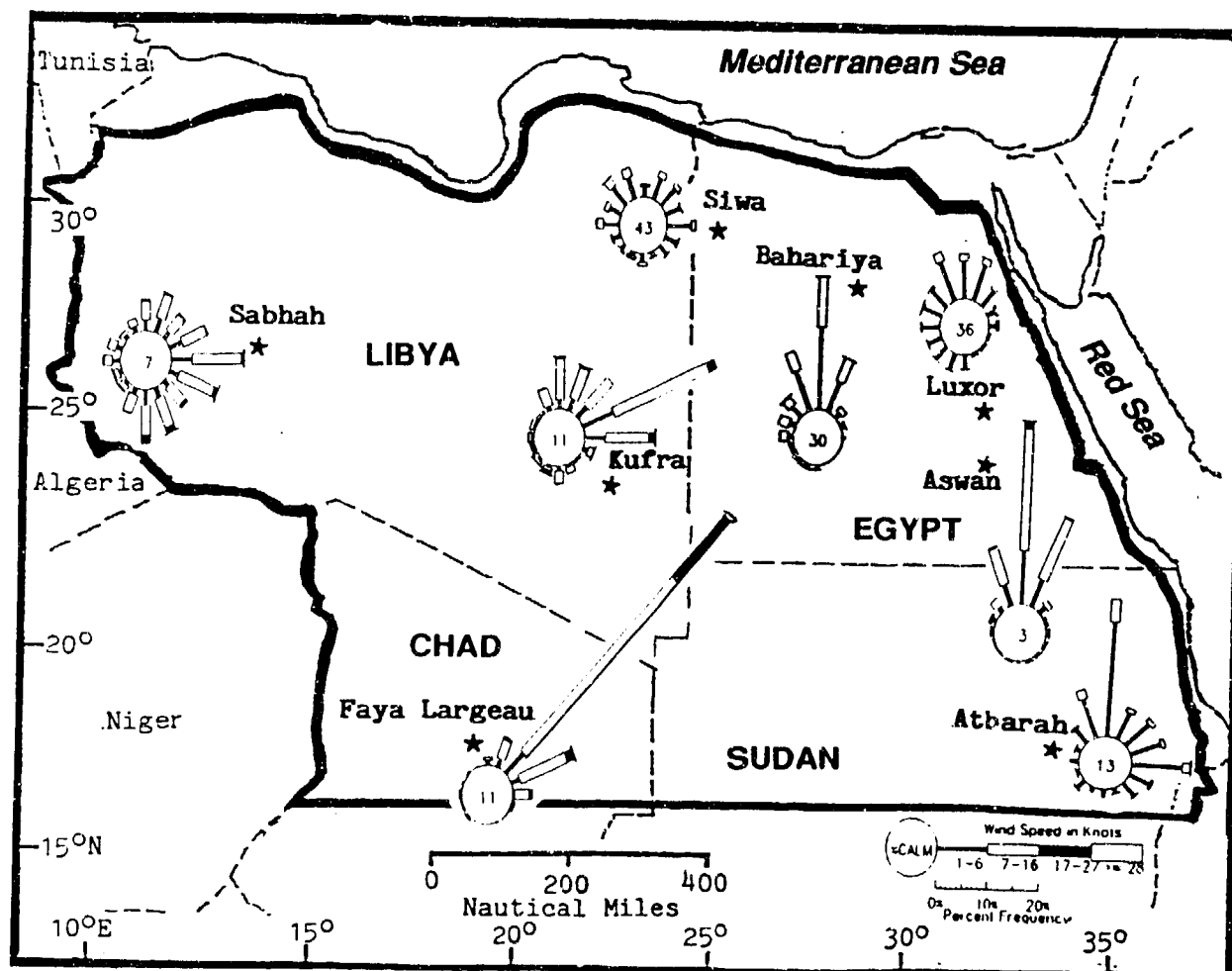


Figure 6-21. October Surface Wind Roses, Eastern Sahara.

PRECIPITATION. Precipitation is concentrated in the north, where late fall fronts produce precipitation, and in the south, where the receding Monsoon Trough produces rainfall south of 21° N in September. Rainfall is erratic over the entire area. Maximum 24-hour

precipitation greatly exceeds mean precipitation for the entire month at most stations. Monsoonal thunderstorms were responsible for the 24-hour rainfall of more than an inch at Atbarah in September. Asyut's 0.8-inch maximum rainfall was from frontal activity.

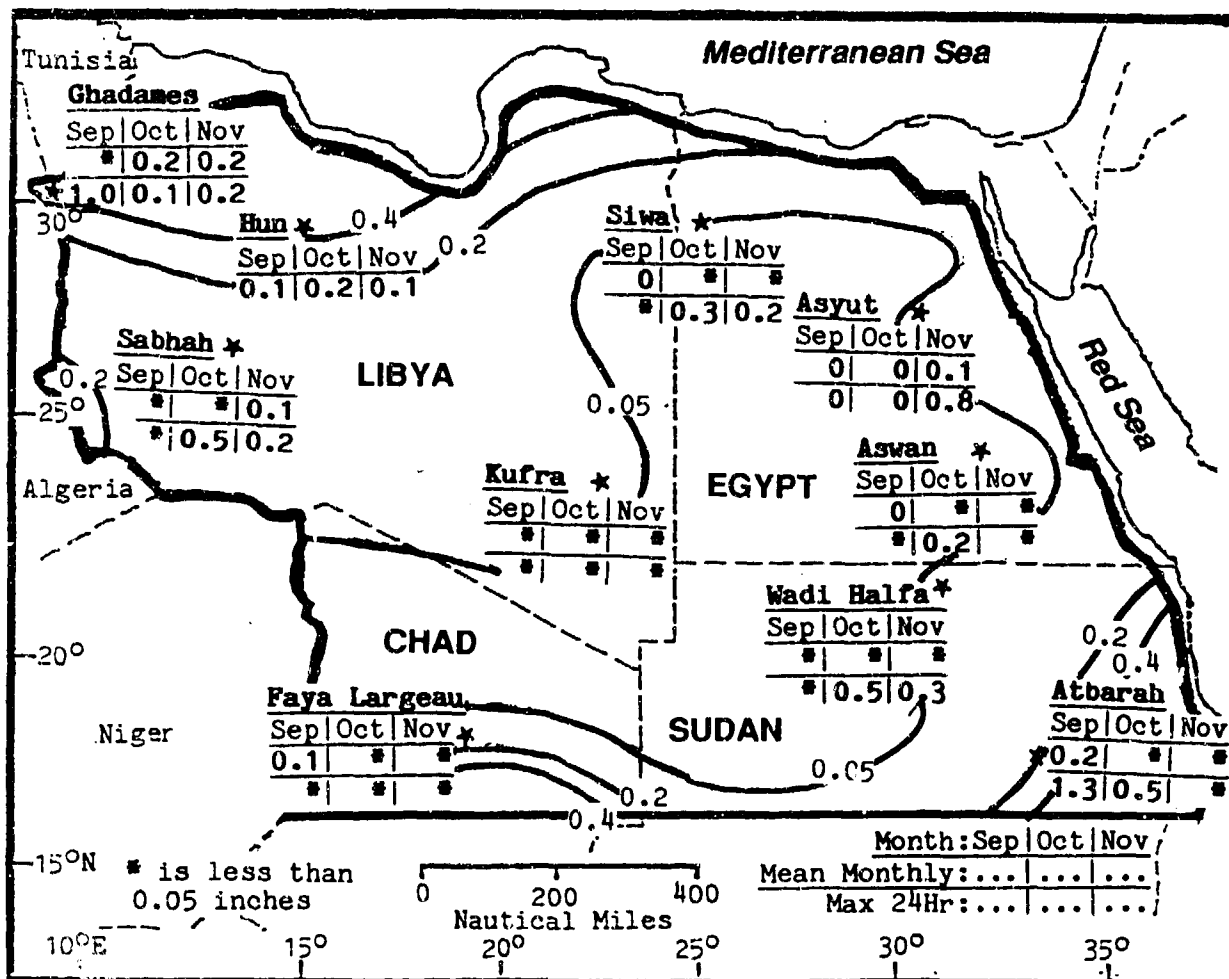


Figure 6-22. Mean Fall Monthly/Maximum 24-hour Precipitation, Eastern Sahara. Isohyets represent mean seasonal rainfall totals.

TEMPERATURE. Mean daily highs decrease by more than 15° F (6° C) through the fall, but they increase between August and September in the south as the Monsoon Trough recedes and the cloud cover decreases.

Record temperatures range from 108° F (42° C) at Kufra to 122° F (50° C) at Ghadames. Late fall polar surges produced record lows of 27° F (-3° C) at Siwa and 54° F (12° C) at Abu Hamed.

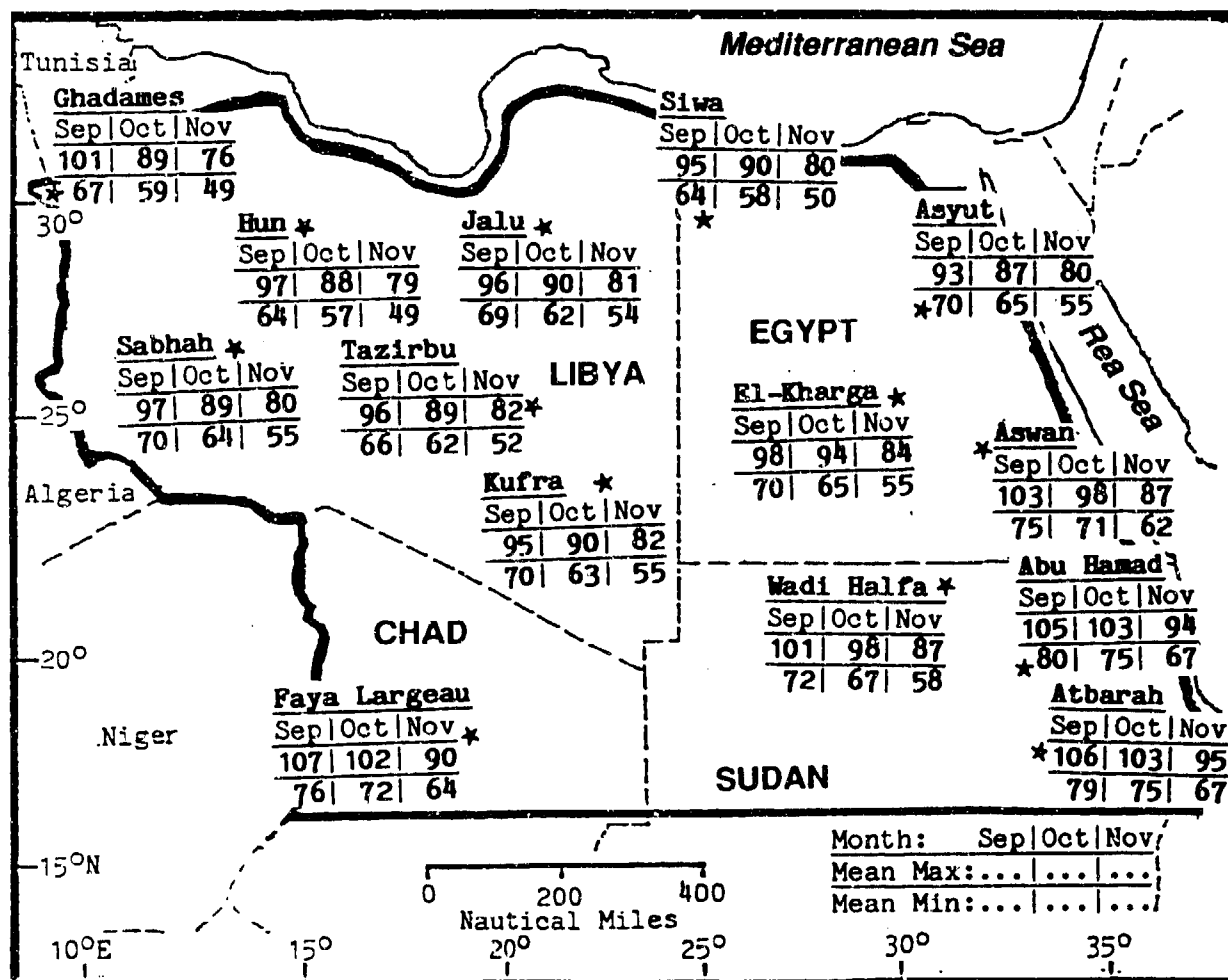


Figure 6-23. Mean Fall Daily Maximum/Minimum Temperatures (F), Eastern Sahara.

Chapter 7

SOUTHERN CHAD AND SUDAN

This region includes those parts of Chad, Sudan, and western Ethiopia that are south of the Sahara. After describing the area's situation and relief, this chapter discusses "general weather conditions" by season.

	Page
Situation and Relief	7-2
Dry Season--November-February	7-4
General Weather	7-4
Sky Cover	7-4
Visibility	7-5
Winds	7-5
Precipitation	7-8
Temperature	7-10
Dry-to-Wet Transition--March-May	7-11
General Weather	7-11
Sky Cover	7-11
Visibility	7-12
Winds	7-13
Precipitation	7-13
Temperature	7-15
Wet Season--June-September	7-16
General Weather	7-16
Sky Cover	7-16
Visibility	7-17
Winds	7-18
Precipitation	7-18
Temperature	7-20
Wet-to-Dry Transition--October	7-21
General Weather	7-21
Sky Cover	7-21
Visibility	7-22
Winds	7-22
Precipitation	7-23
Temperature	7-24

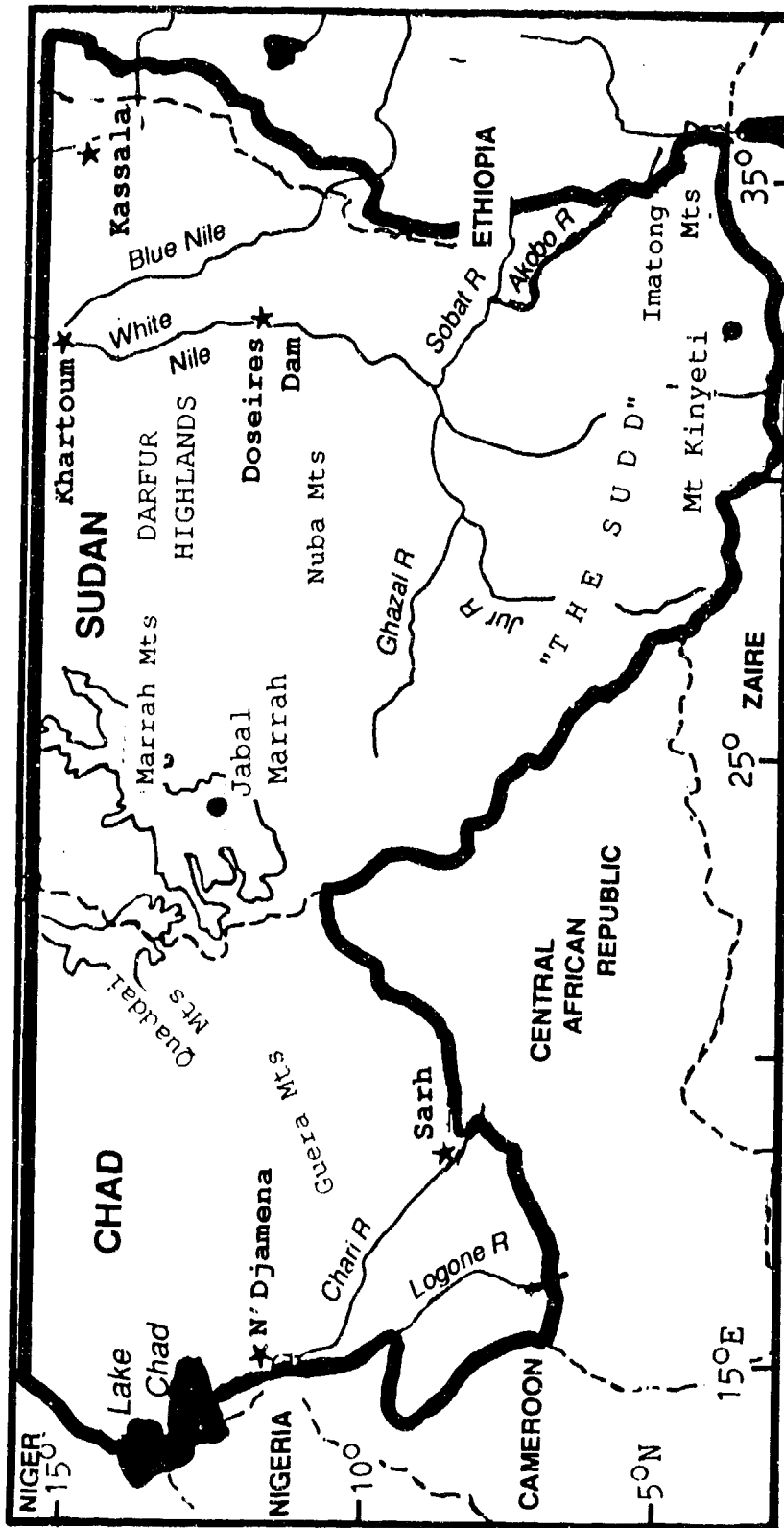


Figure 7-1a. Southern Chad and Sudan. This region includes all of Chad and Sudan south of 16° N and a small part of Ethiopia. The eastern border is formed by the western foothills of the Ethiopian Highlands. The shaded areas are above 3,280 feet (1,000 meters). The western border reaches the eastern shores of Lake Chad. A very poor observing network in Chad and Sudan limits the number of adequate data summaries to two stations, both in the northeastern corner--see Figure 7-1b.

GEOGRAPHY. The entire region lies above 650 feet (200 meters). It is dominated by plateaus dissected with dry intermittent stream beds or wadis. Isolated mountain ranges rise to heights greater than 10,000 feet (3,050 meters). The Sudd, in southern Sudan, is a seasonal drainage basin that covers 50,000 square NM.

Jabal Marrah is the highest point in the Marrah Mountains at 10,073 feet/3,071 meters. It overlooks west-central Sudan's Darfur Highlands, a rolling plateau that covers 138,150 square NM. The smaller and less extensive Quaddai and Guera mountain ranges run north to south along the Chad/Sudan border west of the Darfur Highlands. Quaddai Range elevations are between 4,200 and 4,900 feet (1,280 and 1,495 meters); in the Guera Range, elevations rise to 5,900 feet (1,800 meters).

The Nuba Mountains lie south of the Darfur Highlands. They contain old weathered hills at heights from 3,000 to 4,000 feet (915 to 1,220 meters). Intermittent streams flow toward the White Nile and create large, silt-covered fans on the desert floor.

The northern Imatong Mountains in extreme southeastern Sudan divide the extensive marshlands of the Sudd. Mount Kinyeti, on the northern edge of the Imatong Mountains, is the region's highest peak (10,456 feet/3,187 meters); it extends from Kenya and Uganda northward into extreme southeastern Sudan. Only 400 square NM of this mountain range (including Mt Kinyeti) lies inside the study area.

DRAINAGE AND RIVER SYSTEMS. The largest drainage system in the region is the Nile. It combines the Blue Nile (source: Lake Tana in the Ethiopian Highlands) and the White Nile (source: Lake Victoria).

The White Nile descends 1,970 feet (600 meters) as it flows northward to the Sudd. It loses over half its discharge to evaporation before reaching the Blue Nile at Khartoum. The Sudd floods annually when wet season rains raise the White Nile several feet above flood stage. Major tributaries of the White Nile include the Ghazal, Sobat, Jur, and Akobo.

As the Blue Nile flows northwestward from the Ethiopian Highlands toward Khartoum, it cuts steep gorges into the lower foothills of the Ethiopian Highlands. There is a large dam at Roseires, Sudan. The river's length from Roseires to Khartoum is about 400 NM. South of Khartoum, there is an extensive canal system that links the Blue and White Nile. It provides

navigation and irrigation throughout the adjacent countryside.

The Chari River and its main tributary, the Logone, are Chad's major waterways. The Chari flows northwest and north 500 NM from Sarh (Fort Archambault) to N'Djamena; it forms the border with Cameroon as it enters the southern part of Lake Chad. At times of high water, two channels branch off the main stream, one rejoining the Chari downstream, the other emptying into the large swamplands near Lake Fitri (13° N, 17° E). The Logone River flows 240 NM northwestward in Chad before meeting the Chari at N'Djamena (Ft Lamy). Both rivers are navigable for small steamers north of 11° N during the wet season.

LAKES AND RESERVOIRS. Lake Chad is the fourth largest water body on the African continent. Its surface area varies seasonally from 3,800 to 9,950 square NM. The variations are the result of seasonal rainfall and discharge from the Logone and Chari Rivers. Lake Chad, a fresh-water source, is 787 feet (240 meters) above sea level at its lowest point.

The Bodele Depression (about 9,000 square NM) lies to the northeast of Lake Chad. Its basin averages 820 feet (250 meters) above sea level and occasionally fills from the flooded Chari River. Its southern edge lies within the study area.

VEGETATION. Well-developed woodland and wooded grassland (savannah) grow in areas with greater than 20 inches (500 mm) of rainfall a year in the south. Small areas of tropical rain forest flourish along the Cameroon and Zaire borders.

Between 12° and 14° N, there is a transition from tropical savannah to semidesert steppe. In the very dry extreme north, scattered scrub vegetation grows; this area marks the southern limits of the Sahara. The semidesert steppe contains thorn trees. Large shrubs with only scattered trees are the dominant forms of vegetation above 3,000 feet (915 meters).

Extensive marsh vegetation grows in low-lying areas such as the Sudd, as well as in the areas around most rivers and lakes. Most of these areas become savannah--open, treeless grassland--during the dry season. By the end of the dry season, most grass appears to be dead. The area along the White Nile between 5° and 10° N is permanent swampland.

STATION: KHARTOUM SUDAN														
LAT/LON: 15 36 N					32 33 E					ELEV: 1247 FT				
ELEMENTS	JAN	FEB	MAR	APR	MAY	JUN	JUL	AUG	SEP	OCT	NOV	DEC	ANN	
XTEN MAX	104	111	113	117	117	118	117	110	114	113	108	104	118	
AVG MAX	90	93	100	108	107	107	101	98	101	104	97	92	99	
AVG MIN	60	62	68	72	78	79	75	78	77	78	69	62	71	
XTEN MIN	41	44	49	53	61	67	65	64	61	62	54	43	41	
AVG PRCP	*	*	*	*	0.2	0.3	2.0	2.9	1.1	0.2	*	*	6.7	
MAX MON	*	*	0.6	0.9	0.8	2.3	6.2	6.9	3.8	1.0	0.1	*	11.1	
MAX DAY	*	*	0.6	1.0	0.8	1.4	3.4	3.2	2.0	1.0	0.1	*	4.2	
TS DAYS	0	0	0	0	3	1	5	8	3	2	*	0	20	
DUST DAYS	2	4	6	6	5	7	2	1	1	1	1	2	38	
APP TEMP	87	90	97	102	110	105	102	105	107	104	97	90		

* = LESS THAN 0.05 INCHES OR LESS THAN 0.5 DAYS

STATION: KASSALA SUDAN														
LAT/LON: 15 28 N					36 24 E					ELEV: 1644 FT				
ELEMENTS	JAN	FEB	MAR	APR	MAY	JUN	JUL	AUG	SEP	OCT	NOV	DEC	ANN	
XTEN MAX	107	111	114	114	118	117	108	104	109	110	109	106	117	
AVG MAX	94	97	102	108	107	104	96	93	97	102	100	95	99	
AVG MIN	61	61	67	73	77	77	73	72	73	74	70	64	70	
XTEN MIN	41	43	48	53	52	61	59	59	59	62	51	45	41	
AVG PRCP	*	*	*	0.2	0.5	1.1	3.9	4.9	2.4	0.3	*	*	13.4	
MAX MON	*	0.4	0.5	1.5	2.5	4.1	10.8	9.3	6.3	2.0	0.8	*	19.2	
MAX DAY	*	0.3	0.5	0.8	1.5	2.2	3.2	4.0	3.8	1.0	0.8	*	4.0	
TS DAYS	0	*	*	1	3	3	8	8	8	2	0	0	31	
DUST DAYS	1	1	2	1	2	5	1	*	*	*	*	1	11	
APP TEMP	90	90	98	100	100	103	97	95	93	105	100	95		

* = LESS THAN 0.05 INCHES OR LESS THAN 0.5 DAYS

Figure 7-1b. Climatological Summaries for Two Stations in Southern Chad and Sudan.

GENERAL WEATHER. The dry season is dominated by northeasterly surface flow from the Saharan High and upper-level westerlies. Conditions are stable except in the extreme south where shallow equatorial moisture produces isolated showers associated with a brief Monsoon Trough surge to 5° N in early November and late February. Diurnal showers are widely scattered.

SKY COVER. Dry season cloudiness is lowest of the year. The mean cloud cover pattern (Figure 7-2) shows a distinct north-to-south distribution, with 20% in the north and 60% in the south. The increase to the south is caused by equatorial moisture advection and diurnal convection. Continental tropical (cT) air dominates most of the area, except for a small area near Juba in November and late February when maritime tropical (mT) air dominates. The cT air originates in the Sahara and is dry below 10,000 feet (3,050 meters) MSL. As a result, significant cloud cover is rare during the dry season, but altocumulus and cirrus accompany intense cold fronts; cumulus, cumulonimbus, and altocumulus castellanus occasionally accompany a rare November Atlas Low.

Cirrus is reported at or above 20,000 feet (6 km) MSL but is only about 400 feet (120 meters) thick. Cirrus "blow-off" with frontal thunderstorms may be thicker (1,000 to 2,000 feet/305 to 610 meters) with bases from

40,000 to 50,000 feet (12 to 15 km) MSL. Altocumulus bases range from 10,000 to 18,000 feet (3,050 to 5,485 meters) MSL and 1,000 to 2,000 feet (305 to 610 meters) in thickness. Altocumulus castellanus bases range from 8,000 to 15,000 feet (2,440 to 4,570 meters) MSL, with tops to 40,000 feet (12 km) MSL; virga may fall from these clouds. Fair-weather cumulus may develop with intense afternoon heating in northern Sudan; bases are between 4,000 and 8,000 feet (1,220 and 2,440 meters); average thickness is 2,000 feet (610 meters).

During November and late February, southern Sudan's exposure to mT air generates increased diurnal cloud cover in the form of afternoon fair-weather cumulus with bases from 4,000 to 8,000 feet (1,220 to 2,440 meters). Altocumulus and cirrus form in cross-equatorial, southern hemispheric flow with bases that range from 12,000 to 20,000 feet (3,660 to 6,100 meters) MSL.

Ceilings below 3,000 feet (915 meters) are very rare during the dry season, as shown in Figure 7-2; however, dust obscures skies before and after cold front passage in northern sections. Such rare dust-generated low ceilings are usually reported at 100 to 800 feet (30 to 245 meters). Afternoon cumulus ceilings at 1,500 to 2,500 feet (455 to 760 meters) have been reported in southern Sudan and Chad, but rarely.

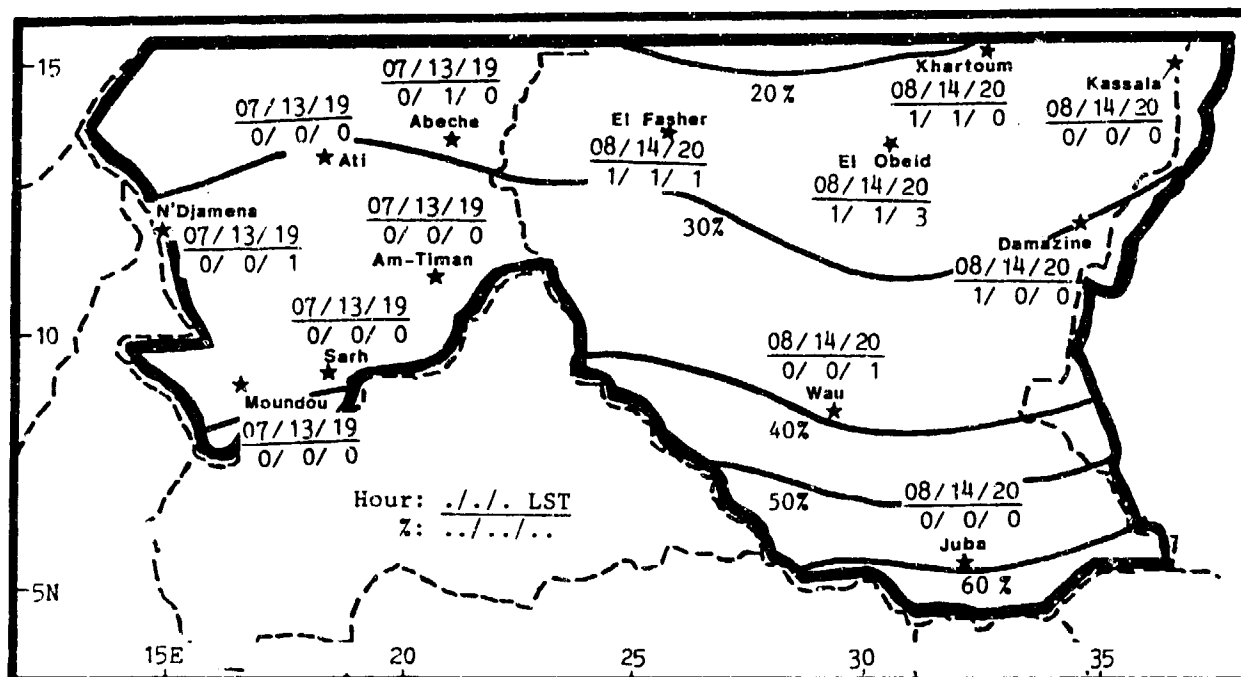


Figure 7-2. Mean Dry Season Cloudiness (isopleths) and Frequencies of Ceilings Below 3,000 Feet (915 meters), Southern Chad and Sudan.

VISIBILITY. The primary dry season visibility restrictions are blowing dust and dust haze. Dry soil conditions near Khartoum, N'Djamena, and Moundou provide noticeable low visibility frequency distributions in the region (Figure 7-3). All these stations are in river valleys and dry lake beds with plenty of fine silt. Rocky or moist areas like Am Timan's rocky highland and Wau's swampland/savannah see very few low visibilities.

Fog, moisture haze, and precipitation only occur south of 10° N, but they rarely lower visibility. Frequency of visibilities below 3 miles varies from 37% at N'Djamena just after sunrise to 0% in the afternoon at Juba and Wau.

Dominant cT air carries Sahara dust and sand into the region. Dust haze reduces visibilities to 3-6 miles on an average of 8 to 18 days a dry season. Polar surges behind intense cold fronts reinforce the Saharan High and tighten the surface pressure gradient between the front and the Monsoon Trough. Strong northeasterlies produce Harmattan conditions (which see); these affect Chad and western Sudan for periods of 1 to 4 days.

Khartoum and El Obeid have duststorm activity with strong northwesterly winds behind active cold fronts. Deep upper-level troughs bring significant polar air advection southward into central Sudan, while turbulent mixing at the surface lowers visibilities to 1 mile for short periods.

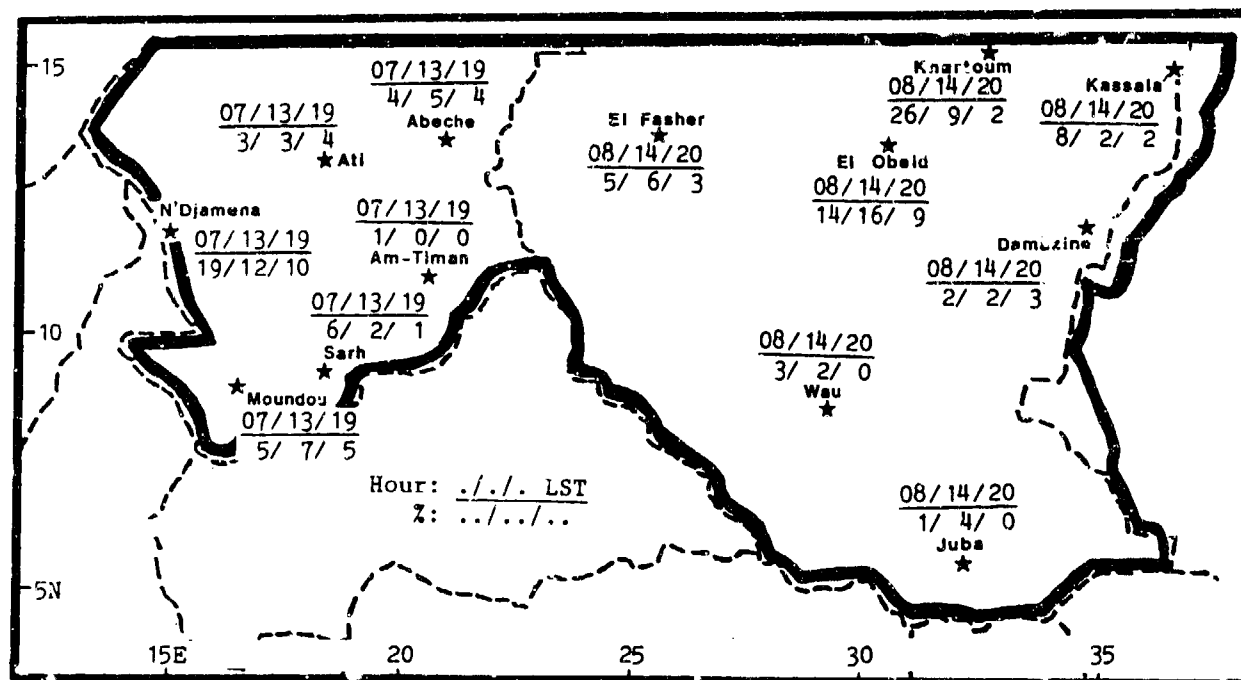


Figure 7-3. Mean Dry Season Frequencies of Visibilities Below 3 Miles, Southern Chad and Sudan.

WINDS. Under the Saharan High's influence, winds are northerly to northeasterly. In Sudan, strong subsidence from the Subtropical Ridge combines with blockage from the Ethiopian Highlands to provide the constant northerly winds shown in Figure 7-4.

Aloft, winds back to westerly under the Subtropical Ridge's influence in the north, but easterly flow persists in the south--see Figures 7-5a-c. This flow allows an intense upper-level disturbance to occasionally affect Sudan.

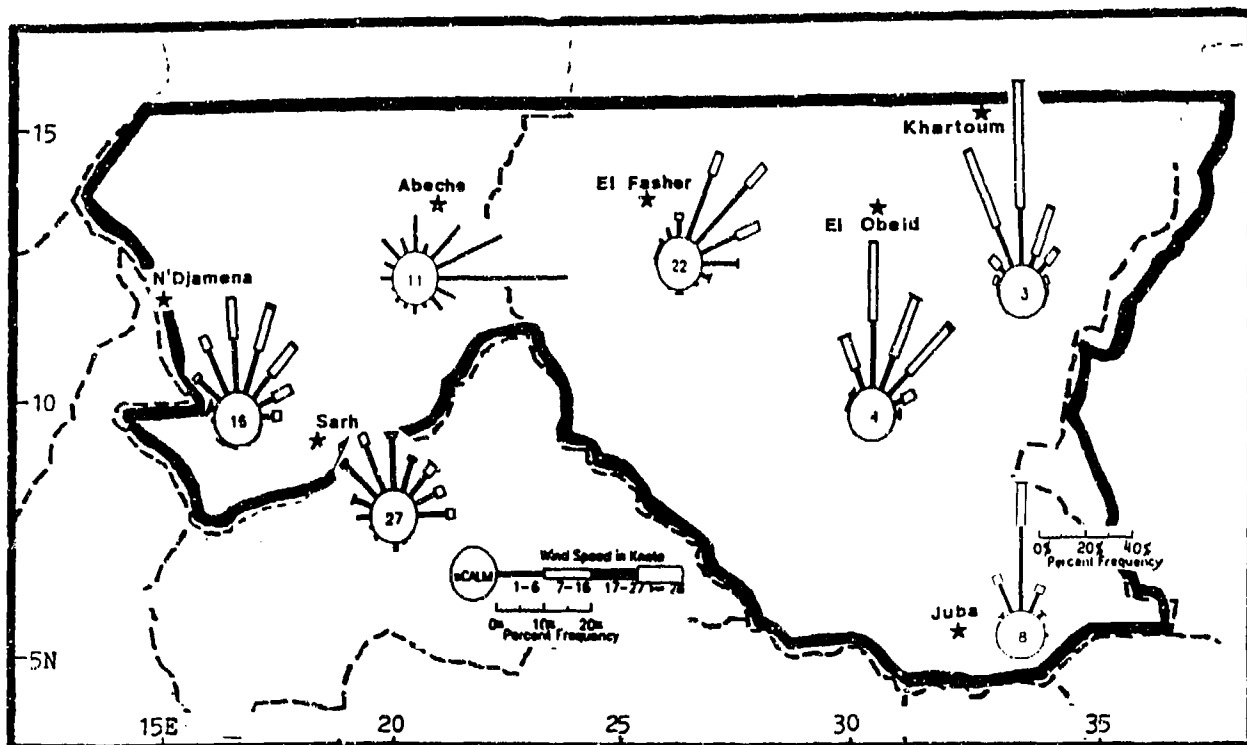


Figure 7-4. January Surface Wind Roses, Southern Chad and Sudan. Note the separate "percent frequency" scale used for Juba.

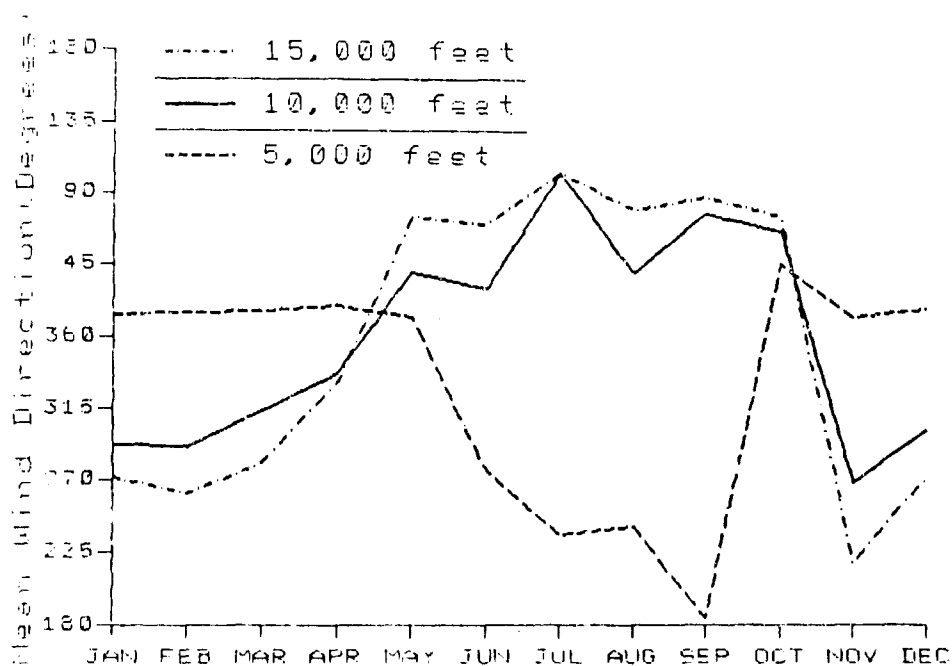


Figure 7-5a. Upper-level Annual Mean Wind Direction, Khartoum, Sudan. Note that the wind direction axis has been shifted to start at 180 degrees.

SOUTHERN CHAD AND SUDAN
DRY SEASON

November-February

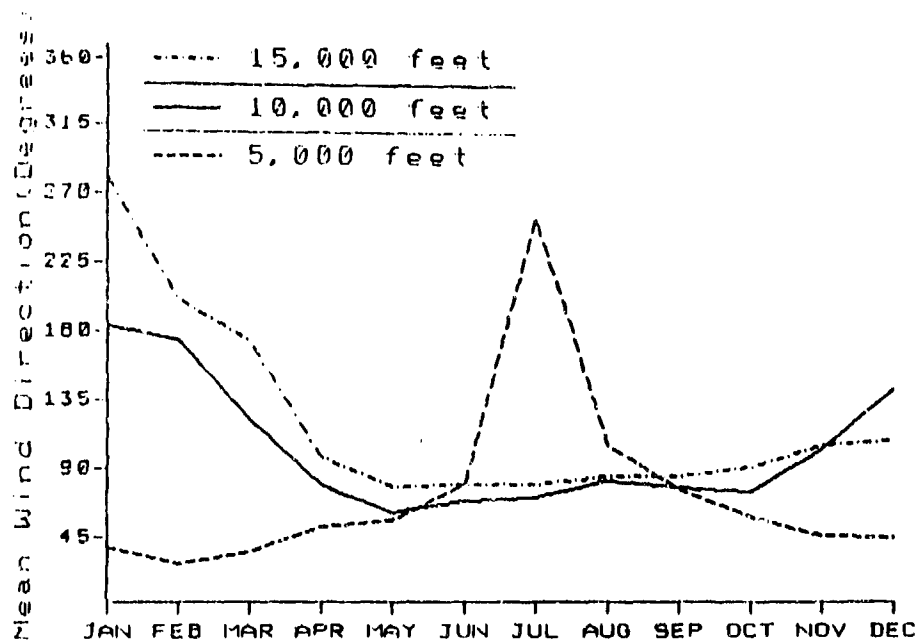


Figure 7-5b. Upper-level Annual Mean Wind Direction, N'Djamena, Chad.

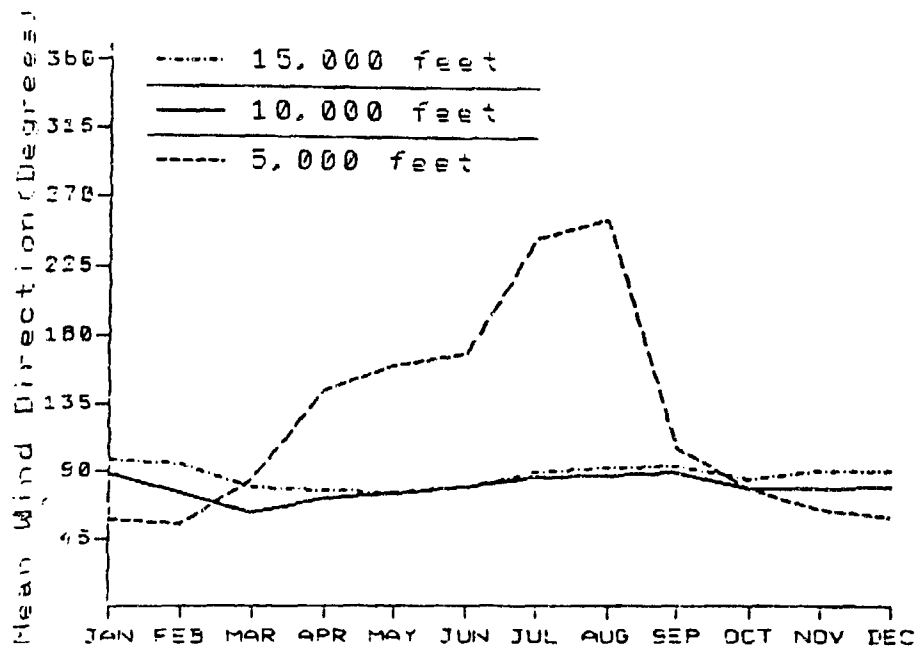


Figure 7-5c. Upper-level Annual Mean Wind Direction, Sarh, Chad.

Wind direction at 30,000 feet (9 km) (Figure 7-6) is dominated by the Subtropical Ridge. Westerly flow is variable from west-southwest to west-northwest in any given month; it persists throughout the dry season north of the Subtropical Ridge. November upper-level easterlies are found in the extreme south; they provide a

good outflow mechanism for isolated convection south of 5° N where low-level moisture remains abundant. Wind speeds at 30,000 feet (9 km) range from 20 to 38 knots, but speeds are higher at El Obeid and Khartoum because of their proximity to the Subtropical Jet Stream.

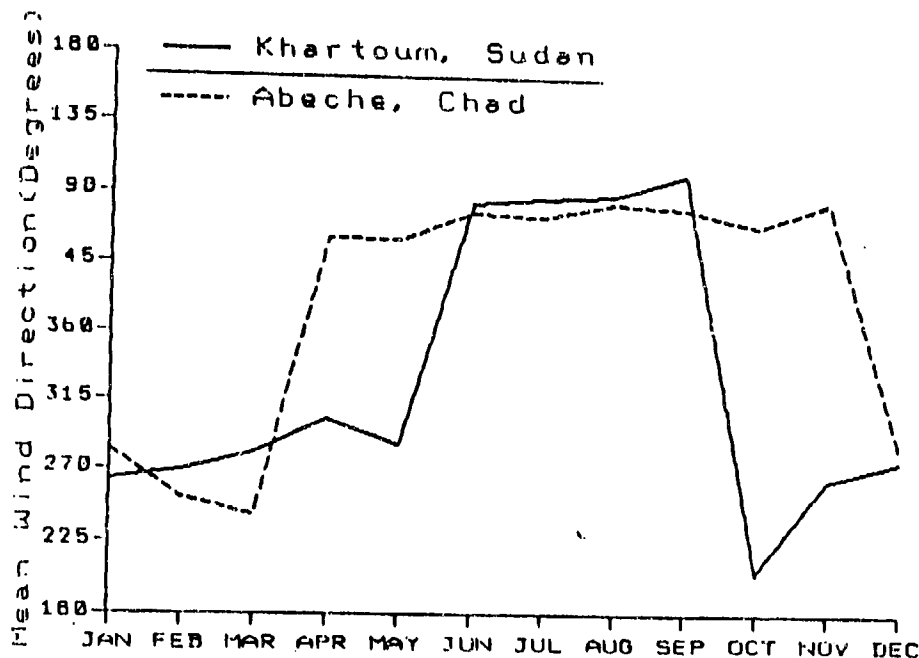


Figure 7-6. Mean Annual 30,000-foot (9 km) Wind Direction, Southern Chad and Sudan. Note that the wind direction axis has been shifted to start at 180 degrees.

PRECIPITATION. Dry season precipitation is rare except for brief surges of equatorial moisture in November, early December, or February. As shown in Figure 7-7, mean precipitation averages less than 1 inch (25 mm) in the dry season except at Juba, which gets 1.4 inches/35 mm in November.

Maximum 24-hour rainfall occurs with intense polar fronts north of 12° N and with isolated convection in the south, where the Monsoon Trough generates isolated

thunderstorms--see Figure 7-8. Thunderstorms tops are above 40,000 feet (12 km) MSL.

Upper-level polar troughs in the Mediterranean Sea area are too dry and weak to penetrate southern Chad and Sudan. Precipitation is rarely recorded north of 7° N in Chad. Light snow is possible on the highest peaks of the Marrah Mountains--polar outbreaks strong enough to produce snow occur once every 50 to 75 years.

SOUTHERN CHAD AND SUDAN
DRY SEASON

November-February

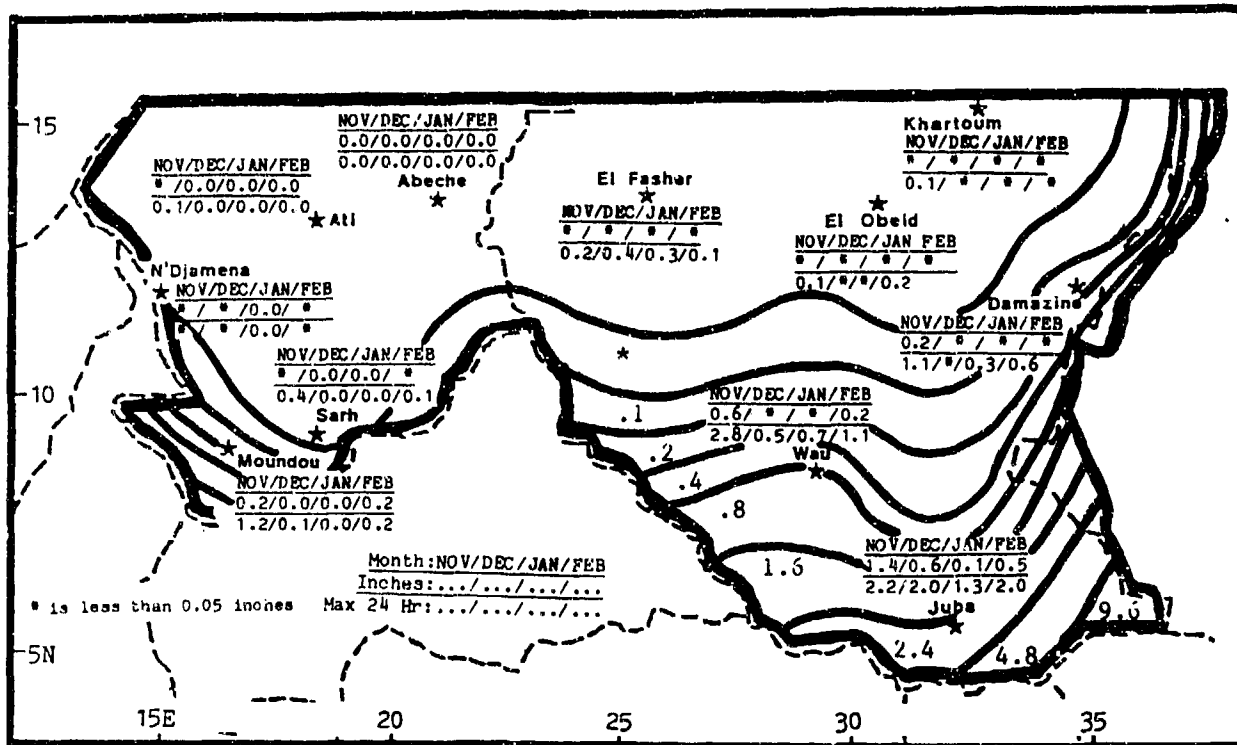


Figure 7-7. Mean Dry Season Monthly/Maximum 24-hour Precipitation, Southern Chad and Sudan. Isohyets represent mean seasonal rainfall totals.

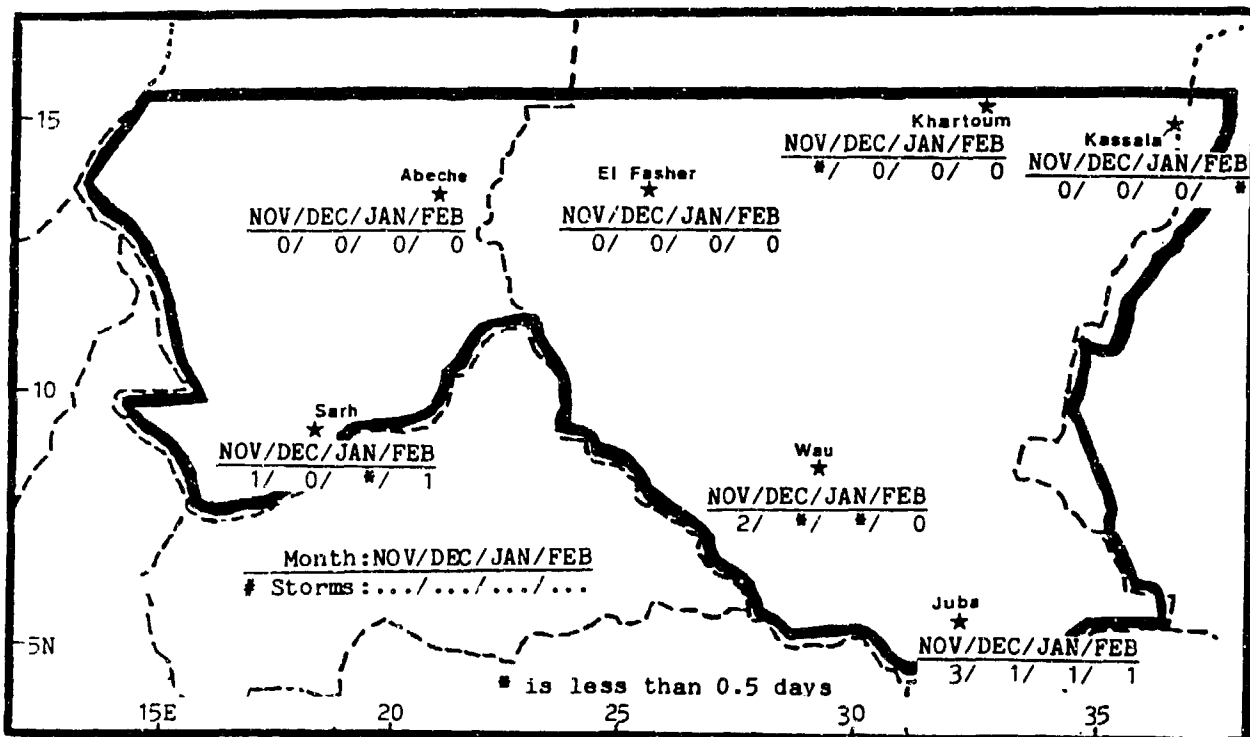


Figure 7-8. Mean Dry Season Thunderstorm Days, Southern Chad and Sudan.

TEMPERATURE. Dry season mean daily highs range from 89° to 104° F (32° to 40° C). Abeche's mean daily highs (Figure 7-9) average 100° F (38° C) or better throughout the dry season. In January, the diurnal temperature range is greater than 40° F (23° C). Record highs include 106° F (41° C) at El Fasher in February

and 113° F (45° C) at Moundou. Mean daily lows range from 50° F (10° C) at El Fasher to 71° F (22° C) at Juba; subfreezing temperatures have been observed at El Obeid and in the Marrah Mountains. Record lows include 31° F (-1° C) at El Obeid and 50° F (10° C) at Sarh. Most stations never report less than 40° F (4° C).

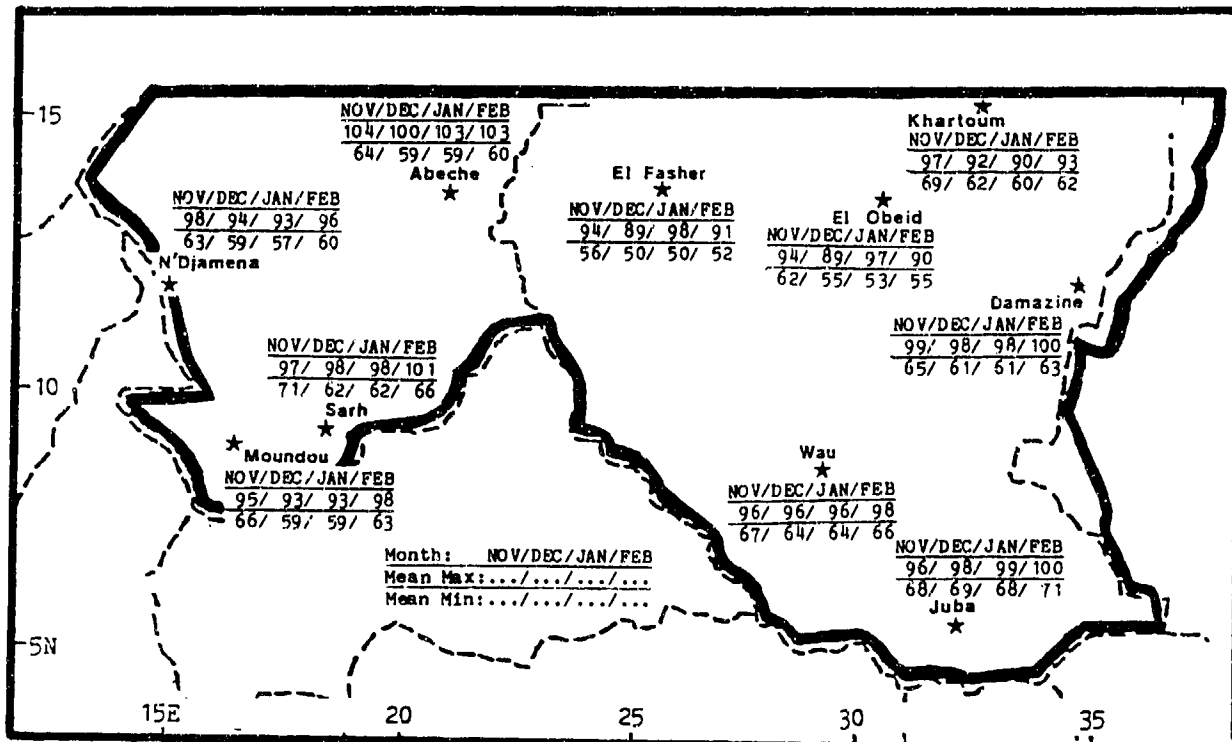


Figure 7-9. Mean Dry Season Daily Maximum/Minimum Temperatures (F), Southern Chad and Sudan.

GENERAL WEATHER. Variable weather during the transition is caused by the Monsoon Trough's slow 3-month migration northward across the region. The Trough moves fastest in extreme eastern Sudan and western Ethiopia because of topography. During the transition, the Trough oscillates northward every 3 to 5 days, then retreats southward for 20 to 50 NM for about a day before another northward surge. The return of the wet season follows Trough passage by 2-4 weeks. Precipitation, cloudiness, and surface wind shifts affect the entire region by late-May. Wet conditions are established at Wau, Juba, and Moundou in March, and at Khartoum, El Fasher, and El Obeid in May. Wetter conditions develop after southerly winds are established for 4 to 6 days in succession.

Another important transition feature is the Subtropical Ridge. Early in the transition, easterly flow aloft is established in the extreme south, where there is good outflow for sustained convection. Westerly flow aloft persists north of the Subtropical Ridge. By late May, easterly flow at the mid- and upper-levels establishes deep convection through most of the region.

SKY COVER. The Monsoon Trough's northward migration increases mean cloudiness south of the

Trough's axis, which separates continental tropical (cT) air from maritime tropical (mT) air. North of the trough, cloud cover patterns are similar to dry season conditions--see Figure 7-10. At Juba, Wau, and Sarh, moist southerly mT air surges northward to 14° N by late May to result in still more cloudiness.

All cloud types are found in the mT air mass. Cirrus develops as outflow "blow-off" from cumulonimbus or within upper-level easterly flow south of the Subtropical Ridge. By late May, altocumulus reappears near the Mid-Tropospheric Easterly Jet (MTEJ) and 100 to 200 NM south of the surface Monsoon Trough. Afternoon heating produces fair-weather cumulus south of the Monsoon Trough; this can grow into towering cumulus and cumulonimbus if enough moisture reaches 700 mb.

Cirrus is reported at or above 20,000 feet (6 km) MSL, but thunderstorm blow-off reaches 40,000 to 60,000 feet (12 to 18 km) MSL and is 1,000 to 1,700 feet (305 to 520 meters) thick. Altocumulus bases are from 10,000 to 18,000 feet (3,050 to 5,485 meters), with tops to 20,000 feet (6 km) MSL north of the surface Monsoon Trough. Altocumulus in mT air forms from 15,000 to 25,000 feet (4,570 to 7,620 meters), with tops to 27,000 feet (8,230 meters) MSL.

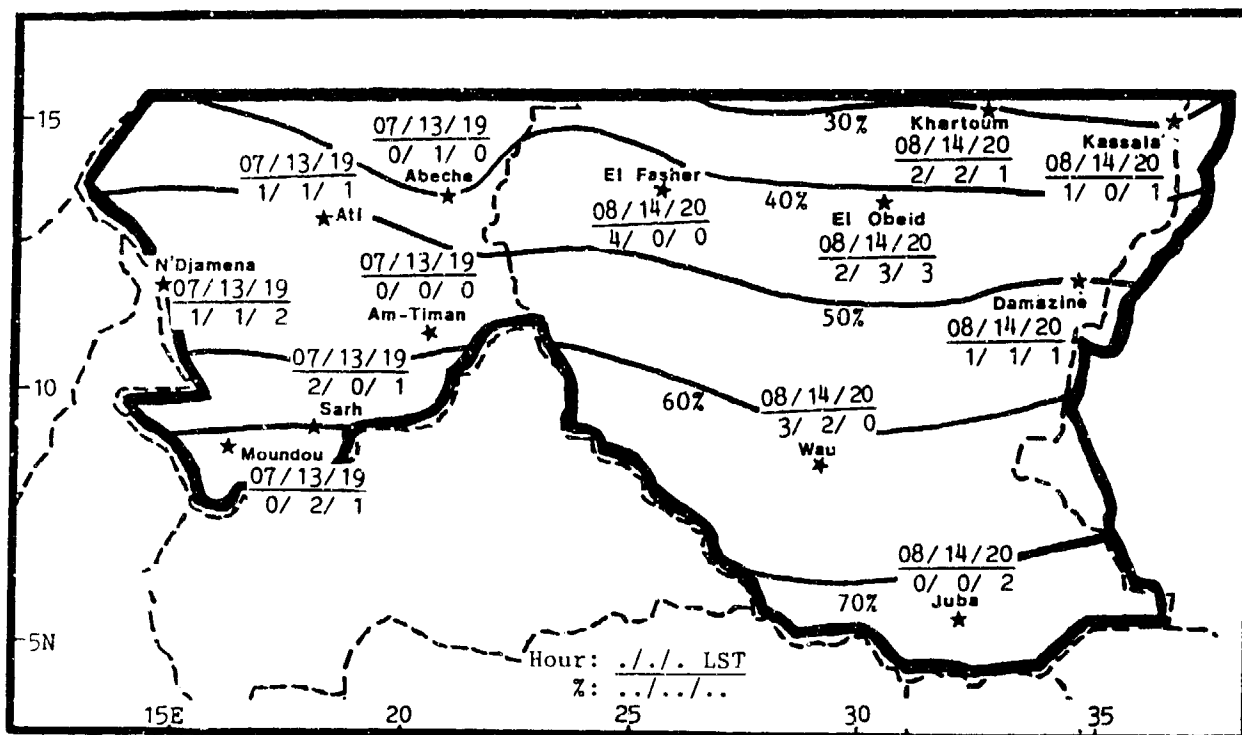


Figure 7-10. Mean Dry-to-Wet Transition Cloudiness (Isopleths) and Frequencies of Ceilings Below 3,000 Feet (915 meters), Southern Chad and Sudan.

Fair-weather cumulus bases range from 4,000 to 8,000 feet (1,220 to 2,440 meters) in mT air and are generally 2,000 feet (610 meters) thick. Cumulonimbus with tops to 60,000 feet (18 km) and towering cumulus with tops at 30,000 feet (9 km) can form with deep low-level moisture support. Heavy thunderstorm clouds may have bases at 500 feet (150 meters).

Ceilings below 3,000 feet (915 meters) can occur along the Monsoon Trough, but rarely. Blowing dust produces obscurations along the Trough axis with ceilings from 200 to 1,000 feet (60 to 305 meters).

Afternoon cumulus with bases from 1,500 to 2,500 feet (450 to 750 meters) forms between Moundou and Juba. By late May, these clouds may occur throughout the region as the surface Monsoon Trough's mean position shifts north of 16° N. Heavy late-season rainfall can produce moisture haze and thin fog in the dense jungles of southern Sudan and Chad. The areas south of Sarh and Wau have cumulus ceilings 15-25% of the time, usually between 5,000 and 7,000 feet (1,525 and 2,135 meters).

VISIBILITY is a function of Monsoon Trough position. Sudden surges often increase surface flow to 10 knots or greater for 3 to 9 hours; gusts can carry dust and sand along the Trough axis and reduce visibility to less than 3 miles.

Polar surges behind Atlas Low cold fronts reinforce northerly flow across the Sahara and often form dense dust haze that reduces visibility to 3-6 miles. Polar surges increase the surface pressure gradient north of the Monsoon Trough and result in strong northeasterlies that produce Harmattan Haze (which see); local visibilities may be reduced to a mile or less.

Northward surges in the Monsoon Trough can produce blowing dust or sand depending on soil condition and wind speed. Wind speeds greater than 10 knots are common 1 to 3 hours before a northward surge. Ground fog forms after a heavy rain. Visibilities can approach zero in thunderstorm downbursts at Juba and Moundou in March, and at Khartoum or Abeche in late May.

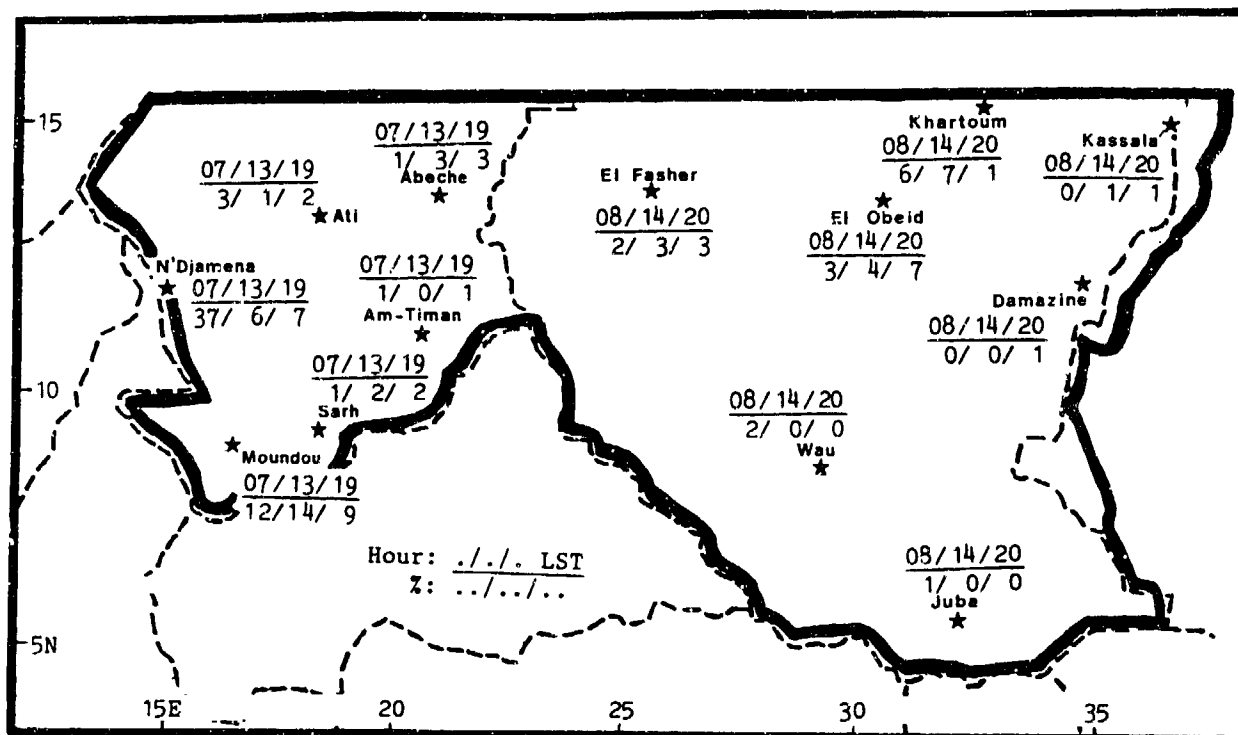


Figure 7-11. Mean Dry-to-Wet Transition Frequencies of Visibilities Below 3 Miles, Southern Chad and Sudan.

Soil condition is also a determinant of visibility. Dense vegetation, such as at Juba, or rocky highlands, like those at Am-Timan, result in low frequencies of visibilities below 3 miles. Precipitation or fog cause nearly all low visibilities south of the Monsoon Trough except for around Khartoum and N'Djamena, where strong winds lift soil easily whenever it is not saturated.

As the Monsoon Trough moves northward, dry soil conditions (and increased chances for duststorms) also move northward. Subsoil moisture and vegetation increase with rainfall south of the Trough. Low-level convective instability causes diurnal variations in visibilities less than 3 miles.

WINDS. Mean surface wind speeds vary from 6 to 12 knots--directions depend on Monsoon Trough position. The high variability of N'Djamena's winds, shown in Figure 7-12, indicates that the Trough fluctuates around this station in April. Early-season southerly surface flow is persistent at southern stations. Strong surface winds (15 knots or greater) frequently occur with mid-latitude frontal passages over the Sahara. Northeasterly flow penetrates southward to N'Djamena, Ati, and El Fasher 24 to 48 hours after the frontal passage.

Winds aloft also reflect the Monsoon Trough's northward progression, as shown in Figures 7-5a-c. Northern stations see dry northerlies at 5,000 feet (1,525 meters) until mid-May.

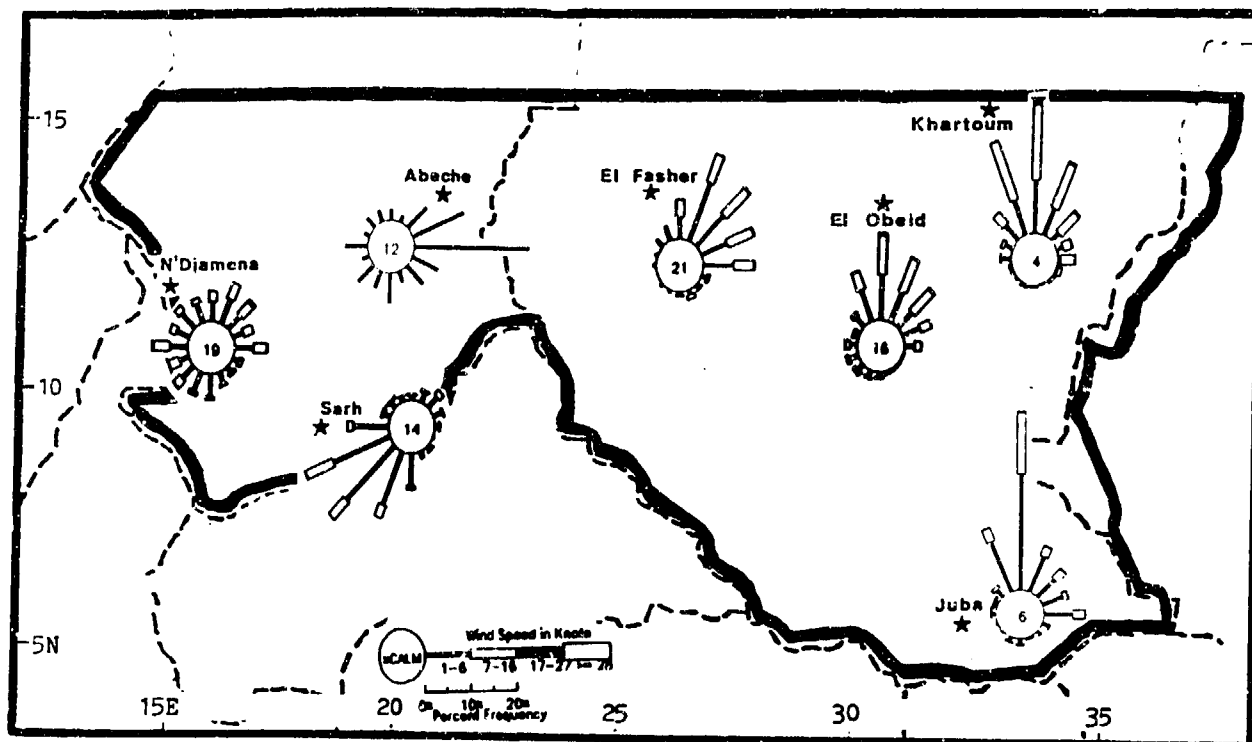
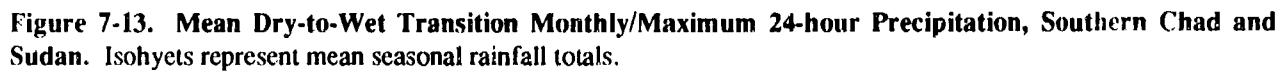


Figure 7-12. April Surface Wind Roses, Southern Chad and Sudan.

PRECIPITATION. Figure 7-13 shows mean monthly precipitation. The rapid increase in rainfall in May shows that deep low-level moisture is established. Heavy convective rainfall does not occur until the surface Trough position is 50 to 250 NM north of the

station. Thunderstorms and squall lines initially develop in April, but squall line activity is not well organized until late May when the MTEJ is established--see Figure 7-14. Tops can exceed 50,000 feet (15 km) MSL by May.

March-May



SOUTHERN CHAD AND SUDAN

DRY-TO-WET TRANSITION

March-May

TEMPERATURE. The mean daily highs shown in Figure 7-15 are similar to wet season temperatures south of 11° N because mean cloud cover distributions are similar. Most southern stations record their warmest temperatures of the year in March and April; mean daily highs increase by 4° to 8° F (2° to 5° C) from those of

the dry season, ranging from 92° to 111° F (33° to 44° C). Record highs include 111° F (44° C) at Juba to 117° F (47° C) at Khartoum and N'Djamena. Mean daily lows range from 58° F (14° C) at El Fasher in March to 78° F (26° C) at Khartoum in May. Record lows are 40° F (4° C) at El Fasher and 60° F (16° C) at Sarh.

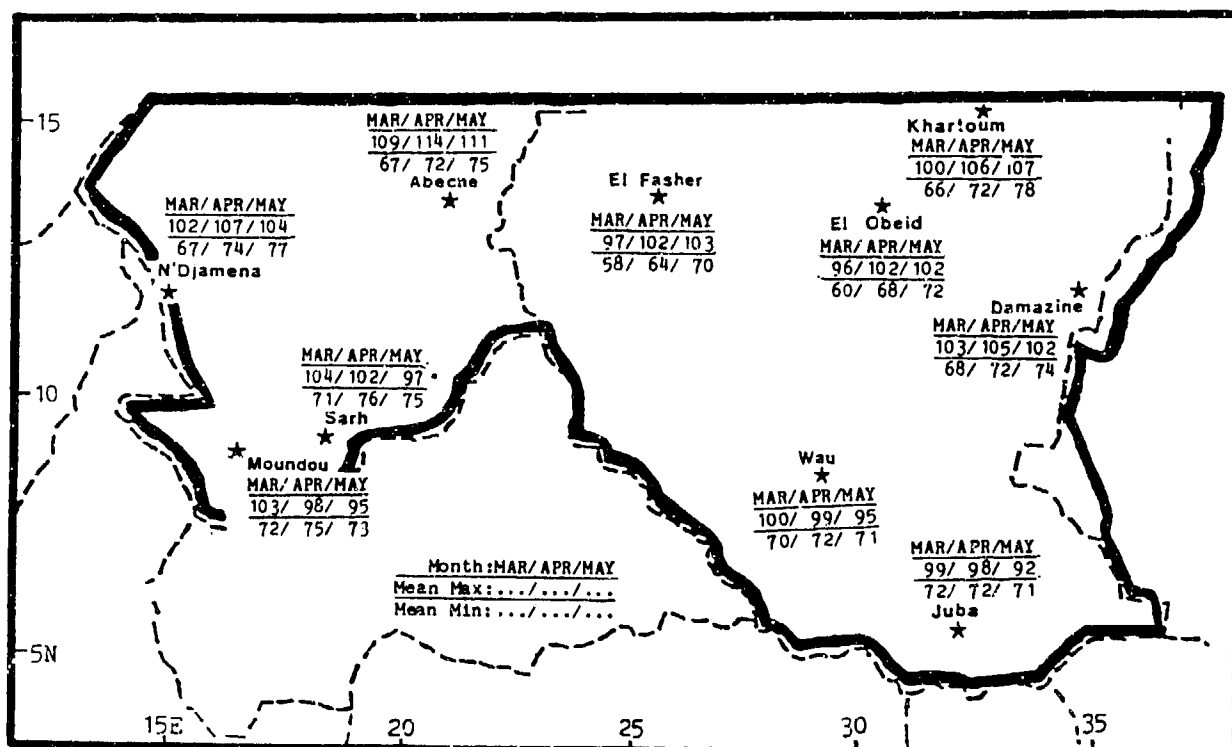


Figure 7-15. Mean Dry-to-Wet Transition Daily Maximum/Minimum Temperatures (F), Southern Chad and Sudan.

GENERAL WEATHER. The Monsoon Trough stays just north of southern Chad and Sudan throughout the wet season, causing scattered showers and thunderstorms. Wet-season weather is dominated by synoptic and mesoscale disturbances caused by mid-level instability (the Mid-Tropospheric Easterly Jet--MTEJ--and African Waves) and the Monsoon Trough. The MTEJ, normally between 13° and 15° N, produces local vorticity maxima through horizontal shearing around 650 mb. Wet-season disturbances include Tropical Squall Lines, Haboobs, and isolated convection near the MTEJ.

Larger scale Easterly Waves propagate westward between 10° and 15° N, frequently spreading cloudiness and precipitation between late June and mid-September.

SKY COVER. The wet season is cloudiest of the year. The highest mean cloud cover percentages are between N'Djamena and Damazine (Figure 7-16). This pattern is caused by the persistence of the MTEJ and the Tropical Easterly Jet at 200 mb. Both jets provide considerable amounts of altocumulus and cirrus.

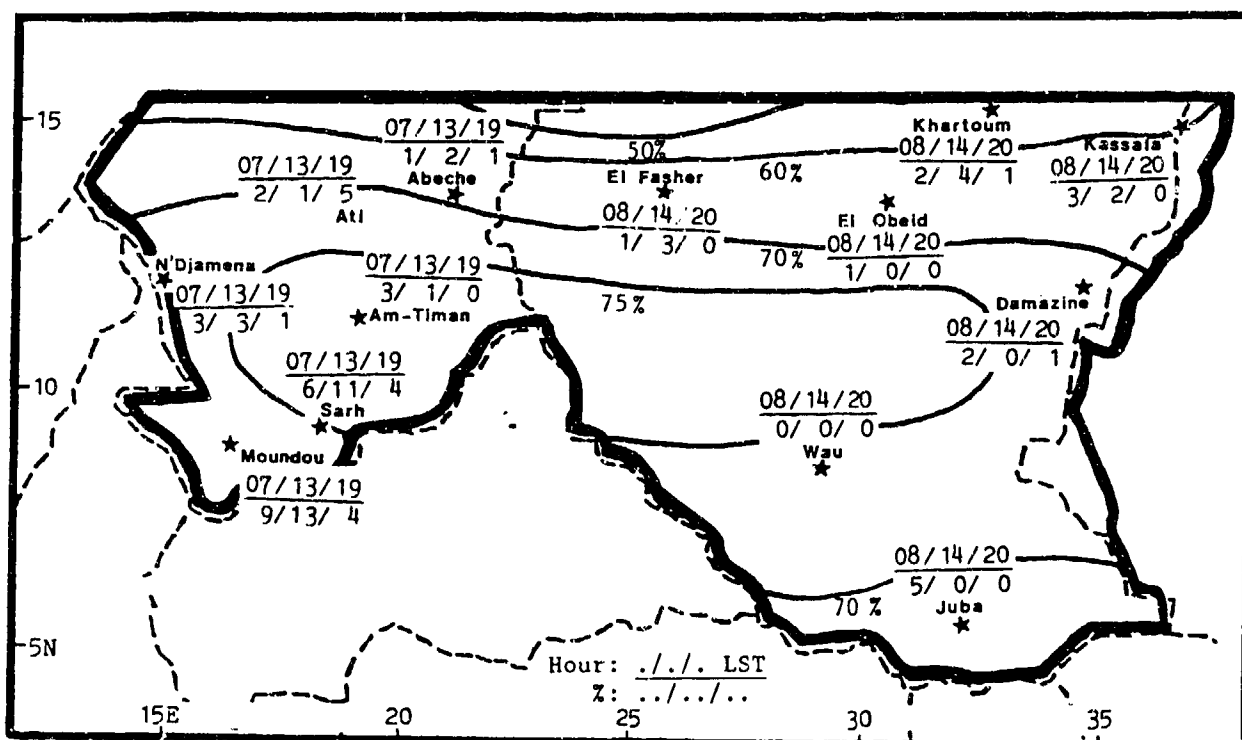


Figure 7-16. Mean Wet Season Cloudiness (Isopleths) and Frequencies of Ceilings Below 3,000 Feet (915 meters), Southern Chad and Sudan.

The mT air south of the surface Monsoon Trough produces convective clouds in the morning. Fair-weather cumulus (about 2,000 feet/610 meters) thick) forms from diurnal instability; bases range from 4,000 to 8,000 feet (1,220 to 2,440 meters). Mid-level disturbances or Easterly Waves trigger greater cumulus development throughout the day, but the MTEJ provides the mid-level divergence necessary for increased cloud development. Heavy convection in a large-scale African Wave, which causes westward-moving squall lines to develop, is common from late June to mid-September between 13° and 15° N and 15° E to 30° E. Cumulonimbus tops reach 60,000 feet (18 km) MSL; towering cumulus reaches only half that. Bases are about the same as fair-weather

cumulus. Altostratus and stratocumulus decks form in the wakes of squall lines with bases between 8,000 and 12,000 feet (2,440 and 3,660 meters) and tops to 20,000 feet (6 km) MSL.

Stratus is rare, but it can form in the early morning after heavy rains; bases are 200-1,000 feet (60-305 meters). Thin fog usually dissipates after sunrise.

Frequency distributions of ceilings below 3,000 feet (915 meters) are 13% or less throughout the region (Figure 7-16). Midday (1300 LST) percentages at Moundou and Sarh reflect abundant low-level moisture. Elsewhere, low ceilings result from isolated cumulus and

SOUTHERN CHAD AND SUDAN

WET SEASON

June-September

morning stratocumulus. Lowest ceilings range from 1,200 to 2,500 feet (365 to 760 meters). Daytime heating can lift morning cloud bases to 8,000 feet (2,440 meters); turbulent surface mixing can dry out the lower layers in all but a few extremely saturated surface conditions. Dust is the primary cause of ceilings below 3,000 feet (915 meters) at El Fasher, Khartoum, and Kassala; however, heavy squall-line showers occasionally result in low ceilings from June to August. Often, dust and sand lifted ahead of a squall line can be observed 30 minutes before it reaches the station. Low ceilings rarely last more than an hour.

VISIBILITY. Considering the high mean cloudiness and abundant moisture, wet season visibilities are generally good. The moist mT air mass, however, does cause some fog, thunderstorms, and damp haze. Duststorms occur at Khartoum, Kassala and El Fasher, but few are observed in July or August during peak squall-line activity. Because the soil is wetter, little dust or sand is raised when speeds are less than 15 knots.

Near-zero visibility is possible during thunderstorms. Light rain, drizzle, and fog can occur with mT air in the stable post-squall environment; visibility can be reduced to less than 3 miles for 6 to 8 hours. Downbursts and strong gust fronts in June squall lines develop walls of dust (known as Haboobs in Sudan) that can lower visibility to zero. Early morning fog and damp haze form after a heavy nocturnal rainshower in the Darfur Highlands, the Sudd, and tropical forests of Southern Chad, but dissipate quickly after sunrise. Bases are 800-1,200 feet (245 to 365 meters); thickness rarely exceeds 200 feet (60 meters).

Frequency of visibilities below 3 miles is less than 4% during any month of the wet season except at Khartoum; there, the frequency can be as high as 11% because Khartoum is located near the confluence of the Blue and White Nile, where there are vast amounts of fine, silty soil and moisture. Squall lines in July and August produce some blowing dust, but visibilities below 3 miles rarely last for more than an hour. Low visibilities at all other stations are attributed to heavy rain and blowing dust.

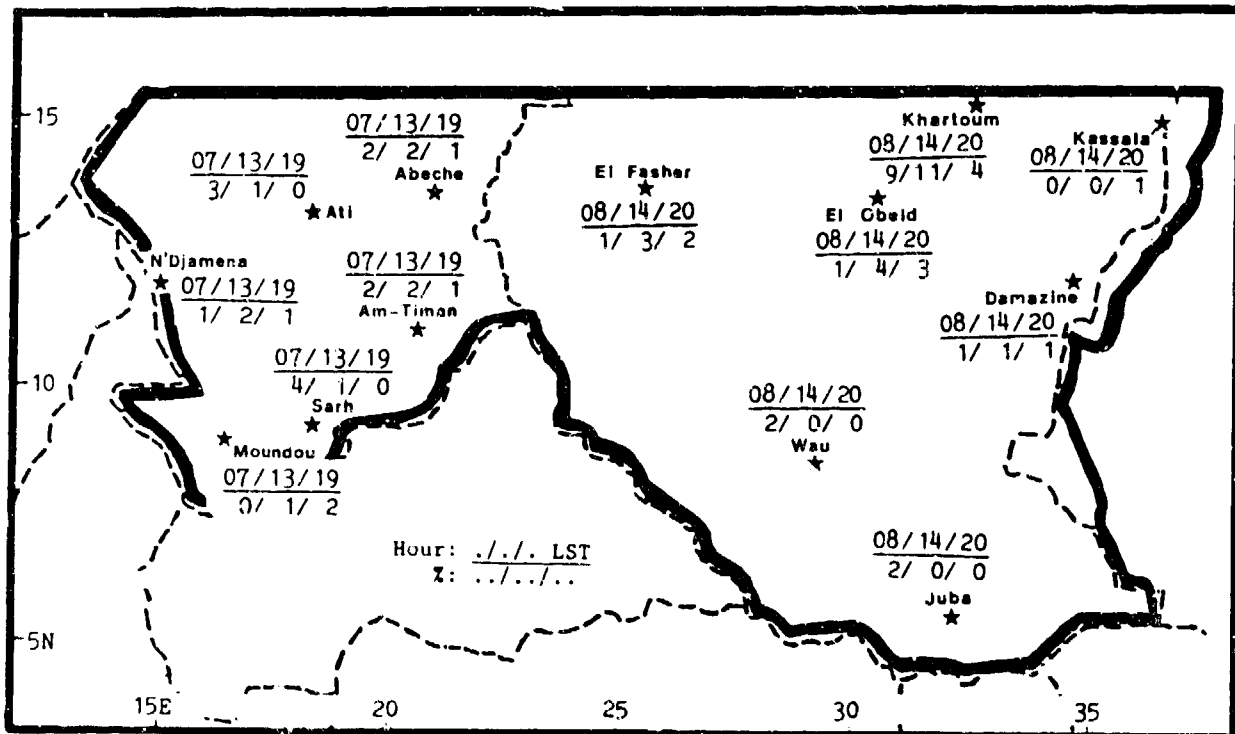


Figure 7-17. Mean Wet Season Frequencies of Visibilities Below 3 Miles, Southern Chad and Sudan.

WINDS. Wet-season mean surface winds are southwesterly at 4 to 10 knots. Winds above 15 knots result from squall lines and heavy isolated convection; gusts can be greater than 40 knots.

15,000-foot (4,570-meter) prevailing wind direction approximates that of the MTEJ; wind speed in the MTEJ averages 10 knots, but occasionally exceeds 40 knots.

Mean low- and mid-level wind directions (Figure 7-5 a-c) illustrate the persistence of southwesterlies with the Monsoon Trough at 5,000 feet (1,520 meters). The

Winds at 30,000 feet (9 km), as shown in Figure 7-6, are consistently easterly from 16 to 24 knots due to the effects of the Tropical Easterly Jet.

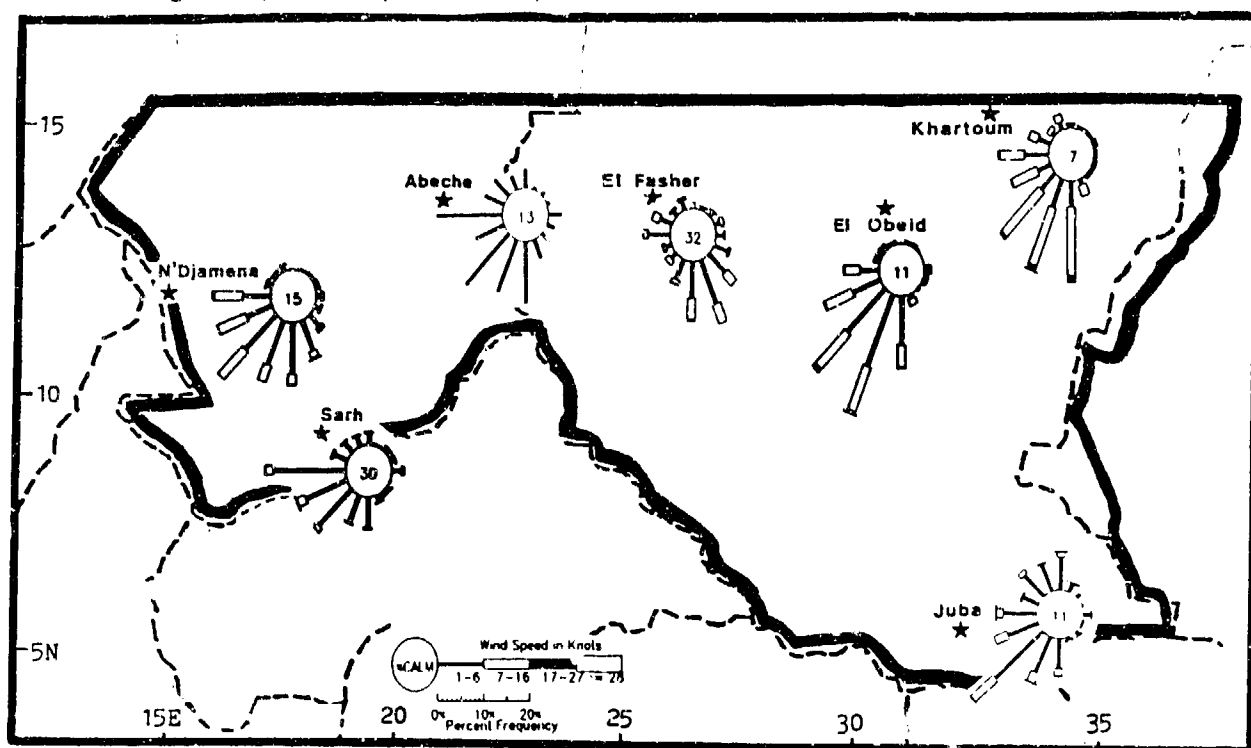


Figure 7-18. July Surface Wind Roses, Southern Chad and Sudan.

PRECIPITATION. Wet season precipitation is the result of persistent southerly flow south of the Monsoon Trough. When the Trough migrates to its northernmost position in August, equatorial moisture (up to 700 mb) advances northward. The MTEJ, located between 13° and 15° N, generates the mid-level insiability necessary for heavy convection; as a consequence, July and August have the highest mean precipitation totals of the year--see Figure 7-19. The rapid southward migration of the Monsoon Trough in late September produces a drop in precipitation in the region's northern half.

Instability along the MTEJ and good convective outflow beneath the Tropical Easterly Jet produce significant shower and thunderstorm clusters from 200 to 300 NM south of the surface Trough. Thunderstorms are common--see Figure 7-20. Most stations have a precipitation maximum in August, the result of diurnal and deep convection.

Orographic uplift of moist southerly low-level flow in the Darfur and Ethiopian Highlands produces variable amounts of scattered late afternoon and evening thundershowers that are irregularly distributed downwind of maximum cloud development. In the Darfur Highlands, Tropical Squall Lines and Easterly Waves proliferate along the MTEJ from July to September.

Late afternoon orographic convection turns into Tropical Squall Lines and convective cloud clusters that move slowly westward into east-central Chad by 1800 LST. As a result, locations immediately west of the Darfur Highlands show a late afternoon or early evening precipitation maximum. Isolated convection dissipates within a 50-NM radius of its origin, but Tropical Squall Lines continuing westward into central and eastern Chad cause a nocturnal precipitation maximum between 2000 and 0600 LST.

SOUTHERN CHAD AND SUDAN

WET SEASON

June-September

Easterly Waves develop over east-central Sudan every 2 to 5 days by early July. Orographic uplift along the Ethiopian Highlands creates thunderstorms and rainshowers similar in distribution to those developing in the Darfur Highlands. They are aligned north to south and move westward between 36° E and 30° E. Isolated cumulonimbus cells account for 30% of total wet-season

rainfall east of El Fasher and north of 11° N. Light, continuous rainshowers occur with thunderstorm blow-off. Significant rainfalls (accounting for 60 to 70% of the wet season total) are associated with diurnally generated convective cells intensifying within Easterly Waves or independently organized squall lines.

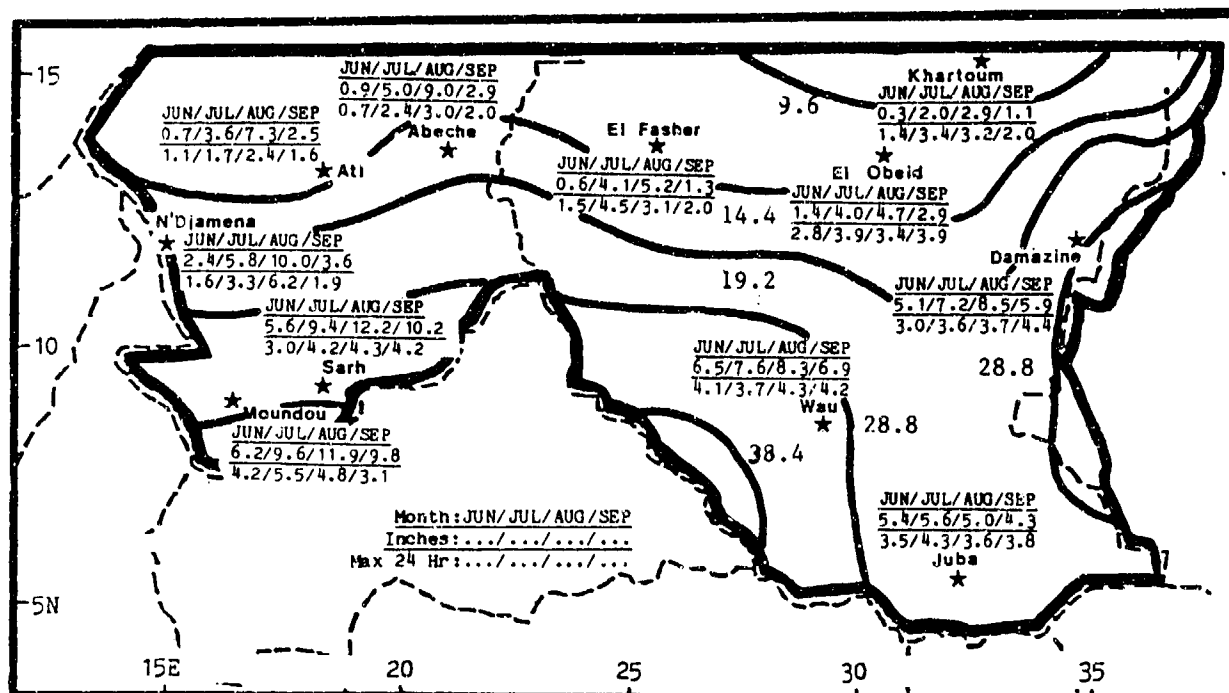


Figure 7-19. Mean Wet Season Monthly/Maximum 24-hour Precipitation, Southern Chad and Sudan. Isohyets represent mean seasonal rainfall totals.

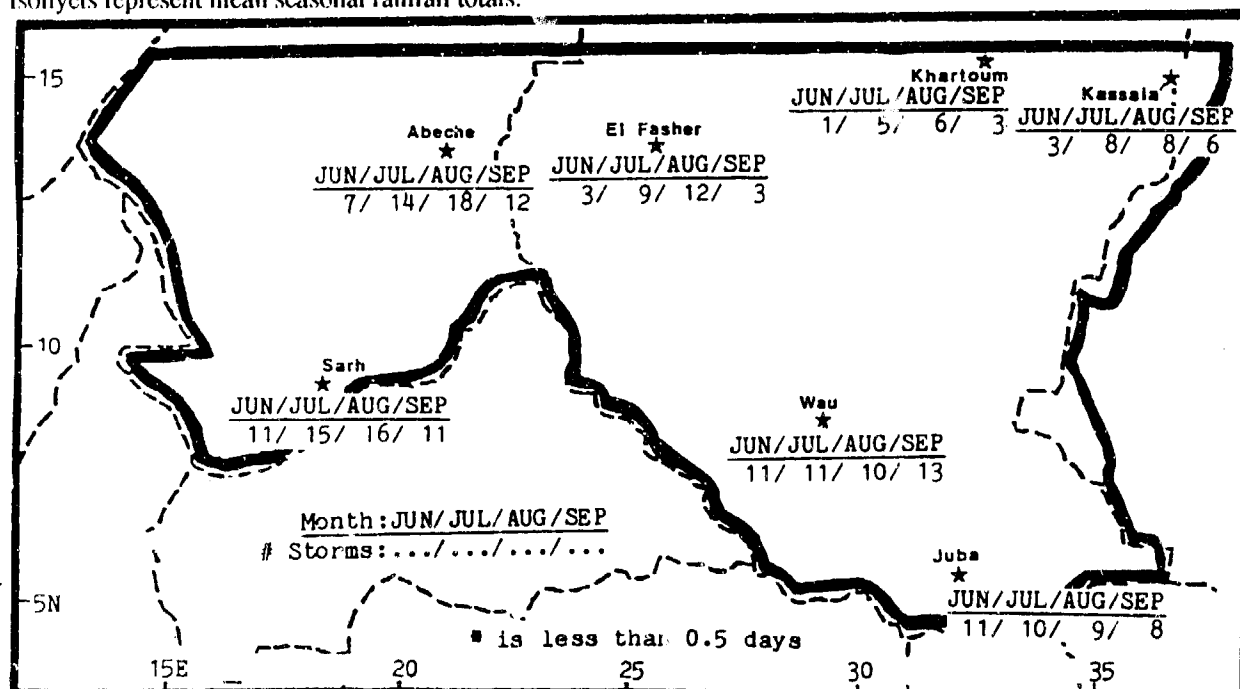


Figure 7-20. Mean Wet-Season Thunderstorm Days, Southern Chad and Sudan.

SOUTHERN CHAD AND SUDAN

WET SEASON

June-September

TEMPERATURE. Wet season mean daily highs are highest in early June before deep equatorial moisture produces persistent mid- and upper-level clouds. Heavy convection and cloud cover cause July and August mean daily highs to be the lowest of the year--see Figure 7-21. June temperatures range from 91° to 109° F (33° to 43°

°C), while July through September means are 86° to 101° F (30° to 38° C). Record highs in early June include 101° F (38° C) at Juba and 118° F (48° C) at Khartoum. Mean daily lows range from 68° F (20° C) at Juba in August to 79° F (26° C) at Khartoum in June. Record lows range from 55° to 62° F (13° to 17° C).

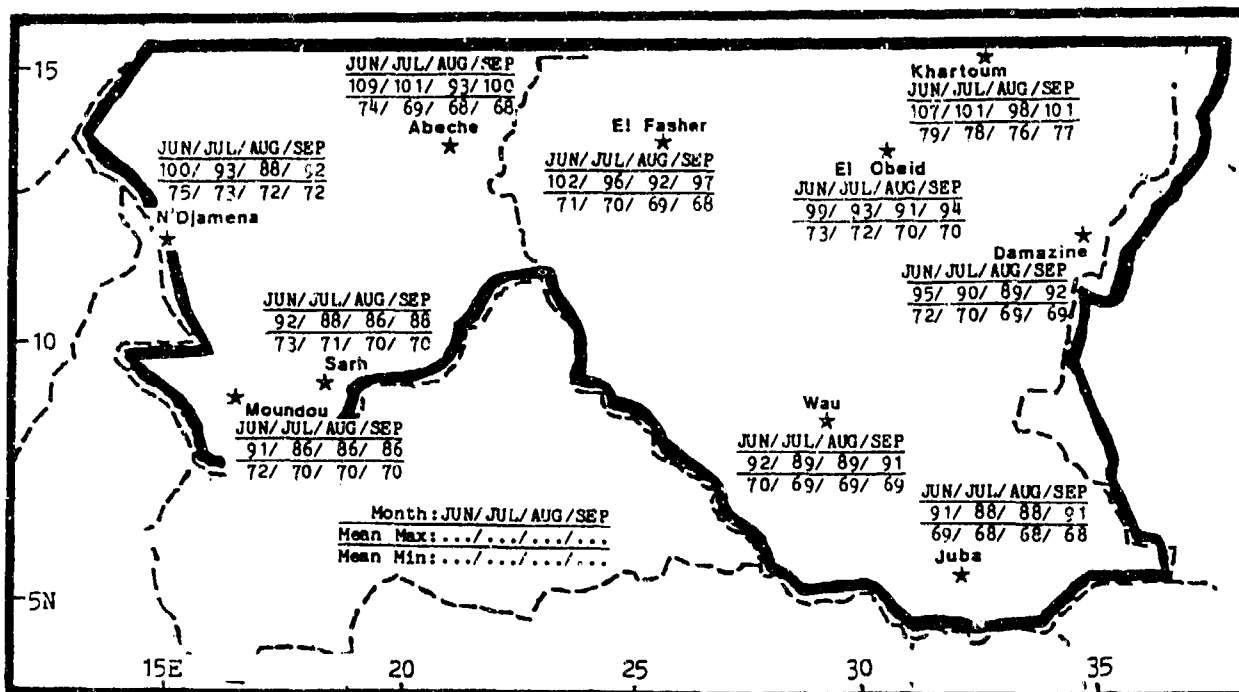


Figure 7-21. Mean Wet-Season Daily Maximum/Minimum Temperatures (F), Southern Chad and Sudan.

SOUTHERN CHAD AND SUDAN

WET-TO-DRY SEASON TRANSITION

October

GENERAL WEATHER. The wet-to-dry transition is very short due to the rapid southward movement of the Monsoon Trough, during which mT air is replaced with cT. In October, the Trough's mean position lies across the region's southern third. Stations to its south get deep, low-level equatorial moisture to fuel heavy convection concentrated south of 5° N.

The Subtropical Ridge migrates south to about 15° N in October, bringing the mid- and upper-level westerlies to the region's northern edge. The Mid-Tropospheric

Easterly Jet (MTEJ) and the Tropical Easterly Jet (TEJ) are weakened. Fair weather is re-established with little rainfall and northeasterly surface flow by mid- to late October north of 7° N.

SKY COVER. North of the Monsoon Trough, the cT airmass is dry Saharan air with little moisture below 10,000 feet (3,050 meters) MSL. The drier air leads to a north to south increase in mean October cloudiness percentages (Figure 7-22).

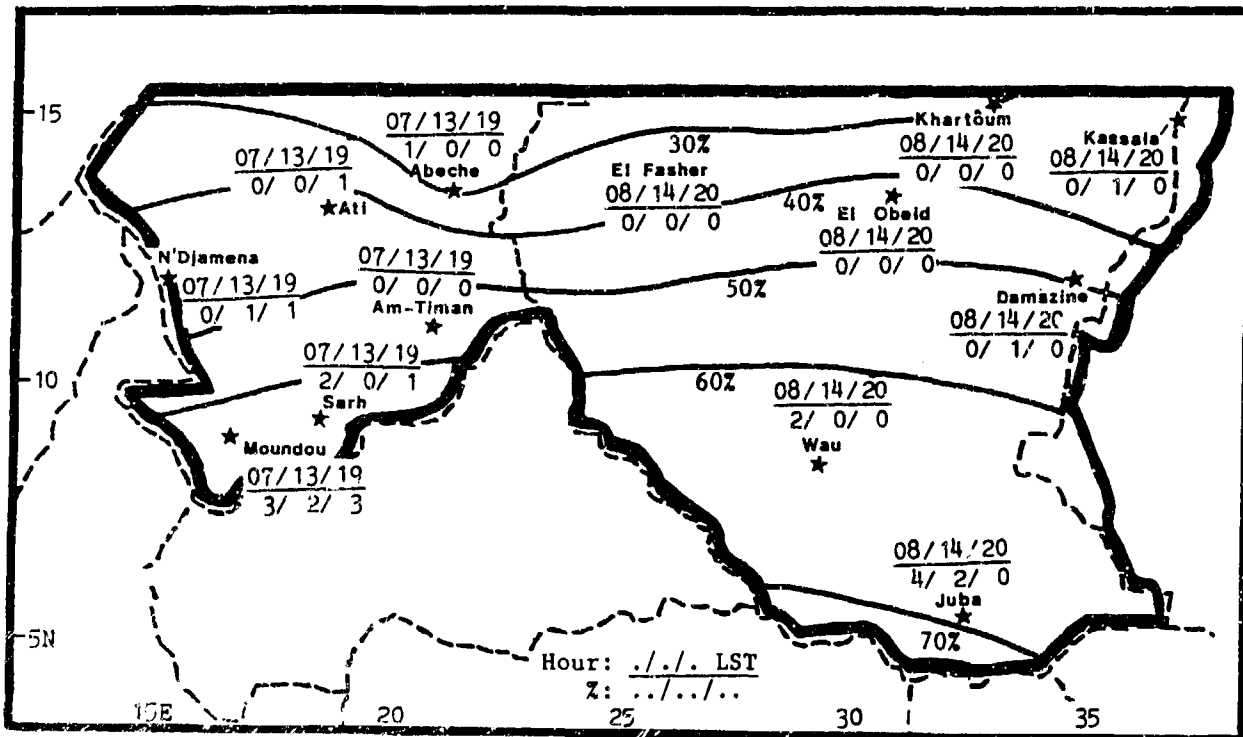


Figure 7-22 Mean Wet-to-Dry Transition Cloudiness (Isolines) and Frequencies of Ceilings Below 3,000 Feet (915 meters), Southern Chad and Sudan.

The cloud types reported near the weak TEJ core and north of the Monsoon Trough in cT air are generally cirrus and altocumulus. Cirrus several hundred feet thick is common above 20,000 feet (6 km) MSL, while altocumulus ranges from 10,000 to 18,000 feet (3,050 to 5,485 meters) MSL with tops between 12,000 and 20,000 feet (3,660 and 6,100 meters) MSL.

Many cloud types may develop in the mT air south of the Monsoon Trough. Cirrus blow-off from cumulonimbus 1,000 to 2,000 feet (305 to 610 meters) thick with tops as high as 60,000 feet (18 km) MSL is common. Altocumulus forming along the Intertropical Discontinuity (ITD) in mT air has bases between 15,000

to 25,000 feet (4,570 to 7,620 meters) MSL with tops ranging 17,000 to 27,000 feet (5,180 to 8,230 meters) MSL. In early October, altostratus may occur behind squall lines with bases between 8,000 and 12,000 feet (2,440 to 3,600 meters) with tops between 15,000 and 20,000 feet (4,570 to 6,100 meters) MSL. Squall-line stratocumulus is 1,000 to 2,000 feet (305 to 610 meters) thick, with bases at 2,000 to 6,000 feet (610 to 1,830 meters). Fair-weather cumulus bases are from 4,000 to 8,000 feet (1,220 to 2,440 meters), tops 2,000 feet (610 meters). Cumulonimbus and towering cumulus bases are similar to fair-weather cumulus, but tops can reach 60,000 feet (18 km).

SOUTHERN CHAD AND SUDAN WET-TO-DRY SEASON TRANSITION

October

Ceiling frequency distributions below 3,000 feet (915 meters) are small; most low-ceiling reports are the result of duststorms. Skies are obscured when the surface pressure gradients tighten either north or south of the Monsoon Trough or with intense thunderstorm outflow boundaries. Ceilings range from 200 to 1,000 feet (60 to 305 meters). Monsoon Trough moisture causes slightly higher low-ceiling frequencies at Wau, Juba, and Moundou. Cumulus and cumulonimbus ceilings range from 1,200 to 2,500 feet (365 to 760 meters).

VISIBILITY. Frequencies of visibilities below 3 miles in the south are lower than in the north because surface soil there is still moist from Monsoon Trough rainfall. High daytime temperatures and decreased rainfall north of the Trough result in drier soil after early October.

Visibilities below 3 miles are infrequent, caused mainly by precipitation and fog. Isolated thunderstorms in early October can produce heavy showers and reduce visibility to near zero for short periods. Duststorms are scarce, but an abnormally dry October increases the possibility.

North of the Monsoon Trough, dry Saharan air dominates and rapidly dries the surface. Visibilities are good except with wind speeds greater than 10 knots, which cause an increase in dust aloft (Harmattan Haze).

October's low-visibility frequencies are less than 13% (Figure 7-23). Slight increases at N'Djamena and Khartoum are caused by more suspended dust, a by-product of the fall harvest.

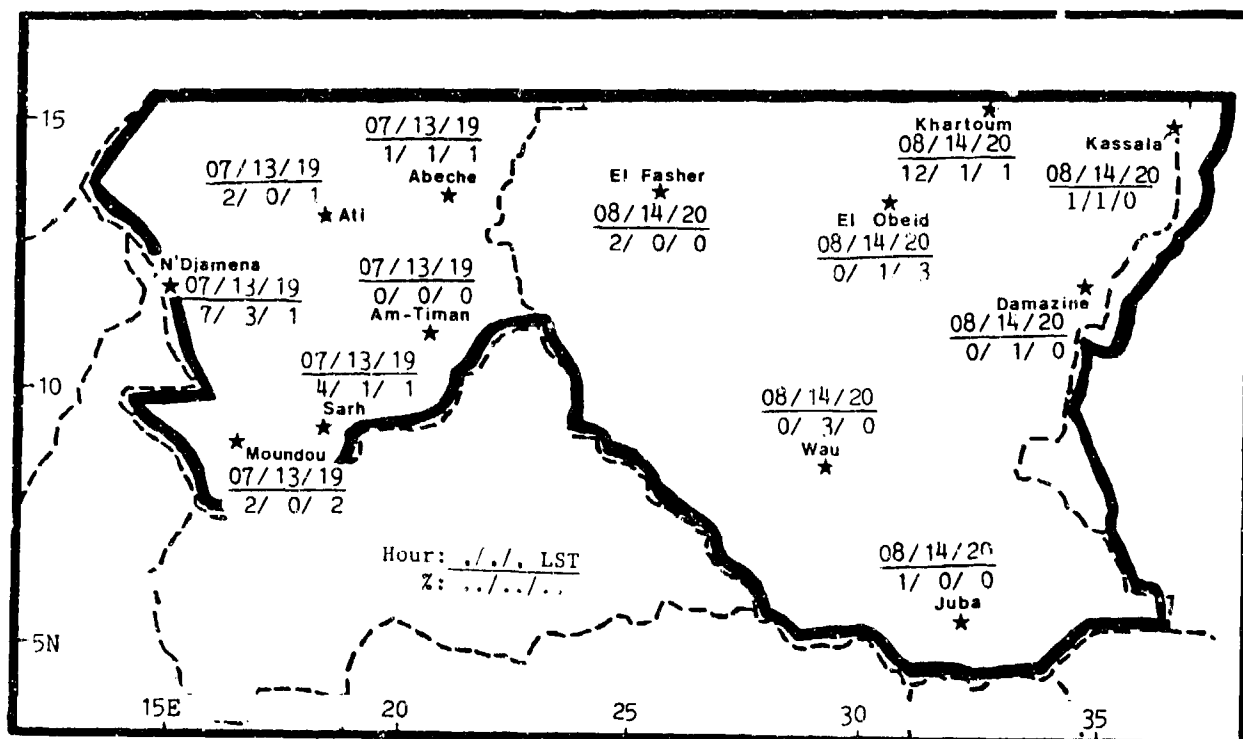


Figure 7-23. Mean Wet-to-Dry Transition Frequencies of Visibilities Below 3 Miles, Southern Chad and Sudan.

WINDS. Prevailing winds shift to northerly as the Monsoon Trough moves southward, but they vary with the Trough's oscillations. Wind direction at N'Djamena is controlled by a lake-breeze circulation off Lake Chad. Speeds average 7 knots.

Winds aloft (Figures 7-5 a-c) are easterly to northeasterly. The easterlies indicate the MTEJ's persistence through October, while the northeasterlies reflect the dry Saharan flow on the north side of the Monsoon Trough.

SOUTHERN CHAD AND SUDAN
WET-TO-DRY SEASON TRANSITION

October

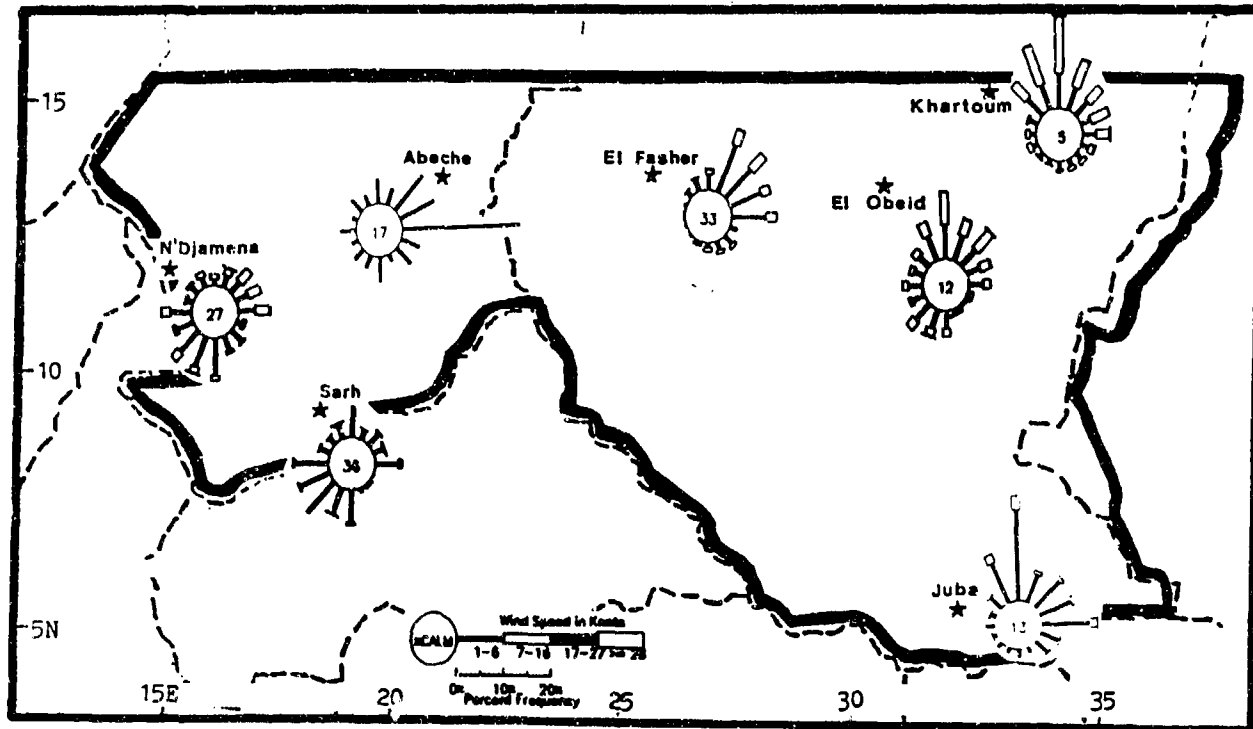


Figure 7-24. October Surface Wind Roses, Southern Chad and Sudan.

PRECIPITATION. Mean transition rainfall (Figure 7-25) is a function of Monsoon Trough position. By late October, the surface Trough is near 6° N over Sudan. Southern locations in Chad and Sudan, where showers and thundershowers prevail, average at least 3 inches (76

mm)--see Figure 7-26. Stations north of 10° N average less than 2 inches (51 mm). Most rain falls in very early October with isolated convection associated with a weakened MTEJ and the rapidly southward-moving surface Monsoon Trough.

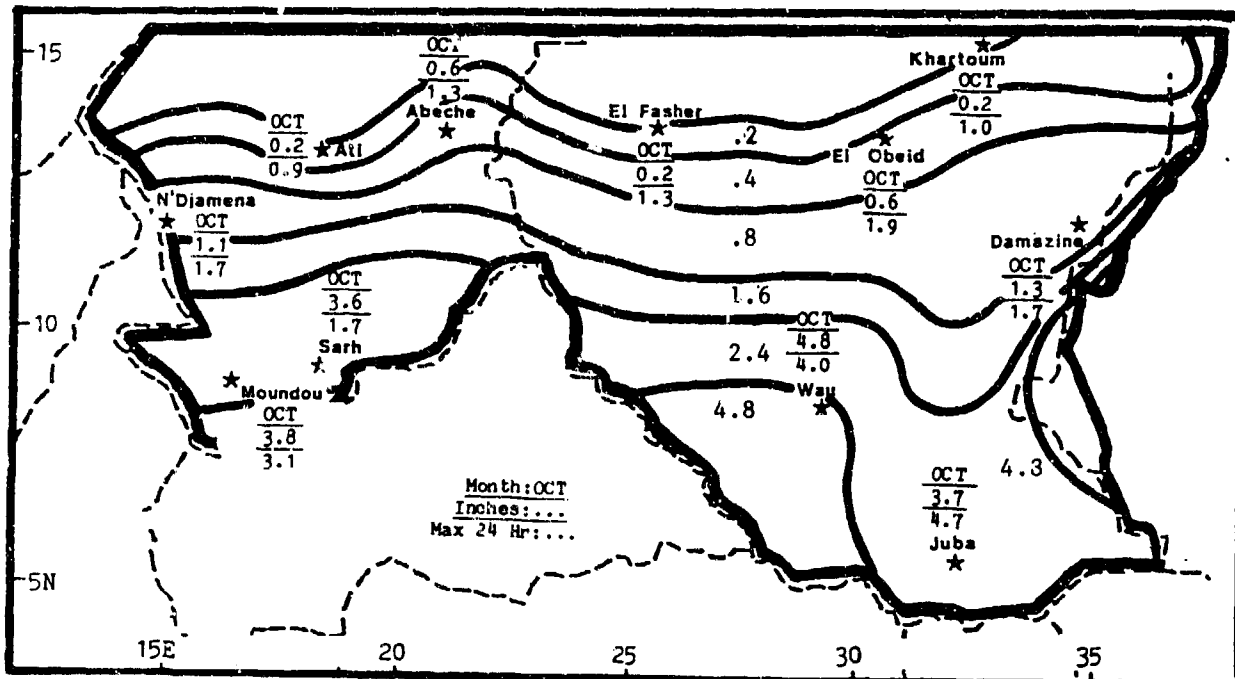


Figure 7-25. Mean Wet-to-Dry Transition Monthly/Maximum 24-hour Precipitation, Southern Chad and Sudan. Isohyets represent mean seasonal rainfall totals.

SOUTHERN CHAD AND SUDAN **WET-TO-DRY SEASON TRANSITION**

October

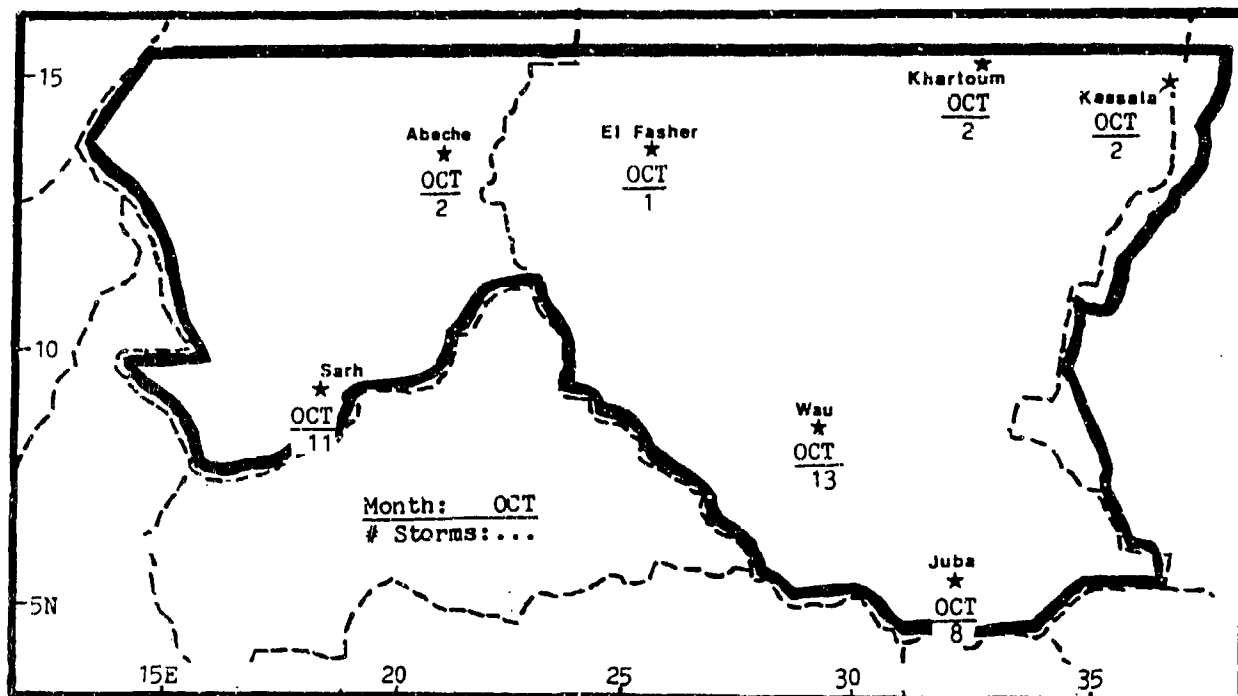


Figure 7-26. Mean Wet-to-Dry Transition Thunderstorm Days, Southern Chad and Sudan.

TEMPERATURE. Mean daily highs (Figure 7-27) range from 90° to 106° F (32° to 41° C). The higher temperatures in the north result from the quick southward migration of the Monsoon Trough, clear skies, and rapid surface heating. South of the Trough, cloud cover keeps

temperatures lower. Record highs include 100° F (38° C) at Moundou and 113° F (45° C) at Khartoum. Mean daily lows range from 64° to 76° F (18° to 24° C). Record lows range from 51° to 62° F (11° to 17° C).

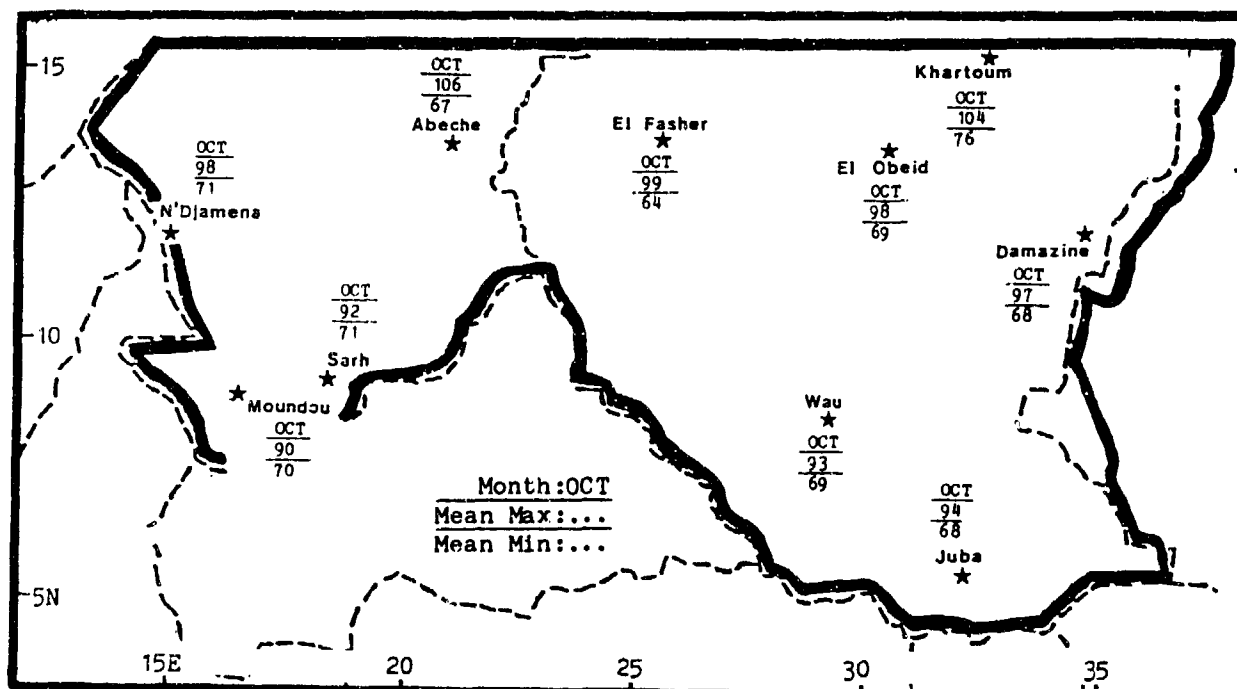


Figure 7-27. Mean Wet-to-Dry Transition Daily Maximum/Minimum Temperatures (F), Southern Chad and Sudan.

BIBLIOGRAPHY

- Ackerman, S.A., and Cox, S.K., "The Saudi Arabian Heat Low: Aerosol Distributions and Thermodynamic Structure," *Journal of Geophysical Research*, Vol. 87, pp. 8991-9002, 1982.
- Adel, A., and Hassan, A., "Characteristics of Khamsin Weather Condition in March 1967," *Meteorological Research Bulletin*, Vol. 4, Arab Republic of Egypt, pp. 63-84, 1972.
- Adel, A., and Hassan, A., and Lasheen, A.M., "Seasonal Changes of Climatological Elements Over Tropical and Subtropical Africa," *Meteorological Research Bulletin*, Vol. 1, Arab Republic of Egypt, pp. 149-179, 1969.
- Aeronautical Climatological Studies, Lod Airport, Series A Meteorological Notes No. 18*, Israel Meteorological Department, pp.45-47, 50-56, date unknown.
- Africa*, AWS/FM-100/001, HQ Air Weather Service, Scott AFB, IL, 1980.
- Alaka, M.A., *Aviation Aspect of Mountain Waves*, TP 26, Tech Note No. 18, Technical Division of the WMO Secretariat, WMO-No. 68, 1958.
- Alpert, P., et al., "A Model Simulation of the Summer Circulation from the Eastern Mediterranean Past Lake Kinneret in the Jordan Valley," *Monthly Weather Review*, Vol. 110, pp. 994-1005, 1982.
- Amer, A., "On the Intertropical Front Over Africa," *Meteorological Research Bulletin*, Vol 1, Arab Republic of Egypt, pp. 151-169.
- Anglo-Egyptian Sudan--El Fasher*, Army Air Forces Weather Division, 1944.
- Anglo-Egyptian Sudan--El Geneina*, Local Forecast Studies, Air Weather Service, 1951.
- Anglo-Egyptian Sudan--Wadi Seidna*, Army Air Forces Weather Division, 1946.
- Atkinson, C.D., *Forecaster's Guide to Tropical Meteorology*, AWS TR 240, HQ Air Weather Service, Scott AFB, IL 1971.
- Atkinson, C.D. and Sadler, J.C., *Mean Cloudiness/Gradient Level Wind Charts Over The Tropics*, AWS TR 215, Volume 2--Charts, HQ Air Weather Service, Scott AFB, IL, 1970.
- Banoub, E.F., *Sandstorms and Duststorms in UAR*, Egypt Met. Dept, Tech Note No.1, pp. 1-30, 1970.
- Barry, R.G., *Mountain Weather and Climate*, Meuthen and Co., London, 1981.
- Bhalotra, Y.P.R., *Aviation Hazards At Malakal and Juba*, Memoir No.4, Sudan Meteorological Service, 1962.
- Bhalotra, Y.P.R., *Meteorology of Sudan*, Memoir No.6, Sudan Meteorological Service, 1963.
- Black, R.E., *Cyclones and Anticyclones in Europe*, 2WW/TN-69/2, 1969.
- Blake, D.W., et al., "Heat Low Over the Saudi Arabian Desert During May 1979 (Summer MONEX)," *Monthly Weather Review*, Vol. 111, pp. 1759-1775, 1983.
- Bryson, R.A., et al., *Normal 500mb Charts for the Northern Hemisphere*, Report No.8, AF 19 (604)-992, 29, 1957.

Burpee, R.W., "The Origin and Structure of Easterly Waves in the Lower Troposphere of North Africa," *Journal of Atmospheric Sciences*, Vol. 29, pp. 77-90, 1972.

Burpee, R.W., "Characteristics of North African Easterly Waves During the Summers of 1968 and 1969," *Journal of Atmospheric Sciences*, Vol. 31, pp. 1556-1570, 1974.

Burpee, R.W., "Weather Forecasting For GATE," *GATE-Preliminary Scientific Results: Volume 1 (of GARP)*, No. 14, pp. 96-99, 1975.

Cairo International Airport (Payne Field), Local Forecast Studies, Air Weather Service, 1955.

Carlson, T.N., "Synoptic Histories of Three African Disturbances That Developed Into Atlantic Hurricanes," *Monthly Weather Review*, Vol. 97, pp. 256-277, 1969.

Climate of Lebanon, Engineer Strategic Intelligence Division Army Map Service, AWS Directorate of Climatology, 1957.

A Climatic Resume of the Mediterranean Sea, NWSED, NAVAIR 50-1C-64, 1975.

Climatological Narrative - Incirlik, Turkey, date unknown.

Components of the 1000mb Winds of the Northern Hemisphere, NAVAIR 50-1C-51, 1966.

Conrad, V., "The Climate of the Mediterranean Region," *Bulletin of the American Meteorological Society*, Vol. 24, pp. 127-145, 1943.

Crutcher, H.L., *Selected Meridional Cross Sections of Heights, Temperatures, and Dew Points of the Northern Hemisphere*, NCDC-NOAA, NAVAIR 50-1C-59, p. 137, 1971.

Delsi, Moayad, *Downdraft Haboob in Khartoum*, Sudan Meteorological Service, 1967.

Dettwiller, J., *Caracteristiques du Jet Subtropical Sur Le N.W. de L'Afrique*, Ministere De L'Equipement, Secretariat D'Etat Aux Transports, Secretariat Genral A L'Aviation Civile, Direction De La Meteorologie Nationale, Monographies De La Meteorologie Nationale, No 58, Rue de l'Universite, Paris 7, 1967.

Development Plan For the Litani River Basin - Republic of Lebanon, Appendix to Section III - Hydrology, Selected Terrain and Climatic Data, U.S. Department of the Interior Bureau of Reclamation, Denver, Colorado, 1954.

Egypt: A Country Study, Foreign Area Studies, American University, 1962.

Eldridge, R.H., "A Synoptic Study of West African Disturbance Lines," *Quarterly Journal of the Royal Meteorological Society*, Vol. 83, pp. 303-314, 1957.

El-Din Harb, M.S., "Widespread Fog Over Egypt and Its Characteristic Pressure Types," *Meteorological Research Bulletin*, Vol. 6, Arab Republic of Egypt, pp. 33-45, 1974.

El-Din, M. I. Shams, *On the Occurrence of Thunderstorms in Early Autumn Along the Western Mediterranean Coast of U.A.R.*, Vol. 2, Arab Republic of Egypt, 1970.

El-Fandy, M.G., "Barometric Lows of Cyprus," *Quarterly Journal of the Royal Meteorological Society*, Vol. 72, pp. 291-306, 1946.

El-Fandy, M.G., "The Formation of Depressions of the Khamsin Type," *Quarterly Journal of the Royal*

- Meteorological Society*, Vol. 66, pp. 323-335, 1940.
- El-Fandy, M.G., "The Effect of the Sudan Monsoon Low on the Development of 'Thundery Conditions in Egypt, Palestine, and Syria," *Royal Meteorological Service Journal*, 74, pp. 31-38, 1948.
- El-Fandy, M.G., and Elnisr, M.K., "On the Conditions Favoring Low Stratus Formation Over the Middle East in Summer," *Bulletin of the American Meteorological Society*, Vol. 30, pp. 357-359, 1949.
- El-Fandy, M.G., "Forecasting the Summer Weather of the Sudan and the Rains That Lead to the Nile Floods," *Quarterly Journal of the Royal Meteorological Service*, Vol. 75, pp. 375-399, 1949.
- El-Fandy, M.G., "Effects of Topography and Other Factors on the Movement of Lows in the Middle East and Sudan," *Bulletin of the American Meteorological Society*, Vol. 31, pp. 375-379, 1950.
- El-Fandy, M.G., "Troughs in the Upper Westerlies and Cyclonic Developments in the Nile Valley," *Royal Meteorological Service Journal*, 76, pp. 166-172, 1950.
- El-Hady, Salama Saleh Abd, *Upper Troughs In the Mediterranean and Middle East*, MSc Thesis, Cairo University, Cairo, Egypt, 1960.
- El-Sawy, K. A., *Cyprus Cyclogenesis*, *Meteorological Research Bulletin*, Vol 3, Arab Republic of Egypt, 1977.
- El-Tantawy, A.H.I., *Jet Streams In The Middle East*, PhD Thesis, Cairo University, Cairo, UB, 1967.
- El-Tantawy, A.H.I., "A Diabatically Induced Deformation of the Tropical African Troposphere in the Rainy Season," *Egypt Meteorological Research Bulletin*, pp. 1-20, 1968.
- El-Tantawy, A.H.I., "On the Genesis and Structure of Spring Desert Depressions in Subtropical Africa," *Egypt Meteorological Research Bulletin*, pp. 70-107, 1968.
- Erdogmus, F., "An Investigation of Winds up to 300hPA Over Turkey Between 1970 and 1984," *Journal of Climatology*, Vol. 8, pp. 509-606, 1988.
- European Theater Weather Orientation*, 2WWP 105-12, 2d Weather Wing, 1977.
- Farr, G.R., *Seasonal and Global Distribution of the Jet Stream and its Kinetic Energies in the Northern Hemisphere*, MS Thesis, Dept of Meteorology, Univ. of Utah, 1964.
- Fegley, Robert S., *Clothing Almanac for Southwest Asia*, Tech Report 69-6-ES, U.S. Army Natick Laboratories, Natick, MA, 1968.
- Fett, R.W. and Bohan, W.A., *Navy Tactical Applications Guide, Vol.5, Part 1, Indian Ocean-Red Sea/Persian Gulf, Weather Analysis and Forecast Applications*, Meteorological Satellite Systems, NEPRF TR 83-02, AD-A134412. 1983.
- Fett, R.W., *North Atlantic and Mediterranean Weather Analysis and Forecast Applications--Volume 3*, NEPRF TN 80-07, 1980.
- Flocas, A.A., "The Annual and Seasonal Distribution of Fronts over Central-Southern Europe and the Mediterranean," *Journal of Climatology*, Vol. 4, pp. 255-267, 1984.
- Flolin, H., "Studies on the Meteorology of Tropical Africa," *Bon Met Abhund*, Heft 5, University of Bonn, Bonn, 1965.

Flohn, H., *Contributions to a Meteorology of the Tibetan Highlands*, Colorado State Univ, Atmospheric Science Paper, No. 130, 1968.

Flohn, H., "Local Wind Systems," *World Survey of Climatology--Volume 2*, Herbert Flohn ed., Elsevier Publ. Co., Amsterdam, 1969.

Fons, M. Claude, *Cyclogenesis in the Western Mediterranean Basin*, FTD-ID(RS)T-0068-81, pp. 57, 1981.

Fortune, M., "Properties of African Squall Lines Inferred from Time-Lapse Satellite Imagery," *Monthly Weather Review*, Vol. 108, pp. 153-168, 1980.

Fouli, R.S., *On the Mean Tropospheric Meridional Circulation over Africa from the Equatorial Area to the Mediterranean*, Meteorological Research Bulletin, Vol 4, Arab Republic of Egypt, pp. 1-15, 1972.

Gamache, J.F., and Houze, R.A., Jr., "Mesoscale Air Motions Associated with a Tropical Squall Line," *Monthly Weather Review*, Vol. 110, pp. 119-135, 1982.

Geiger, R., *Climate Near The Ground*, Harvard Univ. Press, Cambridge, MA., pp. 403-417, 1965.

General Circulation of the Atmosphere., Portuguese Met. Service, DIA LN 783-70, 1970.

General Climatic Information Guide No. 9 Revised, Smyrna, Turkey, Weather Division, Headquarters Army Air Forces, 1944.

Hamilton, R.A., and Archbold, J.W., "Meteorology of Nigeria and Adjacent Territory," *Quarterly Journal of Royal Meteorological Society*, Vol. 71, pp. 231-265, 1945.

Hammer, R.M., "Cloud Development and Distribution Around Khartoum," *Weather (UK)*, Vol. 25, pp. 411-414, 1970.

Hammond Ambassador World Atlas, Hammond Incorporated, Mapiewood, NJ, 1989.

Hance, William A., *The Geography of Modern Africa*, Columbia University Press, New York, NY, 1964.

Hassanein, A.A., *Preliminary Study of the Lower-Tropospheric Inversion Statistics in Cairo*, Meteorological Research Bulletin, Arab Republic of Egypt, pp. 179-193, 1978.

Hastenrath, S., *Climate and Circulation of the Tropics*, Reidel Publ. Co., Dordrecht. 1985.

Hayward, D.F. and Oguntuyinbo, J.S., *The Climatology of West Africa*, Century Hutchinson Ltd, pp. 137-141, 1987.

International Cloud Atlas, Vol 1, World Meteorological Organization, 1956.

Jacobeit, J., "Variations of Trough Positions and Precipitation Patterns in the Mediterranean Area," *Journal of Climatology*, Vol. 7, pp. 453-476, 1987.

Joseph, J.H., Manes, A., and Ashbel, D., "Desert Aerosols Transported by Khamsinic Depressions and Their Weather Effects," *Journal of Applied Meteorology*, Vol. 12, pp. 792-797, 1973.

Kallos, George, Metaxas, Dionyssios A., "Synoptic Processes for the Formation of Cyprus Lows," School of Physics and Mathematics, Meteorology Department, University of Ioannina (Greece), *Rivista De Meteorologia Aeronautica*, Vol XL, No. 2/3, 1980.

- Lahey, J.F., et al., *Atlas of 300mb Wind Characteristics for the Northern Hemisphere*, Final Report, Part 1, AF 19 (604)-2278, Univ of Wisc Press, 1960.
- Leroux, M., *The Climate of Tropical Africa-Part B*, FTD-ID(RS)T-0615-85, pp. 526-566, 1983.
- Leroux, M., *The Climate of Tropical Africa-Atlas*, Volume 2, 1983.
- Levin, Z. and Lindberg, J.D., "Size Distribution, Chemical Composition, and Optical Properties of Urban and Desert Aerosols in Israel," *Journal of Geophysical Research*, Vol. 84, No. C11, 1979.
- Local Forecast Studies, Wheelus AB, Tripoli, Libya*, Air Weather Service, 1949-1962.
- MacCallum, Douglas H., *An Observational Study of Global Upper Tropospheric Jet Streams in Meteorology*, University of California, Los Angeles, CA, 1964.
- Manins, P.C. and Sawford, B.L., "Katabatic Winds: A field case study," *Quarterly Journal of the Royal Meteorological Society*, Vol. 105, pp. 1011-1025, 1979.
- Marine Atlas of the World*, Volume IX, Naval Oceanography Command Detachment, NAVAIR 50-1C-65, 1981.
- Mbele-Mbong, S., *Rainfall in West Central Africa*, Dept of Atmospheric Sciences, Colorado State Univ, Report No.22, NSF GA 29147, 1974.
- McGinley, J.A., "Dynamics of Alpine Lee Cyclogenesis from a Quasi-Geostrophic View," *Rivista Di Meteorologia Aeronautica*, Vol. 44, pp. 45-60, 1984.
- Membery, D.A., "A Unique August Cyclonic Storm Crosses Arabia," *Weather*, Vol. 40, pp. 108-114, 1985.
- Morth, H.T., *Introduction to the Climate of Africa-Notes to Support Lectures on Regional Climatology*, East African Met Service, Nairobi, 1974.
- Naguib, M.K., "Precipitation in the UAR in Relation to Different Synoptic Patterns," *Egypt Meteorological Research Bulletin*, Arab Republic of Egypt, Vol. 2, pp. 207-221, 1971.
- National Intelligence Surveys 25C and 27, Cyprus, Turkey, Section 23, Weather and Climate*, U.S. Central Intelligence Agency, 1970.
- National Intelligence Surveys 28A, 28B, 29, and 31, Syria, Lebanon, Jordan, Israel, Section 23, Weather and Climate*, U.S. Central Intelligence Agency, 1969.
- National Intelligence Survey 49, Libya, Section 23, Weather and Climate*, U.S. Central Intelligence Agency, 1965.
- National Intelligence Survey 52, Equatorial Africa (Chad), Section 23, Weather and Climate*, U.S. Central Intelligence Agency, 1955.
- National Intelligence Survey 53, United Arab Republic, Section 23, Weather and Climate*, U.S. Central Intelligence Agency, 1968.
- National Intelligence Survey 54, Sudan, Section 23, Weather and Climate*, U.S. Central Intelligence Agency, 1965.
- National Intelligence Survey 104, Atlantic Basin, Marine Climate and Oceanography Part IX, The Mediterranean and Black Sea, Section 1, Marine Climate*, U.S. Central Intelligence Agency, 1960.

Naval Air Pilot--Northeast Africa (Including Adjacent Mediterranean Sea and Red Sea Areas), Supplement B to HO No. 262, Hydrographic Office, 1943.

Nieuwolt, S., *Tropical Climatology*, Wiley & Sons, 1977.

Northern Africa, AWS/FM-100/003, HQ Air Weather Service, Scott AFB, IL, 1980.

Omar, M.H., *Some Agroclimatic Factors for the Areas Surrounding Lake Nasser*, WMO Tech Rept #444, pp. 147-149.

Omotosho, J.B., "Spatial and Seasonal Variation of Line Squalls over West Africa," *Archives For Meteorology, Geophysics and Bioclimatology*, Ser A. 33, pp. 143-150, 1984.

Omotosho, J.B., "The Separate Contributions of Line Squalls, Thunderstorms and the Monsoon to the Total Rainfall in Nigeria," *Journal of Climatology*, Vol. 5, pp. 543-552, 1985.

Palmer, T.N. and Zhaobo, S., "A Modelling and Observational Study of the Relationship between Sea Surface Temperature in the North-West Atlantic and the Atmospheric General Circulation," *Quarterly Journal of the Royal Meteorological Society*, Vol. 111, pp. 947-975, 1985.

Palmn E. and Newton, C.W., *Atmospheric Circulation Systems*, Academic Press, New York and London, 1969.

Pedgley, D.E., "Diurnal Variation of the Incidence of Monsoon Rainfall over the Sudan," *Meteorological Magazine*, Vol. 98, pp. 97-107 (Part I); pp. 129-134 (Part II), 1969.

Pedgley, D.E., "Diurnal Incidence of Rain and Thunder at Asmara and Addis Ababa, Ethiopia," *Meteorological Magazine*, Vol. 100, pp. 66-71, 1971.

Pedgley, D.E., "Desert Depressions Over Northeast Africa," *Meteorological Magazine*, Vol. 101, pp. 228-243, 1972.

Pedgley, D.E., "An Exceptional Desert Rainstorm at Kufra, Libya," *Weather*, Vol. 29, pp. 64-70, 1974.

Pruss, W.F., *Climatological Wind Factors Calculator-Charts of Vector Standard Deviation of Winds*, 3WWM 105-5, 1962.

Ramage, C.S., *Monsoon Meteorology*, Academic Press, New York, 1971.

Red Sea and Gulf of Aden-Oceanographical and Meteorological Data, No. 129, Koninklijk Nederlands Meteorologisch Instituut, Amsterdam, 1949.

Reed, R.J., "Principal Frontal Zones of the Northern hemisphere in Winter and Summer," *Bulletin of the American Meteorological Society*, Vol. 41, pp. 591-598, 1960.

Rennick, M.A., "The Generation of African Waves," *Journal of Atmospheric Sciences*, Vol. 33, pp. 1955-1969, 1976.

Riehl, H., *Jet Streams of the Atmosphere*, Dept of Atmospheric Science, Colorado State Univ., Tech Report No. 32, 1962.

Sadler, J.C., *The Upper Tropospheric Circulation Over The Global Tropics*, UHMET 75-05, NSF Grant No. GA-36301, University of Hawaii, 1975.

Sadler, J.C., *The Upper Tropospheric Circulation Over The Global Tropics. Part II-The Statistics*, UHMET 77-02.

NSF Grant No. GA-36301, University of Hawaii, 1977.

Sanders, Frederick, "Life History of Mobile Troughs in the Upper Westerlies," *Monthly Weather Review*, Vol. 116, pp. 2629-2647, 1988.

Sandstorms and Duststorms in the U.A.R., Meteorological Department, Arab Republic of Egypt, Technical Note #1, Cairo, 1970.

Segal, M., et al., "A Study of Meteorological Patterns Associated With A Lake Confined By Mountains-the Dead Sea Case," *Quarterly Journal of the Royal Meteorological Society*, Vol. 109, pp. 549-564, 1983.

Segal, M., et al., "On Some Meteorological Patterns in the Dead Sea Area during Advective Sharav Conditions," *Israel Journ. of Earth Sci.*, Vol. 33, pp. 76-83, 1984.

Segal, M., et al., "Model Evaluation of the Summer Daytime Induced Flows over Southern Israel," *Israel Journ. of Earth Sci.*, Vol. 34, pp. 39-46, 1985.

Sharon, D. and Kutiel, H., "The Distribution of Rainfall Intensity in Israel, Its Regional and Seasonal Variations and Its Climatological Evaluation," *Journal of Climatology*, Vol. 6, pp. 277-291, 1986.

Sivall, T., "Sirocco in the Levant," *Geografiska Annaler*, Vol. 39, pp. 116-142, 1957.

Soliman, K.M., "Khamli Over Egypt," *Royal Meteorological Service*, Vol. 79, pp. 389-397, 1953.

Solot, S.B., "General Circulation Over the Anglo-Egyptian Sudan and Adjacent Regions," *Bulletin of the American Meteorological Society*, Vol. 31, pp. 85-94, 1950.

Solot, S.B., *The Meteorology of Central Africa*, AWSTR 105-50, 1943.

Study of World Wide Occurrence of Fog, Thunderstorms, Supercooled Low Clouds and Freezing Temperatures, NAVAIR 50-1C-60 CH-1, p. 143, 1978.

Sudan Meteorological Service, Climatic Normals--(1921-1950), 1957.

Tantawy, A.H.I., *On the Genesis and Structure of Spring Desert Depressions in Subtropical Africa*, Meteorological Research Bulletin, Arab Republic of Egypt, pp. 70-107, 1963.

Thompson, B.W., *The Climate of Africa*, Oxford Univ. Press, New York, NY, 1965.

Tropical East Africa, AWS/FM-100/006, HQ Air Weather Service, Scott AFB, IL, 1980.

Tropical Meteorology in Africa--4th Seminar, East African Met. Service, Nairobi, 1965.

van de Boogaard, H., *The Mean Circulation of the Tropical and Subtropical Atmosphere-July*, NCAR, NCAR/TN-118+STR, 1977.

Wallace, J.M. and Hobbs, P.V., *Atmospheric Science--An Introductory Survey*, Academic Press, New York, 1977.

Weather In The Black Sea, British Met. Office, Her Majesty's Stationary Office, London, p. 264, 1963.

Weather In The Home Waters and N.E. Atlantic, M.O.446, Meteorological Office, London, pp 16-17, 1943.

Weather In The Mediterranean, Volume 1 (Second Edition) General Meteorology, M.O.391, Meteorological Office.,

London: Her Majesty's Stationary Office, 1962.

Whittaker, L.M. and Horn, L.H., "Northern Hemisphere Extratropical Cyclone Activity for Four Mid-Season Months," *Journal of Climatology*, Vol. 4, pp. 297-310, 1984.

Winstanley, D., "Sharav," *Weather*, Vol. 27, pp. 146-160, 1972.

World Survey of Climatology, Volume 2, General Climatology, Elsevier Publ. Co., Amsterdam, 1969.

World Survey of Climatology, Vol 9, Climates of Southern and Western Asia, Elsevier Scientific Publishing Company, Amsterdam, 1981.

World Survey of Climatology, Vol 10, Climates of Africa, Elsevier Publ. Co., Amsterdam, 1972.

Zambakas, J.D., et al., *The Climate of the Eastern Greek Macedonia*, Academy of Athens--Dept. of Atmos. Physics and Climatology, Sci. Paper No.30, pp. 1-12, 1983.

Zohdy, H., "On the Interaction Between Extratropical and Tropical Disturbances over Africa as Seen From Satellite Pictures," *Meteorological Research Bulletin*, Vol. 3, Arab Republic of Egypt, pp. 87-99, 1971.

DISTRIBUTION

OUSDA/R/AT/E/LS, Pentagon, Washington, DC 20301-3080	1
AF/XOW, Pentagon, Washington, DC 20330-5054	1
AF/XOOCW, Pentagon, Washington, DC 20330-5054	2
AF/XOORF, Pentagon, Washington, DC 20330-5054	1
J-34/ESD, Pentagon, Washington, DC 20318-3000	1
MAC/DOX, Scott AFB, IL 62225-5001	1
AWS/DO, Scott AFB, IL 62225-5008	1
AWS/DOT, Scott AFB, IL 62225-5008	1
AWS/XTJ, Scott AFB, IL 62225-5008	1
AWS/XTX, Scott AFB, IL 62225-5008	1
AWS/PM, Scott AFB, IL 62225-5008	1
AWS/RF, Scott AFB, IL 62225-5008	1
AWS/SC, Scott AFB, IL 62225-5008	1
CSTC/WE, PO Box 3420, Onizuka AFB, CA 94088-3430	1
SSD/WE (Stop 77), Buckley ANGB, Aurora, CO 80011-9599	1
SSD/MWA, PO Box 92960, Los Angeles, CA 90009-2960	1
OL-K, HQ AWS, NEXRAD Opnl Facility, 1200 Westheimer Dr., Norman, OK 73069	1
OL-M, HQ AWS, McClellan AFB, CA 95652-5609	1
Det 1, HQ AWS, Pentagon, Washington, DC 20330-5054	1
Det 9, HQ AWS, PO Box 12297, Las Vegas, NV 89112-0297	1
1WW/DN, Hickam AFB, HI 96853-5000	3
11WS/DON, Elmendorf AFB, AK 99506-5000	1
20WS/DON, APO San Francisco 96328-5000	1
30WS/DON, APO San Francisco 96301-0420	1
2WW/DN, APO New York 09094-5000	3
7WS/DON, APO New York 09403-5000	1
28WS/DON, APO New York 09127-5000	1
31WS/DON, APO New York 09136-5000	1
Det 19, 31WS, APO NY 09289-5000	1
3WW/DN, Offutt AFB, NE 68113-5000	3
9WS/DON, March AFB, CA 92518-5000	1
24WS/DON, Randolph AFB, TX 78150-5000	1
26WS/DON, Barksdale AFB, LA 71110-5002	1
4WW/DN, Peterson AFB, CO 80914-5000	3
2WS/DON, Andrews AFB, MD 20334-5000	20
5WW/DN, Langley AFB, VA 23665-5000	7
1WS/DON, MacDill AFB, FL 33608-5000	5
3WS/DON, Shaw AFB, SC 29152-5000	15
5WS/DON, Ft McPherson, GA 30330-5000	20
25WS/DON, Bergstrom AFB, TX 78743-5000	13
AFGWC/SDSL, Offutt AFB, NE 68113-5000	6
AFGWC/WFG, Offutt AFB, NE 68113-5000	1
USAFETAC, Scott AFB, IL 62225-5438	6
OL-A, USAFETAC, Federal Building, Asheville, NC 28801-2723	3
7WW/DN, Scott AFB, IL 62225-5008	3
6WS/DON, Hurlburt Field, FL 32544-5000	1
15WS/DON, McGuire AFB, NJ 08641-5002	1
17WS/DON, Travis AFB, CA 94535-5986	1
3350 TECH TG/TTGU-W, Stop 62, Chanute AFB, IL 61868-5000	2
3395 TCHTG/TTKO-W, Keesler AFB, MS 39534-5000	2
AFIT/CIR, Wright-Patterson AFB, OH 45433-6583	1
NAVOCEANCOMDET, Federal Building, Asheville, NC 28801-2723	1
NAVOCEANCOMDET, Patuxent River NAS, MD 20670-5103	1
COMNAVOCEANCOM, Code N312, Stennis Space Ctr, MS 39529-5000	1
COMNAVOCEANCOM, Code N332, Stennis Space Ctr, MS 39529-5000	1
NAVOCEANO (Rusty Russum), Stennis Space Ctr, MS 39522-5001	2

NAVOCEANO, Code 9220 (Tony Ortolano), Stennis Space Ctr, MS 39529-5001	1
NAVOCEANO, Code 4601 (Ms Loomis), Stennis Space Ctr, MS 39529-5001	1
FLENUMOCEANCEN, Monterey, CA 93943-5006	1
NOARL West, Monterey, CA 93943-5006	1
Naval Research Laboratory, Code 4323, Washington, DC 20375	1
Naval Postgraduate School, Chmn, Dept of Meteorology, Code 63, Monterey, CA 93943-5000	1
Naval Eastern Oceanography Ctr, U117 McCady Bldg, NAS Norfolk, Norfolk, VA 23511-5000	1
Naval Western Oceanography Ctr, Box 113, Attn: Tech Library, Pearl Harbor, HI 96860-5000	1
Naval Oceanography Command Ctr, COMNAV MAR Box 12, FPO San Francisco, CA 96630-5000	1
Naval Oceanography Command Ctr, Box 31, U.S. NAVSTA FPO NY 09540-3000	1
Pacific Missile Test Center, Geophysics Division, Code 3253, Pt Mugu, CA 93042-5000	1
Dept of Commerce/NOAA/MASC, Library MC5 (Jean Bankhead), 325 Broadway, Boulder, CO 80303	2
OFCM, Suite 900, 6010 Executive Blvd, Rockville, MD 20852	1
NOAA Library-EOC4WSC4, Attn: ACQ, 6009 Executive Blvd, Rockville, MD 20852	1
NOAA/NESDIS (Attn: Capt Pereira), FB #4, Rm 0308, Suitland, MD 20746	1
Armed Forces Medical Intelligence Agency, Info Svcs Div., Bldg 1607, Ft Detrick, Frederick, MD 21701-5004	1
PL OL-AA/SULLA, Hanscom AFB, MA 01731-5000	1
USAF TL, (Attn: GL-AE, Krause), Ft Belvoir, VA 22060-5546	1
Atmospheric Sciences Laboratory, Attn: SLCAS-AT-AB, Aberdeen Proving Grounds, MD 21005-5001	1
Atmospheric Sciences Laboratory, White Sands Missile Range, NM 88002-5501	1
U.S. Army Missile Command, ATTN: AMSMI-RD-TE-T, Redstone Arsenal, AL 35898-5250	1
Technical Library, Dugway Proving Ground, Dugway, UT 84022-5000	1
NWS Training Center, 617 Hardesty, Kansas City, MO 64124	1
NCAR Library, Boulder, CO 80307-3000	1
NCDC Library (D542X2), Federal Building, Asheville, NC 28801-2723	1
NIST Pubs Production, Rm A-405, Admin Bldg, Gaithersburg, MD 20899	1
JSOC/Weather, P.O. Box 70239, Fort Bragg, NC 28307-5000	1
75th RGR (Attn: SWO), Ft Benning, GA 31905-5000	1
HQ 5th U.S. Army, AFKB-OP (SWO), Ft Sam Houston, TX 78234-7000	1
NASA-MSFC-ES44, Attn: Dale Johnson, Huntsville, AL 35812-5000	1
Dept of Atmospheric Sciences, 7127 Math Sciences, UCLA, Los Angeles, CA 90024-5000	1
Dept of Oceanography, A-008, Scripps Inst of Oceanography, Univ of Cal, La Jolla, CA 92093-5000	1
Library, USAFA (DFSEL), Colorado Springs, CO 80840-5000	1
Dept of Atmospheric Sciences, PAS Bldg, Univ of Arizona, Tucson, AZ 85721-5000	1
Dept of Atmospheric Sciences, Atmospheric Science Bldg, Colorado St Univ, Ft Collins, CO 80523-5000	1
Meteorology Unit, NYS College of Ag and Life Science, Bradford Hall, Cornell Univ, Ithaca, NY 14853-5000	1
USDAO/AIRA Cairo, Box 9, FPO New York 09527-0061	2
USDAO/AIRA Tel Aviv, Israel, APO New York 09672-5000	2
USDAO/AIRA, APO New York 09254-0001	2
USDAO Damascus, State Dept Pouch Room, Washington, DC 20520	1
Aeronautical Ctr Library (AAC 64D), PO Box 25082, Oklahoma City, OK 73125-5000	1
Dept of Meteorology, Florida State Univ, Tallahassee, FL 32306-5000	1
Dept of Meteorology, Univ of Hawaii, 2525 Correa Road, Honolulu, HI 96822-5000	1
Dept of Atmospheric and Oceanic Science, Space Research Bldg, Univ of Mich, 2455 Hayward, Ann Arbor, MI 41809-2143	1
Dept of Meteorology and Physical Oceanography, Univ of Miami, Miami, FL 33149-1098	1
Dept of Atmospheric Science, Univ of Missouri, 701 Hiatt St, Columbia, MO 65211-5000	1
Ctr for Ag Meteorology and Climatology, Chase Hall-East Campus, Univ of Nebraska-Lincoln, Lincoln, NE 68583-0728	1
Dept of Marine, Earth, and Atmospheric Sciences, North Carolina St Univ, Box 8208, Raleigh, NC 27695-8208	1
School of Meteorology, Univ of Oklahoma, 200 Felgar St, Norman, OK 73019-5000	1
Dept of Atmospheric Sciences, Stand Agriculture Hall, Oregon St Univ, Corvallis, OR 97331-2209	1
Dept of Meteorology, 503 Walker Bldg, Penn St Univ, University Park, PA 16802-5000	1
Dept of Marine Sciences, Univ of Puerto Rico, Mayaguez, PU 00708-5000	1
Dept of Earth and Atmospheric Sciences, Stadium Hall, Purdue Univ, West Lafayette, IN 47907-5000	1
Library, Rand Corporation, PO Box 2138, Santa Monica, CA 90406-5000	1
Dept of Earth and Atmospheric Sciences, St Louis Univ, PO Box 8099-Laclede Station, St Louis, MO 63156-5000	1
Dept of Meteorology, Univ of St Thomas, 3812 Montrose Blvd, Houston, TX 77006-5000	1
Dept of Meteorology, San Jose St Univ, One Washington Square, San Jose, CA 95192-5000	1
Dept of Meteorology, Texas A&M Univ, College Station, TX 77843-5000	2

US Military Academy, USMA Library, West Point, NY 10996-5000	1
Dept of Oceanography, Stop 9d, US Naval Academy, Annapolis, MD 21402-5000	1
Dept of Meteorology, Univ of Utah, Salt Lake City, UT 84112-5000	1
Dept of Meteorology, Utah St Univ, UMC 4840, Logan, UT 84322-5000	1
Dept of Environmental Sciences, Clark Hall, Univ of Virginia, Charlottesville, VA 22903-5000	1
Dept of Meteorology, Univ of Wisconsin, 1225 W Dayton St, Madison, WI 53706-5000	1
DMTC-FDAC, Cameron Station, Alexandria, VA 22304-6145	2
AUL/LSE, Maxwell AFB, AL 36112-5564	1
AWSTL, Scott AFB, IL 62225-5458	100